MOLECULAR DETERMINANTS OF $\gamma\delta$ T CELL SELECTION, MAINTENANCE AND FUNCTION

EDITED BY: Pierre Vantourout, David Vermijlen and Daniel J. Pennington
PUBLISHED IN: Frontiers in Immunology

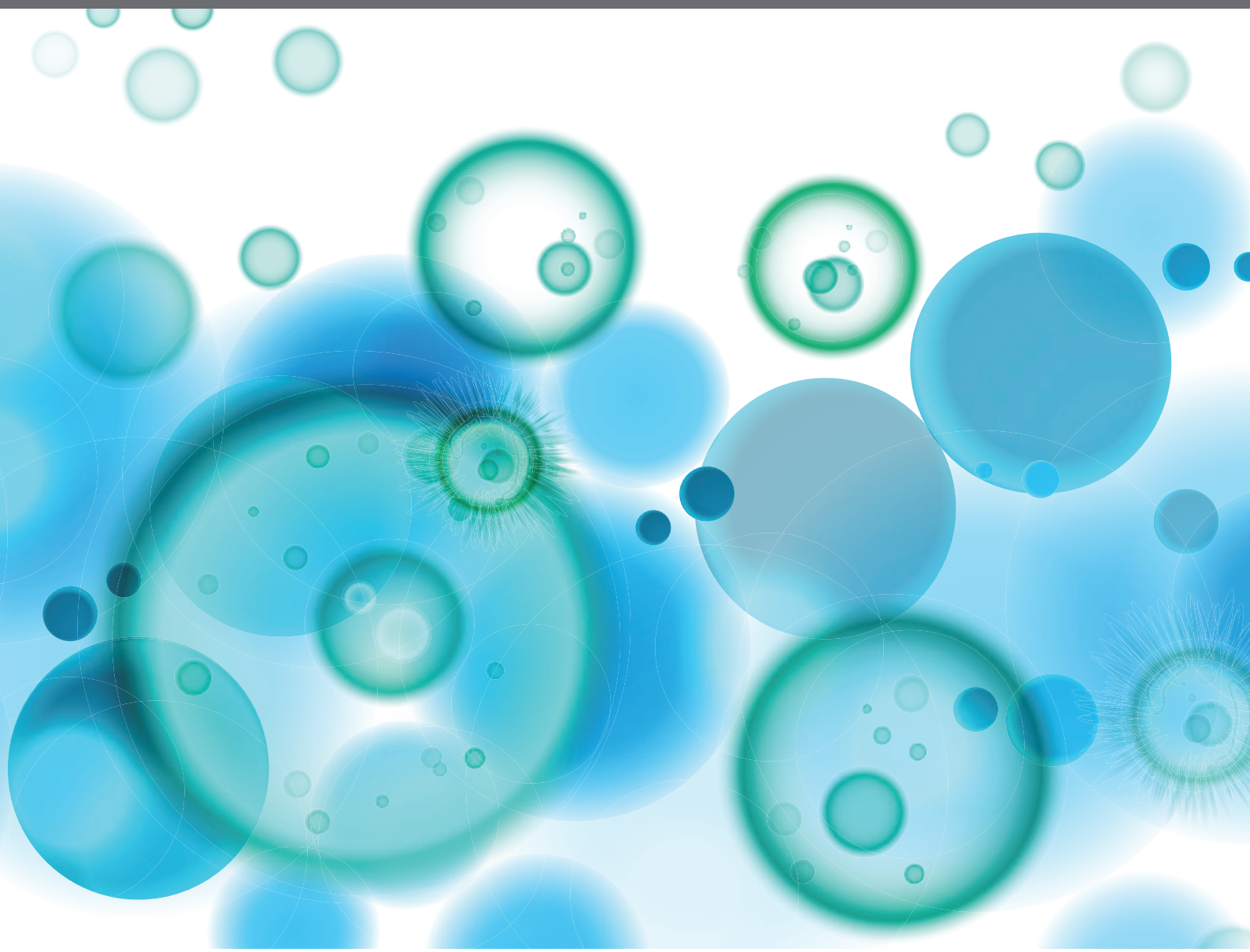

frontiers Research Topics

Frontiers Copyright Statement

© Copyright 2007-2019 Frontiers Media SA. All rights reserved.

All content included on this site, such as text, graphics, logos, button icons, images, video/audio clips, downloads, data compilations and software, is the property of or is licensed to Frontiers Media SA ("Frontiers") or its licensees and/or subcontractors. The copyright in the text of individual articles is the property of their respective authors, subject to a license granted to Frontiers.

The compilation of articles constituting this e-book, wherever published, as well as the compilation of all other content on this site, is the exclusive property of Frontiers. For the conditions for downloading and copying of e-books from Frontiers' website, please see the Terms for Website Use. If purchasing Frontiers e-books from other websites or sources, the conditions of the website concerned apply.

Images and graphics not forming part of user-contributed materials may not be downloaded or copied without permission.

Individual articles may be downloaded and reproduced in accordance with the principles of the CC-BY licence subject to any copyright or other notices. They may not be re-sold as an e-book.

As author or other contributor you grant a CC-BY licence to others to reproduce your articles, including any graphics and third-party materials supplied by you, in accordance with the Conditions for Website Use and subject to any copyright notices which you include in connection with your articles and materials.

All copyright, and all rights therein, are protected by national and international copyright laws.

The above represents a summary only. For the full conditions see the Conditions for Authors and the Conditions for Website Use.

ISSN 1664-8714
ISBN 978-2-88945-991-9
DOI 10.3389/978-2-88945-991-9

About Frontiers

Frontiers is more than just an open-access publisher of scholarly articles: it is a pioneering approach to the world of academia, radically improving the way scholarly research is managed. The grand vision of Frontiers is a world where all people have an equal opportunity to seek, share and generate knowledge. Frontiers provides immediate and permanent online open access to all its publications, but this alone is not enough to realize our grand goals.

Frontiers Journal Series

The Frontiers Journal Series is a multi-tier and interdisciplinary set of open-access, online journals, promising a paradigm shift from the current review, selection and dissemination processes in academic publishing. All Frontiers journals are driven by researchers for researchers; therefore, they constitute a service to the scholarly community. At the same time, the Frontiers Journal Series operates on a revolutionary invention, the tiered publishing system, initially addressing specific communities of scholars, and gradually climbing up to broader public understanding, thus serving the interests of the lay society, too.

Dedication to Quality

Each Frontiers article is a landmark of the highest quality, thanks to genuinely collaborative interactions between authors and review editors, who include some of the world's best academicians. Research must be certified by peers before entering a stream of knowledge that may eventually reach the public - and shape society; therefore, Frontiers only applies the most rigorous and unbiased reviews.
Frontiers revolutionizes research publishing by freely delivering the most outstanding research, evaluated with no bias from both the academic and social point of view. By applying the most advanced information technologies, Frontiers is catapulting scholarly publishing into a new generation.

What are Frontiers Research Topics?

Frontiers Research Topics are very popular trademarks of the Frontiers Journals Series: they are collections of at least ten articles, all centered on a particular subject. With their unique mix of varied contributions from Original Research to Review Articles, Frontiers Research Topics unify the most influential researchers, the latest key findings and historical advances in a hot research area! Find out more on how to host your own Frontiers Research Topic or contribute to one as an author by contacting the Frontiers Editorial Office: researchtopics@frontiersin.org

MOLECULAR DETERMINANTS OF γδ T CELL SELECTION, MAINTENANCE AND FUNCTION

Topic Editors:
Pierre Vantourout, King's College London, United Kingdom
David Vermijlen, Free University of Brussels, Belgium
Daniel J. Pennington, Queen Mary University of London, United Kingdom

Citation: Vantourout, P., Vermijlen, D., Pennington, D. J., eds. (2019). Molecular Determinants of γδ T Cell Selection, Maintenance and Function. Lausanne: Frontiers Media. doi: 10.3389/978-2-88945-991-9

Table of Contents

frontiers in Immunology

ORIGINAL RESEARCH
published: 09 July 2018
doi: 10.3389/fimmu.2018.01579

Anti-CD3 Fab Fragments Enhance Tumor Killing by Human γδ T Cells Independent of Nck Recruitment to the γδ T Cell Antigen Receptor

*Claudia Juraske[1,2,3], Piyamaporn Wipa[1,2,4], Anna Morath[1,2,3,5], Jose Villacorta Hidalgo[6,7], Frederike A. Hartl[1,2,3], Katrin Raute[1,2,3,5], Hans-Heinrich Oberg[8], Daniela Wesch[8], Paul Fisch[6], Susana Minguet[1,2,3], Sutatip Pongcharoen[9,10,11] and Wolfgang W. Schamel[1,2,3]**

[1] Department of Immunology, Faculty of Biology, University of Freiburg, Freiburg, Germany, [2] Centre for Biological Signalling Studies (BIOSS), University of Freiburg, Freiburg, Germany, [3] Center for Chronic Immunodeficiency (CCI), Medical Center – University of Freiburg, Faculty of Medicine, University of Freiburg, Freiburg, Germany, [4] Department of Microbiology and Parasitology, Faculty of Medical Science, Naresuan University, Phitsanulok, Thailand, [5] Spemann Graduate School of Biology and Medicine (SGBM), University of Freiburg, Freiburg, Germany, [6] Department of Pathology, Faculty of Medicine, University of Freiburg, Freiburg, Germany, [7] University Hospital "José de San Martin", University of Buenos Aires, Buenos Aires, Argentina, [8] Institute of Immunology, Christian-Albrechts University of Kiel, Kiel, Germany, [9] Division of Immunology, Department of Medicine, Faculty of Medicine, Naresuan University, Phitsanulok, Thailand, [10] Research Center for Academic Excellence in Petroleum, Petrochemical and Advanced Materials, Faculty of Science, Naresuan University, Phitsanulok, Thailand, [11] Centre of Excellence in Medical Biotechnology, Faculty of Medical Science, Naresuan University, Phitsanulok, Thailand

OPEN ACCESS

Edited by:
Daniel J. Pennington,
Queen Mary University of London,
United Kingdom

Reviewed by:
Christopher E. Rudd,
Université de Montréal, Canada
Pierre Vantourout,
King's College London,
United Kingdom
Maria L. Toribio,
Centro de Biología Molecular
Severo Ochoa (CSIC-UAM), Spain

***Correspondence:**
Wolfgang W. Schamel
wolfgang.schamel@biologie.
uni-freiburg.de

Specialty section:
This article was submitted
to T Cell Biology,
a section of the journal
Frontiers in Immunology

Received: 13 January 2018
Accepted: 26 June 2018
Published: 09 July 2018

Citation:
Juraske C, Wipa P, Morath A,
Hidalgo JV, Hartl FA, Raute K,
Oberg H-H, Wesch D, Fisch P,
Minguet S, Pongcharoen S and
Schamel WW (2018) Anti-CD3
Fab Fragments Enhance Tumor
Killing by Human γδ T Cells
Independent of Nck Recruitment
to the γδ T Cell Antigen Receptor.
Front. Immunol. 9:1579.
doi: 10.3389/fimmu.2018.01579

T lymphocytes expressing the γδ T cell receptor (γδ TCR) can recognize antigens expressed by tumor cells and subsequently kill these cells. γδ T cells are indeed used in cancer immunotherapy clinical trials. The anti-CD3ε antibody UCHT1 enhanced the *in vitro* tumor killing activity of human γδ T cells by an unknown molecular mechanism. Here, we demonstrate that Fab fragments of UCHT1, which only bind monovalently to the γδ TCR, also enhanced tumor killing by expanded human Vγ9Vδ2 γδ T cells or pan-γδ T cells of the peripheral blood. The Fab fragments induced Nck recruitment to the γδ TCR, suggesting that they stabilized the γδ TCR in an active CD3ε conformation. However, blocking the Nck-CD3ε interaction in γδ T cells using the small molecule inhibitor AX-024 neither reduced the γδ T cells' natural nor the Fab-enhanced tumor killing activity. Likewise, Nck recruitment to CD3ε was not required for intracellular signaling, CD69 and CD25 up-regulation, or cytokine secretion by γδ T cells. Thus, the Nck-CD3ε interaction seems to be dispensable in γδ T cells.

Keywords: γδ T cells, T cell antigen receptor, tumor, Nck, activation, signaling, Fab fragments, AX-024

INTRODUCTION

T cells are part of the adaptive immune system and can be divided into αβ and γδ T cells, depending on the T cell antigen receptor (TCR) they express. Whereas most αβ TCRs recognize peptides presented by MHC molecules, γδ TCRs recognize stress-induced self-antigens (1, 2), lipids or pyrophosphates that are secreted by microbes or overproduced in tumor cells (3–7).

The main subset of γδ T cells in human blood is Vγ9Vδ2, which accounts for 2–10% of all T cells. The Vγ9Vδ2 TCR recognizes self and foreign non-peptidic phosphorylated small organic

compounds of the isoprenoid pathway, collectively termed phosphoantigens (8–12). It is known that Vγ9Vδ2 T cells are also stimulated by certain tumor cells, such as the Daudi B cell lymphoma (13), which most likely expresses high levels of phosphoantigens (14). Alternatively, γδ T cells recognize cell surface molecules that are differentially expressed on transformed solid tumors or lymphomas and leukemias (7, 15). An enhanced production of phosphoantigens in transformed cells can be further increased by therapeutically administered nitrogen-containing bisphosphonates, such as zoledronate, which inhibit the farnesyl pyrophosphate synthase of the isoprenoid pathway (16, 17). Several studies demonstrated that a repetitive stimulation of γδ T cells *in vivo* is necessary to reduce tumor growth (18–20). While sustained stimulation of Vγ9Vδ2 γδ T cells by phosphoantigens or nitrogen-containing bisphosphonates often leads to their exhaustion, bispecific antibodies provide a newly tool to target γδ T cells to antigens expressed by tumor cells and enhanced their cytotoxic activity (19, 21–23). Although the exact molecular mechanism leading to phosphoantigen recognition is a matter of debate (24, 25), this recognition is clearly mediated by cognate interaction with the Vγ9Vδ2 TCR.

T cell antigen receptors consist of a clonotypic TCRαβ or TCRγδ heterodimer, and the CD3δε, CD3γε, and CD3ζζ dimers. TCRαβ and TCRγδ bind to the antigen and the CD3 chains transduce the signal of antigen binding into the cell by phosphorylation of the tyrosines in their cytoplasmic tails by Src-family kinases. Consequently, the tyrosine kinase ZAP70 can bind to phosphorylated CD3 and the signal of ligand binding is transmitted further to intracellular signaling cascades, such as Ca^{2+} influx and the Ras/Erk pathway, ultimately resulting in the activation of the T cell. This includes the execution of the cytotoxic activity to kill infected or tumor cells, up-regulation of CD69 and CD25, as well as secretion of cytokines.

How antigen binding to the TCR is communicated to the cytosolic tails of CD3 is not well understood. The αβ TCR is in equilibrium between two reversible conformations: the antigen-stabilized active CD3 conformation and the resting conformation adopted by non-engaged TCRs (26–28). The active CD3 conformation is stabilized by peptide-MHC or anti-CD3 antibody binding to the αβ TCR (29, 30), and it is absolutely required (but not sufficient) for TCR activation (27, 30–32). This active CD3 conformation is defined by the exposure of a proline-rich sequence (PRS) in CD3ε that then binds to the SH3.1 domain of the adaptor protein Nck [SH3.1(Nck)] (26, 33). Blocking the CD3ε–Nck interaction by the small molecule inhibitor AX-024 or by other means diminished ligand-induced CD3 phosphorylation and downstream signaling events (34–36). Shifting to the active CD3 conformation is necessary for αβ TCR triggering, however, it is not sufficient (30, 37). Fab fragments of anti-CD3 antibodies stabilize the active conformation, but are unable to elicit biochemical signals leading to T cell activation (30, 38, 39). In addition, antigen-induced αβ TCR clustering and/or phosphatase exclusion are required, most likely to elicit stable phosphorylation of the ITAMs and thus, T cell activation (30, 37, 40).

How antigen binding to the γδ TCR is transmitted to the cytosolic tails of CD3 is even more obscure. Antigen binding to TCRγδ failed to expose the CD3ε's PRS, in sharp contrast to the αβ TCR, but efficiently activated the γδ T cell (41). Artificial induction of the active conformation by binding the anti-CD3ε antibody UCHT1 to the γδ TCR enhanced the cytotoxic activity of human γδ T cells against a pancreatic tumor cell line (41). Whether Nck is recruited to γδ TCRs in the natural or the UCHT1 enhanced activity and whether this plays a role in the increased tumor killing is to date unknown.

Here, we used expanded γδ T cells from human peripheral blood of healthy donors and show that UCHT1 and Fab fragments of UCHT1 lead to the recruitment of Nck to the γδ TCR. Further, we stimulated the γδ T cells with B cell lymphomas and demonstrate that UCHT1 Fab fragments increase the tumor killing by the γδ T cells and that Nck binding to the γδ TCR is not involved in this tumor killing.

MATERIALS AND METHODS

Expansion of Human γδ T Cells

Informed consent for the performed studies was obtained from the donors in accordance with the Declaration of Helsinki and Institutional Review Board approval from the University of Freiburg Ethics Committee (412/9). Human peripheral blood mononuclear cells were isolated from healthy donors by using a Ficoll–Hypaque gradient. Cells were adjusted to 10^6 cells/ml and cultured in RPMI 1640 supplemented with 10% fetal calf serum (FCS) and antibiotics.

To expand Vγ9Vδ2 γδ T cells, cells were stimulated with 2.5 μM zoledronate and 50 U/ml rIL-2 (Novartis). Additionally, rIL-2 was added every 2 days over a culture period of 21 days. After 14 days the purity of expanded γδ T cells was analyzed by flow cytometry and was >95% Vγ9Vδ2 T cells.

To expand different γδ T cell subsets, cells were stimulated with 1 μg/ml concanavalin A and rIL-2 and rIL-4 (both 100 U/ml) were added to the cell suspensions. Additionally, rIL-2 and IL-4 were added every 3–4 days over a culture period of 21 days. After 14 days γδ T cells were enriched by negative isolation using the human TCRγ/δ$^+$ T Cell Isolation Kit (Miltenyi Biotech). Cultures were composed of 20–40% Vδ1$^+$ and 60–80% Vδ2$^+$ T cells and the purity of the enriched γδ T cells was evaluated by flow cytometry. Cultures with a purity >95% were used for the experiments.

^{51}Cr Release Assay

Daudi or Raji tumor cells (5,000 cells/well in a 96-well plate) were incubated with 50 μl ^{51}Cr for 1 h at 37°C. After labeling, cells were washed two times and the cell concentration was adjusted to 5×10^4 cells/ml in RPMI 1640 supplemented with 10% FCS, antibiotics, and 50 U/ml rIL-2 (Novartis). The assay was performed in U bottom 96-well plate, with an effector (γδ T cell) to target (Daudi or Raji cells) ratio of 12.5:1, in triplicates and with six replicates for spontaneous (^{51}Cr release from target cells in medium alone) and maximum release (^{51}Cr release from target cells lysed with the detergent Trition X-100). The required amount of effector cells (6.25×10^4 cells/well) was harvested and the concentration was adjusted to 1.25×10^6 cells/ml in RPMI 1640 supplemented with 10% FCS and 50 U/ml rIL-2 (Novartis). To the labeled tumor cells the expanded γδ T cells were added, and left untreated (−)

or treated with 5 μg/ml UCHT1, 3.33 μg/ml Fab, or 3.33 μg/ml Fab_{red} (to obtain equimolar amounts). Additionally, DMSO or different concentrations of the inhibitor AX-024 (36) solubilized in DMSO were added. Cells were incubated at 37°C and 5% CO_2 for 5 h. After incubation, 50 μl of the supernatant was transferred into ^{51}Cr filter plates (Lumaplate). The plates were measured in a microplate scintillation γ-ray counter and data were acquired in counts per minute (cpm). Cytotoxicity was calculated according to the formula: specific lysis (%) = (experimental cpm − spontaneous cpm): (maximum cpm − spontaneous cpm) × 100.

SH3.1(Nck) Pull Down Assay

Zoledronate-expanded γδ T cells were starved for 1 h at 37°C in RPMI 1640 without FCS and left unstimulated or stimulated with 5 μg/ml anti-CD3 antibody UCHT1. Cells were lysed in lysis buffer containing 20 mM Tris–HCl pH 8, 137 mM NaCl, 2 mM EDTA, 10% glycerol, protease inhibitor cocktail, and 0.3% Brij96V. Subsequently, insoluble material was removed by centrifugation. Postnuclear fractions were incubated with glutathione beads coupled to GST-SH3.1(Nck) at 4°C as described (26). Beads, including the bound proteins, were washed and proteins separated by non-reducing SDS-PAGE. Western blotting was performed with anti-CD3ζ and anti-GST antibodies.

Preparation of Fab and Fab_{red} Fragments

UCHT1 Fab fragments were prepared using the Pierce® Fab Micro Preparation Kit from Thermo Fisher Scientific, which uses the enzyme papain to cleave the complete UCHT1 antibody and protein A coupled beads to purify the Fab fragments. The purified Fab fragments were analyzed by SDS-PAGE and Coomassie staining. To generate reduced Fab fragments (Fab_{red}) the purified Fab fragment was incubated with 10 mM dithiothreitol for 30 min at room temperature. Afterward, 1 mM iodoacetamide was added and incubated for further 30 min at room temperature. The Fab_{red} were then immediately used. Purity of Fab and Fab_{red} was further tested by their inability to induce Ca^{2+} influx in T cells.

Flow Cytometry

Concanavalin A expanded γδ T cells were incubated with 5 μg/ml UCHT1, 3.33 μg/ml Fab, or 3.33 μg/ml Fab_{red} or left untreated at 37°C and 5% CO_2 for 5 h. Cells were washed two times and stained with APC-labeled anti-mouse IgG antibody on ice (Southern Biotech). The labeled cell suspension was analyzed by the Gallios™ flow cytometer and the data were analyzed with FlowJo software.

Jurkat and G8 γδ TCR-expressing Jurkat cells were stained with APC-labeled anti-mouse γδ TCR (GL3; eBioscience). Cells were analyzed as described above.

Measurement of Ca^{2+} Influx

Five million cells were resuspended in 1 ml RPMI 1640 medium supplemented with 1% FCS in the presence or absence of 10 nM AX-024, antibiotics, and labeled in the dark with 0.1% pluronic acid, 2.6 μM Fluo-3 AM, and 5.5 μM Fura Red AM (Life Technologies) for 45 min at 37°C. The stained cells were washed and kept on ice in the dark until the measurement. For calcium influx, cells were diluted 1:20 with pre-warmed medium and maintained at 37°C during the event collection on a CyAn ADP flow cytometer (Beckman Coulter). Baseline fluorescence was monitored for 1.5 min, then the stimuli were added as indicated (the Fab and Fab_{red} fragments were added 30 s earlier to ensure binding to the γδ TCR when the other stimuli were added). The stimulation was recorded for further 5 min. Data were analyzed with the FlowJo software.

Intracellular Staining for Phospho-ZAP70 and Phospho-Erk

Peripheral blood mononuclear cells were isolated from healthy donors using a Ficoll–Hypaque gradient. T cells were obtained by negative isolation using the Pan T cell Isolation Kit (Miltenyi Biotech). Cells were taken in RPMI 1640 supplemented with 10% FCS and were rested for 1 h at 37°C in the presence or absence of different concentrations of the inhibitor AX-024 (36). Cells were left unstimulated or stimulated with 10 μg/ml anti-CD3 antibody UCHT1 for 2 min or 5 min and were fixed with 2% paraformaldehyde for 30 min on ice. Subsequently, cells were permeabilized with 87.7% methanol for 30 min on ice and stained with rabbit anti-phospho-ZAP70 (Cell Signaling) or rabbit phospho-Erk (Cell Signaling) overnight. Next, cells were stained with biotin-labeled anti-CD3 (UCHT1; BioLegend), PE-labeled anti-γ/δTCR antibodies (Life Technologies), and DyLight-labeled anti-rabbit IgG (Thermo Scientific) and subsequently with eFluor 450-labeled Streptavidin (eBioscience). Cells were measured by flow cytometry and gated on CD3- and TCRγδ-positive cells for analysis.

In Situ Proximity Ligation Assay (PLA)

Cells were grown on diagnostic microscopic slides (Thermo Scientific). They were left unstimulated, stimulated with 5 μg/ml UCHT1, 3.33 μg/ml Fab, or 3.33 μg/ml Fab_{red} and simultaneously treated with 10 nM AX-024 at 37°C for 5 min. Cells were then fixed with 4% paraformaldehyde, permeabilized with 0.5% saponin, and blocked with blocking solution. Subsequently, cells were co-incubated with the goat anti-CD3ε (M20ε, Santacruz) and a rabbit anti-Nck1 antibody (Cell Signaling). PLA between the CD3ε and Nck1 molecules was performed with the Duolink kit according to the manufacturer's instructions (Olink Bioscience), resulting in red fluorescence signals. Cell nuclei were stained with DAPI. A confocal microscope (C2, Nikon) was used for imaging and analysis. The number of the PLA signal dots was scored with the BlobFinder program (Uppsala University).

CD25 and CD69 Up-Regulation

To each well of a U bottom 96-well plate 2×10^4 Daudi or Raji tumor cells, 2.5×10^5 expanded γδ T cells, and 5 μg/ml UCHT1, 3.33 μg/ml Fab, 3.33 μg/ml Fab_{red}, or medium (unstimulated) were given. In addition, the cells were left untreated or treated with different concentrations of AX-024. The plate was incubated at 37°C and 5% CO_2 for 18 h. After incubation, the supernatants were kept at −80°C to quantify the amounts of TNFα and IFNγ (see below). Cells were stained with APC-labeled anti-CD25 (eBioscience) or APC-labeled anti-CD69 (Life Technologies) together with PE-labeled anti-γ/δTCR antibodies (Life Technologies). Cells were analyzed by flow cytometry gating on γδTCR-positive cells.

TNFα and IFNγ Secretion

The concentrations of TNFα and IFNγ in the culture supernatants were measured by standard enzyme linked immunosorbent assay (ELISA).

Statistical Analysis

Data are represented as mean ± SEM or ± SD. All differences between experimental groups were analyzed with the Student's *t*-test. Significant differences were considered when the *p* values were less than 0.05. (n.s. = non significant, $^{*}p < 0.05$, $^{**}p < 0.01$, $^{***}p < 0.001$, and $^{****}p < 0.0001$). *n* refers to the number of independently performed experiments.

RESULTS

The Anti-CD3ε Antibody UCHT1 Enhances Tumor Killing by Human γδ T Cells

Human short-term expanded Vγ9Vδ2 γδ T cells can kill pancreatic ductal adenocarcinoma Panc89 cells *in vitro* (21, 23), which was enhanced by co-incubation with the anti-CD3ε antibody UCHT1 (41). In order to test target cells from different origins, we used now the ^{51}Cr-labeled human B cell lymphoma lines Daudi or Raji (13) and incubated them with zoledronate-expanded peripheral blood human γδ T cells in the presence or absence of UCHT1. Release of ^{51}Cr to the cell culture supernatant is a measure for the lysis of the tumor cells and was quantified with a scintillation γ-ray counter. Approximately 40% of the Daudi and 5% of the Raji cells were specifically killed by the γδ T cells in the absence of exogenously added antibody (**Figure 1**). The addition of the UCHT1 antibody strongly enhanced tumor killing by the γδ T cells reaching 75% of specific killing for both cell lines (**Figure 1**).

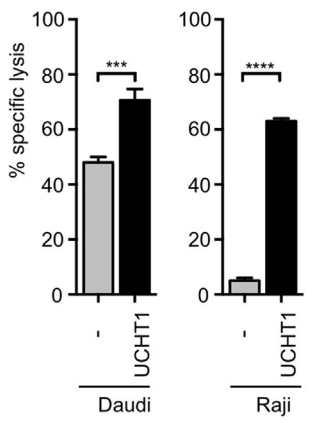

FIGURE 1 | UCHT1 increased tumor killing by γδ T cells. ^{51}Cr-labeled Daudi and Raji cells were incubated with zoledronate-expanded human γδ T cells without (–) or with the addition of 5 μg/ml UCHT1 using an effector to target (T cell to tumor cell) ratio of 12.5:1. After 5 h of co-culture, the amount of released ^{51}Cr was measured in the supernatant by γ-ray spectroscopy. Data represent mean ± SD of triplicate wells ($n = 3$). Significance was determined by unpaired *t*-test, two-tailed between untreated γδ T cells and treated samples.

Using Its SH3.1(Nck) Domain, Nck Is Recruited to the UCHT1-Stimulated γδ TCR

UCHT1 stabilizes the γδ TCR in the active CD3 conformation, in which the CD3ε PRS is exposed (41). Since only the exposed PRS binds to SH3.1(Nck), PRS exposure can be measured with the SH3.1(Nck) pull down assay (**Figure 2A**). To test whether the UCHT1-bound γδ TCR can bind to SH3.1(Nck) in our zoledronate-expanded γδ T cells, we incubated the cells with or without UCHT1 and lysed them. Performing a pull down assay using SH3.1(Nck)-coupled beads, we found that UCHT1 increased the amount of γδ TCR that bound to the beads (**Figures 2B,C**). This indicated that SH3.1(Nck) can bind to the γδ TCR and that UCHT1 stabilizes the γδ TCR in the active CD3 conformation.

To date it is unknown whether endogenous Nck is recruited to the γδ TCR upon stimulation. To test this, we used the *in situ* PLA. PLA is a technique that allows visualization of the close proximity between endogenous proteins in fixed cells by a red fluorescent dot (42). Recently, we established the PLA to quantify the proximity of Nck with the αβ TCR using anti-CD3ε and anti-Nck antibodies (33). Here we applied this assay to γδ T cells. To this end, we incubated expanded human γδ T cells with UCHT1 and performed PLA (**Figure 2D**). Indeed, CD3ε–Nck proximity was increased in UCHT1-stimulated cells compared to unstimulated cells (**Figures 2E,F**) suggesting that Nck is indeed recruited to the γδ TCR upon UCHT1 binding.

To test whether endogenous Nck uses its SH3.1 domain to bind to the CD3ε PRS in the γδ TCR, we made use of the small molecule inhibitor AX-024. In αβ T cells AX-024 was shown to specifically bind to SH3.1(Nck) and hence block the SH3.1(Nck)–PRS interaction (36). Using αβ T cells as a control, we made sure that PLA is a suitable assay to test the inhibition of the SH3.1(Nck)–PRS interaction mediated by AX-024 (Figure S1 in Supplementary Material). Next, we incubated the γδ T cells with UCHT1 in the absence or presence of 10 nM AX-024. Indeed, the CD3ε–Nck proximity was reduced to background levels after AX-024 treatment (**Figures 2E,F**), indicating that the PRS–SH3.1 interaction is necessary for the recruitment of Nck to the γδ TCR upon UCHT1 binding. This finding was corroborated with a PLA experiment in which CD3 phosphorylation was blocked using the Src kinase inhibitor PP2 (Figure S2 in Supplementary Material). Indeed, Nck was recruited to the γδ TCR in the presence of PP2, suggesting that an SH2(Nck)-phospho-CD3 interaction was not required.

Preparation of Pure UCHT1 Fab Fragments

Complete anti-CD3ε antibodies bind bivalently to the TCR leading to T cell activation, whereas Fab fragments of the same antibodies bind monovalently and fail to activate T cells (30, 37–39). The use of complete anti-CD3ε antibodies in therapeutical settings might have the drawback of unspecific polyclonal T cell activation. Thus, we aimed here to investigate whether UCHT1 Fab fragments that only bind monovalently to the TCR might enhance tumor killing by human γδ T cells in the absence of undesired unspecific T cell activation. To this end,

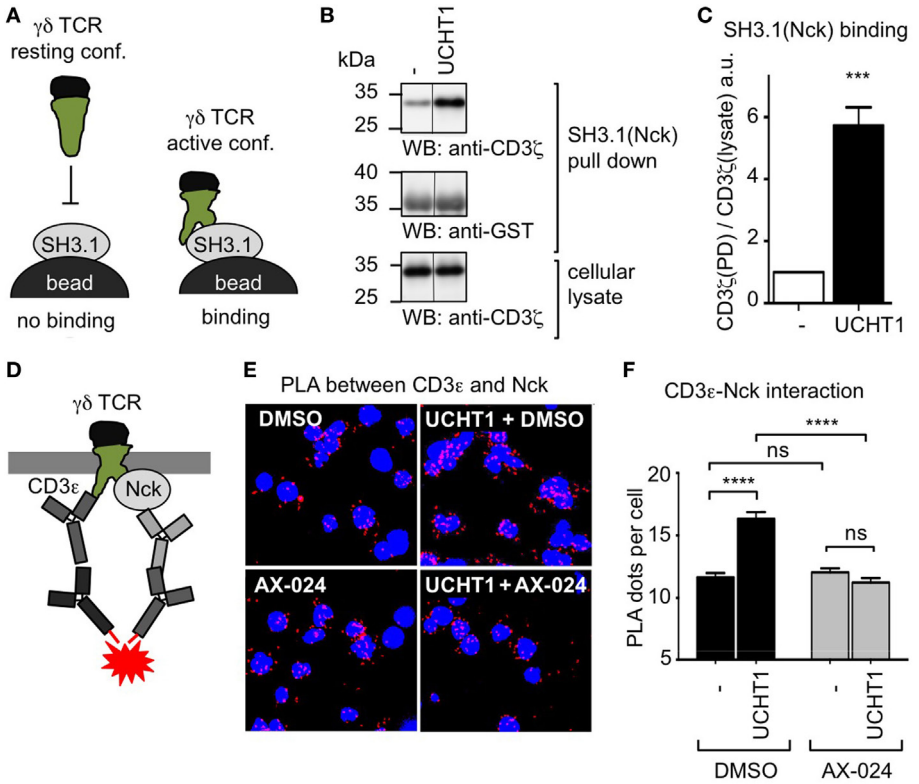

FIGURE 2 | Using its SH3.1(Nck) domain Nck binds to the UCHT1-stimulated γδ T cell antigen receptor (TCR). **(A)** Schematic of the SH3.1(Nck) pull down assay. **(B)** Zoledronate-expanded γδ T cells were left untreated (–) or stimulated with 5 μg/ml UCHT1 at 37°C for 5 min. The cellular lysates were incubated with SH3.1(Nck)-coupled beads and bound proteins separated by SDS-PAGE along with aliquots of the cellular lysate. Western blotting was done using anti-CD3ζ and anti-GST antibodies. **(C)** The normalized ratio of the band intensities of CD3ζ to GST in the SH3.1(Nck) pull down is plotted. Data of three independent experiments were used to calculate the mean ± SD; statistics was done by two-tailed *t*-test. **(D)** Schematic of the *in situ* proximity ligation assay (PLA) using anti-CD3ε and anti-Nck antibodies. **(E)** Close proximity between the TCR and Nck was detected by *in situ* PLA. Zoledronate-expanded γδ T cells were either left untreated (–) or treated with 5 μg/ml UCHT1 in the absence or presence of 10 nM AX-024 at 37°C for 5 min. After fixation and permeabilization, PLA was performed using the primary antibodies goat anti-CD3ε (M20) and rabbit anti-Nck1, and the corresponding secondary antibodies. Nuclei were stained with DAPI. **(F)** The corresponding quantification of the red PLA dots and the mean ± SEM is displayed; statistics was done by two-tailed *t*-test. For each condition 500 cells were analyzed. Three independent experiments were performed ($n = 3$).

we generated pure Fab fragments by cleaving UCHT1 antibodies with papain and subsequently purifying the Fab fragments using the Pierce Fab Micro Preparation kit. The complete UCHT1 antibody before and after digestion and the purified Fab fragments were analyzed by reducing SDS-PAGE and Coomassie staining (**Figure 3A**). We found that the complete immunoglobulin heavy chain (HC) at 50 kDa was not detectable in the Fab fragments, but the light chain (LC) was traceable at 24 kDa (lane 4). As the variable and CH1 parts of the HC have the same size as the LC, they are not visible as an additional band in SDS-PAGE (**Figure 3A**, Fab).

We found earlier that very small amounts of $F(ab')_2$ fragments might contaminate the Fab preparation. They are not detectable by SDS-PAGE and Coomassie staining, but due to their cross-linking ability they can lead to TCR activation in functional assays (30). $F(ab')_2$ fragments can be reduced to Fab fragments by the use of dithiothreitol (DTT) followed by quenching of DTT with iodoacetamide (30). To test for the presence of small amounts of contaminating UCHT1 or UCHT1 $F(ab')_2$ fragments in the Fab preparation, we incubated our reagents with TCRαβ-negative Jurkat T cells expressing the human Vγ9Vδ2 TCR (43, 44) and measured calcium influx into the cytosol as a read-out for TCR activity. The unreduced Fab fragments either did not induce any or just a very small increase in cytosolic calcium (**Figure 3B**, upper panel), indicating that some preparations were contaminated with tiny amounts of $F(ab')_2$. However, the reduced Fab fragments never induced any calcium response (**Figure 3B**, second panel). As a control, the reduced Fab fragment cross-linked by anti-κ LC antibodies, resulted in calcium influx, indicating that the reduced Fab fragments were functional. Treatment of the cells with the complete UCHT1 antibody resulted in the strongest calcium response (**Figure 3B**, lowest panel). From now on, UCHT1 Fab fragments will be called "Fab" and the reduced fragments "Fab_{red}."

By using staining and flow cytometry, we show that Fab and Fab_{red} can equally well bind to human γδ T cells (**Figure 3C**).

In conclusion, Fab_{red} preparations contained functional Fab fragments that are purely monovalent and failed to crosslink and activate the TCR.

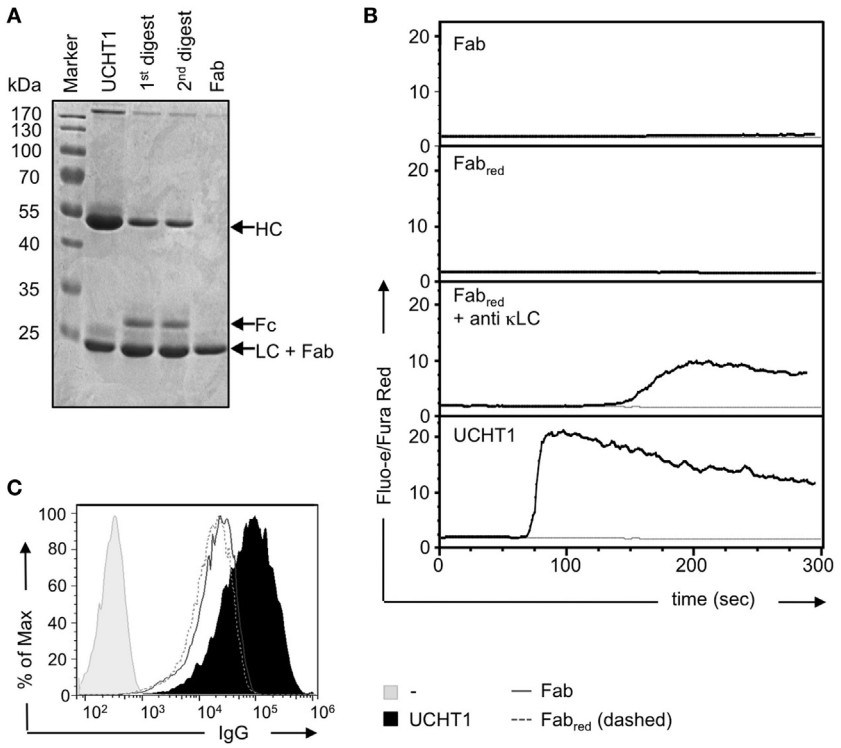

FIGURE 3 | Preparation of UCHT1 Fab fragments. **(A)** The anti-CD3ε antibody UCHT1 was digested with papain using a kit from Thermo Fisher Scientific. The Fab fragments were purified with protein A coupled beads. The complete antibody (lane 1), the first and second digestions (lanes 2 and 3), and the purified Fab fragment (lane 4) were separated by reducing SDS-PAGE followed by Coomassie staining ($n > 3$). **(B)** Jurkat Vγ9Vδ2 cells were labeled with Fluo-3 AA and Fura Red AM and the baseline of cellular Ca^{2+} was measured by flow cytometry for 1 min. The indicated reagents were then added and Ca^{2+} levels were measured for additional 6 min (black lines). The gray lines represent baseline Ca^{2+} level without addition of any stimuli ($n > 3$). **(C)** Concanavalin A expanded γδ T cells were stained with UCHT1, Fab, Fab_{red}, or left untreated, followed by an APC-labeled anti-mouse IgG antibody as a secondary reagent. Fluorescence intensities were quantified by flow cytometry ($n > 3$).

UCHT1 Fab Fragments Enhance Tumor Killing by Human γδ T Cells

Next, we tested whether Fab and Fab_{red} enhance tumor killing by γδ T cells. To this end, we co-cultured zoledronate-expanded γδ T cells with Daudi or Raji cells as in **Figure 1**. Both, Fab and Fab_{red} increased killing of the tumor cells (**Figure 4A**). In Daudi cells, which were more susceptible to the cytotoxic activity of the γδ T cells, Fab, and Fab_{red} were almost as active as UCHT1. In Raji cells, which were only killed to 5% by γδ T cells, Fab and Fab_{red} enhanced the cytotoxic activity, so that 30% of the cells were killed.

Zoledronate and IL-2 specifically expand human Vγ9Vδ2 γδ T cells (16, 23). γδ T cells can also be expanded from human peripheral blood using the lectin concanavalin A, IL-4, and IL-2, resulting in cultures containing both, Vδ1 and Vδ2 γδ T cells (45). Concanavalin A, IL-4, and IL-2 expanded γδ T cells (here called concanavalin A expanded γδ T cells) also killed Daudi and Raji cells, and this activity was increased by UCHT1, Fab, and Fab_{red} (**Figure 4B**). This effect was not donor-specific, since the enhanced tumor killing mediated by UCHT1, Fab, and Fab_{red} was also observed when using concanavalin A expanded γδ T cell from blood of four different healthy donors (HD, **Figure 4C**).

Nck Is Recruited to the γδ TCR Upon Binding to Fab and Fab_{red}

Fab and Fab_{red} do not cross-link the γδ TCR, but might enhance tumor killing by stabilizing the active CD3 conformation of the γδ TCR—just as the complete UCHT1 antibody does (**Figure 2**). Hence, we used PLA to test whether Fab and Fab_{red} induced the recruitment of Nck to the γδ TCR. Indeed, treatment of the γδ T cells with Fab and Fab_{red} resulted in an increase in TCR–Nck proximity (**Figures 5A,B**). Again, the incubation with the small molecule inhibitor AX-024 reduced Nck binding to the γδ TCR to background levels. This finding suggests that binding of Fab and Fab_{red} to the γδ TCR artificially stabilizes the active CD3 conformation and results in the recruitment of Nck to the γδ TCR using the SH3.1(Nck) domain.

Tumor Killing by γδ T Cells Is Independent of Nck Recruitment to the γδ TCR

We next analyzed whether Nck recruitment to the γδ TCR upon UCHT1, Fab, or Fab_{red} treatment was involved in γδ T cell activation mediated by tumor cells, and for the cytotoxic activity of γδ T cells. Concanavalin A expanded γδ T cells (**Figure 6A**) or zoledronate-expanded γδ T cells (**Figure 6B**) were incubated with

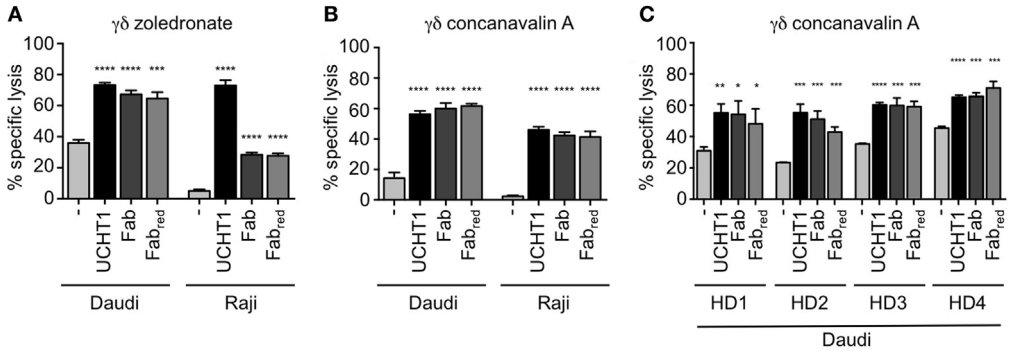

FIGURE 4 | Fab and Fab_{red} fragments enhanced tumor killing by γδ T cells. ^{51}Cr-labeled Daudi and Raji cells were incubated with zoledronate **(A)** or concanavalin A **(B)** expanded γδ T cells in triplicates without (–) or with 5 μg/ml UCHT1, 3.33 μg/ml Fab, or 3.33 μg/ml Fab_{red} (these concentrations were chosen to obtain equimolar amounts of the different reagents). The effector to target ratio was 12.5:1. After 5 h of co-culture, the amount of released ^{51}Cr was measured in the supernatant by γ-ray spectroscopy ($n = 3$). **(C)** Concanavalin A expanded γδ T cells from four different donors (HD1, 2, 3, and 4) were used in a chromium-release assay using Daudi cells as target as in **(A)** ($n = 1$). Data represent mean ± SD of triplicate wells. Significance was determined by unpaired *t*-test, two-tailed between untreated γδ T cells and UCHT1, Fab or Fab_{red}-treated samples.

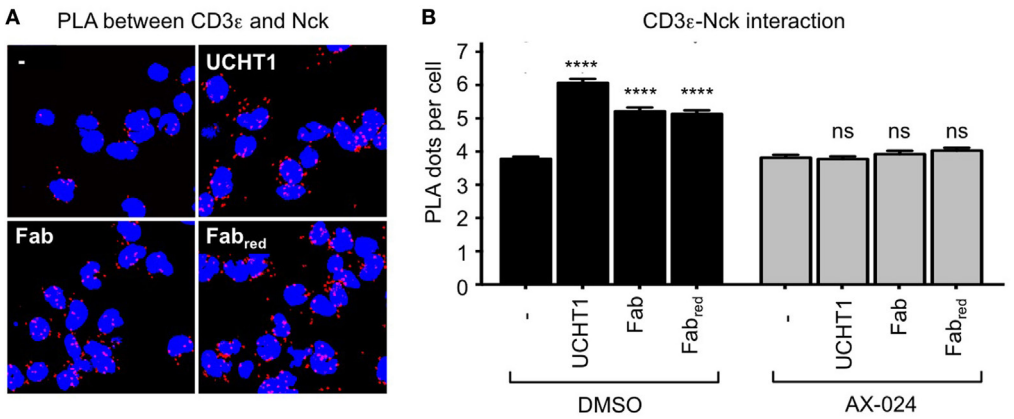

FIGURE 5 | UCHT1 Fab induced the recruitment of Nck to the γδ T cell antigen receptor. **(A)** The proximity ligation assay as in **Figure 2** was performed using 5 μg/ml UCHT1, 3.33 μg/ml Fab, and 3.33 μg/ml Fab_{red} in the absence or presence of 10 nM AX-024. **(B)** The data of **(A)** were analyzed as in **Figure 2F**; 700 cells were analyzed per condition. Two independent experiments were performed ($n = 2$).

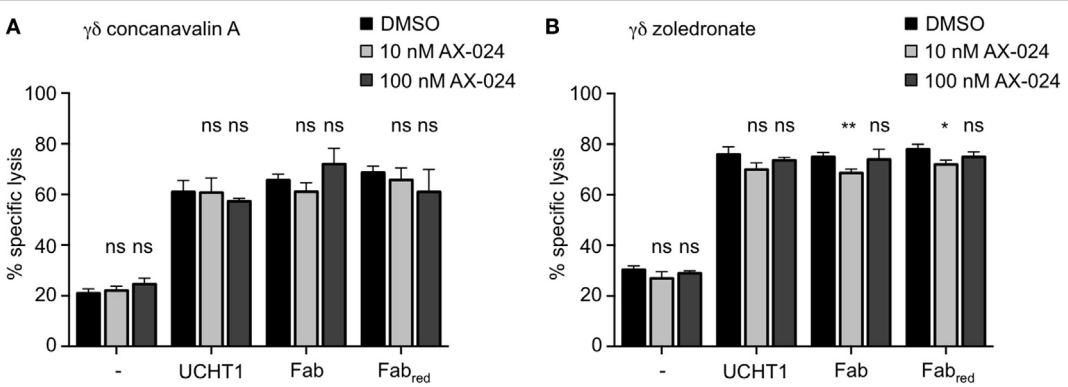

FIGURE 6 | Tumor killing by γδ T cells is independent of Nck recruitment to the γδ T cell antigen receptor. ^{51}Cr-labeled Daudi cells were incubated with concanavalin A **(A)** or zoledronate **(B)** expanded γδ T cells without (–) or with 5 μg/ml UCHT1, 3.33 μg/ml Fab, or 3.33 μg/ml Fab_{red}. In addition, 10 or 100 nM of AX-024 was included or not. The effector to target ratio was 12.5:1. After 5 h of co-culture, the amount of released ^{51}Cr was measured in the supernatant by γ-ray spectroscopy. Data represent mean ± SD of triplicates ($n = 3$). Significance was determined by unpaired *t*-test, two-tailed between untreated samples and samples treated with AX-024.

Daudi cells in the presence or absence of UCHT1, Fab, or Fab_{red} with or without AX-024 to block the PRS–SH3.1 interaction. Two concentrations of AX-024 were used, 10 nM AX-024 as in **Figure 5** and 100 nM AX-024. All three anti-CD3 reagents significantly enhanced tumor killing by the γδ T cells. AX-024 did not disturb the γδ T cell-mediated "basal" tumor cell killing (without anti-CD3 reagents). Importantly, AX-024 did also not influence the enhanced killing activity in the presence of the anti-CD3 reagents for the concanavalin A expanded γδ T cells (**Figure 6A**). In case of the zoledronate-expanded γδ T cells (**Figure 6B**) very small reductions with 10 nM, but not with 100 nM AX-024, can be detected. Hence, we concluded that AX-024 did also not diminish tumor killing for the zoledronate-expanded γδ T cells.

These findings indicate that Nck recruitment to the γδ TCR is dispensable for the cytotoxic activity of γδ T cells stimulated by tumor cells.

Activation of γδ T Cells Is Independent of Nck Recruitment to the γδ TCR

In addition to cytotoxic activity, γδ T cell activation involves up-regulation of the expression of the high affinity IL-2 receptor CD25 and of the activation marker CD69 (46). Next, we sought to analyze whether Fab can also enhance these activation events in γδ T cells and whether Nck binding to the γδ TCR was required for that. Zoledronate-expanded γδ T cells were stimulated with Daudi or Raji cells in the presence or absence of UCHT1, Fab, or Fab_{red} with or without AX-024. As with tumor cell killing, all three anti-CD3 reagents enhanced CD25 (**Figures 7A,B**) or CD69 (**Figure 7C**) up-regulation by the γδ T cells. Blocking the γδ TCR–Nck interaction with AX-024 did neither affect the expression of CD25 nor of CD69 independently of the anti-CD3 reagents (Note that the decrease of UCHT1 enhanced CD69 expression by AX-024 was not seen in other experiments).

We have also tested whether AX-024 impacts on CD69 up-regulation in fresh, naive γδ T cells from human blood. As with the expanded cells, AX-024 did not change the extent of CD69 expression when the cells were stimulated with UCHT1 (Figure S3 in Supplementary Material).

Furthermore, γδ T cells secrete pro-inflammatory cytokines, such as TNFα and IFNγ, upon activation by tumor cells (47). Finally, we show that TNFα and IFNγ production induced by Daudi or Raji cells was enhanced by UCHT1, Fab, or Fab_{red} (**Figures 7D,E**). AX-024 neither diminished TNFα and IFNγ secretion in the absence nor in the presence of the anti-CD3 reagents.

Together, our data indicate that UCHT1, Fab, or Fab_{red} binding to the γδ TCR enhances the tumor cell-induced activation of γδ T cells. Although Nck is recruited to the anti-CD3 bound γδ TCR, this recruitment seems to be dispensable for γδ T cell activation events, such as cytotoxicity, CD25, and CD69 up-regulation, as well as TNFα and IFNγ secretion.

Fab Fragments Enhance Intracellular Signaling Independent of the Nck-γδ TCR Interaction

If Nck recruitment to the γδ TCR is not involved in tumor killing and the up-regulation of activation markers, it might also not be required for the γδ TCR induced induction of intracellular signaling. To test this, we stimulated fresh human γδ T cells with UCHT1 in the absence or presence of AX-024 and measured the phosphorylation of the kinases ZAP70 and Erk by flow cytometry (Figures S4A,B in Supplementary Material). As expected, γδ TCR stimulation increased the amount of phospho-ZAP70 and phospho-Erk. Importantly, treatment of the cells with AX-024 did not influence the extent of ZAP70 or Erk phosphorylation, indicating that recruitment of Nck to the γδ TCR was not required for the induction of signaling by the UCHT1-stimulated γδ TCR.

Next we asked whether Fab fragments would also increase signaling by an antigen-triggered γδ TCR. In order to use a cognate ligand for the γδ TCR, we switched to a different γδ TCR system, namely the G8 γδ TCR where a clearly defined ligand, namely MHC class I-like T22, can be used (48, 49). In fact, stimulation of G8 γδ TCR-expressing cells with soluble T22 tetramers leads to T cell stimulation without stabilizing the CD3 conformational change at the γδ TCR (41). Here, we expressed the G8 γδ TCR in Jurkat T cells, similar to as we did with a chimeric γδ TCR in a Jurkat-derived cell (27). Indeed, the G8 γδ TCR was expressed on the surface of the Jurakt cells (**Figure 8A**).

Next, we stimulated the G8 γδ TCR-expressing Jurkat cells with soluble T22 tetramers and measured the amount of intracellular calcium as a signaling read-out. As expected, the Fab fragments hardly induced calcium signaling downstream of the γδ TCR, whereas T22 tetramers did (**Figure 8B**). Importantly, adding Fab to the T22 tetramers augmented the calcium response, most likely by stabilizing the γδ TCR in the active CD3 conformation. The same result was obtained when using Fab_{red} fragments (Figure S5A in Supplementary Material).

To test whether the enhanced calcium response was sensitive to the recruitment of Nck to the γδ TCR, we stimulated the G8 γδ TCR-expressing Jurkat cells with the T22 tetramers and Fab in the absence or presence of AX-024. Clearly, AX-024 treatment did reduce the calcium response (**Figure 8C**), suggesting that the Nck–γδ TCR interaction was not required for the enhanced calcium signaling. The same result was obtained when using Fab_{red} fragments (Figure S5B in Supplementary Material).

Together our data suggest that Fab fragments enhance signaling *via* the γδ TCR by stabilizing the active CD3 conformation, independent of the Nck–γδ TCR interaction.

DISCUSSION

The potential use of cytotoxic γδ T cells in immunotherapy against cancer is particularly attractive. Since γδ T cells are independent of antigen presentation by MHC class I and of the presence of mutated epitopes, they are ideal effectors against tumors with low mutation loads. Cytotoxic γδ T cells display afferent responses and have been recognized as the best favorable prognosis marker for solid tumors when infiltrated immune cells were analyzed (50). This suggested that γδ T cells play an important role in the defense against tumors in human patients. Therefore, γδ T cells are currently tested as cellular reagents in cancer immunotherapy clinical trials (51–53).

We have previously shown that the tumor killing activity of γδ T cells can be increased by addition of the anti-CD3ε antibody

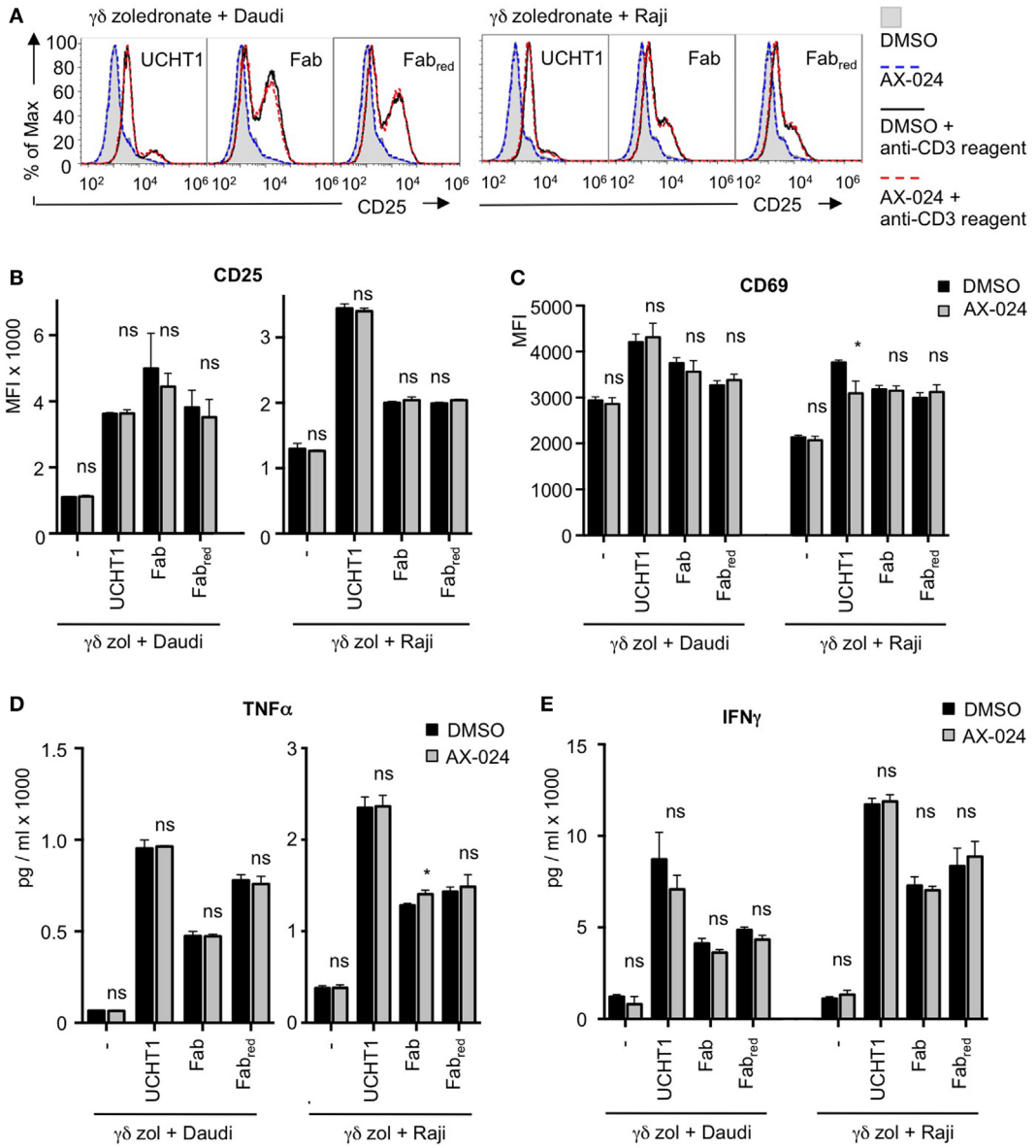

FIGURE 7 | The up-regulation of activation markers and cytokines is independent of Nck recruitment to the γδ T cell antigen receptor (TCR). Daudi and Raji cells were incubated with zoledronate-expanded γδ T cells without (–) or with 5 μg/ml UCHT1, 3.33 μg/ml Fab, or 3.33 μg/ml Fab$_{red}$. In addition, 10 nM AX-024 was included or not. The γδ T cell to target cell ratio was 12.5:1. The cells were co-cultured at 37°C and 5% CO_2 for 18 h. Subsequently, cells were either stained with anti-CD25 and anti-γ/δTCR **(A,B)** or with anti-CD69 and anti-γ/δTCR **(C)** antibodies. Fluorescence intensities were quantified by flow cytometry **(A)** and the mean fluorescence intensity is displayed **(B,C)**. Data represent mean ± SD of triplicates ($n = 3$). Significance was determined by unpaired *t*-test, two-tailed between untreated samples and samples treated with AX-024. **(D,E)** The experiments were performed as in **(A)**. After co-culturing of the cells for 18 h, the supernatants were harvested. TNFα **(D)** and IFNγ **(E)** concentrations were quantified by enzyme linked immunosorbent assay.

UCHT1. However, UCHT1 is a potent T cell activating agent due to its intrinsic capability to induce cross-linking of TCRs and to stabilize the active CD3 conformation (27, 41). Thus, UCHT1 activates all T cells (αβ and γδ), regardless of their specificity, possibly resulting in an unspecific polyclonal T cell response and a potential life-threatening cytokine storm. These drawbacks profoundly limit the use of UCHT1 as a therapeutical agent to enhance tumor cell killing by cytotoxic γδ T cells that recognize tumor antigens by their γδ TCR. Here, we aimed to explore the use of UCHT1 Fab fragments as an alternative to enhance tumor killing by γδ T cells. UCHT1 Fab fragments do not activate αβ TCRs by themselves due to their monovalent binding (30, 38, 39) and here we show that this is also the case with the γδ TCR. Importantly, we demonstrate that UCHT1 Fab fragments significantly boosted tumor cell killing by γδ T cells, suggesting the use of UCHT1 Fab fragments as specific co-stimulation agents in γδ T cell immunotherapy approaches.

All three ligands that were previously tested for the γδ TCR (Daudi and phosphoantigens for the human Vγ9Vδ2 TCR and

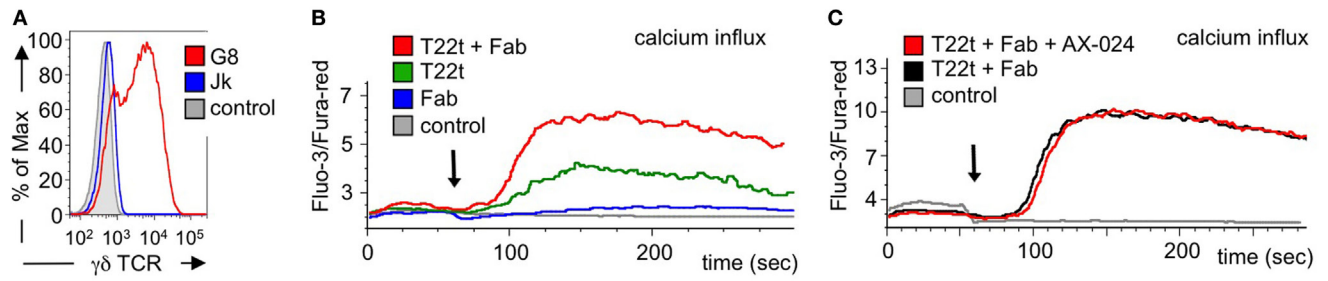

FIGURE 8 | Calcium signaling is enhanced by Fab fragments and does not require the Nck-γδ T cell antigen receptor (TCR) interaction. **(A)** G8 γδ TCR-expressing Jurkat cells were stained with the γδ TCR-specific antibody GL3 and analyzed by flow cytometry. As controls, the GL3-stained parental Jurkat cells and unstained G8 γδ TCR-expressing cells are shown ($n > 3$). **(B)** Jurkat cells expressing the G8 γδ TCR were stimulated with the G8 ligand T22 tetramers (T22t), UCHT1 Fab, or a combination of both T22t and Fab. Intracellular calcium was measured using the dyes Fluo-3 and Fura-red by flow cytometry. Calcium influx is depicted as the median ratio of Fluo-3 to Fura-red fluorescence over time. As a negative control, steptavidin was added to the cells. The arrow indicates addition of the stimuli ($n = 3$). **(C)** The experiment was performed as in **(C)** with the difference that cells without and with 10 nM AX-024 were stimulated with the combination of T22t and Fab. As a control, PBS was added to the cells ($n = 3$).

T22 tetramers for the murine G8 TCR) did not stabilize the active CD3 conformation, as defined by the exposure of the CD3ε PRS (41). In contrast, UCHT1 did stabilize the γδ TCR in its active conformation (41). In addition, UCHT1 binds simultaneously to two TCRs and thereby crosslinks γδ TCRs, leading to γδ TCR and T cell activation. Thus, by using UCHT1, it is not possible to distinguish whether cross-linking of TCRs or stabilization of the CD3 active conformation is the event enhancing tumor killing by γδ T cells. To answer this mechanistic question, we used here monovalent UCHT1 Fab fragments, which only have one binding site per molecule and, therefore, do not cross-link TCRs. Our data show that UCHT1 Fab fragments also enhanced the cytotoxic activity of human γδ T cells. Thus, a cross-linking activity is not required to boost γδ T cell cytotoxic activity. We next tested whether UCHT1 Fab fragments also stabilize the active γδ CD3 conformation and thereby, induce the recruitment of Nck to the CD3ε PRS. The treatment of the γδ T cells with the Fab fragments or with UCHT1 led to the recruitment of Nck to the γδ TCR. This induced recruitment was abrogated in the presence of the inhibitor AX-024, which blocks the interaction of the CD3ε PRS with SH3.1(Nck) (36). And indeed SH3.1(Nck) can bind to the CD3ε PRS in γδ TCRs [(41) and this study]. These data provide strong mechanistic evidence demonstrating that Nck binds to the γδ TCR *via* the CD3ε PRS upon stabilization of the active CD3 conformation, like in the αβ TCR (26, 33).

Human Vγ9Vδ2 γδ T cells modestly killed the B cell lymphoma lines Daudi and Raji. This killing was enhanced in the presence of UCHT1 Fab. Daudi and other tumor cells express high levels of phosphoantigens (14), which together with butyrophilin 3A1 most likely constitute (part of) the ligand for the Vγ9Vδ2 TCR (24, 25). Thus, the γδ TCR was likely to be bound to the natural phosphoantigen/butyrophilin 3A1 ligand in our experimental settings. This potential binding stimulated the γδ TCR, but without stabilizing the γδ TCR in its active CD3 conformation (41). Here, we show that, in addition to stimulation by the natural ligands, the γδ TCR was stabilized in its active conformation when we used the UCHT1 Fab fragments. This treatment not only enhance the tumor cell killing, but also the activation of γδ T cells as seen by augmented CD69, CD25, IFNγ, and TNFα expression. Enhanced up-regulation of CD69 and CD25 was also seen with the complete UCHT1 antibody ((41) and this study). However, increased production of IFNγ and TNFα by UCHT1 was not seen earlier (41) and this could be due to differences in the cells used (expanded γδ T cells versus a γδ T cell clone). Our data thus support the idea that enforcing the γδ TCR to adopt the active CD3 conformation in the presence of its natural ligand might generate a quantitatively or/and qualitatively distinct set of activation signals that ultimately enhance γδ T cell activation.

One mechanism to promote such distinct signals might have been the recruitment of Nck to the γδ TCR. We found, however, that Nck recruitment was dispensable for the enhanced activation of the γδ T cells in the presence of the Fab fragments or the complete antibody. This suggests that a so far unknown effect of the active CD3 conformation in the γδ TCR increases γδ T cell activity. One possibility might be enhanced phosphorylation of the CD3 tails on tyrosines in analogy to the αβ TCR (27, 28), which might lead to a stronger T cell stimulation. Indeed, the kinase ZAP70 that binds to doubly phosphorylated CD3 subunits (54) and is recruited to the γδ TCR (55) was phosphorylated upon stimulation of γδ T cells with UCHT1. Since this phosphorylation was independent of Nck recruitment, it might be a downstream effect of the active CD3 conformation that we were looking for.

ZAP70 is important to trigger signaling cascades in αβ T cells, such as the Erk and calcium pathways (54), and these pathways are also triggered by stimulation of the Vγ9Vδ2 TCR by phosphoantigens or anti-CD3 antibodies (41, 55–59). Here, we show that calcium influx stimulated by the cognate ligand–γδ TCR interaction was increased upon stabilization of the active CD3 conformation. This is in line with our earlier finding that trapping the γδ TCR in the resting CD3 conformation by using CD3ε mutants [CD3εK76T and CD3εC80G (31, 32)] reduced γδ TCR calcium signaling (41). Similarly UCHT1 enhanced phosphorylation of Erk [(41) and this study], and this again was independent of Nck recruitment to the γδ TCR. Since the Erk pathway is involved

in the antitumor activity of Vγ9Vδ2 T cells (56), an increase in phospho-Erk might explain the enhanced tumor killing when the active CD3 conformation was stabilized. In conclusion, stabilization of the active CD3 conformation in a ligand-triggered γδ TCR leads to enhanced downstream signaling.

Taken together, this study might help to design therapeutical agents, such as the Fab fragments of UCHT1, to specifically enhance tumor cell killing by γδ T cells while preventing unspecific activation of all T cells.

ETHICS STATEMENT

Informed consent for the performed studies was obtained from the donors in accordance with the Declaration of Helsinki and Institutional Review Board approval from the University of Freiburg Ethics Committee (412/9).

AUTHOR CONTRIBUTIONS

CJ performed the killing assays as well as the CD69 and CD25 up-regulation experiments. CJ and AM prepared and tested the Fab fragments and performed the signaling assays. CJ, KR, H-HO, DW, and AM expanded human γδ T cells. PW, CJ, and FH performed the PLA experiments and JH performed the ELISA. PF, SM, SP, and WS conceived the experiments. CJ, WS, PW, DW, PF, SM, and SP wrote or edited the manuscript.

ACKNOWLEDGMENTS

We thank the BIOSS toolbox for preparing antibodies for this work and for running the robotic platform (INST 39/899-1 FUGG) to conduct the calcium equipments as well as Sylvia Kock for technical assistance. We thank Balbino Alarcon, Damia Tormo, and Andy Gagete from Artax Biopharma for providing the AX-024 inhibitor and Erin J. Adams and Andrew Sandstrom for the T22 tetramers. This work was funded by the Deutsche Forschungsgemeinschaft (DFG) through EXC294 (the Center for Biological Signaling Studies, BIOSS, WWS), GSC-4 (Spemann Graduate School, AM and KR), SFB1160 (PF, SM), SFB850 (SM), and MI1942/2-1 (SM). FAH was supported by the Elite programme of the Baden-Württemberg Stiftung to SM. JH was supported by a Ph.D. fellowship from the Deutscher Akademischer Austauschdienst (DAAD) and PW by the Royal Golden Jubilee Ph.D. programme of the Thailand Research Fund (TRF). WS was supported by the German Federal Ministry of Education and Research (BMBF 01EO1303). SP received research grants from Naresuan University (R2560B044) and the TRF (RSA5880009).

SUPPLEMENTARY MATERIAL

The Supplementary Material for this article can be found online at https://www.frontiersin.org/article/10.3389/fimmu.2018.01579/full#supplementary-material.

REFERENCES

1. Groh V, Steinle A, Bauer S, Spies T. Recognition of stress-induced MHC molecules by intestinal epithelial γδ T cells. *Science* (1998) 279:1737–40. doi:10.1126/science.279.5357.1737
2. Uldrich AP, Le Nours J, Pellicci DG, Gherardin NA, McPherson KG, Lim RT, et al. CD1d-lipid antigen recognition by the γδ TCR. *Nat Immunol* (2013) 14:1137–45. doi:10.1038/ni.2713
3. Vantourout P, Hayday A. Six-of-the-best: unique contributions of γδ T cells to immunology. *Nat Rev Immunol* (2013) 13:88–100. doi:10.1038/nri3384
4. Chien Y, Konigshofer Y. Antigen recognition by γδ T cells. *Immunol Rev* (2007) 215:46–58. doi:10.1111/j.1600-065X.2006.00470.x
5. Bonneville M, O'Brien RL, Born WK. γδ T cell effector functions: a blend of innate programming and acquired plasticity. *Nat Rev Immunol* (2010) 10:467–78. doi:10.1038/nri2781
6. Zou C, Zhao P, Xiao Z, Han X, Fu F, Fu L. γδ T cells in cancer immunotherapy. *Oncotarget* (2017) 8:8900–9. doi:10.18632/oncotarget.13051
7. Chitadze G, Oberg HH, Wesch D, Kabelitz D. The ambiguous role of γδ T lymphocytes in antitumor immunity. *Trends Immunol* (2017) 38:668–78. doi:10.1016/j.it.2017.06.004
8. Bukowski JF, Morita CT, Band H, Brenner MB. Crucial role of TCR γ chain junctional region in prenyl pyrophosphate antigen recognition by γδ T cells. *J Immunol* (1998) 161:286–93.
9. Bukowski JF, Morita CT, Tanaka Y, Bloom BR, Brenner MB, Band H. Vγ2Vδ2 TCR-dependent recognition of non-peptide antigens and Daudi cells analyzed by TCR gene transfer. *J Immunol* (1995) 154:998–1006.
10. Constant P, Davodeau F, Peyrat MA, Poquet Y, Puzo G, Bonneville M, et al. Stimulation of human γδ T cells by nonpeptidic mycobacterial ligands. *Science* (1994) 264:267–70. doi:10.1126/science.8146660
11. Tanaka Y, Morita CT, Tanaka Y, Nieves E, Brenner MB, Bloom BR. Natural and synthetic non-peptide antigens recognized by human γδ T cells. *Nature* (1995) 375:155–8. doi:10.1038/375155a0
12. Espinosa E, Belmant C, Pont F, Luciani B, Poupot R, Romagne F, et al. Chemical synthesis and biological activity of bromohydrin pyrophosphate, a potent stimulator of human γδ T cells. *J Biol Chem* (2001) 276:18337–44. doi:10.1074/jbc.M100495200
13. Fisch P, Meuer E, Pende D, Rothenfusser S, Viale O, Kock S, et al. Control of B cell lymphoma recognition via natural killer inhibitory receptors implies a role for human Vγ9/Vδ2 T cells in tumor immunity. *Eur J Immunol* (1997) 27:3368–79. doi:10.1002/eji.1830271236
14. Gober HJ, Kistowska M, Angman L, Jenö P, Mori L, De Libero G. Human T cell receptor γδ cells recognize endogenous mevalonate metabolites in tumor cells. *J Exp Med* (2003) 197:163–8. doi:10.1084/jem.20021500
15. Silva-Santos B, Serre K, Norell H. γδ T cells in cancer. *Nat Rev Immunol* (2015) 15:683–91. doi:10.1038/nri3904
16. Roelofs AJ, Jauhiainen M, Monkkonen H, Rogers MJ, Monkkonen J, Thompson K. Peripheral blood monocytes are responsible for γδ T cell activation induced by zoledronic acid through accumulation of IPP/DMAPP. *Br J Haematol* (2009) 144:245–50. doi:10.1111/j.1365-2141.2008.07435.x
17. Benzaid I, Monkkonen H, Bonnelye E, Monkkonen J, Clezardin P. In vivo phosphoantigen levels in bisphosphonate-treated human breast tumors trigger Vgamma9Vdelta2 T-cell antitumor cytotoxicity through ICAM-1 engagement. *Clin Cancer Res* (2012) 18:6249–59. doi:10.1158/1078-0432.CCR-12-0918
18. Kabelitz D, Wesch D, Pitters E, Zoller M. Characterization of tumor reactivity of human Vγ9Vδ2 γδ T cells in vitro and in SCID mice in vivo. *J Immunol* (2004) 173:6767–76. doi:10.4049/jimmunol.173.11.6767
19. Dieli F, Vermijlen D, Fulfaro F, Caccamo N, Meraviglia S, Cicero G, et al. Targeting human γδ T cells with zoledronate and interleukin-2 for immunotherapy of hormone-refractory prostate cancer. *Cancer Res* (2007) 67:7450–7. doi:10.1158/0008-5472.CAN-07-0199
20. Meraviglia S, Eberl M, Vermijlen D, Todaro M, Buccheri S, Cicero G, et al. In vivo manipulation of Vγ9Vδ2 T cells with zoledronate and low-dose IL-2 for immunotherapy of advanced breast cancer patients. *Clin Exp Immunol* (2010) 161:290–7. doi:10.1111/j.1365-2249.2010.04167.x
21. Oberg HH, Grage-Griebenow E, dam-Klages SA, Jerg E, Peipp M, Kellner C, et al. Monitoring and functional characterization of the lymphocytic compartment in pancreatic ductal adenocarcinoma patients. *Pancreatology* (2016) 16:1069–79. doi:10.1016/j.pan.2016.07.008
22. Oberg HH, Kellner C, Gonnermann D, Peipp M, Peters C, Sebens S, et al. γδ T cell activation by bispecific antibodies. *Cell Immunol* (2015) 296:41–9. doi:10.1016/j.cellimm.2015.04.009

23. Oberg HH, Peipp M, Kellner C, Sebens S, Krause S, Petrick D, et al. Novel bispecific antibodies increase γδ T-cell cytotoxicity against pancreatic cancer cells. *Cancer Res* (2014) 74:1349–60. doi:10.1158/0008-5472.CAN-13-0675
24. Vavassori S, Kumar A, Wan GS, Ramanjaneyulu GS, Cavallari M, El Daker S, et al. Butyrophilin 3A1 binds phosphorylated antigens and stimulates human γδ T cells. *Nat Immunol* (2013) 14:908–16. doi:10.1038/ni.2665
25. Sandstrom A, Peigne CM, Leger A, Crooks JE, Konczak F, Gesnel MC, et al. The intracellular B30.2 domain of butyrophilin 3A1 binds phosphoantigens to mediate activation of human Vγ9Vδ2 T cells. *Immunity* (2014) 40:490–500. doi:10.1016/j.immuni.2014.03.003
26. Gil D, Schamel WW, Montoya M, Sanchez-Madrid F, Alarcon B. Recruitment of Nck by CD3 epsilon reveals a ligand-induced conformational change essential for T cell receptor signaling and synapse formation. *Cell* (2002) 109:901–12. doi:10.1016/S0092-8674(02)00799-7
27. Swamy M, Beck-Garcia K, Beck-Garcia E, Hartl FA, Morath A, Yousefi OS, et al. A cholesterol-based allostery model of T cell receptor phosphorylation. *Immunity* (2016) 44:1091–101. doi:10.1016/j.immuni.2016.04.011
28. Schamel WW, Alarcon B, Hofer T, Minguet S. The allostery model of TCR regulation. *J Immunol* (2017) 198:47–52. doi:10.4049/jimmunol.1601661
29. Risueno RM, Gil D, Fernandez E, Sanchez-Madrid F, Alarcon B. Ligand-induced conformational change in the T-cell receptor associated with productive immune synapses. *Blood* (2005) 106:601–8. doi:10.1182/blood-2004-12-4763
30. Minguet S, Swamy M, Alarcon B, Luescher IF, Schamel WW. Full activation of the T cell receptor requires both clustering and conformational changes at CD3. *Immunity* (2007) 26:43–54. doi:10.1016/j.immuni.2006.10.019
31. Martínez-Martín N, Risueño RM, Morreale A, Zaldívar I, Fernández-Arenas E, Herranz F, et al. Cooperativity between T cell receptor complexes revealed by conformational mutants of CD3epsilon. *Sci Signal* (2009) 2:ra43. doi:10.1126/scisignal.2000402
32. Blanco R, Borroto A, Schamel WW, Pereira P, Alarcon B. Conformational changes in the T cell receptor differentially determine T cell subset development in mice. *Sci Signal* (2014) 7:ra115. doi:10.1126/scisignal.2005650
33. Paensuwan P, Hartl FA, Yousefi OS, Ngoenkam J, Wipa P, Beck-Garcia E, et al. Nck binds to the T cell antigen receptor using its SH3.1 and SH2 domains in a cooperative manner, promoting TCR functioning. *J Immunol* (2016) 196:448–58. doi:10.4049/jimmunol.1500958
34. Borroto A, Arellano I, Dopfer EP, Prouza M, Suchanek M, Fuentes M, et al. Nck recruitment to the TCR required for ZAP70 activation during thymic development. *J Immunol* (2013) 190:1103–12. doi:10.4049/jimmunol.1202055
35. Borroto A, Arellano I, Blanco R, Fuentes M, Orfao A, Dopfer EP, et al. Relevance of Nck-CD3epsilon interaction for T cell activation in vivo. *J Immunol* (2014) 192:2042–53. doi:10.4049/jimmunol.1203414
36. Borroto A, Reyes-Garau D, Jimenez MA, Carrasco E, Moreno B, Martinez-Pasamar S, et al. First-in-class inhibitor of the T cell receptor for the treatment of autoimmune diseases. *Sci Transl Med* (2016) 8:370ra184. doi:10.1126/scitranslmed.aaf2140
37. Minguet S, Schamel WWA. A permissive geometry model for TCR-CD3 activation. *Trends Biochem Sci* (2008) 33:51–7. doi:10.1016/j.tibs.2007.10.008
38. Chang TW, Kung PC, Gingras SP, Goldstein G. Does OKT3 monoclonal antibody react with an antigen-recognition structure on human T cells? *Proc Natl Acad Sci U S A* (1981) 78:1805–8. doi:10.1073/pnas.78.3.1805
39. Kaye J, Janeway CA Jr. The Fab fragment of a directly activating monoclonal antibody that precipitates a disulfide-linked heterodimer from a helper T cell clone blocks activation by either allogeneic Ia or antigen and self-Ia. *J Exp Med* (1984) 159:1397–412. doi:10.1084/jem.159.5.1397
40. Cordoba SP, Choudhuri K, Zhang H, Bridge M, Basat AB, Dustin ML, et al. The large ectodomains of CD45 and CD148 regulate their segregation from and inhibition of ligated T-cell receptor. *Blood* (2013) 121:4295–302. doi:10.1182/blood-2012-07-442251
41. Dopfer EP, Hartl FA, Oberg HH, Siegers GM, Yousefi OS, Kock S, et al. The CD3 conformational change in the γδ T cell receptor is not triggered by antigens but can be enforced to enhance tumor killing. *Cell Rep* (2014) 7:1704–15. doi:10.1016/j.celrep.2014.04.049
42. Soderberg O, Gullberg M, Jarvius M, Ridderstrale K, Leuchowius KJ, Jarvius J, et al. Direct observation of individual endogenous protein complexes in situ by proximity ligation. *Nat Methods* (2006) 3:995–1000. doi:10.1038/nmeth947
43. Alibaud L, Arnaud J, Llobera R, Rubin B. On the role of CD3δ chains in TCRγδ/CD3 complexes during assembly and membrane expression. *Scand J Immunol* (2001) 54:155–62. doi:10.1046/j.1365-3083.2001.00938.x
44. Siegers GM, Swamy M, Fernandez-Malave E, Minguet S, Rathmann S, Guardo AC, et al. Different composition of the human and the mouse γδ T cell receptor explains different phenotypes of CD3γ and CD3δ-immunodeficiencies. *J Exp Med* (2007) 204:2537–44. doi:10.1084/jem.20070782102207c
45. Siegers GM, Ribot EJ, Keating A, Foster PJ. Extensive expansion of primary human γδ T cells generates cytotoxic effector memory cells that can be labeled with Feraheme for cellular MRI. *Cancer Immunol Immunother* (2012) 62:571–83. doi:10.1007/s00262-012-1353-y
46. Wesch D, Marx S, Kabelitz D. Comparative analysis of alpha beta and γδ T cell activation by *Mycobacterium tuberculosis* and isopentenyl pyrophosphate. *Eur J Immunol* (1997) 27:952–6. doi:10.1002/eji.1830270422
47. Kondo M, Sakuta K, Noguchi A, Ariyoshi N, Sato K, Sato S, et al. Zoledronate facilitates large-scale ex vivo expansion of functional γδ T cells from cancer patients for use in adoptive immunotherapy. *Cytotherapy* (2008) 10:842–56. doi:10.1080/14653240802419328
48. Crowley MP, Fahrer AM, Baumgarth N, Hampl J, Gutgemann I, Teyton L, et al. A population of murine γδ T cells that recognize an inducible MHC class Ib molecule. *Science* (2000) 287:314–6. doi:10.1126/science.287.5451.314
49. Adams EJ, Chien YH, Garcia KC. Structure of a γδ T cell receptor in complex with the nonclassical MHC T22. *Science* (2005) 308:227–31. doi:10.1126/science.1106885
50. Gentles AJ, Newman AM, Liu CL, Bratman SV, Feng W, Kim D, et al. The prognostic landscape of genes and infiltrating immune cells across human cancers. *Nat Med* (2015) 21:938–45. doi:10.1038/nm.3909
51. Deniger DC, Moyes JS, Cooper LJ. Clinical applications of γδ T cells with multivalent immunity. *Front Immunol* (2014) 5:636. doi:10.3389/fimmu.2014.00636
52. Fournie JJ, Sicard H, Poupot M, Bezombes C, Blanc A, Romagne F, et al. What lessons can be learned from γδ T cell-based cancer immunotherapy trials? *Cell Mol Immunol* (2013) 10:35–41. doi:10.1038/cmi.2012.39
53. Paul S, Lal G. Regulatory and effector functions of γδ T cells and their therapeutic potential in adoptive cellular therapy for cancer. *Int J Cancer* (2016) 139:976–85. doi:10.1002/ijc.30109
54. Courtney AH, Lo WL, Weiss A. TCR signaling: mechanisms of initiation and propagation. *Trends Biochem Sci* (2018) 43:108–23. doi:10.1016/j.tibs.2017.11.008
55. Lafont V, Liautard J, Sable-Techene M, Sainte-Marie Y, Favero J. Isopentenyl pyrophosphate, a mycobacterial non-peptidic antigen, triggers delayed and highly sustained signaling in human γδ T lymphocytes without inducing down-modulation of T cell antigen receptor. *J Biol Chem* (2001) 276:15961–7. doi:10.1074/jbc.M008684200
56. Correia DV, d'Orey F, Cardoso BA, Lanca T, Grosso AR, deBarros A, et al. Highly active microbial phosphoantigen induces rapid yet sustained MEK/Erk- and PI-3K/Akt-mediated signal transduction in anti-tumor human γδ T-cells. *PLoS One* (2009) 4:e5657. doi:10.1371/journal.pone.0005657
57. Nedellec S, Sabourin C, Bonneville M, Scotet E. NKG2D costimulates human V gamma 9V delta 2 T cell antitumor cytotoxicity through protein kinase C theta-dependent modulation of early TCR-induced calcium and transduction signals. *J Immunol* (2010) 185:55–63. doi:10.4049/jimmunol.1000373
58. Thedrez A, Sabourin C, Gertner J, Devilder MC, Allain-Maillet S, Fournie JJ, et al. Self/non-self discrimination by human γδ T cells: simple solutions for a complex issue? *Immunol Rev* (2007) 215:123–35. doi:10.1111/j.1600-065X.2006.00468.x
59. Cipriani B, Knowles H, Chen L, Battistini L, Brosnan CF. Involvement of classical and novel protein kinase C isoforms in the response of human Vγ9Vδ2 T cells to phosphate antigens. *J Immunol* (2002) 169:5761–70. doi:10.4049/jimmunol.169.10.5761

Conflict of Interest Statement: The authors declare that the research was conducted in the absence of any commercial or financial relationships that could be construed as a potential conflict of interest.

Copyright © 2018 Juraske, Wipa, Morath, Hidalgo, Hartl, Raute, Oberg, Wesch, Fisch, Minguet, Pongcharoen and Schamel. This is an open-access article distributed under the terms of the Creative Commons Attribution License (CC BY). The use, distribution or reproduction in other forums is permitted, provided the original author(s) and the copyright owner(s) are credited and that the original publication in this journal is cited, in accordance with accepted academic practice. No use, distribution or reproduction is permitted which does not comply with these terms.

frontiers in Immunology

MINI REVIEW
published: 02 July 2018
doi: 10.3389/fimmu.2018.01501

Development and Selection of the Human Vγ9Vδ2$^+$ T-Cell Repertoire

Carrie R. Willcox, Martin S. Davey and Benjamin E. Willcox**

Cancer Immunology and Immunotherapy Centre, Institute for Immunology and Immunotherapy, University of Birmingham, Birmingham, United Kingdom

Vγ9Vδ2$^+$ lymphocytes are among the first T-cells to develop in the human fetus and are the predominant peripheral blood γδ T-cell population in most adults. Capable of broad polyclonal responses to pyrophosphate antigens (pAg), they are implicated in immunity to a diverse range of infections. Previously Vγ9Vδ2$^+$ development was thought to involve postnatal selection and amplification of public Vγ9 clonotypes in response to microbial stimuli. However, recent data indicate the Vγ9Vδ2$^+$ T-cell receptor (TCR) repertoire, which is generated early in gestation, is dominated by public Vγ9 clonotypes from birth. These chains bear highly distinct features compared to Vγ9 chains from Vδ1$^+$ T-cells, due either to temporal differences in recombination of each subset and/or potentially prenatal selection of pAg-reactive clonotypes. While these processes result in a semi-invariant repertoire featuring Vγ9 sequences preconfigured for pAg recognition, alterations in TCRδ repertoires between neonate and adult suggest either peripheral selection of clonotypes responsive to microbial antigens or altered postnatal thymic output of Vγ9Vδ2$^+$ T-cells. Interestingly, some individuals demonstrate private Vγ9Vδ2$^+$ expansions with distinct effector phenotypes, suggestive of selective expansion in response to microbial stimulation. The Vγ9Vδ2$^+$ T-cell subset, therefore, exhibits many features common to mouse γδ T-cell subsets, including early development, a semi-invariant TCR repertoire, and a reliance on butyrophilin-like molecules in antigen recognition. However, importantly Vγ9Vδ2$^+$ T-cells retain TCR sensitivity after acquiring an effector phenotype. We outline a model for Vγ9Vδ2$^+$ T-cell development and selection involving innate prenatal repertoire focusing, followed by postnatal repertoire shifts driven by microbial infection and/or altered thymic output.

Keywords: gamma/delta T-cell, T-cell receptor repertoire, Vγ9Vδ2$^+$ T-cell, phosphoantigen, HMBPP

OPEN ACCESS

Edited by:
Daniel J. Pennington, Queen Mary University of London, United Kingdom

Reviewed by:
Bruno Silva-Santos, Instituto de Medicina Molecular (IMM), Portugal
Immo Prinz, Hannover Medical School, Germany

****Correspondence:***
Carrie R. Willcox
c.r.willcox@bham.ac.uk;
Benjamin E. Willcox
b.willcox@bham.ac.uk

Specialty section:
This article was submitted to T Cell Biology, a section of the journal Frontiers in Immunology

Received: *03 May 2018*
Accepted: *18 June 2018*
Published: *02 July 2018*

Citation:
Willcox CR, Davey MS and Willcox BE (2018) Development and Selection of the Human Vγ9Vδ2$^+$ T-Cell Repertoire. Front. Immunol. 9:1501. doi: 10.3389/fimmu.2018.01501

DEVELOPMENT OF THE Vγ9Vδ2$^+$ T-CELL COMPARTMENT

Vγ9Vδ2$^+$ lymphocytes are the predominant γδ T-cell subset in healthy adult peripheral blood. Essentially all Vγ9Vδ2$^+$ T-cells respond to small pyrophosphate antigens (pAg) (1) in a T-cell receptor (TCR)-dependent manner (2), a process dependent on target cell expression of the butyrophilin (BTN) family member BTN3A1 (3). The population expands during childhood (4), typically comprising ~1–10% of total peripheral blood T-cells in healthy adults.

The Vγ9 and Vδ2 variable (V) gene segments are the first γ/δ chains to undergo rearrangement in development, detected in fetal liver from as early as 5–6 weeks gestation (5), and in fetal thymus after 8 weeks gestation (6). By mid-gestation (20–30 weeks), Vγ9Vδ2$^+$ T-cells dominate the γδ repertoire (7) (**Figure 1**). However, Vδ1$^+$ T-cell generation increases later in gestation, and Vδ1$^+$ T-cells comprise

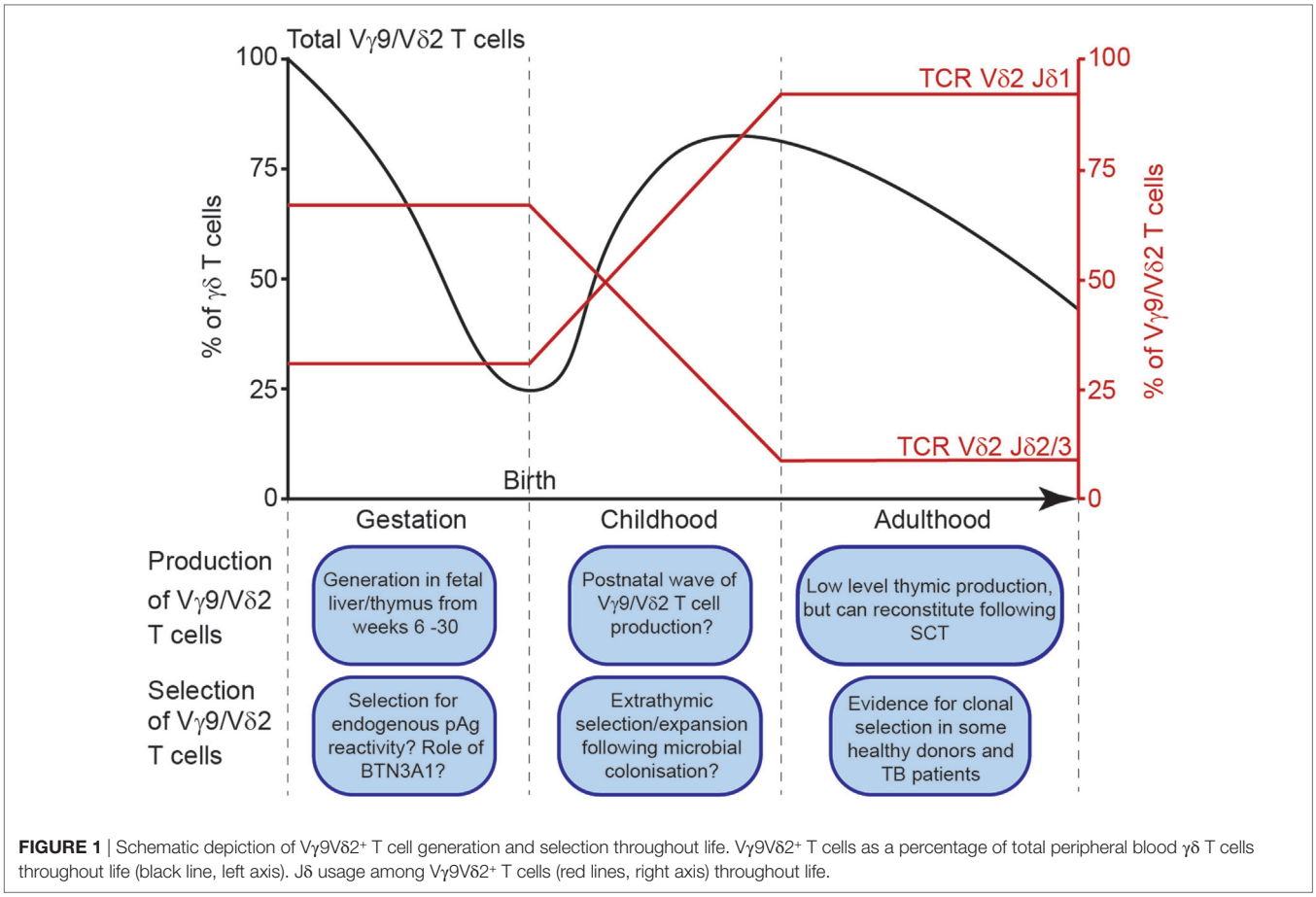

FIGURE 1 | Schematic depiction of Vγ9Vδ2+ T cell generation and selection throughout life. Vγ9Vδ2+ T cells as a percentage of total peripheral blood γδ T cells throughout life (black line, left axis). Jδ usage among Vγ9Vδ2+ T cells (red lines, right axis) throughout life.

the majority of the γδ repertoire in cord blood (7, 8), and in pediatric thymus (9). It is unclear whether gestationally produced Vγ9Vδ2+ cells persist in fetal blood, and become outnumbered by subsequent Vδ1+ T-cell production, or whether most Vγ9Vδ2+ T-cells exit circulation and populate the tissues. However, the dramatic postnatal numerical expansion of Vγ9Vδ2+ T-cells likely occurs following microbial exposure, with the Vγ9Vδ2+ subset ultimately dominating the circulating γδ T-cell repertoire during childhood (4, 10). Consistent with this, Vγ9Vδ2+ T-cells mature in phenotype early after birth concomitant with their numerical expansion (4); moreover, several infections stimulate Vγ9Vδ2+ expansion, and tellingly, identical twins have different Vγ9Vδ2+ profiles (4).

THE Vγ9Vδ2+ TCR REPERTOIRE IN HEALTHY ADULTS

Early studies identified Vγ9Vδ2+ TCR features required for pAg responsiveness. Interestingly, adult Vδ2 CDR3s were highly diverse, composed of Vδ2 joined to one (or occasionally two) diversity (D) segments (usually Dδ3), and typically used joining (J) segment Jδ1 (11, 12). A hydrophobic amino acid, typically Val/Leu/Ile at position 97 of the Vδ2 framework (position 5 of the CDR3, defined as the amino acids between the Vδ2 segment C-terminal Cys and the conserved Phe of the J segment), generated by N-nucleotide addition, was required for pAg recognition (12, 13).

Conversely, Vγ9 gene segments were relatively restricted in CDR3γ sequence and length, and exclusively utilized JγP and constant region Cγ1 (11,14,15). One clonotype (CALW**EVQ**ELGKKIKVF), generated by germline Vγ9-JγP recombination with minimal nucleotide trimming and no N-nucleotide addition, was present in many healthy donors (15). Further low-throughput analyses detected many "public" Vγ9 clonotypes in multiple individuals (16). Although peripheral blood γδ T-cell numbers vary widely between individuals and are influenced by age and sex (17), public clonotypes are conserved irrespective of age, sex, and race (16), and between cord blood and adult (18). Although the presence of such public Vγ9 sequences was thought to reflect strong postnatal peripheral selection and amplification of specific clonotypes following microbial exposure (19), an improved understanding of the Vγ9Vδ2+ TCR repertoire suggests alternative possibilities.

EVIDENCE FOR CONVERGENT RECOMBINATION IN THE Vγ9 TCR REPERTOIRE

Deep sequencing analyses of Vγ9Vδ2+ TCR repertoires (20–23) have confirmed a high frequency of public Vγ9 clonotypes in adult Vγ9Vδ2+ T-cells, and reveal the basis for Vγ9 TCR publicity. The most prevalent of these, CALW**EVQ**ELGKKIKVF, highlighted in many previous studies (7, 11, 15, 16, 18), comprised

between 4 and 45% of the Vγ9 repertoire (20–22). As noted (15), this amino acid sequence can be generated by near-germline recombination of Vγ9 and JγP gene segments with minimal nucleotide trimming and no N-nucleotide addition. However, it can also result from several different nucleotide sequences: (1) involving trimming of nucleotides at the 3′ end of the V region and/or 5′ end of the J region, (2) incorporation of one or more palindromic (P)-nucleotides, and/or (3) addition of one or several non-templated (N)-nucleotides by terminal deoxynucleotide transferase (TdT), resulting in the same amino acid sequence (**Table 1**). Moreover, other public Vγ9 clonotypes can be generated in multiple ways depending on the extent of V and J gene segment trimming, and N/P-nucleotide addition (**Table 1**) (23).

These features suggest the publicity of the Vγ9 repertoire is due to convergent recombination, a phenomenon proposed for generation of public TCRβ repertoires (24), whereby distinct recombination events "converge" to generate the same nucleotide sequences, and multiple nucleotide sequences "converge" to encode the same amino acid sequence. Venturi et al. proposed that public TCRβ responses arise from clonotypes with a high precursor frequency in two ways. Public sequences could arise independently multiple times in each individual by convergent recombination. Alternatively, precursor frequency could be increased if a single TCRβ rearrangement, which undergoes several rounds of proliferation after pre-TCR selection, could pair with many TCRα chains. Importantly, γδ T-cells do not undergo pre-TCR selection or proliferate after successful TCRγ rearrangement (but before TCRδ rearrangement) during T-cell development. Public Vγ9 sequences observed in adults must, therefore, result from convergent recombination.

High throughput Vδ2 TCR repertoire sequencing analyses provide corroborating evidence for convergent Vγ9 recombination. CDR3δ2 repertoires are more diverse than CDR3γ9 repertoires derived from Vγ9Vδ2+ T-cells from most adults (21, 23). Therefore, prevalent Vγ9 clonotypes (e.g., CALW**EVQ**ELGKKIKVF) do not reflect clonal expansion (if so equally large Vδ2 clonotypes would also be observed), but are likely recombined independently multiple times and pair with distinct Vδ2 chains. Single cell PCR in several individuals has substantiated the feasibility of this hypothesis, establishing unequivocally that public Vγ9 CDR3 clonotypes each paired with multiple Vδ2 clonotypes (23), confirming that public Vγ9 sequences arise frequently and independently. These findings prove that "convergent recombination" is an inherent feature of the Vγ9 repertoire, in keeping with public sequences exhibiting high precursor frequency because they have arisen *via* many independent recombination events in each donor. They also raise the question of whether, rather than requiring selective postnatal clonotypic expansion, the prevalence of public Vγ9 sequences may be preconfigured since birth.

TABLE 1 | Common public Vγ9-JγP sequences can be generated by convergent recombination.

	Vγ9						P	N	P		JγP										P nt	N nt
Germline	**TGT**	**GCC**	**TTG**	**TGG**	**GAG**	**GTG**				**T**	**GGG**	**CAA**	**GAG**	**TTG**	**GGC**	**AAA**	**AAA**	**ATC**	**AAG**	**GTA**	**TTT**	
CALW**EVQ**ELGKKIKVF																						
	TGT	GCC	TTG	TGG	GAG	GTG						CAA	GAG	TTG	GGC	AAA	AAA	ATC	AAG	GTA	TTT	0	0
	TGT	GCC	TTG	TGG	GAG	GT		C				CAA	GAG	TTG	GGC	AAA	AAA	ATC	AAG	GTA	TTT	0	1
	TGT	GCC	TTG	TGG	GAG	GT		A				CAA	GAG	TTG	GGC	AAA	AAA	ATC	AAG	GTA	TTT	0	1
	TGT	GCC	TTG	TGG	GAG	GT		T				CAA	GAG	TTG	GGC	AAA	AAA	ATC	AAG	GTA	TTT	0	1
	TGT	GCC	TTG	TGG	GAG	GTG	CA	G					GAG	TTG	GGC	AAA	AAA	ATC	AAG	GTA	TTT	2	1
CALW**EVR**ELGKKIKVF																						
	TGT	GCC	TTG	TGG	GAG	GTG	C	G				A	GAG	TTG	GGC	AAA	AAA	ATC	AAG	GTA	TTT	1	1
	TGT	GCC	TTG	TGG	GAG	GTG		AG				A	GAG	TTG	GGC	AAA	AAA	ATC	AAG	GTA	TTT	0	2
	TGT	GCC	TTG	TGG	GAG	GTG	C	GT					GAG	TTG	GGC	AAA	AAA	ATC	AAG	GTA	TTT	1	2
	TGT	GCC	TTG	TGG	GAG	GTG	C	GC					GAG	TTG	GGC	AAA	AAA	ATC	AAG	GTA	TTT	1	2
	TGT	GCC	TTG	TGG	GAG	GTG	C	GG					GAG	TTG	GGC	AAA	AAA	ATC	AAG	GTA	TTT	1	2
CALW**EAQ**ELGKKIKVF																						
	TGT	GCC	TTG	TGG	GAG	G		CA				CAA	GAG	TTG	GGC	AAA	AAA	ATC	AAG	GTA	TTT	0	2
	TGT	GCC	TTG	TGG	GAG	G		CC				CAA	GAG	TTG	GGC	AAA	AAA	ATC	AAG	GTA	TTT	0	2
	TGT	GCC	TTG	TGG	GAG	G		CG				CAA	GAG	TTG	GGC	AAA	AAA	ATC	AAG	GTA	TTT	0	2
	TGT	GCC	TTG	TGG	GAG	G		CT				CAA	GAG	TTG	GGC	AAA	AAA	ATC	AAG	GTA	TTT	0	2
CALW**EVL**ELGKKIKVF																						
	TGT	GCC	TTG	TGG	GAG	GTG	C	T				A	GAG	TTG	GGC	AAA	AAA	ATC	AAG	GTA	TTT	1	1
	TGT	GCC	TTG	TGG	GAG	GTG	C	TG					GAG	TTG	GGC	AAA	AAA	ATC	AAG	GTA	TTT	1	2
	TGT	GCC	TTG	TGG	GAG	GTG	C	TT					GAG	TTG	GGC	AAA	AAA	ATC	AAG	GTA	TTT	1	2
	TGT	GCC	TTG	TGG	GAG	GTG	C	TC					GAG	TTG	GGC	AAA	AAA	ATC	AAG	GTA	TTT	1	2
CALW**EQ**ELGKKIKVF																						
	TGT	GCC	TTG	TGG	GAG							CAA	GAG	TTG	GGC	AAA	AAA	ATC	AAG	GTA	TTT	0	0
	TGT	GCC	TTG	TGG	GA			A				CAA	GAG	TTG	GGC	AAA	AAA	ATC	AAG	GTA	TTT	0	1

Vγ9 and JγP gene segments are subject to nuclease activity, non-templated (N) nucleotide addition, and incorporation of palindromic (P) nucleotides, during recombination. Above are shown some of the possible different nucleotide sequences observed that generate the same CDR3 amino acid sequences, for five of the most common public Vγ9 sequences. N-nucleotides are shown in red and P-nucleotides are shown in blue.

SHAPING OF THE ADULT Vγ9Vδ2 TCR REPERTOIRE: POSTNATAL SELECTION

An intriguing question is whether Vγ9Vδ2$^+$ T-cells expand *en masse* following microbial exposure during early childhood, concurrent with phenotypic maturation (4, 10), or whether dominant clonotypic selection operates, resulting in prevalent public Vγ9 clonotypes in adults (19). Of relevance, a recent study has compared adult peripheral blood with cord blood Vγ9Vδ2$^+$ TCR repertoires (23). Importantly, the most prevalent public Vγ9 clonotype (CALW**EVQ**ELGKKIKVF) in the fetus (7) was also prevalent in cord (18, 23) and remains dominant in most adults (18, 20, 21). Moreover, other public Vγ9 clonotypes are frequently found in all these populations (16, 23). Also, the CDR3δ lengths in cord blood and adult peripheral blood are similar (23). Therefore, the public Vγ9 clonotypes present in adult peripheral blood Vγ9Vδ2$^+$ T-cells are present at similar relative frequencies in cord blood Vγ9Vδ2$^+$ T-cells. Furthermore, there were relatively subtle changes in the diversity of Vδ2-associated Vγ9 TCR repertoire from neonate to adult (23).

Despite these observations, postnatal changes in the Vδ2 repertoire are ultimately inconsistent with the concept of Vγ9Vδ2$^+$ T-cell expansion *en masse*. Crucially, most Vγ9Vδ2$^+$ cells in adult peripheral blood express Vδ2 recombined with Jδ1 (12), whereas in the cord blood most Vδ2 rearrangements use Jδ3, and to a lesser degree Jδ2 (12, 23) (**Figure 1**). This difference could be explained in two ways. One possibility is that extrathymic selection of specific clonotypes may occur in response to microbial exposure. Of relevance, it is currently unclear whether cord blood Vγ9Vδ2-Jδ3 cells are reactive to common pAg. While most Vδ2-Jδ1$^+$ sequences in cord blood do generally contain a hydrophobic amino acid at position 5 (a motif previously linked to pAg reactivity) (23), fewer Vδ2-Jδ3$^+$ sequences contain this motif (23). Consistent with this, Vγ9Vδ2$^+$ T-cells from cord blood are generally less responsive to pAg than adult Vγ9Vδ2$^+$ T-cells (10, 18, 25), however, the Vδ2 repertoire of responsive cells has not been reported, and conceivably only Vδ2-Jδ1 TCRs were responding in these assays.

A second possibility that could explain postnatal alterations in the Vδ2 TCR repertoire is a second wave of Vγ9Vδ2$^+$ T-cell production after birth. Thymic Vγ9Vδ2$^+$ T-cell output is thought to decrease after birth, based on failure to detect Vγ9 or Vδ2 gene expression in pediatric thymus samples (26), or detection of <10% of thymocytes expressing Vδ2 in thymi from children (4, 9). Surprisingly, Vγ9 expression was not detected in the thymus during childhood, despite its co-expression by Vδ1$^+$ cells (21), which continue to be generated after birth (4, 26). Conceivably this issue warrants reinvestigation, and perhaps postnatal thymic Vγ9Vδ2$^+$ T-cell generation has been underappreciated. Consistent with this, Ravens (22) and others (27, 28) have shown Vγ9Vδ2$^+$ T-cell reconstitution following stem cell transplantation. Newly generated Vγ9Vδ2$^+$ T-cells presumably originate in the recipient's thymus (22). Detailed comparison of Vδ2-Jδ1 sequences in cord blood and adult repertoires (23) also hints at postnatal Vγ9Vδ2$^+$ T-cell production. Although Vδ2-Jδ1 clonotypes are relatively uncommon in cord blood (most use Vδ2-Jδ3 at that time), those present often have shorter CDR3s, incorporating fewer N-nucleotides [as observed in fetal liver (5)] in comparison to the longer, more private Vδ2-Jδ1 clonotypes observed in adults. However, if the Vγ9Vδ2$^+$ T-cells that predominate in adults are indeed generated in the postnatal thymus, we have observed no obvious differences in the Vγ9 repertoire of these cells, suggesting that the thymus continues to generate Vγ9-JγP rearrangements with low diversity even when TdT is expressed and when Vγ9 CDR3s found in Vδ1$^+$ cells are highly diverse (21).

EVIDENCE FOR PRENATAL SHAPING OF THE Vγ9Vδ2$^+$ TCR REPERTOIRE

Postnatal processes clearly strongly influence the Vγ9Vδ2$^+$ T-cell compartment. However, other events may also shape the prenatal Vγ9Vδ2$^+$ repertoire (**Figure 1**). The Vγ9 repertoire is already highly restricted in CDR3 length during gestation, with public clonotypes evident (7), consistent with the cord blood Vγ9 repertoire (23). This indicates postnatal pAg exposure is not required for the selection of these features. However, the possibility that there might be some selection for pAg-reactive semi-invariant Vγ9Vδ2$^+$ T cells before postnatal microbial exposure has been suggested previously (7), which potentially could operate intra- or extra-thymically. Conceivably, this could involve elevated levels of endogenous pAgs such as IPP derived from fetal isoprenoid metabolism, or pAg derived from placental microbiota; in addition, a specific selecting element, such as one or more of the BTN3 gene products could be involved (7). Bearing these possibilities in mind, enrichment of Jδ3 within cord blood Vδ2 sequences relative to adult peripheral blood could relate to more permissive positive selection of clonotypes responding to such fetal-specific selection events relative to postnatal responsiveness to exogenous microbially derived pAg. However, alternatively, genetic processes may explain the restricted nature of the Vγ9 repertoire in fetal and cord blood Vδ2$^+$ cells. Consistent with this suggestion, the mouse OP9-DL1 thymic organ culture system can support Vγ9Vδ2$^+$ T cell generation (9), arguing against a stringent positive selection step involving BTN3A1/pAg-mediated events. Of relevance to inherent genetic bias in Vγ9 chain recombination, whereas Vδ1-associated Vγ9 chains are diverse in length and rarely use JγP, Vδ2-associated Vγ9 CDR3 sequences are restricted in length, and exclusively utilize JγP, including in adults. These differences could merely reflect changes in gene segment accessibility during Vγ9Vδ2$^+$ T-cell generation in early gestation, or regulation of Vγ9 chain recombination that favor simpler public Vγ9 rearrangements during the earlier timescale of fetal Vγ9Vδ2$^+$ T-cell generation, before TdT is expressed (i.e., before 20 weeks of gestation) (29).

COMPARISONS BETWEEN Vγ9Vδ2$^+$ T-CELLS AND SEMI-INVARIANT MOUSE γδ T-CELL SUBSETS

Several features of the Vγ9Vδ2$^+$ compartment suggest similarities to mouse γδ T-cell subsets (30). The early fetal wave of Vγ9Vδ2$^+$ production, combined with the semi-invariant Vγ9Vδ2$^+$ TCR repertoire, mirrors early waves of semi-invariant mouse γδ T-cells. The first T-cells to develop in mouse fetal thymus are Vγ5Vδ1$^+$ dendritic epidermal T-cells, which have limited junctional

diversity in both TCR chains (31). This is followed by production of Vγ6Vδ1 TCRs, also of limited diversity, then postnatal production of more diverse γδ T-cell populations using Vγ4, Vγ1, and Vγ7 chains (32). Some of these γδ populations undergo intrathymic or extrathymic selection events. DETC cells undergo intrathymic selection involving the BTN family member Skint1 (33, 34); the Vγ7 repertoire requires the presence of BTNL1/6 for extrathymic intestinal selection (35). Another semi-invariant mouse population expresses Vγ4 sequences of restricted length and diversity (analogous to public human Vγ9 sequences) with a germline-encoded Vδ5-Dδ2-Jδ1 sequence (36, 37), although its role and the signals that drive selection are unknown. The presence of γδ T-cells expressing semi-invariant TCRs in both mice and humans suggests this may reflect a shared paradigm for generation of T-cell populations with uniform reactivity to particular antigenic epitopes. Consistent with a related immunobiology, both BTN3A1 and BTN3A2/3 are important for Vγ9Vδ2+ T-cell recognition (38). However, while some semi-invariant mouse γδ T-cell populations can become hyporesponsive to TCR triggering following initial strong TCR signaling during development (39), this does not apparently apply to human Vγ9Vδ2+ T-cells. Notably Vγ9Vδ2+ T-cells remain responsive to both pAg and anti-CD3 stimulation, a feature which underlies their potential use in several cancer immunotherapy applications (40), and they also exhibit the potential for further TCR-mediated plasticity (41–44).

POTENTIAL FOR CLONAL FOCUSING IN RESPONSE TO INFECTIOUS/STRESS CHALLENGE

Although clear evidence supports a broad polyclonal Vγ9Vδ2+ T-cell response to pAg, the extent to which clonotype-specific responses occur remains unclear. Vγ9Vδ2+ T-cells expand in various infections (1) but TCR clonality is uncharacterized in most scenarios. While most healthy donors have similar Vγ9 repertoires composed of up to 80% public Vγ9 clonotypes and diverse Vδ2 clonotypes (23), a minority of healthy donors have one or several expanded Vγ9 and Vδ2 clonotypes reminiscent of Vδ1 expansions (21), with the top clone comprising 20–40% of all Vγ9 and Vδ2 CDR3s (23). These clones express Vγ9 clonotypes shared less frequently between adult donors, often with longer or more complex CDR3s containing more added N-nucleotides. In these donors, a Vδ2 clonotype of similar frequency is detected, and pairing of the top Vγ9 and Vδ2 clonotypes can be confirmed by single cell PCR. This clonal expansion correlated with a change in Vδ2+ T-cell phenotype to $CD45RA^{neg}CD27^{neg}$ (23), distinct from the $CD45RA^{neg}CD45RO^{+}CD27^{+}$ phenotype observed in most healthy donors (45). The factors driving this clonal expansion and phenotypic maturation in these seemingly healthy donors are unclear. Ryan et al. (46) have also observed healthy donors with Vγ9Vδ2+ T-cells of differing effector phenotypes, although the clonality of Vγ9Vδ2+ T-cells was not examined. Expansion of particular Vδ2 clonotypes has also been noted in tuberculosis (47, 48), human leprosy (49), and in a macaque tuberculosis model (50). Public Vγ9 clonotypes were not shown to change during BCG infection in macaques (51), however, a lack of Vδ TCR clonotype data could have obscured the presence of clonotypic expansions with distinct Vδ2 chains. Conceivably clonal expansion may occur after Epstein–Barr virus or other common viral infections, and may underlie clonal expansions observed in otherwise healthy donors. Moreover, it is unclear how expansion of particular Vγ9Vδ2+ clonotypes helps protect the host, given the polyclonal response of Vγ9Vδ2+ T-cells to pAg. Conceivably expanded clones could respond with higher avidity, or alternatively could be reactive to different pathogen-specific stimuli, such as chemically diverse antigens. Additional work will no doubt address these questions.

CONCLUSION

In summary, we suggest Vγ9Vδ2+ T-cell development is shaped by both prenatal and postnatal events (**Figure 1**), which impact TCR repertoire and pAg reactivity. Importantly, the human Vγ9Vδ2+ TCR repertoire is composed of highly public Vγ9 chains produced by frequent recombination events that occur in every individual, resulting in a semi-invariant repertoire largely preconfigured from birth for pAg reactivity. These Vγ9 chains may undergo prenatal selection based on pAg reactivity, or unknown factors may constrain Vγ9-JγP rearrangements. Alongside public Vγ9 sequences, the Vδ2 repertoire is very diverse and private, and changes between neonatal and adult Vδ2 TCR repertoires suggest several selection events throughout life. Vδ2-Jδ3 TCRs are prevalent in cord blood and these may be positively selected in fetal development for recognition of host pAgs, or these rearrangements may be preferentially generated in early gestation. Vδ2-Jδ1 chains with longer CDR3 and hydrophobic amino acids at position 5 ultimately dominate the Vδ2 repertoire in adults, and these may be selected from rare rearrangements in cord blood following microbial pAg exposure, or further Vγ9Vδ2+ T-cell generation may occur in the postnatal thymus. Nevertheless, these selection events produce a repertoire that exploits the somatically recombined Vγ9Vδ2+ TCR as a surrogate pattern recognition receptor to sense pAgs. Further clonal selection appears to occur in some healthy adults and during some infections, however, exactly what protection such favored clonotypes provide that are not provided already by the broad Vγ9Vδ2+ TCR repertoire is an intriguing question future studies can address.

AUTHOR CONTRIBUTIONS

CW, MD, and BW jointly conceived the concepts presented in this review. CW analyzed data, prepared figures, and wrote the first draft; MD prepared figures and helped finalize the manuscript; BW helped plan and write the final manuscript.

ACKNOWLEDGMENTS

We thank Taher Taher and Ameenah Zeglam for reading this manuscript.

FUNDING

This work was supported by a Wellcome Trust Investigator award (099266/Z/12/Z to BW), supporting MD and CW.

REFERENCES

1. Morita CT, Jin C, Sarikonda G, Wang H. Nonpeptide antigens, presentation mechanisms, and immunological memory of human Vgamma2Vdelta2 T cells: discriminating friend from foe through the recognition of prenyl pyrophosphate antigens. *Immunol Rev* (2007) 215:59–76. doi:10.1111/j.1600-065X.2006.00479.x
2. Bukowski JF, Morita CT, Tanaka Y, Bloom BR, Brenner MB, Band H. V gamma 2V delta 2 TCR-dependent recognition of non-peptide antigens and Daudi cells analyzed by TCR gene transfer. *J Immunol* (1995) 154(3):998–1006.
3. Harly C, Guillaume Y, Nedellec S, Peigne CM, Monkkonen H, Monkkonen J, et al. Key implication of CD277/butyrophilin-3 (BTN3A) in cellular stress sensing by a major human gammadelta T-cell subset. *Blood* (2012) 120(11):2269–79. doi:10.1182/blood-2012-05-430470
4. Parker CM, Groh V, Band H, Porcelli SA, Morita C, Fabbi M, et al. Evidence for extrathymic changes in the T cell receptor gamma/delta repertoire. *J Exp Med* (1990) 171(5):1597–612. doi:10.1084/jem.171.5.1597
5. McVay LD, Carding SR. Extrathymic origin of human gamma delta T cells during fetal development. *J Immunol* (1996) 157(7):2873–82.
6. McVay LD, Jaswal SS, Kennedy C, Hayday A, Carding SR. The generation of human gammadelta T cell repertoires during fetal development. *J Immunol* (1998) 160(12):5851–60.
7. Dimova T, Brouwer M, Gosselin F, Tassignon J, Leo O, Donner C, et al. Effector Vgamma9Vdelta2 T cells dominate the human fetal gammadelta T-cell repertoire. *Proc Natl Acad Sci U S A* (2015) 112(6):E556–65. doi:10.1073/pnas.1412058112
8. Morita CT, Parker CM, Brenner MB, Band H. TCR usage and functional capabilities of human gamma delta T cells at birth. *J Immunol* (1994) 153(9):3979–88.
9. Ribot JC, Ribeiro ST, Correia DV, Sousa AE, Silva-Santos B. Human gammadelta thymocytes are functionally immature and differentiate into cytotoxic type 1 effector T cells upon IL-2/IL-15 signaling. *J Immunol* (2014) 192(5):2237–43. doi:10.4049/jimmunol.1303119
10. De Rosa SC, Andrus JP, Perfetto SP, Mantovani JJ, Herzenberg LA, Herzenberg LA, et al. Ontogeny of gamma delta T cells in humans. *J Immunol* (2004) 172(3):1637–45. doi:10.4049/jimmunol.172.3.1637
11. Davodeau F, Peyrat MA, Hallet MM, Gaschet J, Houde I, Vivien R, et al. Close correlation between Daudi and mycobacterial antigen recognition by human gamma delta T cells and expression of V9JPC1 gamma/V2DJC delta-encoded T cell receptors. *J Immunol* (1993) 151(3):1214–23.
12. Davodeau F, Peyrat MA, Hallet MM, Houde I, Vie H, Bonneville M. Peripheral selection of antigen receptor junctional features in a major human gamma delta subset. *Eur J Immunol* (1993) 23(4):804–8. doi:10.1002/eji.1830230405
13. Wang H, Fang Z, Morita CT. Vgamma2Vdelta2 T cell receptor recognition of prenyl pyrophosphates is dependent on all CDRs. *J Immunol* (2010) 184(11):6209–22. doi:10.4049/jimmunol.1000231
14. Casorati G, De Libero G, Lanzavecchia A, Migone N. Molecular analysis of human gamma/delta+ clones from thymus and peripheral blood. *J Exp Med* (1989) 170(5):1521–35. doi:10.1084/jem.170.5.1521
15. Delfau MH, Hance AJ, Lecossier D, Vilmer E, Grandchamp B. Restricted diversity of V gamma 9-JP rearrangements in unstimulated human gamma/delta T lymphocytes. *Eur J Immunol* (1992) 22(9):2437–43. doi:10.1002/eji.1830220937
16. Cairo C, Armstrong CL, Cummings JS, Deetz CO, Tan M, Lu C, et al. Impact of age, gender, and race on circulating gammadelta T cells. *Hum Immunol* (2010) 71(10):968–75. doi:10.1016/j.humimm.2010.06.014
17. Caccamo N, Dieli F, Wesch D, Jomaa H, Eberl M. Sex-specific phenotypical and functional differences in peripheral human Vgamma9/Vdelta2 T cells. *J Leukoc Biol* (2006) 79(4):663–6. doi:10.1189/jlb.1105640
18. Cairo C, Sagnia B, Cappelli G, Colizzi V, Leke RG, Leke RJ, et al. Human cord blood gammadelta T cells expressing public Vgamma2 chains dominate the response to bisphosphonate plus interleukin-15. *Immunology* (2013) 138(4):346–60. doi:10.1111/imm.12039
19. Pauza CD, Cairo C. Evolution and function of the TCR Vgamma9 chain repertoire: It's good to be public. *Cell Immunol* (2015) 296(1):22–30. doi:10.1016/j.cellimm.2015.02.010
20. Sherwood AM, Desmarais C, Livingston RJ, Andriesen J, Haussler M, Carlson CS, et al. Deep sequencing of the human TCRgamma and TCRbeta repertoires suggests that TCRbeta rearranges after alphabeta and gammadelta T cell commitment. *Sci Transl Med* (2011) 3(90):90ra61. doi:10.1126/scitranslmed.3002536
21. Davey MS, Willcox CR, Joyce SP, Ladell K, Kasatskaya SA, McLaren JE, et al. Clonal selection in the human Vdelta1 T cell repertoire indicates gammadelta TCR-dependent adaptive immune surveillance. *Nat Commun* (2017) 8:14760. doi:10.1038/ncomms14760
22. Ravens S, Schultze-Florey C, Raha S, Sandrock I, Drenker M, Oberdorfer L, et al. Human gammadelta T cells are quickly reconstituted after stem-cell transplantation and show adaptive clonal expansion in response to viral infection. *Nat Immunol* (2017) 18(4):393–401. doi:10.1038/ni.3686
23. Davey MS, Willcox CR, Hunter S, Kasatskaya SA, Remmerswaal EB, Salim M, et al. The human Vδ2+ T cell compartment comprises distinct innate-like Vγ9+ and adaptive Vγ9- subsets. *Nat Commun* (2018). 9:1760. doi:10.1038/s41467-018-04076-0
24. Venturi V, Price DA, Douek DC, Davenport MP. The molecular basis for public T-cell responses? *Nat Rev Immunol* (2008) 8(3):231–8. doi:10.1038/nri2260
25. Tomchuck SL, Leung WH, Dallas MH. Enhanced cytotoxic function of natural killer and CD3+CD56+ cells in cord blood after culture. *Biol Blood Marrow Transplant* (2015) 21(1):39–49. doi:10.1016/j.bbmt.2014.10.014
26. McVay LD, Carding SR, Bottomly K, Hayday AC. Regulated expression and structure of T cell receptor gamma/delta transcripts in human thymic ontogeny. *EMBO J* (1991) 10(1):83–91.
27. Villers D, Milpied N, Gaschet J, Davodeau F, Hallet MM, Bonneville M, et al. Alteration of the T cell repertoire after bone marrow transplantation. *Bone Marrow Transplant* (1994) 13(1):19–26.
28. Gorski J, Yassai M, Keever C, Flomenberg N. Analysis of reconstituting T cell receptor repertoires in bone marrow transplant recipients. *Arch Immunol Ther Exp (Warsz)* (1995) 43(2):93–7.
29. Bodger MP, Janossy G, Bollum FJ, Burford GD, Hoffbrand AV. The ontogeny of terminal deoxynucleotidyl transferase positive cells in the human fetus. *Blood* (1983) 61(6):1125–31.
30. Vermijlen D, Prinz I. Ontogeny of innate T lymphocytes – some innate lymphocytes are more innate than others. *Front Immunol* (2014) 5:486. doi:10.3389/fimmu.2014.00486
31. Asarnow DM, Goodman T, LeFrancois L, Allison JP. Distinct antigen receptor repertoires of two classes of murine epithelium-associated T cells. *Nature* (1989) 341(6237):60–2. doi:10.1038/341060a0
32. Carding SR, Egan PJ. Gammadelta T cells: functional plasticity and heterogeneity. *Nat Rev Immunol* (2002) 2(5):336–45. doi:10.1038/nri797
33. Boyden LM, Lewis JM, Barbee SD, Bas A, Girardi M, Hayday AC, et al. Skint1, the prototype of a newly identified immunoglobulin superfamily gene cluster, positively selects epidermal gammadelta T cells. *Nat Genet* (2008) 40(5):656–62. doi:10.1038/ng.108
34. Turchinovich G, Hayday AC. Skint-1 identifies a common molecular mechanism for the development of interferon-gamma-secreting versus interleukin-17-secreting gammadelta T cells. *Immunity* (2011) 35(1):59–68. doi:10.1016/j.immuni.2011.04.018
35. Di Marco Barros R, Roberts NA, Dart RJ, Vantourout P, Jandke A, Nussbaumer O, et al. Epithelia use butyrophilin-like molecules to shape organ-specific gammadelta T cell compartments. *Cell* (2016) 167(1):203–18.e17. doi:10.1016/j.cell.2016.08.030
36. Kashani E, Fohse L, Raha S, Sandrock I, Oberdorfer L, Koenecke C, et al. A clonotypic Vgamma4Jgamma1/Vdelta5Ddelta2Jdelta1 innate gammadelta T-cell population restricted to the CCR6(+)CD27(-) subset. *Nat Commun* (2015) 6:6477. doi:10.1038/ncomms7477
37. Wei YL, Han A, Glanville J, Fang F, Zuniga LA, Lee JS, et al. A highly focused antigen receptor repertoire characterizes gammadelta T cells that are poised to make IL-17 rapidly in naive animals. *Front Immunol* (2015) 6:118. doi:10.3389/fimmu.2015.00118
38. Vantourout P, Laing A, Woodward MJ, Zlatareva I, Apolonia L, Jones AW, et al. Heteromeric interactions regulate butyrophilin (BTN) and BTN-like molecules governing gammadelta T cell biology. *Proc Natl Acad Sci U S A* (2018) 115(5):1039–44. doi:10.1073/pnas.1701237115
39. Wencker M, Turchinovich G, Di Marco Barros R, Deban L, Jandke A, Cope A, et al. Innate-like T cells straddle innate and adaptive immunity by altering antigen-receptor responsiveness. *Nat Immunol* (2014) 15(1):80–7. doi:10.1038/ni.2773
40. Gomes AQ, Martins DS, Silva-Santos B. Targeting gammadelta T lymphocytes for cancer immunotherapy: from novel mechanistic insight to clinical

application. *Cancer Res* (2010) 70(24):10024–7. doi:10.1158/0008-5472.CAN-10-3236
41. Vermijlen D, Ellis P, Langford C, Klein A, Engel R, Willimann K, et al. Distinct cytokine-driven responses of activated blood gammadelta T cells: insights into unconventional T cell pleiotropy. *J Immunol* (2007) 178(7):4304–14. doi:10.4049/jimmunol.178.7.4304
42. Davey MS, Morgan MP, Liuzzi AR, Tyler CJ, Khan MWA, Szakmany T, et al. Microbe-specific unconventional T cells induce human neutrophil differentiation into antigen cross-presenting cells. *J Immunol* (2014) 193(7):3704–16. doi:10.4049/jimmunol.1401018
43. Tyler CJ, Doherty DG, Moser B, Eberl M. Human Vgamma9/Vdelta2 T cells: Innate adaptors of the immune system. *Cell Immunol* (2015) 296(1):10–21. doi:10.1016/j.cellimm.2015.01.008
44. Peters C, Hasler R, Wesch D, Kabelitz D. Human Vdelta2 T cells are a major source of interleukin-9. *Proc Natl Acad Sci U S A* (2016) 113(44):12520–5. doi:10.1073/pnas.1607136113
45. Dieli F, Gebbia N, Poccia F, Caccamo N, Montesano C, Fulfaro F, et al. Induction of gammadelta T-lymphocyte effector functions by bisphosphonate zoledronic acid in cancer patients in vivo. *Blood* (2003) 102(6):2310–1. doi:10.1182/blood-2003-05-1655
46. Ryan PL, Sumaria N, Holland CJ, Bradford CM, Izotova N, Grandjean CL, et al. Heterogeneous yet stable Vdelta2(+) T-cell profiles define distinct cytotoxic effector potentials in healthy human individuals. *Proc Natl Acad Sci U S A* (2016) 113(50):14378–83. doi:10.1073/pnas.1611098113
47. Xi X, Han X, Li L, Zhao Z. gammadelta T cells response to *Mycobacterium tuberculosis* in pulmonary tuberculosis patients using preponderant complementary determinant region 3 sequence. *Indian J Med Res* (2011) 134:356–61.
48. Ding Y, Ma F, Wang Z, Li B. Characteristics of the Vdelta2 CDR3 sequence of peripheral gammadelta T cells in patients with pulmonary tuberculosis and identification of a new tuberculosis-related antigen peptide. *Clin Vaccine Immunol* (2015) 22(7):761–8. doi:10.1128/CVI.00612-14
49. Uyemura K, Deans RJ, Band H, Ohmen J, Panchamoorthy G, Morita CT, et al. Evidence for clonal selection of gamma/delta T cells in response to a human pathogen. *J Exp Med* (1991) 174(3):683–92. doi:10.1084/jem.174.3.683
50. Huang D, Chen CY, Zhang M, Qiu L, Shen Y, Du G, et al. Clonal immune responses of *Mycobacterium*-specific gammadelta T cells in tuberculous and non-tuberculous tissues during *M. tuberculosis* infection. *PLoS One* (2012) 7(2):e30631. doi:10.1371/journal.pone.0030631
51. Cairo C, Hebbeler AM, Propp N, Bryant JL, Colizzi V, Pauza CD. Innate-like gammadelta T cell responses to *Mycobacterium* Bacille Calmette-Guerin using the public V gamma 2 repertoire in *Macaca fascicularis*. *Tuberculosis (Edinb)* (2007) 87(4):373–83. doi:10.1016/j.tube.2006.12.004

Conflict of Interest Statement: The authors declare that the research was conducted in the absence of any commercial or financial relationships that could be construed as a potential conflict of interest.

Copyright © 2018 Willcox, Davey and Willcox. This is an open-access article distributed under the terms of the Creative Commons Attribution License (CC BY). The use, distribution or reproduction in other forums is permitted, provided the original author(s) and the copyright owner are credited and that the original publication in this journal is cited, in accordance with accepted academic practice. No use, distribution or reproduction is permitted which does not comply with these terms.

frontiers in Immunology

ORIGINAL RESEARCH
published: 22 June 2018
doi: 10.3389/fimmu.2018.01430

Epidermal T Cell Dendrites Serve as Conduits for Bidirectional Trafficking of Granular Cargo

*Grzegorz Chodaczek[1,2], Monika Toporkiewicz[2], M. Anna Zal[1] and Tomasz Zal[1]**

[1] Department of Immunology, University of Texas MD Anderson Cancer Center, Houston, TX, United States,
[2] Confocal Microscopy Laboratory, Wroclaw Research Centre EIT+, Wroclaw, Poland

Dendritic epidermal T cells (DETCs) represent a prototypical lineage of intraepithelial γδ T cells that participate in the maintenance of body barrier homeostasis. Unlike classical T cells, DETCs do not recirculate and they remain persistently activated through their T cell receptors (TCR) at steady state, i.e., in absence of infection or tissue wounding. The steady state TCR signals sustain the formation of immunological synapse-like phosphotyrosine-rich aggregates located on projections (PALPs) which act to anchor and polarize DETC's long cellular projections toward the apical epidermis while the cell bodies reside in the basal layers. The PALPs are known to contain pre-synaptic accumulations of TCR-containing and lysosomal granules, but how this cargo accumulates there remains unclear. Here, we combined anti-Vγ5 TCR, cholera toxin subunit B (CTB), and LysoTracker (LT)-based intravital labeling of intracellular granules, with high resolution dynamic microscopy and fluorescence recovery after photobleaching (FRAP) to characterize the steady state composition and transport of DETC granules in steady state epidermis. Intradermal fluorescent Vγ5 antibody decorated DETCs without causing cellular depletion, dendrite mobilization or rounding up and became slowly internalized over 48 h into intracellular granules that, after 6 days, colocalized with LAMP-1 and less so with LT or early endosomal antigen-1. Intradermal CTB was likewise internalized predominantly by DETCs in epidermis, labeling a partly overlapping set of largely LAMP-1$^+$ intracellular granules. These as well as LT-labeled granules readily moved into newly forming dendrites and accumulated at the apical endings. FRAP and spatiotemporal tracking showed that the inside tubular lengths of DETC cellular projections supported dynamic trafficking of lysosomal cargo toward and away from the PALPs, including internalized TCR and lipid raft component ganglioside GM1 (labeled with CTB). By contrast, the rate of GM1 granules transport through comparable dendrites of non-DETCs was twice slower. Our observations suggest that DETCs use chronic TCR activation to establish a polarized conduit system for long-range trans-epithelial transport aimed to accumulate mature lysosomes at the barrier-forming apical epidermis. The biological strategy behind the steady state lysosome polarization by DETCs remains to be uncovered.

Keywords: gamma delta (gammadelta) T cells, dendritic epidermal T cell, lysosomes, intracellular transport, intravital microscopy, fluorescence recovery after photobleaching

OPEN ACCESS

Edited by:
Pierre Vantourout, King's College London, United Kingdom

Reviewed by:
Björn Önfelt, Royal Institute of Technology, Sweden
Immo Prinz, Hannover Medical School, Germany

***Correspondence:**
Tomasz Zal
tzal@mdanderson.org

Specialty section:
This article was submitted to T Cell Biology, a section of the journal Frontiers in Immunology

Received: *23 February 2018*
Accepted: *08 June 2018*
Published: *22 June 2018*

Citation:
Chodaczek G, Toporkiewicz M, Zal MA and Zal T (2018) Epidermal T Cell Dendrites Serve as Conduits for Bidirectional Trafficking of Granular Cargo. Front. Immunol. 9:1430. doi: 10.3389/fimmu.2018.01430

INTRODUCTION

Considered a member of the innate body barrier defense system, murine dendritic epidermal T cells (DETCs) contribute to skin repair and homeostasis (1–3). These cells extend long cellular processes from the mid-body in the basal epidermis toward the apical epidermis thereby spanning across the whole epidermis thickness and interacting with both the immature (basal) and mature (squamous) keratinocytes. The striking apical polarity of DETCs results from the formation of dendrite-anchoring phosphotyrosine-rich aggregates located on projections (PALPs) which are sustained at inter-squamous keratinocyte junctions by the local chronic activation of the cell's unique Vγ5-Vδ1 T cell receptors (TCR) [according to the Tonegawa nomenclature (4, 5)]. The dendrite-terminal cytoplasm underneath the PALPs harbors distinct accumulations of intracellular granules some of which contain TCR and/or lysosomal and exocytic pathway markers LysoTracker (LT), GM1, and LAMP-1 (5). The presence of intracellular granules inside DETCs was uncovered as early as in 1985 by Romani et al. who described electron-dense cores and small vesicles surrounded by less electron-dense material in isolated Thy-1$^+$ epidermal cells (DETC) (6). Thereafter, and consistent with the capacity of DETCs to kill their targets, Krähenbühl et al. demonstrated that some DETC granules contained granzyme A (BLT esterase activity) and perforin (Ca^{2+}-dependent hemolytic activity) (7) and Ibusuki et al. demonstrated *in vitro* cytotoxic granule exocytosis in response to stimulation of short-term DETC lines (8). The steady state accumulations of dendrite-terminal granular cargo at the PALPs could signify a local formative process, such as TCR and/or other membrane component internalization and/or a long-range transport from the cell bodies, and the cargo could be poised for localized secretion. However, the *in vivo* behavior of DETC's intracellular cargo has remained unknown.

In this work, we establish a methodology for the labeling and DETC-selective analysis of intracellular cargo transport *in vivo*, and we apply it to examine the dynamic behavior of DETC's intracellular granules at steady state conditions. Using time-lapse fluorescence microscopy and fluorescence recovery after photobleaching (FRAP), we show that DETC TCR and GM1 membrane components are readily internalized and that the content of resulting cargo enters the lysosomal and LAMP-1 granule pools. Furthermore, we show that DETCs transport their intracellular granules along the lengths of the cell's a dendrites, at steady state, both away from and toward the apical epidermis, and more dynamically than similarly labeled dendritic-form dermal cells. Our observations demonstrate a novel approach to study DETC cargo dynamics and suggest that DETCs use chronic, dendrite-terminal TCR activation to establish a polarized conduit system for trans-epithelial cargo transport.

MATERIALS AND METHODS

Mice

IL2p8-GFP mice were obtained from M. Yui and E. Rothenberg (California Institute of Technology, Pasadena, CA, USA) (9) and used at 6–24 weeks of age. In these mice, the epidermal GFP is present solely in DETCs (5, 9). CD11c-YFP mice (10) were obtained from M. Nussenzweig (The Rockefeller University, New York, NY, USA) and were crossed with IL2p8-GFP mice to simultaneously visualize DETCs and Langerhans cells. The mice were housed at the University of Texas MD Anderson Cancer Center (UT MDACC), Houston, TX, USA and the Wroclaw Research Centre EIT+ and the Institute of Immunology and Experimental Therapy, Wroclaw, Poland in individually ventilated cages in 12:12 h light-dark cycle under specific pathogen-free conditions. All animal manipulations were approved by the UT MDACC Institutional Animal Care and Use Committee or the Local Ethics Committee for Experiments on Animals at the Institute of Immunology and Experimental Therapy.

Antibodies and Reagents

LysoTracker Red DND-99, cholera toxin subunit B (CTB)-Alexa Fluor (AF)555 or AF647 conjugates (Cat. No A20187, A10470, and A20186), and anti-rabbit IgG-AF647 antibody were from ThermoFisher Scientific. Unlabeled anti-TCR Vγ3 (Vγ5 according to Tonegawa's nomenclature) antibody (clone 536) was from Santa Cruz Biotechnology and its isotype control (Syrian hamster IgG, clone SHG-1) was from BioLegend. These antibodies were labeled in house using AF555 and AF647 labeling kits according to manufacturer's instructions (ThermoFisher Scientific). Anti-LAMP-1-AF647 clone 1D4B was from BioLegend and anti-early endosome antigen-1 (EEA-1) (#2411) was from Cell Signaling.

Ex Vivo Immunofluorescence of Mouse Epidermis

Mouse ears were split laterally and immediately fixed for 1 h at 20–22°C with 3.7% (wt/vol) formaldehyde. The subcutaneous cartilage was removed and the skin was made permeable for at least 18 h with 0.5% (wt/vol) saponin in 2% (vol/vol) FBS and 0.03% (wt/vol) azide in PBS. Samples were stained for at least 18 h at 22–37°C with antibodies diluted in 2% (vol/vol) FBS and 0.5% (vol/vol) saponin in PBS and, after being washed in PBS, were mounted in ProLong Gold (ThermoFisher Scientific). Fluorescence imaging was performed using a Leica SP8 confocal microscope with 63× NA1.4 and 40× NA1.3 oil objectives (Leica Microsystems).

Intravital Labeling and Microscopy

Mice were anesthetized and the ear pinnae was injected, using 31 G insulin syringe, with 20 µl of the following labeling solutions, in PBS: 10 µM LT Red, 10 µg/ml CTB-AF555 or AF647 conjugate, ~1.4 µg/ml fluorescently labeled anti-Vγ5 antibody, or ~1.4 µg/ml of fluorescently labeled isotype control antibody. In some experiments, CTB and anti-Vγ5 antibody were mixed together. Intravital imaging was performed 1 h later for LT, or several days later for the antibodies. Mice were anesthetized by isoflurane inhalation and placed on a heated microscope stage. Ear pinna was immobilized on a metal pedestal with a dab of silicone paste, moistened with a drop of PBS and covered with a 0.17-mm glass coverslip. The imaging was performed using upright Leica SP5 or

SP8 resonant scanning confocal systems equipped with piezoelectric z-drive (Piezosystem, Jena) and 40× NA1.3 oil objective. The pinhole was set to 1–2 AU and image pixel size at 0.09–0.150 µm. Stacks of confocal images, spaced 0.1–1 µm apart, were acquired every 10–30 s for up to 2 h with line averaging to diminish noise.

Image Processing

3-D and temporal image stacks were smoothed by kernel 3 median filtering and autofluorescence background was removed by thresholding followed by contrast stretching. Tissue drift was corrected using Imaris software (Bitplane) in 3-D or Stackreg plugin (11) of Fiji software (National Institutes of Health) in 2-D maximum intensity projections. For granule tracking, the GFP signal of DETCs was binarized and used to gate other fluorescence channels. Granule surfaces were identified and tracked in 2-D and shape parameters were measured using the Imaris software (Bitplane). The automated tracking algorithm was the autoregressive motion with 3 µm maximum one frame travel distance. Alternatively, granules were tracked manually. Two-dimensional projections of 3-D z-stacks were generated based on maximum intensities. Depth was color-coded using Leica Application Suite Advanced Fluorescence software or Temporal Color Code plugin in Fiji with "Rainbow RGB" look-up table. Co-localization analysis and Pearson coefficient calculations were performed in Imaris. All fluorescence intensity measurements in regions of interest (ROI) and line profiling were done using Fiji. To delineate mid-body regions, the GFP-based cell regions were eroded until dendrite disappearance followed by dilation. Dendrite regions were obtained by subtracting the perinuclear regions from the initial cell regions.

Statistical Analysis

Statistical significance of differences between two experimental groups were determined using a nonparametric Mann–Whitney *U*-test (two-group comparison) with *p*-values of less than 0.05 considered significant, in GraphPad Prism (GraphPad Software).

RESULTS

In Vivo Labeling of DETC Granules

In our previous report, we described the *in vivo* phenomenon of DETC steady state apical polarization through the dendrite-terminal TCR activation in the PALPs (5). Among other findings, we observed that besides in the PALPs membrane, TCR was present along with GM1 in juxtaposed cytoplasmic foci, and that much of DETC's lysosomes (LT) and GM1 [cholera toxin subunit B (CTB) binding] were accumulating at steady state at the PALPs. We also noticed that intravital anti-CD3 cross-linking did not activate DETCs to round up. Therefore, to visualize TCR-containing DETC intracellular granules *in vivo*, we injected the dermis with AF647-labeled anti-Vγ5 TCR antibody [Tonegawa's nomenclature (4)], also known as Vγ3 in Garman's nomenclature (12). In addition, or separately, to label GM1-containing granules, we injected CTB-AF555. Both reagents diffused into the epidermis and stained preferentially DETCs within 10 min and delineated the plasma membranes with strong accumulations at the apical dendrite ends (**Figure 1A**; Figure S1 in Supplementary Material), thereby confirming *in vivo* the staining of the PALPs in fixed epidermis (5). We also noted that whereas the cellular specificity of Vγ5-AF647 and CTB was almost exclusive for DETCs in the epidermis (**Figure 1**, $Z = 3.6$–9.6 µm; Figure S2 in Supplementary Material), CTB also labeled a network of other, currently unidentified cells in the underlying dermis, many of them remarkably dendritic (**Figure 1A**, $Z = 15$–19.8 µm). CTB-AF555 became internalized into cytoplasmic granules within 90 min and Vγ5-AF647 was partially internalized after 24 h (Figure S1 in Supplementary Material) and completely after 6 days thereby highlighting a collection of intracellular granules (**Figures 1B,D**). The intravital labeling of DETC granules by Vγ5 antibody and CTB persisted for at least 16 days and we did not observe any loss of DETC cellularity or any signs of acute activation such as dendrite motility or cells rounding up.

Using intradermal Vγ5 and/or CTB fluorescence labeling, we focused further studies on the steady state, i.e., at least 6 days after the intradermal injection. Vγ5 fluorescence was found in ellipsoidal shaped granules measuring, in the XY image planes, respectively, 0.25 ± 0.007 µm × 0.48 ± 0.012 µm on the short and long axes (mean ± SEM). Given that the antibody could be proteolytically degraded over the time, the observed signals did not necessarily indicate a continued presence of TCR. Likewise, CTB-AF555 fluorescence delineated small granules dispersed throughout DETC body and prominent granular accumulations in the apical dendrite endings (**Figure 1B**; Figure S3 in Supplementary Material). These granules ellipsoid size was 0.27 ± 0.001 and 0.48 ± 0.001 µm (mean ± SEM). The Vγ5 and CTB fluorescence signals partly colocalized in a subset of intracellular granules, especially at the ends of dendrites (**Figure 1C**). The intracellular localization of the granules was ascertained by 3-D confocal sectioning (**Figure 1D**).

To characterize the *in vivo* Vγ5 and CTB steady state DETC granules, we co-labeled the skin of IL2p8-GFP mice with intradermal LT *in vivo* followed by GFP-based image gating. We also stained the steady state Vγ5 and CTB-labeled epidermis *ex vivo* for the EEA-1 and LAMP-1 (**Figure 2**). In agreement with our prior report (5), LT-stained lysosomes were predominantly localized at the ends of dendrites. Within the limits of confocal resolution, LT granule's diameters ranged from 0.25–0.45 ± 0.001 µm (mean ± SEM) to 0.8–1.0 µm [full width at half maximum (FWHM)]. Both Vγ5 and CTB signals most substantially colocalized with LAMP-1 and less so with EEA-1 and LT (**Figures 2A–C**; Figure S3 in Supplementary Material) and CTB/LT co-localization was significantly higher at dendrite ends than in mid-bodies (**Figure 2C**). Vγ5/LT co-localization in dendrites vs. mid-bodies was not significantly different, at the current statistical power. The Pearson's coefficients in **Figures 2B,C** lower panels are not averages of the corresponding whole-cell values in the upper panels due to using a subset of cells with clearly defined mid-bodies, and ROI differences. Taken together, these results revealed a propensity of DETCs to internalize cell membrane TCR and GM1 into partially overlapping pools of lysosomal and exocytic pathway (LAMP-1) intracellular granules.

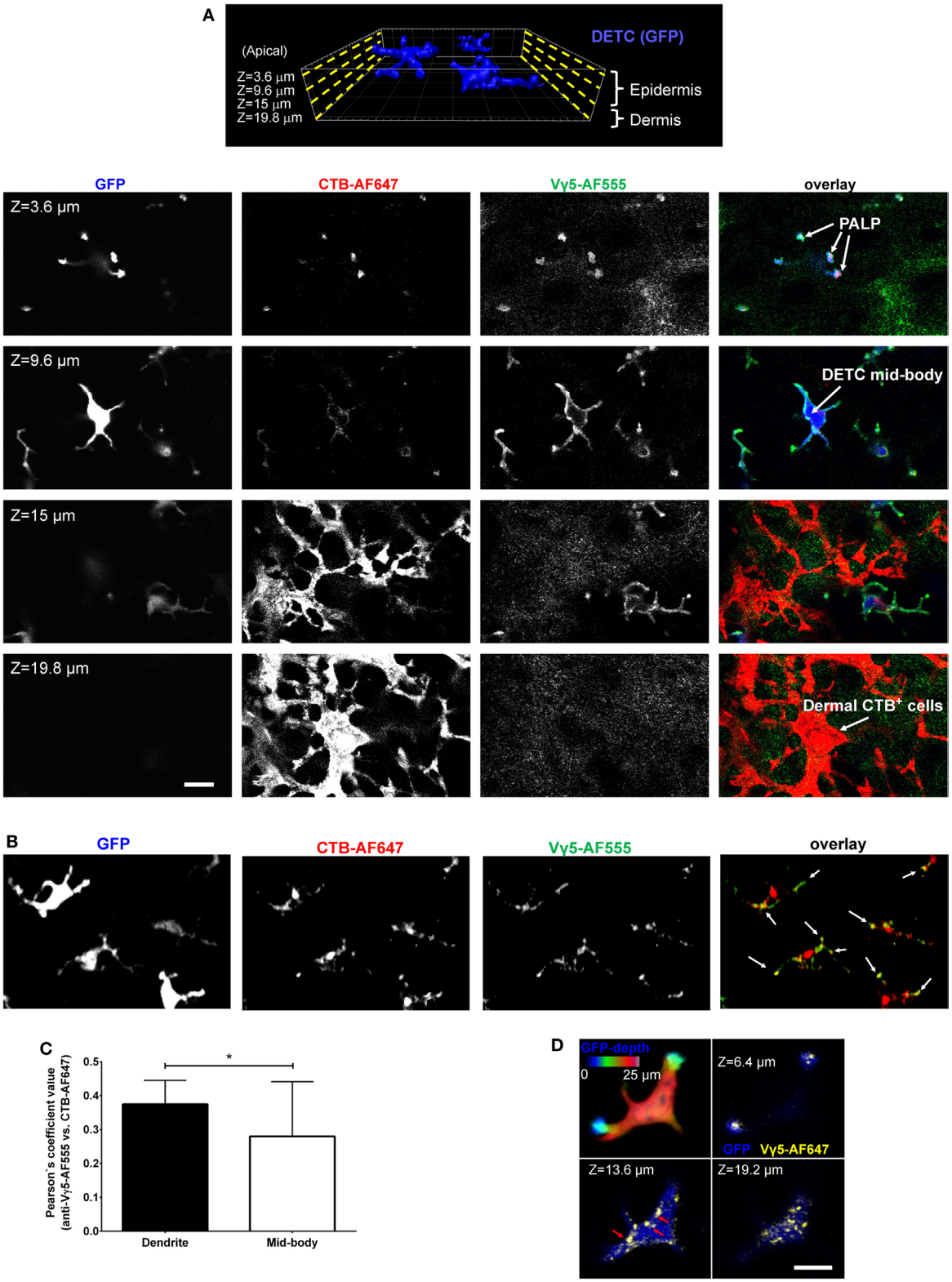

FIGURE 1 | Intravital skin labeling by intradermal injection of fluorescent anti-Vγ5 antibody and CTB in IL2p8-GFP mouse ear. **(A)** One hour from the injection. Four representative confocal image z-planes from a 3-D z-stack at the indicated z-depth positions measured from the apical skin surface. **(B)** Six days after injection (different site). Maximum intensity projection of a confocal image z-stack. The white arrows point to the apical dendrite positions. **(C)** Quantification of Vγ5 and CTB signal co-localization after 6 days. **(D)** 3-D confocal sectioning to demonstrate the cytoplasmic localization of the granules 6 days after labeling. The color-coded depth projection shows the entire dendritic epidermal T cell (DETC) body. Scale bars = 10 µm.

Dynamics of LT-Stained Granules

Having established three methods for intravital labeling of DETC granules (i.e., using Vγ5 antibody, CTB, or LT), we proceeded to characterize the steady state granule dynamics. The LT labeling method was rapid and not expected to interfere with any cellular processes, but could not exclude the possibility of the dye leakage between cells. The Vγ5 and CTB labeling required a 6-day rest, but excluded fluorescence leakage and highlighted a somewhat different range of granules. Intravital mouse time-lapse microscopy of LT-stained granules revealed highly dynamic behavior, the lysosomes seemingly fusing with each other and splitting (**Figure 3**; Movies S1 and S2 in Supplementary Material). The median instantaneous velocity was 0.84 μm/min (0.35–2.04 μm/min—25–75% percentile, respectively), while the fastest vesicles

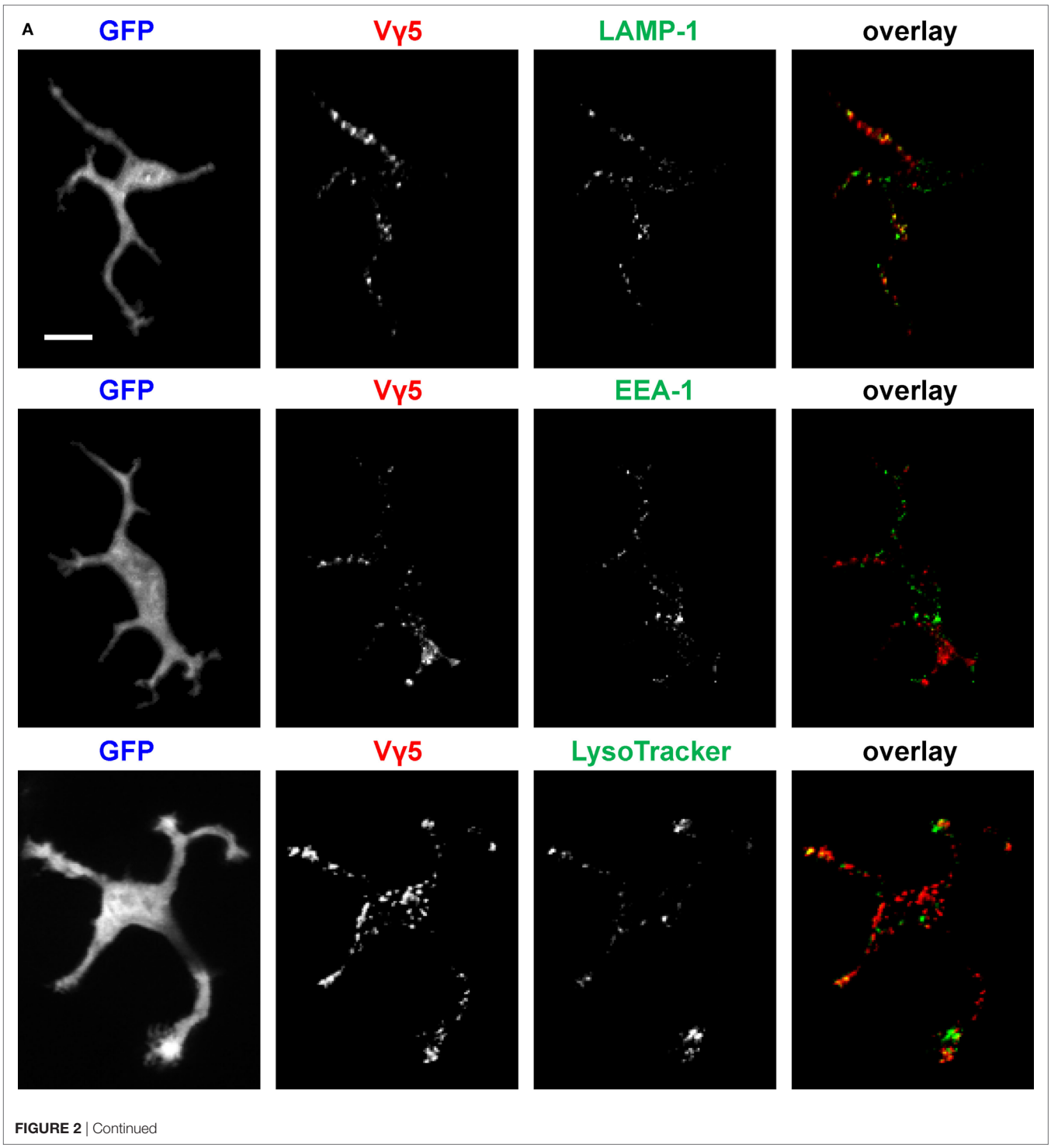

FIGURE 2 | Continued

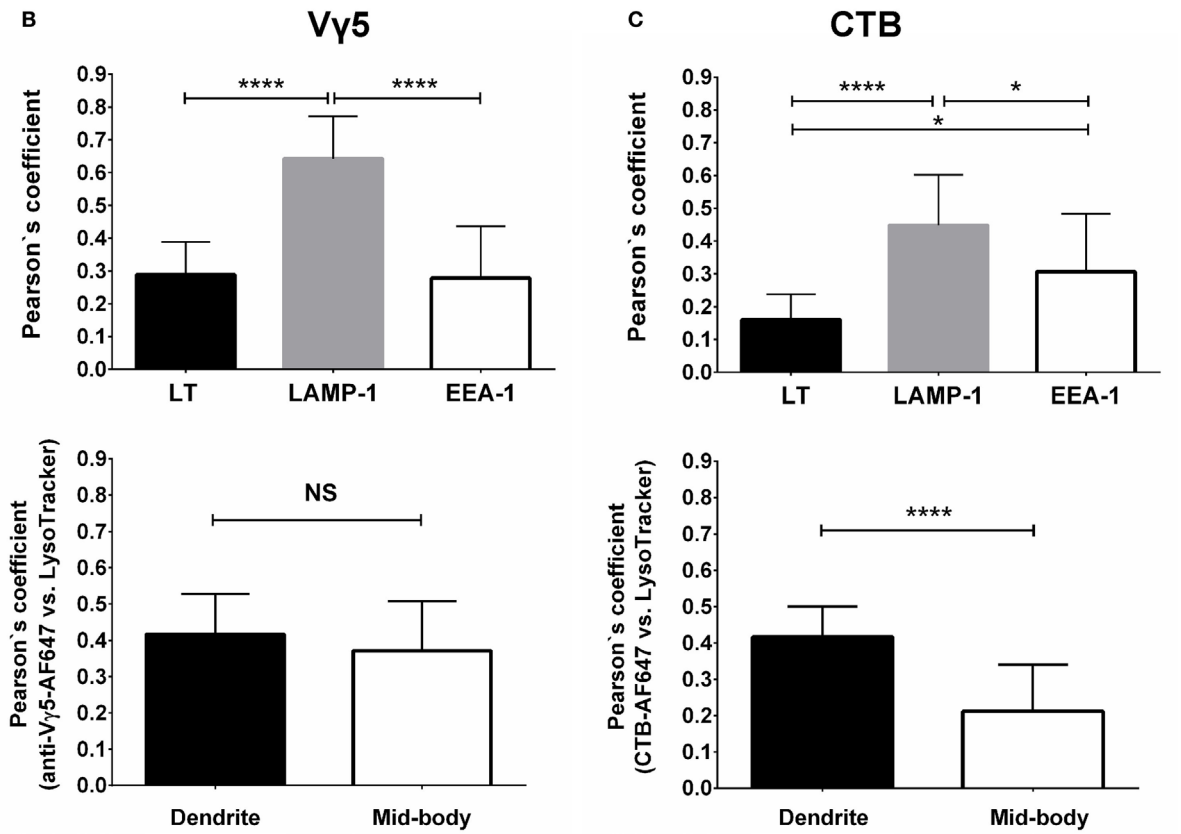

FIGURE 2 | Characterization of dendritic epidermal T cell (DETC) granules containing internalized Vγ5 or CTB fluorescence. IL2p8-GFP mouse ear was injected with Vγ5-AF555 antibody or CTB-AF555 and, 6 days later, stained with LT or harvested for immunofluorescence. **(A)** Representative DETC examples. **(B)** Analysis of Vγ5$^+$ granule co-localization with endosomal [early endosome antigen-1 (EEA-1)] and lysosomal [LAMP-1 and LysoTracker (LT)] markers in whole DETC bodies (upper panel) or in dendrites and mid-bodies (lower panel). **(C)** Similar as in **(B)**, but for CTB. *N* = 20–30 cells/mouse in five mice. The dendrite vs. mid-body co-localization analyses [**(B,C)** lower panels] were performed on a subset of the cells in upper panels (i.e., where mid-bodies could be clearly delineated). Scale bar = 10 μm.

were typically small (FWHM ≤ 0.3 μm) and moved at 8.5 μm/min. The maximum instantaneous speed of the largest lysosomes was within the range of 1.1–2.4 μm/min and their short-range motions seemed to be random over the relatively short observation time. On occasion, we observed the process of a new dendrite forming by localized budding off followed by back and forth length changes ending with the distal end anchoring, presumably through a PALP. During this process, which took several to tenths of minutes, lysosomes entered into the new dendrite soon after the budding off and then accumulated at the end after the length of dendrite has stabilized (**Figure 3**; Movies S1 and S2 in Supplementary Material). These observations suggested that the accumulations of lysosomes in DETC's apical dendrite endings was a result of granule transport.

Dynamics of CTB-Labeled Granules and Comparison With Non-DETC

We used steady state CTB and Vγ5 labeling to evaluate the dynamics of intracellular cargo transport by measuring the kinetics of intravital FRAP. Lack of intercellular fluorophore diffusion was ascertained by the lack of signal recovery upon whole-cell FRAP (Figure S4 in Supplementary Material). Using CTB, we compared DETCs to the CTB$^+$ non-DETC cells in the dermis. **Figure 4A** and Movie S3 in Supplementary Material show an example of FRAP experiment whereby the photobleaching was localized in a DETC apical dendrite end characteristic of a PALP, and **Figure 4B** and Movie S4 in Supplementary Material show a similar experiment on a dendrite of a dermal non-DETC CTB$^+$ cell. In DETCs, fluorescence re-emerged in the photobleached dendrite with the recovery half-life estimated for 10–45 min (**Figure 4C**, blue curve). By contrast, similar distance and shape FRAP kinetics in non-DETC dendrites were about twice slower (**Figure 4C**, red curve), also in comparison to non-DETC mid-bodies (Figure S5 in Supplementary Material). Although granule transport in cell bodies is not unexpected *per se*, this comparison showed that the capacity of DETC for dendrite-guided cargo transport was more profound than in non-DETCs.

Time-lapse recordings of steady state CTB granules in DETCs revealed individual granule motilities. The median instantaneous velocity was 1.22 μm/min (0.51–2.50 μm/min—25–75% percentile, respectively). CTB granules moved from the mid-body along the

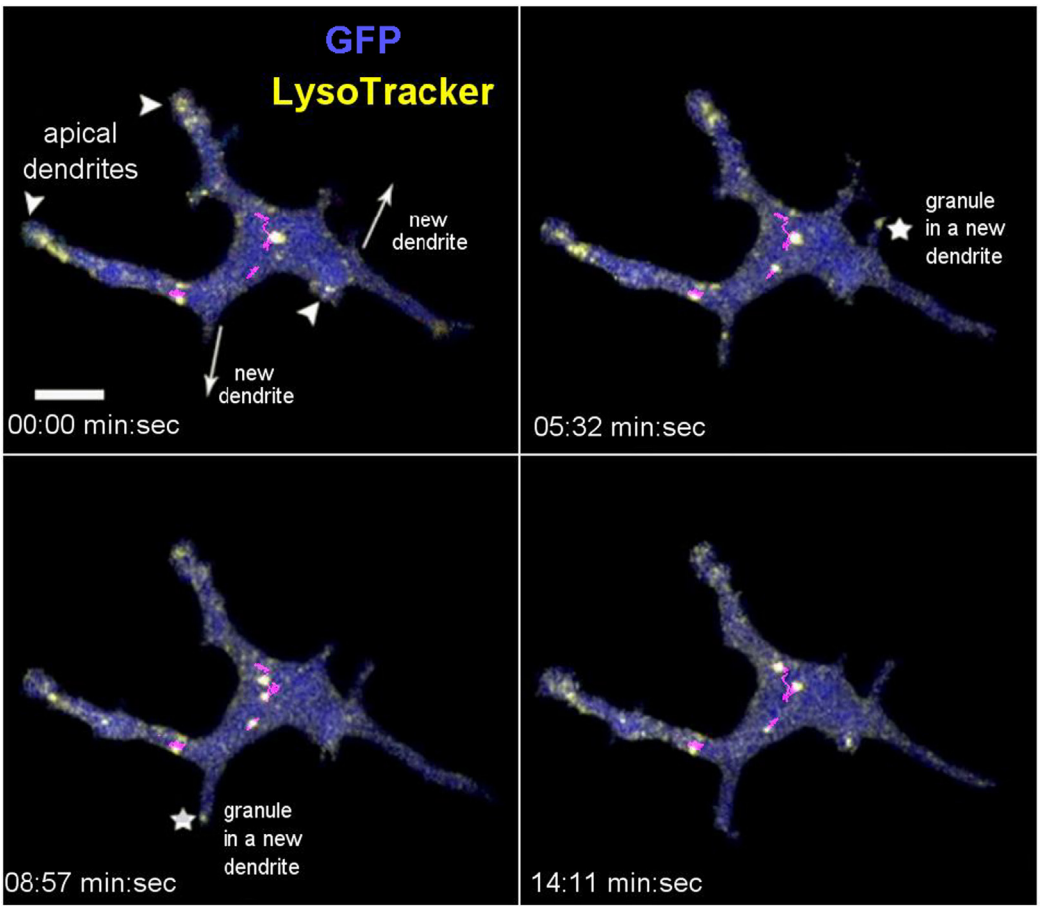

FIGURE 3 | *In vivo* dynamics of dendritic epidermal T cell granules labeled with LysoTracker. The panel shows maximum intensity projections from a video sequence. The arrowheads point to the apical dendrites (based on 3-D inspection), the arrows indicate the direction of new dendrite growths, and the asterisks indicate the accumulating granules. The magenta lines represent tracks of several mid-body granules (see Movie S1 in Supplementary Material). Scale bar = 5 μm.

lengths of dendrites in jumping fashion and the fluorescence accumulated at the apical end (**Figure 4D**). In this example, fluorescence intensity spiked sequentially through the regions 1–4 as the vesicle moved through the branched dendrite from 24 to 37 min. These recordings demonstrated that CTB-labeled vesicles were transported from the mid-body through dendrites toward dendrite ends.

Dynamics of TCR-Labeled Granules and Retrograde Transport

Finally, we evaluated the steady state dynamics of DETC granules that were labeled by anti-Vγ5-TCR antibody internalization. Given that CTB-based labeling could be associated with a degree of inflammatory activation, Vγ5 labeling should be free from such effects. As for CTB, we waited for 6 days from the intradermal injection to allow for complete internalization and washout and for the skin to return to a steady state. After photobleaching the apical dendrite endings, we observed movement of vesicles from DETC bodies toward the photobleached dendrites within 6 min (Movies S5 and S6 in Supplementary Material). **Figure 5A** depicts the movement of individual vesicles that are arriving at a photobleached dendrite end. Based on multiple FRAP experiments, the median instantaneous velocity of granule movement was 1.07 μm/min (0.44–2.27 μm/min—25–75% percentile, respectively) and maximum instantaneous velocity was 4.23 μm/min (1.75–7.66 μm/min—25–75% percentile, respectively). As for LT labeling, we observed that newly formed dendrites were quickly filled with Vγ5-labeled vesicles migrating into the emergent tips (Movie S7 in Supplementary Material).

To test for the presence of retrograde granule movement, i.e., from dendrite ends toward the mid-bodies, we photobleached mid-cell body areas such that the only remaining fluorescence was located in dendrite endings (**Figure 5B**; Movies S8 and S9 in Supplementary Material). In this setting, we observed fluorescence entering the mid-body regions from dendrite ends. However, the retrograde transport kinetics was about half of the anterograde movements and the extrapolated FRAP half time was approximately 80 min (**Figure 5C**). Based on individual Vγ5 granule tracking in multiple cells, the instantaneous velocities of the granules were somewhat higher in dendrites compared to mid-bodies (**Figure 5D**). The instantaneous velocities of CTB, TCR, and LT granules were not statistically different (**Figure 5E**).

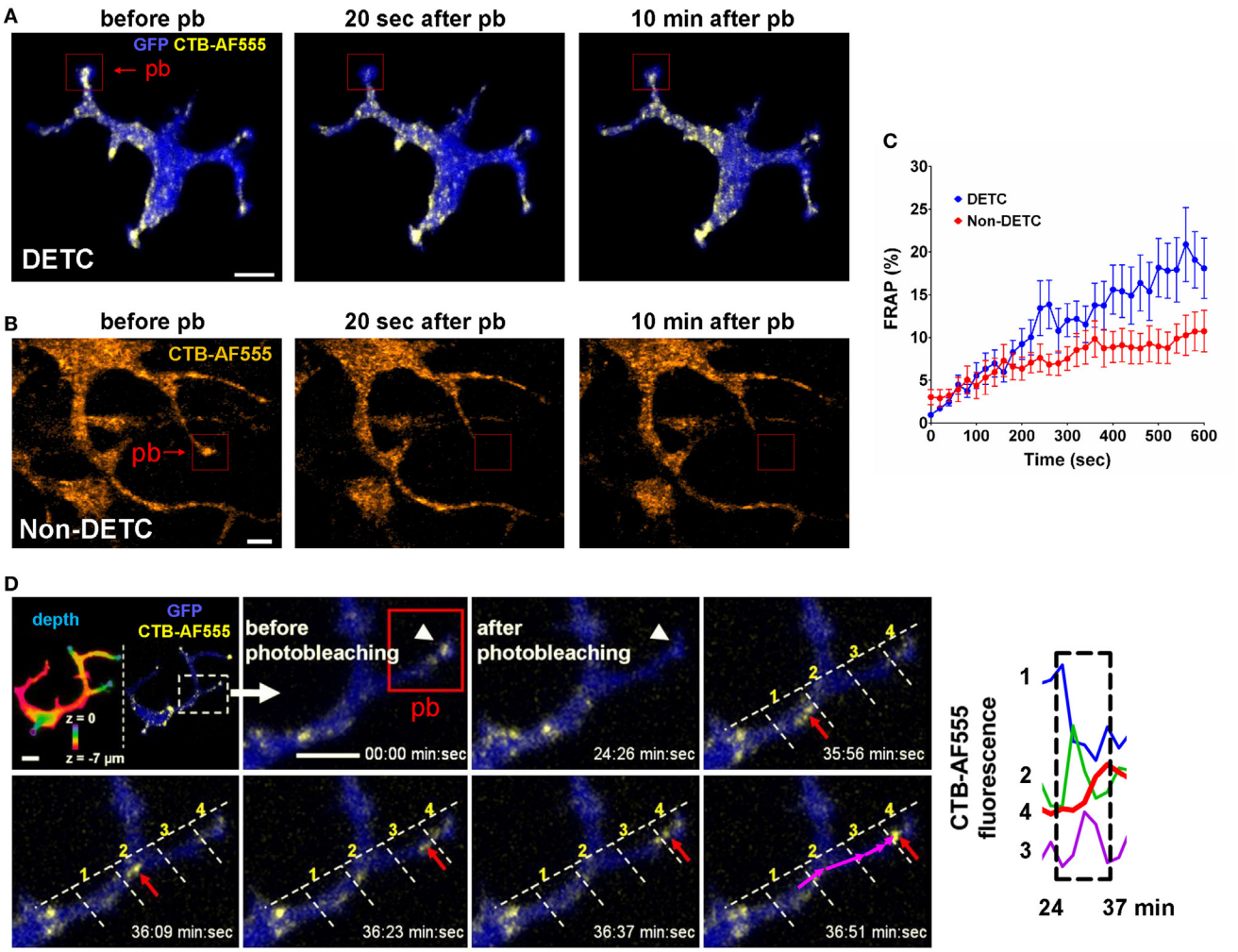

FIGURE 4 | *In vivo* dynamics of dendritic epidermal T cell (DETC) granules labeled with CTB-AF555 in IL2p8-GFP mouse ear. **(A)** Fluorescence recovery after photobleaching (FRAP) in a DETC dendrite end. The red rectangle area was photobleached (pb) and the cell was imaged for 10 min (see Movie S3 in Supplementary Material). **(B)** FRAP in a dermal non-DETC dendrite end. The red rectangle area was photobleached and the cell was imaged for 10 min (see Movie S4 in Supplementary Material). **(C)** Cumulative analysis of FRAP kinetics for multiple dendrite ends (n = 15 cells in five mice). Each point is a mean ± SEM. **(D)** Example of cargo movement along dendrite length. Upper left: color-coded depth—the apical localizations are blue-green and basal localizations are red. The dashed rectangle indicates zoom area. AF555 was photobleached in the red rectangle area. AF555 signal was measured in the four regions of interest (ROI) along the dendrite. The red arrow points to granule movement. The graph shows a rapid transition of AF555 (granule) intensity through the four ROIs, this movement starting after 24 min. Scale bars = 5 µm.

DISCUSSION

This study follows upon the discovery of DETC *in vivo* trans-epidermal polarization through the steady state TCR activation in the PALPs (5). The apical-polarized dendritic morphology of DETCs is a puzzling feature of this T cell lineage, reminiscent of their epidermal dendritic cohabitants, Langerhans cells. It is thought to facilitate a remote probing of the surrounding microenvironment including the barrier-forming apical squamous keratinocyte layers while maintaining cell body residence at a safe distance (13). A distinctive feature of DETCs, the PALPs contain distinct accumulations of cytoplasmic granules containing varying amounts of TCR, GM1, and LAMP-1 (5). In this report, we focused on the intracellular dynamics of DETC granules in the physiological microenvironment of intact skin at steady state. Our results demonstrate that DETC's long cellular projections sustain trans-epidermal trafficking of intracellular cargo, both in anterograde and retrograde fashion, i.e., toward and away from the PALPs. This way, DETCs can be considered a conduit system for cargo transport across the epidermis. To the best of our knowledge, this aspect of intraepithelial γδ T cell biology, i.e., *in vivo* intracellular granule transport, has not been studied before in DETCs or other intraepithelial T cell systems. The comparison of FRAP kinetics in DETC dendrites with that in nearby comparable cellular protrusions of dermal cells showed that the rate of transport in DETCs is higher. We could not compare DETCs to Langerhans cells because we did not find a common scheme for granule labeling in these cells other than with LT, which is not suitable for FRAP.

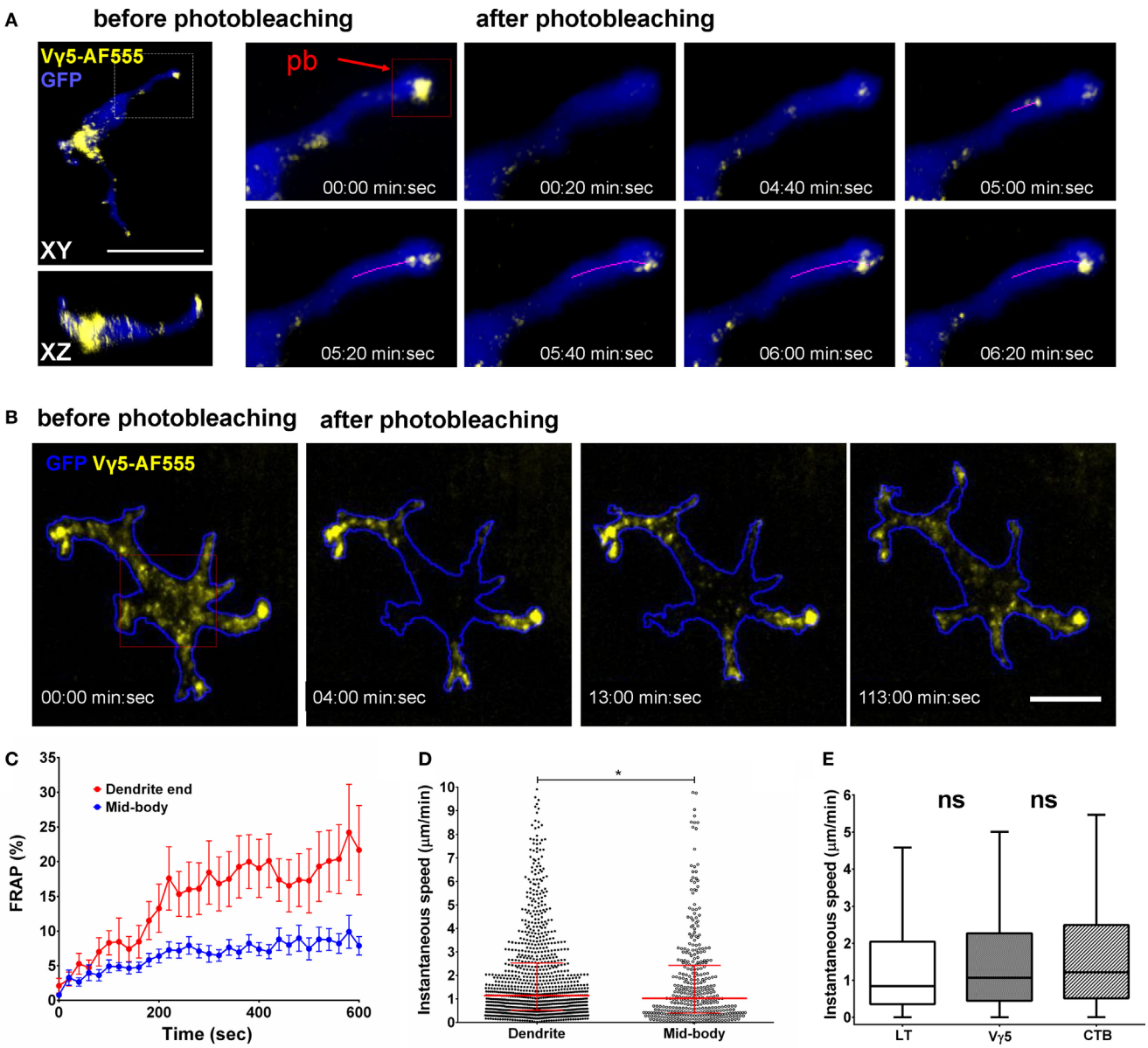

FIGURE 5 | *In vivo* dynamics of dendritic epidermal T cell (DETC) granules labeled by intradermal anti-Vγ5-AF555. **(A)** Fluorescence recovery after photobleaching (FRAP) in an apical dendrite end. AF555 fluorescence was photobleached in the red rectangle area centered on the end of an apical-facing dendrite (pb) and the entire cell was imaged, in 3-D, every 20 s for 10 min. The magenta line represents a track of moving granule. **(B)** FRAP in DETC mid-body. The photobleaching was located in the red rectangle area. Cell outline based on GFP signal. **(C)** FRAP analysis, $n = 15$ cells in five mice. **(D)** Comparison of instantaneous granule velocities in DETC dendrites vs. mid-bodies. Each dot is the speed of a single vesicle, data pooled from $n = 15$ cells in five mice. The horizontal line and whiskers are the median and interquartile ranges. **(E)** Comparison of instantaneous granule velocities depending on labeling method. Data pooled from $n = 15$ cells in five mice, shown as box with median and interquartile range with Tukey whiskers. Scale bars = 10 μm.

One tantalizing question that remains to be addressed is about the exact functional biological purpose of the apical dendrite granule accumulations, which has to be considered in the context of the PALPs. The presence of LT and mature lysosome/exocytosis marker LAMP-1 in DETC apical granules that also colocalized with Vγ5 and/or CTB fluorescence (**Figure 2**) suggests that some of the granules represent mature lysosomes, which could be poised for externalization, and that TCR and GM1/CTB internalization pathways ultimately feed into mature lysosomes. The latter notion and the relatively lower CTB/LT co-localization in mid-bodies compared to dendrites, where most LT fluorescence accumulated, is consistent with the process of membrane GM1 recycling by lysosomal sorting (14). This and other dissimilarities between the intracellular fates and steady state localizations of Vγ5 antibody and CTB fluorescence likely reflect expected variances in ligand and label trafficking and degradation. Considering that DETCs produce granzymes and perforin and can kill target cells by cytotoxic/LAMP-1 granule

release (6–8, 15), and that cytolytic granules are a subset of lysosomes, one exciting proposition is that some of the PALP's lysosomal and LAMP-1 granules that accumulate in PALPs contain cytotoxic factors. The presence of lysosomal and TCR-containing granules just underneath the sites of DETC TCR steady state activation, i.e., the PALPs (5) and now the presence of steady state transport for dendrite end granule accumulation and retrograde transport resemble the immunological synapses that form, albeit transiently, between antigen-specific cytotoxic T lymphocytes and their cellular targets (5, 16, 17). Another resemblance is with NK cell's remote synapse-like structures that form at the tips of "membrane nanotubes" and appear to support target cell killing (18). Other possible functions of DETC granule transport to the apical epidermis could be to facilitate targeted secretion of keratinocyte differentiation or repair factors. By demonstrating three methods for intravital DETC granule labeling, and by revealing the pattern of granule dynamics in otherwise un-manipulated/steady state, the current study should facilitate further functional and mechanistic investigations. An interesting aspect of any biological function of dendrite-guided DETC cargo transport is that it will be lost when DETCs are activated and round up.

Our demonstration of the existence of granule transport in DETC dendrites was enabled by the intravital granule labeling and tracking and by FRAP technique. The use of LT required independent labeling of DETCs with cytoplasmic fluorescent protein reporter (IL2p8-GFP) for digital 3-D gating, but it was convenient, rapid, and practically non-disturbing. LT labeling was suitable for granule tracking but less so for FRAP because the small molecule dye could, in principle, diffuse between granules or cells rather freely. Another limitation was that LT-based granule tracking was strictly limited to the inside of DETC bodies due to the need for image digital gating. By contrast, Vγ5 and CTB-based intravital labeling was not expected to allow for fluorescence diffusion (although carrier protein degradation would eventually ensue) thereby enabling FRAP experimentation. These methods should be useful to follow granules fates outside DETC bodies. One disadvantage of these labeling schemes was the possibility of transient cellular responses to the ligands hence the need for several days of steady state re-establishment. As mentioned earlier, anti-DETC TCR antibody did not deplete these cells *in vivo*—of note for experiments where DETC depletion might be desired.

The magnitude of CTB selectivity for DETCs among other cells in the epidermis was quite remarkable, suggesting that DETCs represent a major source (or recipient) of GM1 ganglioside in epidermis. While DETC-bound Vγ5 antibody was internalized relatively slowly, over more than 24 h, CTB internalization occurred much faster, within one and a half hour. This could reflect the underlying dynamics of GM1 ganglioside or CTB pentameric structure hence stronger avidity and capacity for cross-linking. Alternatively, the rapid labeling of DETC granules by CTB internalization could be related to the previously described process of physiological transport of gangliosides from the plasma membrane to intralysosomal membranes in cultured fibroblasts (14). If secreted, GM1 production by DETCs could be of local consequence for keratinocyte differentiation (19).

The dynamic imaging here confirmed our prior findings of the apical dendrite-terminal lysosome accumulation and it demonstrated that these lysosomal clusters are relatively long-lived and confined, as opposed to diffusing randomly in and out of the end-terminal dendrite swellings. Interestingly, these experiments revealed highly dynamic movement of lysosomal granules within the dendrites and cell bodies, including directional inflow into newly formed dendrites. This anterograde transport was reminiscent of "long processive runs," as if it followed tracks, described by Rodionov et al. (20), likely driven by molecular motors and cytoskeletal structures such as microtubules. In this respect, an interesting puzzle arises when one considers the known role of the microtubule-organizing center (MTOC) in the movement of cargo at the immunological synapse of classical αβ T cells. Therefore, the directional movement of granule subsets is associated with the MTOC relocalization toward the synapse (21, 22). This mechanism clearly cannot operate in DETCs at steady state because of the multiplicity of the PALPs.

Given that intradermal anti-Vγ5-TCR antibody (or CTB) did not cause perceptible morphological changes that would indicate acute cellular activation, such as cell rounding up, and consistent with the presence of non-phosphorylated TCR in submerged clusters underneath the PALPs surface (5), our results demonstrate that DETC TCR can be readily internalized without perturbing the cell behavior in a gross manner. Considering the ultimate trafficking of Vγ5 antibody fluorescence into lysosomal and LAMP-1 granules including in the PALPs, and knowing that TCRs of classical αβ T cells are continuously internalized and recycled back to the cell surface (23, 24), it is possible that the physiological accumulation of TCR in the PALPs is in part maintained by endosome-mediated TCR recycling. However, we could not yet establish if the PALPs are the sites of physiological TCR internalization. DETCs could use TCR and/or other cell membrane component internalization to efficiently probe their extracellular surroundings. In this respect, it would be interesting to know whether steady state and/or acute TCR binding to endogenous ligands, which remain to be discovered, would be associated with TCR internalization similar to that by anti-Vγ5 antibody, and weather the endogenous ligands would remain bound to the TCR and co-internalized. The retrograde transport could serve multiple purposes such as to simply retrieve molecules for disposal or recycling, or to probe the molecular composition of epidermal barrier for communication into the dermis. The uncovering of DETC's dendrite-mediated cargo transport opens a host of new directions for further functional studies.

ETHICS STATEMENT

All animal manipulations were approved by the Institutional Animal Care and Use Committee, The University of Texas MD Anderson Cancer Center, Houston, TX, USA, or the Local Ethics Committee for Experiments on Animals at the Institute of Immunology and Experimental Therapy, Wroclaw, Poland.

AUTHOR CONTRIBUTIONS

GC and TZ designed the studies, analyzed and interpreted the results. GC, MT, and MZ obtained and analyzed the data. GC, MT, and TZ wrote the manuscript.

ACKNOWLEDGMENTS

We thank E. Rothenberg and M. Yui (Caltech) for IL2p8–GFP mice and M. Nussenzweig for CD11c-YFP mice. This work was supported by the National Science Centre of Poland grant (2014/15/B/NZ6/03502), University of Texas MD Anderson Institutional Research Grant 3-0026138, and The National Institutes of Health grants AI065688 and 1S10RR029552.

SUPPLEMENTARY MATERIAL

The Supplementary Material for this article can be found online at https://www.frontiersin.org/articles/10.3389/fimmu.2018.01430/full#supplementary-material.

FIGURE S1 | Internalization of Vγ5-AF647 and CTB-AF555 in dendritic epidermal T cells (DETCs). Images show examples of DETCs after 10 min, 90 min, or 24 h from intradermal co-injection of CTB-AF555 and anti-Vγ5-AF647. The white arrows point to the apical dendrites (based on 3-D z-stack inspection). Scale bar = 10 μm.

FIGURE S2 | Vγ5 labeling is specific for dendritic epidermal T cells (DETCs). **(A)** Accumulation of anti-Vγ5-AF555 antibody in DETCs but not in Langerhans (LC) or other cells. Left panel: dual reporter IL2p8-GFP (bright) and CD11c-YFP (dim) mouse skin imaged in the same channel. Middle panel: DETC and LC identification. **(B)** Comparison of anti-Vγ5-AF555 antibody (upper panel) with the isotype control (lower panel). Fluorescence intensity profiles are drawn along dashed regions to relate AF555 signals to GFP-labeled DETC bodies. Scale bar = 10 μm.

FIGURE S3 | Identification of CTB-labeled granules. Immunofluorescence on skin samples 6 days after injection of fluorescent CTB. Steady state CTB-labeled granules colocalize with LAMP-1. The white arrows point to apical dendrite endings, determined by 3-D z-stack inspection.

FIGURE S4 | Whole-cell fluorescence recovery after photobleaching (FRAP). The lack of fluorescence recovery in the whole-cell photobleached areas demonstrates that CTB **(A)** and Vγ5 **(B)** labeling did not diffuse from the intercellular spaces or by leaking from the neighboring cells. Fluorescence intensity profiles are based on AF555 signal measured in the whole cell.

FIGURE S5 | Mid-body fluorescence recovery after photobleaching (FRAP) in dermal non-dendritic epidermal T cells (DETCs) labeled by CTB-AF555 (related to **Figure 4B**). Ear skin of a mouse was labeled with intradermal CTB-AF555. Laser scanning microscope was focused in the dermis and the area in the red rectangle was photobleached followed by time-lapse imaging of the FRAP. Lower panel: FRAP quantification for dendrite ends and mid-bodies for multiple FRAP experiments on 10–13 cells in two mice each. Images in "orange hot" intensity color palette. Scale bar = 10 μm.

MOVIE S1 | Dynamics of lysosomes in a dendritic epidermal T cell (DETC) *in vivo*. Imaging was performed 1 h after intradermal injection of LysoTracker (LT) Red into a healthy IL2p8-GFP mouse. Depth color coding indicates apical layers in purple, also shown with the arrowheads. The arrows point to the direction of a new dendrite formation. The new dendrites are quickly populated by LT-stained granules. LT signal based on GFP gate.

MOVIE S2 | Dynamics of lysosomes in a dendritic epidermal T cell (DETC) *in vivo*. Imaging was performed 1 h after intradermal injection of LysoTracker (LT) Red into a healthy IL2p8-GFP mouse. Four optical sections from a z-stack are shown with raw (non-GFP-gated) LT signal. Right top side: maximum intensity projection of the z-stack with LT signal based on GFP gate. Right bottom side: LT signal based on GFP gate in "fire" intensity palette.

MOVIE S3 | *In vivo* dynamics of dendritic epidermal T cell (DETC) intracellular granules labeled by CTB-AF555 internalization. Imaging was performed 11 days after intradermal injection of CTB-AF555 into a healthy IL2p8-GFP mouse. Depth color coding indicates apical layers in purple, also shown with the arrowheads. The white squares indicate the areas subjected to photobleaching. The arrows point to newly arrived granules.

MOVIE S4 | *In vivo* dynamics of intracellular granules labeled by CTB-AF555 internalization in dermal non-dendritic epidermal T cells (DETCs). The white squares indicate the areas (dendrite end or mid-body) subjected to photobleaching.

MOVIE S5 | *In vivo* dynamics of dendritic epidermal T cell (DETC) intracellular granules labeled by internalized anti-Vγ5-AF647. Imaging was performed 6 days after the antibody intradermal injection into a healthy IL2p8-GFP mouse. Individual video frames represent temporal projections of 376 s sequences. The white rectangle indicates the area subjected to photobleaching.

MOVIE S6 | *In vivo* dynamics of anti-Vγ5-T cell receptors (TCR)-AF555 labeled granules at dendritic epidermal T cell (DETC) dendrite ends. Imaging was performed 6 days after intradermal injection of anti-Vγ5-AF555 antibody into a healthy IL2p8-GFP mouse. The white rectangles indicate the areas subjected to photobleaching. GFP-based depth color coding indicates apical layers in blue. AF555 signal is represented in "fire" intensity palette. Movie is a combined recording of three cells.

MOVIE S7 | *In vivo* dynamics of anti-T cell receptors (TCR)-AF647 labeled granules in new dendrites and in a dendritic epidermal T cell (DETC) mid-body area that is not connected to a dendrite. Imaging was performed 6 days after intradermal injection of anti-Vγ5 TCR-AF647 antibody into one ear of a healthy IL2p8-GFP mouse. Bottom panels show the AF647 channel intensity using the "fire" intensity palette. The white rectangle indicates the area subjected to photobleaching, also indicated with the white arrow. For this cell, the photobleached area is located over a part of cell mid-body that is not a dendrite, and not connected to a dendrite. The insets shown on the right side represent zoomed-in areas to point to the dendrite ends labeled with the corresponding numbers. The red arrows point to the areas of new dendrite appearance, which are quickly populated by fluorescent granules.

MOVIE S8 | *In vivo* dynamics of anti-Vγ5-T cell receptors (TCR)-AF555 labeled granules at dendritic epidermal T cell (DETC) mid-body. Imaging was performed 6 days after intradermal injection of anti-Vγ5-AF555 antibody into a healthy IL2p8-GFP mouse. The white rectangles indicate the areas subjected to photobleaching. GFP-based depth color coding indicates apical layers in blue. AF555 signal is represented in "fire" intensity palette. Movie is a combined recording of three cells.

MOVIE S9 | *In vivo* dynamics of anti-Vγ5-T cell receptors (TCR)-AF647 labeled granules at dendritic epidermal T cell (DETC) dendrite base. Imaging was performed 6 days after intradermal injection of anti-Vγ5-AF647 antibody into a healthy IL2p8-GFP mouse. The white rectangle indicates the area subjected to photobleaching.

REFERENCES

1. Ramirez K, Witherden DA, Havran WL. All hands on DE(T)C: epithelial-resident γδ T cells respond to tissue injury. *Cell Immunol* (2015) 296:57–61. doi:10.1016/j.cellimm.2015.04.003
2. Komori HK, Witherden DA, Kelly R, Sendaydiego K, Jameson JM, Teyton L, et al. Cutting edge: dendritic epidermal γδ T cell ligands are rapidly and locally expressed by keratinocytes following cutaneous wounding. *J Immunol* (2012) 188:2972–6. doi:10.4049/jimmunol.1100887
3. Vantourout P, Hayday A. Six-of-the-best: unique contributions of γδ T cells to immunology. *Nat Rev Immunol* (2013) 13:88–100. doi:10.1038/nri3384
4. Heilig JS, Tonegawa S. Diversity of murine gamma genes and expression in fetal and adult T lymphocytes. *Nature* (1986) 322:836–40. doi:10.1038/322836a0

5. Chodaczek G, Papanna V, Zal MA, Zal T. Body-barrier surveillance by epidermal γδ TCRs. *Nat Immunol* (2012) 13:272–82. doi:10.1038/ni.2240
6. Romani N, Stingl G, Tschachler E, Witmer MD, Steinman RM, Shevach EM, et al. The Thy-1-bearing cell of murine epidermis. A distinctive leukocyte perhaps related to natural killer cells. *J Exp Med* (1985) 161:1368–83. doi:10.1084/jem.161.6.1368
7. Krähenbühl O, Gattesco S, Tschopp J. Murine Thy-1+ dendritic epidermal T cell lines express granule-associated perforin and a family of granzyme molecules. *Immunobiology* (1992) 184:392–401. doi:10.1016/S0171-2985(11)80596-6
8. Ibusuki A, Kawai K, Yoshida S, Uchida Y, Nitahara-Takeuchi A, Kuroki K, et al. NKG2D triggers cytotoxicity in murine epidermal γδ T cells via PI3K-dependent, Syk/ZAP70-independent signaling pathway. *J Invest Dermatol* (2014) 134:396–404. doi:10.1038/jid.2013.353
9. Yui MA, Sharp LL, Havran WL, Rothenberg EV. Preferential activation of an IL-2 regulatory sequence transgene in TCRγδ and NKT cells: subset-specific differences in IL-2 regulation. *J Immunol* (2004) 172:4691–9. doi:10.4049/jimmunol.172.8.4691
10. Lindquist RL, Shakhar G, Dudziak D, Wardemann H, Eisenreich T, Dustin ML, et al. Visualizing dendritic cell networks in vivo. *Nat Immunol* (2004) 5:1243–50. doi:10.1038/ni1139
11. Thévenaz P, Ruttimann UE, Unser M. A pyramid approach to subpixel registration based on intensity. *IEEE Trans Image Process* (1998) 7:27–41. doi:10.1109/83.650848
12. Garman RD, Doherty PJ, Raulet DH. Diversity, rearrangement, and expression of murine T cell gamma genes. *Cell* (1986) 45:733–42. doi:10.1016/0092-8674(86)90787-7
13. Kubo A, Nagao K, Yokouchi M, Sasaki H, Amagai M. External antigen uptake by Langerhans cells with reorganization of epidermal tight junction barriers. *J Exp Med* (2009) 206:2937–46. doi:10.1084/jem.20091527
14. Mobius W, Herzog V, Sandhoff K, Schwarzmann G. Gangliosides are transported from the plasma membrane to intralysosomal membranes as revealed by immuno-electron microscopy. *Biosci Rep* (1999) 19(4):307–16. doi:10.1023/A:1020502525572
15. Whang MI, Guerra N, Raulet DH. Costimulation of dendritic epidermal γδ T cells by a new NKG2D ligand expressed specifically in the skin. *J Immunol* (2009) 182:4557–64. doi:10.4049/jimmunol.0802439
16. Dustin ML, Chakraborty AK, Shaw AS. Understanding the structure and function of the immunological synapse. *Cold Spring Harb Perspect Biol* (2010) 2:a002311. doi:10.1101/cshperspect.a002311
17. Stinchcombe JC, Bossi G, Booth S, Griffiths GM. The immunological synapse of CTL contains a secretory domain and membrane bridges. *Immunity* (2001) 15:751–61. doi:10.1016/S1074-7613(01)00234-5
18. Chauveau A, Aucher A, Eissmann P, Vivier E, Davis DM. Membrane nanotubes facilitate long-distance interactions between natural killer cells and target cells. *Proc Natl Acad Sci U S A* (2010) 107:5545–50. doi:10.1073/pnas.0910074107
19. Seishima M, Takagi H, Okano Y, Mori S, Nozawa Y. Ganglioside-induced terminal differentiation of human keratinocytes: early biochemical events in signal transduction. *Arch Dermatol Res* (1993) 285(7):397–401. doi:10.1007/BF00372132
20. Rodionov VI, Hope AJ, Svitkina TM, Borisy GG. Functional coordination of microtubule-based and actin-based motility in melanophores. *Curr Biol* (1998) 8:165–8. doi:10.1016/S0960-9822(98)70064-8
21. Stinchcombe JC, Majorovits E, Bossi G, Fuller S, Griffiths GM. Centrosome polarization delivers secretory granules to the immunological synapse. *Nature* (2006) 443:462–5. doi:10.1038/nature05071
22. Kupfer A, Dennert G. Reorientation of the microtubule-organizing center and the Golgi apparatus in cloned cytotoxic lymphocytes triggered by binding to lysable target cells. *J Immunol* (1984) 133:2762–6.
23. Alcover A, Alarcón B. Internalization and intracellular fate of TCR-CD3 complexes. *Crit Rev Immunol* (2000) 20:325–46. doi:10.1615/CritRevImmunol.v20.i4.20
24. Das V, Nal B, Dujeancourt A, Thoulouze M-I, Galli T, Roux P, et al. Activation-induced polarized recycling targets T cell antigen receptors to the immunological synapse; involvement of SNARE complexes. *Immunity* (2004) 20:577–88. doi:10.1016/S1074-7613(04)00106-2

Conflict of Interest Statement: The authors declare that the research was conducted in the absence of any commercial or financial relationships that could be construed as a potential conflict of interest.

Copyright © 2018 Chodaczek, Toporkiewicz, Zal and Zal. This is an open-access article distributed under the terms of the Creative Commons Attribution License (CC BY). The use, distribution or reproduction in other forums is permitted, provided the original author(s) and the copyright owner are credited and that the original publication in this journal is cited, in accordance with accepted academic practice. No use, distribution or reproduction is permitted which does not comply with these terms.

frontiers in Immunology

MINI REVIEW
published: 08 June 2018
doi: 10.3389/fimmu.2018.01246

ABCA1, apoA-I, and BTN3A1: A Legitimate Ménage à Trois in Dendritic Cells

*Chiara Riganti[1], Barbara Castella[2] and Massimo Massaia[2,3]**

[1] Dipartimento di Oncologia, Università degli Studi di Torino, Turin, Italy, [2] Laboratorio di Immunologia dei Tumori del Sangue (LITS), Centro Interdipartimentale di Ricerca in Biologia Molecolare (CIRBM), Università degli Studi di Torino, Turin, Italy, [3] SC Ematologia, AO S. Croce e Carle, Cuneo, Italy

Human Vγ9Vδ2 T cells have the capacity to detect supra-physiological concentrations of phosphoantigens (pAgs) generated by the mevalonate (Mev) pathway of mammalian cells under specific circumstances. Isopentenyl pyrophosphate (IPP) is the prototypic pAg recognized by Vγ9Vδ2 T cells. B-cell derived tumor cells (i.e., lymphoma and myeloma cells) and dendritic cells (DCs) are privileged targets of Vγ9Vδ2 T cells because they generate significant amounts of IPP which can be boosted with zoledronic acid (ZA). ZA is the most potent aminobisphosphonate (NBP) clinically available to inhibit osteoclast activation and a very potent inhibitor of farnesyl pyrophosphate synthase in the Mev pathway. ZA-treated DCs generate and release in the supernatants picomolar IPP concentrations which are sufficient to induce the activation of Vγ9Vδ2 T cells. We have recently shown that the ATP-binding cassette transporter A1 (ABCA1) plays a major role in the extracellular release of IPP from ZA-treated DCs. This novel ABCA1 function is fine-tuned by physical interactions with IPP, apolipoprotein A-I (apoA-I), and butyrophilin-3A1 (BTN3A1). The mechanisms by which soluble IPP induces Vγ9Vδ2 T-cell activation remain to be elucidated. It is possible that soluble IPP binds to BTN3A1, apoA-I, or other unknown molecules on the cell surface of bystander cells like monocytes, NK cells, Vγ9Vδ2 T cells, or any other cell locally present. Investigating this scenario may represent a unique opportunity to further characterize the role of BTN3A1 and other molecules in the recognition of soluble IPP by Vγ9Vδ2 T cells.

Keywords: Vγ9Vδ2 T cells, phosphoantigens, isopentenyl pyrophosphate, ATP-binding cassette transporter A1, apolipoprotein A-I, butyrophilin-3A1

OPEN ACCESS

Edited by:
Pierre Vantourout, King's College London, United Kingdom

Reviewed by:
Gennaro De Libero, Universität Basel, Switzerland
Martin S. Davey, University of Birmingham, United Kingdom

****Correspondence:***
Massimo Massaia
massimo.massaia@unito.it

Specialty section:
This article was submitted to T Cell Biology, a section of the journal Frontiers in Immunology

Received: *25 February 2018*
Accepted: *17 May 2018*
Published: *08 June 2018*

Citation:
Riganti C, Castella B and Massaia M (2018) ABCA1, apoA-I, and BTN3A1: A Legitimate Ménage à Trois in Dendritic Cells. Front. Immunol. 9:1246. doi: 10.3389/fimmu.2018.01246

INTRODUCTION

A very peculiar feature of Vγ9Vδ2 T cells is their TCR-dependent, MHC-independent recognition of phosphoantigens (pAgs) (1). pAgs are pyrophosphorylated isoprenoids generated in the mevalonate (Mev) pathway of mammalian cells. Isopentenyl pyrophosphate (IPP) is the prototypic pAg recognized by Vγ9Vδ2 T cells (2). Increased Mev pathway dysregulation has been reported in many types of cancer cells (3). This metabolic derangement leads to increased IPP production which is sensed by Vγ9Vδ2 T cells laying the basis of their multifaceted contribution to immune surveillance and antitumor immunity (4).

Vγ9Vδ2 T cells also recognize pAgs generated in Mev and non-Mev pathway of microbial pathogens [i.e., hydroxyl dimethylallyl pyrophosphate (HDMAPP), hydroxy-methyl-butyl-pyrophosphate (HMBPP)] (5, 6); this capacity confers to Vγ9Vδ2 T cells a critical role in innate and adaptive antimicrobial immune responses (7).

The third pAg category recognized by Vγ9Vδ2 T cells are the synthetic pAgs developed for therapeutic purposes [i.e., bromohydrinpyrophosphate, (2E)-1-hydroxy-2-methylpent-2-enyl pyrophosphate (CHDMAPP)] (8, 9). Some of these compounds have been investigated in clinical trials with alternating success (10) and are currently used as research tools to directly or indirectly activate Vγ9Vδ2 T cells *in vitro* (11–13). More recently, several technologies have been used to generate pAg prodrugs with the aim to overcome the poor cell membrane permeability and limited *in vivo* stability of pyrophosphate containing pAgs (14, 15).

Another strategy which has been used *in vivo* and *in vitro* to activate Vγ9Vδ2 T cells is to intentionally increase intracellular IPP concentrations in tumor cells and/or antigen-presenting cells (APCs) like monocytes or dendritic cells (DCs) with aminobisphosphonates (NBP) (16), and alkylamines (17, 18). These compounds inhibit farnesylpyrophosphate synthase (FPPS) in the Mev pathway causing intracellular IPP accumulation (18–20). Prodrug technology has also been used to develop an highly hydrophobic NBP prodrug [tetrakis-pivaloyloxymethyl 2-(thiazole-2-ylamino) ethylidene-1,1-bis-phosphonate (PTA)] to facilitate intracellular uptake and, after conversion into the active form, to induce FPPS blockade and IPP accumulation (21).

The fate of supra-physiological IPP concentrations is different according to cell type and tissue localization. Intracellular formation of the pro-apoptotic ATP analog 1-adenosin-5-yl 3-(3-methylbut-3-enyl) triphosphoric acid diester (ApppI) formation depends on the activity of FPPS, aminoacyl-tRNA synthetases, dosage, and potency of NBP (22). Zoledronic acid (ZA), the most potent NBP clinically available, is commonly used to treat bone disease in myeloma and solid cancers with bone metastases (23–25). In osteoclasts, ZA-induced supra-physiological IPP concentrations leads to intracellular ApppI formation (26). ApppI initiates the apoptotic program in osteoclasts explaining the therapeutic efficacy of ZA in this setting. Tumor cells also accumulate intracellular apoptotic ApppI concentrations when exposed to ZA concentrations similar to those achieved in the mineralized bone (from 50 μM to 1 mM). Much lower ZA concentrations (0.5–1 μM) are used to boost the capacity of tumor cells, monocytes, and DCs to activate Vγ9Vδ2 T cells (19, 27, 28). Under these conditions, ZA-induced IPP accumulation is insufficient to induce enough ApppI to trigger apoptosis. It is highly conceivable that APCs like monocytes and DCs have developed mechanisms to resist the toxic effects of intracellular IPP accumulation and converted this resilience to survive and recruit Vγ9Vδ2 T cells. Upregulation of IPP extruders like ABCA1 could contribute to this resilience (see also below).

Zoledronic acid-treated mature DCs are better Vγ9Vδ2 T-cell activators than ZA-treated monocytes or ZA-treated immature DCs (29). This superiority is directly related to their capacity to accumulate high intracellular IPP concentrations and to release IPP in the supernatants (SNs) at concentrations up to 1,000× higher (nanomolar range) than intracellular concentrations (picomolar range) (29, 30). These extracellular IPP concentrations are sufficient to induce Vγ9Vδ2 T-cell proliferation in the absence of cell-to-cell contact with ZA-treated DCs (30, 31). How IPP is released in the extracellular microenvironment and delivered to Vγ9Vδ2 T cells has been a matter of investigation and partially decoded over the last year (31). This review is aimed at discussing the role played by ABCA1, apo-AI, and BTN3A1 in the extracellular IPP release from ZA-treated DCs.

LOOKING FOR MEMBRANE-ASSOCIATED pAg TRANSPORTERS

F1-ecto-ATPase has been the first cell surface protein associated with IPP presentation to Vγ9Vδ2 T cells. Interest was driven by the discovery that apoA-I and F1-ecto-ATPase discriminate between Vγ9Vδ2 T-cell sensitive or insensitive tumor cell lines (32). The association between IPP and F1-eco-ATPase was reported a few years later in 721.221 B cells (33). This B-cell line is unable to activate Vγ9Vδ2 T cells, unless incubated with high-dose ZA to induce apoptosis. ZA stimulation induces intracellular IPP accumulation, ApppI formation and binding to F1-ecto-ATPase. Allosteric F1-ecto-ATPase modification induced by ApppI leads to Vγ9Vδ2 T-cell activation *via* TCR-dependent recognition (33).

Although very attractive, this model left the field open to several questions. IPP does not directly bind to F1-ecto-ATPase, but it requires ApppI formation; a nucleotide pyrophosphatase (NPP) is then required to release IPP from ApppI and make it available to Vγ9Vδ2 T cells. It is currently unknown whether NPP activity is provided *in cis* by the same cells which have accumulated IPP or *in trans* by neighboring cells. Thus, the IPP/ApppI/F1-ecto-ATPase pathway appears to work as a multistep process in which IPP is initially transformed into ApppI which is relocated to the plasma membrane bound to F1-ecto-ATPase. Next, IPP is made available to bystander Vγ9Vδ2 T cells by NPP which releases IPP from ApppI. Vγ9Vδ2 T cells themselves have been reported to express CD39 ecto-ATPase after activation, but with the opposite goal, i.e., to destroy locally available IPP and downregulate their activation (34). Another issue is that ApppI is mainly generated in apoptotic cells, whereas Vγ9Vδ2 T cells are also activated by non-apoptotic cells (35–37). Finally, HMBPP, HDMAPP, and all HDMAPP-adenylated, thymidylated, and uridylated pyrophosphoric derivatives are potent Vγ9Vδ2 T-cell activators without any capacity to bind F1-ecto-ATPase (9, 38). These nucleotides are released in the extracellular microenvironment by non-apoptotic cells or bacteria and cleaved by extracellular pyrophosphatase (39).

A major advance has been the discovery that F1-ecto-ATPase is a receptor for apolipoprotein A-I (apoA-I) (32, 39) and that apoA-I is necessary for Vγ9Vδ2 T-cell activation by tumor cells expressing IPP/ApppI-loaded F1-ecto-ATPase (32). Since it is very unlikely that F1-ecto-ATPase is released from the plasma membrane, it has been hypothesized that soluble apoA-I may activate Vγ9Vδ2 T cells remotely. Interestingly, chronic inflammation is associated with reduced levels of circulating apoA-I and lower immune competence of Vγ9Vδ2 T cells (40). All these findings have enforced the idea that apoA-I is a necessary player in the efflux, delivery and pAg presentation to Vγ9Vδ2 T cells (32).

LOOKING FOR SOLUBLE pAg TRANSPORTERS

ApoA-I is physiologically involved in the assembly of nascent high-density lipoproteins (HDL), which mediate the reverse cholesterol transport. The first step in this process is the interaction of apoA-I with the extracellular domain of the ATP-binding cassette transporter A1 (ABCA1), a member of the ABC transmembrane transporter family, abundant in liver, gastrointestinal tract, and macrophages (41). Cholesterol and phospholipids are physiologically effluxed by ABCA1 and loaded by apoA-I, but they are not the only lipids handled by this pathway; α-tocopherol (42), dolichol, and retinoic acid are also effluxed by ABCA1 and transported by apoA-I to nascent HDL (43, 44). Interestingly, all these molecules share multiple isoprenoid moieties identical to that contained in IPP and other Vγ9Vδ2 T-cell activating pAgs.

This structural similarity prompted us to investigate whether the ABCA1/apoA-I system could also extrude intracellular IPP, especially when potentially harmful intracellular concentrations are reached. ZA-treated DCs turned out to be a very convenient and highly reproducible tool to investigate this issue. We have found that ABCA1 plays a major role in the extracellular IPP release from ZA-treated DCs and other cells, and that IPP cannot be released in the SNs of ZA-treated DCs if ABCA1 is not present or functionally active.

So far, we cannot exclude that other isoprenoids structurally related to IPP, like dimethylallyl pyrophosphate, geranyl pyrophosphate, FPP, or geranylgeranyl pyrophosphate (GGPP), are also effluxed by the ABCA1/apoA-I system in DCs and/or other cells. These isoprenoids can also activate Vγ9Vδ2 T cells (45, 46) and regulate the cross-talk between immune cells, cancer cells, and bystander cells in the tumor microenvironment (TME) (47, 48). To exert their mitogenic or regulatory functions in the TME, these metabolites must reach adequate intracellular concentrations to be released in replace of cholesterol and/or phospholipids that are the privileged molecules conveyed by ABCA1/apoA-I. We have shown that IPP extracellular release by ABCA1 overcomes that of cholesterol only when supra-physiological concentration of IPP are reached as a consequence of ZA-induced FPPS inhibitions (31). It is possible that ABCA1 takes the lead in extruding alternative pAgs like HMBPP only when supra-physiological concentrations are reached as reported in neutrophils after internalization of HMBPP-producing bacteria (49). Structure–activity relation studies, cross-linking of radiolabeled pAgs different from IPP should help to clarify this unexplored and exciting issue.

Interestingly, single-nucleotide polymorphisms and post-translational modifications (i.e., methionine oxidation) reduce apoA-I affinity for cholesterol and increase the affinity for other lipids (50). Since oxidation commonly occurs in the inflammatory microenvironment, it is possible that oxidized apoA-I behave more efficiently as pAg carrier and provide adequate pAg concentrations in inflamed tissues to induce the activation of Vγ9Vδ2 T cells (**Figure 1**).

BTN3A1: A KEY PLAYER IN Vγ9Vδ2 T-CELL RESPONSES TO pAg

One major advance in understanding pAg-induced Vγ9Vδ2 T-cell activation has been the identification of the butyrophilin-3 (BTN3) protein family as a key mediator in this process (53). BTN3 proteins, also known as CD277, are type I transmembrane proteins with two immunoglobulin (Ig)-like extracellular domains (IgV and IgC) and close structural homology with the B7-superfamily of proteins (54, 55). Three isoforms of BTN3A are present in humans: BTN3A1, BTN3A2, and BTN3A3, each encoded by a separate gene. BTN3A1 and BTN3A3 both contain the intracellular B30.2 domains, but BTN3A1 only has the capacity to induce pAg-dependent Vγ9Vδ2 T-cell activation. Recent findings from Vantourout et al. (56) indicate that BTN3A2 also is deeply involved in pAg-induced activation of Vγ9Vδ2 T cells (see also **Figure 2**) by regulating the appropriate routing, kinetics, and/or stability of BTN3A1.

Two mechanisms have been proposed to explain the interactions between BTN3A1 and pAgs and how these interactions are sensed by Vγ9Vδ2 T cells. Reports about how BTN3A proteins interact with pAgs are very conflicting and still represent an unsolved and intriguing question. The first mechanism postulates that pAgs are presented to Vγ9Vδ2 T cells *via* the membrane-distal IgV-like domain within the BTN3A1 ectodomain (57, 58). This model is reminiscent of the classical Ag-presentation model and implies that pAgs are made available in the extracellular space from endogenous or exogenous sources. However, following reports have demonstrated that pAgs interact directly with the intracellular B30.2 domain and failed to detect any association with the extracellular domains of BTN3A1 nor with the Vγ9Vδ2 TCRs (59–63).

The other mechanism is an inside-out mechanism initiated by interactions of the intracellular B30.2 domain with pAgs (59–63). Opposite to the antigen-presenting model, the allosteric model implies that signaling is operated by endogenous pAgs or exogenous pAgs after internalization from external sources. Within cells, pAgs are discriminated from non-antigenic small molecules because the former only may induce the conformational switch of the intracellular B30.2 domain (64). These changes determine the structural reorganization of BTN3A1 dimers on the cell surface which adopt a V-shaped conformation which is avidly recognized by Vγ9Vδ2 T cells. The inside-out signaling can be mimicked by agonistic (20.1) or antagonistic (103.2) antibodies which can induce or block the active conformation of BTN3A dimers on the cell surface (65) (**Figure 2**). It is still unclear how conformational changes of the intracellular B30.2 domain are transmitted to the cell surface. The juxtamembrane domain located close to the B30.2 domain has recently been reported to play an important role in the inside-out signal propagation (66, 67). The recruitment of other proteins like RhoB and periplakin has been proposed to participate to the structural reorganization of BTN3A1 dimers on the cell surface (61, 68). More recently, BTN3A2 also has been reported to be involved in the induction of active BTN3A1 conformation (56) (**Figure 2**). However, existing data require a cautious interpretation since

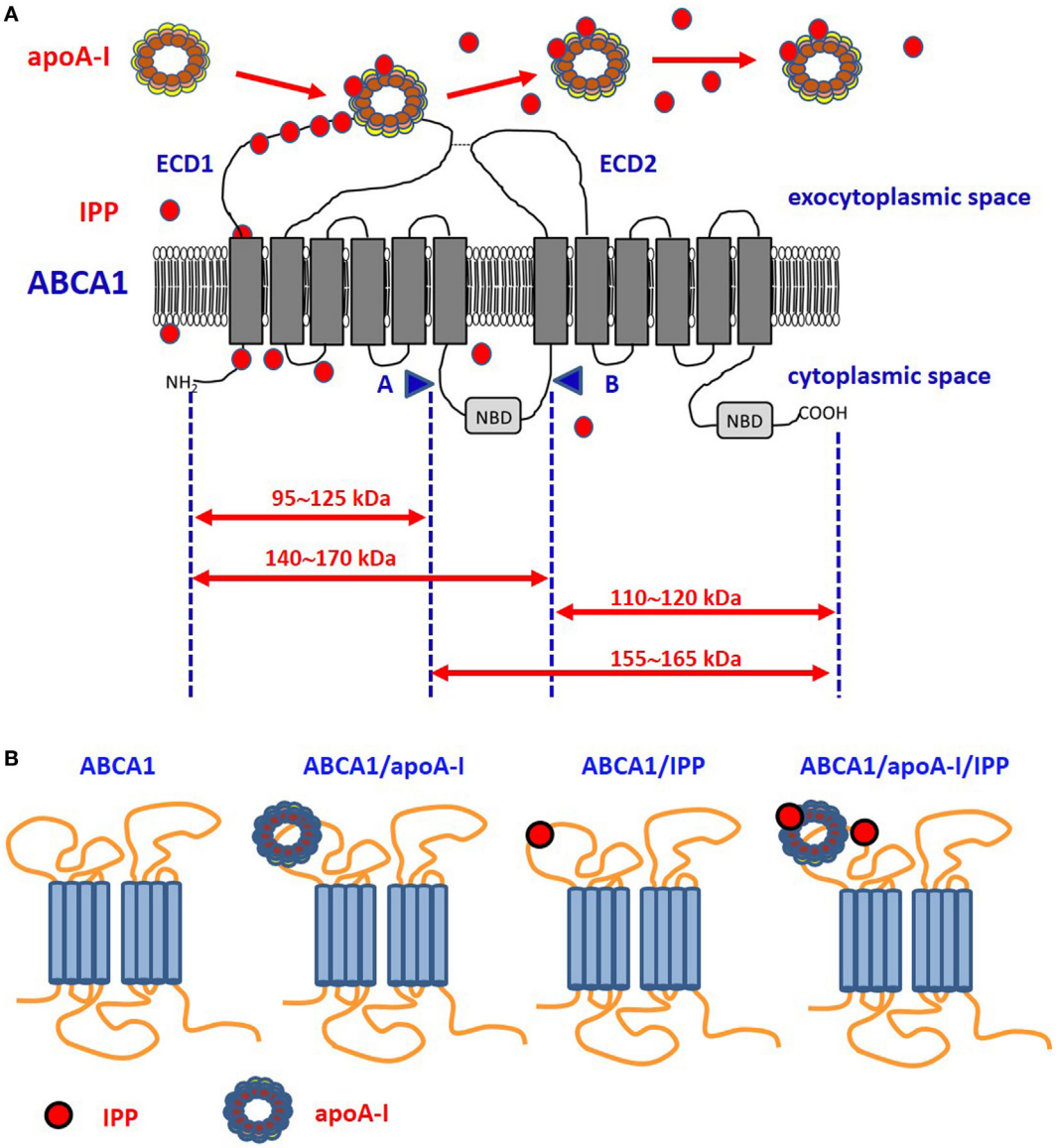

FIGURE 1 | Proposed model of ABCA1, apoA-I, and isopentenyl pyrophosphate (IPP) interactions**. (A)** It is unknown whether intracellular IPP binds to intracellular ABCA1 domains as it does with the intracellular B30.2 domain of BTN3A1 (see **Figure 2**). IPP is extruded across ABCA1 pore and reaches the extracellular environment. Limited trypsin-digestion cleaves ABCA1 into four fragments, corresponding to different extracellular and intracellular domains (51). The schematic diagram of trypsin-limited digestion of ABCA1 and the molecular sizes of the fragments produced are shown. We have found that IPP is associated with the amino-terminal extracellular portion of ABCA1 (31). Interestingly, apoA-I has been reported to interact with the same portion (52). We propose that IPP and apoA-I meet and associate within the amino-terminal portion of ABCA1 in the ECD1. IPP locally competes with cholesterol and other phospholipids for apoA-I binding and transportation. Local concentrations and the oxidized status of apoA-I, especially if IPP-producing cells are embedded in an inflammatory microenvironment, may favor IPP binding vs other metabolites. It is also possible that IPP is released in the extracellular space unbound to apoA-I. It is currently unknown whether IPP/apoA-I is more resistant to degradation by serum nucleotide pyrophosphatases than soluble IPP and more effective in the activation of Vγ9Vδ2 T cells faraway from IPP-producing cells. **(B)** ABCA1 is schematically represented from left to the right without any extra-loaded molecule, loaded with apoA-I only, with IPP only, and with IPP/apoA-I + IPP. It has been shown that apoA-I and IPP can bind to ABCA1, and that ABCA1 can bind to BTN3A1 (31). It is currently unknown whether ABCA1 has different affinity for BTN3A1 depending on IPP and/or apoA-I loading. Arrows: moleculare weight of fragments derived from trypsin-cleavage sites; COOH, carboxyterminal domain; ECD1, extracellular domain 1; ECD2, extracellular domain 2; NBD, nucleotide binding domain; NH2, amino-terminal domain.

in most cases they have been obtained using recombinant proteins and/or immobilized Vγ9Vδ2 TCRs. These experimental conditions do not recapitulate the dynamic situation going on under physiological or pathological conditions when much lower amounts of pAgs, binding proteins, and Vγ9Vδ2 TCRs are available. Likewise, some unsolved issues remain regarding the conformational switch induced by agonistic or antagonistic anti-BTN3A1 mAbs that may not fully mimic the conformational switch induced by pAgs, at least in some experimental models like the murine Vγ9Vγ2 TCR-transfectants reported by Starick

et al (69). This variegate scenario is the propellant of an exciting debate about how BTN3A proteins interact with pAgs and stimulate Vγ9Vδ2 T cells.

Both the antigen presentation and the allosteric model implies pAg transportation across the cell membrane: the former implies that pAgs are made available in the extracellular space from

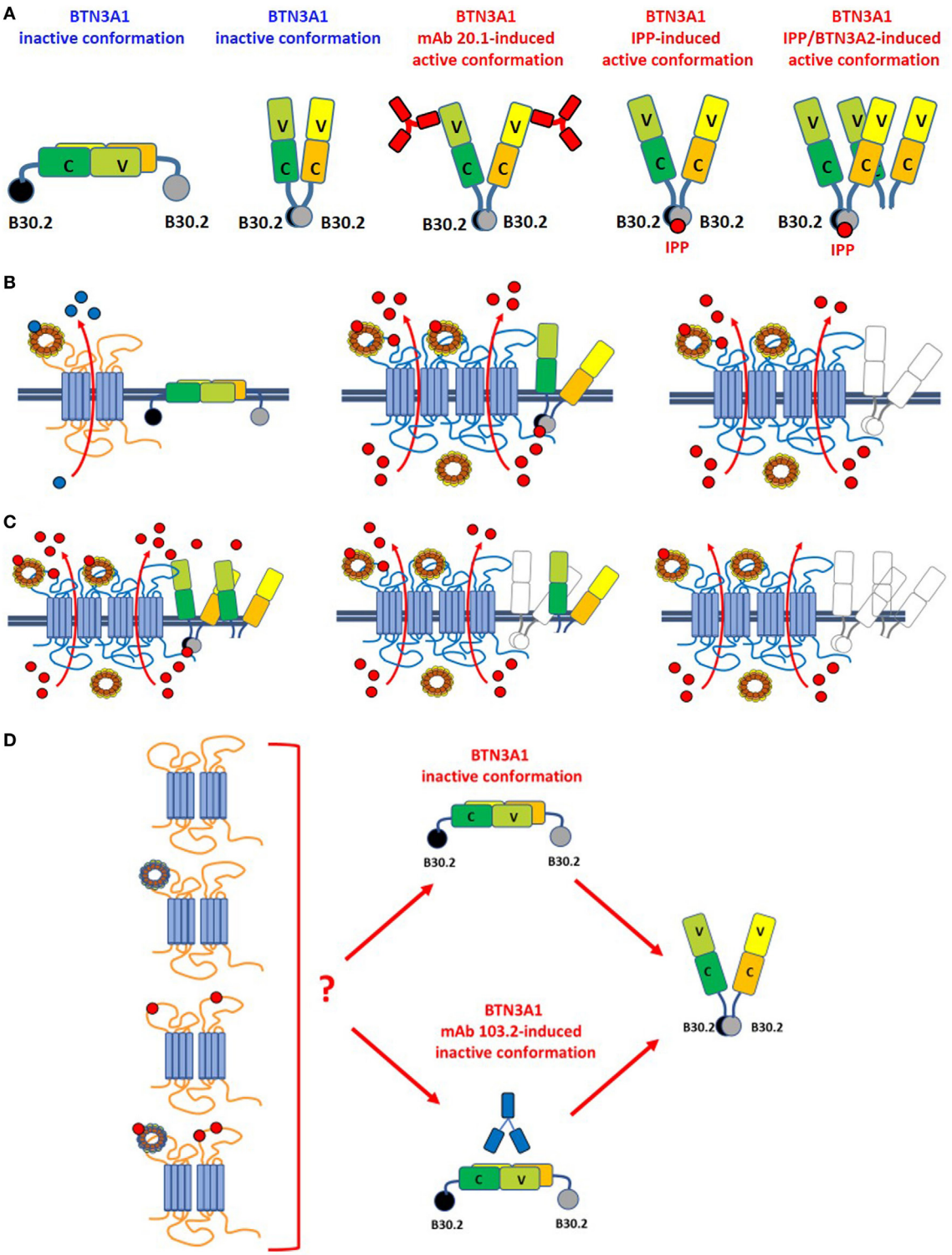

FIGURE 2 | Continued

FIGURE 2 | Leads of the ménage à trois between ABCA1, apoA-I, and BTN3A1. **(A)** BTN3A1 inactive and active dimer conformations are represented from left to the right. Models are derived from crystallographic-based models using recombinant proteins and/or immobilized Vγ9Vδ2 TCRs, and tested using Fluorescence Resonance Energy Transfer-based measurements or proximity-ligation assays. These models are inspiring but still unproved in living cells under physiological or pathological conditions. The inactive conformations include both the head-to-tail conformation (left) and a V-shaped conformation (right) (65). Active conformations are characterized by loss of the head-to-tail conformation or by a rotational shift in the V-shaped dimer induced by the agonistic 20.1 mAb (which binds to extracellular IGHV-like domains), isopentenyl pyrophosphate (IPP) (which binds to the intracellular B30.2 domain), or by BTN3A1/BTN3A2 interactions as recently reported by Vantourout et al. (56). **(B)** Hypothetical configuration of ABCA1/apoA-I/BTN3A1 interactions are represented from left to right. *Left*: in the absence of zoledronic acid (ZA)-induced supra-physiological IPP concentrations, BTN3A1 maintains the inactive dimer conformation (for simplicity only the head-to-tail dimer is shown); ABCA1 in cooperation with apoA-I is mainly committed to extrude cholesterol (blue dots). ABCA1 and BTN3A1 are not physically associated under these conditions. *Middle*: hypothetical configuration of ABCA1/apoA-I/BTN3A1 interactions driven by ZA-induced intracellular IPP accumulation (red dots). ABCA1 and apoA-I expressions are increased, BTN3A1 expression is not increased, but BTN3A1 acquires the active dimer conformation because IPP is bound to the intracellular B30.2 domain; the mutually supportive cooperation between ABCA1, apoA-I, and active BTN3A1 leads to the release of picomolar IPP amounts in the extracellular fluids. Whether extracellular IPP (red dots) binds to extracellular IGHV-like domain of BTN3A1 (as shown) and participate to the activation of Vγ9Vδ2 T cells according to the antigen-presentation presentation model proposed by Vavassori (57) is unknown; *Right*: hypothetical scenario in *Btn3a1*-silenced ZA-treated dendritic cells. Desertion of BTN3A1 from the ménage à trois decreases the efficiency of extracellular IPP release by ABCA1/apoA-I even if they remain upregulated (31). These data indicate that the expression of BTN3A1 is useful but dispensable and that the main role is played by ABCA1/apoA-I; **(C)** hypothetical models of ABCA1/apoA-I/BTN3A1-BTN3A2 interactions are represented from left to right. Active BTN3A1 conformation is induced by interactions between BTN3A1/BTN3A2 and IPP bound to the B30.2 domains of BTN3A1. No data are currently available to support the hypothesis that BTN3A2 is physically bound to ABCA1. *Left*: ABCA1 and apoA-I expressions are increased, and BTN3A1 acquires the active dimer conformation because of BTN3A1/BTN3A2/IPP interactions. It is unknown whether this is the most effective complex to extrude IPP. *Middle*: in the experiments reported in Ref. (31), we have silenced BTN3A1 expression only and we know that this complex is still able to release IPP although with a lower efficiency [see also **(B)**, right panel]. One possible explanation is that BTN3A2 partially substitutes for BTN3A1. *Right*: it is conceivable, although yet unproved, that desertion of both BTN3A1 and BTN3A2 from the complex compromises even more extracellular IPP release. **(D)** It is currently unknown whether unloaded ABCA1 or IPP/apoA-I-loaded ABCA1 can switch BTN3A1 from its inactive conformation to the active dimer conformation in the absence of IPP bound to the intracellular B30.2 domain. For simplicity only the head-to-tail dimer is shown. It is also unknown whether unloaded or IPP/apoA-I-loaded ABCA1 can overcome the inactive BTN3A1 conformation locked by the antagonist 103.2 mAb.

endogenous sources; the latter that exogenous pAgs are internalized from external sources. BTN3A molecules are devoid of the capacity to transport pAgs across the membrane suggesting that interactions with other transporters are needed. The existence of an inside-out transporter was anticipated by De Libero and coworkers to support the antigen presentation model. Interestingly, these Authors have hypothesized the existence of a dedicated IPP transporter supervening only when there is an excessive IPP accumulation within APCs, but not when IPP is provided exogenously (58).

Based on these data, we have hypothesized that ABCA1, apoA-I, and BTN3A1 cooperate in the extracellular IPP release from ZA-treated cells. We believe that, whatever the mechanisms responsible for the conformational switch driven by intracellular IPP and/or agonistic/antagonistic anti-BTN3A1 mAb, it is mainly the active BTN3A1 conformation to participate to the ménage à trois and to facilitate extracellular IPP release in cooperation with ABCA1 and apoA-I. Intracellular IPP accumulation is boosted by ZA stimulation and this is propaedeutic to the acquisition of the active conformation fuctionally confirmed by the excellent ability of ZA-treated DCs to activate Vγ9Vδ2 T cells.

THE COOPERATION BETWEEN ABCA1, apoA-I AND BTN3A1

After screening the expression and activity of a large number of plasma membrane-associated ATPases, ABC transporters involved in lipid efflux and phosphate transporters, we found that ABCA1 only is upregulated by ZA treatment in DCs. Interestingly, this upregulation is accompanied by the simultaneous increase of apoA-I and IPP in the SNs (31). The highly significant correlation between the release of extracellular IPP and the expression of ABCA1 in many different cell types prompted us to further investigated the role of ABCA1/apoA-I in IPP efflux. The 3D structure of human ABCA1 has not yet been solved; the only available data indicate that apoA-I binds the extracellular amino-terminal domain of ABCA1 (52). Of note, we found that, in ZA-treated DCs, IPP binds to the same domain (31) (**Figure 1**). Only further proteo-lipidomic analysis of DC-derived SNs can provide the direct demonstration that IPP is physically associated to apoA-I. This will be a solid step toward the next challenge, i.e., understanding how extracellular IPP is presented to Vγ9Vδ2 T-cells (i.e., in soluble form, bound to Apo-AI, bound to BTN3A1). Our opinion is that ABCA1 extrudes IPP, but it cannot be an effective IPP-presenting molecule in a soluble form because it is a transmembrane protein unreleasable from viable cells. Whether the ABCA1/IPP/apoA-I complex can be released from apoptotic cells to provide activatory signals to Vγ9Vδ2 T cells is unknown. We have not determined the capacity of ZA-treated DCs to activate Vγ9Vδ2 T cells in cell-to-cell contact experiments after *Abca1* and/or *Btn3a1* silencing or knock-out. Additional experiments are needed to determine whether ABCA1 is just a safety valve supervening when potentially dangerous intracellular IPP concentrations are reached in DCs or whether ABCA1 is directly involved in pAg presentation.

As far as BTN3A1 is concerned, it appears to play the "third actor role" in the ABCA1/apoA-I/BTN3A1 ménage à trois (**Figure 2**). Contrarily to apoA-I, cross-linking experiments demonstrate that BTN3A1 does not bind to apoA-I, but co-immunoprecipitation and proximity-ligation assays indicate

that BTN3A1 is physically associated with ABCA1 in DCs. It is really intriguing that, among all the possible partners available, BTN3A1 is physically and functionally associated with ABCA1 which extrudes IPP and whose expression is upregulated by IPP.

Zoledronic acid-treated *Abca1*-silenced DCs have a significant reduction in the ability to release extracellular IPP, whereas ZA-treated *Btn3A1*-silenced DCs are only marginally affected. However, when both genes are silenced in *Btn3a1/Abca1*-double silenced DCs, a statistically significant reduction in extracellular IPP release is observed compared with ZA-treated *Abca1*-silenced DCs (31).

We are aware that siRNA determine a partial and transient downregulation of BTN3A1 that can be different in different cell types. So far, data generated in our lab are sufficient to conclude that BTN3A1 participates to the ménage à trois facilitating extracellular IPP release by ABCA1 and apoA-I in ZA-treated DCs. A comparison between single and double *Abca1* and *Btn3a1* permanent knock-out cells could provide a more definitive conclusion about BTN3A1 involvement in IPP efflux.

Very recently, it has been reported that BTN3A2 also is required for optimal BTN3A1-mediated activation of Vγ9Vδ T cells (56). The interaction between these isoforms regulates the appropriate routing, kinetics, and stability of BTN3A1. Thus, we have envisaged an hypothetical scenario in which both BTN3A1 and BTN3A2 collaborate with ABCA1 and apoA-I to induce extracellular IPP release (**Figure 2**).

It is currently unknown whether the physical interaction between ABCA1 and BTN3A1 is a late event arising after that IPP-induced conformational changes have occurred or whether this is an early event contributing with IPP to the induction of BTN3A1 conformational changes. Since no physical interactions are detected between ABCA1 and BTN3A1 in the absence of ZA stimulation, and silencing *Abca1*, *Btn3a1*, or both genes, has no effect on extracellular IPP release in untreated DCs (31), the IPP/ABCA1/apoA-I/BTN3A1 cross-talk is likely initiated only after that supra-physiological IPP concentrations has been induced by ZA treatment. As of today, we cannot exclude that BTN3A1 interacts with other proteins, including BTN3A2 or other ABC transporters, to promote extracellular IPP release. Highly conserved and ubiquitous proteins like BTN3A1 are often part of multiprotein complexes where they may exert functions of adaptors, scaffold proteins or allosteric modulators of their interactors. Investigation of this putative BTN3A1 role is still in its infancy, but it could unravel very interesting and unexpected discoveries. Only an in-depth interactome study of BTN3A1 may identify other interactors involved in IPP efflux. Crystallography studies of BTN3A1-interactors complexes will provide additional information on the putative domains involved in IPP binding and subsequent IPP delivery to the interactors. Functional assays investigating IPP efflux, after selectively silencing the putative interactors, will shed light on the hierarchical function of each molecule in the process.

INTRACELLULAR SIGNALING INVOLVED IN ABCA1/apoA-I UPREGULATION

Intracellular IPP binding to the B30.2 domain to induce BTN3A1 conformational changes and the concurrent upregulation of apoA-I and ABCA1 appear as a nicely coordinated process. 500 pM IPP, which is in the range of intracellular concentrations detected in ZA-treated DCs, is sufficient to activate the liver X receptor α (LXRα) and promote LXRα-induced transcription of *Abca1* and *apoA-I* (31). Putative ligands of LXRα in macrophages include several isoprenoid compounds, such as retinoic acid (70), astaxanthin (71), allyl-cysteine (72), or zerumbone (73). In DCs, however, the effect of IPP is highly specific and neither exogenously added FPP or GGPP induce LXRα activation (31). The different chain length and tridimensional conformation may account for the different ability to induce LXRα activation. Moreover, ZA decreases intracellular FPP and GGPP concentrations to sub-picomolar values (74–76) which are insufficient to induce LXRα activation (31).

These data also point out how different can be the transcriptional regulation of Abca1/apoA-I and lipid metabolism in immune cells. In DCs, *Abca1* expression is mainly regulated by LXRα and IPP-induced ABCA1 upregulation is finalized to extrude IPP in cooperation with apoA-I and BTN3A1; moreover, DCs express very low levels of LXRβ (77) which remains unmodulated by ZA (31). By contrast, *Abca1* expression in T cells is governed mainly by LXRβ and ABCA1 upregulation induces cholesterol depletion and impairs T-cell functions (78). It is currently unknown whether a similar ménage à trois occurs in T cells as a consequence of LXRβ-induced ABCA1 activation.

A second IPP-independent mechanism by which ZA upregulates ABCA1/apoA-I complex in DCs is the intracellular shortage of FPP generated by FPPS inhibition, decreased Ras prenylation (74) and decreased activity of the Ras-dependent PI3K/Akt/mTOR pathway (79) which constitutively inhibits LXRα activation (31, 80). PI3K/Akt-activity also reduces the amount of surface ABCA1, likely interfering with recycling mechanisms (81). ERK1/2, other Ras-downstream effectors (73), negatively regulate ABCA1 expression in macrophages (82). Although not yet explored in DCs, also this Ras-dependent pathway may be involved in ABCA1 expression and ABCA1-dependent IPP efflux.

CONCLUSION

In conclusion, the ménage à trois between apoA-I, ABCA1, and BTN3A1 in ZA-treated DCs is finalized to extrude very efficiently intracellular IPP after that supra-physiological concentrations have been reached as a consequence of a deranged Mev pathway. The relationships between these partners are hierarchically not equivalent because ABCA1 and apoA-I are physically associated (as expected), ApoA-I and BTN3A1 are physically associated, whereas BTN3A1 and apoA-I are not physically associated. IPP binds to ABCA1, BTN3A1, and apoA-I, further promoting interactions between these molecules. We speculate that the aim of this mènage à trois is twofold: the first is to extend the range of immune regulation also to Vγ9Vδ2 T cells which are not in close proximity to pAg-presenting cells. Under this perspective,

IPP efflux can be included in the number of the damage-associated molecular patterns, as microbial pAgs can be considered part of pathogen-associated molecular patterns, i.e., highly conserved pathways that trigger and sustain immune activity in response to danger signals (83). The second is to protect pAg-presenting cells from apoptosis due to intracellular ApppI accumulation. It is reasonable that immune cells have developed pleiotropic mechanisms to protect themselves from IPP accumulation. A redundancy of mechanisms controlling the IPP efflux may ensure that the immune activation of Vγ9Vδ2 T cells operated by pAg-presenting cells is not prematurely terminated.

AUTHOR CONTRIBUTIONS

All authors have made substantial contributions to text and figures and have approved the manuscript for submission.

FUNDING

This study was supported by the Italian Association for Cancer Research (AIRC) (IG15232 to CR and IG 16985 to MM). BC is a post-doc research fellow supported by American Association for Cancer Research (AACR).

REFERENCES

1. Constant P, Davodeau F, Peyrat MA, Poquet Y, Puzo G, Bonneville M, et al. Stimulation of human gamma delta T cells by nonpeptidic mycobacterial ligands. *Science* (1994) 264:267–70. doi:10.1126/science.8146660
2. Tanaka Y, Morita CT, Tanaka Y, Nieves E, Brenner MB, Bloom BR. Natural and synthetic non-peptide antigens recognized by human gamma delta T cells. *Nature* (1995) 375:155–8. doi:10.1038/375155a0
3. Gruenbacher G, Thurnher M. Mevalonate metabolism in cancer. *Cancer Lett* (2015) 356:192–6. doi:10.1016/j.canlet.2014.01.013
4. Silva-Santos B, Serre K, Norell H. γδ T cells in cancer. *Nat Rev Immunol* (2015) 15(11):683–91. doi:10.1038/nri3904
5. Eberl M, Hintz M, Reichenberg A, Kollas AK, Wiesner J, Jomaa H. Microbial isoprenoid biosynthesis and human gammadelta T cell activation. *FEBS Lett* (2003) 544:4–10. doi:10.1016/S0014-5793(03)00483-6
6. Amslinger S, Hecht S, Rohdich F, Eisenreich W, Adam P, Bacher A, et al. Stimulation of Vgamma9/Vdelta2 T-lymphocyte proliferation by the isoprenoid precursor, (E)-1-hydroxy-2-methyl-but-2-enyl 4-diphosphate. *Immunobiology* (2007) 212:47–55. doi:10.1016/j.imbio.2006.08.003
7. Riganti C, Massaia M, Davey MS, Eberl M. Human γδ T-cell responses in infection and immunotherapy: common mechanisms, common mediators? *Eur J Immunol* (2012) 42(7):1668–76. doi:10.1002/eji.201242492
8. Espinosa E, Belmant C, Pont F, Luciani B, Poupot R, Romagné F, et al. Chemical synthesis and biological activity of bromohydrin pyrophosphate, a potent stimulator of human gamma delta T cells. *J Biol Chem* (2001) 276:18337–44. doi:10.1074/jbc.M100495200
9. Moulin M, Alguacil J, Gu S, Mehtougui A, Adams EJ, Peyrottes S, et al. Vγ9Vδ2 T cell activation by strongly agonistic nucleotidic phosphoantigens. *Cell Mol Life Sci* (2017) 74(23):4353–67. doi:10.1007/s00018-017-2583-0
10. Bennouna J, Levy V, Sicard H, Senellart H, Audrain M, Hiret S, et al. Phase I study of bromohydrin pyrophosphate (BrHPP, IPH 1101), a Vgamma9Vdelta2 T lymphocyte agonist in patients with solid tumors. *Cancer Immunol Immunother* (2010) 59(10):1521–30. doi:10.1007/s00262-010-0879-0
11. Burjanadzé M, Condomines M, Reme T, Quittet P, Latry P, Lugagne C, et al. In vitro expansion of gamma delta T cells with anti-myeloma cell activity by Phosphostim and IL-2 in patients with multiple myeloma. *Br J Haematol* (2007) 39(2):206–16. doi:10.1111/j.1365-2141.2007.06754.x
12. Gertner-Dardenne J, Bonnafous C, Bezombes C, Capietto AH, Scaglione V, Ingoure S, et al. Bromohydrin pyrophosphate enhances antibody-dependent cell-mediated cytotoxicity induced by therapeutic antibodies. *Blood* (2009) 113(20):4875–84. doi:10.1182/blood-2008-08-172296
13. Vermijlen D, Gatti D, Kouzeli A, Rus T, Eberl M. γδ T cell responses: how many ligands will it take till we know? *Semin Cell Dev Biol* (2018). doi:10.1016/j.semcdb.2017.10.009
14. Davey MS, Malde R, Mykura RC, Baker AT, Taher TE, Le Duff CS, et al. Synthesis and biological evaluation of (E)-4-hydroxy-3-methylbut-2-enyl phosphate (HMBP) aryloxy triester phosphoramidate prodrugs as activators of Vγ9/Vδ2 T-cell immune responses. *J Med Chem* (2018) 61(5):2111–7. doi:10.1021/acs.jmedchem.7b01824
15. Foust BJ, Poe MM, Lentini NA, Hsiao CC, Wiemer AJ, Wiemer DF. Mixed aryl phosphonate prodrugs of a butyrophilin ligand. *ACS Med Chem Lett* (2017) 8(9):914–8. doi:10.1021/acsmedchemlett.7b00245
16. Kunzmann V, Bauer E, Feurle J, Weissinger F, Tony HP, Wilhelm M. Stimulation of gammadelta T cells by aminobisphosphonates and induction of antiplasma cell activity in multiple myeloma. *Blood* (2000) 96:384–92.
17. Bukowski JF, Morita CT, Brenner MB. Human gamma delta T cells recognize alkylamines derived from microbes, edible plants, and tea: implications for innate immunity. *Immunity* (1999) 11:57–65. doi:10.1016/S1074-7613(00)80081-3
18. Thompson K, Rojas-Navea J, Rogers MJ. Alkylamines cause Vgamma9Vdelta2 T-cell activation and proliferation by inhibiting the mevalonate pathway. *Blood* (2006) 107:651–4. doi:10.1182/blood-2005-03-1025
19. Gober HJ, Kistowska M, Angman L, Jeno P, Mori L, De Libero G. Human T cell receptor gammadelta cells recognize endogenous mevalonate metabolites in tumor cells. *J Exp Med* (2003) 197:163–8. doi:10.1084/jem.20021500
20. Thompson K, Rogers MJ. Statins prevent bisphosphonate-induced gamma, delta-T-cell proliferation and activation in vitro. *J Bone Miner Res* (2004) 19:278–88. doi:10.1359/JBMR.0301230
21. Tanaka Y, Murata-Hirai K, Iwasaki M, Matsumoto K, Hayashi K, Kumagai A, et al. Expansion of human γδ T cells for adoptive immunotherapy using a bisphosphonate prodrug. *Cancer Sci* (2018) 109(3):587–99. doi:10.1111/cas.13491
22. Mönkkönen H, Kuokkanen J, Holen I, Evans A, Lefley DV, Jauhiainen M, et al. Bisphosphonate-induced ATP analog formation and its effect on inhibition of cancer cell growth. *Anticancer Drugs* (2008) 19(4):391–9. doi:10.1097/CAD.0b013e3282f632bf
23. Alegre A, Gironella M, Bailén A, Giraldo P. Zoledronic acid in the management of bone disease as a consequence of multiple myeloma: a review. *Eur J Haematol* (2014) 92(3):181–8. doi:10.1111/ejh.12239
24. Das M. Long interval zoledronic acid use in bone metastases. *Lancet Oncol* (2017) 18(2):e72. doi:10.1016/S1470-2045(17)30019-0
25. Karim SM, Brown J, Zekri J. Efficacy of bisphosphonates and other bone-targeted agents in metastatic bone disease from solid tumors other than breast and prostate cancers. *Clin Adv Hematol Oncol* (2013) 11(5):281–7.
26. Monkkonen H, Auriola S, Lehenkari P, Kellinsalmi M, Hassinen IE, Vepsalainen J, et al. A new endogenous ATP analog (ApppI) inhibits the mitochondrial adenine nucleotide translocase (ANT) and is responsible for the apoptosis induced by nitrogen-containing bisphosphonates. *Br J Pharmacol* (2006) 147:437–45. doi:10.1038/sj.bjp.0706628
27. Li J, Herold MJ, Kimmel B, Muller I, Rincon-Orozco B, Kunzmann V, et al. Reduced expression of the mevalonate pathway enzyme farnesyl pyrophosphate synthase unveils recognition of tumor cells by Vgamma9Vdelta2 T cells. *J Immunol* (2009) 182:8118–24. doi:10.4049/jimmunol.0900101
28. Wang H, Sarikonda G, Puan KJ, Tanaka Y, Feng J, Giner JL, et al. Indirect stimulation of human Vgamma2Vdelta2 T cells through alterations in isoprenoid metabolism. *J Immunol* (2011) 187:5099–113. doi:10.4049/jimmunol.1002697
29. Fiore F, Castella B, Nuschak B, Bertieri R, Mariani S, Bruno B, et al. Enhanced ability of dendritic cells to stimulate innate and adaptive immunity on short-term incubation with zoledronic acid. *Blood* (2007) 110(3):921–7. doi:10.1182/blood-2006-09-044321
30. Castella B, Riganti C, Fiore F, Pantaleoni F, Canepari ME, Peola S, et al. Immune modulation by zoledronic acid in human myeloma: an advantageous cross-talk between Vγ9Vδ2 T cells, αβ CD8+ T cells, regulatory T cells, and dendritic cells. *J Immunol* (2011) 187:1578–90. doi:10.4049/jimmunol.1002514

31. Castella B, Kopecka J, Sciancalepore P, Mandili G, Foglietta M, Mitro N, et al. The ATP-binding cassette transporter A1 regulates phosphoantigen release and Vγ9Vδ2 T cell activation by dendritic cells. *Nat Commun* (2017) 8:15663. doi:10.1038/ncomms15663
32. Scotet E, Martinez LO, Grant E, Barbaras R, Jenö P, Guiraud M, et al. Tumor recognition following Vgamma9Vdelta2 T cell receptor interactions with a surface F1-ATPase-related structure and apolipoprotein A-I. *Immunity* (2005) 22(1):71–80. doi:10.1016/j.immuni.2004.11.012
33. Mookerjee-Basu J, Vantourout P, Martinez LO, Perret B, Collet X, Périgaud C, et al. F1-adenosine triphosphatase displays properties characteristic of an antigen presentation molecule for Vgamma9Vdelta2 T cells. *J Immunol* (2010) 184:6920–8. doi:10.4049/jimmunol.0904024
34. Gruenbacher G, Gander H, Rahm A, Idzko M, Nussbaumer O, Thurnher M. Ecto-ATPase CD39 inactivates isoprenoid-derived Vγ9Vδ2 T cell phosphoantigens. *Cell Rep* (2016) 16:444–56. doi:10.1016/j.celrep.2016.06.009
35. Mariani S, Muraro M, Pantaleoni F, Fiore F, Nuschak B, Peola S, et al. Effector gammadelta T cells and tumor cells as immune targets of zoledronic acid in multiple myeloma. *Leukemia* (2005) 19(4):664–70. doi:10.1038/sj.leu.2403693
36. Mitrofan LM, Pelkonen J, Mönkkönen J. The level of ATP analog and isopentenyl pyrophosphate correlates with zoledronic acid-induced apoptosis in cancer cells in vitro. *Bone* (2009) 45(6):1153–60. doi:10.1016/j.bone.2009.08.010
37. Räikkönen J, Crockett JC, Rogers MJ, Mönkkönen H, Auriola S, Mönkkönen J. Zoledronic acid induces formation of a pro-apoptotic ATP analogue and isopentenyl pyrophosphate in osteoclasts in vivo and in MCF-7 cells in vitro. *Br J Pharmacol* (2009) 157(3):427–35. doi:10.1111/j.1476-5381.2009.00160.x
38. Nerdal PT, Peters C, Oberg HH, Zlatev H, Lettau M, Quabius ES, et al. Butyrophilin 3A/CD277-dependent activation of human γδ T cells: accessory cell capacity of distinct leukocyte populations. *J Immunol* (2016) 197:3059–68. doi:10.4049/jimmunol.1600913
39. Martinez LO, Jacquet S, Esteve JP, Rolland C, Cabezón E, Champagne E, et al. Ectopic beta-chain of ATP synthase is an apolipoprotein A-I receptor in hepatic HDL endocytosis. *Nature* (2003) 421:75–9. doi:10.1038/nature01250
40. Champagne E, Martinez LO, Vantourout P, Collet X, Barbaras R. Role of apolipoproteins in gammadelta and NKT cell-mediated innate immunity. *Immunol Res* (2005) 33:241–55. doi:10.1385/IR:33:3:241
41. Hafiane A, Genest J. HDL, atherosclerosis, and emerging therapies. *Cholesterol* (2013) 2013:891403. doi:10.1155/2013/891403
42. Shichiri M, Takanezawa Y, Rotzoll DE, Yoshida Y, Kokubu T, Ueda K, et al. ATP-binding cassette transporter A1 is involved in hepatic alpha-tocopherol secretion. *J Nutr Biochem* (2010) 21:451–6. doi:10.1016/j.jnutbio.2009.02.002
43. Shiota Y, Kiyota K, Kobayashi T, Kano S, Kawamura M, Matsushima T, et al. Distribution of dolichol in the serum and relationships between serum dolichol levels and various laboratory test values. *Biol Pharm Bull* (2008) 31:340–7. doi:10.1248/bpb.31.340
44. Summers JA, Harper AR, Feasley CL, Van-Der-Wel H, Byrum JN, Hermann M, et al. Identification of apolipoprotein A-I as a retinoic acid-binding protein in the eye. *J Biol Chem* (2016) 291:18991–9005. doi:10.1074/jbc.M116.725523
45. Nussbaumer O, Gruenbacher G, Gander H, Komuczki J, Rahm A, Thurnher M. Essential requirements of zoledronate-induced cytokine and γδ T cell proliferative responses. *J Immunol* (2013) 191:1346–55. doi:10.4049/jimmunol.1300603
46. Gruenbacher G, Nussbaumer O, Gander H, Steiner B, Leonhartsberger N, Thurnher M. Stress-related and homeostatic cytokines regulate Vγ9Vδ2 T-cell surveillance of mevalonate metabolism. *Oncoimmunology* (2014) 3:e953410. doi:10.4161/21624011.2014.953410
47. Gruenbacher G, Thurnher M. Mevalonate metabolism governs cancer immune surveillance. *Oncoimmunology* (2017) 6:1342917. doi:10.1080/2162402X.2017.1342917
48. Gruenbacher G, Thurnher M. Mevalonate metabolism in immuno-oncology. *Front Immunol* (2017) 8:1714. doi:10.3389/fimmu.2017.01714
49. Davey MS, Lin CY, Roberts GW, Heuston S, Brown AC, Chess JA, et al. Human neutrophil clearance of bacterial pathogens triggers anti-microbial γδ T cell responses in early infection. *PLoS Pathog* (2011) 7(5):e1002040. doi:10.1371/journal.ppat.1002040
50. Cukier AMO, Therond P, Didichenko SA, Guillas I, Chapman MJ, Wright SD, et al. Structure-function relationships in reconstituted HDL: focus on antioxidative activity and cholesterol efflux capacity. *Biochim Biophys Acta* (2017) 1862:890–900. doi:10.1016/j.bbalip.2017.05.010
51. Takahashi K, Kimura Y, Kioka N, Matsuo M, Ueda K. Purification and ATPase activity of human ABCA1. *J Biol Chem* (2006) 281:10760–8. doi:10.1074/jbc.M513783200
52. Nagao K, Zhao Y, Takahashi K, Kimura Y, Ueda K. Sodium taurocholate-dependent lipid efflux by ABCA1: effects of W590S mutation on lipid translocation and apolipoprotein A-I dissociation. *J Lipid Res* (2009) 50:1165–72. doi:10.1194/jlr.M800597-JLR200
53. Harly C, Guillaume Y, Nedellec S, Peigne CM, Monkkonen H, Monkkonen J, et al. Key implication of CD277/butyrophilin-3 (BTN3A) incellular stress sensing by a major human gammadelta T-cell subset. *Blood* (2012) 120:2269–79. doi:10.1182/blood-2012-05-430470
54. Rhodes DA, Stammers M, Malcherek G, Beck S, Trowsdale J. The cluster of BTN gene sin the extended major histocompatibility complex. *Genomics* (2001) 71:351–62. doi:10.1006/geno.2000.6406
55. Palakodeti A, Sandstrom A, Sundaresan L, Harly C, Nedellec S, Olive D, et al. The molecular basis for modulation of human Vgamma9Vdelta2 T cell responses by CD277/butyrophilin-3 (BTN3A)-specific antibodies. *J Biol Chem* (2012) 287:32780–90. doi:10.1074/jbc.M112.384354
56. Vantourout P, Laing A, Woodward MJ, Zlatareva I, Apolonia L, Jones AW, et al. Heteromeric interactions regulate butyrophilin (BTN) and BTN-like molecules governing γδ T cell biology. *Proc Natl Acad Sci U S A* (2018) 115(5):1039–44. doi:10.1073/pnas.1701237115
57. Vavassori S, Kumar A, Wan GS, Ramanjaneyulu GS, Cavallari M, ElDaker S, et al. Butyrophilin 3A1 binds phosphorylated antigens and stimulates human gammadelta T cells. *Nat Immunol* (2013) 14(9):908–16. doi:10.1038/ni.2665
58. De Libero G, Lau SY, Mori L. Phosphoantigen presentation to TCR γδ cells, a conundrum getting less gray zones. *Front Immunol* (2015) 15(5):679. doi:10.3389/fimmu.2014.00679
59. Hsiao CH, Lin X, Barney RJ, Shippy RR, Li J, Vinogradova O, et al. Synthesis of a phosphoantigen prodrug that potently activates Vgamma9Vdelta2 T-lymphocytes. *Chem Biol* (2014) 21:945–54. doi:10.1016/j.chembiol.2014.06.006
60. Sandstrom A, Peigne CM, Leger A, Crooks JE, Konczak F, Gesnel MC, et al. The intracellular B30.2 domain of butyrophilin 3A1 binds hosphoantigens to mediate activation of human Vgamma9Vdelta2 T cells. *Immunity* (2014) 40:490–500. doi:10.1016/j.immuni.2014.03.003
61. Rhodes DA, Chen HC, Price AJ, Keeble AH, Davey MS, James LC, et al. Activation of human gammadelta T cells by cytosolic interactions of BTN3A1 with soluble phosphoantigens and the cytoskeletal adaptor periplakin. *J Immunol* (2015) 194:2390–8. doi:10.4049/jimmunol.1401064
62. Wang H, Morita CT. Sensor function for butyrophilin 3A1 in prenyl pyrophosphate stimulation of human Vgamma2Vdelta2 T cells. *J Immunol* (2015) 195:4583–94. doi:10.4049/jimmunol.1500314
63. Harly C, Peigné CM, Scotet E. Molecules and mechanisms implicated in the peculiar antigenic activation process of human Vγ9Vδ2 T cells. *Front Immunol* (2015) 5:657. doi:10.3389/fimmu.2014.00657
64. Salim M, Knowles TJ, Baker AT, Davey MS, Jeeves M, Sridhar P, et al. BTN3A1 discriminates γδ T cell phosphoantigens from nonantigenic small molecules via a conformational sensor in its B30.2 domain. *ACS Chem Biol* (2017) 12(10):2631–43. doi:10.1021/acschembio.7b00694
65. Gu S, Nawrocka W, Adams EJ. Sensing of pyrophosphate metabolites by Vgamma9Vdelta2 T cells. *Front Immunol* (2014) 5:688. doi:10.3389/fimmu.2014.00688
66. Peigné CM, Léger A, Gesnel MC, Konczak F, Olive D, Bonneville M, et al. The juxtamembrane domain of butyrophilin BTN3A1 controls phosphoantigen-mediated activation of human Vγ9Vδ2 T cells. *J Immunol* (2017) 198(11):4228–34. doi:10.4049/jimmunol.1601910
67. Nguyen K, Li J, Puthenveetil R, Lin X, Poe MM, Hsiao CC, et al. The butyrophilin 3A1 intracellular domain undergoes a conformational change involving the juxtamembrane region. *FASEB J* (2017) 31(11):4697–706. doi:10.1096/fj.201601370RR
68. Sebestyen Z, Scheper W, Vyborova A, Gu S, Rychnavska Z, Schiffler M, et al. RhoB mediates phosphoantigen recognition by Vc9Vd2 T cell receptor. *Cell Rep* (2016) 15:1973–85. doi:10.1016/j.celrep.2016.04.081
69. Starick L, Riano F, Karunakaran MM, Kunzmann V, Li J, Kreiss M, et al. Butyrophilin 3A (BTN3A, CD277)-specific antibody 20.1 differentially

activates Vγ9Vδ2 TCR clonotypes and interferes with phosphoantigen activation. *Eur J Immunol* (2017) 47(6):982–92. doi:10.1002/eji.201646818
70. Manna PR, Sennoune SR, Martinez-Zaguilan R, Slominski AT, Pruitt K. Regulation of retinoid mediated cholesterol efflux involves liver X receptor activation in mouse macrophages. *Biochem Biophys Res Commun* (2015) 464:312–37. doi:10.1016/j.bbrc.2015.06.150
71. Iizuka M, Ayaori M, Uto-Kondo H, Yakushiji E, Takiguchi S, Nakaya K, et al. Astaxanthin enhances ATP-binding cassette transporter A1/G1 expressions and cholesterol efflux from macrophages. *J Nutr Sci Vitaminol (Tokyo)* (2012) 58:96–104. doi:10.3177/jnsv.58.96
72. Malekpour-Dehkordi Z, Javadi E, Doosti M, Paknejad M, Nourbakhsh M, Yassa N, et al. S-allylcysteine, a garlic compound, increases ABCA1 expression in human THP-1 macrophages. *Phytother Res* (2013) 27:357–61. doi:10.1002/ptr.4713
73. Zhu S, Liu JH. Zerumbone, A natural cyclic sesquiterpene, promotes ABCA1-dependent cholesterol efflux from human THP-1 macrophages. *Pharmacology* (2015) 95:258–63. doi:10.1159/000381722
74. Riganti C, Castella B, Kopecka J, Campia I, Coscia M, Pescarmona G, et al. Zoledronic acid restores doxorubicin chemosensitivity and immunogenic cell death in multidrug-resistant human cancer cells. *PLoS One* (2013) 8:60975. doi:10.1371/journal.pone.0060975
75. Rigoni M, Riganti C, Vitale C, Griggio V, Campia I, Robino M, et al. Simvastatin and downstream inhibitors circumvent constitutive and stromal cell-induced resistance to doxorubicin in IGHV unmutated CLL cells. *Oncotarget* (2015) 6:29833–46. doi:10.18632/oncotarget.4006
76. Kopecka J, Porto S, Lusa S, Gazzano E, Salzano G, Giordano A, et al. Self-assembling nanoparticles encapsulating zoledronic acid revert multidrug resistance in cancer cells. *Oncotarget* (2015) 6:31461–78. doi:10.18632/oncotarget.5058
77. Geyeregger R, Zeyda M, Bauer W, Kriehuber E, Säemann MD, Zlabinger GJ, et al. Liver X receptors regulate dendritic cell phenotype and function through blocked induction of the actin-bundling protein fascin. *Blood* (2007) 109:4288–95. doi:10.1182/blood-2006-08-043422
78. Thurnher M, Gruenbacher G. T lymphocyte regulation by mevalonate metabolism. *Sci Signal* (2015) 8:4. doi:10.1126/scisignal.2005970
79. Moriceau G, Ory B, Mitrofan L, Riganti C, Blanchard F, Brion R, et al. Zoledronic acid potentiates mTOR inhibition and abolishes the resistance of osteosarcoma cells to RAD001 (everolimus): pivotal role of the prenylation process. *Cancer Res* (2010) 70:10329–39. doi:10.1158/0008-5472.CAN-10-0578
80. Dong F, Mo Z, Eid W, Courtney KC, Zha X. Akt inhibition promotes ABCA1-mediated cholesterol efflux to ApoA-I through suppressing mTORC1. *PLoS One* (2014) 9:113789. doi:10.1371/journal.pone.0113789
81. Huang CX, Zhang YL, Wang JF, Jiang JY, Bao JL. MCP-1 impacts RCT by repressing ABCA1, ABCG1, and SR-BI through PI3K/Akt posttranslational regulation in HepG2 cells. *J Lipid Res* (2013) 54:1231–40. doi:10.1194/jlr.M032482
82. Mulay V, Wood P, Manetsch M, Darabi M, Cairns R, Hoque M, et al. Inhibition of mitogen-activated protein kinase Erk1/2 promotes protein degradation of ATP binding cassette transporters A1 and G1 in CHO and HuH7 cells. *PLoS One* (2013) 8:62667. doi:10.1371/journal.pone.0062667
83. Garg AD, Galluzzi L, Apetoh L, Baert T, Birge RB, Bravo-San Pedro JM, et al. Molecular and translational classifications of DAMPs in immunogenic cell death. *Front Immunol* (2015) 6:588. doi:10.3389/fimmu.2015.00588

Conflict of Interest Statement: The authors declare that the research was conducted in the absence of any commercial or financial relationships that could be construed as a potential conflict of interest.

Copyright © 2018 Riganti, Castella and Massaia. This is an open-access article distributed under the terms of the Creative Commons Attribution License (CC BY). The use, distribution or reproduction in other forums is permitted, provided the original author(s) and the copyright owner are credited and that the original publication in this journal is cited, in accordance with accepted academic practice. No use, distribution or reproduction is permitted which does not comply with these terms.

frontiers in Immunology

REVIEW
published: 08 May 2018
doi: 10.3389/fimmu.2018.00981

Thymic Program Directing the Functional Development of γδT17 Cells

*Youenn Jouan[1,2,3], Emmanuel C. Patin[4], Maya Hassane[5], Mustapha Si-Tahar[1,2], Thomas Baranek[1,2] and Christophe Paget[1,2]**

[1] INSERM, Centre d'Etude des Pathologies Respiratoires (CEPR), UMR 1100, Tours, France, [2] Université de Tours, Tours, France, [3] Service de Médecine Intensive Réanimation, Centre Hospitalier Régional Universitaire de Tours, Tours, France, [4] Division of Radiotherapy and Imaging, Targeted Therapy Team, The Institute of Cancer Research, London, United Kingdom, [5] Department of Biochemistry and Molecular Genetics, Faculty of Medicine, American University of Beirut, Beirut, Lebanon

OPEN ACCESS

Edited by:
Pierre Vantourout,
King's College London,
United Kingdom

Reviewed by:
Melanie Wencker,
UMR5308 Centre International de Recherche en Infectiologie (CIRI), France
Marie-Laure Michel,
INRA Centre Jouy-en-Josas, France
Julie Ribot,
Instituto de Medicina Molecular (IMM), Portugal

***Correspondence:**
Christophe Paget
christophe.paget@inserm.fr

Specialty section:
This article was submitted to T Cell Biology, a section of the journal Frontiers in Immunology

Received: 22 February 2018
Accepted: 20 April 2018
Published: 08 May 2018

Citation:
Jouan Y, Patin EC, Hassane M, Si-Tahar M, Baranek T and Paget C (2018) Thymic Program Directing the Functional Development of γδT17 Cells. Front. Immunol. 9:981. doi: 10.3389/fimmu.2018.00981

γδT cells comprise a unique T cell sublineage endowed with a wide functional repertoire, which allow them to play important—sometimes opposite—roles in many immune responses associated with infection, cancer, and inflammatory processes. This is largely dependent on the existence of pre-programmed discrete functional subsets that differentiate within the thymus at specific temporal windows of life. Since they represent a major early source of interleukin-17A in many models of immune responses, the γδT17 cell population has recently gained considerable interest. Thus, a better dissection of the developmental program of this effector γδT subset appears critical in understanding their associated immune functions. Several recent reports have provided new exciting insights into the developmental mechanisms that control γδT cell lineage commitment and differentiation. Here, we review the importance of thymic cues and intrinsic factors that shape the developmental program of γδT17 cells. We also discuss the potential future areas of research in γδT17 cell development especially in regards to the recently provided data from deep RNA sequencing technology. Pursuing our understanding into this complex mechanism will undoubtedly provide important clues into the biology of this particular T cell sublineage.

Keywords: γδT cells, innate immunity, interleukin-17A, thymus, transcription factor, development

Interleukin-17 (IL-17) is a highly conserved cytokine in vertebrates that plays a critical role in host homeostasis and immune response to pathogens especially at barrier sites (1, 2). Recent evidence indicates that IL-17 also emerges as a key contributor in immunity beyond the scope of infection, such as inflammation and cancer (3, 4). Given the pivotal role of lymphoid cell-derived IL-17 in orchestrating immune responses, its cellular sources have been extensively searched over the last decade. Initially believed to be mainly produced by conventional $CD4^+$ T (Th17) cells (5, 6), the discovery of innate and innate-like lymphocytes endowed with potent capacities to produce IL-17 (7) suggests that this cytokine is well poised at the border between innate and adaptive immunity. These populations include γδT cells (8), natural killer T (NKT) cells (9), mucosal-associated invariant T (MAIT) cells (10), and group 3 innate lymphoid cells (ILC3) (11). Among those, γδT cells have been

Abbreviations: Ag, antigen; APC, Ag presenting cells; Blk, B lymphocyte kinase; DETC, dendritic epidermal γδT cell; IL, interleukin; IFN, interferon; ILC, innate lymphoid cells; Lef1, lymphoid enhancer-binding factor; MAIT, mucosal-associated invariant T; NKT, Natural Killer T; TCR, T cell receptor; TEC, thymic epithelial cells; TF, transcription factor.

demonstrated to be the main contributors in IL-17 production in many settings, such as infection, autoimmunity, and cancer. Here, we discuss the recent advances on our understanding of IL-17-producing γδT (γδT17) cell biology with a particular emphasis on the transcriptional road maps that drives their innately "pre-programmed" effector fate.

CHARACTERISTICS OF γδT17 CELLS

Mouse γδT cells consist of a heterogeneous population of thymus-derived T lymphocytes characterized by distinct functional properties (e.g., cytokine profile and/or cytotoxic properties) and tissue distribution (12). Within this subset diversity, γδT17 cells can be defined based on their T cell receptor (TCR) repertoire usage and surface markers. Thus, γδT17 cells are almost exclusively restricted to γδT cells expressing either a Vγ6 or a Vγ4 TCR (N.B.: The Heilig and Tonegawa's nomenclature (13) has been used in this review) (**Table 1**). In addition, many cell surface antigens (Ags) have been shown to distinguish γδT17 cells and can be defined as $CD27^{-}$, $NK1.1^{-}$, $IL\text{-}7R\alpha^{high}$, $IL\text{-}18R^{high}$, $CD122^{-}$, and $CCR6^{+}$ cells (14–16). γδT17 cells mainly establish residency at barrier sites including lung, skin, vagina, and oral cavity. However, they can recirculate in particular pathological situations including infections and cancer (17). The migratory capacity of γδT17 cells is regulated by the chemokine receptors CCR2 (during inflammation) and CCR6 (at homeostasis) (18). This preferential location at barrier sites might indicate a preferential interplay between γδT17 cells and the endogenous flora (19) as exemplified by the strong reduction in frequency of lung resident γδT17 cells in germ-free mice (20). Interestingly, while $V\gamma4^{+}$ γδT17 cells can be detected in the gastrointestinal tract (21), we and others failed to detect $V\gamma6^{+}$ γδT17 cells in this tissue in adult mice under steady-state condition (20, 22). This might suggest that the nature and/or diversity of commensals in the various mucosa could differentially influence the maintenance of γδT17 cell subsets.

γδT17 cells are characterized by their ability to promptly produce copious amounts of IL-17A/F, IL-22, IL-21, and GM-CSF (8, 23–25). This rapid capacity to produce these cytokines can be mainly attributed to their innate-like feature. Despite expressing a fully functional rearranged TCR, γδT17 cells can respond to activating cytokines (IL-1β, IL-23, and IL-18) even in absence of concomitant TCR engagement (8, 16). However, TCR ligation on naive γδT17 cells has been shown to license them by increasing activating cytokine receptor expression (e.g., IL-1R1 and IL-23R) and thus rendering them permissive to "innate" stimulation (26). The nature of these Ags is yet to be determined. Notably, the unprocessed form of the red algae protein phycoerythrin has been shown to interact with a small proportion of naive γδT cell TCRs irrespectively of their TCR repertoire (26). Even if the physiological relevance of phycoerythrin in the biology of mammalian cells is difficult to conceive, it is tempting to speculate that structurally related Ags could be relevant in the general selection and licensing of γδT cells. In addition, the fact that a single Ag can be recognized by various γδTCRs harboring distinct CDR3 regions is reminiscent with the NKT cell biology (27) and can suggest the existence of a restricted conformational "hot-spot" comprising few amino acid residues in CDR3 regions responsible for γδT cell antigenicity in mice. This structural basis for Ag recognition by innate-like T cells might have been conserved all through the evolution from jawless vertebrates (28).

Despite leaving the thymus with a pre-programmed effector fate, γδT17 cells have been shown to conserve a certain degree of plasticity in the periphery. This characteristic originates from an epigenetic regulation program for specific genes in γδT17 cells such as Dickkopf-related protein 3 (29). Thus, along with IL-17, γδT17 cells can also produce interferon (IFN)-γ under inflammatory conditions. The biological relevance of this plasticity has been revealed in various settings including *Listeria monocytogenes* infection (22). In this later model, long-lasting accumulation of $V\gamma6^{+}$ IFN-γ/IL-17 double producers was observed within intestinal lamina propria (22, 30). Since $V\gamma6^{+}$ γδT17 cells were reported to be absent from the gastrointestinal tract at steady-state (20), it is possible that the combination of the γδT17 cell epigenome and local environment modifications under this inflammatory condition favors their homing and survival in the gut tissue. On the other hand, it is interesting to mention that IFN-γ-producing pre-programmed γδT cells (γδT1) do not possess the capacity to

TABLE 1 | Origin, tissue distribution, and TCR repertoire of γδT17 cells.

Subset	Windows of development	Steady-state tissue distribution	Origin	V(D)J diversity
$V\gamma1^{+}$	Mainly perinatal (day 3–8)	Barrier sites and lymphoid tissues	Natural	Intermediate to high
$V\gamma2/3^{+}$	Late embryonic and perinatal (from E17 to day8)	Barrier sites and lymphoid tissues	Natural	–
$V\gamma4^{+}$	Late embryonic and postnatal (E18 onward)	Barrier sites and lymphoid tissues	Natural: for $V\gamma4^{+}$ T cells of fetal origin including at least the Vγ4Vδ5 subset	Invariant for natural γδT17: Vγ4Jγ1/Vδ5Dδ2Jδ1
			Inducible: after Ag encounter in the periphery without extensive clonal expansion	Intermediate to high for inducible γδT17
$V\gamma5^{+}$	Embryonic only (from E13 to E16)	Epidermis	Reprogrammed: unknown mechanism (TCR?)	Invariant: Vγ5Jγ1Cγ1/Vδ1Dδ2Jδ2
$V\gamma6^{+}$	Embryonic only (from E14 to birth)	Barrier sites at the exception of the gut	Natural	Invariant: Vγ6Jγ1Cγ1/Vδ1Dδ2Jδ2

E, embryonic day; V, variable gene segment; D, diversity gene segment; J, junction gene segment; Ag, antigen; TCR, T cell receptor.

produce IL-17 (31). However, a small proportion of epidermal γδT1 (e.g., Vγ5$^+$) cells has been demonstrated to produce IL-17 *in vivo* upon skin wounding (32). The molecular determinants involved in giving rise to this cytokine production capacity are currently unknown but seem to rely on TCR signaling (33).

The existence of γδT17 cells in humans is still a matter of debate (34). Actually, the thymic program of γδT cells in humans seems to differ from the one described in mice (35). Most of the data available suggest that human γδT cells might not be "innately" programmed to produce IL-17 during their thymic development but rather acquire this capacity under inflammatory conditions once in the periphery akin to CD4$^+$ Th17 cells. Thus, circulating Vγ9Vδ2$^+$ [using Lefranc's nomenclature (36)] T cells from adult healthy donors produce no or little IL-17 (37) except under complex stimulatory protocol including both activating cytokines and TCR engagement (38). However, it is important to mention that purified Vγ9$^+$ γδT cells from cord blood seem more prone to produce IL-17 (37, 39, 40) that could suggest an embryonic origin for human γδT17 cells similar to the murine situation. It is, therefore, possible that these putative γδT17 cells occupy particular niches of the body that render them difficult to assess under homeostatic conditions. Murine pre-committed γδT17 cells are often characterized by the expression of an almost clonal TCR (41). Thanks to next-generation sequencing, the existence of clonal TCR-expressing γδT cell subsets in humans has recently emerged. Upon cytomegalovirus reactivation, a recent study demonstrated the massive proliferation of diverse γδT cell clones in patients after allogeneic-hematopoietic-stem-cell transplantation (42). However, the *TRG* and *TRD* sequences of these clones were not shared among individuals at the nucleotide level (42). In addition, analysis of the human Vδ1$^+$ T cells in healthy adults indicates that this repertoire is dominated by few private clonotypes (43). Determining the cytokine profile of these clones will be helpful to better appreciate the existence and origins of γδT17 cells in humans. Whatever the mechanisms that drive their emergence in humans, the capacity of human γδT cells to produce IL-17 has been demonstrated in various immune responses including infection, cancer, and autoimmunity (38, 44–46).

DEVELOPMENT OF γδT17 CELLS

Dealing With the Concept of "Innate/Natural" vs "Adaptive/Inducible" Origins of γδT17 Cells

Mouse γδT cells develop in a standardized manner by sequential waves that can be conveniently followed based on their Vγ chain usage (47). This process starts during embryonic life from day 13 (E13) onward. The first wave is exclusively constituted of the IFN-γ-producing Vγ5$^+$ cells and lasts for about 4 days. This is shortly followed by a developmental wave of "natural" IL-17-producers comprising both canonical Vγ6$^+$ (from E14 to birth) and restricted subsets of Vγ4$^+$ (E18 onward) (48, 49). Around birth, IFN-γ-producing Vγ1$^+$ and Vγ4$^+$ subsets start to develop along with the IL-4/IFN-γ-double producers Vγ1$^+$Vδ6$^+$ subset. After birth, developing γδT cells mainly exhibit a naive uncommitted profile (47).

According to this scheme, natural γδT17 cell development is believed to be restricted to the gestational period. To support this notion, Haas and colleagues demonstrated that transplantation of bone marrow from IL-17-competent mice into lethally irradiated *Il17af*-deficient adult recipients failed to induce γδT17 cell development (49). Partial γδT17 cell development in the thymus could be achieved in reconstituted *Il17af*-deficient neonate recipients but failed to give rise to γδT17 cells in the periphery. In addition, inducible expression of *Rag1* in T cell precursors in adult mice did not restore *de novo* generation of γδT17 cells (49). Likewise, CCR6$^+$ IL-17-producing dermal γδT cells failed to reconstitute 8 weeks after bone marrow transplantation unless the mice received an additional transfer of neonatal thymocytes (33). Surprisingly, the same lab reported the presence of Vγ4$^+$ CCR6$^+$ (but not Vγ4$^-$ CCR6$^+$) γδT17 cells in lymph nodes of recipient TCRδ$^{-/-}$ mice following bone marrow transplantation in absence of neonatal thymocytes at 12 weeks post-grafting (50). The basis for this difference remains unclear but one can argue that, in the 12 weeks model, authors have reconstituted "inducible" γδT17 cells only. Several studies have also reported that the peripheral pool of γδT17 cells decreased with age (51, 52), which further support the embryonic origin of natural γδT17 cells.

Despite suggesting a strict favorable temporal window for natural γδT17 cell development during fetal life, these studies also raised some additional interrogations. Is this developmental model imposed by intrinsic (nature of γδT precursors) or extrinsic (embryonic vs adult thymic environment) factors? Zúñiga-Pflücker's team recently started to provide an answer to this question. Culture of γδTCR-transduced fetal or adult hematopoietic precursors with OP9-Delta-like protein 4 (Dll4) cells led to the development of γδT cells with IL-17 production capacity in a similar manner (53). Thus, these data suggest that adult progenitors conserve their intrinsic capacity to develop as γδT17 cells once in an appropriate environment. However, since the authors used a clonal TCR (Vγ4Vδ5) (54) for transfection, it cannot be excluded that in addition to the favorable environment, the nature of the TCR expressed plays a role in the IL-17 effector fate, in particular regarding the recent discovery of clonal Vγ4Jγ1/Vδ5Dδ2Jδ1 T cells with a strongly biased IL-17-producing profile (55). In addition, recent studies have shown that adult peripheral γδT cells (from adult bone marrow-derived precursors) can convert into "induced" γδT17 cells upon inflammatory conditions (56, 57). Both studies highlighted a critical role for the cytokines IL-23 and IL-1β, and to a lesser extent TCR signaling, in this process (56, 57). Importantly, the potential to give rise to inducible γδT17 cells seems to be restricted to the IL-2Rβ$^-$ γδT cell subset (57). To further illustrate this peripheral polarization capacity, Buus and colleagues recently provided a RNA-Seq analysis of adult γδ thymocytes indicating IL-17 potential in certain subsets including notably IL-2Rα$^+$ Clec12A$^+$ Vγ1$^+$ and Vγ4$^+$ cells (58).

This situation illustrates the recent concept of "natural" vs "inducible" γδT17 cells (48). While "natural" (Vγ6$^+$ and Vγ4$^+$ subsets) γδT17 cells are committed to this effector fate during their embryonic/perinatal thymic developmental program, "inducible" γδT17 cells stem from naive (Vγ1$^+$ and Vγ4$^+$ subsets) γδT cells within the periphery upon inflammatory conditions through cytokine, and/or Ag recognition akin to conventional CD4$^+$

Th17 cells (26). Thus, it is tempting to view "natural" γδT17 cells as innate-like T cells whereas "inducible" γδT17 cells can rather be considered adaptive. This is reminiscent with the situation in the αβ lineage comprising innate-like T17 (NKT17 and MAIT17) cells and adaptive conventional Th17 cells.

Thymic Molecular Determinants of γδT17 Cell Effector Fate

In this section, we will review the thymic determinants that drive γδT cell differentiation into an IL-17 effector fate by deciphering how "natural" IL-17-committed γδT cells emerge from the rest of the γδT cell compartment. Before commitment into γδT17 cell sublineage, thymic precursors have to first undergo a bifurcation into αβ or γδ lineages. Mechanisms driving this initial dichotomy are beyond the scope of this review, but it is worth mentioning that the strength of TCR engagement in thymocytes emerges as a driving force in this process [see Ref. (53, 59) for reviews]. However, requirement for TCR ligation in IL-17-commited γδT cell differentiation is still an intense matter of debates that will be discussed later. Commitment toward the γδT lineage happens at double negative (DN)2 and DN3 stages (60, 61). Interestingly, the effector fate of "natural" γδT cell subsets (IFN-γ- vs IL-17A-producing) appears to be already predetermined at this stage. Thus, commitment to "natural" γδT17 cells exclusively arises from the late DN2 stage in a B cell leukemia/lymphoma 11b-dependent manner (46).

Further differentiation into the IL-17 effector fate is a complex and highly dynamic process involving multiple molecular and cellular interactions. For the salve of clarity, we distinguish here the (1) extrinsic factors (e.g., thymic environmental cues) and (2) intrinsic factors [e.g., intracellular signaling pathways and transcription factors (TFs)] that tune γδT17 precursors into mature γδT17 cells.

Extrinsic Factors

Molecular and cellular players within the thymic microenvironment are crucial for acquisition of γδT cell effector fate (**Figure 1**). Anatomically, precursors migrate from the cortex to the medulla during this process, where they receive multiple signals that dictate their differentiation. In this three-dimensional environment, it is important to keep in mind that time should be considered as a fourth dimension when deciphering the "natural" γδT17 cells ontogeny.

Cytokines

Many cytokines have been reported to directly or indirectly regulate thymic γδT17 cell differentiation/development.

IL-7 is a critical and non-redundant cytokine in lymphopoiesis (62). IL-7Rα-deficient mice completely lack γδT cells (63, 64) partly due to the role of IL-7 in V-J recombination of TCRγ genes (63, 65). Its specific role in survival and proliferation of γδT17 cells

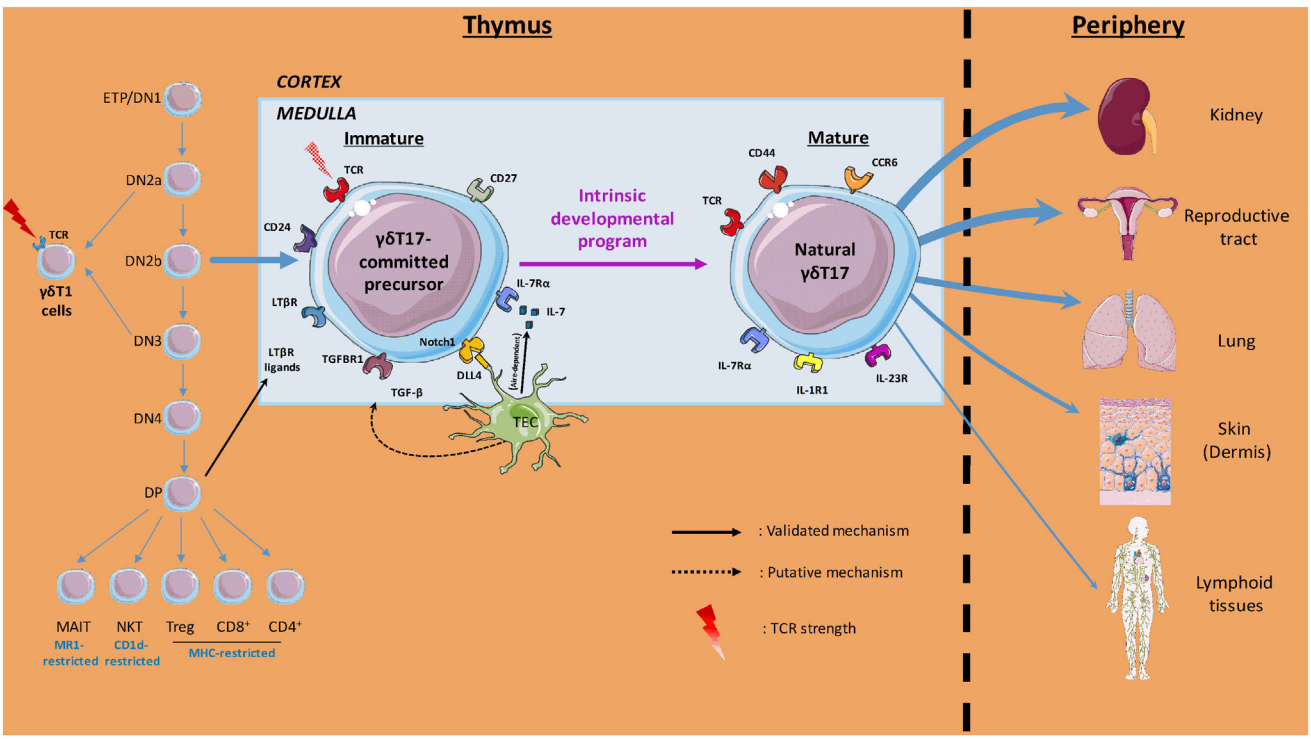

FIGURE 1 | Overview of thymic γδT17 cell ontogeny. Initial intrathymic pathways leading to pre-committed γδT17 cells divergence from other T cell lineages are illustrated. The thymic (cortical and medullary) environmental cues involved in γδT17 cell effector fate and the preferential peripheral niches of mature γδ17 cells are also depicted. Labels indicate the cells, soluble factors, proteins, surface markers, and T cell receptor (TCR) signal strength involved in the γδT17 cell program of differentiation.

in peripheral tissues under homeostatic and pathological situations has been demonstrated (37, 66, 67). Even if this question has never been directly addressed, many studies imply a requirement for IL-7 in the proper natural γδT17 cell development. First, in a model of conditional abrogation (RBP-Jκ) that precludes IL-7Rα (CD127) expression, but in which the initial generation of γδ precursors (DN2 and DN3 stages) is maintained, the pool of both thymic and peripheral γδT17 cells is markedly reduced (68). Second, addition of recombinant IL-7 in fetal thymic organ culture from E16 thymus promotes γδT17 cell expansion over IFN-γ-producing γδT cells (37). Understanding whether IL-7 directly participates in the differentiation program or solely in the post-differentiation expansion of γδT17 cells will require further investigations. In line with the favorable temporal window for γδT17 cell development around birth, it is important to mention that thymus is particularly enriched for IL-7 [especially in thymic epithelial cells (TECs)] in neonates and its presence declines with age (69, 70).

Akin to conventional αβ Th17 cells, TGF-β1 has also been proposed to participate in γδT17 cell development (71). In addition, this report indicates that some other Th17-driving cytokines, such as IL-23 and IL-21, appear to be dispensable. However, since the authors have performed their investigation in 11-day-old mice, a time at which natural γδT17 cells already egressed the thymus, it is difficult to precisely evaluate the contribution of TGF-β1 in natural γδT17 cell differentiation.

The role of IL-6 in γδT17 cell development is somehow controversial. While several studies indicated that IL-6 deficiency did not influence γδT17 cell homeostasis and cytokine production capacity (71, 72), others reported a defect in γδT17 cells in both thymus (73) and peripheral organs (74). Thus, the contribution of IL-6 in natural γδT17 cell differentiation remains unclear. In addition, mRNAs for IL-6Rα (CD126) are barely expressed on both immature and mature thymic natural γδT17 cells (from the ImmGen database). However, it cannot be firmly excluded that IL-6 influences the thymic microenvironment to support γδT17 cell differentiation as previously hypothesized (73).

Thus, this indicates that the cytokine network within the thymic microenvironment has to be tightly regulated in a time-dependent manner to allow natural γδT17 cell differentiation.

Thymic Epithelial Cells

Akin to other thymocytes, interaction with TEC is likely critical in γδT17 cell differentiation, even though few experimental data are currently available. Thus, medullary (m)TEC has been implicated in regulating Vγ6$^+$ γδT17 cell development through the TF autoimmune regulator (Aire) (69). In *Aire*$^{-/-}$ mice, IL-7 production is up-regulated in mTEC, and this is accompanied by an overproduction of Vγ6$^+$ γδT17 thymocytes. Interestingly, other subsets of natural γδT17 cells, especially Vγ4$^+$ subsets were not affected by specific Aire deletion in mTEC (69). This feature also indicates that the various natural γδT17 cell subsets probably require different signals to develop.

Cortical (c)TEC has also been recently shown to control γδT17 cell development. Using a mouse model with specific cTEC ablation, Nitta and colleagues observed a strong dysregulation in the proportion of natural γδT17 cell subsets (75). Specifically, absence of cTEC skewed the γδT17 TCR repertoire toward Vγ6 expression at the expense of the Vγ4$^+$ T cell subset during the postnatal period while the proportions of Vγ6$^+$ and Vγ4$^+$ γδT17 cells remained normal during embryonic life. Authors hypothesize that in their mouse model, the postnatal thymic microenvironment resembles to the fetal microenvironment, which in turn favors the Vγ6$^+$ subset. In addition, since they have been proposed to be a prime source of TGFβ (76), cTEC could also participate in thymic development of γδT17 cells through this mechanism (71).

The importance of Dll4, a Notch ligand expressed by TEC (77) has also been proposed in γδT17 cell differentiation (78). In a co-culture model of E15 thymocytes with stromal cells, absence of Dll4 expression by stromal cells led to an abrogation in γδT17 cell development (78). This phenotype indicates that Dll4 is likely to be a common factor for the differentiation of all natural γδT17 cell subsets.

Finally, a recent study proposed that signaling through NF-κB-inducing kinase (NIK) in TEC is essential for the generation of a fully functional pool of γδT17 cells (79). However, the molecular factors regulated by NIK in TEC are yet to be determined. Understanding the NIK-dependent pathways in TEC will certainly provide important clues in the TEC-γδT17 precursor interaction mechanisms that drive γδT17 cell effector fate.

Altogether, the fetal and perinatal thymic environment offers a temporal window of opportunity for γδT17 cell differentiation. However, the available literature indicates the requirement for differential factors according to the subset of naturally occurring γδT17 cells. This might somewhat rely on the intrinsic nature of the γδT17 precursors. It can also be hypothesized that these precursors (Vγ6$^+$ and Vγ4$^+$) require timely expressed TCR ligands in the thymic environment. However, no host-derived Ags have been proposed to date to participate in γδT17 cell differentiation.

Intrinsic Factors

A Requirement for TCR Ligation: Still an Open Question?

Beyond its importance into γδ lineage commitment, TCR signal strength is also involved in the functional maturation of γδ-committed thymocytes. Specifically, TCR signal strength drives the IL-17- vs IFN-γ-producing γδT cell dichotomy. However, it appears difficult to clearly attribute a specific strength to a specific effector fate. While the literature tends to demonstrate consensually that a strong TCR signaling in γδ thymocytes drives their commitment toward a Th1-like effector fate (31, 80–82), the situation in γδT17 cell differentiation remains highly debated.

Chronologically, a first set of data suggested that γδT17 cell differentiation occurred in the absence of TCR cognate ligands (80). However, (1) this study used adult thymocytes and focused on peripheral organs that are weakly if not populated with natural γδT17 cells and (2) it cannot be excluded that ligand-independent TCR signaling plays a part in this model. Therefore, these results are likely to provide specific information about the requirement of TCR signals for inducible γδT17 cells. In this sense, these data perfectly fit with the concept that inducible γδT17 cells egress the thymus with a naive uncommitted profile and need further encounter with peripheral Ags to gain their capacity to produce IL-17. Few years later, the lab of Adrian Hayday highlighted the butyrophilin-like molecule Skint-1 as a molecular determinant in

Th1-like effector fate of Vγ5$^+$ T cells (31). Interestingly, in absence of Skint-1, the differentiation of Vγ5$^+$ T cells resulted in the generation of cells displaying a phenotype of natural γδT17 cells (31). Indeed, Skint-1 engagement in Vγ5$^+$ thymocytes induces the upregulation of TCR-dependent genes that subsequently repress the transcriptional differentiation program of natural γδT17 cells. In line, Pennington and colleagues recently demonstrated that differentiation of E15 γδ thymocytes in presence of an anti-TCRδ mAb (GL3) blunted their commitment toward a γδT17 cell profile (82). Altogether, weak or no TCR signals seem required to allow proper γδT17 cell development. Thus, the developmental program of natural γδT17 cells appears to be a TCR Ag-free process acquired by "neglect."

On the other hand, mice presenting a reduced function in the TCR proximal signaling kinase ZAP-70 displayed a reduced pool of both IL-17A-producing Vγ6$^+$ and to a lesser extent Vγ4$^+$ T cells in neonate thymocytes (83). In the same line, Silva-Santos and colleagues observed a reduction in the frequency of IL-17A-producing Vγ6$^+$ subset using double-heterozygous mice for the CD3 subunits γ and δ in which TCR signaling is attenuated (81).

These apparently contradictory results may have multiple explanations. Notably, it is assumable that the different subsets of γδT17 precursors may require a specific and fine-tuned TCR signals to engage in their differentiation program. Specifically, Vγ6$^+$ may require an "intermediate" TCR signals while Vγ4$^+$ subsets may need weak or no signals. Moreover, intensity of TCR signaling can be hardly compared from one experimental setting to another, making any generalization risky. In this context, the importance of TCR signaling in programming γδT17 cell differentiation is still an open question. This also raises the putative existence of TCR self-ligands for natural γδT17 cells. The recent discovery of butyrophilin-like molecules as Ags for mouse γδT cells (84, 85) opens a new exciting avenue of research in the field. Identification of the enlarged butyrophilin family in both mouse and human γδT cell biology might offer an interesting anchoring point for future translational studies.

Costimulatory Molecules

On top of the TCR, its accessory receptors have been proposed to participate in γδT cell differentiation. In addition to be a convenient marker to distinguish γδT functional subsets, the costimulatory receptor CD27 has been shown to participate in γδT cell development (14). Indeed, γδ thymocytes from *Cd27*$^{-/-}$ mice presented altered expression of *ifng*. Although CD27 deficiency did not influence the pool of γδT17 cells, CD27 gain of function in thymic cultures resulted in lower IL-17 transcripts by CD27$^-$ γδ thymocytes (14). Thus, CD27 appears as a thymic regulator in γδT cell effector fate.

Inducible T cell co-stimulator (ICOS) signaling pathway has also recently emerged as a possible determinant in γδT17 cell (at least for the Vγ4$^+$ subset) development (86). Agonistic activity of anti-ICOS mAb in fetal thymic organ culture significantly impaired Vγ4$^+$ γδT17 development. In line, genetic ablation of ICOS tends to increase the pool of thymic Vγ4$^+$ γδT17 cells (86). Thus, this study indicates that ICOS-dependent intracellular pathways in thymocytes controls γδT17 cell effector fate.

Besides, one must keep in mind, that, alongside with TCR and costimulation receptor signaling, multiple other signals have to be integrated by embryonic thymocytes to, *in fine*, engage toward the γδT17 effector fate.

Soluble Mediator Receptor Signaling Pathways

γδT17 precursors express specific receptors for various soluble factors produced in the thymic environment by hematopoietic and non-hematopoietic cells. Signals provided by these mediators have to be integrated by γδT cells to fully develop.

For instance, TGFβ receptor (TGFβR) signaling pathway in developing γδT17 cells could be important in their effector fate. Mice deficient for Smad3, a critical component of the TGFβR signaling pathway presented a striking defect in frequency of thymic γδT17 cells compared with littermate controls (71). However, since the authors did not provide direct evidence (bone marrow chimera and OP-9 models) for an intrinsic role of the TGFβR signaling pathway, it cannot be excluded that this pathway is indirectly linked to γδT17 cell development.

In addition, the targeting of lymphotoxin-β receptor through double positive thymocytes-derived ligands (87) also controls the generation of γδT17 cells by regulating the expression of TFs from the NF-κB family namely RelA and RelB (88).

As mentioned above, the IL-7/IL-7Rα axis is important to generate a normal pool of γδT17 cells. However, a better understanding of the downstream molecular cascade involved will be helpful to understand whether this axis controls the differentiation program or the homeostasis of γδT17 cells.

On the other hand, IL-15Rα signaling disruption favors the development of γδT17 cells in thymus of neonates (65). The molecular mechanisms responsible for this are currently unknown but might rely on the activation of repressing factors in the IL-15Rα signaling pathway or could be indirect by reducing the competition with γδT17-driving γ-chain-dependent cytokines such as IL-7.

The expression of the prostacyclin (PGI2) receptor (IP) on thymocytes has also been demonstrated to control γδT17 cell development. This was evidenced by a failure to generate γδT17 cells in the thymus of IP$^{-/-}$ mice (89). However, the molecular determinants involved in this process are yet to be defined.

The γδT17 Cell Transcriptional Program

The dynamic integration of these multiple signals leads to the implementation of a complex transcriptional program that dictates γδT17 cell effector fate (**Figure 2**). The aim of this program is ultimately to maintain and/or to favor the expression of Rorc (encoding RORγt), the cardinal TF for IL-17-secreting cells (90) including γδT cells (72). The recent advances in RNA deep sequencing analysis allowed a better understanding of the transcriptional regulation involved in γδT17 development.

Thus, SRY-related HMG-box (SOX) 4 and SOX13, two members of the high mobility group box TF family constitute a central node of regulation in this program (50, 91, 92). SOX4/13 are paramount in the acquisition of the γδT17 effector fate by (1) directly controlling *Rorc* transcription, (2) possibly enhancing important γδT17 cell-driving pathways such as IL-7Rα signaling, and (3) possibly inhibiting *Rorc*-repressing TFs (31, 92).

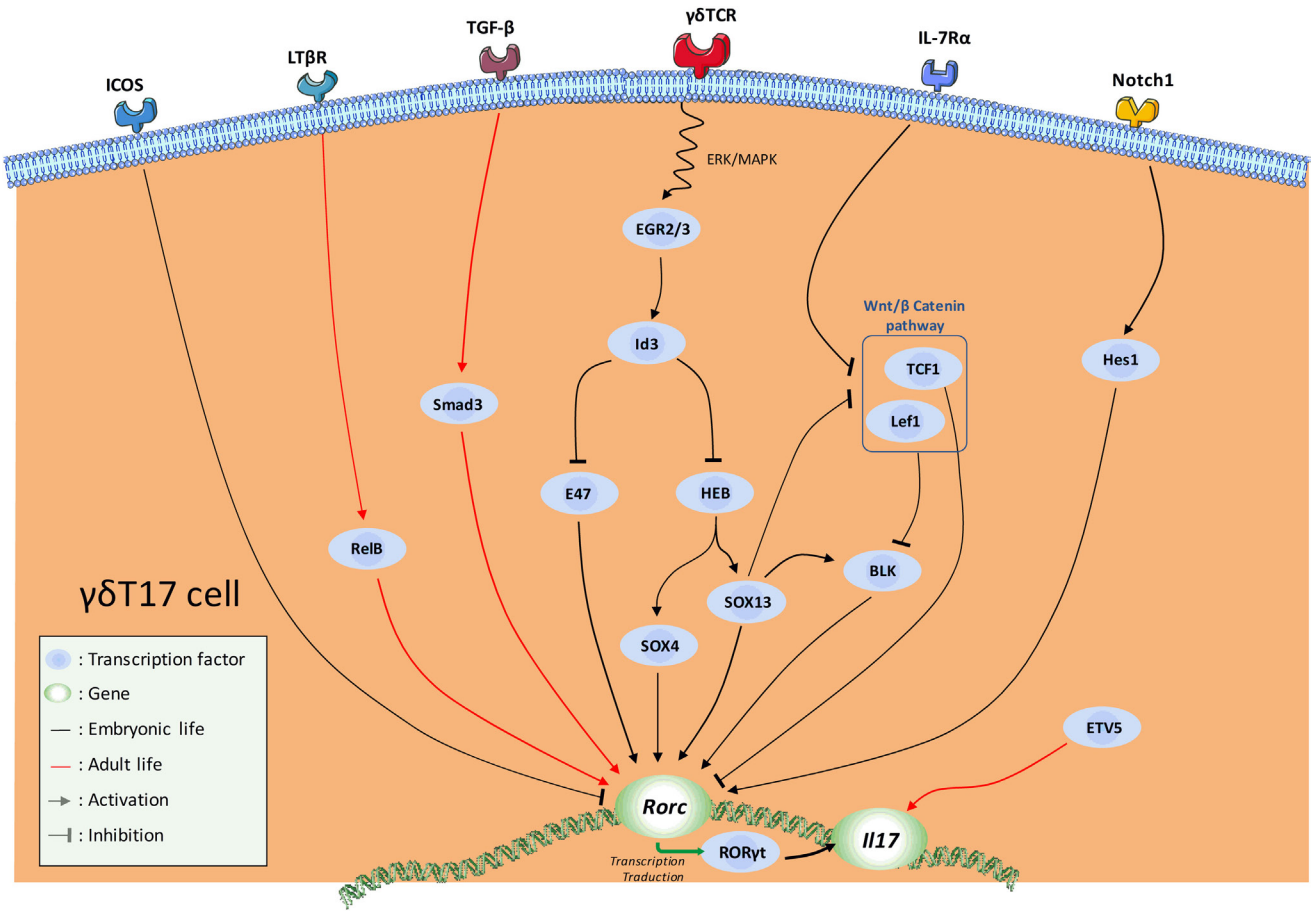

FIGURE 2 | Schematic overview of the current knowledge in the transcription factor (TF) network involved in natural γδT17 cell effector fate. Major activating and repressing pathways implicated during γδ17 effector fate acquisition are depicted.

In this later mechanism, SOX13 was suggested to inhibit the *Rorc*-repressing activity of two downstream mediators of the Wnt/β-catenin signaling pathway namely lymphoid enhancer-binding factor 1 (Lef1) and transcription factor 1 (TCF1) (92). In this context, *Tcf7* (encoding for TCF1) deficiency leads to an aberrant high proportion of γδT17 cells (92). At this stage, it is also important to mention that this pathway also regulates the development of the IFN-γ-producing Vγ1Vδ6.3$^+$ and Vγ5$^+$ cells (92). The mechanisms by which the TCF1–Lef1 axis counteracts the γδT17 transcriptional program are not fully understood. First, it is possible that TCF1 and Lef1 control *Rorc* expression through epigenetic (histone deacetylase) activity as suggested in conventional T cells (93). Alternatively, this axis could also indirectly repress *Rorc* expression by inhibiting the transcription of B lymphocyte kinase (Blk) (92), an important signal transducer in γδT17 cell development (94). However, how Blk controls RORγt expression is currently unknown. It is noteworthy that, using *blk*$^{-/-}$ mice, Vγ6$^+$ T cells were shown to be more Blk-dependent than Vγ4$^+$ (94). As SOX13 was shown to regulate Blk expression and to control Vγ4$^+$, but minimally Vγ6$^+$, subset development (92), these results appear somewhat contradictory. However, Vγ4 and Vγ6 subsets develop at different temporal windows; therefore, they are likely to integrate different thymic signals. As a result, this might modulate the relative importance of a same regulatory axis, and eventually leading to different effects on their respective transcriptional program. Thus, regulatory network required for Vγ4$^+$ ontogeny may be more SOX13-dependent than Vγ6$^+$ subset. Regarding the differential contribution of the TCR signaling in the γδT17 effector fate of these populations, Blk may play a role at this stage. According to its regulatory activity on TCR signaling, Blk could act as a "rheostat" to fine-tune signals delivered by the thymic γδT cell ligands. Thus, Blk deficiency might affect more Vγ6$^+$ ontogeny as TCR signaling has been proposed to control the development of these latter but not Vγ4$^+$. Of note, Blk overexpression has been shown to enhance IL-7 responsiveness in B cells (95).

As stated earlier, the TCR signaling pathway strongly influences the acquisition of the γδT17 effector fate. Mechanistically, TCR engagement induces upregulation of proteins of the early growth response (Egr) family namely Egr2 and Egr3 (31, 81). These two TFs positively regulate the DNA-binding protein inhibitor Id3. Thus, Id3 impairs γδT17 cell differentiation through (1) inhibition of HeLa E-box binding protein (HEB)-dependent *Sox4* and *Sox13* expressions (96) and (2) inhibition of the *Rorc* promoter

E47 (91). This scheme is also in line with the differential requirement for TCR strength in γδT17 cell effector fate of Vγ6$^+$ and Vγ4$^+$ further emphasizing the differences in the developmental programs of Vγ6$^+$ *vs* Vγ4$^+$ γδT17 cells.

In addition, the promyelocytic leukemia zinc finger (PLZF) protein is a key TF in the development of some innate and innate-like lymphocytes that dictates their acquisition of a Th-like effector program (97–99). PLZF was shown to control Vγ6$^+$ differentiation into γδT17 cells (100). The molecular mechanisms that govern PLZF activity in Vγ6$^+$ development are currently unknown and require further investigations. PLZF contribution in Vγ4$^+$ γδT17 cell development has not been assessed yet. However, it is noteworthy that PLZF does not appear to be expressed in neonates Vγ4$^+$ precluding a role of this TF for this particular subset (100).

Among the intracellular pathways that dictate the γδT17 effector fate, Notch signaling contributes to the generation of γδT17 cells through the helix-loop-helix protein Hes1 (78). Since it mainly exerts transcriptional repressing activities, it is possible that Hes1 acts in one of the pathways discussed above. Unrevealing the Hes1 interactome in developing γδT17 cells will be informative to get insight into the molecular factors that regulate this mechanism. An additional pathway by which the Notch signaling pathway could influence γδT17 cell development is by promoting IL-7Rα expression through the RBP-Jκ pathway (68). However, this pathway was only described in peripheral γδT17 cells of adult mice to control their homeostasis and self-renewal.

In addition to its role in proliferation/survival of γδT17 cells during development, the IL-7Rα signaling pathway is also likely to contribute to their transcriptional program. Indeed, IL-7/IL-7Rα signaling in fetal thymocytes was demonstrated to blunt both *Lef1* and *Tcf7* expression (101).

In silico analyses have also been fruitful to understand the transcriptional program of γδT17 cells. Using an algorithm that predicts important regulators across various lineages, the TF ETV5, along with SOX13 was proposed as a master regulator in Vγ4$^+$ γδT17 cell differentiation (102). Conditional ablation of ETV5 in T cells confirmed the role of this TF in Vγ4$^+$ γδT17 effector fate (102). Absence of ETV5 in developing Vγ4$^+$ slightly reduced RORγt expression but severely impaired IL-17 secretion. This is reminiscent with the situation for Th17 cell differentiation in which ETV5 directly promotes *il17a* and *il17f* expressions but has no influence on *Rorc* (103). The role of ETV5 in Vγ6$^+$ development remains to be determined; however, ETV5 is highly expressed on immature fetal Vγ6$^+$ and strongly repressed upon maturation (http://www.immgen.org/databrowser/index.html).

Originally thought to be acquired by "neglect," this literature underlines that the γδT17 effector fate is under the control of a very active process in which the SOX4/13 axis acts as a guardian for proper RORγt expression. In addition, the discrepancies in the phenotypes observed for Vγ4$^+$ and Vγ6$^+$ γδT17 cells imply different programs for natural γδT17 cell development. Thus, further transcriptomic analyses at single cell resolution are clearly required to better decipher the overlapping and/or specific developmental "trajectories" that drive the effector fate of these subsets.

What Can We Learn From Transcriptomic Analysis of Developing Natural γδT17 Cells?

As stated above, the recent advances in the quality of whole genome analyses allowed to validate and/or to predict the involvement of numerous genes in the transcriptional signature of many cell populations including γδT cells. In addition, normalized and comparative analysis of various gene sets among lymphocyte lineages led to the identification of conserved and/or distinct signature pathways in their effector program including Th17(-like) effector fate (104).

However, *in silico* analysis of the transcriptional program of γδT17 cells has been mainly discussed regarding the maturation of the Vγ4$^+$ cell subset in adult mice (91, 92, 104). Thus, this population comprises both "inducible" γδT17 cells as well as non-IL-17-producing subsets. To focus on "natural" γδT17 cells that develop during embryonic life, we reanalyzed the datasets of developing Vγ6$^+$ T cells (immature/CD24^{hi} vs mature/CD24^{low}) (GSE37448). Bioinformatic analysis generated a gene set of the top 1,000 transcripts significantly regulated during the effector fate acquisition of this subset (Table S1 in Supplementary Material). Interestingly, while similar analysis on developing fetal Vγ5$^+$ T cells (GSE15907) indicated that 87.8% of the 1,000 top regulated genes were up-regulated, only 48.7% did so in the Vγ6$^+$ dataset (**Figure 3**). This emphasizes the fact that, unlike γδT1, γδT17 cell effector fate is rather acquired using a repressing model.

As expected, among the list of gene generated, we found many up-regulated genes shared with other innate(-like) or adaptive IL-17-producing lymphocytes including *Rorc*, *Il17a*, and *Il17f* and the cytokine/chemokine receptors *Il1r1*, *Il2rb*, *Il7r*, *Il17rc*, *Il17re*, *Il23r*, *Il18r1*, *Ccr6*, and *Cxcr6*. This is paralleled by a silencing of genes involved in Th1 and Th2 differentiation, such as *Il2ra*, *Il12rb2*, *Lck*, *Gata3*, and *Maml2*.

In addition, we noted numerous genes involved in TCR signaling including *Lck*, *Nck2*, *Pak1*, *Plcg*, *Prkcq, Ptpn22*, and *Nfkbie*. Notably, all these transcripts were down-modulated during Vγ6$^+$ maturation. Moreover, genes involved in costimulation, such as *Cd27*, *Cd28*, *Icos*, *Themis, Slamf1*, *Slamf6*, and *Pik3r2,* were also repressed upon differentiation. In line, it is noteworthy that the transcript encoding for the nuclear receptor Nur77 (*Nr4a1*), a faithful marker of TCR strength (105) is strongly repressed during Vγ6$^+$ maturation. Given the controversy discussed previously, these observations clearly suggest that the TCR signaling pathway has to be maintained under tight regulation to allow Vγ6$^+$ T cell differentiation.

More importantly, using advanced pathway analysis, we pinpointed, in the Vγ6$^+$ T cell gene set, multiple family of genes involved in biological processes and molecular pathways that might be involved in their developmental program (**Figure 4**).

Nutrient Metabolism

Along with *Nr4a1*, other genes encoding for nuclear receptors such as receptors of vitamin A (*Rarg*) and D (*Vdr*), two vitamins reported to participate in ILC, γδT and NKT (25, 106) homeostasis and development are up-regulated during Vγ6$^+$ maturation.

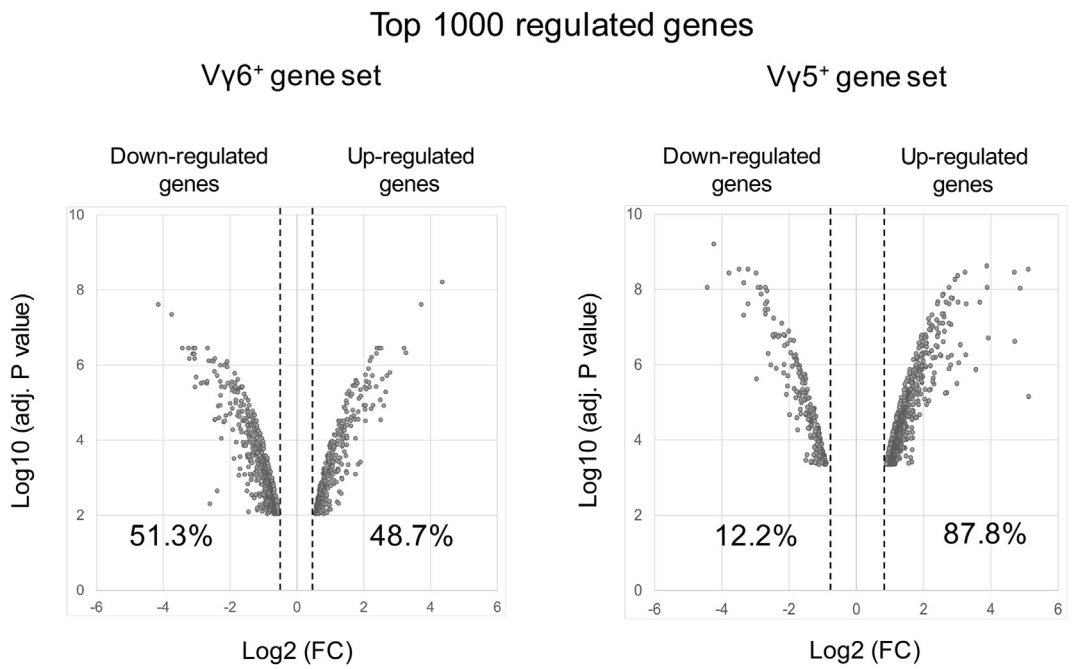

FIGURE 3 | Volcano plots of the top 1,000 regulated genes during Vγ6 and Vγ5 maturation. Raw data were extracted from datasets (GSE37448 and GSE15907) downloaded from the NCBI's data repositories. Vγ6+ and Vγ5+ gene sets were generated by comparing gene expression in immature ($CD24^{high}$) vs mature ($CD24^{low}$) thymocytes at E17 for both populations (2–3 replicates/subset). The top 1,000 regulated genes ($P < 0.05$) were used to constitute the two gene sets (Table S1 in Supplementary Material). Volcano plots represent either positively or negatively regulated genes (as fold change) according to their respective *P* value. Labels indicate the percentage of genes that are either positively or negatively regulated in each dataset. FC, fold change.

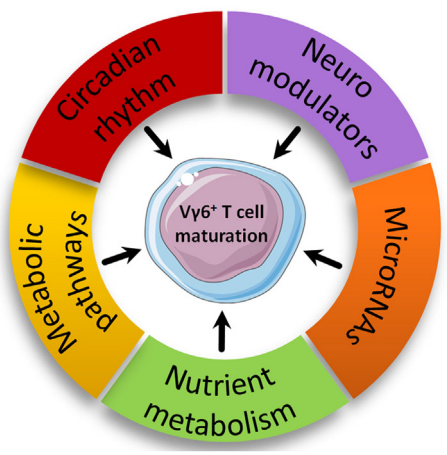

FIGURE 4 | Proposed new biological pathways involved in intrathymic Vγ6+ maturation. Biological pathways with enriched modulated genes in the Vγ6+ dataset are represented based on advanced pathway analysis using the trial version of iPathwayGuide (©Advaita Corporation).

In addition, genes encoding for vitamin transporters (*Slc23a2* and *Slc2a3*) were also modulated in the Vγ6+ gene set. This could imply an important role for vitamins in γδT17 cell development. Somewhat related, expression of *gpr183*, a sensor of oxysterols was strongly up-regulated (3.6 fold) in developing Vγ6+ T cells. Interestingly, GPR183 has recently emerged as a critical player in the control of ILC3 homeostasis (107). Moreover, oxysterols are ligands for RORγt and drive Th17 cell differentiation (108). The influence of nutrient-derived metabolites on lymphocyte immunity including early development has recently gained considerable attention (2). The recent discovery of vitamin B2 metabolites as Ags for MAIT cells (109) will certainly reinforce the interest of immunologists for nutrient metabolism. The availability of vitamins *in utero* has also been shown to control the quality of the immune system in later life (110). According to these arguments and the temporal window of development for γδT17 cells, investigating the nutrient metabolism in γδT17 cell biology will be likely to provide new interesting data on the influence of maternal diet in shaping immunity.

Neuroimmunology

In line with the emerging concept of neuroimmunology, numerous members of the "neuroactive ligand-receptor interaction" pathway were present in the Vγ6+ gene set including genes encoding for neuroactive substance receptors of neuropeptide (*Gpr83*), hormones (*Sstr2*, *Rxfp1*, and *Calcrl*), prostanoids (*Ptger4*, *Ptgfrn*, and *Ptgir*), leukotrienes (*Cysltr2* and *Ltb4r1*), nucleotides (*P2rx7*, *Adora2a*, and *Lpar4*), and amino acids (*Gabbr1*, *Gabbr2*, and *Gria3*). Interestingly, the above-mentioned genes encoding for prostanoids, hormones, and nucleotide receptors are down-regulated during Vγ6+ T cell maturation, while those encoding for leukotrienes are up-regulated.

The relationship between neuromodulators and immune cell development is largely unexplored. However, there are evidence for an expression of neuromodulators and their associated-receptors in TEC and on thymocytes, respectively (111). Furthermore, *ex vivo* somatostatin (ligand for *Sstr2*) addition in FTOC increased thymocyte numbers and maturation. By contrast, both neuropeptide Y (ligand for *Gpr83*) and calcitonin (ligand for *Calcrl*) reduced thymocyte numbers (112). Last, *Ptgir* (encoding for the prostaglandin I2 receptor) has already been biologically validated to participate in natural γδT17 cell development (89). Regarding this, a broad analysis of the eicosanoid family in γδT17 cell development should be encouraged.

Circadian Rhythm

Among highly regulated genes, our analysis also retrieved genes related to circadian rhythm. Thus, we found that *Nr1d1*, *Nr1d2*, and *Bhlhe40,* which encodes for REV-ERBα, REV-ERBβ, and Dec1 proteins, respectively, were all up-regulated in mature Vγ6$^+$ T cells. These proteins are critical repressors of *Arntl* (encoding for Bmal1), *Npas2*, and *Clock*, three master clock genes (113, 114). Of note, *Arntl*, *Npas2*, and *Clock* were also significantly regulated in developing Vγ6$^+$ T cells. Recent literature has emphasized the importance of circadian rhythms in fine-tuning immune responses (113, 115). Interestingly, RORγt expression has been shown to be under circadian regulation through a REV-ERBα-dependent mechanism (116). Thus, these data may suggest a role for the circadian rhythm in Vγ6$^+$ T cell biology. Of note, NFIL3 (E4BP4), a repressor of the circadian clock, is implicated in the differentiation/development of ILCs and NK cells (117–119). In addition, we can speculate that the regulation of these clock genes helps mature Vγ6$^+$ T cells to integrate and to regulate circadian cues once in the periphery, as demonstrated for many other cellular actors of innate immunity (113).

Immunometabolism

Regarding the growing interest for understanding immunometabolic pathways implicated in leukocyte biology, we searched for genes involved in metabolic pathways. Our analysis revealed that many genes involved in the six major metabolic pathways specifically glycolysis (*Aldh2*, *Ldhb*, *Acss1*, and *Acss2*), tricarboxylic acid cycle (*Idh1*, *Idh2*, and *Aco1*), pentose phosphate pathway (*Fbp1*), fatty acid oxidation (*Cpt1a*, *Nr4a3*, *Peci*, *Auh*, *Pex5*, and *Ivd*), fatty acid synthesis (*Fads2* and *Slc45a3*), and amino acid metabolism (*Aco1* and *Bcat1*) are down-regulated in mature Vγ6$^+$ T cells.

Interestingly, fatty acid oxidation is associated with regulatory T cell differentiation while glycolysis is a major metabolic pathway in effector T cell differentiation (120, 121). Of note, expression of *Cpt1a* was reduced in Th17 cells compared with regulatory T cells (120). Enhanced fatty acid synthesis and glycolysis in immune cells, especially T cells, have been regarded as markers of inflammatory cells required for acquisition of effector functions upon inflammatory conditions (122). This adds a metabolic argument into the fact that Vγ6$^+$ T cells are "preset" cells with metabolic programing occurring during development, to be immediately and fully functional once in peripheral tissues.

MicroRNAs

To date, there is limited literature on the role of microRNAs in leukocyte development. In our gene set, we detected the presence of five microRNAs (*mir15b*, *mir181a-1*, *mir181a-2*, *mir181b-1*, and *mir181b-2*), all of them being down-regulated in mature Vγ6$^+$ T cells. Of note, miR-181 was reported to be essential in NKT cell development (123, 124). Interestingly, the group of Immo Prinz studied the impact of miR-181a/b-1 deficiency on γδT cell development. While thymic Vγ1$^+$ and Vγ4$^+$ T cell subsets were unaltered in the absence of miR-181a/b-1, authors reported a higher frequency of thymic, but not peripheral Vγ6$^+$ cells in miR-181a/b-1-deficient mice (125). The reason that underlines this feature is currently unknown. However, since miR-181 is a well-known positive regulator of the TCR signal strength (126), it is tempting to hypothesize that a reduced TCR signaling confers an advantage for Vγ6$^+$ T cell differentiation. Thus, defining the miRome of developing γδT17 cells will potentially bring a novel layer of complexity in their developmental program.

Even if these *in silico* analyses suggest a role for scantily explored biological pathways in γδT17 cell development and/or maintenance, supportive experimental data are clearly required to explore these predictive hypotheses. It is noteworthy that these proposed biological pathways are not meant to be Vγ6$^+$ cell-specific and, therefore, it does not preclude that other cell types including other γδT cell subsets may rely on similar biological pathways to develop. In addition, instruction that drives γδT17 effector fate is likely to start early in thymocyte development [even before TCR rearrangement (49)]; therefore, comparing immature vs mature populations probably induced an important bias in our analysis.

CONCLUDING REMARKS

Despite the considerable body of work performed in the field of γδT17 cell ontogeny, many questions remain unsolved and sometimes appear more complex than initially thought. Even if revealing bulk transcriptomes have been informative to predict the developmental program of γδT17 cells, they present a major drawback since this kind of analysis does not reflect the dynamic aspect of the development. In this context, the recent and rapid evolution in single cell deep RNA sequencing and bioinformatics technologies will undoubtedly help to reveal the developmental "trajectories" that dictate γδT17 cell effector fate. In addition, other layers of regulation such as post-transcriptional (especially epigenetic) regulation and implication of microRNAs deserve further investigations and will have to be integrated in order to better decipher the general mechanism(s) driving γδT17 cell development. Given the critical role of γδT17 cells in major health concerns such as infections and cancer, advances in these fundamental biological processes are clearly mandatory.

AUTHOR CONTRIBUTIONS

YJ, EP, MH, MS-T, TB, and CP prepared and wrote the manuscript.

ACKNOWLEDGMENTS

YJ is a recipient of a PhD scholarship (poste d'acceuil) from INSERM. MS-T and CP are supported by INSERM. TB is supported by the University of Tours. We apologize to colleagues whose works could not be cited due to space constraints. This work benefited from data assembled by the ImmGen consortium. Some of the figures were created using the vector image bank of Servier Medical Art (http://smart.servier.com/). Servier Medical Art by Servier is licensed under a Creative Commons Attribution 3.0 Unported License (https://creativecommons.org/licenses/by/3.0/).

FUNDING

This work was supported by the recurrent annual financial support from INSERM and by a grant from the "Institut National du Cancer" (INCa, PLBIO14-155) as well as a grant from the Région Centre-Val-de-Loire (project 7UP).

SUPPLEMENTARY MATERIAL

The Supplementary Material for this article can be found online at https://www.frontiersin.org/articles/10.3389/fimmu.2018.00981/full#supplementary-material.

REFERENCES

1. Gaffen SL, Jain R, Garg AV, Cua DJ. The IL-23-IL-17 immune axis: from mechanisms to therapeutic testing. *Nat Rev Immunol* (2014) 14:585–600. doi:10.1038/nri3707
2. Veldhoen M. Interleukin 17 is a chief orchestrator of immunity. *Nat Immunol* (2017) 18:612–21. doi:10.1038/ni.3742
3. Zou W, Restifo NP. T(H)17 cells in tumour immunity and immunotherapy. *Nat Rev Immunol* (2010) 10:248–56. doi:10.1038/nri2742
4. Miossec P, Kolls JK. Targeting IL-17 and TH17 cells in chronic inflammation. *Nat Rev Drug Discov* (2012) 11:763–76. doi:10.1038/nrd3794
5. Harrington LE, Hatton RD, Mangan PR, Turner H, Murphy TL, Murphy KM, et al. Interleukin 17-producing CD4+ effector T cells develop via a lineage distinct from the T helper type 1 and 2 lineages. *Nat Immunol* (2005) 6:1123–32. doi:10.1038/ni1254
6. Langrish CL, Chen Y, Blumenschein WM, Mattson J, Basham B, Sedgwick JD, et al. IL-23 drives a pathogenic T cell population that induces autoimmune inflammation. *J Exp Med* (2005) 201:233–40. doi:10.1084/jem.20041257
7. Cua DJ, Tato CM. Innate IL-17-producing cells: the sentinels of the immune system. *Nat Rev Immunol* (2010) 10:479–89. doi:10.1038/nri2800
8. Sutton CE, Lalor SJ, Sweeney CM, Brereton CF, Lavelle EC, Mills KHG. Interleukin-1 and IL-23 induce innate IL-17 production from gammadelta T cells, amplifying Th17 responses and autoimmunity. *Immunity* (2009) 31:331–41. doi:10.1016/j.immuni.2009.08.001
9. Michel M-L, Keller AC, Paget C, Fujio M, Trottein F, Savage PB, et al. Identification of an IL-17-producing NK1.1(neg) iNKT cell population involved in airway neutrophilia. *J Exp Med* (2007) 204:995–1001. doi:10.1084/jem.20061551
10. Dusseaux M, Martin E, Serriari N, Péguillet I, Premel V, Louis D, et al. Human MAIT cells are xenobiotic-resistant, tissue-targeted, CD161hi IL-17-secreting T cells. *Blood* (2011) 117:1250–9. doi:10.1182/blood-2010-08-303339
11. Crellin NK, Trifari S, Kaplan CD, Satoh-Takayama N, Di Santo JP, Spits H. Regulation of cytokine secretion in human CD127(+) LTi-like innate lymphoid cells by toll-like receptor 2. *Immunity* (2010) 33:752–64. doi:10.1016/j.immuni.2010.10.012
12. Nielsen MM, Witherden DA, Havran WL. γδ T cells in homeostasis and host defence of epithelial barrier tissues. *Nat Rev Immunol* (2017) 17:733–45. doi:10.1038/nri.2017.101
13. Heilig JS, Tonegawa S. Diversity of murine gamma genes and expression in fetal and adult T lymphocytes. *Nature* (1986) 322:836–40. doi:10.1038/322836a0
14. Ribot JC, deBarros A, Pang DJ, Neves JF, Peperzak V, Roberts SJ, et al. CD27 is a thymic determinant of the balance between interferon-gamma- and interleukin 17-producing gammadelta T cell subsets. *Nat Immunol* (2009) 10:427–36. doi:10.1038/ni.1717
15. Haas JD, González FHM, Schmitz S, Chennupati V, Föhse L, Kremmer E, et al. CCR6 and NK1.1 distinguish between IL-17A and IFN-gamma-producing gammadelta effector T cells. *Eur J Immunol* (2009) 39:3488–97. doi:10.1002/eji.200939922
16. Lalor SJ, Dungan LS, Sutton CE, Basdeo SA, Fletcher JM, Mills KHG. Caspase-1-processed cytokines IL-1beta and IL-18 promote IL-17 production by gammadelta and CD4 T cells that mediate autoimmunity. *J Immunol* (2011) 186:5738–48. doi:10.4049/jimmunol.1003597
17. Papotto PH, Ribot JC, Silva-Santos B. IL-17+ γδ T cells as kick-starters of inflammation. *Nat Immunol* (2017) 18:604–11. doi:10.1038/ni.3726
18. McKenzie DR, Kara EE, Bastow CR, Tyllis TS, Fenix KA, Gregor CE, et al. IL-17-producing γδ T cells switch migratory patterns between resting and activated states. *Nat Commun* (2017) 8:15632. doi:10.1038/ncomms15632
19. Duan J, Chung H, Troy E, Kasper DL. Microbial colonization drives expansion of IL-1 receptor 1-expressing and IL-17-producing gamma/delta T cells. *Cell Host Microbe* (2010) 7:140–50. doi:10.1016/j.chom.2010.01.005
20. Paget C, Chow MT, Gherardin NA, Beavis PA, Uldrich AP, Duret H, et al. CD3bright signals on γδ T cells identify IL-17A-producing Vγ6Vδ1+ T cells. *Immunol Cell Biol* (2015) 93:198–212. doi:10.1038/icb.2014.94
21. Muzaki ARBM, Soncin I, Setiagani YA, Sheng J, Tetlak P, Karjalainen K, et al. Long-lived innate IL-17-producing γ/δ T cells modulate antimicrobial epithelial host defense in the colon. *J Immunol* (2017) 199:3691–9. doi:10.4049/jimmunol.1701053
22. Sheridan BS, Romagnoli PA, Pham Q-M, Fu H-H, Alonzo F, Schubert W-D, et al. γδ T cells exhibit multifunctional and protective memory in intestinal tissues. *Immunity* (2013) 39:184–95. doi:10.1016/j.immuni.2013.06.015
23. Barros-Martins J, Schmolka N, Fontinha D, Pires de Miranda M, Simas JP, Brok I, et al. Effector γδ T cell differentiation relies on master but not auxiliary Th cell transcription factors. *J Immunol* (2016) 196:3642–52. doi:10.4049/jimmunol.1501921
24. Lukens JR, Barr MJ, Chaplin DD, Chi H, Kanneganti T-D. Inflammasome-derived IL-1β regulates the production of GM-CSF by CD4(+) T cells and γδ T cells. *J Immunol* (2012) 188:3107–15. doi:10.4049/jimmunol.1103308
25. Mielke LA, Jones SA, Raverdeau M, Higgs R, Stefanska A, Groom JR, et al. Retinoic acid expression associates with enhanced IL-22 production by γδ T cells and innate lymphoid cells and attenuation of intestinal inflammation. *J Exp Med* (2013) 210:1117–24. doi:10.1084/jem.20121588
26. Zeng X, Wei Y-L, Huang J, Newell EW, Yu H, Kidd BA, et al. γδ T cells recognize a microbial encoded B cell antigen to initiate a rapid antigen-specific interleukin-17 response. *Immunity* (2012) 37:524–34. doi:10.1016/j.immuni.2012.06.011
27. Scott-Browne JP, Matsuda JL, Mallevaey T, White J, Borg NA, McCluskey J, et al. Germline-encoded recognition of diverse glycolipids by natural killer T cells. *Nat Immunol* (2007) 8:1105–13. doi:10.1038/ni1510
28. Deng L, Velikovsky CA, Xu G, Iyer LM, Tasumi S, Kerzic MC, et al. A structural basis for antigen recognition by the T cell-like lymphocytes of sea lamprey. *Proc Natl Acad Sci U S A* (2010) 107:13408–13. doi:10.1073/pnas.1005475107
29. Schmolka N, Serre K, Grosso AR, Rei M, Pennington DJ, Gomes AQ, et al. Epigenetic and transcriptional signatures of stable versus plastic differentiation of proinflammatory γδ T cell subsets. *Nat Immunol* (2013) 14:1093–100. doi:10.1038/ni.2702
30. Hamada S, Umemura M, Shiono T, Hara H, Kishihara K, Tanaka K, et al. Importance of murine Vdelta1gammadelta T cells expressing interferon-gamma and interleukin-17A in innate protection against *Listeria monocytogenes* infection. *Immunology* (2008) 125:170–7. doi:10.1111/j.1365-2567.2008.02841.x
31. Turchinovich G, Hayday AC. Skint-1 identifies a common molecular mechanism for the development of interferon-γ-secreting versus interleukin-17-secreting γδ T cells. *Immunity* (2011) 35:59–68. doi:10.1016/j.immuni.2011.04.018

32. MacLeod AS, Hemmers S, Garijo O, Chabod M, Mowen K, Witherden DA, et al. Dendritic epidermal T cells regulate skin antimicrobial barrier function. *J Clin Invest* (2013) 123:4364–74. doi:10.1172/JCI70064
33. Gray EE, Suzuki K, Cyster JG. Cutting edge: identification of a motile IL-17-producing gammadelta T cell population in the dermis. *J Immunol* (2011) 186:6091–5. doi:10.4049/jimmunol.1100427
34. Deknuydt F, Scotet E, Bonneville M. Modulation of inflammation through IL-17 production by gammadelta T cells: mandatory in the mouse, dispensable in humans? *Immunol Lett* (2009) 127:8–12. doi:10.1016/j.imlet.2009.08.003
35. Ribot JC, Ribeiro ST, Correia DV, Sousa AE, Silva-Santos B. Human γδ thymocytes are functionally immature and differentiate into cytotoxic type 1 effector T cells upon IL-2/IL-15 signaling. *J Immunol* (2014) 192:2237–43. doi:10.4049/jimmunol.1303119
36. LeFranc MP, Forster A, Baer R, Stinson MA, Rabbitts TH. Diversity and rearrangement of the human T cell rearranging gamma genes: nine germline variable genes belonging to two subgroups. *Cell* (1986) 45:237–46. doi:10.1016/0092-8674(86)90388-0
37. Michel M-L, Pang DJ, Haque SFY, Potocnik AJ, Pennington DJ, Hayday AC. Interleukin 7 (IL-7) selectively promotes mouse and human IL-17-producing γδ cells. *Proc Natl Acad Sci U S A* (2012) 109:17549–54. doi:10.1073/pnas.1204327109
38. Caccamo N, La Mendola C, Orlando V, Meraviglia S, Todaro M, Stassi G, et al. Differentiation, phenotype, and function of interleukin-17-producing human Vγ9Vδ2 T cells. *Blood* (2011) 118:129–38. doi:10.1182/blood-2011-01-331298
39. Ness-Schwickerath KJ, Jin C, Morita CT. Cytokine requirements for the differentiation and expansion of IL-17A- and IL-22-producing human Vgamma2Vdelta2 T cells. *J Immunol* (2010) 184:7268–80. doi:10.4049/jimmunol.1000600
40. Moens E, Brouwer M, Dimova T, Goldman M, Willems F, Vermijlen D. IL-23R and TCR signaling drives the generation of neonatal Vgamma9Vdelta2 T cells expressing high levels of cytotoxic mediators and producing IFN-gamma and IL-17. *J Leukoc Biol* (2011) 89:743–52. doi:10.1189/jlb.0910501
41. O'Brien RL, Roark CL, Jin N, Aydintug MK, French JD, Chain JL, et al. gammadelta T-cell receptors: functional correlations. *Immunol Rev* (2007) 215:77–88. doi:10.1111/j.1600-065X.2006.00477.x
42. Ravens S, Schultze-Florey C, Raha S, Sandrock I, Drenker M, Oberdörfer L, et al. Human γδ T cells are quickly reconstituted after stem-cell transplantation and show adaptive clonal expansion in response to viral infection. *Nat Immunol* (2017) 18:393–401. doi:10.1038/ni.3686
43. Davey MS, Willcox CR, Joyce SP, Ladell K, Kasatskaya SA, McLaren JE, et al. Clonal selection in the human Vδ1 T cell repertoire indicates γδ TCR-dependent adaptive immune surveillance. *Nat Commun* (2017) 8:14760. doi:10.1038/ncomms14760
44. Fenoglio D, Poggi A, Catellani S, Battaglia F, Ferrera A, Setti M, et al. Vdelta1 T lymphocytes producing IFN-gamma and IL-17 are expanded in HIV-1-infected patients and respond to *Candida albicans*. *Blood* (2009) 113:6611–8. doi:10.1182/blood-2009-01-198028
45. Wu P, Wu D, Ni C, Ye J, Chen W, Hu G, et al. γδT17 cells promote the accumulation and expansion of myeloid-derived suppressor cells in human colorectal cancer. *Immunity* (2014) 40:785–800. doi:10.1016/j.immuni.2014.03.013
46. Shibata K, Yamada H, Nakamura M, Hatano S, Katsuragi Y, Kominami R, et al. IFN-γ-producing and IL-17-producing γδ T cells differentiate at distinct developmental stages in murine fetal thymus. *J Immunol* (2014) 192:2210–8. doi:10.4049/jimmunol.1302145
47. Prinz I, Silva-Santos B, Pennington DJ. Functional development of γδ T cells. *Eur J Immunol* (2013) 43:1988–94. doi:10.1002/eji.201343759
48. Chien Y, Zeng X, Prinz I. The natural and the inducible: IL-17 producing gamma delta T cells. *Trends Immunol* (2013) 34:151–4. doi:10.1016/j.it.2012.11.004
49. Haas JD, Ravens S, Düber S, Sandrock I, Oberdörfer L, Kashani E, et al. Development of interleukin-17-producing γδ T cells is restricted to a functional embryonic wave. *Immunity* (2012) 37:48–59. doi:10.1016/j.immuni.2012.06.003
50. Gray EE, Ramírez-Valle F, Xu Y, Wu S, Wu Z, Karjalainen KE, et al. Deficiency in IL-17-committed Vγ4(+) γδ T cells in a spontaneous Sox13-mutant CD45.1(+) congenic mouse substrain provides protection from dermatitis. *Nat Immunol* (2013) 14:584–92. doi:10.1038/ni.2585
51. Roark CL, Aydintug MK, Lewis J, Yin X, Lahn M, Hahn Y-S, et al. Subset-specific, uniform activation among V gamma 6/V delta 1+ gamma delta T cells elicited by inflammation. *J Leukoc Biol* (2004) 75:68–75. doi:10.1189/jlb.0703326
52. Shibata K, Yamada H, Nakamura R, Sun X, Itsumi M, Yoshikai Y. Identification of CD25+ gamma delta T cells as fetal thymus-derived naturally occurring IL-17 producers. *J Immunol* (2008) 181:5940–7. doi:10.4049/jimmunol.181.9.5940
53. Zarin P, Chen ELY, In TSH, Anderson MK, Zúñiga-Pflücker JC. Gamma delta T-cell differentiation and effector function programming, TCR signal strength, when and how much? *Cell Immunol* (2015) 296:70–5. doi:10.1016/j.cellimm.2015.03.007
54. Bonneville M, Ito K, Krecko EG, Itohara S, Kappes D, Ishida I, et al. Recognition of a self major histocompatibility complex TL region product by gamma delta T-cell receptors. *Proc Natl Acad Sci U S A* (1989) 86:5928–32. doi:10.1073/pnas.86.15.5928
55. Kashani E, Föhse L, Raha S, Sandrock I, Oberdörfer L, Koenecke C, et al. A clonotypic Vγ4Jγ1/Vδ5Dδ2Jδ1 innate γδ T-cell population restricted to the $CCR6^{+}CD27^{-}$ subset. *Nat Commun* (2015) 6:6477. doi:10.1038/ncomms7477
56. Papotto PH, Gonçalves-Sousa N, Schmolka N, Iseppon A, Mensurado S, Stockinger B, et al. IL-23 drives differentiation of peripheral γδ17 T cells from adult bone marrow-derived precursors. *EMBO Rep* (2017) 18:1957–67. doi:10.15252/embr.201744200
57. Muschaweckh A, Petermann F, Korn T. IL-1β and IL-23 promote extrathymic commitment of CD27+CD122-γδ T cells to γδT17 cells. *J Immunol* (2017) 199:2668–79. doi:10.4049/jimmunol.1700287
58. Buus TB, Ødum N, Geisler C, Lauritsen JPH. Three distinct developmental pathways for adaptive and two IFN-γ-producing γδ T subsets in adult thymus. *Nat Commun* (2017) 8:1911. doi:10.1038/s41467-017-01963-w
59. Ciofani M, Zúñiga-Pflücker JC. Determining γδ versus αß T cell development. *Nat Rev Immunol* (2010) 10:657–63. doi:10.1038/nri2820
60. Carpenter AC, Bosselut R. Decision checkpoints in the thymus. *Nat Immunol* (2010) 11:666–73. doi:10.1038/ni.1887
61. Hayday AC, Saito H, Gillies SD, Kranz DM, Tanigawa G, Eisen HN, et al. Structure, organization, and somatic rearrangement of T cell gamma genes. *Cell* (1985) 40:259–69. doi:10.1016/0092-8674(85)90140-0
62. Fry TJ, Mackall CL. The many faces of IL-7: from lymphopoiesis to peripheral T cell maintenance. *J Immunol* (2005) 174:6571–6. doi:10.4049/jimmunol.174.11.6571
63. Maki K, Sunaga S, Ikuta K. The V-J recombination of T cell receptor-gamma genes is blocked in interleukin-7 receptor-deficient mice. *J Exp Med* (1996) 184:2423–7. doi:10.1084/jem.184.6.2423
64. He YW, Malek TR. Interleukin-7 receptor alpha is essential for the development of gamma delta + T cells, but not natural killer cells. *J Exp Med* (1996) 184:289–93. doi:10.1084/jem.184.1.289
65. Appasamy PM, Kenniston TW, Weng Y, Holt EC, Kost J, Chambers WH. Interleukin 7-induced expression of specific T cell receptor gamma variable region genes in murine fetal liver cultures. *J Exp Med* (1993) 178:2201–6. doi:10.1084/jem.178.6.2201
66. Patin EC, Soulard D, Fleury S, Hassane M, Dombrowicz D, Faveeuw C, et al. Type I IFN receptor signaling controls IL7-dependent accumulation and activity of protumoral IL17A-producing γδT cells in breast cancer. *Cancer Res* (2018) 78:195–204. doi:10.1158/0008-5472.CAN-17-1416
67. Rei M, Gonçalves-Sousa N, Lança T, Thompson RG, Mensurado S, Balkwill FR, et al. Murine CD27(-) Vγ6(+) γδ T cells producing IL-17A promote ovarian cancer growth via mobilization of protumor small peritoneal macrophages. *Proc Natl Acad Sci U S A* (2014) 111:E3562–70. doi:10.1073/pnas.1403424111
68. Nakamura M, Shibata K, Hatano S, Sato T, Ohkawa Y, Yamada H, et al. A genome-wide analysis identifies a notch-RBP-Jκ-IL-7Rα axis that controls IL-17-producing γδ T cell homeostasis in mice. *J Immunol* (2015) 194:243–51. doi:10.4049/jimmunol.1401619
69. Fujikado N, Mann AO, Bansal K, Romito KR, Ferre EMN, Rosenzweig SD, et al. Aire inhibits the generation of a perinatal population of interleukin-17A-producing γδ T cells to promote immunologic tolerance. *Immunity* (2016) 45:999–1012. doi:10.1016/j.immuni.2016.10.023
70. Alves NL, Richard-Le Goff O, Huntington ND, Sousa AP, Ribeiro VSG, Bordack A, et al. Characterization of the thymic IL-7 niche in vivo. *Proc Natl Acad Sci U S A* (2009) 106:1512–7. doi:10.1073/pnas.0809559106

71. Do J, Fink PJ, Li L, Spolski R, Robinson J, Leonard WJ, et al. Cutting edge: spontaneous development of IL-17-producing gamma delta T cells in the thymus occurs via a TGF-beta 1-dependent mechanism. *J Immunol* (2010) 184:1675–9. doi:10.4049/jimmunol.0903539
72. Lochner M, Peduto L, Cherrier M, Sawa S, Langa F, Varona R, et al. In vivo equilibrium of proinflammatory IL-17+ and regulatory IL-10+ Foxp3+ RORgamma t+ T cells. *J Exp Med* (2008) 205:1381–93. doi:10.1084/jem.20080034
73. Hayes SM, Laird RM. Genetic requirements for the development and differentiation of interleukin-17-producing γδ T cells. *Crit Rev Immunol* (2012) 32:81–95. doi:10.1615/CritRevImmunol.v32.i1.50
74. Petermann F, Rothhammer V, Claussen MC, Haas JD, Blanco LR, Heink S, et al. γδ T cells enhance autoimmunity by restraining regulatory T cell responses via an interleukin-23-dependent mechanism. *Immunity* (2010) 33:351–63. doi:10.1016/j.immuni.2010.08.013
75. Nitta T, Muro R, Shimizu Y, Nitta S, Oda H, Ohte Y, et al. The thymic cortical epithelium determines the TCR repertoire of IL-17-producing γδT cells. *EMBO Rep* (2015) 16:638–53. doi:10.15252/embr.201540096
76. Takahama Y, Letterio JJ, Suzuki H, Farr AG, Singer A. Early progression of thymocytes along the CD4/CD8 developmental pathway is regulated by a subset of thymic epithelial cells expressing transforming growth factor beta. *J Exp Med* (1994) 179:1495–506. doi:10.1084/jem.179.5.1495
77. Ribeiro AR, Rodrigues PM, Meireles C, Di Santo JP, Alves NL. Thymocyte selection regulates the homeostasis of IL-7-expressing thymic cortical epithelial cells in vivo. *J Immunol* (2013) 191:1200–9. doi:10.4049/jimmunol.1203042
78. Shibata K, Yamada H, Sato T, Dejima T, Nakamura M, Ikawa T, et al. Notch-Hes1 pathway is required for the development of IL-17-producing γδ T cells. *Blood* (2011) 118:586–93. doi:10.1182/blood-2011-02-334995
79. Mair F, Joller S, Hoeppli R, Onder L, Hahn M, Ludewig B, et al. The NFκB-inducing kinase is essential for the developmental programming of skin-resident and IL-17-producing γδ T cells. *Elife* (2015) 4:e10087. doi:10.7554/eLife.10087
80. Jensen KDC, Su X, Shin S, Li L, Youssef S, Yamasaki S, et al. Thymic selection determines gammadelta T cell effector fate: antigen-naive cells make interleukin-17 and antigen-experienced cells make interferon gamma. *Immunity* (2008) 29:90–100. doi:10.1016/j.immuni.2008.04.022
81. Muñoz-Ruiz M, Ribot JC, Grosso AR, Gonçalves-Sousa N, Pamplona A, Pennington DJ, et al. TCR signal strength controls thymic differentiation of discrete proinflammatory γδ T cell subsets. *Nat Immunol* (2016) 17:721–7. doi:10.1038/ni.3424
82. Sumaria N, Grandjean CL, Silva-Santos B, Pennington DJ. Strong TCRγδ signaling prohibits thymic development of IL-17A-secreting γδ T cells. *Cell Rep* (2017) 19:2469–76. doi:10.1016/j.celrep.2017.05.071
83. Wencker M, Turchinovich G, Di Marco Barros R, Deban L, Jandke A, Cope A, et al. Innate-like T cells straddle innate and adaptive immunity by altering antigen-receptor responsiveness. *Nat Immunol* (2014) 15:80–7. doi:10.1038/ni.2773
84. Vantourout P, Laing A, Woodward MJ, Zlatareva I, Apolonia L, Jones AW, et al. Heteromeric interactions regulate butyrophilin (BTN) and BTN-like molecules governing γδ T cell biology. *Proc Natl Acad Sci U S A* (2018) 115:1039–44. doi:10.1073/pnas.1701237115
85. Di Marco Barros R, Roberts NA, Dart RJ, Vantourout P, Jandke A, Nussbaumer O, et al. Epithelia use butyrophilin-like molecules to shape organ-specific γδ T cell compartments. *Cell* (2016) 167:203–218.e17. doi:10.1016/j.cell.2016.08.030
86. Buus TB, Schmidt JD, Bonefeld CM, Geisler C, Lauritsen JPH. Development of interleukin-17-producing Vγ2+ γδ T cells is reduced by ICOS signaling in the thymus. *Oncotarget* (2016) 7:19341–54. doi:10.18632/oncotarget.8464
87. Silva-Santos B, Pennington DJ, Hayday AC. Lymphotoxin-mediated regulation of gammadelta cell differentiation by alphabeta T cell progenitors. *Science* (2005) 307:925–8. doi:10.1126/science.1103978
88. Powolny-Budnicka I, Riemann M, Tänzer S, Schmid RM, Hehlgans T, Weih F. RelA and RelB transcription factors in distinct thymocyte populations control lymphotoxin-dependent interleukin-17 production in γδ T cells. *Immunity* (2011) 34:364–74. doi:10.1016/j.immuni.2011.02.019
89. Jaffar Z, Ferrini ME, Shaw PK, FitzGerald GA, Roberts K. Prostaglandin I_2 promotes the development of IL-17-producing γδ T cells that associate with the epithelium during allergic lung inflammation. *J Immunol* (2011) 187:5380–91. doi:10.4049/jimmunol.1101261
90. Ivanov II, McKenzie BS, Zhou L, Tadokoro CE, Lepelley A, Lafaille JJ, et al. The orphan nuclear receptor RORgammat directs the differentiation program of proinflammatory IL-17+ T helper cells. *Cell* (2006) 126:1121–33. doi:10.1016/j.cell.2006.07.035
91. Narayan K, Sylvia KE, Malhotra N, Yin CC, Martens G, Vallerskog T, et al. Intrathymic programming of effector fates in three molecularly distinct γδ T cell subtypes. *Nat Immunol* (2012) 13:511–8. doi:10.1038/ni.2247
92. Malhotra N, Narayan K, Cho OH, Sylvia KE, Yin C, Melichar H, et al. A network of high-mobility group box transcription factors programs innate interleukin-17 production. *Immunity* (2013) 38:681–93. doi:10.1016/j.immuni.2013.01.010
93. Xing S, Li F, Zeng Z, Zhao Y, Yu S, Shan Q, et al. Tcf1 and Lef1 transcription factors establish CD8(+) T cell identity through intrinsic HDAC activity. *Nat Immunol* (2016) 17:695–703. doi:10.1038/ni.3456
94. Laird RM, Laky K, Hayes SM. Unexpected role for the B cell-specific Src family kinase B lymphoid kinase in the development of IL-17-producing γδ T cells. *J Immunol* (2010) 185:6518–27. doi:10.4049/jimmunol.1002766
95. Tretter T, Ross AE, Dordai DI, Desiderio S. Mimicry of pre-B cell receptor signaling by activation of the tyrosine kinase Blk. *J Exp Med* (2003) 198:1863–73. doi:10.1084/jem.20030729
96. In TSH, Trotman-Grant A, Fahl S, Chen ELY, Zarin P, Moore AJ, et al. HEB is required for the specification of fetal IL-17-producing γδ T cells. *Nat Commun* (2017) 8:2004. doi:10.1038/s41467-017-02225-5
97. Savage AK, Constantinides MG, Han J, Picard D, Martin E, Li B, et al. The transcription factor PLZF directs the effector program of the NKT cell lineage. *Immunity* (2008) 29:391–403. doi:10.1016/j.immuni.2008.07.011
98. Constantinides MG, McDonald BD, Verhoef PA, Bendelac A. A committed precursor to innate lymphoid cells. *Nature* (2014) 508:397–401. doi:10.1038/nature13047
99. Kovalovsky D, Uche OU, Eladad S, Hobbs RM, Yi W, Alonzo E, et al. The BTB-zinc finger transcriptional regulator PLZF controls the development of invariant natural killer T cell effector functions. *Nat Immunol* (2008) 9:1055–64. doi:10.1038/ni.1641
100. Lu Y, Cao X, Zhang X, Kovalovsky D. PLZF controls the development of fetal-derived IL-17+Vγ6+ γδ T cells. *J Immunol* (2015) 195:4273–81. doi:10.4049/jimmunol.1500939
101. Yu Q, Erman B, Park J-H, Feigenbaum L, Singer A. IL-7 receptor signals inhibit expression of transcription factors TCF-1, LEF-1, and RORgammat: impact on thymocyte development. *J Exp Med* (2004) 200:797–803. doi:10.1084/jem.20032183
102. Jojic V, Shay T, Sylvia K, Zuk O, Sun X, Kang J, et al. Identification of transcriptional regulators in the mouse immune system. *Nat Immunol* (2013) 14:633–43. doi:10.1038/ni.2587
103. Pham D, Sehra S, Sun X, Kaplan MH. The transcription factor Etv5 controls TH17 cell development and allergic airway inflammation. *J Allergy Clin Immunol* (2014) 134:204–14. doi:10.1016/j.jaci.2013.12.021
104. Lee YJ, Starrett GJ, Lee ST, Yang R, Henzler CM, Jameson SC, et al. Lineage-specific effector signatures of invariant NKT cells are shared amongst γδ T, innate lymphoid, and Th cells. *J Immunol* (2016) 197:1460–70. doi:10.4049/jimmunol.1600643
105. Sekiya T, Kashiwagi I, Yoshida R, Fukaya T, Morita R, Kimura A, et al. Nr4a receptors are essential for thymic regulatory T cell development and immune homeostasis. *Nat Immunol* (2013) 14:230–7. doi:10.1038/ni.2520
106. Yu S, Bruce D, Froicu M, Weaver V, Cantorna MT. Failure of T cell homing, reduced CD4/CD8alphaalpha intraepithelial lymphocytes, and inflammation in the gut of vitamin D receptor KO mice. *Proc Natl Acad Sci U S A* (2008) 105:20834–9. doi:10.1073/pnas.0808700106
107. Emgård J, Kammoun H, García-Cassani B, Chesné J, Parigi SM, Jacob J-M, et al. Oxysterol sensing through the receptor GPR183 promotes the lymphoid-tissue-inducing function of innate lymphoid cells and colonic inflammation. *Immunity* (2018) 48:120–132.e8. doi:10.1016/j.immuni.2017.11.020
108. Soroosh P, Wu J, Xue X, Song J, Sutton SW, Sablad M, et al. Oxysterols are agonist ligands of RORγt and drive Th17 cell differentiation. *Proc Natl Acad Sci U S A* (2014) 111:12163–8. doi:10.1073/pnas.1322807111
109. Kjer-Nielsen L, Patel O, Corbett AJ, Le Nours J, Meehan B, Liu L, et al. MR1 presents microbial vitamin B metabolites to MAIT cells. *Nature* (2012) 491:717–23. doi:10.1038/nature11605
110. van de Pavert SA, Ferreira M, Domingues RG, Ribeiro H, Molenaar R, Moreira-Santos L, et al. Maternal retinoids control type 3 innate lymphoid

cells and set the offspring immunity. *Nature* (2014) 508:123–7. doi:10.1038/nature13158
111. Silva AB, Palmer DB. Evidence of conserved neuroendocrine interactions in the thymus: intrathymic expression of neuropeptides in mammalian and non-mammalian vertebrates. *Neuroimmunomodulation* (2011) 18:264–70. doi:10.1159/000329493
112. Solomou K, Ritter MA, Palmer DB. Somatostatin is expressed in the murine thymus and enhances thymocyte development. *Eur J Immunol* (2002) 32:1550–9. doi:10.1002/1521-4141(200206)32:6<1550::AID-IMMU1550>3.0.CO;2-W
113. Bass J, Lazar MA. Circadian time signatures of fitness and disease. *Science* (2016) 354:994–9. doi:10.1126/science.aah4965
114. Honma S, Kawamoto T, Takagi Y, Fujimoto K, Sato F, Noshiro M, et al. Dec1 and Dec2 are regulators of the mammalian molecular clock. *Nature* (2002) 419:841–4. doi:10.1038/nature01123
115. Scheiermann C, Kunisaki Y, Frenette PS. Circadian control of the immune system. *Nat Rev Immunol* (2013) 13:190–8. doi:10.1038/nri3386
116. Yu X, Rollins D, Ruhn KA, Stubblefield JJ, Green CB, Kashiwada M, et al. TH17 cell differentiation is regulated by the circadian clock. *Science* (2013) 342:727–30. doi:10.1126/science.1243884
117. Seillet C, Huntington ND, Gangatirkar P, Axelsson E, Minnich M, Brady HJM, et al. Differential requirement for Nfil3 during NK cell development. *J Immunol* (2014) 192:2667–76. doi:10.4049/jimmunol.1302605
118. Gascoyne DM, Long E, Veiga-Fernandes H, de Boer J, Williams O, Seddon B, et al. The basic leucine zipper transcription factor E4BP4 is essential for natural killer cell development. *Nat Immunol* (2009) 10:1118–24. doi:10.1038/ni.1787
119. Xu W, Domingues RG, Fonseca-Pereira D, Ferreira M, Ribeiro H, Lopez-Lastra S, et al. NFIL3 orchestrates the emergence of common helper innate lymphoid cell precursors. *Cell Rep* (2015) 10:2043–54. doi:10.1016/j.celrep.2015.02.057
120. Gerriets VA, Kishton RJ, Nichols AG, Macintyre AN, Inoue M, Ilkayeva O, et al. Metabolic programming and PDHK1 control CD4+ T cell subsets and inflammation. *J Clin Invest* (2015) 125:194–207. doi:10.1172/JCI76012
121. Michalek RD, Gerriets VA, Jacobs SR, Macintyre AN, MacIver NJ, Mason EF, et al. Cutting edge: distinct glycolytic and lipid oxidative metabolic programs are essential for effector and regulatory CD4+ T cell subsets. *J Immunol* (2011) 186:3299–303. doi:10.4049/jimmunol.1003613
122. O'Neill LAJ, Kishton RJ, Rathmell J. A guide to immunometabolism for immunologists. *Nat Rev Immunol* (2016) 16:553–65. doi:10.1038/nri.2016.70
123. Henao-Mejia J, Williams A, Goff LA, Staron M, Licona-Limón P, Kaech SM, et al. The microRNA miR-181 is a critical cellular metabolic rheostat essential for NKT cell ontogenesis and lymphocyte development and homeostasis. *Immunity* (2013) 38:984–97. doi:10.1016/j.immuni.2013.02.021
124. Ziętara N, Łyszkiewicz M, Witzlau K, Naumann R, Hurwitz R, Langemeier J, et al. Critical role for miR-181a/b-1 in agonist selection of invariant natural killer T cells. *Proc Natl Acad Sci U S A* (2013) 110:7407–12. doi:10.1073/pnas.1221984110
125. Sandrock I, Ziętara N, Łyszkiewicz M, Oberdörfer L, Witzlau K, Krueger A, et al. MicroRNA-181a/b-1 Is Not Required for Innate γδ NKT Effector Cell Development. *PLoS One* (2015) 10:e0145010. doi:10.1371/journal.pone.0145010
126. Li Q-J, Chau J, Ebert PJR, Sylvester G, Min H, Liu G, et al. miR-181a is an intrinsic modulator of T cell sensitivity and selection. *Cell* (2007) 129:147–61. doi:10.1016/j.cell.2007.03.008

Conflict of Interest Statement: The authors declare that the research was conducted in the absence of any commercial or financial relationships that could be construed as a potential conflict of interest.

Copyright © 2018 Jouan, Patin, Hassane, Si-Tahar, Baranek and Paget. This is an open-access article distributed under the terms of the Creative Commons Attribution License (CC BY). The use, distribution or reproduction in other forums is permitted, provided the original author(s) and the copyright owner are credited and that the original publication in this journal is cited, in accordance with accepted academic practice. No use, distribution or reproduction is permitted which does not comply with these terms.

frontiers in Immunology

ORIGINAL RESEARCH
published: 07 May 2018
doi: 10.3389/fimmu.2018.00717

Variegated Transcription of the WC1 Hybrid PRR/Co-Receptor Genes by Individual γδ T Cells and Correlation With Pathogen Responsiveness

*Payal Damani-Yokota[1], Janice C. Telfer[1,2] and Cynthia L. Baldwin[1,2]**

[1] Program in Molecular and Cellular Biology, University of Massachusetts, Amherst, MA, United States, [2] Department of Veterinary and Animal Sciences, University of Massachusetts, Amherst, MA, United States

γδ T cells have broad reactivity and actively participate in protective immunity against tumors and infectious disease-causing organisms. In γδ-high species such as ruminants and other artiodactyls many γδ T cells bear the lineage-specific markers known as WC1. WC1 molecules are scavenger receptors coded for by a multigenic array and are closely related to SCART found on murine γδ T cells and CD163 found on a variety of cells. We have previously shown that WC1 molecules are hybrid pattern recognition receptors thereby binding pathogens as well as signaling co-receptors for the γδ T cell receptor. WC1$^+$ γδ T cells can be divided into two major subpopulations differentiated by the WC1 genes they express and the pathogens to which they respond. Therefore, we hypothesize that optimal γδ T cell responses are contingent on pathogen binding to WC1 molecules, especially since we have shown that silencing WC1 results in an inability of γδ T cells from primed animals to respond to the pathogen *Leptospira*, a model system we have employed extensively. Despite this knowledge about the crucial role WC1 plays in γδ T cell biology, the pattern of WC1 gene expression by individual γδ T cells was not known but is critical to devise methods to engage γδ T cells for responses to specific pathogens. To address this gap, we generated 78 γδ T cell clones. qRT-PCR evaluation showed that approximately 75% of the clones had one to three WC1 genes transcribed but up to six per cell occurred. The co-transcription of WC1 genes by clones showed many combinations and some WC1 genes were transcribed by both subpopulations although there were differences in the overall pattern of WC1 genes transcription. Despite this overlap, *Leptospira*-responsive WC1$^+$ memory γδ T cell clones were shown to have a significantly higher propensity to express WC1 molecules that are known to bind to the pathogen.

Keywords: γδ T cells, co-receptors, WC1, T cell receptor, pattern recognition receptors

OPEN ACCESS

Edited by:
David Vermijlen,
Free University of Brussels, Belgium

Reviewed by:
Domenico Mavilio,
Università degli Studi di Milano, Italy
Brandon Lee Plattner,
University of Guelph, Canada

***Correspondence:**
Cynthia L. Baldwin
cbaldwin@umass.edu

Specialty section:
This article was submitted to T Cell Biology, a section of the journal Frontiers in Immunology

Received: *13 January 2018*
Accepted: *22 March 2018*
Published: *07 May 2018*

Citation:
Damani-Yokota P, Telfer JC and Baldwin CL (2018) Variegated Transcription of the WC1 Hybrid PRR/Co-Receptor Genes by Individual γδ T Cells and Correlation With Pathogen Responsiveness. Front. Immunol. 9:717. doi: 10.3389/fimmu.2018.00717

INTRODUCTION

WC1 family members are T cell co-receptors and pathogen recognition receptors uniquely expressed by the majority of γδ T cells in the blood of ruminants (1). Structurally they are Group B scavenger receptor cysteine rich (SRCR) molecules (2) and belong to the CD163 family (2, 3) which also includes the murine γδ T cell marker SCART (3, 4). WC1-expressing γδ T cells in cattle, a γδ T cell high species and our experimental model, are classified into two main subpopulations

referred to as WC1.1$^+$ or WC1.2$^+$ based on expression of different WC1 molecules that react with monoclonal antibodies (mAb) that recognize epitopes in their N-terminal SRCR domains (5). We and others have previously shown that these subpopulations also differ in their responses to pathogens. For example, following *in vivo* priming of cattle cells in the WC1.1$^+$ subpopulation respond by proliferation and interferon-γ production to *Leptospira* spp. in *in vitro* recall responses (6, 7) whereas cells in the WC1.2$^+$ subpopulation respond *in vitro* to other pathogens such as *Anaplasma marginale* following infection (8). When cattle are infected with virulent strains of *Mycobacterium bovis* both WC1$^+$ lineages are recruited to the granulomas in infected cattle (9) but only the WC1.1$^+$ cells respond to the vaccine strain BCG (10). Following *in vivo*-sensitization, these WC1$^+$ mycobacterial-responsive bovine γδ T cells also have been shown to respond in recall responses *in vitro* to both protein and non-protein antigens while WC1$^+$ and CD8$^+$ γδ T cells respond to BCG-infected macrophages (9, 11). Adaptive-like memory γδ T cells are not confined to the bovine model having been described for specific subpopulations of murine γδ T cells (12, 13) and to be sensitized by *Listeria monocytogenes* (14) and *Staphyloccus aureus* (15) *in vivo* while in humans and non-human primates memory γδ T cells responses to mycobacteria (16–18), influenza (19), and malaria (20) have been reported.

The 13 WC1 molecules can be divided into 10 WC1.1-types and 3 WC1.2-types based on signature insertions or deletions of amino acids in their most membrane-distal SRCR domain known as the a1 domain (Figure S1 in Supplementary Material). The first sequenced WC1 genes (21) and therefore considered to be the archetypal WC1.1 [coded for by *WC1-3* (22)] and WC1.2 molecules [coded for by *WC1-4* (22)] differ in their binding to *Leptospira*. As many as five of WC1-3's 11 SRCR domains are engaged, including the a1 domain, while none of the SRCR domains of its WC1.2 counterpart, WC1-4, bind *Leptospira* despite considerable sequence similarity (23). Binding can be disrupted by a single amino acid mutation (23). Four other WC1.1 type molecules also have SRCR domains that bind *Leptospira* but none of the WC1.2 molecules have such domains. This knowledge contributed to our understanding of the dichotomy in the ability of cells in the subpopulations to respond to particular pathogens. We hypothesize that the WC1 molecules expressed by a γδ T cell contribute to its pathogen responsiveness and that co-expression of multiple WC1 gene products that bind the same pathogen could result in increased avidity for the pathogen and amplify the signal in a dose-dependent manner (i.e., the more WC1's of the same or multiple types that bind the pathogen, the stronger the cellular activation signal). The latter is based on our findings that when all (vs. a proportion of) the WC1 receptors are co-crosslinked in conjunction with the γδ T cell receptor (TCR) augmentation of the cellular activation is enhanced (24). Conversely, when WC1 expression is downregulated by RNA silencing there is an abrogation of γδ T cell response (25).

The previous analyses of WC1 transcripts in the subpopulations suggest co-expression of WC1 genes in a variegated pattern. While the WC1.2$^+$ population has transcripts for all three WC1.2-type genes, only two of the three WC1.2-type gene products react with the population-defining mAb (5, 26). This suggests the non-mAb-reactive gene product is co-expressed in cells expressing the mAb-reactive gene product. WC1.3$^+$ cells, a subpopulation of the WC1.1$^+$ population, express at least two WC1 genes based on reactivity with two mAbs: mAb CACT21A that reacts with WC1-8 only and mAb BAG25A that reacts with WC1.1-like molecules but not WC1-8 (5, 24). However, the following questions remained: is there a specific number of different WC1 genes that all WC1$^+$ γδ T cells express and are there set combinations of WC1 genes always expressed together? Understanding the expression of WC1 genes on individual γδ T cells is necessary to build models of how to induce cellular immune responses to specific pathogens. By analyzing WC1$^+$ γδ T cell clones here, we showed that the WC1 locus is permissive for transcription of more than one gene by an individual cell and describe the many combinations of WC1 gene transcription. Finally, using the *Leptospira*-responsive WC1$^+$ memory γδ T cell clones we showed these cells have a high propensity to express WC1 molecules that bind to the pathogen.

MATERIALS AND METHODS

Isolation of Cells and RNA

Whole blood was collected with heparin by jugular venipuncture from a single adult Holstein heifer that had been vaccinated against *Leptospira* serovar Hardjo with a commercial inactivated vaccine (Spirovac, Pfizer) using an initial two-dose regime during calfhood and subsequently boosted intermittently with a single dose during adulthood as approved by the University of Massachusetts IACUC. Rabies vaccines were given. This vaccination procedure in cattle has been shown previously to result in γδ T cells in blood that respond in recall responses when stimulated *in vitro* with *Leptospira* (6, 7, 27). Peripheral blood mononuclear cells (PBMC) were isolated from blood by Ficoll-hypaque density gradient centrifugation. Total RNA was isolated from cells using TRIzol (Invitrogen) with 20 μg of glycogen carrier added after the chloroform step. 0.5–1 μg RNA was treated with 1 U of DNase enzyme (Promega) for 30 min at 37°C, then 70°C for 5 min. RNA purity and concentration were determined by Nanodrop spectrophotometry (Thermo-Fisher). cDNA synthesis was done using a commercial reverse-transcriptase kit (Promega) according to the manufacturer's protocol. For T cell clone cDNA samples, we used Single Cell PreAmp Mix with random primers (Fisher Scientific), at 95°C for 10 min, followed by 14 cycles of 15 s at 95°C and 4 min at 60°C with a final inactivation at 99°C for 10 min.

Lymphocyte Cultures

Lymphocytes were cultured with a modification of the protocol for generating bovine central memory T cells (T_{CM}) (28). Briefly, 2.5×10^6 PBMC were stimulated in a 24-well culture plates in 1 ml of complete RPMI (c-RPMI) medium [RPMI-1640 supplemented with 10% heat-inactivated fetal bovine serum (Hyclone), 200 mM L-glutamine (Sigma), 5×10^{-5} M 2-mercaptoethanol (Sigma) and 10 mg/ml gentamycin (Invitrogen)] with 0.16 μg/ml of sonicated *Leptospira borgpetersenii* serovar Hardjobovis. On days 3 and 7, 0.5 ml of supernatant was removed from each well and replenished with 0.5 ml of c-RPMI containing 30 U/ml of recombinant

bovine IL-2 (rBoIL-2; R&D Systems). On days 10 and 12, 0.5 ml of the supernatant was removed and replaced with fresh c-RPMI medium. This protocol is referred to as the T_{CM} protocol throughout. On day 14, cultures were pooled and washed with sterile PBS and then dye-loaded with 0.5 μM efluor-670 cell division dye (eBioSciences) according to the manufacturer's protocol. Cells were cultured with sonicated *Leptospira* for an additional 7 days; this modification is referred to as the T_{EM} protocol.

Immunofluorescence Staining and Flow Cytometric Sorting

WC1.1$^+$ and WC1.2$^+$ γδ T cell subpopulations were obtained by staining lymphocytes with anti-WC1.1 mAb (BAG25A with anti-Mu IgM-FITC) and anti-WC1.2 mAb (CACTB32A with anti-Mu IgG1-PE). For WC1.3$^+$ cells, lymphocytes were stained with anti-WC1.1 mAb and anti-WC1.3 mAb (CACT21A with anti-Mu IgG1-PE). Double or single-stained cells were sorted using FACS ARIA (BD). To obtain cell populations for T cell expansion, efluor670 dye-loaded cells were washed and stained as above, but sorted on efluor670-APC low cells (indicating multiple cell divisions had occurred in culture) to obtain WC1.1, WC1.2, and WC1.3 cell populations. Evaluation of memory markers by indirect immunofluorescence with mAbs against TCRδ (mAb GB21A, IgG2b), CD44 (mAb BAQ40A, IgG3-PE), and CD62L (mAb BAQ92A, IgG1-PE) and appropriate secondary Abs conjugated to fluorophores was conducted and evaluated by flow cytometry. MAbs were purchased from Washington State University Monoclonal Antibody Center (Pullman, WA, USA), and fluorophore-conjugated secondary polyclonal antibodies were purchased from Southern Biotechnology. All analyses were done using FlowJo v10 (TreeStar, Inc.).[1]

Generation of T Cell Clones

On day 21 of the T_{EM} protocol, sorted WC1$^+$ γδ T cell populations were plated into 96-well round-bottom tissue culture plates at a concentration of 1 cell/well in 100 μl volume. Plated cells were stimulated by adding 5×10^4 irradiated (5,000 rads) autologous PBMC and 10 U/ml rBoIL-2 with or without 0.5 ng/ml rHuIL-15 (R&D Systems) with or without 0.16 μg/ml sonicated *Leptospira borgpetersenii* serovar Hardjbovis. Every 10 days, 100 μl of supernatant from each well was removed and replaced with 100 μl medium containing the same components until cells were harvested. Cell colonies were visible by 20 days after plating in 96-well plates and were harvested in TRIzol for RNA isolation about 7 weeks post-plating. The likelihood that any of the cell colonies had arisen from a single cell was determined by the method of de St. Groth (29). For each putative T cell clone, we harvested between 5×10^4 and 5×10^5 cells for cDNA synthesis. Viable cells were counted in a hemocytometer by microscopy using Trypan Blue exclusion.

Primer Design and qRT-PCR

ClustalW2[2] was used for multiple sequence alignment for bovine WC1 SRCR a1 domains based on accession numbers as published (26) to design TaqMan assays for individual WC1 genes (Figure S1 in Supplementary Material). Custom designed primers and the FAM/MGB fluorophore/quencher system (referred to as TaqMan assays) were prepared by Invitrogen. Additionally, commercially available TaqMan assays for the bovine TCRδ constant gene (TRDC), GAPDH, beta-2 microglobulin, CD4 and CD8α were obtained from Invitrogen (**Table 1**). GAPDH and beta-2 microglobulin were used as housekeeping genes to determine template concentrations while CD4 and CD8α were used as negative controls (data not shown). Amplicons were generated using the Stratagene qPCR system with the following settings: an initial 2 min UDG step followed by 10 min at 95°C and 40 cycles of 15 s at 95°C, and 30 s at 60°C. The mean and SEM of replicate wells for WC1 and TRDC TaqMan assays was calculated for each target.

Amplicons were run on 2% TAE-agarose gels, purified by gel extraction (Qiagen) (Figure S2A in Supplementary Material), cloned into pCR2.1 vector using TOPO-TA (Invitrogen), transformed into ONE-SHOT competent cells (Invitrogen), and plated on LB-kanamycin plates. Bacterial colonies were selected and the plasmids purified using the mini-prep plasmid purification kit (Qiagen). Selected cDNA clones were commercially sequenced by Genewiz (South Plainfield, NJ, USA) and results were analyzed using BioEdit (Version 7.0.5.3) and sequences aligned using Clustalw2 (see text footnote 2) (Figure S2B in Supplementary Material). The primers occasionally amplified a secondary SRCR a1 domain as well as the targeted one, determined by cloning and sequencing the amplicons. We tested for and found no off-target detection with the TaqMan assays (**Table 2**) when using previously generated constructs of WC1 SRCR a1-domain-coding sequences cloned into the pSecTag2 vector (23) as templates (WC1-pST2A). Thus, we interpreted this to mean that the FAM probe corrects any spurious transcript amplification by the primers. For generating standard curves, WC1-pST2A plasmids were diluted to equal concentrations by

TABLE 1 | TaqMan primer/probe assays.

Gene ID	Genbank accession #	TaqMan assay ID	Corresponding plasmid for producing standard curves
wc1-1	FJ031186	AIRSAUH	pSecTag2A-WC1-1
wc1-2	JN998897	AIS080P	pSecTag2A-WC1-2
wc1-3	FJ031191	AIT966X	pSecTag2A-WC1-3
wc1-4	FJ031202	AIVI5C5	pSecTag2A-WC1-4
wc1-5	JQ900627	AIWR3JD	pSecTag2A-WC1-5
wc1-6	JN234380	AIX01PL	pSecTag2A-WC1-6
wc1-7	JN234377	AIY9ZVT	pSecTag2A-WC1-7
wc1-8	JN998896	AI0IX11	pSecTag2A-WC1-8
wc1-9	FJ031208	AI1RV79	pSecTag2A-WC1-9
wc1-10	JQ900628	AI20UEH	pSecTag2A-WC1-10
wc1-11	FJ031209	AI39SKP	pSecTag2A-WC1-11
wc1-12	JN234378	AI5IQQX	pSecTag2A-WC1-12
wc1-13	FJ031187	AI6ROW5	pSecTag2A-WC1-13
trdc	D90419	AIGJR3Q	pCR2.1-TRDC
gapdh	NM_001034034	Bt03210913	pCR2.1-GAPDH
cd4	NM_001103225	Hs01058407	n.d.
cd8	NM_174015	Bt03212361	n.d.

n.d., not done.

[1]https://www.flowjo.com (Accessed: December, 2017).

[2]http://www.ebi.ac.uk/Tools/clustalw2/index.html (Accessed: December, 2017).

TABLE 2 | Evaluation of WC1 TaqMan assays for specificity.

TaqMan assays for	WC1 a1 domain in the pST2a vector as templates (WC1-x)												
	1	**2**	**3**	**4**	**5**	**6**	**7**	**8**	**9**	**10**	**11**	**12**	**13**
WC1-1	31.90[a]												
WC1-2		32.15											
WC1-3			30.94										
WC1-4				32.34									
WC1-5					29.97								
WC1-6						29.07							
WC1-7							30.02						
WC1-8								33.13					
WC1-9									26.87				
WC1-10										28.16			
WC1-11											30.05		
WC1-12												26.33	
WC1-13													29.28

[a]*Each number is a Ct value with blank cells meaning no Ct detected during amplification.*

spectrophotometric quantification; primers to the vector backbone and qPCR were used to confirm the concentration of the constructs. TRDC amplified from PBMC was cloned into pCR2.1 and used to generate a standard curve.

Statistics

Pearson's *r* correlation was used to determine the relationship between the number of WC1 genes transcribed and the moles of either TRDC or WC1 gene transcripts measured. Student's *t*-test was used to determine significant differences in the proportion of cells in the WC1 subpopulations with transcripts for WC1 genes whose products bind *Leptospira*.

RESULTS

Derivation and Analysis of WC1$^+$ γδ T Cell Lines and Clones

While previous studies indicated that bulk γδ T cell subpopulations can express more than one WC1 gene (9, 24), expression of WC1 genes by individual γδ T cells has been largely undefined. To fill this gap, we evaluated WC1 gene transcription by clones of WC1$^+$ γδ T cells using a customized TaqMan assay system. Due to a high degree of sequence similarity among WC1 genes (Figure S1 in Supplementary Material), a number of experiments were performed to validate the specificity of the TaqMan assays (see M&M: **Table 2**; Figure S2 in Supplementary Material) and differences in efficiency (*Ct* values using the plasmids with cloned WC1 SRCR a1 domains ranged from *Ct* 26 to 33 when equal concentrations of template were used) were compensated for by constructing standard curves (**Figure 1**); the difference in efficiency was accepted as a necessary compromise to maintain the ability of the TaqMan assays to distinguish among WC1 transcripts. Bulk cell lines were generated from which to derive γδ T cell clones using a mixture of *Leptospira* and cytokine cocktail stimulations. γδ T cells in PBMC from *Leptospira*-vaccinated animals but not unvaccinated animals (6) are known from our previous studies to have recall responses *in vitro* (27). We evaluated the γδ T cells in the expansion cultures with *Leptospira* for changes in expression of memory markers as we have shown previously these differ from the expression by naïve cells from unvaccinated cattle (27). An increase in CD44 and decrease in CD62L was seen in the initial round of stimulation using a protocol to generate bovine T_{CM} cells (28) (**Figure 2**, day 0–day 12). There was an even greater increase in CD44 expression and decrease in CD62L by day 21 (**Figure 2**) when the dividing cells were sorted for T cell cloning (a time when the cells would be ready to respond to a new round of stimulation). Variations in the cloning protocol after day 14 were tried with a total of four distinct strategies and included sorting populations of dividing cells to enhance the chance of clonal diversity (Table S1 in Supplementary Material). Clones were generated from 12 cycles of expansion (Table S1 in Supplementary Material) with purity of all the flow cytometry sorts ranging from 87.9 to 99.3% (Figure S3 and Table S1 in Supplementary Material). WC1.1$^+$ and WC1.1$^+$/WC1.3$^+$ sorted cells were cultured with IL-2 and *Leptospira* (Table S1 in Supplementary Material, Strategy 3) since we knew that some WC1.1$^+$ (7) and WC1.3$^+$ cells (Chen C and Baldwin CL, unpublished data) from vaccinated animals are *Leptospira* responsive. Clones from these sorted populations that were expanded by re-stimulation with *Leptospira* grew more efficiently than those without. To obtain WC1.2$^+$ clones IL-2 alone or in combination with IL-15 with or without IL-18 was used, since IL-15 is known to stimulate γδ T cells (30, 31). In total, we generated 78 clones (**Table 3**). The cloning efficiency of each cycle showed that the probability that any individual T cell line was actually a clonal population was 96–99% based on the maximum likelihood method of de St Groth [Table S2 in Supplementary Material; (29)].

Variegated WC1 Gene Transcription by γδ T Cell Clones

Analysis of the gene transcription by the γδ T cell clones showed the number of WC1 genes transcribed per clone varied and that many more combinations occurred than expected (**Table 3**). If the mean and SE was at zero, the gene was not included in the tally of transcription since this indicated it was not measurable in all replicate samples. T cell clones expressing only 1–3 WC1

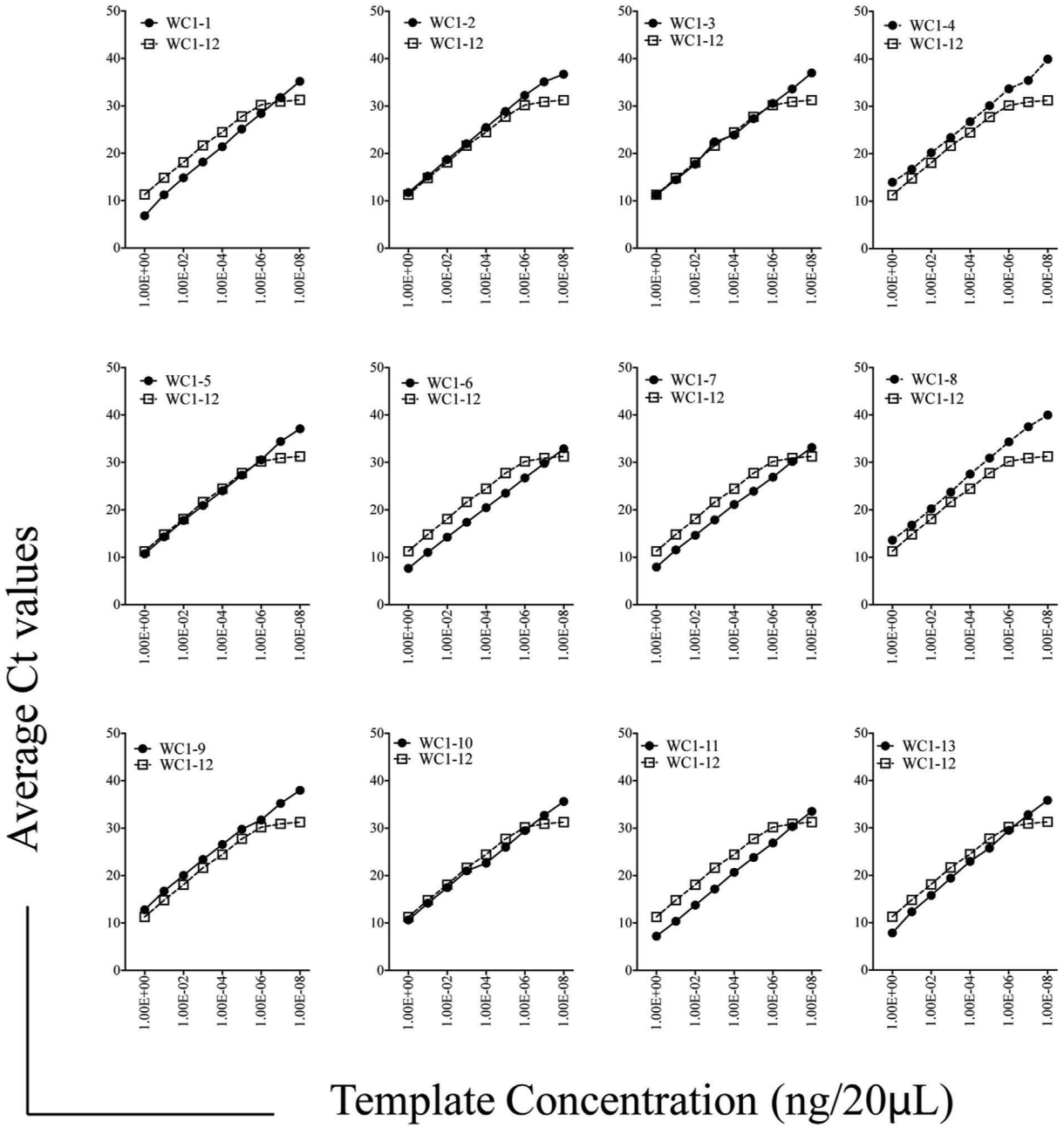

FIGURE 1 | Efficiency of Taqman assays for WC1 transcripts. Standard curves for individual WC1 genes' scavenger receptor cysteine rich a1 domains were amplified and detected with the Taqman primer/probe assays using serially diluted pST2a-WC1 templates. In each case, *WC1-12* efficiency is shown as a benchmark.

genes accounted for ~75% of all γδ T cell clones (**Figure 3**) with 8 of the 13 WC1 genes found to be transcribed alone in individual clones. The consistency of transcription over time for sample clones was evaluated (**Figure 4**) and showed that while the magnitude of transcription was not identical (e.g., see Clone 6: at Wk 0 WC1-1 has the greatest level of transcription while at Wk4 WC1-4 did) the transcription of specific genes was generally consistent. While cDNA preparations from clones had different molar concentrations of transcripts for WC1 genes and TRDC (shown for representative clones in Figure S4 in Supplementary Material), neither correlated with the number of different WC1 gene transcripts detected (Pearson's *r* correlations were 0.01662 and 0.00016, respectively). While evaluation of all putative clones showed that the frequency that had transcripts from five or six different WC1 genes was low (11% of the colonies) (**Figure 5**), based on the prediction that only 1–4% of the colonies that arose are not clonal populations using the maximum likelihood method (29) then at least some of the colonies transcribing five or

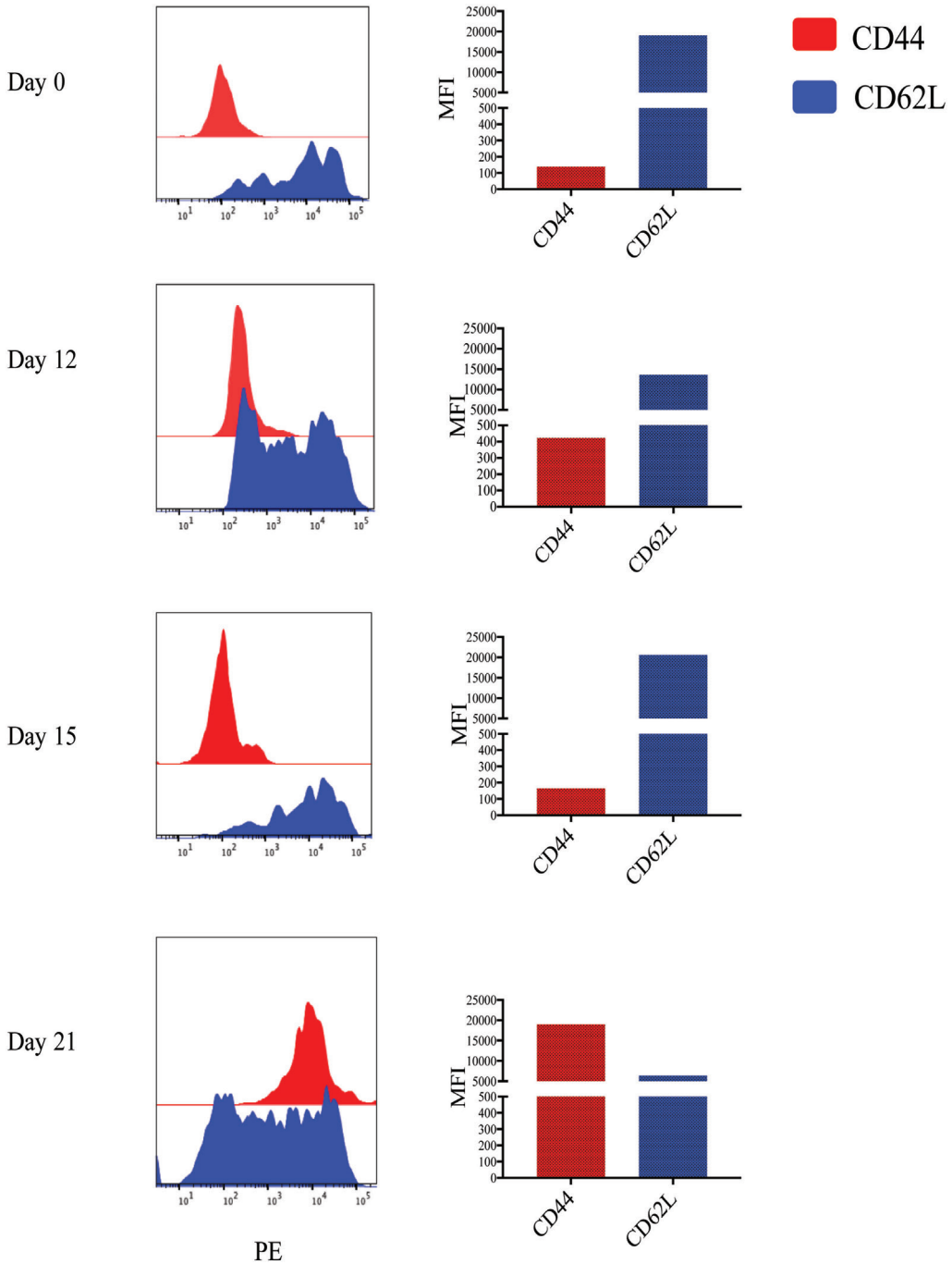

FIGURE 2 | Memory markers of *Leptospira* stimulated cultures. Cultures of peripheral blood mononuclear cells from a vaccinated animal subjected to the T_{CM} and T_{EM} protocol and cells stained for T cell receptor (TCR)δ with monoclonal antibody (mAb) GB21A (FITC) at the times indicated. The TCRδ$^+$ cells were flow cytometrically gated on mAb GB21A$^+$ and evaluated for their surface marker expression of either CD44 or CD62L (PE) by two-color immunofluorescence shown as histograms. The mean fluorescence intensity (MFI) is shown in the bar graphs.

six different WC1 genes would be expected to have been derived from a single cell.

Previous analyses of bulk-sorted WC1$^+$ subpopulations indicated that the WC1 genes with the highest levels of transcription differed between the WC1.1 and WC1.2 subpopulations (9, 24). Here, we found the transcription of WC1 genes overlapped among clones from the two subpopulations (**Figure 5**) but when just the gene with the highest WC1 transcript level for each T cell clone was considered and re-aggregated (**Figure 6A**) the pattern of relative transcription was generally similar to what we reported for bulk-sorted subpopulations previously. The diversity index also showed that there are differences in WC1 gene transcription

TABLE 3 | Summary of WC1 transcripts expressed by γδ T cell clones.

Clone #	# of WC1 genes transcribed	WC1.2-like WC1 transcripts (WC1-)	WC1.1-like WC1 transcripts (WC1-)
A86	1	4	–
23		4	–
13M-20-2D		7	–
A6C		7	–
101F		7	–
8D2		7	–
3-E11		7	–
PY08C		–	1
2D10-21A		–	1
3-10H		–	3
5-11G		–	3
131-6-11B		–	6
B11D		–	10
6-7C		–	10
28-9H		–	12
A93		–	13
AC06		–	13
BG08		–	13
5	2	4, 7	–
33		4, 7	–
17		4, 7	–
AE05		4, 7	–
159E		4, 7	–
3-7G		–	3, 8
2-7C		–	3, 8
8I		–	1, 11
501K/D		–	6, 13
25-1F		4	8
8G-31		4	10
2		4	11
26-3F-13N		4	11
7H5		4	11
87-30		4	13
7		7	6
5-11F		7	8
21		7	1
209E		9	10
1-3H	3	–	1, 8, 11
13L-10-5E		–	1, 11, 12
17-10A		–	2, 12, 13
B7B		–	8, 10, 11
18-10F		–	3, 8, 13
PY01G		4, 7	1
4-E6		4, 7	6
B9D		4, 7	11
10		4, 7	11
16		4, 7	11
4-E8		4, 7	11
21-3E		4, 7	12
9		4	7, 11
8E-29		4	6, 11
23-9H-13E		7	8, 11
7-10A-13C		7	8, 11
AF08		7	11, 13
8M		9	1, 11
101G		9	3, 10
24		9	6, 10
8P	4	–	3, 6, 10, 11
9H11		4	3, 6, 10
B8F		4	1, 8, 11
20-7H		7	3, 11, 12
6		4,7	1, 11
13		4,7	9,11
7H5		4, 7	1, 3
2D10		4, 7	1, 3
22-9H		4, 7	3, 12
27-5F		4, 7	3, 12
6-9D-13B		4, 7	8, 11
13K-13-9B		4, 7	11, 13
3G6		4, 9	11, 12
PYO1E		7, 9	1, 11
1B5-21A	5	7	1, 6, 11, 13
PY100		4, 7	1, 6, 8
4		4, 7	8, 11, 13
11-9F		4, 9	1, 8, 11
A5F	6	4	3, 8, 11, 12, 13
9H10		4, 7	1, 3, 6, 10
20-9G		4, 7	2, 10, 11, 12

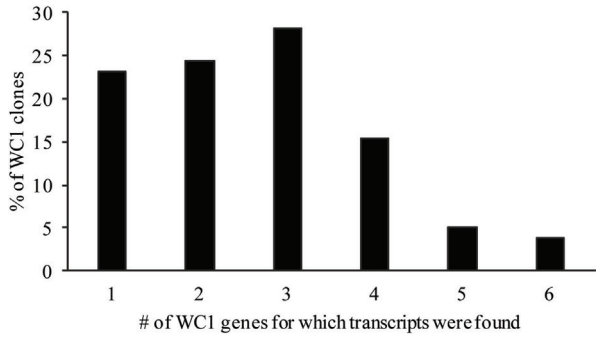

FIGURE 3 | Percentage of WC1 transcripts expressed per γδ T cell clone. The percentage of clones with a particular number of different WC1 gene transcripts is shown.

between WC1.1 and WC1.2 clones (**Figure 6B**). Nevertheless, unexpected combinations of transcripts were found together, although the archetypal genes for the WC1.1 and WC1.2 subpopulations (*WC1-3* and *WC1-4*, respectively) were only detected together in cell lines that had transcripts for four or more WC1 genes (**Table 3**). The infrequent occurrence of this phenomenon considering all 78 clones evaluated largely supports our previous findings that WC1.1 and WC1.2 are the two foundational sublineages of WC1$^+$ γδ T cells expressing an array of WC1 genes that enable them to respond to specific pathogens differently.

WC1 Gene Transcript by Pathogen-Specific Memory γδ T Cells

A proportion of the cells in the WC1.1$^+$ subpopulation of γδ T cells from animals that have been primed by vaccination specifically proliferate and produce IFNγ in response to stimulation with *Leptospira* in recall assays indicating their role as adaptive-like memory lymphocytes (27). In contrast, many fewer in the WC1.2$^+$ subpopulation do so. Based on these observations, we sought to determine if the WC1 gene transcription was different among clones that responded to *Leptospira* (WC1.1 cohort) compared

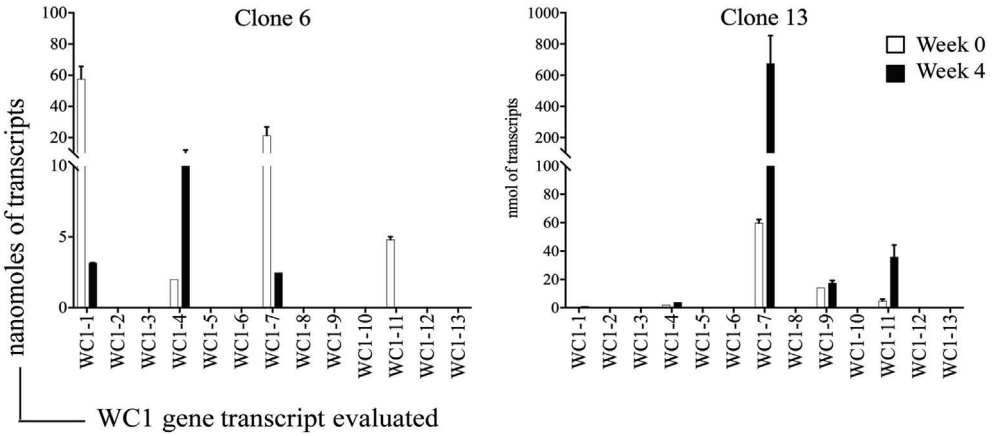

FIGURE 4 | Time-course evaluation of WC1 gene transcription. Evaluation of WC1 gene transcription by selected clones at two different time-points 4 weeks apart are shown. Filled bars show earlier time point and open bars the later. Transcripts are represented as moles of the mean ± SE of replicates. This was done three times with triplicate samples.

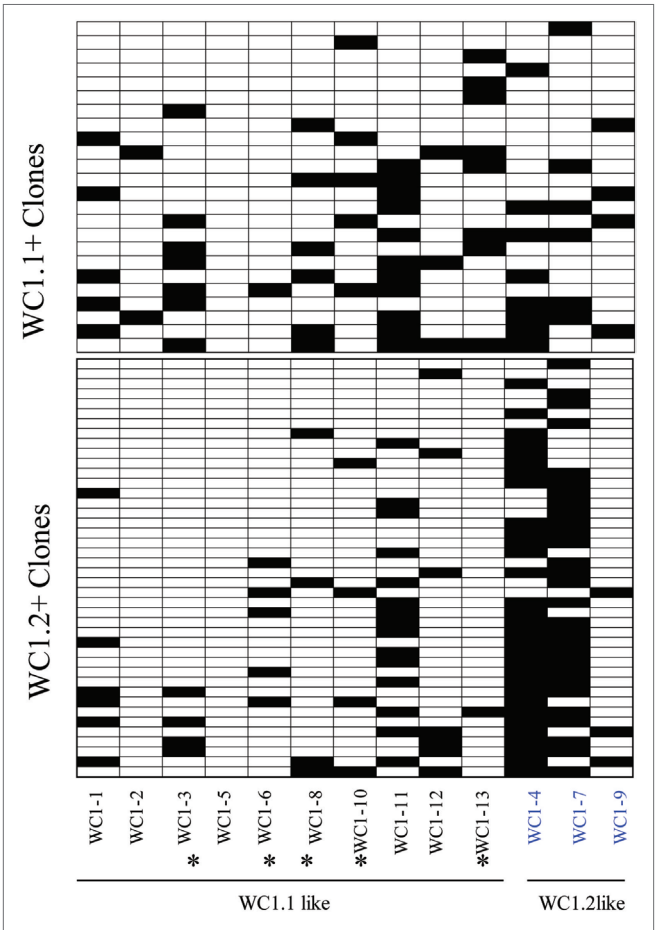

FIGURE 5 | WC1 gene transcripts associated with individual WC1.1$^+$ or WC1.2$^+$ clones. The various combinations of WC1 gene transcripts are shown for clones derived by flow cytometrically sorted cell subpopulations in a heat map. * = WC1 gene products that bind *Leptospira*.

with those that generally did not (WC1.2 cohort) since we have shown previously that 5 of the 13 bovine WC1 molecules have SRCR domains that directly bind *Leptospira* (i.e., WC1-3, WC1-6, WC1-8, WC1-10, and WC1-13) (23). Since antibody-mediated co-ligation of WC1 and TCR/CD3 results in augmented proliferation and IFNγ production, it suggests that pathogen-mediated co-ligation of WC1 and TCR/CD3 would also and thus that WC1 expression and pathogen binding specificity would influence γδ T cell responsiveness (24, 25, 32). 80% of the WC1.1 cohort of clones that were generated with cells from a primed animal and continually cultured with *Leptospira* had transcripts for at least one WC1 gene that had a binding domain for *Leptospira* (**Figure 5**). Clones from the WC1.2 cohort were necessarily developed with cytokine stimulation here and only 37% of those clones had transcripts coding for WC1 molecules with a binding domain for *Leptospira*. This was significantly different ($p < 0.008$). The observation that some WC1.2$^+$ cells do have transcripts for *Leptospira*-binding WC1 molecules is consistent with the minor population of WC1.2$^+$ γδ T cells that have been found to respond to *Leptospira* stimulation (7) and that would be preferentially expanded under these conditions given the initial culture was with *Leptospira*.

DISCUSSION

We previously hypothesized that within the WC1.1$^+$ and WC1.2$^+$ subpopulations there would be set WC1 gene programming that broke down these cohorts into even smaller populations. This was rejected based on the results here because few clones had the same pattern of WC1 gene transcription. This mix of patterns occurred even though all the clones were derived from a single animal. We would expect similar complex patterns in other animals since unlike the gene numbers for Ly49 and KIR (other multigenic arrays of immune system cell receptors) that are highly variable among the genomes of mouse strains (33) and humans (34), respectively, the WC1 family is highly conserved with regard to

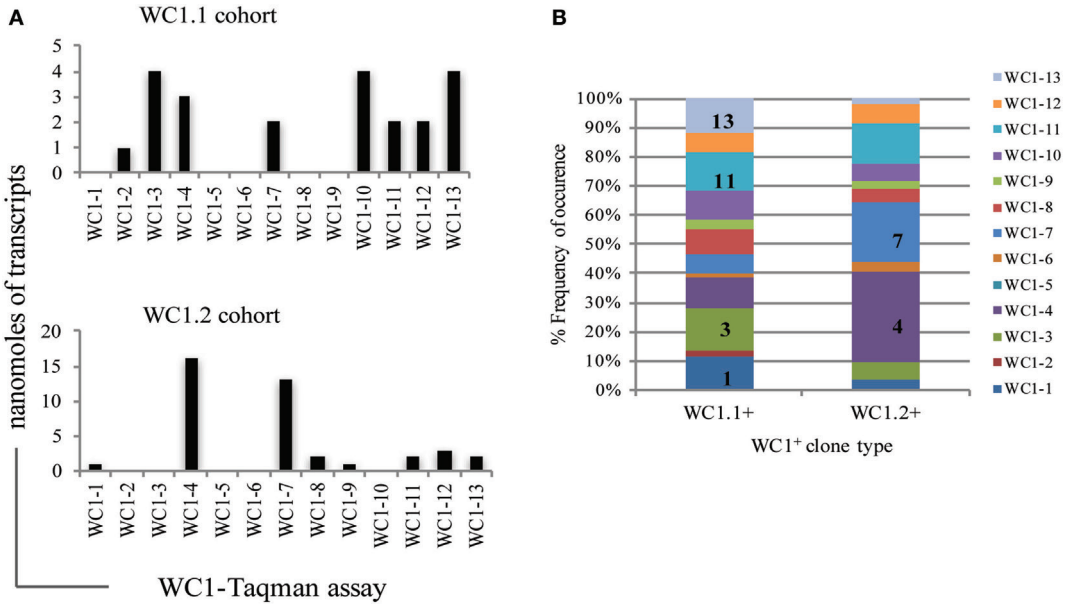

FIGURE 6 | Diversity index of individual WC1 gene transcription by γδ T cell clones in each WC1 cohort. **(A)** For each clone the predominately expressed WC1 gene, based on highest mean transcript level, was noted and the total number of times a WC1 gene was the predominant is plotted. **(B)** Diversity index shows the percentage of times transcripts for the WC1 genes occurred in a cohort of clones (*y*-axis). WC1 genes most frequently transcribed within the repertoire of WC1 transcripts is indicated as a number *x* (e.g., WC1-*x*) in appropriate boxes to add emphasis.

gene number and sequence among cattle breeds including for *Bos taurus* and *Bos indicus* (3, 26). Although the gene transcription and presumably expression of the WC1 multigenic array was more complex and variable than predicted it is similar to the 30 different Ly49 patterns seen for 62 clones of murine NK cells (35) and agrees with TLR gene expression by human and murine CD4 and CD8 T cells which ranges from four to seven TLR [reviewed in Ref. (36)] and with transcription of one to eight KIR family genes by human NK clones (37). However, for NK cells the number of different KIR genes transcribed/cell is normally distributed (37) while our results indicated transcription of fewer WC1 genes per cell is favored.

Variegated gene expression of immune cell receptors that sense the environment, including KIR, Ly49, and TLR, is common and allows individual cells to detect specific stimuli (38). Some multigenic arrays of PRR such as TLR have some genes constitutively expressed on lymphocytes while expression of other genes is induced in response to environmental cues such as microbes and cytokines (39). In contrast, the WC1 transcription patterns appear to be stable since among animals there is a largely consistent ratio of WC1.1$^+$ and WC1.2$^+$ cells, defined by their WC1 gene expression, that changes according to age (7) and which first appears during thymic development (Damani-Yokota, unpublished data). This is similar to the set proportion of cells expressing specific KIR genes in human or Ly49 genes in mice (40–42). Variegated gene expression of these multigenic arrays has been shown to be controlled by differential methylation of CpG islands around the transcriptional start site (43), by bidirectional promoter switches that are controlled by noncoding RNA (38, 42, 44), and by differences in 5′ upstream regulatory regions (41) which ensure stability of gene expression. Finally, there is precedent for the SRCR receptor transcriptome in a population of immune cells changing in response to bacterial injection into sea urchins (45), suggesting that the clonal expansion of cells with stable expression of SRCR receptors in response to infection is an ancient and conserved mechanism.

The WC1 transcriptome of the two major subpopulations of WC1$^+$ γδ T cells (WC1.1$^+$ and WC1.2$^+$) isolated from either *ex vivo* PBMC or following culture with antigens have signature WC1 genes dominantly transcribed but they also have lower levels of transcripts for additional WC1 genes (9, 24). These minor transcripts could represent low-level sterile transcription since their gene products were not evident by immunofluorescence. For example, sterile transcripts for TLR are found in CD4 T cells (46). Nevertheless, some of the clones had transcripts that coded for WC1 genes normally expressed by the other cohort that may have arisen from impurities in the flow cytometric sorting process (i.e., WC1.1$^+$ cells in the WC1.2$^+$ sorted population) while others may be cell lines, i.e., not of single cell origin. The presence of two or more clonal populations of cells in a culture could convey a growth advantage to cells including some not activated directly by antigen. These issues are unresolved but would account for only a small percentage of the colonies or cell lines derived since the maximum likelihood method (29) indicates that there is 96–99% probability that they are derived from a single cell.

Our previous studies support a model of γδ T cell activation in which pathogen ligation of the WC1 co-receptors along with the TCR is necessary for optimal cellular responses (32, 47). Moreover, crosslinking of the γδ TCR with WC1s using an mAb that recognizes most WC1 molecules (mAb CC15) has been

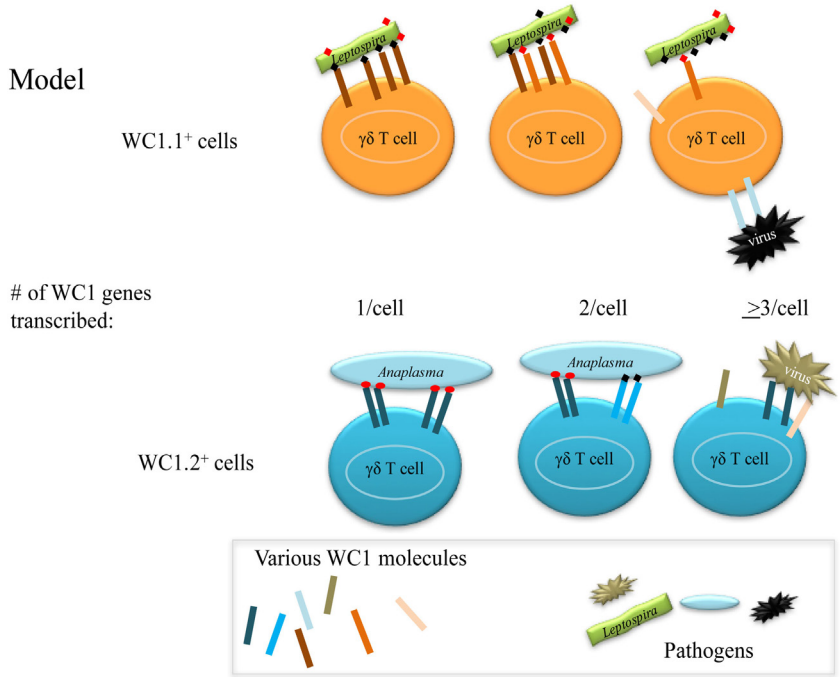

FIGURE 7 | Model for WC1 interaction with pathogens. γδ T cells may express variable numbers of different WC1 molecules thus potentially enabling them to interact with more than one ligand on the same or different pathogens. However, since the number of WC1 co-receptors is necessarily limited on a cell an increase in receptor diversity could affect the avidity of the interaction with any particular ligand.

shown to give a stronger and more amplified signal compared with crosslinking with an mAb that recognizes a specific WC1 molecule within the family of 13 (i.e., WC1-8 by mAb CACT21A) (24). Thus, co-crosslinking of all WC1 molecules on a cell with the γδ TCR by natural ligand binding would be expected to provide an advantage to the cell while multiple different WC1 molecules increase the potential for WC1 molecules to bind more than one ligand of a pathogen. Also expression of WC1 molecules in various combinations could increase the types of pathogens to which an individual cell could respond. Conversely, expression of multiple WC1 genes could decrease avidity for a particular pathogen if some of the WC1 molecules did not bind a ligand on the particular pathogen. We present these alternatives in a model (**Figure 7**).

Since much of our work has used the recall response to *Leptospira* as the model to elucidate the role of WC1 molecules in directing γδ T cell responses, we framed the results in that context. Our hypothesis that the individual or combination of WC1 molecules being expressed by a γδ T cell contributes to its pathogen responsiveness is supported by our finding that the majority of memory γδ WC1.1$^+$ T cell clones had transcripts for WC1 molecules that bind *Leptospira* (23). Since we were unable to grow WC1.1$^+$ clones without repeated stimulation with *Leptospira*, we suggest that the remaining clones that did not express WC1 molecules with known *Leptospira*-binding domains may have a TCR with higher affinity for the bacteria and thus do not need co-ligation of WC1 for activation. With regard to the WC1.2$^+$ population, it is known to be characterized by dominant transcription of genes *WC1-4*, *WC1-7*, and *WC1-9*, none of which have been found to bind *Leptospira* (23). However, some WC1.2$^+$ γδ T cell clones had transcripts for WC1 genes whose products bind *Leptospira* which agrees with the small proportion of WC1.2$^+$ γδ T cells in PBMC that do in fact respond to *Leptospira* (7).

The cloning system yielded valuable insights into the variegated WC1 gene transcription but the question of how stable WC1 transcriptional programming is established in thymocytes remains unresolved. We are currently investigating differential occupancy of WC1 enhancers in the WC1.1 and WC1.2 loci by transcription factors implicated in γδ T cell development (12) and consequent epigenetic modification of the loci to help resolve this question. It also will be important to characterize the TCR repertoires of those *Leptospira*-responsive WC1.1$^+$ γδ T cell clones that did not have transcripts for *Leptospira*-binding WC1 molecules. We predict that the CDR3 repertoires for these cells will be significantly different from those with *Leptospira*-binding WC1 co-receptors and are the subject of current studies.

ETHICS STATEMENT

All animal use was approved by the University of Massachusetts' Institutional Animal Care and Use Committee.

AUTHOR CONTRIBUTIONS

PD-Y contributed to the design of experiments, acquisition, analysis, and interpretation of the data and helped draft the manuscript. CB and JT contributed to the conception and design of the research, analysis and interpretation of the data, and

drafting the manuscript. All authors critically revised, read and approved the final manuscript, and agreed to be fully accountable for ensuring the integrity and accuracy of the work.

ACKNOWLEDGMENTS

We thank Dr. Amy Burnside for assistance with the flow cytometry cell sorting in the Institute of Applied Life Sciences at University of Massachusetts Amherst. We thank Alexandria Gillespie and Samuel Black for reading the manuscript.

FUNDING

This research was supported by grant no. 2011-67015-30736 under NIFA-USDA/NIH "Dual Purpose with Dual Benefit Research in Biomedicine and Agriculture Using Agriculturally Important Domestic Animals" and USDA National Institute for Food and Agriculture grant no. 2017-67015-26631 to Drs. Cynthia L. Baldwin and Janice C. Telfer.

SUPPLEMENTARY MATERIAL

The Supplementary Material for this article can be found online at https://www.frontiersin.org/articles/10.3389/fimmu.2018.00717/full#supplementary-material.

FIGURE S1 | Sequence alignment of bovine WC1 genes. General structure of bovine WC1 molecules is shown for 6 and 11 scavenger receptor cysteine rich (SRCR)-containing molecules along with the transmembrane (TM) and endodomain. Multiple sequence alignment of the deduced amino acids of the SRCR a1 domains (the most membrane distal) of the 13 bovine WC1 molecules using ClustalW with identical amino acids shown as dots and gaps as dashes. Variable regions 1 and 2 (VR1 and VR2, respectively) are marked to show regions of greatest sequence variability among the different WC1 sequences. WC1-4, WC1-7, and WC1-9 are considered WC1.2-type molecules while the rest are WC1.1 based on amino acid deletions or additions at positions 75, 76, and 89.

FIGURE S2 | Establishment of TaqMan primer assays. **(A)** Evaluation of TaqMan primer amplified PCR products on 2% TAE-agarose gel showing amplicon size ranging from 100 to 200 bp for WC1 transcripts labeled WC1-1 to WC1-13 and other genes as indicated. **(B)** PCR products were gel-purified and cloned into pCR2.1 and subsequently analyzed with Sanger sequencing. Multiple sequence alignment using BioEdit shows nucleotide sequences of TaqMan assay-amplified WC1 genes from cDNA relative to the reference gene sequence found in Genbank (see **Table 1** for accession numbers).

FIGURE S3 | Sorting strategy to obtain WC1$^+$ γδ T cell subpopulations for single cell cloning. **(A)** Single-positive WC1.1$^+$ or WC1.2$^+$ and **(B)** double positive WC1.1$^+$/WC1.3$^+$ γδ T cells were flow cytometrically analyzed and gates applied. The three gated cell populations were then evaluated for their level of cell division dye and the efluor-670^{low} cells (indicative of multiple cell divisions) were collected as shown. This is representative of multiple flow cytometric sorts.

FIGURE S4 | Representative clones with variable numbers of WC1 gene transcripts. Examples (from the 78 total clones) that had transcripts for one to five WC1 gene transcripts. If the mean was less than 2 and SE was at below zero, the gene was not included in the tally of transcripts in **Figures 5** and **6** or **Table 3**. **(A)** WC1.1 cohort of γδ T cell clones from monoclonal antibodies (mAb) BAG25A$^+$/CACTB32A$^-$ sorted cells expanded using expansion strategy 3 (*Leptospira* and IL-2) or **(B)** WC1.2 cohort of γδ T cell clones from mAb BAG25A$^-$/CACTB32A$^+$ sorted cells expanded with IL-2 with or without IL-15 and IL-18 supplementation. Moles of transcripts for each clone (mean ± SE) for WC1 and TRDC (hatched bars) are shown.

REFERENCES

1. Telfer JC, Baldwin CL. Bovine gamma delta T cells and the function of gamma delta T cell specific WC1 co-receptors. *Cell Immunol* (2015) 296:76–86. doi:10.1016/j.cellimm.2015.05.003
2. PrabhuDas MR, Baldwin CL, Bollyky PL, Bowdish DME, Drickamer K, Febbraio M, et al. Classification of scavenger receptors and their roles in health and disease. *J Immunol* (2017) 198:3775–89. doi:10.4049/jimmunol.1700373
3. Herzig CT, Waters RW, Baldwin CL, Telfer JC. Evolution of the CD163 family and its relationship to the bovine gamma delta T cell co-receptor WC1. *BMC Evol Biol* (2010) 10:181. doi:10.1186/1471-2148-10-181
4. Kisielow J, Kopf M, Karjalainen K. SCART scavenger receptors identify a novel subset of adult gammadelta T cells. *J Immunol* (2008) 181:1710–6. doi:10.4049/jimmunol.181.3.1710
5. Chen C, Herzig CT, Telfer JC, Baldwin CL. Antigenic basis of diversity in the gammadelta T cell co-receptor WC1 family. *Mol Immunol* (2009) 46(13):2565–75. doi:10.1016/j.molimm.2009.05.010
6. Naiman BM, Alt D, Bolin CA, Zuerner R, Baldwin CL. Protective killed *Leptospira borgpetersenii* vaccine induces potent Th1 immunity comprising responses by CD4 and gammadelta T lymphocytes. *Infect Immun* (2001) 69:7550–8. doi:10.1128/IAI.69.12.7550-7558.2001
7. Rogers AN, Vanburen DG, Hedblom EE, Tilahun ME, Telfer JC, Baldwin CL. Gammadelta T cell function varies with the expressed WC1 coreceptor. *J Immunol* (2005) 174:3386–93. doi:10.4049/jimmunol.174.6.3386
8. Lahmers KK, Norimine J, Abrahamsen MS, Palmer GH, Brown WC. The CD4+ T cell immunodominant *Anaplasma marginale* major surface protein 2 stimulates gammadelta T cell clones that express unique T cell receptors. *J Leukoc Biol* (2005) 77:199–208. doi:10.1189/jlb.0804482
9. McGill JL, Sacco RE, Baldwin CL, Telfer JC, Palmer MV, Waters WR. Specific recognition of mycobacterial protein and peptide antigens by gammadelta T cell subsets following infection with virulent *Mycobacterium bovis*. *J Immunol* (2014) 192:2756–69. doi:10.4049/jimmunol.1302567
10. Price S, Davies M, Villarreal-Ramos B, Hope J. Differential distribution of WC1(+) gammadelta TCR(+) T lymphocyte subsets within lymphoid tissues of the head and respiratory tract and effects of intranasal *M. bovis* BCG vaccination. *Vet Immunol Immunopathol* (2010) 136:133–7. doi:10.1016/j.vetimm.2010.02.010
11. Hogg AE, Worth A, Beverley P, Howard CJ, Villarreal-Ramos B. The antigen-specific memory CD8+ T-cell response induced by BCG in cattle resides in the CD8+gamma/deltaTCR-CD45RO+ T-cell population. *Vaccine* (2009) 27:270–9. doi:10.1016/j.vaccine.2008.10.053
12. Munoz-Ruiz M, Sumaria N, Pennington DJ, Silva-Santos B. Thymic determinants of gammadelta T cell differentiation. *Trends Immunol* (2017) 38:336–44. doi:10.1016/j.it.2017.01.007
13. Lombes A, Durand A, Charvet C, Riviere M, Bonilla N, Auffray C, et al. Adaptive immune-like gamma/delta T lymphocytes share many common features with their alpha/beta T cell counterparts. *J Immunol* (2015) 195:1449–58. doi:10.4049/jimmunol.1500375
14. Sheridan BS, Pham QM, Lee YT, Cauley LS, Puddington L, Lefrancois L. Oral infection drives a distinct population of intestinal resident memory CD8(+) T cells with enhanced protective function. *Immunity* (2014) 40:747–57. doi:10.1016/j.immuni.2014.03.007
15. Murphy AG, O'Keeffe KM, Lalor SJ, Maher BM, Mills KH, McLoughlin RM. *Staphylococcus aureus* infection of mice expands a population of memory gammadelta T cells that are protective against subsequent infection. *J Immunol* (2014) 192:3697–708. doi:10.4049/jimmunol.1303420
16. Shen Y, Zhou D, Qiu L, Lai X, Simon M, Shen L, et al. Adaptive immune response of Vgamma2Vdelta2+ T cells during mycobacterial infections. *Science* (2002) 295:2255–8. doi:10.1126/science.1068819
17. Hoft DF, Brown RM, Roodman ST. Bacille Calmette-Guerin vaccination enhances human gamma delta T cell responsiveness to mycobacteria suggestive of a memory-like phenotype. *J Immunol* (1998) 161:1045–54.
18. Li L, Wu CY. CD4+ CD25+ Treg cells inhibit human memory gammadelta T cells to produce IFN-gamma in response to *M tuberculosis* antigen ESAT-6. *Blood* (2008) 111:5629–36. doi:10.1182/blood-2008-02-139899

19. Qin G, Liu Y, Zheng J, Xiang Z, Ng IH, Malik Peiris JS, et al. Phenotypic and functional characterization of human gammadelta T-cell subsets in response to influenza A viruses. *J Infect Dis* (2012) 205:1646–53. doi:10.1093/infdis/jis253
20. Teirlinck AC, McCall MB, Roestenberg M, Scholzen A, Woestenenk R, de Mast Q, et al. Longevity and composition of cellular immune responses following experimental *Plasmodium falciparum* malaria infection in humans. *PLoS Pathog* (2011) 7(12):e1002389. doi:10.1371/journal.ppat.1002389
21. Clevers H, MacHugh ND, Bensaid A, Dunlap S, Baldwin CL, Kaushal A, et al. Identification of a bovine surface antigen uniquely expressed on CD4-CD8- T cell receptor gamma/delta+ T lymphocytes. *Eur J Immunol* (1990) 20:809–17. doi:10.1002/eji.1830200415
22. Herzig CT, Baldwin CL. Genomic organization and classification of the bovine WC1 genes and expression by peripheral blood gamma delta T cells. *BMC Genomics* (2009) 10:191. doi:10.1186/1471-2164-10-191
23. Hsu H, Chen C, Nenninger A, Holz L, Baldwin CL, Telfer JC. WC1 is a hybrid gammadelta TCR coreceptor and pattern recognition receptor for pathogenic bacteria. *J Immunol* (2015) 194:2280–8. doi:10.4049/jimmunol.1402021
24. Chen C, Hsu H, Hudgens E, Telfer JC, Baldwin CL. Signal transduction by different forms of the gammadelta T cell-specific pattern recognition receptor WC1. *J Immunol* (2014) 193:379–90. doi:10.4049/jimmunol.1400168
25. Wang F, Herzig CT, Chen C, Hsu H, Baldwin CL, Telfer JC. Scavenger receptor WC1 contributes to the gammadelta T cell response to Leptospira. *Mol Immunol* (2011) 48:801–9. doi:10.1016/j.molimm.2010.12.001
26. Chen C, Herzig CT, Alexander LJ, Keele JW, McDaneld TG, Telfer JC, et al. Gene number determination and genetic polymorphism of the gamma delta T cell co-receptor WC1 genes. *BMC Genet* (2012) 13:86. doi:10.1186/1471-2156-13-86
27. Blumerman SL, Herzig CT, Baldwin CL. WC1+ gammadelta T cell memory population is induced by killed bacterial vaccine. *Eur J Immunol* (2007) 37:1204–16. doi:10.1002/eji.200636216
28. Maggioli MF, Palmer MV, Thacker TC, Vordermeier HM, Waters WR. Characterization of effector and memory T cell subsets in the immune response to bovine tuberculosis in cattle. *PLoS One* (2015) 10(4):e0122571. doi:10.1371/journal.pone.0122571
29. de St Groth F. The evaluation of limiting dilution assays. *J Immunol Methods* (1982) 49:R11–23. doi:10.1016/0022-1759(82)90269-1
30. Conlon KC, Lugli E, Welles HC, Rosenberg SA, Fojo AT, Morris JC, et al. Redistribution, hyperproliferation, activation of natural killer cells and CD8 T cells, and cytokine production during first-in-human clinical trial of recombinant human interleukin-15 in patients with cancer. *J Clin Oncol* (2015) 33:74–82. doi:10.1200/JCO.2014.57.3329
31. Van Acker HH, Anguille S, Willemen Y, Van den Bergh JM, Berneman ZN, Lion E, et al. Interleukin-15 enhances the proliferation, stimulatory phenotype, and antitumor effector functions of human gamma delta T cells. *J Hematol Oncol* (2016) 9:101. doi:10.1186/s13045-016-0329-3
32. Hsu H, Baldwin CL, Telfer JC. The endocytosis and signaling of the gammadelta T cell coreceptor WC1 are regulated by a dileucine motif. *J Immunol* (2015) 194:2399–406. doi:10.4049/jimmunol.1402020
33. Carlyle JR, Mesci A, Fine JH, Chen P, Belanger S, Tai LH, et al. Evolution of the Ly49 and Nkrp1 recognition systems. *Semin Immunol* (2008) 20:321–30. doi:10.1016/j.smim.2008.05.004
34. Wilson MJ, Torkar M, Haude A, Milne S, Jones T, Sheer D, et al. Plasticity in the organization and sequences of human KIR/ILT gene families. *Proc Natl Acad Sci U S A* (2000) 97:4778–83. doi:10.1073/pnas.080588597
35. Kubota A, Kubota S, Lohwasser S, Mager DL, Takei F. Diversity of NK cell receptor repertoire in adult and neonatal mice. *J Immunol* (1999) 163:212–6.
36. Kabelitz D. Expression and function of toll-like receptors in T lymphocytes. *Curr Opin Immunol* (2007) 19:39–45. doi:10.1016/j.coi.2006.11.007
37. Valiante NM, Uhrberg M, Shilling HG, Lienert-Weidenbach K, Arnett KL, D'Andrea A, et al. Functionally and structurally distinct NK cell receptor repertoires in the peripheral blood of two human donors. *Immunity* (1997) 7:739–51. doi:10.1016/S1074-7613(00)80393-3
38. Anderson SK. Transcriptional regulation of NK cell receptors. *Curr Top Microbiol Immunol* (2006) 298:59–75.
39. Zarember KA, Godowski PJ. Tissue expression of human toll-like receptors and differential regulation of toll-like receptor mRNAs in leukocytes in response to microbes, their products, and cytokines. *J Immunol* (2002) 168:554–61. doi:10.4049/jimmunol.168.2.554
40. Belanger S, Tai LH, Anderson SK, Makrigiannis AP. Ly49 cluster sequence analysis in a mouse model of diabetes: an expanded repertoire of activating receptors in the NOD genome. *Genes Immun* (2008) 9:509–21. doi:10.1038/gene.2008.43
41. Takei F, McQueen KL, Maeda M, Wilhelm BT, Lohwasser S, Lian RH, et al. Ly49 and CD94/NKG2: developmentally regulated expression and evolution. *Immunol Rev* (2001) 181:90–103. doi:10.1034/j.1600-065X.2001.1810107.x
42. Li H, Pascal V, Martin MP, Carrington M, Anderson SK. Genetic control of variegated KIR gene expression: polymorphisms of the bi-directional KIR3DL1 promoter are associated with distinct frequencies of gene expression. *PLoS Genet* (2008) 4:e1000254. doi:10.1371/journal.pgen.1000254
43. Santourlidis S, Trompeter HI, Weinhold S, Eisermann B, Meyer KL, Wernet P, et al. Crucial role of DNA methylation in determination of clonally distributed killer cell Ig-like receptor expression patterns in NK cells. *J Immunol* (2002) 169:4253–61. doi:10.4049/jimmunol.169.8.4253
44. Anderson SK. Probabilistic bidirectional promoter switches: noncoding RNA takes control. *Mol Ther Nucleic Acids* (2014) 3:e191. doi:10.1038/mtna.2014.42
45. Pancer Z. Dynamic expression of multiple scavenger receptor cysteine-rich genes in coelomocytes of the purple sea urchin. *Proc Natl Acad Sci U S A* (2000) 97:13156–61. doi:10.1073/pnas.230096397
46. Mansson A, Adner M, Cardell LO. Toll-like receptors in cellular subsets of human tonsil T cells: altered expression during recurrent tonsillitis. *Respir Res* (2006) 7:36. doi:10.1186/1465-9921-7-36
47. Hanby-Flarida MD, Trask OJ, Yang TJ, Baldwin CL. Modulation of WC1, a lineage-specific cell surface molecule of gamma/delta T cells augments cellular proliferation. *Immunology* (1996) 88:116–23. doi:10.1046/j.1365-2567.1996.d01-649.x

Conflict of Interest Statement: The authors declare that the research was conducted in the absence of any commercial or financial relationships that could be construed as a potential conflict of interest.

Copyright © 2018 Damani-Yokota, Telfer and Baldwin. This is an open-access article distributed under the terms of the Creative Commons Attribution License (CC BY). The use, distribution or reproduction in other forums is permitted, provided the original author(s) and the copyright owner are credited and that the original publication in this journal is cited, in accordance with accepted academic practice. No use, distribution or reproduction is permitted which does not comply with these terms.

frontiers in Immunology

ORIGINAL RESEARCH
published: 01 May 2018
doi: 10.3389/fimmu.2018.00930

Functional Alleles of Chicken BG Genes, Members of the Butyrophilin Gene Family, in Peripheral T Cells

Lei Chen[1], Michaela Fakiola[1†], Karen Staines[2,3], Colin Butter[2,3] and Jim Kaufman[1,4]*

[1] Department of Pathology, University of Cambridge, Cambridge, United Kingdom, [2] Pirbright Institute, Compton, United Kingdom, [3] School of Life Sciences, University of Lincoln, Lincoln, United Kingdom, [4] Department of Veterinary Medicine, University of Cambridge, Cambridge, United Kingdom

γδ T cells recognize a wide variety of ligands in mammals, among them members of the butyrophilin (BTN) family. Nothing is known about γδ T cell ligands in chickens, despite there being many such cells in blood and lymphoid tissues, as well as in mucosal surfaces. The major histocompatibility complex (MHC) of chickens was discovered because of polymorphic BG genes, part of the BTN family. All but two BG genes are located in the BG region, oriented head-to-tail so that unequal crossing-over has led to copy number variation (CNV) as well as hybrid (chimeric) genes, making it difficult to identify true alleles. One approach is to examine BG genes expressed in particular cell types, which likely have the same functions in different BG haplotypes and thus can be considered "functional alleles." We cloned nearly full-length BG transcripts from peripheral T cells of four haplotypes (B2, B15, B19, and B21), and compared them to the BG genes of the B12 haplotype that previously were studied in detail. A dominant BG gene was found in each haplotype, but with significant levels of subdominant transcripts in three haplotypes (B2, B15, and B19). For three haplotypes (B15, B19, and B21), most sequences are closely-related to BG8, BG9, and BG12 from the B12 haplotype. We found that variation in the extracellular immunoglobulin-variable-like (Ig-V) domain is mostly localized to the membrane distal loops but without evidence for selection. However, variation in the cytoplasmic tail composed of many amino acid heptad repeats does appear to be selected (although not obviously localized), consistent with an intriguing clustering of charged and polar residues in an apparent α-helical coiled-coil. By contrast, the dominantly-expressed BG gene in the B2 haplotype is identical to BG13 from the B12 haplotype, and most of the subdominant sequences are from the BG5-BG7-BG11 clade. Moreover, alternative splicing leading to intron read-through results in dramatically truncated cytoplasmic tails, particularly for the dominantly-expressed BG gene of the B2 haplotype. The approach of examining "functional alleles" has yielded interesting data for closely-related genes, but also thrown up unexpected findings for at least one haplotype.

Keywords: B-G, membrane protein, adaptive immunity, innate immunity, B7 family

OPEN ACCESS

Edited by:
Pierre Vantourout, King's College London, United Kingdom

Reviewed by:
Daniel Olive, Aix Marseille Université, France
Jacques Robert, University of Rochester, United States

***Correspondence:**
Jim Kaufman
jfk31@cam.ac.uk

†Present address:
Michaela Fakiola, National Institute of Molecular Genetics (INGM), Milan, Italy

Specialty section:
This article was submitted to T Cell Biology, a section of the journal Frontiers in Immunology

Received: *23 February 2018*
Accepted: *16 April 2018*
Published: *01 May 2018*

Citation:
Chen L, Fakiola M, Staines K, Butter C and Kaufman J (2018) Functional Alleles of Chicken BG Genes, Members of the Butyrophilin Gene Family, in Peripheral T Cells. Front. Immunol. 9:930. doi: 10.3389/fimmu.2018.00930

INTRODUCTION

The chicken major histocompatibility complex (MHC) was first described as the B blood group, based on serological reactions mainly with the so-called BG antigen on erythrocytes. Later experiments showed that recombination events could separate most of the BG antigen reactivity in the BG region from the antigens encoded by classical class I and class II genes in the BF-BL region

(1–5). The fact is that BG molecules, like class I and class II molecules, are highly polymorphic cell surface antigens with wide tissue distributions and encoded in the MHC led one eminent researcher to refer to them as the class IV antigens and to the early speculation that they might be the ligands of the newly discovered chicken γδ T cells, but various approaches to demonstrate this possibility failed (6, 7).

Now it is clear that some homologs of the BG molecules, such as the butyrophilin (BTN) and butyrophilin-like (BTNL) molecules, may indeed to be the ligands of mammalian γδ cells (8–11). The discovery of myelin oligodendrocyte glycoprotein (MOG) in the nervous system of rodents and of BTN in lipid droplets of cow milk (12–14) eventually led to the description of the BTN gene family. This BTN family includes BTN, BTNL, skin T cell (SKINT), and BG genes, based mainly on the sequence relationships of the immunoglobulin-variable-like (Ig-V) extracellular domain, and is overall part of the larger B7 gene family (15). Certain BTN family members are known to be involved in immunological reactions, including some expressed on T cells reported to be involved in negative co-stimulation and some expressed as heterodimers on epithelial cells involved in recognition by T cells with certain restricted γδ TCRs (8, 10, 16, 17).

There are similarities but also differences between the mammalian BTN family members and chicken BG molecules. Both the BTN and BG genes are multigene families with wide tissue distribution, some members being expressed on hemopoietic cells, and others being expressed on other cell types, particularly epithelial cells (8–11, 18, 19). Some BTN family genes are known to function as heterodimeric glycoproteins in recognition by mammalian γδ T cells (16, 17); BG molecules have long been known to be disulfide-linked dimers, although without apparent glycosylation, and the presence of homo- versus hetero-dimers has not been resolved (20–22). However, there are various intron–exon and domain organizations within the mammalian BTN family (8–11), none of which are identical to the BG genes (20, 23, 24). In particular, the cytoplasmic tails of mammalian BTN family members have only a few heptad repeats and typically end with a 30.2 (also called PRY-SPRY) domain; by comparison the BG molecules all have long cytoplasmic tails composed of many heptad repeats. Moreover, high serologic polymorphism, copy number variation (CNV) and rapid evolution of BG genes in the BG region have been reported compared with the mammalian BTN family members (24).

At the moment, it is not clear whether the polymorphism of the BG genes is functionally important. Comparison of alleles of BG loci was easy for the two singleton genes: a nearly monomorphic BG0 gene on chromosome 2 and the polymorphic BG1 gene in the BF-BL region on chromosome 16 (25). All other known BG genes are located head-to-tail in the BG region on chromosome 16, which renders them targets for apparent gene conversion (meaning that the polymorphism might be due to drift rather than selection) and also subject to unequal crossing-over (meaning that the CNV makes it hard to unequivocally identify orthologous alleles in different BG haplotypes) (24, 25). To approach these problems, we have assumed that the genes from different haplotypes expressed in particular cell types could be considered alleles in a functional sense. If such "functional alleles" could be reliably identified, then the sequences could be compared for amount and location of variation, and assessed for selection at the protein level.

The BG genes of the B12 haplotype are the most intensely studied, and one of the simplest patterns was from peripheral T cells, in which the BG9 gene was strongly expressed and the BG12 gene was weakly expressed, as assessed by reverse-transcriptase polymerase chain reaction (RT-PCR) with SS-TM primers that amplified the signal sequence to transmembrane region, followed by cloning and sequencing (24). In this study, we developed "HU" primers from near the beginning of the 5′ untranslated region (5′UTR) of hemopoietic ("H") BG genes to near the end of the 3′ untranslated region (3′UTR) of all known (universal or "U") BG genes, and sequenced the nearly full-length amplicons from four chicken lines with other B haplotypes: line 6_1 (B2), line 15I (B15), line P2a (B19), and line N (B21). We expected to find a single or dominantly expressed BG gene in each haplotype that would be closely related to the BG9 gene found in the B12 haplotype, which would allow us to determine whether the sequence variation between haplotypes is localized and/or selected in the extracellular region, the cytoplasmic tail, both, or neither.

MATERIALS AND METHODS

Chicken Lines and Haplotypes

Four lines of White Leghorn chickens were maintained under specific pathogen-free condition at the Pirbright Institute (formerly the Institute for Animal Health) in Compton, UK: line N, line P2a, line 15I, and line 6_1, with the MHC haplotypes of B21, B19, B15, and B2, respectively. The history of these lines is described (26).

Isolation of Cells

Peripheral blood was taken from wing veins with heparin and washed twice with cold PBS by centrifugation at 300 *g* at 4°C for 5 min and resuspension in cold PBS. Cells were counted using a hemocytometer, and around 5×10^7 lymphocytic cells in 2 ml were stained at 4°C in the dark for 1 h using T cell specific antibodies [10 µl mouse anti-chicken CD4-FITC and 10 µl of mouse anti-chicken CD8b-FITC for lines N and P2a; 10 µl mouse anti-chicken CD4-RPE and 10 µl of mouse anti-chicken CD8-RPE for lines 15I and 6_1 (all antibodies from Southern Biotech)]. Then the cells were washed 3–4 times with cold PBS and resuspended into 1 ml cold PBS for sorting, using magnetic-activated cell sorting (MACS, Miltenyi Biotec) for line N and P2a, and a DakoCytomation MoFlo MLS high-speed cell sorter (Beckman Coulter) for fluorescence-activated cell sorting (FACS, performed by Mr. Nigel Miller in the Department of Pathology) for line 15I and 6_1.

RNA Isolation, cDNA Synthesis, and PCR Amplification

Roughly 1×10^6 sorted T cells were extracted for total RNA following the manufacturer's protocol for the NucleoSpin RNA II RNA extraction kit (Machery-Nagel). First strand cDNA was produced from 5 to 10 ng RNA following the manufacturer's

protocol for the Maxima H Minus First Strand cDNA Synthesis Kit (ThermoFisher). Briefly, the RNA was mixed with oligo-$(dT)_{18}$ primer and dNTP mixtures, heated at 65°C for 5 min, chilled on ice for 3 min, RT buffer and Maxima H Minus Enzyme Mix added, and the reaction mixture incubated at 55°C for 45 min, followed by 85°C for 45 min to inactivate the enzyme.

PCR amplification was carried out using Phusion® Hot Start Flex DNA Polymerase (NEB) in a 50 µl reaction mixture with 0.5 µl (5–10 ng) cDNA, 200 µM total dNTPs (1 µl of 10 mM stock), Phusion buffer (10 µl of 5× stock), 1 U Phusion enzyme (0.5 µl of 200 U/ml), 250 nM forward primer and 250 nM reverse primer (both 1.25 µl of 10 µM stocks), and nuclease-free water (35.5 µl), and with reaction conditions of 2 min at 98°C, 35 cycles of 98°C 10 s, 66.5°C 20 s and 72°C 60 s, and finally 10 min at 72°C.

The SS forward (UC74) and TM reverse (UC76) primers (5′CTCCTGCCTTATCTCRTGGCTCTGCAC 3′and 5′CACAG CCAGAGCCACYKTCCAG 3′) to amplify the signal sequence to transmembrane region (**Figure 1**) have been described (24). The H forward (UC206) primer (5′TCCGCTCGAGCTCT CTYCTCCTACAG3′) has been described (25). The U reverse (UC650) primer (5′TAACACCCAAAGCAGTTTTCTNCC3′) was designed by inspection. The location of the HU primer pair to amplify nearly full-length cDNA is indicated (**Figure 1**).

Cloning and Sequencing

Several bands were generated after HU–PCR reaction, as illustrated by 1% agarose gel electrophoresis of a representative example (**Figure 1**). Amplification with SS-TM primers in pilot experiments revealed that all bands from 1,500 to 3,000 bp contained BG cDNA sequences. For the final experiments, a single region was cut out of the gel after shorter times of electrophoresis (20 min at 100 V), so that sequences of all these sizes were treated in parallel. DNA was extracted using the ISOLATE II PCR and Gel Kit (Bioline).

DNA fragments were cloned into the pJET vector (CloneJET PCR cloning kit, ThermoFisher), 92–96 colonies were picked for colony PCR using HU primers, and DNA from the 40–60 positive clones was prepared by Miniprep (PureLink Quick Plasmid Miniprep Kit, Invitrogen) and sent for dideoxy chain termination sequencing (DNA Sequencing Facility, Department of Biochemistry, University of Cambridge). Sequencing primers

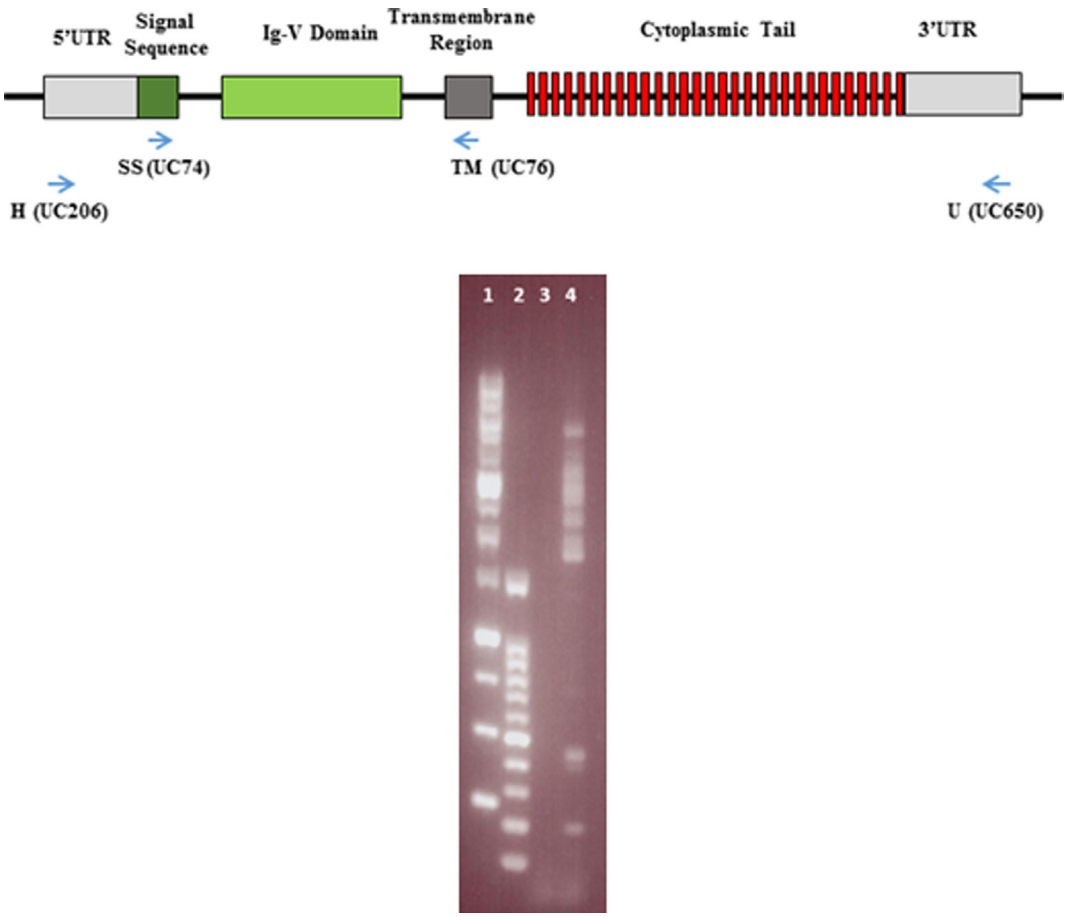

FIGURE 1 | Representation of the intron–exon structure of a typical BG gene, with the encoded mRNA regions and protein domains indicated, as well as the location of the primers for the SS-TM and HU amplifications (top). Picture of agarose gel with the results of a representative amplification using HU primers (bottom). Lane 1, GeneDireX 1 kB markers (10, 8, 6, 5, 4, 3, 2.5, 2, 1.5, 1, 0.75, 0.5, and 0.25 kB); lane 2, GeneDireX 100 bp markers (1500, 1000, 900, 800, 700, 600, 500, 400, 300, 200, and 100 bp); lane 3, no template control PCR; lane 4, PCR with line N T cell cDNA.

wereT7(5′TAATACGACTCACTATAGGG3′),pJETR(5′AAGAACATCGATTTTCCATGGCAG3′),UC699(5′TTTTCTATGATCATCC 3′), UC700 (5′ TTTTCTATGATCATCC 3′), UC701 (5′ TGGCTCTGCACYTCCTCS 3′), and UC703 (5′ TGRACCTGGAGGTGTCAG 3′). Sequencing identified 35–45 BG clones, some of which were BG0 and BG1 and therefore were not further analyzed. Names were given to the sequences from the remaining clones, according to the following convention: abbreviated line name, "T" for T cells, "BG," a letter representing the exon 2 sequence with "a" being the most frequently detected exon 2 sequence (and "b" being the second most frequently detected exon 2 sequence, and so forth), a dash and then a number representing the alternative splicing variant with "1" being the most frequently detected clone (and "2" the second most frequently detected clone, and so forth). Some of these clones were eventually found to be chimeras, and were not further considered in the analyses, leading to 57 final sequences (Figure S1 in Supplementary Material).

Sequence Analysis

Sequencing trace data were viewed, trimmed, and assembled in CLC DNA Workbench 5 (QIAGEN). Primary sequence alignments were carried out in CLC and finished sequences were exported into MEGA7[1] for Clustal W alignment, from which the ".meg" file was generated and used for phylogenetic analysis using Neighbor Joining method in MEGA7 with bootstrap (1000) for phylogeny test. Sequence alignments were imported into BioEdit Sequence Alignment Editor,[2] then exported as a "rich text with current shaded view setting," opened in Word (Microsoft) and modified manually by adding annotations. Helical wheel analysis for the cytoplasmic tails was done using online program DrawCoil10[3] and **Figure 8** and Figure S5 in Supplementary Material were modified from the diagrams generated from this program. The model for Ig-V domain of BG8 in **Figure 7** was built by Swiss-Model[4] based on the template of the MOG molecule (PDB ID 3csp.1) sharing 40.35% identity in amino acid sequences. The structure was then viewed, edited, and annotated in PyMOL.[5] All the other figures were designed and manipulated in Word or Powerpoint (Microsoft).

RESULTS

One Dominant and Several Other BG Genes Are Expressed in Peripheral T Cells of Each B Haplotype, With Most Part of the BG8-BG9-BG12-BG13 Clade

Peripheral T cells were isolated from the blood of four chickens from lines with different B haplotypes: line 6_1 (B2) and line 15I (B15) by FACS and line P2a (B19) and line N (B21) by MACS, and both with a cocktail of monoclonal antibodies (mAb) to CD4 and CD8. Total RNA was converted to cDNA using reverse-transcriptase and an oligo-dT primer, and then nearly full-length transcripts were amplified by PCR using HU primers, cloned and sequenced on both strands. Two independent PCR reactions were analysed, and for line 6_1 (B2) a third PCR reaction was carried out using SS-TM primers, expected to detect all BG transcripts.

For each chicken line, 26–84 BG cDNA clones (excluding BG0 and BG1 clones) were isolated and then sequenced with a variety of primers, with the reads assembled and analysed (**Figure 2**). Fifty-seven unique sequences were found (Figure S1 in Supplementary Material). Assuming that each unique sequence of the extracellular Ig-V domain (encoded by exon 2) corresponds to a gene, the 57 unique sequences originate from 16 genes, with 3–5 genes expressed in each haplotype, none of which were shared between any two of the four haplotypes (**Figure 2**). Comparison of the nearly full-length sequences within each gene based on exon 2 sequences revealed that almost all differences were due to alternative splicing events in the cytoplasmic tail, which will be further described in a later section of the Results. However, some exon 2 sequences within a line differ in only one nucleotide and were only found in a single PCR (see Figure S1 in Supplementary Material). It seems likely that some of these clones are due to nucleotide mis-incorporation during amplification, but they were considered as separate genes since there are examples of separate genes with single nucleotide differences within the B12 haplotype (24). Based on the number of clones with different exon 2 sequences, there is one gene expressed more than the others in all four samples, but only in the N line (B21) was one gene really overwhelmingly dominant as found previously for the B12 haplotype (**Figure 2**).

Based on the intron–exon structures of BG genes (**Figure 1**) from the well-characterized B12 haplotype, the cDNA sequences from the four haplotypes could be organized conceptually into transcript sequences without introns, which could be used for the first stage of analysis. By comparison with the 14 BG genes of the B12 haplotype (24), the conceptual transcript sequences from these cDNA clones were mainly from the phylogenetic clade of BG8-BG9-BG12-BG13 genes of the B12 haplotype (**Figure 3**). The sequences of this clade have a 5′UTR characteristic of hemopoietic BG genes (as expected for genes amplified with an H forward primer) with a cytoplasmic tail and 3′UTR characteristic of the so-called type 2 sequence, quite different from the 5′UTR sequences of tissue BG genes and those genes with so-called type 1 cytoplasmic region and 3′UTR sequences (**Figure 4**).

Some features of the BG genes from line 6_1 (B2) are different from those of the other three haplotypes. Throughout the length of the sequences, the dominantly expressed conceptual transcripts (as defined in the previous paragraph) from B15, B19, and B21 (BG8, BG9, and BG12 gene sequences from B12) are much more closely related with each other than with the dominantly expressed conceptual transcript from B2 (and the BG13 gene sequence) (**Figures 3** and **5**). The BG13 gene had already been seen to have an apparent gene conversion in exon 2 (25), but based on these latest data, we now consider the BG8-BG9-BG12 clade as having a type 2a cytoplasmic tail, with the BG13 (and other sequences such as BG3, BG4, and BG6) having a type 2b cytoplasmic tail (but not for the 3′UTR, which are nearly identical in all these sequences). Another surprise was the fact that many of the cDNA sequences isolated from line 6_1 (B2) are in fact identical (or very nearly so) to BG genes from the B12 haplotype (**Figure 3**), an unexpected finding for us since

[1]http://www.megasoftware.net/ (Accessed: January, 2018).
[2]http://en.bio-soft.net/format/BioEdit.html (Accessed: January, 2018).
[3]http://www.grigoryanlab.org/drawcoil/ (Accessed: January, 2018).
[4]https://swissmodel.expasy.org/ (Accessed: January, 2018).
[5]https://pymol.org/2/ (Accessed: January, 2018).

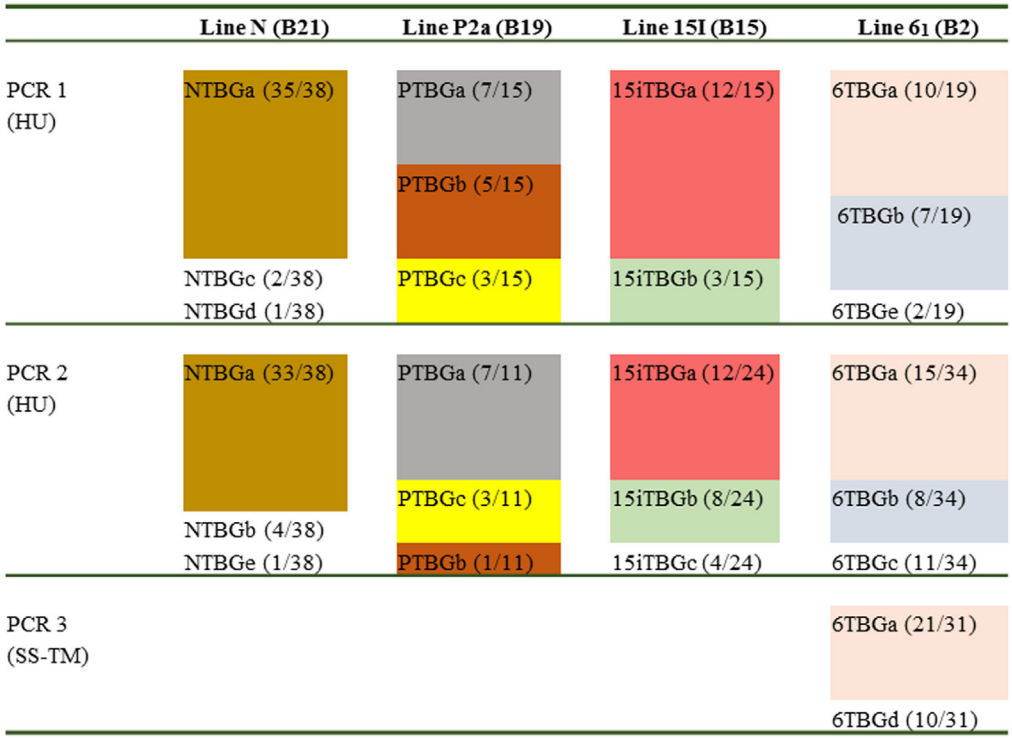

Line CB (B12)	Line N (B21)	Line P2a (B19)	Line 15I (B15)	Line 61 (B2)
BG9 (25/28)	NTBGa (68/76)	P2aTBGa (14/26)	15iTBGa (24/39)	6TBGa (46/84)
BG12 (3/28)	NTBGb (4/76)	P2aTBGb (6/26)	15iTBGb (11/39)	6TBGb (15/84)
	NTBGc (2/76)	P2aTBGc (6/26)	15iTBGc (4/39)	6TBGc (11/84)
	NTBGd (1/76)			6TBGd (10/84)
	NTBGe (1/76)			6TBGe (2/84)

FIGURE 2 | Overall results for the number of genes (based on exon 2 sequences) amplified from cDNA preparations derived from blood T cells isolated from various chicken lines (with different B haplotypes): line CB (B12), line N (B21), line P2a (B19), line 15I (B15), and line 6_1 (B2). Top panel, independent amplifications from the four chicken lines; HU, hemopoietic forward and "universal" reverse primers to give nearly full-length sequences; SS–TM, signal sequence forward and transmembrane reverse primers to give SS, extracellular Ig-V domain and TM regions. Different colors indicate different exon 2 sequences, except those sequences that are only found in one PCR reaction. Names follow the convention: abbreviated line name, "T" for T cells, "BG" and a letter representing the exon 2 sequence with "a" being the most frequently detected exon 2 sequence (and "b" being the second most frequently detected exon 2 sequence, and so forth); numbers in parentheses indicate the number of clones found for a particular exon 2 sequence out of the total number for the particular PCR reaction. Bottom panel, the total results for four chicken lines from this paper and for the CB line (B12) from Ref. (24).

the B haplotype was originally defined by serology predominantly of the BG region. In fact, the serological identity of B2 and B12 molecules on erythrocytes was noted long ago (5), and confirmed by two-dimensional gel analysis (27). The mystery deepens with the realization that the dominantly expressed BG gene from B12 T cells is BG9 (despite the presence of a BG13 gene), whereas the dominantly expressed BG transcript from B2 T cells is identical in sequence to BG13, with no BG9 sequence found (**Figures 2** and **3**).

Finally, the subdominant cDNA sequences varied between haplotypes. Most of these subdominant sequences are also most closely related to the BG8, BG9, and BG12 sequences, but some are more closely related to the BG5-BG7-BG11 clade (**Figures 3** and **4**), which has 5′UTR sequences characteristic of hemopoietic BG genes but with a cytoplasmic tail and 3′UTR characteristic of the so-called type 1 sequence (24). In particular, of the four subdominant transcripts in line 6_1 (B2), one is identical and another nearly identical to BG7 while a third (for which only the V domain sequence is complete) is identical to BG11 (**Figures 3** and **4**).

The Dominantly Expressed BG Genes for Three Haplotypes Show Evidence for Clustering of Variation but Not Selection in the Extracellular Domain Compared With Selection but Not Clear Clustering in the Cytoplasmic Tail

All BG genes can be divided up into the 5′UTR and signal sequence encoded by exon 1, the Ig-V extracellular domain

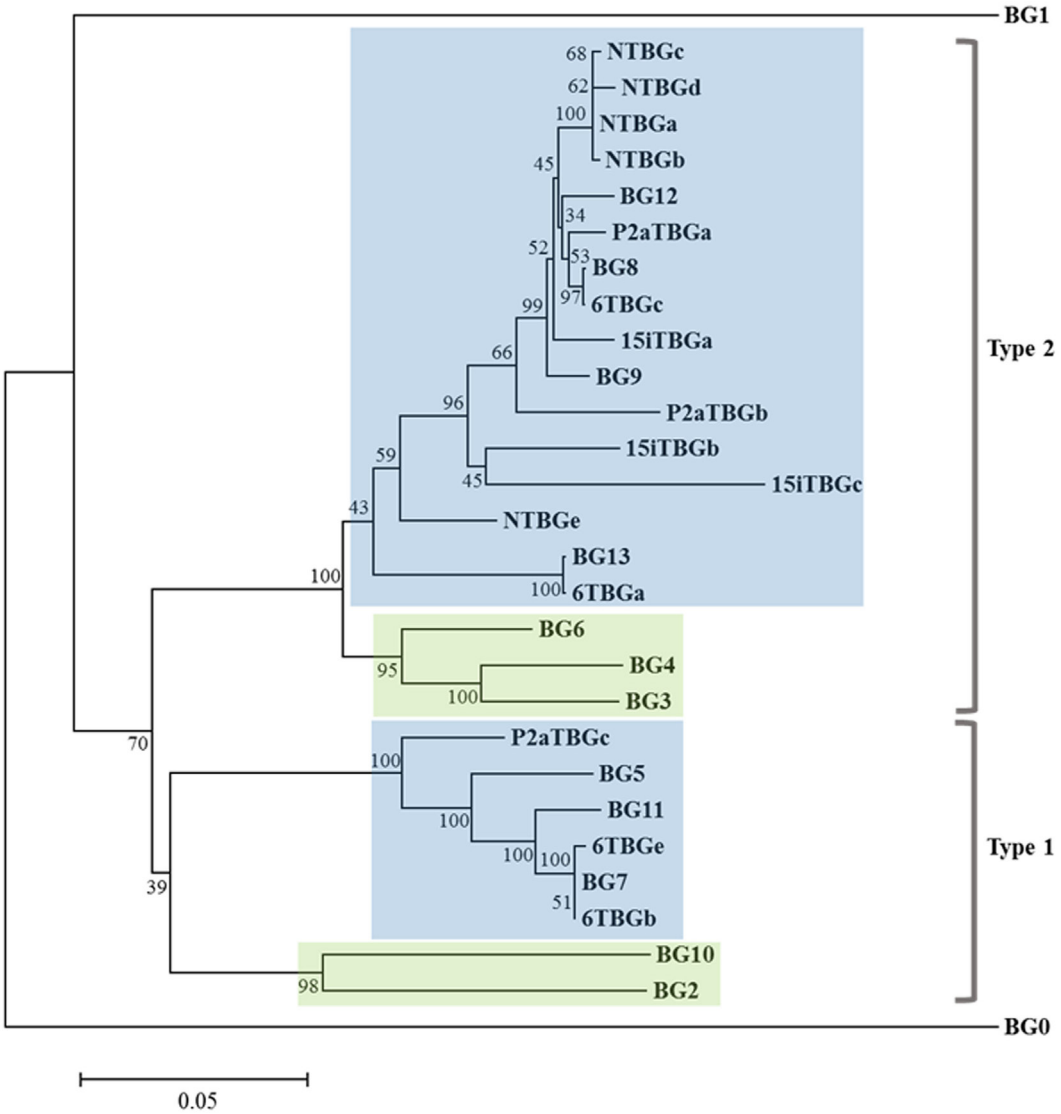

FIGURE 3 | Phylogenetic tree of nucleotide sequences for the "(nearly) full-length conceptual transcripts" (i.e., exons without introns) for the 16 genes from four chicken lines identified in this paper, and for the 14 BG genes of the B12 haplotype from Ref. (24). Names of the transcripts follow the convention: abbreviated line name, "T" for T cells, "BG" and the letter "a" representing the most frequently detected clone from the most frequently detected exon 2 sequence (and "b" representing the most frequently detected clone from the second most frequently detected exon 2 sequence, and so forth). Names of the genes follow the convention "BG" and the number of the gene locus from the B12 haplotype. Indicated by color are those clades with 5′ ends of hemopoietic (blue) and tissue (green), and by brackets for 3′ ends of type 1 and type 2. Branch lengths are scaled by genetic distance, and percentage bootstrap values are indicated at the nodes. 6TBGd is not present in this tree since it was only detected by the SS–TM amplification, and some sequences may be due to nucleotide mis-incorporation during amplification (for instance, NTBGa may have given rise to NTBGb and NTBGc, see Figure S1 in Supplementary Material).

encoded by exon 2, the transmembrane region encoded in exon 3, a cytoplasmic tail of heptad repeats mostly encoded by many 21 nucleotide exons, and 3′UTR encoded within the final exon (**Figure 1**) (24). The phylogenetic relationships seen for exon 2 are true for the whole of the conceptual transcripts, except for the few that have a type 1 cytoplasmic tail and 3′UTR.

It is of interest to gain insight into the features of the sequences at the nucleotide and amino acid level, including the location and potential clustering of the sequence variation as well as any evidence for selection. As mentioned above, the dominantly expressed conceptual transcript from line 6_1 (B2) is identical to the BG13 sequence of the B12 haplotype, so there is no allelic variation to consider (**Figures 3** and **5**). However, there is variation throughout the conceptual transcripts of the dominantly expressed cDNAs from the three other haplotypes, which can be compared with the BG genes of the B12 haplotype (**Figure 5**; Figure S3 in Supplementary Material).

The 5′UTR of the dominantly expressed BG sequences expressed in T cells, like all other hemopoietic BG genes, has a large indel compared with those BG genes of the B12 haplotype

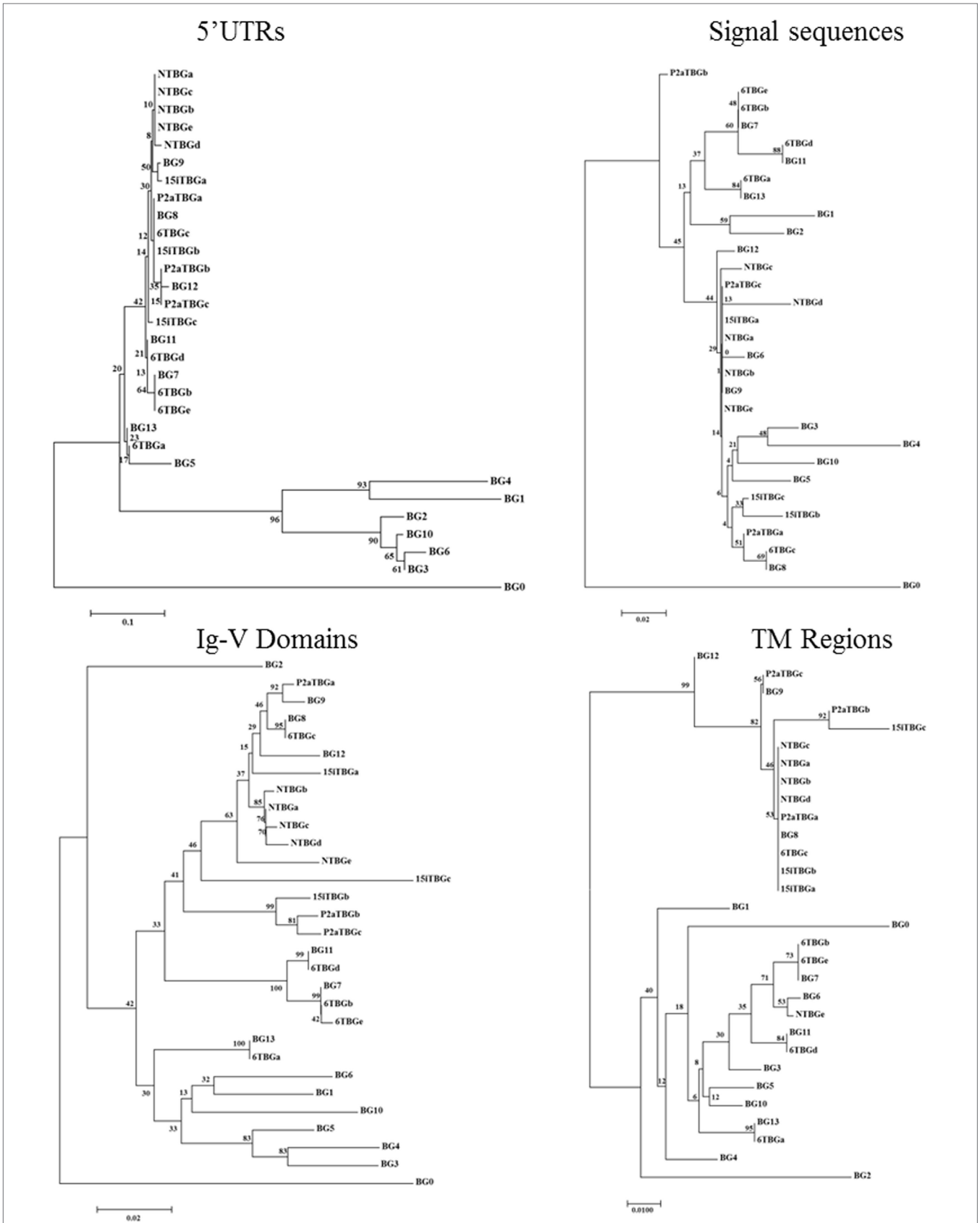

FIGURE 4 | Continued

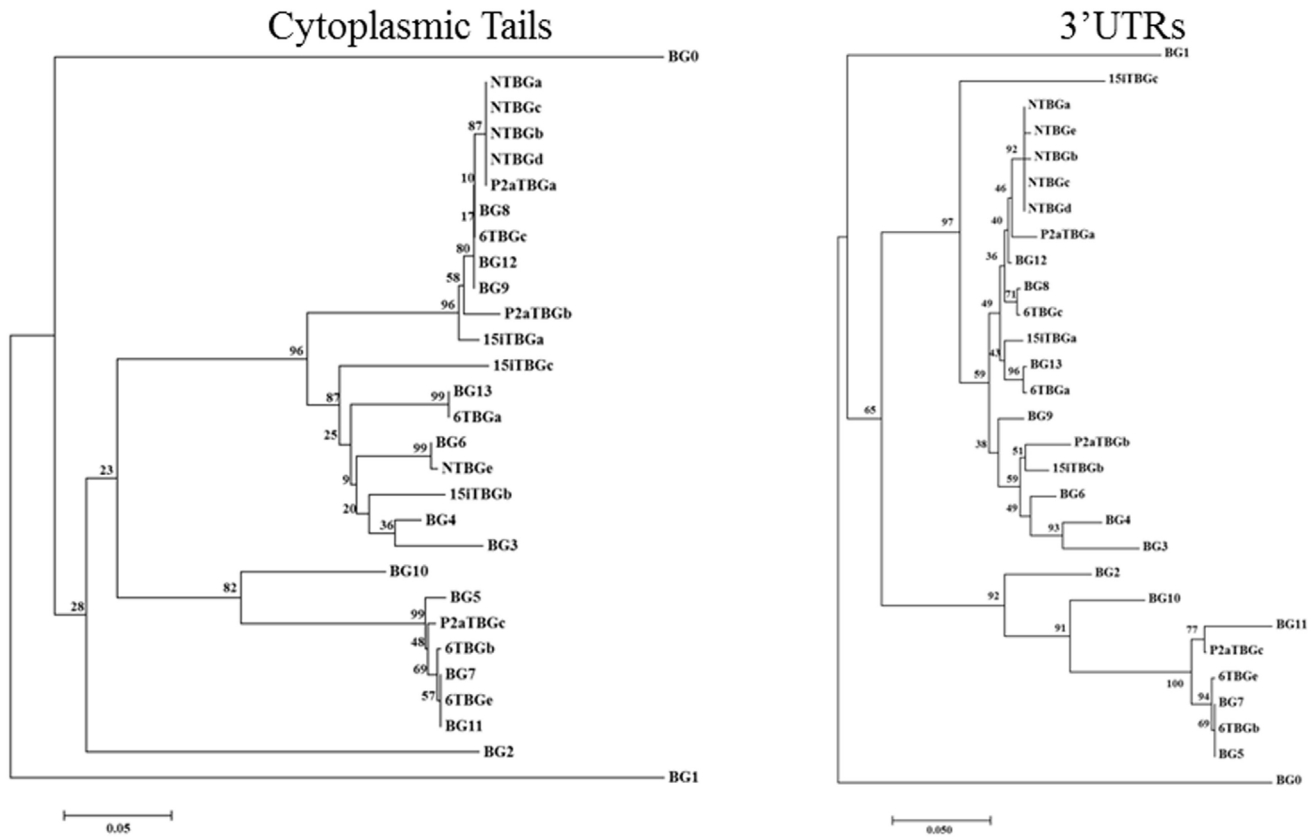

FIGURE 4 | Phylogenetic trees of nucleotide sequences for portions of the "(nearly) full-length conceptual transcripts" (i.e., exons without introns) for the 16 genes (based on exon 2 sequences) from four chicken lines identified in this paper, and for the 14 BG genes of the B12 haplotype from Ref. (24). Trees include 5′ untranslated region (5′UTR) from exon 1, signal sequence from exon 1, exon 2 (two nucleotides from the signal sequence and then the nucleotides encoding the Ig-V domain), exon 3 (transmembrane region), the exons corresponding to the cytoplasmic tail (excluding any nucleotides in the final exon that encode amino acids), and the final exon [which is exactly the 3′ untranslated region (3′UTR) in some sequences, but for which the first nucleotides encode the last amino acids of the cytoplasmic tail in most sequences]. Other details are in the **Figure 3**.

that are expressed primarily in tissues (Figure S3 in Supplementary Material). Only 15 positions out of 137 nucleotides in the 5′UTR (excluding the primer binding site) differ in one or another of the dominantly expressed sequences from the four haplotypes (including B2) as well as the BG8, BG9, BG12, and BG13 genes of the B12 haplotype, and this variation is of unknown significance.

In the portion of exon 1 encoding most of the signal sequence (**Figure 6**; Figure S4 in Supplementary Material), only 1–6 differences out of 99 nucleotides leading to 0–4 changes in 33 amino acids are found in the dominantly expressed sequences from the four haplotypes (including B2) as well as the BG8, BG9, BG12, and BG13 genes of the B12 haplotype. There is only one (silent) nucleotide change that fails to lead to an amino acid change, so the variation might appear to be selected. However, this variation does not change the overall hydrophobic sequence nor does it change the signal peptidase site of three small amino acids (the last codon of which is split, with the second and third positions located in exon 2).

Compared with the BG8 gene of the B12 haplotype, the variation in the part of exon 2 encoding the extracellular Ig-V domain ranges from 4 to 9 differences out of 342 nucleotides leading to 1–5 changes in 114 amino acids in the three haplotypes (B15, B19, and B21), and 22 nucleotides and 12 amino acids for line 6_1 (B2) and BG13 (B12) (**Figure 7**; Figure S4 in Supplementary Material). The location of the variation is not clustered along the sequence, but for the three haplotypes (and BG8, BG9, and BG12 of the B12 haplotype), a structural model (**Figure 7**) shows that nearly all the amino acid variation is located in the membrane distal loops presumably pointing away from the cell surface, with one position in the β-strands and one in the loops underneath the Ig-V domain. For line 6_1 (B2) and BG13 (B12), there is more variation away from the distal loops. However, there was no change in the cysteines that form the intra-domain disulfide bond, or the cysteine located in the equivalent of complementarity determining region 1 (CDR1) that form a disulfide bond between the two chains of a BG dimer.

Comparison of the codons in the extracellular Ig-V domain for which there is nucleotide variation (**Figure 6**; Figure S4 in Supplementary Material) shows that for each sequence of the three haplotypes, the nucleotide changes that lead to no change in the amino acid (silent or synonymous changes) versus those that lead to a change in the amino acid (replacement or non-synonymous

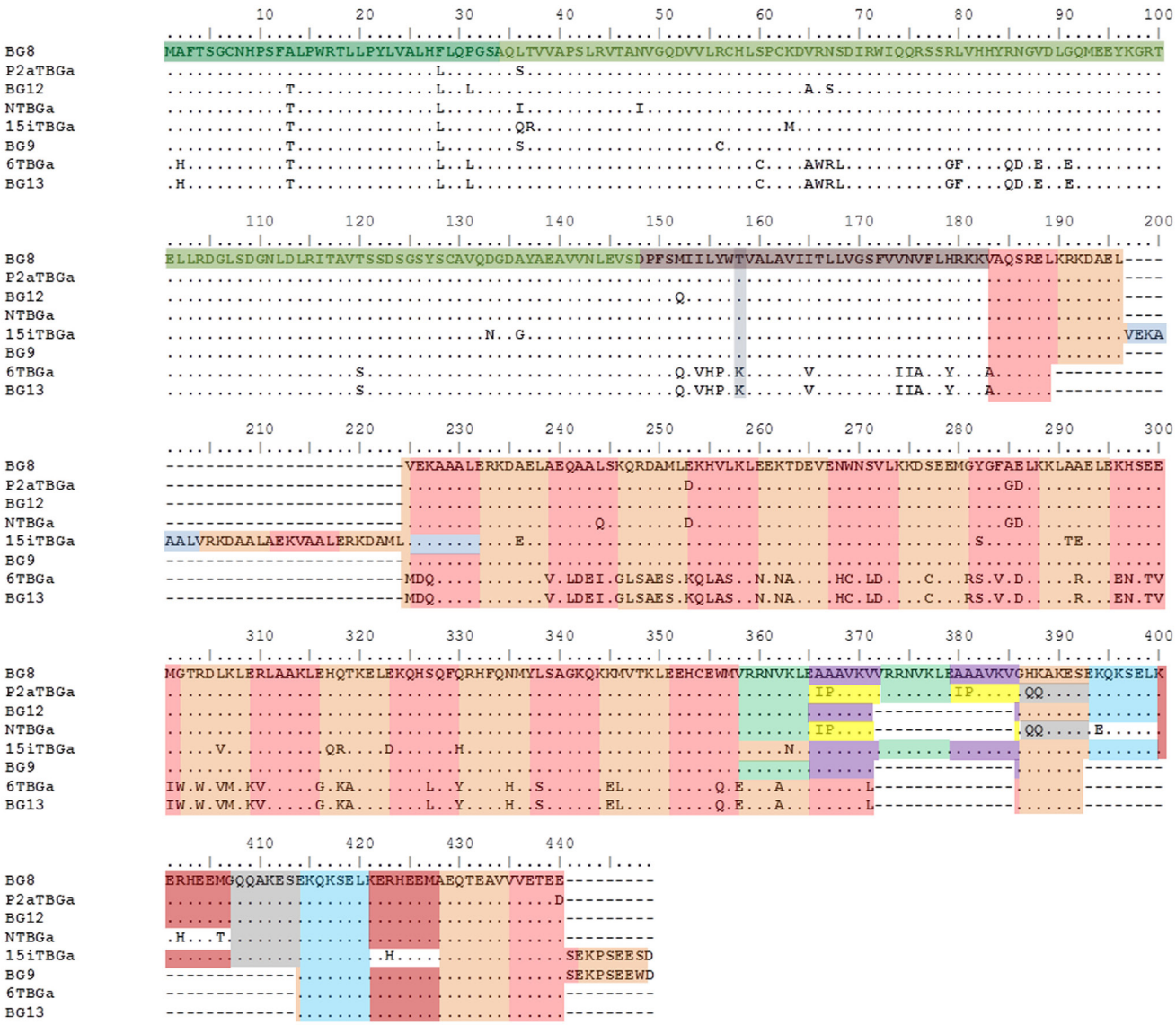

FIGURE 5 | Alignment of amino acid sequences from the "(nearly) full-length conceptual transcripts" (i.e., exons without introns) for the dominantly expressed genes from four chicken lines identified in this paper, and for the appropriate BG genes (BG8, BG9, BG12, and BG13) of the B12 haplotype from Ref. (24). Names of the transcripts follow the convention: abbreviated line name, "T" for T cells, "BG" and the letter "a" representing the most frequently detected clone from the most frequently detected exon 2 sequence. Names of the genes follow the convention "BG" and the number of the gene locus from the B12 haplotype. Regions of the amino acid sequence are indicated with colors (but with amino acids split between two exons indicated by both colors): signal sequence, darker green; Ig-V domain, bright green; transmembrane region, darker brown (with lysine/threonine dimorphism in gray-blue); heptad repeats based on 21 nucleotide exons, alternating orange and light brown (except for some repeated exons in gray, light green, purple yellow, and light blue). Letters indicate amino acids by single letter code, dots indicate identities with BG8 sequence, dashes indicate no sequence present (deletion). Cytoplasmic tail of 6TBGa is conceptual, as alternative splicing leads to intron read-through and an early stop codon.

changes) range from two silent and one replacement change to three silent and five replacement changes. Comparison of the dominantly expressed BG from line 6_1 (B2) and BG13 (B12) with the other three haplotypes (and BG8, BG9, and BG12) shows 7 silent and 12 replacement changes. Given that random changes would be expected to lead to only twice as many replacements as silent changes, these data are not consistent with strong selection.

There are two kinds of transmembrane regions described for BG genes, which are also found in the conceptual transcripts of the four haplotypes (Figure S3 in Supplementary Material). The dominantly expressed BG sequence for line 6_1 (B2) is identical to BG13, with the transmembrane region bearing a lysine in the otherwise hydrophobic region. The dominantly expressed BG sequences from the other three haplotypes (and BG8, BG9, and BG12) all have with a threonine instead of the lysine along with nine other amino acid differences compared to BG13. There is no variation between the transmembrane region sequences of the three haplotypes (and only one amino acid difference in BG12).

		S (1)	S (2)	S (3)	N (1)	N (2)	N (3)	N (1+2)	N (1+3)	N (2+3)	N (1+2+3)
Signal Sequence	NTBGa				2						
	P2aTBGa				1						
	15iTBGa				2						
	BG9				2						
	BG12				2	1					
	BG13-6TBGa			1	2	1		1			
Ig-V Domain	NTBGa			2	1					1	
	P2aTBGa			2				1			
	15iTBGa			3	1	3				1	
	BG9			2	1			1			
	BG12	1		3		1				1	
	BG13-6TBGa			7	3	6			1	2	
TM Region	NTBGa										
	P2aTBGa										
	15iTBGa										
	BG9			1							
	BG12			2				1			
	BG13-6TBGa			3	4	3		1		1	1
Cytoplasmic Tail	NTBGa			2	3	4	3	1		1	
	P2aTBGa			2	3	2	4	2			
	15iTBGa	1		1	4	8	5	2		2	
	BG9						1			1	
	BG12										
	BG13-6TBGa	2			20	16	7	6	4	3	2

FIGURE 6 | Compared with BG8 of the B12 haplotype, the number of silent and replacement changes by codon position for the "(nearly) full-length conceptual transcripts" (i.e., exons without introns) of the dominantly expressed genes from four chicken lines identified in this paper, and of the other appropriate BG genes (BG9, BG12, and BG13) of the B12 haplotype from Ref. (24). Names of the transcripts follow the convention: abbreviated line name, "T" for T cells, "BG" and the letter "a" representing the most frequently detected clone from the most frequently detected exon 2 sequence. Names of the genes follow the convention "BG" and the number of the gene locus from the B12 haplotype. Values are based on the alignments in Figure S4 in Supplementary Material, and amino acids from split codons at the edges of the exons are assigned to the exon with two of the three nucleotides of the codon (for instance, last amino acid of the signal sequence is assigned to the Ig-V domain, which in fact starts with glutamine in the mature protein).

By contrast, there are only three silent nucleotide changes out of 17 total in line 6_1 (B2) and BG13, and three codons have multiple nucleotide changes, again consistent with some selection between the BG8-BG9-BG12 sequences and the BG13 sequences (**Figure 6**; Figure S4 in Supplementary Material).

The cytoplasmic tail is composed of amino acid heptad repeats encoded by 21 nucleotide exons (with a few exons of 18 or 24 nucleotides), the numbers of which vary between BG genes (**Figure 5**; Figures S2 and S3 in Supplementary Material). Besides different numbers of the exons that code for these heptad repeats, the location of the first stop codon either in the penultimate exon or at the beginning of the last exon affects the numbers of repeats. The dominantly expressed BG sequence for line 6_1 (B2) is like BG13, with 27 such exons in the conceptual transcript. The conceptual transcripts of the other three haplotypes have dominantly expressed BG sequences that are similar to BG8 (33 exons), BG9 (28 exons but a stop codon after a repeat in final exon, giving 29 apparent heptad repeats), and BG12 (31 exons): 37 exons for line 15I (B15) that has an apparent insertion of 4 exons but in addition a stop codon after a repeat in the final exon (giving 38 apparent repeats), 33 repeats for line P2a (B19), and 29 repeats for line N (B21).

The presence of amino acid heptad repeats encoded by 21 nucleotide exons strongly suggests that the two cytoplasmic tails of a BG dimer form an α-helical coiled-coil, similar to what is sometimes called a leucine zipper (28, 29). In such coiled-coils, the first and fourth amino acids in a true heptad repeat (which from here will be called *a* and *d* positions) act as the interface between the two chains, with some contribution by the neighboring amino acids (*e* and *g* positions) (30). To better understand the sequence features of the cytoplasmic tail, as well as location of any variation, representations of helical wheels were inspected.

It seems unlikely that *a* and *d* amino acids forming the interface of the two chains in the coiled-coil would involve the first amino acid of each 21 nucleotide exon, since that amino acid is encoded by one nucleotide from the previous exon followed by two nucleotides from the exon under consideration, and thus the first amino acid encoded by this split codon would vary depending on the previous exon. In fact, the helical wheels of both BG8 and BG13 revealed a clear pattern (**Figure 8**): the amino acids from the fourth codon and the last codon of the 21 nucleotide repeat are mostly hydrophobic, presumably corresponding to the *a* and *d* amino acids of the true heptad repeat that would form a hydrophobic interface between the two chains. Moreover, there

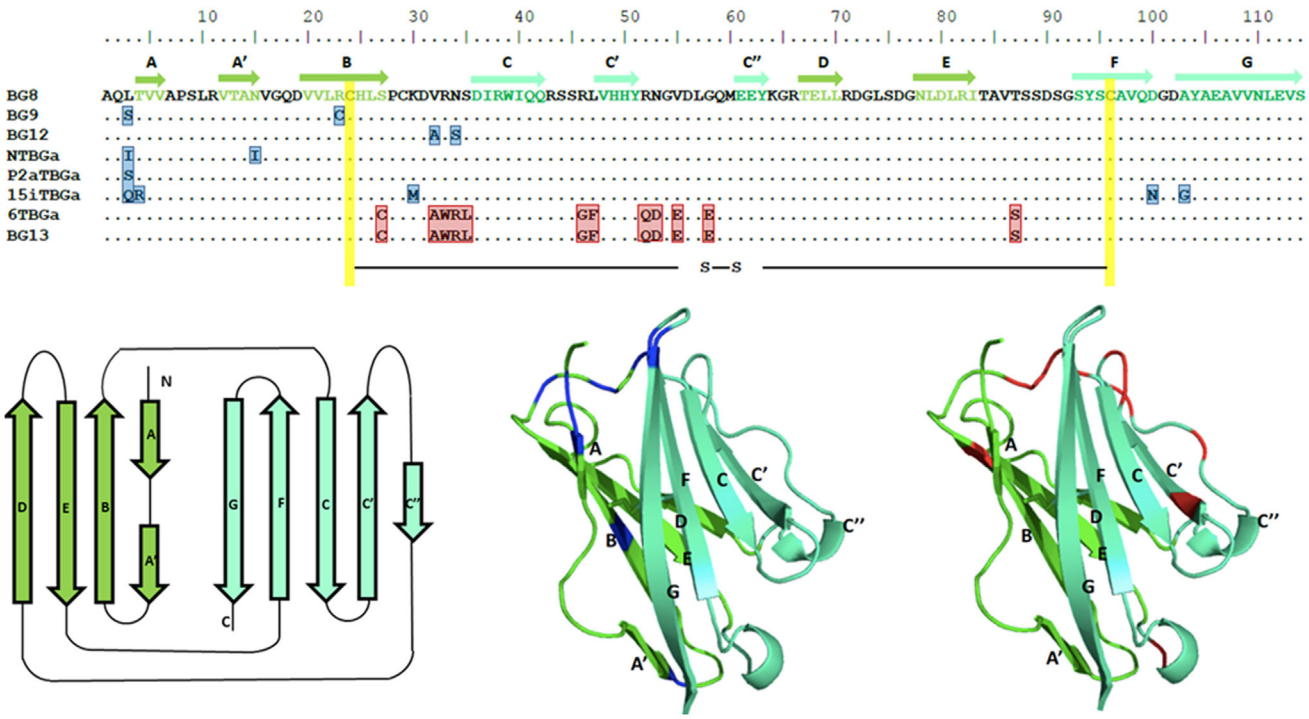

FIGURE 7 | Alignment of amino acid sequences for the Ig-V domains of the dominantly expressed genes from four chicken lines identified in this paper, and for the appropriate genes of the B12 haplotype from Ref. (24), along with structural models of the Ig-V domains with the location of variation compared with the BG8 sequence of the B12 haplotype indicated. Names of the transcripts follow the convention: abbreviated line name, "T" for T cells, "BG" and the letter "a" representing the most frequently detected exon 2 sequence. Names of the genes follow the convention "BG" and the number of the gene locus from the B12 haplotype. In the top panel, letters indicate amino acids by single letter code, dots indicate identities with BG8 sequence, residues that differ from BG8 are boxed in blue for the three lines, and red for line 6_1 and BG13; yellow indicates the intra-domain cysteines. The β-strands of the V region are indicated by arrows in the top panel, and are colored dark green for one face of the domain and light green for the other face. The same color scheme is used for the three panels below, with the positions of residues for the three lines (and BG9 and BG12) that differ from BG8 colored blue in the middle panel, and positions of residues for line 6_1 and BG13 that differ from BG8 colored red in the right hand panel.

are many fewer hydrophobic amino acids at the other positions, with many of the amino acids from the first and third codon (corresponding to the *e* and *g* positions) charged, potentially allowing salt bridges between oppositely charged amino acids of the two chains (30). It is not immediately clear from the data whether the potential salt bridges might be for homodimers or for heterodimers with some of the subdominantly expressed chains. However, the charges in the five positions other than those forming the hydrophobic stripe between the chains are clustered into acidic, basic, and polar patches along the coiled-coil, with a particularly clear acidic patch at the C-terminus. Also striking is the presence of a cysteine residue in the same position of the cytoplasmic tail of the conceptual transcripts of all the dominantly expressed BG molecules.

There is no sequence variation in the cytoplasmic tail between the dominantly expressed BG conceptual transcripts for line 6_1 (B2) and BG13 from the B12 haplotype, but the variation in the three other haplotypes, BG8, BG9, and BG12 is scattered along the sequence (except for an apparent insertion in the B15 sequence from line 15I), with only one *a* and one *d* position being variable out of 25 variable positions total (**Figure 8**; Figures S2 and S3 in Supplementary Material). This variation is all di-allelic, most of which is arguably conservative changes (A/T, M/T, E/D, Q/H, A/G, L/V, Y/S, A/I, and A/P) with only a few arguably radical changes (A/E, K/E, L/Q, K/N, Q/R, K/Q, and R/H). Decorating the coiled-coil representation of the cytoplasmic tail sequence revealed that much of the variation is located in two parts of the coil, 11–18 and 23–26 of 33 heptads (**Figure 8**), but whether this constitutes clustering is not yet clear. The cytoplasmic tail from the dominantly expressed conceptual transcript of line 6_1 (B2) and from the BG13 gene (B12) is shorter (27 heptads) than the dominantly expressed genes from B15, B19, and B21 and the BG8, BG9, and BG12 genes from B12 haplotype (**Figure 8**). Interestingly, the actual cytoplasmic tails of the dominant and some subdominant sequences of line 6_1 (B2) are much shorter (**Figure 8**; Figure S5 in Supplementary Material), as discussed below.

Unlike the protein coding regions including the cytoplasmic tail, the final exon (which includes the 3′UTR) of the dominantly expressed BG genes of all four haplotypes as well as the BG8, BG9, BG12, and BG13 genes are co-linear (except for a 20 nucleotide insertion in BG9 that is shared with most BG genes not in the BG8-BG9-BG12-BG13 clade) and nearly identical in sequence (Figures S3 and S4 in Supplementary Material). Including the 27 nucleotides that code for protein in BG9 and the dominantly expressed

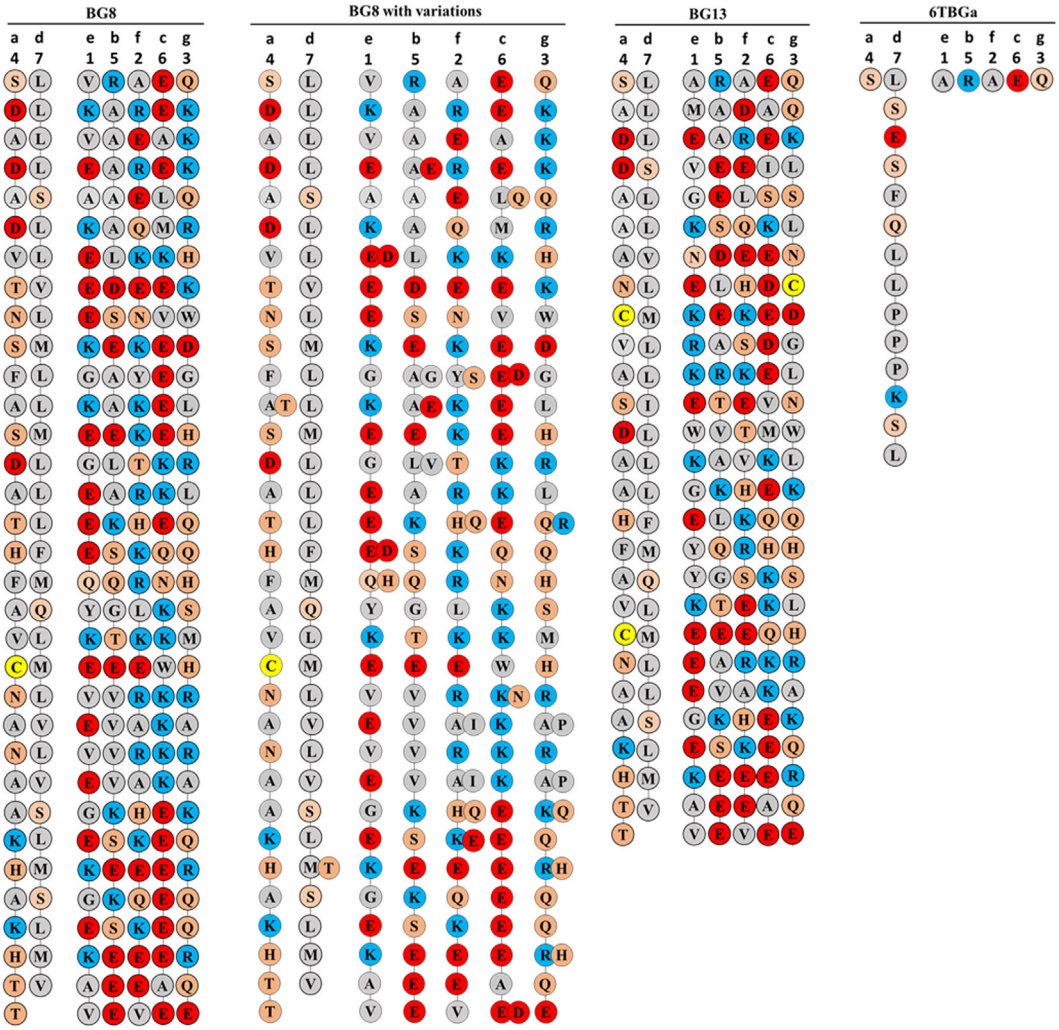

FIGURE 8 | Coiled-coil representations of the cytoplasmic tails of BG8; BG8 with the different amino acids found in BG9 and BG12 of the B12 haplotype and in the "(nearly) full-length conceptual transcripts" (i.e., exons without introns) of the dominant sequences of line 15I (B15), line P2a (B19), line N (B21); B13 which is identical to the "(nearly) full-length conceptual transcript" (i.e., exons without introns) of the dominant sequence of line 6_1 (B2); and the dominant sequence of line 6_1 (B2) with the expected amino acid sequence from the most frequent clone using the real transcript (i.e., exons with the intron read-throughs leading to an early stop codon, sequence 6TBGa-1). The transmembrane region would be at the top of the page, so the C-terminus of the BG protein is at the bottom of the page. The positions of the seven codons in the 21 nucleotide repeat are indicated with numbers at the top, and the position of the seven amino acid positions of the "true heptad repeat" are indicated with letters. Colors of circles surrounding the amino acids (single letter code) indicate features of the amino acids (red, acidic; blue, basic; orange, polar; and gray, hydrophobic except for yellow, cysteine), with the understanding that these features do not correspond to full descriptions of the properties of the amino acids.

BG from line 15I (B15) but are untranslated in the other members of this clade, there are only 26 positions out of 411 nucleotides that vary between the eight sequences, with unknown significance.

Alternative Splicing and Intron Read-Through Lead to Truncated Cytoplasmic Tails, Particularly for the Dominantly Expressed BG Gene From Line 6_1 (B2)

The analysis thus far has assumed that the RNA transcripts correspond to the exons as identified by their sequence features without any introns that were present, a minimal length for the mRNA. However, many of the 57 unique sequences actually isolated include stretches of sequence that are clearly introns, based on comparison with known genes in the B12 haplotype (**Figure 9**; Figures S1 and S3 in Supplementary Material).

Almost all of the retained introns lead to in-frame stop codons, some of which are long before the stop codon expected from the conceptual transcripts (**Figure 9**; Figures S1 and S3 in Supplementary Material). The dominantly expressed BG sequence from line 6_1 (B2) retains the intron directly after the first 21 nucleotide exon, which truncates the cytoplasmic tail after only 13 amino acids (**Figure 8**; Figure S1 in Supplementary Material). Thus, the dominantly expressed BG sequence from line 6_1 (B2) has

a different sequence from the other three haplotypes, but also lacks the long cytoplasmic tail. Some of the subdominant sequences also have truncated cytoplasmic tails, some with clusters of cysteines (**Figures 8** and **9**; Figure S5 in Supplementary Material).

DISCUSSION

To overcome the difficulty of identifying truly orthologous alleles in the ever-shifting panoply of BG genes in the BG region, we

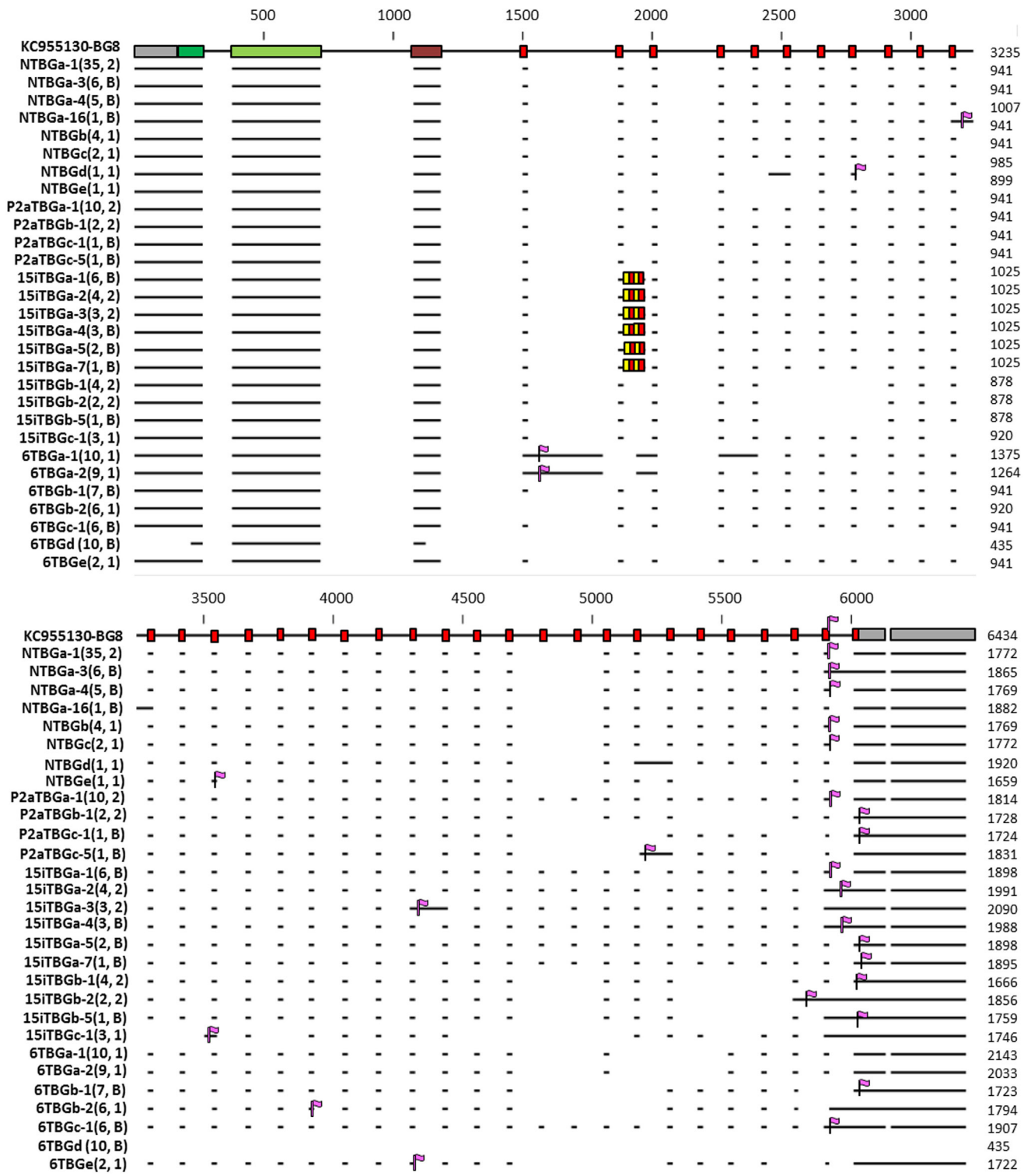

FIGURE 9 | Continued

FIGURE 9 | Representation of the intron–exon structure of the BG genes (based on exon 2 sequences) inferred from 29 sequences (representative of each of the 16 genes based on exon 2, as well as those alternatively expressed transcripts identified in more than one independent PCR) from line 6_1 (B2), line 15I (B15), line P2a (B19), and line N (B21), indicating the actual mRNA transcripts as horizontal lines and stop codons as vertical purple flags. In 15iTBGa, the alternating red and yellow boxes indicate the four additional heptad repeats found for this gene, compared with BG8 (B12). Names of the transcripts follow the convention: abbreviated line name, "T" for T cells, "BG" and the letter "a" representing the most frequently detected clone from the most frequently detected exon 2 sequence (and "b" representing the most frequently detected clone from the second most frequently detected exon 2 sequence, and so forth), a dash and then a number representing the alternative splicing variant with "1" being the most frequently detected clone (and "2" the second most frequently detected clone, and so forth). Numbers in parentheses indicate the number of clones found for a particular full sequence, followed by the number of independent PCRs in which the sequence was identified (1, found in one PCR; 2, found in two PCRs; B, found in one PCR described in this paper and one using B cell cDNA, data not shown).
The 29 sequences were deposited in GenBank, with the accession numbers as follows: NTBGa-1, MH156615; NTBGa-3, MH156616; NTBGa-4, MH156617; NTBGa-16, MH156618; NTBGb, MH156619; NTBGc, MH156620; NTBGd, MH156621; NTBGe, MH156622; P2aTBGa-1, MH156623; P2aTBGb-1, MH156624; P2aTBGc-1, MH156625; P2aTBGc-5, MH156626; 15iTBGa-1, MH156627; 15iTBGa-2, MH156628; 15iTBGa-3, MH156629; 15iTBGa-4, MH156630; 15iTBGa-5, MH156631; 15iTBGa-7, MH156632; 15iTBGb-1, MH156633; 15iTBGb-2, MH156634; 15iTBGb-5, MH156635; 15iTBGc-1, MH156636; 6TBGa-1, MH156637; 6TBGa-2, MH156638; 6TBGb-1, MH156639; 6TBGb-2, MH156640; 6TBGc-1, MH156641; 6TBGd, MH156642; 6TBGe, MH156643.

adopted the approach of looking at the BG transcripts in single cell types to identify "functional alleles." Based on our limited examination of the transcripts in cells and tissues of the B12 haplotype (24), we began with peripheral T cells from chicken lines bearing four additional haplotypes. The overall results are summarized as a cartoon (**Figure 10**).

Based on our previous results, we expected a single dominantly expressed BG transcript (perhaps with another subdominant transcript at a low level) for each haplotype. We hoped that the transcripts from the five haplotypes would be similar enough that we could identify limited variation and determine whether such variation was clustered in regions of the protein with functional significance and/or under selective pressure. In particular, we wanted to ascertain whether such variation in the extracellular Ig-V domain and the cytoplasmic tail showed evidence for selected function, since there is no evidence that the serological polymorphism found in the extracellular Ig-V domain has functional significance while the two reported examples of function have been localized to the cytoplasmic tail. In fact, we found a series of surprises.

First, only line N (B21) cells had one really dominantly expressed BG gene, as we had found with the CB (B12) line. The other three lines with different haplotypes had one dominant gene expressed, but the subdominantly expressed genes were present in significant amounts. We were so concerned about this result that we carried out a third amplification of the cDNA from line 6_1 (B2) using SS–TM primers (the same used for the B12 experiments), which gave the same dominantly expressed BG gene but a completely different subdominant BG gene compared with the amplifications with HU primers. Therefore, we are not completely convinced that our amplifications are without bias. Unbiased approaches such as RNAseq or proteomics might be suitable for answering this question.

The significant levels of subdominant BG transcripts in three of the four haplotypes did lead us to wonder whether the dominantly expressed BG protein in some haplotypes might associate with subdominant BG proteins to make heterodimers. Another possibility is that some or all of these expressed proteins might associate as heterodimers with BG0 or BG1 chains, which were found in all cells at significant amounts. We were unable to see an obvious pattern from our helical wheel analyses. Careful analyses at the protein level of *ex vivo* cells as well as flow cytometry and biochemical analysis of cells transfected with one versus two BG genes might help answer this question.

Second, three of the four haplotypes have dominantly expressed BG genes with sequences close enough with each other (and to the gene strongly expressed in the B12 haplotype) to allow good comparisons for allelic variability, but one haplotype is rather different. The dominantly expressed BG gene from all four haplotypes came from one clade of BG genes in B12 chickens (BG8-BG9-BG12-BG13, hemopoietic 5′ UTR with type 2 cytoplasmic tail and 3′UTR). The T cells from line 15I (B15), line P2a (B19), and line N (B21) expressed BG genes that are very closely related to the BG9 gene (and also to BG8 and BG12). By contrast, the dominantly expressed BG gene from line 6_1 (B2) has many differences throughout the sequence (except in the 3′UTR). This B2 gene seems identical with the BG13 gene of the B12 haplotype (as presaged by serology of erythrocytes (5)), which is not expressed in B12 T cells (at least as assessed by amplification with the SS-TM primers (24)) despite being present in the B12 haplotype.

Among the subdominant BG genes expressed at significant levels, most are closely related to BG8, BG9, and BG12, with none that clustered with BG13. However, there were several subdominant BG genes whose overall sequences clustered with the BG5-BG7-BG11 clade (hemopoietic 5′ UTR with type 1 cytoplasmic tail and 3′UTR), three from line 6_1 (B2) and one from line P2a (B19). The potential significance of these different sequences is unclear.

Third, the comparison of the Ig-V domains from closely related BG genes showed clustering of the variation but no evidence for selection at the protein level. Only low levels of variation were found in the Ig-V domain of the dominantly expressed BG genes of the three haplotypes along with the closely related BG8, BG9, and BG12 genes of the B12 haplotype. This variation is mainly localized to the distal loops, which could suggest selection for functional interactions with other molecules, but there was no evidence for selection of variation based on non-synonymous (replacement) versus synonymous (silent) changes; perhaps data from additional haplotypes will help. By contrast, the dominantly expressed BG gene of line 6_1 (B2) is identical to the BG13 gene of the B12 haplotype, the differences with the other three haplotypes and three other genes of the B12 haplotype were scattered throughout the structure, and again there was no support for selection at the protein level.

Fourth, by contrast to the extracellular Ig-V domain, there was clear support for selection of variation in the cytoplasmic tail, which could be mapped to a conceptual model of an α-helical coiled-coil. The presence of exons with 21 nucleotide repeats

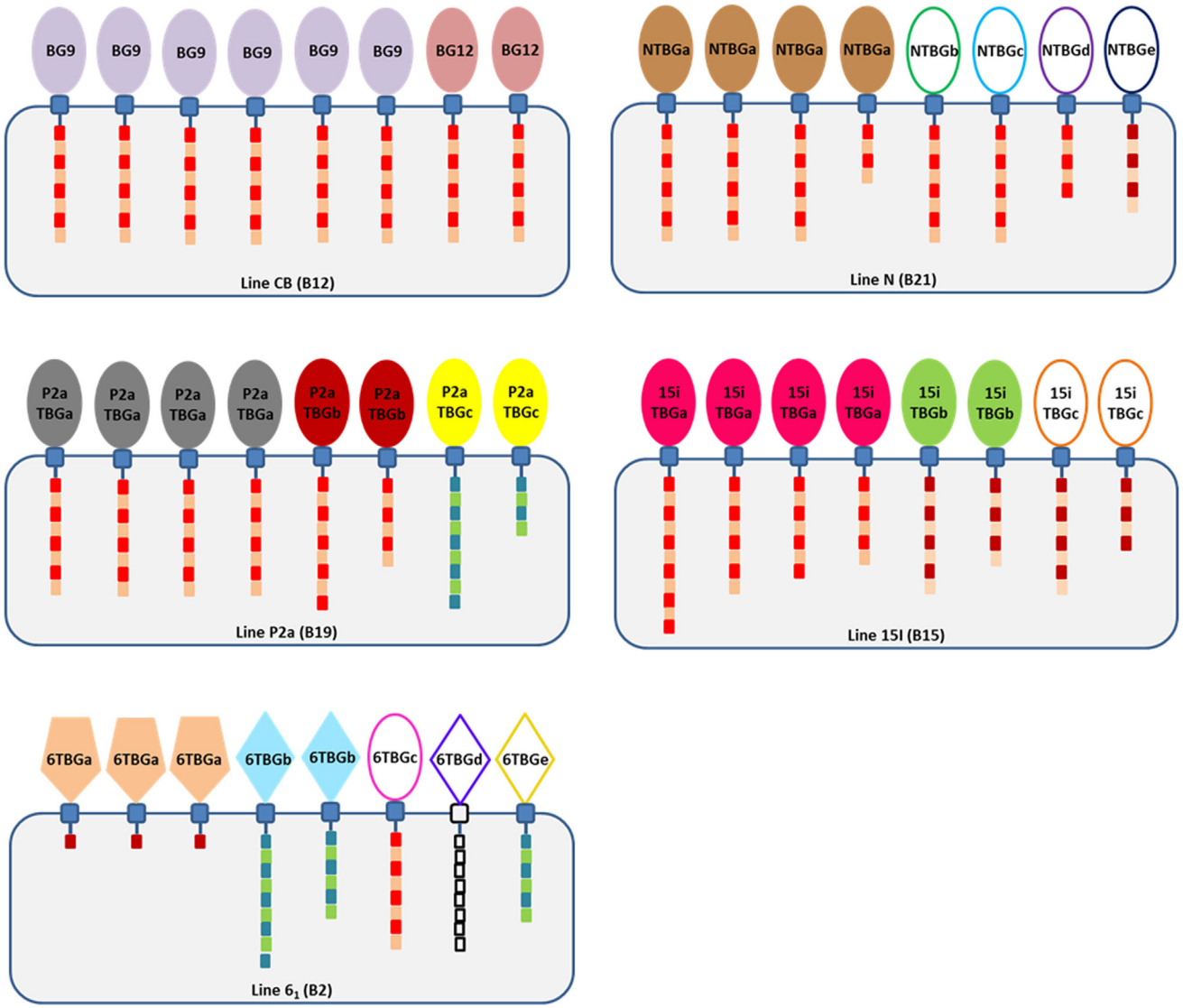

FIGURE 10 | Cartoon summary of the findings, showing that there are no expressed sequences identical between the four chicken lines but that line 6_1 has sequences identical to genes of the B12 haplotype (which, however, are not expressed in T cells of the B12 haplotype), that most expressed sequences are from the B8-B9-B12 clade although line 6_1 (B2) has a dominantly expressed BG sequence of the BG13 clade and two subdominant sequences from the BG5-BG7-BG11 clade, and that cytoplasmic tails are mostly type 2a and that the length varies due to alternative splicing (intron read-through). The cartoon shows BG proteins in cells of each haplotype, with the numbers of each protein reflecting the ratio of different sequences in that haplotype. Extracellular Ig-V domains are represented by shapes to indicate relationship to clades of BG genes from the B12 haplotype (ovals, BG8-BG9-BG12 clade; pentagons, BG13 clade; and diamonds, BG5-BG7-BG11 clade) and by color (colors as in **Figure 2**, with those sequences found in only one PCR represented by ovals and diamonds not filled with color); cytoplasmic tails indicated by boxes representing heptad repeats, with lengths correlated with the length of the tail taking into account alternative splicing and with colors representing the clade (type 1, blue and green; type 2a, bright red and brown; type 2b, dark red and brown; and 6TBGd, white since no data are available).

encoding heptad amino acid repeats in a molecule known to be a dimer originally prompted the view that this portion of the molecule is a coiled-coil of two α-helices (20, 24, 31). This view was supported by the isolation of a soluble BG cytoplasmic tail as a molecule that displaces tropomyosin (32, 33), an actin-myosin regulator composed of a coiled-coil (34).

Visualization of the repeats in the BG cytoplasmic tails by forms of helical wheels (30) identified the amino acid encoded by the fourth codon and the last codon of each 21 nucleotide exon as predominantly hydrophobic, and thus likely to be the first ("*a*") and fourth ("*d*") amino acids of the true heptad. The fact that the true heptad repeat spans two exons was unexpected, but perhaps obvious in retrospect, given that the first codon is split and thus depends on two exons. This finding is most easily interpreted as a hydrophobic stripe on one α-helix interacting with a hydrophobic stripe on the other α-helix, buried between the two chains, whether as a homo- or a hetero-dimer. The other residues would project into the cytoplasm and, in the dominantly

expressed BG genes, are present as patches of highly charged residues, along with a highly conserved cysteine. In some of the subdominantly expressed BG genes, there are clusters of cysteine residues. It is very likely that these various patches interact with other molecules, which might be identified by proteomics. Another possibility for the cysteines is modification, for instance palmitoylation (35) which could bring the α-helical coiled-coil to the underside of the membrane.

The variation in the cytoplasmic tail for the conceptual transcripts from the three haplotypes with similar BG sequences (and the BG8, BG9, and BG12 genes from the B12 haplotype) is predominantly located in two stretches at the five positions that are not in the hydrophobic stripe between the two α-helices of the coiled-coil. The functional significance of this variation is not clear, but the evidence from silent versus replacement substitutions supports selection for this variation. The only two known examples of function for BG molecules, regulation of actin-myosin by "zipper protein" in intestinal epithelial cells and effect of the BG1 gene on viral disease (32, 33, 36), are both associated with the cytoplasmic tail rather than the extracellular Ig-V domain, which may fit with the notion that the cytoplasmic tail is under selection for variation.

Fifth, many of the real transcripts had intron read-through that shortened the cytoplasmic tail compared to what was expected from the conceptual gene sequence, most dramatically truncating nearly the whole cytoplasmic tail of the dominantly expressed BG gene of line 6_1 (B2). Such intron read-through, a form of alternative splicing, was first noticed long ago in the cytoplasmic tails encoded by BG cDNAs (20, 31). Some intron read-through seems to have become fixed, for example BG1 genes in which an active immunotyrosine inhibition motif (ITIM) is located in an exon bounded by two 21 nucleotide repeats (25, 36). A bioinformatic analysis of the 14 BG genes of the B12 haplotype found many read-through introns that led to in-frame stop codons, but no additional signaling motifs were obvious in those introns that read through in-frame (24).

The large proportion of transcripts with intron read-through was unexpected. One possibility that cannot be ruled out from our data is that these RNAs are incompletely spliced nuclear RNAs which would never be translocated to the cytoplasm or be translated. However, the RNA was primed with oligo-dT for the reverse transcription step and the amplicons are nearly full-length, so it seems most likely that these RNAs are polyadenylated. Ultimately, isolation and analysis of cytoplasmic or polysome RNA and/or analysis at the protein level is required to be sure that these transcripts encode real BG molecules.

Assuming that the intron read-through leads to truncated cytoplasmic tails in a real BG dimer, this kind of alternative splicing could be a way to regulate the interaction of the BG dimer with other molecules (i.e., the interactome) between different cell types. One possible interaction might be with orphan 30.2 (PRY-SPRY) domains (37), which would result in BG-30.2 complexes reminiscent of BTN and BTNL proteins. It is also possible that the truncated cytoplasmic tail of the dominantly expressed BG from line 6_1 (B2) serves to ensure that the type 2b tail is not present in T cells, if it is type 2a tails that are necessary.

In summary, the work described in this report provides a first basis from which additional experiments can clarify the nature of the BG molecules found on the surface of different cell types, with the ultimate aim of determining the function of different domains of the molecules and the selection pressure under which they evolve. The unexpected results lead to many questions, which eventually will be answered in our quest to understand the structure, function and evolution of the BG genes and molecules.

DATA AVAILABILITY STATEMENT

Twenty-nine sequences generated in this work have been deposited in GenBank, and given accession numbers are from MH156615 to MH156643.

ETHICS STATEMENT

This study was carried out in accordance with the recommendations of Home Office guidelines. The protocol was approved by the Local Ethics committee of the Pirbright Institute.

AUTHOR CONTRIBUTIONS

LC carried out most of the experimental procedures; MF, KS, and CB isolated the cells; LC and JK made the figures and wrote the text.

ACKNOWLEDGMENTS

The authors thank Dr. Samer Halabi and Mr. Tom (C. H. T.) Yip for help and insight with the structural models, and also thank Dr. Hassnae Afrache, Ms. Rebecca Martin, Ms. Ellen Palmer, and Dr. Clive Tregaskes for critical reading of the manuscript.

FUNDING

This work was supported by funds from a Wellcome Trust programme grant (089305/Z/09/Z) and then a Wellcome Trust Investigator Award (110106/Z/15/Z).

SUPPLEMENTARY MATERIAL

The Supplementary Material for this article can be found online at https://www.frontiersin.org/articles/10.3389/fimmu.2018.00930/full#supplementary-material.

REFERENCES

1. Briles WE, McGibbon WH, Irwin MR. On multiple alleles effecting cellular antigens in the chicken. *Genetics* (1950) 35(6):633–52.
2. Gilmour DG. Segregation of genes determining red cell antigens at high levels of inbreeding in chickens. *Genetics* (1959) 44(1):14–33.
3. Schierman LW, Nordskog AW. Relationship of blood type to histocompatibility in chickens. *Science* (1961) 134(3484):1008–9. doi:10.1126/science.134.3484.1008
4. Simonsen M, Hála K, Nicolaisen EM. Linkage disequilibrium of MHC genes in the chicken. I. The B-F and B-G loci. *Immunogenetics* (1980) 10(2):103–12. doi:10.1007/BF01561559

5. Simonsen M, Crone M, Koch C, Hála K. The MHC haplotypes of the chicken. *Immunogenetics* (1982) 16(6):513–32. doi:10.1007/BF00372021
6. Skjødt K, Koch C, Crone M, Simonsen M. Analysis of chickens for recombination within the MHC (B-complex). *Tissue Antigens* (1985) 25(5):278–82. doi:10.1111/j.1399-0039.1985.tb00450.x
7. Kaufman J, Skjødt K, Salomonsen J. The B-G multigene family of the chicken major histocompatibility complex. *Crit Rev Immunol* (1991) 11(2):113–43.
8. Abeler-Dörner L, Swamy M, Williams G, Hayday AC, Bas A. Butyrophilins: an emerging family of immune regulators. *Trends Immunol* (2012) 33(1):34–41. doi:10.1016/j.it.2011.09.007
9. Afrache H, Gouret P, Ainouche S, Pontarotti P, Olive D. The butyrophilin (BTN) gene family: from milk fat to the regulation of the immune response. *Immunogenetics* (2012) 64(11):781–94. doi:10.1007/s00251-012-0619-z
10. Arnett HA, Viney JL. Immune modulation by butyrophilins. *Nat Rev Immunol* (2014) 14(8):559–69. doi:10.1038/nri3715
11. Rhodes DA, Reith W, Trowsdale J. Regulation of Immunity by Butyrophilins. *Annu Rev Immunol* (2016) 34:151–72. doi:10.1146/annurev-immunol-041015-055435
12. Habib AA, Marton LS, Allwardt B, Gulcher JR, Mikol DD, Högnason T, et al. Expression of the oligodendrocyte-myelin glycoprotein by neurons in the mouse central nervous system. *J Neurochem* (1998) 70(4):1704–11. doi:10.1046/j.1471-4159.1998.70041704.x
13. Jack LJ, Mather IH. Cloning and analysis of cDNA encoding bovine butyrophilin, an apical glycoprotein expressed in mammary tissue and secreted in association with the milk-fat globule membrane during lactation. *J Biol Chem* (1990) 265(24):14481–6.
14. Mather IH, Jack LJ. A review of the molecular and cellular biology of butyrophilin, the major protein of bovine milk fat globule membrane. *J Dairy Sci* (1993) 76(12):3832–50. doi:10.3168/jds.S0022-0302(93)77726-7
15. Henry J, Miller MM, Pontarotti P. Structure and evolution of the extended B7 family. *Immunol Today* (1999) 20(6):285–8. doi:10.1016/S0167-5699(98)01418-2
16. Di Marco Barros R, Roberts NA, Dart RJ, Vantourout P, Jandke A, Nussbaumer O, et al. Epithelia use butyrophilin-like molecules to shape organ-specific γδ T cell compartments. *Cell* (2016) 167(1):203.e–18.e. doi:10.1016/j.cell.2016.08.030
17. Vantourout P, Laing A, Woodward MJ, Zlatareva I, Apolonia L, Jones AW, et al. Heteromeric interactions regulate butyrophilin (BTN) and BTN-like molecules governing γδ T cell biology. *Proc Natl Acad Sci U S A* (2018) 115(5):1039–44. doi:10.1073/pnas.1701237115
18. Miller MM, Goto R, Young S, Liu J, Hardy J. Antigens similar to major histocompatibility complex B-G are expressed in the intestinal epithelium in the chicken. *Immunogenetics* (1990) 32(1):45–50. doi:10.1007/BF01787328
19. Salomonsen J, Dunon D, Skjødt K, Thorpe D, Vainio O, Kaufman J. Chicken major histocompatibility complex-encoded B-G antigens are found on many cell types that are important for the immune system. *Proc Natl Acad Sci U S A* (1991) 88(4):1359–63. doi:10.1073/pnas.88.4.1359
20. Kaufman J, Salomonsen J, Skjødt K, Thorpe D. Size polymorphism of chicken major histocompatibility complex-encoded B-G molecules is due to length variation in the cytoplasmic heptad repeat region. *Proc Natl Acad Sci U S A* (1990) 87(21):8277–81. doi:10.1073/pnas.87.21.8277
21. Kline K, Briles WE, Bacon L, Sanders BG. Characterization of two distinct disulfide-linked B-G molecules in the chicken. *J Hered* (1988) 79(4):249–56. doi:10.1093/oxfordjournals.jhered.a110505
22. Salomonsen J, Skjødt K, Crone M, Simonsen M. The chicken erythrocyte-specific MHC antigen. Characterization and purification of the B-G antigen by monoclonal antibodies. *Immunogenetics* (1987) 25(6):373–82. doi:10.1007/BF00396103
23. Miller MM, Goto R, Young S, Chirivella J, Hawke D, Miyada CG. Immunoglobulin variable-region-like domains of diverse sequence within the major histocompatibility complex of the chicken. *Proc Natl Acad Sci U S A* (1991) 88(10):4377–81. doi:10.1073/pnas.88.10.4377
24. Salomonsen J, Chattaway JA, Chan AC, Parker A, Huguet S, Marston DA, et al. Sequence of a complete chicken BG haplotype shows dynamic expansion and contraction of two gene lineages with particular expression patterns. *PLoS Genet* (2014) 10(6):e1004417. doi:10.1371/journal.pgen.1004417
25. Chattaway J, Ramirez-Valdez RA, Chappell PE, Caesar JJ, Lea SM, Kaufman J. Different modes of variation for each BG lineage suggest different functions. *Open Biol* (2016) 6(9):160188. doi:10.1098/rsob.160188
26. Shaw I, Powell TJ, Marston DA, Baker K, van Hateren A, Riegert P, et al. Different evolutionary histories of the two classical class I genes BF1 and BF2 illustrate drift and selection within the stable MHC haplotypes of chickens. *J Immunol* (2007) 178(9):5744–52. doi:10.4049/jimmunol.178.9.5744
27. Miller MM, Goto R, Abplanalp H. Analysis of the B-G antigens of the chicken MHC by two-dimensional gel electrophoresis. *Immunogenetics* (1984) 20(4):373–85. doi:10.1007/BF00345612
28. Crick FH. Is alpha-keratin a coiled coil? *Nature* (1952) 170(4334):882–3. doi:10.1038/170882b0
29. Alber T. Structure of the leucine zipper. *Curr Opin Genet Dev* (1992) 2(2):205–10. doi:10.1016/S0959-437X(05)80275-8
30. Aronsson C, Dånmark S, Zhou F, Öberg P, Enander K, Su H, et al. Self-sorting heterodimeric coiled coil peptides with defined and tuneable self-assembly properties. *Sci Rep* (2015) 5:14063. doi:10.1038/srep14063
31. Kaufman J, Salomonsen J, Skjødt K. B-G cDNA clones have multiple small repeats and hybridize to both chicken MHC regions. *Immunogenetics* (1989) 30(6):440–51. doi:10.1007/BF02421176
32. Bikle DD, Munson S, Morrison N, Eisman J. Zipper protein, a newly described tropomyosin-like protein of the intestinal brush border. *J Biol Chem* (1993) 268(1):620–6.
33. Bikle DD, Munson S, Komuves L. Zipper protein, a B-G protein with the ability to regulate actin/myosin 1 interactions in the intestinal brush border. *J Biol Chem* (1996) 271(15):9075–83. doi:10.1074/jbc.271.15.9075
34. Hitchcock-DeGregori SE, Barua B. Tropomyosin structure, function, and interactions: a dynamic regulator. *Subcell Biochem* (2017) 82:253–84. doi:10.1007/978-3-319-49674-0_9
35. Kaufman JF, Krangel MS, Strominger JL. Cysteines in the transmembrane region of major histocompatibility complex antigens are fatty acylated via thioester bonds. *J Biol Chem* (1984) 259(11):7230–8.
36. Goto RM, Wang Y, Taylor RL Jr, Wakenell PS, Hosomichi K, Shiina T, et al. BG1 has a major role in MHC-linked resistance to malignant lymphoma in the chicken. *Proc Natl Acad Sci U S A* (2009) 106(39):16740–5. doi:10.1073/pnas.0906776106 Erratum in: *Proc Natl Acad Sci U S A*. 2010 Apr 27;107(17):8041.
37. Kaufman J, Milne S, Göbel TW, Walker BA, Jacob JP, Auffray C, et al. The chicken B locus is a minimal essential major histocompatibility complex. *Nature* (1999) 401(6756):923–5. doi:10.1038/44856

Conflict of Interest Statement: The authors declare that the research was conducted in the absence of any commercial or financial relationships that could be construed as a potential conflict of interest.

Copyright © 2018 Chen, Fakiola, Staines, Butter and Kaufman. This is an open-access article distributed under the terms of the Creative Commons Attribution License (CC BY). The use, distribution or reproduction in other forums is permitted, provided the original author(s) and the copyright owner are credited and that the original publication in this journal is cited, in accordance with accepted academic practice. No use, distribution or reproduction is permitted which does not comply with these terms.

frontiers in Immunology

MINI REVIEW
published: 24 April 2018
doi: 10.3389/fimmu.2018.00851

Working in "NK Mode": Natural Killer Group 2 Member D and Natural Cytotoxicity Receptors in Stress-Surveillance by γδ T Cells

Bruno Silva-Santos[1]* *and Jessica Strid*[2]*

[1] Instituto de Medicina Molecular – João Lobo Antunes, Faculdade de Medicina, Universidade de Lisboa, Lisboa, Portugal,
[2] Division of Immunology and Inflammation, Department of Medicine, Imperial College London, London, United Kingdom

Natural killer cell receptors (NKRs) are germline-encoded transmembrane proteins that regulate the activation and homeostasis of NK cells as well as other lymphocytes. For γδ T cells, NKRs play critical roles in discriminating stressed (transformed or infected) cells from their healthy counterparts, as proposed in the "lymphoid stress-surveillance" theory. Whereas the main physiologic role is seemingly fulfilled by natural killer group 2 member D, constitutively expressed by γδ T cells, enhancement of their therapeutic potential may rely on natural cytotoxicity receptors (NCRs), like NKp30 or NKp44, that can be induced selectively on human Vδ1$^+$ T cells. Here, we review the contributions of NCRs, NKG2D, and their multiple ligands, to γδ T cell biology in mouse and human.

Keywords: γδ T cells, natural killer cell receptors, natural killer group 2 member D, natural cytotoxicity receptors, immunotherapy

OPEN ACCESS

Edited by:
Pierre Vantourout, King's College London, United Kingdom

Reviewed by:
Olivier Toutirais, University of Caen Normandy, France
Paul Austin Moss, University of Birmingham, United Kingdom
Daniela Wesch, Christian-Albrechts University (CAU) of Kiel, Germany

***Correspondence:**
Bruno Silva-Santos
bssantos@medicina.ulisboa.pt;
Jessica Strid
j.strid@imperial.ac.uk

Specialty section:
This article was submitted to T Cell Biology, a section of the journal Frontiers in Immunology

Received: *23 February 2018*
Accepted: *06 April 2018*
Published: *24 April 2018*

Citation:
Silva-Santos B and Strid J (2018) Working in "NK Mode": Natural Killer Group 2 Member D and Natural Cytotoxicity Receptors in Stress-Surveillance by γδ T Cells. Front. Immunol. 9:851. doi: 10.3389/fimmu.2018.00851

INTRODUCTION

Natural killer cell receptors (NKRs) comprise various germline-encoded transmembrane proteins characterized for their capacity to regulate NK cell activation and homeostasis. This large family includes lectin-type receptors, natural cytotoxicity receptors (NCRs), and killer immunoglobulin receptors. The balance between activating and inhibitory signals derived from these receptors controls NK cell functionality. Besides their roles for NK cells, some NKRs, most notably natural-killer group 2 member D (NKG2D), have been known for long to be expressed by some subsets of T cells (1), including γδ T cells (2). In fact, nearly all human γδ T cells, and most mouse γδ T cells, express NKG2D. Importantly, we, and others, have shown that NKG2D is a key determinant of tumor cell recognition by murine intraepithelial γδ T cells (3, 4), as well as human peripheral blood (2, 5) and tumor-infiltrating (6) γδ T cells.

By contrast to NKG2D, NCRs were initially thought to be NK cell-specific (7), although this has changed particularly with the discovery of innate lymphoid cells (ILCs) (8). In fact, the acquisition of an NK-like phenotype and functionality was earlier reported on human intestinal intraepithelial lymphocytes (IELs), particularly in celiac disease (9, 10). The NCRs expressed on αβ IELs triggered interferon-γ (IFN-γ) secretion and degranulation (10), thus suggesting that IEL activation under inflammatory conditions favored the differentiation of "NK-like" effectors performing type 1 cytotoxic functions in an NKR-mediated (and TCR-independent) manner. We have recently built on this to show that human γδ T cells, specifically of the Vδ1$^+$ subset, can be induced to express NCRs upon TCR plus IL-15 (or IL-2) stimulation *in vitro*, and these NCRs enhanced the capacity to target tumor cells of multiple origins, both *in vitro* and *in vivo* [(11, 12), and unpublished data].

In this mini-review, we will focus on the roles of NCRs, NKG2D, and their ligands for γδ T cell biology in mouse and human.

NKG2D AND ITS LIGANDS

The best-characterized activating NKR is NKG2D. NKG2D is a C-type lectin-like transmembrane receptor, which recognizes a range of different major histocompatibility complex class (MHC) I-related self-ligands induced or upregulated by a variety of cellular stress events, and notably on infected or transformed epithelial cells (ECs) (13). In mice, two isoforms of NKG2D exist, NKG2D-short (S) or NKG2D-long (L), while only the counterpart to the NKG2D-L isoform is expressed in human. The receptor functions as an activating receptor only through its association with signaling adaptor proteins, which are determined by the isoform of NKG2D expressed. NKG2D-S can associate with both DAP10 (recruits phosphatidylinositol 3-kinase) and DAP12 (activates tyrosine kinases Syk and ZAP70) while NKG2D-L is structurally incapable of associating with DAP12 and NKG2D-mediated signaling is mediated solely through DAP10 (14–16).

Engagement of NKG2D can trigger degranulation, cytotoxicity, and/or cytokine production—the distinct outcome of the receptor ligation may be explained by differential isoform and adaptor protein expression. Whereas, mouse $CD8^+$ αβ T cells do not express DAP12 (and the exclusive NKG2D-DAP10 association serves as a costimulatory receptor), mouse epidermal γδ IELs constitutively express NKG2D-S, NKG2D-L, DAP10, and DAP12, and NKG2D ligation may trigger activity without TCR engagement (17).

Despite the different isoforms of NKG2D, the receptor is highly conserved with the receptors being 70% homologous between human and mouse, for example. NKG2D from one species can bind ligands from another (18). This is curious as the ligands are multiple and are both highly diverse in their amino-acid sequence, domain structure, membrane anchoring as well as exhibiting considerable allelic variation, and a wide range of receptor-binding affinities (**Figure 1A**). NKG2D ligands identified so far in humans include the MHC class I-chain-related proteins A and B (MICA and MICB) and six different UL16-binding proteins. In mice, three subgroups of NKG2D ligands have been identified: five isoforms of retinoic acid early-inducible 1 (Rae-1) proteins, one murine UL16-binding protein-like transcript 1 (MULT1), and three different isoforms of H60 proteins (**Figure 1A**). Why the NKG2D receptor is so promiscuous and engaging with so many ligands is not know, however, there are indications that not all ligands are functionally equivalent and that the diversity may allow for unique tissue-specific and contextual functions (1).

NKG2D AS A CRITICAL DETERMINANT OF MOUSE γδ T CELL ACTIVATION

Study of the NKG2D receptor is not only of huge academic interest, but clearly has therapeutic importance both within cancer, infection, and autoimmunity. Study of this receptor has also given us fundamental insight into γδ T cell biology. The capacity of murine tissue γδ T cells to act solely on alterations of autologous stress-antigens, such as those of the NKG2D receptor, and thus survey the "health-status" of a given EC has been termed lymphoid stress-surveillance (LSS) (4, 20, 21) (**Figure 1Bi**,ii). LSS highlights an important function of γδ T cells as afferent sensors of cellular dysregulations and as initiators of local and systemic immunity—a clear distinction from conventional αβ T cell biology. The activation of tissue γδ T cells during LSS *in situ* occurs seemingly without TCR stimulation (4). However, an alternative explanation could be that the TCR is constitutively engaged in the tissue as was suggested by an elegant study visualizing the γδ TCR continually signaling in the skin epidermis (22). The self-ligand recognized by the Vγ5Vδ1 TCR was not identified in this study, however, the implication of a possible constitutive TCR engagement in the tissue could be a predisposition to respond rapidly to stress-induced ligands recognized by co-stimulatory receptors, such as NKG2D. Whether substituting or synergizing with TCR signaling, these (co)stimulators are of pivotal importance in initiating and tuning the γδ T cell response. Interestingly, while epidermal γδ IEL activate and respond rapidly *in vivo* to transgenic acute upregulation of Rae-1 on ECs (4) (**Figure 1Bi**), prolonged constitutive expression of Rae-1 (19) renders them hyporesponsive and they remain in a resting state (**Figure 1Biii**). It is not clear how this tuning of the γδ IEL responsiveness is regulated according to the length of NKG2D-ligand expression, but the "beneficial autoimmunity" displayed during acute stress responses may be detrimental in chronicity and could be regulated by negative signals mediated by inhibitory NKRs, such as Ly49E and CD94-NKG2A (23). It would be of therapeutic value to understand when and how NKG2D-ligand hyporesponsiveness may occur as solid tumors, for example, can have long-term display of these ligands, which paradoxically could switch off resident tissue immune surveillance.

Natural killer group 2 member D clearly is a cytotoxic receptor and its engagement on γδ T cells has been shown in many murine studies to induce degranulation, cytotoxicity, and sometimes cytokine production (3, 17, 24). These studies all assessed γδ T cell function in isolation *in vitro* using γδ T cell lines. However, NKG2D ligands may not always function to generate cytotoxic responses *in situ* and the outcome of NKG2D receptor ligation is almost certainly context dependent. The different ligands have variable affinity for the receptor and may invoke differential responses. For example, the relatively low affinity ligand H60c is constitutively (and exclusively) expressed in the skin without evoking apparent cytotoxicity *in vivo* although it could induce cytotoxicity in γδ IEL cell lines *in vitro* (25). Moreover, while inducible expression of the high affinity Rae-1 ligand in the epidermis *in vivo* clearly activates the epidermal γδ IEL (**Figure 1Bii**) no overt cytotoxicity of the ECs was observed (4). Rather, a possible role for NKG2D-ligation in EC repair was indicated as this pathway was shown to induce potent expression of type 2 cytokines, particularly IL-13, from the γδ IEL, which functions to potentiate EC turnover, maintain an intact barrier, and thereby enhance resistance to carcinogenesis (26, 27). Further, Rae-1 transcripts were initially reported in mouse embryonic tissues and NKG2D ligands are also expressed in cells of the bone marrow (28, 29). Interestingly, MICA is also expressed by trophoblasts during normal human

A

Human NKG2D ligands

NKG2D ligands	Cell-surface anchor	NKG2D binding affinity (K_D)
MICA	TM	1 mM*
MICB	TM	0.8 mM
ULBP1	GPI	1.1 mM
ULBP2	GPI	ND
ULBP3	GPI	ND
ULBP4	TM	ND
ULBP5	TM	ND
ULBP6	GPI	ND

Mouse NKG2D ligands

NKG2D ligands	Cell-surface anchor	NKG2D binding affinity (K_D)
MICA	TM	1 mM*
MICB	TM	0.8 mM
ULBP1	GPI	1.1 mM
ULBP2	GPI	ND
ULBP3	GPI	ND
ULBP4	TM	ND
ULBP5	TM	ND
ULBP6	GPI	ND

B

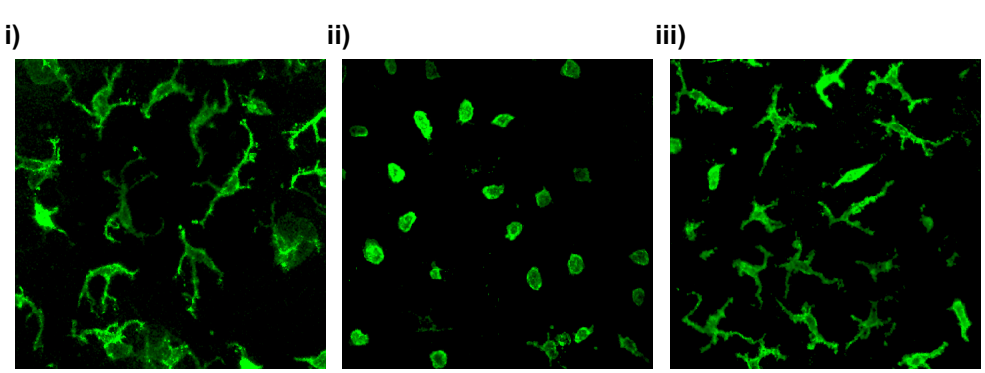

FIGURE 1 | NKG2D ligands and a timely response to alteration in their expression by epidermal γδTCR$^+$ intraepithelial lymphocytes (IELs). **(A)** Human and mouse NKG2D ligands, their cell surface anchor and their affinity to NKG2D are shown. **(B)** Representative confocal images of murine epidermal Vγ5Vδ1$^+$ IELs in whole epidermal sheets following transgenic upregulation of Rae-1 under the involucrin promoter. (i) Single-transgenic and (ii) bi-transgenic mice were fed with doxycycline for 72 h, inducing expression of Rae-1 only in bi-transgenic mice (4). (iii) Mice with sustained expression of Rae-1 under the involucrin promoter (19). The images depict how acute expression of Rae-1 on epithelial cells induces morphological and activational changes in the neighboring IELs, whereas constitutive expression of Rae-I renders them hyporesponsive. Abbreviations: *allele-dependent NKG2D, natural killer group 2 member D; MIC, MHC class I-chain-related protein; ULBP, cytomegalovirus UL16-binding protein; Rae-1, retinoic acid early-inducible 1; MULT1, murine UL16-binding protein-like transcript 1; al, a2, and a3, analogous to the a1, a2, and a3 domains of MHC 1a proteins; TM, transmembrane protein; GPI, glycosylphosphatidylinositol-linked protein; ND, not determined.

pregnancy, which may be sensed by uterine NK cells (which are not cytolytic). Together these observations suggest that NKG2D-ligand expression does not always evoke cytotoxicity *in vivo*, but may have an additional and relatively unexplored role in development and/or tissue repair.

NKG2D-DEPENDENT ACTIVATION OF HUMAN γδ T CELLS

Most (60–95%) human peripheral blood γδ T cells express Vγ9Vδ2 TCRs that are uniquely activated by non-peptidic prenyl pyrophosphate antigens (phosphoantigens, PAg) such as isopenthenyl pyrophosphate, which is abundant in tumor cells; or (E)-4-hydroxy-3-methyl-but-enyl pyrophosphate, that is produced by bacteria and parasites [reviewed in Ref. (30)]. PAg-activated Vγ9Vδ2 T cells play important protective roles in infections, such as tuberculosis (31–34); and can kill a variety of tumor cell lines (35, 36).

Recent research has clarified how PAg may be "sensed" by Vγ9Vδ2 TCRs. This involves butyrophilin 3A1 (BTN3A1; also known as CD277), a B7 superfamily member that binds PAg in its intracellular B30.2 domain, which leads to significant conformational changes in the extracellular domains of the protein (37–43). Importantly, the effects of both agonist and blocking anti-BTN3A1 mAbs on Vγ9Vδ2 TCR transductants indicated that the TCR is necessary for the activation process (44, 45).

Besides TCR-dependent sensing of intracellular PAg accumulation, the discrimination between tumor and healthy cells by Vγ9Vδ2 T cells seemingly also involves NKG2D, which is expressed on the cell surface of nearly all Vγ9Vδ2 T cells, as it is on peripheral CD8$^+$ αβ T cells. We have observed that NKG2D blockade reduces by circa 50%, the capacity of (PAg-activated) Vγ9Vδ2 T cells to target leukemic cells (as measured by apoptosis induction *in vitro*) (5). Moreover, when we looked for NKG2D ligands whose expression could account for leukemia cell recognition, we found ULBP1 to be the strongest candidate (5, 35). Consistent with this, the

downregulation of ULBP1 impaired, whereas its overexpression enhanced, Vγ9Vδ2 T cell-mediated killing of leukemia/lymphoma cells (5). In independent studies, other NKG2D ligands have emerged as major determinants of tumor cell targeting by γδ T cells: ULBP4 in ovarian and colon carcinomas (46); and ULBP3 in B-cell chronic lymphocytic leukemia (CLL) (47). In the latter report, the critical γδ T cell subpopulation were Vδ1$^+$ (rather than Vδ2$^+$) T cells and Vδ1$^+$ T cell counts as well as detectable/inducible ULBP3 expression both associated positively with disease control in CLL patients (47). Along the same lines, a recent study showed that ULBP1 and NKG2D expression associated (positively) with longer overall survival of gastric cancer patients (48). Thus, enhancement of NKG2D ligand expression, as achieved by bortezomib or temozolomide treatment of multiple myeloma (49) and glioblastoma multiforme (50) cells, respectively, may have important therapeutic potential, even if NKG2D ligand shedding may constitute an important immune evasion mechanism (51). On the other hand, tumor-directed recombinant ligands that engage NKG2D may also enhance tumor cell targeting, as recently documented against malignant B cells for bispecifics composed of CD20-binding and NKG2D ligand (MICA or ULBP2) domains (52).

The relative importance of NKG2D *versus* TCR stimulation of γδ T cells in human is still debated (53). Some studies reported the ability of Vγ9Vδ2 T cells to trigger effector responses through NKG2D stimulation alone (i.e., similarly to NK cells) (36, 54, 55). However, others have failed to show NKG2D-induced activation without simultaneous TCR stimulation (56). In this later case, NKG2D would function in γδ T cells like in CD8$^+$ αβ T cells, i.e., as a costimulatory receptor accessory to the TCR. Future research should clarify whether the capacity to deploy NKG2D independently of the TCR varies between Vδ2$^+$ versus Vδ1$^+$ γδ T cells. The latter are preferentially found in mucosal tissues and can often be more abundant than Vδ2$^+$ T cells within solid tumors (57). Unlike Vγ9Vδ2 T cells, Vδ1$^+$ T cells do not recognize PAg; instead, intestinal epithelial Vδ1$^+$ T cells were shown to bind MICA (and MICB) *via* a diverse set of Vδ1$^+$ TCRs (58, 59), including on transfectants lacking NKG2D (60). Interestingly, our own data have identified a key difference between Vδ2$^+$ and Vδ1$^+$ T cells with regards to the ability to enhance their cytotoxic potential through the upregulation of a distinct class of NK cell receptors—the NCRs.

INDUCED NCRs ON HUMAN Vδ1$^+$ T CELLS

In contrast with NKG2D, NCRs were until recently thought to be NK-specific. However, reports on the acquisition of NCR expression by activated IELs (9, 10), and the subsequent identification of ILCs constitutively expressing NCRs, particularly NKp46 (8), have clearly demonstrated that NCR expression is not an exclusive property of NK cells. Although mouse γδ T cells seemingly do not express NKp46, we reported that the continued (>2 weeks) activation by TCR agonists (or mitogens-like PHA) in the presence of IL-15 or IL-2 induced NCR expression in a large fraction (>50%) of human γδ T cells (11). Interestingly, NCR induction was mostly restricted to Vδ1$^+$ T cells, as Vδ2$^+$ T cells failed to express any of the NCRs above background levels. And, in Vδ1$^+$ T cells, the main induced NCRs were NKp30 and NKp44, with NKp46 limited to a smaller fraction (<20%) of activated cells. Antibody-mediated modulation and redirected lysis assays demonstrated the capacity of NKp30 and, to a lesser extent, NKp44, but not NKp46, to enhance Vδ1$^+$ T cell cytotoxicity against tumor cell targets (11). Furthermore, NCR triggering increased IFN-γ expression in Vδ1$^+$ T cells, consistent with their role in NK cells (61). Based on these findings, we have developed and established the pre-clinical proof-of-concept for a new (NCR$^+$ Vδ1$^+$) cellular product, delta one T (DOT) cells, for adoptive immunotherapy of cancer (12) (**Figure 2**). Moreover, we also demonstrated that this NKp30-mediated activation of Vδ1$^+$ T cells was able to inhibit HIV viral replication, through the production of CCL3/MIP-1α, CCL4/MIP-1β, and CCL5/RANTES (62). These three CC-chemokines can inhibit viral replication by binding to CCR5, one of the primary co-receptors that HIV-1 uses for entry into CD4$^+$ T cells. Collectively, these studies showed that the induced expression of NCRs on Vδ1$^+$ T cells enhances their anti-tumor and anti-viral functions.

The acquisition of NCR expression by peripheral blood Vδ1$^+$ T cells strictly requires strong TCR activation (11). This is consistent with previous work on human IELs, since the ability to upregulate NKp46 and NKp44 in the gut environment only occurred in effector T cells, and the expanded population of NCR$^+$ αβ IELs in celiac disease displayed a highly restricted TCR repertoire indicative of oligoclonal expansion (10). Thus, the major current working hypothesis is that the expression of NCRs in T cells may derive from chronic activation *via* the TCR. This may allow pre-activated T lymphocytes to circumvent antigen-restricted responses, instead employing NCRs to respond continuously against "danger" or "stress," which clearly fits the concept of LSS by γδ T cells (4, 20, 21).

In this context, it will be critical to identify the NCR ligands that are relevant to NCR$^+$ Vδ1$^+$ T cell biology, presumably associated with the processes of cellular transformation or viral infection. Thus, the hemagglutinin (HA) protein of the influenza and vaccinia virus binds NKp46 to stimulate NK cells to lyse virus-infected cells (63, 64). Conversely, a HCMV protein, pp65, was reported to inhibit NK cytotoxicity by dissociating the signaling chain, CD3ζ, from its complex with NKp30 (65).

Self-derived molecules have also been identified as ligands for NCRs, which underlies their capacity to target tumor and/or stressed cells. One of the first self-molecules identified to interact with NKp30 is the human leukocyte antigen-B-associated transcript 3 (BAT3) (66). The expression of this molecule on the tumor cell surface triggers NKp30-mediated killing and the production of IFN-γ and TNF-α. The anti-tumor role of BAT3 was confirmed *in vivo* by showing that peripheral blood NK cells were less efficient at clearing tumors when an anti-BAT3 blocking antibody was administered in mice.

A member of the B7 receptor family, B7-H6, was also shown to bind NKp30 (67). B7-H6 is present on cell surface of both primary tumor and tumor cell lines, while neither healthy nor stressed cells seemingly expressing it. Interestingly, while the presence of B7-H6 on the surface of tumor cells makes them

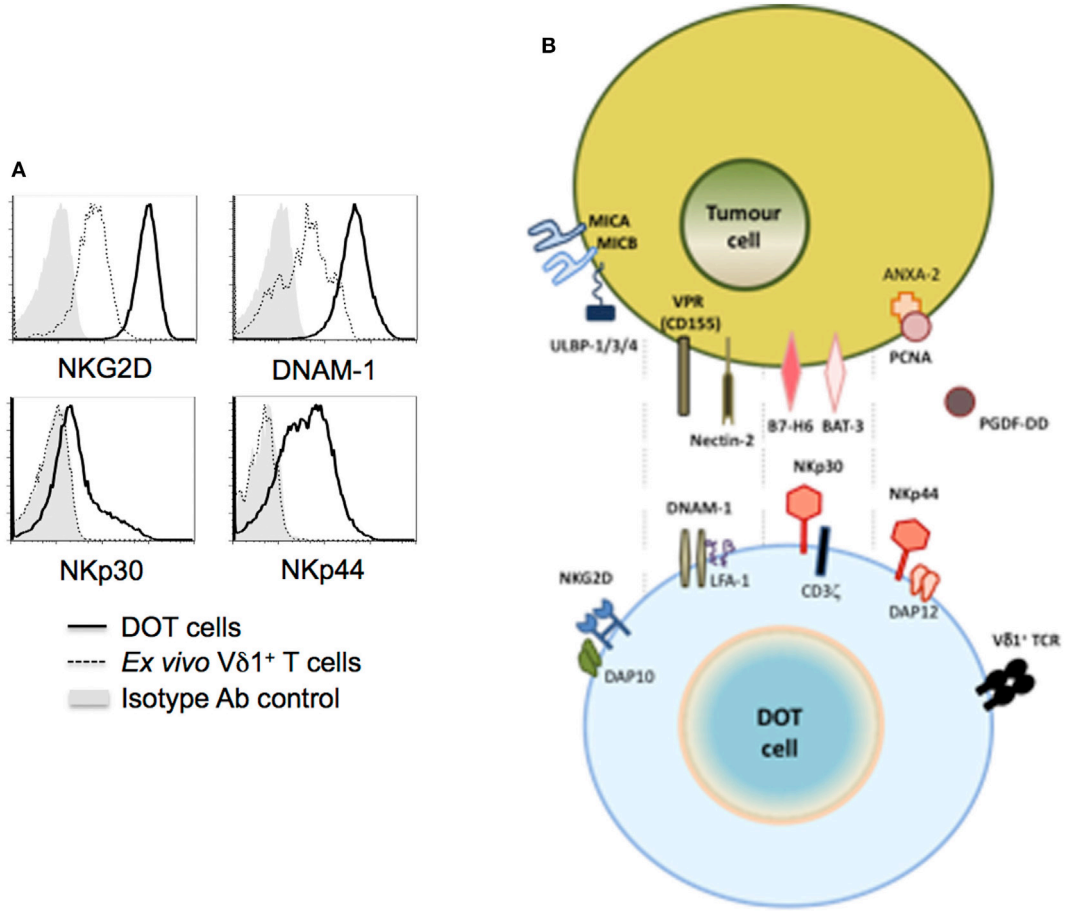

FIGURE 2 | NK cell receptors and ligands for delta one T (DOT) cells. DOT cells are expanded/activated Vδ1+ T cells that upregulate NKG2D and DNAM-1 levels, and induce *de novo* NKp30 and NKp44 expression [**(A)** from Ref. (12)]. **(B)** The figure depicts putative ligands for those NK cell receptors known to be (over) expressed on tumor cells.

susceptible to NKp30-mediated killing (67), the binding of B7-H6 to the alternative splice variant, NKp30c, reduces cytotoxicity and IFN-γ production, instead inducing NK cells to produce the immunoregulatory cytokine IL-10 (68). Moreover, the expression of the NKp30c isoform associated with poor clinical prognosis in gastrointestinal sarcoma.

As for NKp44, until recently its best-characterized ligand was an inhibitory molecule, proliferating cell nuclear antigen, that is commonly expressed by tumor cells, and strongly inhibited by NK cell cytotoxicity and IFN-γ production, likely *via* the inhibitory ITIM motif atypically present in the intracellular domain of NKp44 (69). However, a very recent study showed that NKp44 binds to platelet-derived growth factor-DD, a key promoter of tumor cell proliferation, epithelial–mesenchymal transition, and angiogenesis (70). The interaction provoked NK cell activation and the secretion of IFN-γ and TNF-α, which induced tumor cell growth arrest, including in *in vivo* cancer models. This may be a seminal finding in our understanding of how immune cells can recognize tumor cells. Future research should clarify the repertoire of NCR ligands that underlie the enhanced anti-tumor functions of NCR+ Vδ1+ T cells (**Figure 2**).

CONCLUSION AND PERSPECTIVES

Our current working model includes two stages of γδ T cell activation and target cell recognition: first, γδ T cells are activated by γδTCR ligands (many of which are still unknown); but then NKRs may play the key role in identifying stressed (transformed or infected) targets. This role is physiologically fulfilled by NKG2D (25), constitutively expressed by γδ T cells (3, 4); but therapeutically it can rely on induced NCRs, particularly for the human Vδ1+ T cell subset whose clinical potential is still to be realized (57). For these, the expression of both NKG2D and NCRs provides two functional layers of innate stress-surveillance, particularly of tumors. From a clinical perspective, we have established a clinical-grade protocol to differentiate NCR+ Vδ1+ T cells *in vitro*, from peripheral blood of cancer patients, toward the development of a new adoptive cell immunotherapy ("DOT cells") (12). Of note, concomitant with TCR stimulation, IL-15 seems to be the key cytokine for NCR induction on Vδ1+ T cells (12), which is consistent with previous data on NK cells and IELs (61). Given that the gut is an IL-15-rich environment, it will be interesting to investigate the expression of NCRs on intestinal γδ T cells, especially since these compose a

large fraction of the IEL compartment; and are highly enriched in Vδ1$^+$ (compared to Vδ2$^+$) T cells. Such future research should also clarify the enigmatic role of NKp46, since it was not evident from our studies on blood-derived Vδ1$^+$ T cells (12); and address the potential relevance of NCRs for the reported regulatory functions of Vδ1$^+$ TILs (71, 72).

Besides cancer, another potential application for NCR$^+$ Vδ1$^+$ T cells is the control of viral infection. Our demonstration that NKp30 engagement on *in vitro* activated Vδ1$^+$ T cells is able to suppress HIV-1 replication through the production of CCL3/MIP-1α, CCL4/MIP-1β, and CCL5/RANTES, opens new avenues for the manipulation of γδ T cells in HIV-1 disease. This is particularly interesting because HIV-1 infection is characterized by a marked expansion of Vδ1$^+$ T cells (73–75). This may be even more relevant in mucosal tissues, namely intestinal and cervical mucosa that are sites of HIV-1 entry, where Vδ1$^+$ T cells are particularly abundant (76), while CD4$^+$ T cells are strongly depleted (77). Of additional great potential is the use of NCR$^+$ Vδ1$^+$ T cells in CMV infection, given the well-established anti-CMV activity and long-term expansion of Vδ1$^+$ T cells (78–81), including post-allogeneic stem cell transplantation (80–81).

In conclusion, we propose that NK cell receptor expression by γδ T cells contributes decisively to their role as a "bridge" between innate and adaptive immunity, both physiologically (*via* constitutive NKG2D) and therapeutically (through induced NCRs). We believe this entails great potential for future γδ T cell-based immunotherapies against viral infections or cancer.

AUTHOR CONTRIBUTIONS

BS-S and JS contributed equally to the inception and writing of the manuscript.

ACKNOWLEDGMENTS

We thank Adrian Hayday, Domenico Mavilio, Kelly Hudspeth, and Daniel Correia for insightful discussions on this topic; and Natacha Gonçalves-Sousa for her help to write the manuscript. We acknowledge funding from the Wellcome Trust (100999/Z/13/Z) and Cancer Research UK (C21010/A19788) (to JS) and Fundação para a Ciência e a Tecnologia (PTDC/DTP-PIC/4931/2014) (to BS-S). This publication was sponsored by LISBOA-01-0145-FEDER-007391, project cofunded by FEDER, through POR Lisboa 2020—Programa Operacional Regional de Lisboa, PORTUGAL 2020, and Fundação para a Ciência e a Tecnologia.

REFERENCES

1. Eagle RA, Trowsdale J. Promiscuity and the single receptor: NKG2D. *Nat Rev Immunol* (2007) 7:737–44. doi:10.1038/nri2144
2. Bauer S, Groh V, Wu J, Steinle A, Phillips JH, Lanier LL, et al. Activation of NK cells and T cells by NKG2D, a receptor for stress-inducible MICA. *Science* (1999) 285:727–9. doi:10.1126/science.285.5428.727
3. Girardi M, Oppenheim DE, Steele CR, Lewis JM, Glusac E, Filler R, et al. Regulation of cutaneous malignancy by gammadelta T cells. *Science* (2001) 294:605–9. doi:10.1126/science.1063916
4. Strid J, Roberts SJ, Filler RB, Lewis JM, Kwong BY, Schpero W, et al. Acute upregulation of an NKG2D ligand promotes rapid reorganization of a local immune compartment with pleiotropic effects on carcinogenesis. *Nat Immunol* (2008) 9:146–54. doi:10.1038/ni1556
5. Lanca T, Correia DV, Moita CF, Raquel H, Neves-Costa A, Ferreira C, et al. The MHC class Ib protein ULBP1 is a nonredundant determinant of leukemia/lymphoma susceptibility to gammadelta T-cell cytotoxicity. *Blood* (2010) 115:2407–11. doi:10.1182/blood-2009-08-237123
6. Groh V, Rhinehart R, Secrist H, Bauer S, Grabstein KH, Spies T. Broad tumor-associated expression and recognition by tumor-derived gamma delta T cells of MICA and MICB. *Proc Natl Acad Sci U S A* (1999) 96:6879–84. doi:10.1073/pnas.96.12.6879
7. Moretta A, Bottino C, Vitale M, Pende D, Cantoni C, Mingari MC, et al. Activating receptors and coreceptors involved in human natural killer cell-mediated cytolysis. *Annu Rev Immunol* (2001) 19:197–223. doi:10.1146/annurev.immunol.19.1.197
8. Satoh-Takayama N, Vosshenrich CAJ, Lesjean-Pottier S, Sawa S, Lochner M, Rattis F, et al. Microbial flora drives interleukin 22 production in intestinal NKp46+ cells that provide innate mucosal immune defense. *Immunity* (2008) 29:958–70. doi:10.1016/j.immuni.2008.11.001
9. Meresse B, Chen Z, Ciszewski C, Tretiakova M, Bhagat G, Krausz TN, et al. Coordinated induction by IL15 of a TCR-independent NKG2D signaling pathway converts CTL into lymphokine-activated killer cells in celiac disease. *Immunity* (2004) 21:357–66. doi:10.1016/j.immuni.2004.06.020
10. Meresse B, Curran SA, Ciszewski C, Orbelyan G, Setty M, Bhagat G, et al. Reprogramming of CTLs into natural killer-like cells in celiac disease. *J Exp Med* (2006) 203:1343–55. doi:10.1084/jem.20060028
11. Correia DV, Fogli M, Hudspeth K, da Silva MG, Mavilio D, Silva-Santos B. Differentiation of human peripheral blood Vdelta1+ T cells expressing the natural cytotoxicity receptor NKp30 for recognition of lymphoid leukemia cells. *Blood* (2011) 118:992–1001. doi:10.1182/blood-2011-02-339135
12. Almeida AR, Correia DV, Fernandes-Platzgummer A, Da Silva CL, Da Silva MG, Anjos DR, et al. Delta one T cells for immunotherapy of chronic lymphocytic leukemia: clinical-grade expansion/differentiation and preclinical proof of concept. *Clin Cancer Res* (2016) 22:5795–804. doi:10.1158/1078-0432.CCR-16-0597
13. Raulet DH, Gasser S, Gowen BG, Deng W, Jung H. Regulation of ligands for the NKG2D activating receptor. *Annu Rev Immunol* (2013) 31:413–41. doi:10.1146/annurev-immunol-032712-095951
14. Diefenbach A, Tomasello E, Lucas M, Jamieson AA, Hsia JK, Vivier E, et al. Selective associations with signaling proteins determine stimulatory versus costimulatory activity of NKG2D. *Nat Immunol* (2002) 3:1142–9. doi:10.1038/ni858
15. Wu J, Song Y, Bakker AB, Bauer S, Spies T, Lanier LL, et al. An activating immunoreceptor complex formed by NKG2D and DAP10. *Science* (1999) 285:730–2. doi:10.1126/science.285.5428.730
16. Rosen DB, Araki M, Hamerman JA, Chen T, Yamamura T, Lanier LL. A Structural basis for the association of DAP12 with mouse, but not human, NKG2D. *J Immunol* (2004) 173:2470–8. doi:10.4049/jimmunol.173.4.2470
17. Nitahara A, Shimura H, Ito A, Tomiyama K, Ito M, Kawai K. NKG2D ligation without T cell receptor engagement triggers both cytotoxicity and cytokine production in dendritic epidermal T cells. *J Invest Dermatol* (2006) 126:1052–8. doi:10.1038/sj.jid.5700112
18. Lilienfeld BG, Garcia-Borges C, Crew MD, Seebach JD. Porcine UL16-binding protein 1 expressed on the surface of endothelial cells triggers human NK cytotoxicity through NKG2D. *J Immunol* (2006) 177:2146–52. doi:10.4049/jimmunol.177.4.2146
19. Oppenheim DE, Roberts SJ, Clarke SL, Filler R, Lewis JM, Tigelaar RE, et al. Sustained localized expression of ligand for the activating NKG2D receptor impairs natural cytotoxicity in vivo and reduces tumor immunosurveillance. *Nat Immunol* (2005) 6:928–37. doi:10.1038/ni1239
20. Strid J, Tigelaar RE, Hayday AC. Skin immune surveillance by T cells-a new order? *Semin Immunol* (2009) 21:110–20. doi:10.1016/j.smim.2009.03.002
21. Hayday AC. Gammadelta T cells and the lymphoid stress-surveillance response. *Immunity* (2009) 31:184–96. doi:10.1016/j.immuni.2009.08.006
22. Chodaczek G, Papanna V, Zal MA, Zal T. Body-barrier surveillance by epidermal gammadelta TCRs. *Nat Immunol* (2012) 13:272–82. doi:10.1038/ni0612-621d

23. Van Beneden K, De Creus A, Stevenaert F, Debacker V, Plum J, Leclercq G. Expression of inhibitory receptors Ly49E and CD94/NKG2 on fetal thymic and adult epidermal TCR V gamma 3 lymphocytes. *J Immunol* (2002) 168:3295–302. doi:10.4049/jimmunol.168.7.3295
24. Ibusuki A, Kawai K, Yoshida S, Uchida Y, Nitahara-Takeuchi A, Kuroki K, et al. NKG2D triggers cytotoxicity in murine epidermal γδ T cells via PI3K-dependent, Syk/ZAP70-independent signaling pathway. *J Invest Dermatol* (2014) 134:396–404. doi:10.1038/jid.2013.353
25. Whang MI, Guerra N, Raulet DH. Costimulation of dendritic epidermal T cells by a new NKG2D ligand expressed specifically in the skin. *J Immunol* (2009) 182:4557–64. doi:10.4049/jimmunol.0802439
26. Strid J, Sobolev O, Zafirova B, Polic B, Hayday A. The intraepithelial T cell response to NKG2D-ligands links lymphoid stress surveillance to atopy. *Science* (2011) 334:1293–7. doi:10.1126/science.1211250
27. Dalessandri T, Crawford G, Hayes M, Castro Seoane R, Strid J. IL-13 from intraepithelial lymphocytes regulates tissue homeostasis and protects against carcinogenesis in the skin. *Nat Commun* (2016) 7:12080. doi:10.1038/ncomms12080
28. Nomura M, Zou Z, Joh T, Takihara Y, Matsuda Y, Shimada K. Genomic structures and characterization of Rae1 family members encoding GPI-anchored cell surface proteins and expressed predominantly in embryonic mouse brain. *J Biochem* (1996) 120:987–95. doi:10.1093/oxfordjournals.jbchem.a021517
29. Ogasawara K, Benjamin J, Takaki R, Phillips JH, Lanier LL. Function of NKG2D in natural killer cell-mediated rejection of mouse bone marrow grafts. *Nat Immunol* (2005) 6:938–45. doi:10.1038/ni1236
30. Morita CT, Jin C, Sarikonda G, Wang H. Nonpeptide antigens, presentation mechanisms, and immunological memory of human Vgamma2Vdelta2 T cells: discriminating friend from foe through the recognition of prenyl pyrophosphate antigens. *Immunol Rev* (2007) 215:59–76. doi:10.1111/j.1600-065X.2006.00479.x
31. Shen Y, Zhou D, Qiu L, Lai X, Simon M, Shen L, et al. Adaptive immune response of Vgamma2Vdelta2+ T cells during mycobacterial infections. *Science* (2002) 295:2255–8. doi:10.1126/science.1068819
32. Qaqish A, Huang D, Chen CY, Zhang Z, Wang R, Li S, et al. Adoptive transfer of phosphoantigen-specific γδ T cell subset attenuates *Mycobacterium tuberculosis* infection in nonhuman primates. *J Immunol* (2017) 198:4753–63. doi:10.4049/jimmunol.1602019
33. Chen ZW. Protective immune responses of major Vγ2Vδ2 T-cell subset in *M. tuberculosis* infection. *Curr Opin Immunol* (2016) 42:105–12. doi:10.1016/j.coi.2016.06.005
34. Kabelitz BYD, Bender A, Schondelmaier S, Schoel B, Kaufmann SHE. A large fraction of human peripheral blood gamma/delta + T cells is activated by *Mycobacterium tuberculosis* but not by its 65-kD heat shock protein. *J Exp Med* (1990) 171:667–79.
35. Gomes AQ, Correia DV, Grosso AR, Lança T, Ferreira C, Lacerda JF, et al. Identification of a panel of ten cell surface protein antigens associated with immunotargeting of leukemias and lymphomas by peripheral blood γδ t cells. *Haematologica* (2010) 95:1397–404. doi:10.3324/haematol.2009.020602
36. Wrobel P, Shojaei H, Schittek B, Gieseler F, Wollenberg B, Kalthoff H, et al. Lysis of a broad range of epithelial tumour cells by human gamma delta T cells: involvement of NKG2D ligands and T-cell receptor- versus NKG2D-dependent recognition. *Scand J Immunol* (2007) 66:320–8. doi:10.1111/j.1365-3083.2007.01963.x
37. Sandstrom A, Peigné C-M, Léger A, Crooks JE, Konczak F, Gesnel M-C, et al. The intracellular B30.2 domain of butyrophilin 3A1 binds phosphoantigens to mediate activation of human Vγ9Vδ2 T cells. *Immunity* (2014) 40:490–500. doi:10.1016/j.immuni.2014.03.003
38. Gu S, Sachleben JR, Boughter CT, Nawrocka WI, Borowska MT, Tarrasch JT, et al. Phosphoantigen-induced conformational change of butyrophilin 3A1 (BTN3A1) and its implication on Vγ9Vδ2 T cell activation. *Proc Natl Acad Sci U S A* (2017) 114:E7311–20. doi:10.1073/pnas.1707547114
39. Peigné C-M, Léger A, Gesnel M-C, Konczak F, Olive D, Bonneville M, et al. The juxtamembrane domain of butyrophilin BTN3A1 controls phosphoantigen-mediated activation of human Vγ9Vδ2 T cells. *J Immunol* (2017) 198:4228–34. doi:10.4049/jimmunol.1601910
40. Salim M, Knowles TJ, Baker AT, Davey MS, Jeeves M, Sridhar P, et al. BTN3A1 discriminates γδ T cell phosphoantigens from nonantigenic small molecules via a conformational sensor in its B30.2 domain. *ACS Chem Biol* (2017) 12:2631–43. doi:10.1021/acschembio.7b00694
41. Nguyen K, Li J, Puthenveetil R, Lin X, Poe MM, Hsiao CHC, et al. The butyrophilin 3A1 intracellular domain undergoes a conformational change involving the juxtamembrane region. *FASEB J* (2017) 31:4697–706. doi:10.1096/fj.201601370RR
42. Sebestyen Z, Scheper W, Vyborova A, Gu S, Rychnavska Z, Schiffler M, et al. RhoB mediates phosphoantigen recognition by Vγ9Vδ2 T cell receptor. *Cell Rep* (2016) 15:1973–85. doi:10.1016/j.celrep.2016.04.081
43. Wang H, Morita CT. Sensor function for butyrophilin 3A1 in prenyl pyrophosphate stimulation of human Vγ2Vδ2 T cells. *J Immunol* (2015) 195:4583–94. doi:10.4049/jimmunol.1500314
44. Harly C, Guillaume Y, Nedellec S, Peigne CM, Monkkonen H, Monkkonen J, et al. Key implication of CD277/butyrophilin-3 (BTN3A) in cellular stress sensing by a major human gammadelta T cell subset. *Blood* (2012) 120(11):2269–79. doi:10.1182/blood-2012-05-430470
45. Gu S, Nawrocka W, Adams EJ. Sensing of pyrophosphate metabolites by Vγ9Vδ2 T cells. *Front Immunol* (2015) 5:688. doi:10.3389/fimmu.2014.00688
46. Kong Y, Cao W, Xi X, Ma C, Cui L, He W. The NKG2D ligand ULBP4 binds to TCRgamma9/delta2 and induces cytotoxicity to tumor cells through both TCRgammadelta and NKG2D. *Blood* (2009) 114:310–7. doi:10.1182/blood-2008-12-196287
47. Poggi A, Venturino C, Catellani S, Clavio M, Miglino M, Gobbi M, et al. Vdelta1 T lymphocytes from B-CLL patients recognize ULBP3 expressed on leukemic B cells and up-regulated by trans-retinoic acid. *Cancer Res* (2004) 64:9172–9. doi:10.1158/0008-5472.CAN-04-2417
48. Kamei R, Yoshimura K, Yoshino S, Inoue M, Asao T, Fuse M, et al. Expression levels of UL16 binding protein 1 and natural killer group 2 member D affect overall survival in patients with gastric cancer following gastrectomy. *Oncol Lett* (2018) 15:747–54. doi:10.3892/ol.2017.7354
49. Niu C, Jin H, Li M, Zhu S, Zhou L, Jin F, et al. Low-dose bortezomib increases the expression of NKG2D and DNAM-1 ligands and enhances induced NK and γδ T cell-mediated lysis in multiple myeloma. *Oncotarget* (2017) 8:5954–64. doi:10.18632/oncotarget.13979
50. Chitadze G, Lettau M, Luecke S, Wang T, Janssen O, Fürst D, et al. NKG2D- and T-cell receptor-dependent lysis of malignant glioma cell lines by human γδ T cells: modulation by temozolomide and A disintegrin and metalloproteases 10 and 17 inhibitors. *Oncoimmunology* (2016) 5:1–13. doi:10.1080/2162402X.2015.1093276
51. Chitadze G, Bhat J, Lettau M, Janssen O, Kabelitz D. Generation of soluble NKG2D ligands: proteolytic cleavage, exosome secretion and functional implications. *Scand J Immunol* (2013) 78:120–9. doi:10.1111/sji.12072
52. Peipp M, Wesch D, Oberg HH, Lutz S, Muskulus A, van de Winkel JGJ, et al. CD20-specific immunoligands engaging NKG2D enhance γδ T cell-mediated lysis of lymphoma cells. *Scand J Immunol* (2017) 86:196–206. doi:10.1111/sji.12581
53. Correia DV, Lopes AC, Silva-Santos B. Tumor cell recognition by γδ T lymphocytes. *Oncoimmunology* (2013) 2:e22892. doi:10.4161/onci.22892
54. Das H, Groh V, Kuijl C, Sugita M, Morita CT, Spies T, et al. MICA engagement by human Vgamma2Vdelta2 T cells enhances their antigen-dependent effector function. *Immunity* (2001) 15:83–93. doi:10.1016/S1074-7613(01)00168-6
55. Rincon-Orozco B, Kunzmann V, Wrobel P, Kabelitz D, Steinle A, Herrmann T. Activation of V gamma 9V delta 2 T cells by NKG2D. *J Immunol* (2005) 175:2144–51. doi:10.4049/jimmunol.175.4.2144
56. Nedellec S, Sabourin C, Bonneville M, Scotet E. NKG2D costimulates human V gamma 9V delta 2 T cell antitumor cytotoxicity through protein kinase C theta-dependent modulation of early TCR-induced calcium and transduction signals. *J Immunol* (2010) 185:55–63. doi:10.4049/jimmunol.1000373
57. Silva-Santos B, Serre K, Norell H. gammadelta T cells in cancer. *Nat Rev Immunol* (2015) 15:683–91. doi:10.1038/nri3904
58. Groh V, Steinle A, Bauer S, Spies T. Recognition of stress-induced MHC molecules by intestinal epithelial γδ T cells. *Science* (1998) 279:1737–40. doi:10.1126/science.279.5357.1737
59. Xu B, Pizarro JC, Holmes MA, McBeth C, Groh V, Spies T, et al. Crystal structure of a gammadelta T-cell receptor specific for the human MHC class I homolog MICA. *Proc Natl Acad Sci U S A* (2011) 108:2414–9. doi:10.1073/pnas.1015433108
60. Wu J, Groh V, Spies T. T cell antigen receptor engagement and specificity in the recognition of stress-inducible MHC class I-related chains by human epithelial gd T cells. *J Immunol* (2002) 169:1236–40. doi:10.4049/jimmunol.169.3.1236

61. Hudspeth K, Silva-Santos B, Mavilio D. Natural cytotoxicity receptors: Broader expression patterns and functions in innate and adaptive immune cells. *Front Immunol* (2013) 4:69. doi:10.3389/fimmu.2013.00069
62. Hudspeth K, Fogli M, Correia DV, Mikulak J, Roberto A, Della Bella S, et al. Engagement of NKp30 on Vdelta1 T-cells induces the production of CCL3, CCL4 and CCL5 and suppresses HIV-1 replication. *Blood* (2012) 119(17):4013–6. doi:10.1182/blood-2011-11-390153
63. Mandelboim O, Lieberman N, Lev M, Paul L, Arnon TI, Bushkin Y, et al. Recognition of haemagglutinins on virus-infected cells by NKp46 activates lysis by human NK cells. *Nature* (2001) 409:1055–60. doi:10.1038/35059110
64. Jarahian M, Fiedler M, Cohnen A, Djandji D, Hämmerling GJ, Gati C, et al. Modulation of nkp30- and nkp46-mediated natural killer cell responses by poxviral hemagglutinin. *PLoS Pathog* (2011) 7:e1002195. doi:10.1371/journal.ppat.1002195
65. Arnon TI, Achdout H, Levi O, Markel G, Saleh N, Katz G, et al. Inhibition of the NKp30 activating receptor by pp65 of human cytomegalovirus. *Nat Immunol* (2005) 6:515–23. doi:10.1038/ni1190
66. Pogge von Strandmann E, Simhadri VR, von Tresckow B, Sasse S, Reiners KSS, Hansen HP, et al. Human leukocyte antigen-B-associated transcript 3 is released from tumor cells and engages the NKp30 receptor on natural killer cells. *Immunity* (2007) 27:965–74. doi:10.1016/j.immuni.2007.10.010
67. Brandt CS, Baratin M, Yi EC, Kennedy J, Gao Z, Fox B, et al. The B7 family member B7-H6 is a tumor cell ligand for the activating natural killer cell receptor NKp30 in humans. *J Exp Med* (2009) 206:1495–503. doi:10.1084/jem.20090681
68. Delahaye NF, Rusakiewicz S, Martins I, Menard C, Roux S, Lyonnet L, et al. Alternatively spliced NKp30 isoforms affect the prognosis of gastrointestinal stromal tumors. *Nat Med* (2011) 17:700–7. doi:10.1038/nm.2366
69. Rosental B, Brusilovsky M, Hadad U, Oz D, Appel MY, Afergan F, et al. Proliferating cell nuclear antigen is a novel inhibitory ligand for the natural cytotoxicity receptor NKp44. *J Immunol* (2011) 187:5693–702. doi:10.4049/jimmunol.1102267
70. Barrow AD, Edeling MA, Trifonov V, Luo J, Goyal P, Bohl B, et al. Natural killer cells control tumor growth by sensing a growth factor. *Cell* (2018) 172:534–48. doi:10.1016/j.cell.2017.11.037
71. Ye J, Ma C, Wang F, Hsueh EC, Toth K, Huang Y, et al. Specific recruitment of γδ regulatory T cells in human breast cancer. *Cancer Res* (2013) 73:6137–48. doi:10.1158/0008-5472.CAN-13-0348
72. Ye J, Ma C, Hsueh EC, Eickhoff CS, Zhang Y, Varvares MA, et al. Tumor-derived regulatory T cells suppress innate and adaptive immunity through the induction of immunosenescence. *J Immunol* (2013) 190:2403–14. doi:10.4049/jimmunol.1202369
73. Poccia F, Boullier S, Lecoeur H, Cochet M, Poquet Y, Colizzi V, et al. Peripheral V gamma 9/V delta 2 T cell deletion and anergy to nonpeptidic mycobacterial antigens in asymptomatic HIV-1-infected persons. *J Immunol* (1996) 157:449–61.
74. De Paoli P, Gennari D, Martelli P, Basaglia G, Crovatto M, Battistin S, et al. Subset of gamma delta lymphocytes is increased during HIV-1 infection. *Clin Exp Immunol* (1991) 83:187–91. doi:10.1111/j.1365-2249.1991.tb05612.x
75. Hinz T, Wesch D, Friese K, Reckziegel A, Arden B, Kabelitz D. T cell receptor gamma delta repertoire in HIV-1-infected individuals. *Eur J Immunol* (1994) 24:3044–9. doi:10.1002/eji.1830241219
76. Poles MA, Barsoum S, Yu W, Yu J, Sun P, Daly J, et al. Human immunodeficiency virus type 1 induces persistent changes in mucosal and blood gammadelta T cells despite suppressive therapy. *J Virol* (2003) 77:10456–67. doi:10.1128/JVI.77.19.10456-10467.2003
77. Brenchley JM, Price DA, Schacker TW, Asher TE, Silvestri G, Rao S, et al. Microbial translocation is a cause of systemic immune activation in chronic HIV infection. *Nat Med* (2006) 12:1365–71. doi:10.1038/nm1511
78. Halary F, Pitard V, Dlubek D, Krzysiek R, de la Salle H, Merville P, et al. Shared reactivity of Vδ2 ^{neg} γδ T cells against cytomegalovirus-infected cells and tumor intestinal epithelial cells. *J Exp Med* (2005) 201:1567–78. doi:10.1084/jem.20041851
79. Pitard V, Roumanes D, Lafarge X, Couzi L, Garrigue I, Lafon ME, et al. Long-term expansion of effector/memory V{delta}2- {gamma}-{delta} T cells is a specific blood signature of CMV infection. *Blood* (2008) 112:1317–24. doi:10.1182/blood-2008-01-136713
80. Ravens S, Schultze-Florey C, Raha S, Sandrock I, Drenker M, Oberdörfer L, et al. Human γδ T cells are quickly reconstituted after stem-cell transplantation and show adaptive clonal expansion in response to viral infection. *Nat Immunol* (2017) 18:393–401. doi:10.1038/ni.3686
81. Knight A, Madrigal AJ, Grace S, Sivakumaran J, Kottaridis P, Mackinnon S, et al. The role of Vdelta2-negative gammadelta T cells during cytomegalovirus reactivation in recipients of allogeneic stem cell transplantation. *Blood* (2010) 116:2164–72. doi:10.1182/blood-2010-01-255166

Conflict of Interest Statement: BS-S is a co-founder and share holder of Lymphact—Lymphocyte Activation Technologies S.A. Jessica Strid declares that the research was conducted in the absence of any commercial or financial relationships that could be construed as a potential conflict of interest.

Copyright © 2018 Silva-Santos and Strid. This is an open-access article distributed under the terms of the Creative Commons Attribution License (CC BY). The use, distribution or reproduction in other forums is permitted, provided the original author(s) and the copyright owner are credited and that the original publication in this journal is cited, in accordance with accepted academic practice. No use, distribution or reproduction is permitted which does not comply with these terms.

frontiers in Immunology

REVIEW
published: 20 April 2018
doi: 10.3389/fimmu.2018.00828

Towards Deciphering the Hidden Mechanisms That Contribute to the Antigenic Activation Process of Human Vγ9Vδ2 T Cells

Lola Boutin[1,2]* *and Emmanuel Scotet*[1,3]*

[1] CRCINA, INSERM, CNRS, Université d'Angers, Université de Nantes, Nantes, France, [2] Sanofi R&D, Biologics Research, Centre de Recherche Vitry Alfortville, Paris, France, [3] LabEx IGO "Immunotherapy, Graft, Oncology", Nantes, France

OPEN ACCESS

Edited by:
Pierre Vantourout,
King's College London,
United Kingdom

Reviewed by:
Eric Champagne,
UMR5282 Centre de Physiopathologie de Toulouse Purpan (CPTP), France
Andrew Wiemer,
University of Connecticut, United States
Jean Jacques Fournie,
ERL5294 Centre de Recherches en Cancérologie de Toulouse, France

***Correspondence:**
Lola Boutin
lola.boutin@univ-nantes.fr;
Emmanuel Scotet
emmanuel.scotet@inserm.fr

Specialty section:
This article was submitted to T Cell Biology, a section of the journal Frontiers in Immunology

Received: 15 February 2018
Accepted: 05 April 2018
Published: 20 April 2018

Citation:
Boutin L and Scotet E (2018) Towards Deciphering the Hidden Mechanisms That Contribute to the Antigenic Activation Process of Human Vγ9Vδ2 T Cells. Front. Immunol. 9:828. doi: 10.3389/fimmu.2018.00828

Vγ9Vδ2 T cells represent a major unconventional γδ T cell subset located in the peripheral blood of adults in humans and several non-human primates. Lymphocytes that constitute this transitional subset can sense subtle level changes of intracellular phosphorylated intermediates of the isoprenoid biosynthesis pathway (phosphoantigens, pAg), such as isopentenyl pyrophosphate, during cell stress events. This unique antigenic activation process operates in a rigorous framework that requires the expression of butyrophilin 3A1 (BTN3A1/CD277) molecules, which are type I glycoproteins that belong to the B7 family. Several studies have further shown that pAg specifically bind to the intracellular B30.2 domain of BTN3A1 linked to the antigenic activation of Vγ9Vδ2 T cells. Here, we highlight the recent advances in BTN3A1 dynamics induced upon the binding of pAg and the contribution of the different subunits to this activation process. Recent reports support that conformational modifications of BTN3A1 might represent a key step in the detection of infection or tumorigenesis by Vγ9Vδ2 T cells. A better understanding of this mechanism will help optimize novel immunotherapeutical approaches that target defined functions of this unique γδ T cell subset.

Keywords: human γδ T cell, T cell receptor, antigenic activation, phosphoantigens, butyrophilin, B30.2

1. γδ T CELLS COMPOSE A SPECIAL IMMUNOLOGICAL UNIT

Discovered in the mid-1980s, gamma delta (γδ) T lymphocytes still puzzle and fascinate by their unconventional features. During thymic ontogeny, γδ T cell subsets originating from common lymphoid precursor cells emerge before αβ T cells to represent the predominant $CD3^+$ population at the fetal development. Their relative frequency then decreases after birth, while αβ T cells progressively predominate. Importantly, for yet unclear reasons, the expression of particular TCR Vγ and Vδ regions is associated with preferential tissue locations. Hence, the major human peripheral γδ T cell subset (frequency >80%) in healthy adult expresses a heterodimeric TCR composed of Vγ9and Vδ2 chains, and represents about 5% of total lymphoïd cells (1, 2). By contrast, Vδ1 and Vδ3 subsets are mainly detected in epithelial tissues, liver, spleen, tonsils, lymph nodes, and thymus (3). Interestingly, γδ T cells compose the majority of circulating T lymphocytes in some non-primate species (i.e., cattle, sheep, pigs, and birds), which raises questions about evolutionary processes and the biology of this subset (4).

From a functional point of view, γδ T cells are involved in the control of microbial infections (e.g., bacteria, virus, and parasite), cell transformation, homeostasis, and tissue repair already reviewed in Ref. (5, 6). Their activation during these physiopathological contexts induces the release of cytotoxic and bacteriostatic molecules, such as perforin, granzymes, granulysin, and defensins, death-inducing receptor, and TNF-related apoptosis-inducing ligand receptor (TRAIL). Activated γδ T cells also regulate immune responses by secreting a large panel of soluble molecules, such as cytokines, that can promote the clearance of either intracellular pathogens (e.g., TNFα, IFNγ), extracellular bacteria, fungi (IL-17) or parasites (e.g., IL-4, IL-5, and IL-13); inflammatory (e.g., TNFα, IFNγ) or anti-inflammatory responses (e.g., TGFβ, IL-10); tissue healing, epithelium repair, and cell survival. Interestingly, complementary studies have shown that activated γδ T cells, through type I IFN sensitizations, also promote dendritic cells (DC) maturation and, therefore, could represent adjuvant cells (7–9). Moreover, some γδ T cell subset, like human Vγ9Vδ2 T cells, can acquire an antigen-presenting cell (APC)-like phenotype and regulate conventional $CD4^+$/$CD8^+$ αβ T cell responses (10).

In contrast to most conventional αβ T cells which directly recognize antigenic structures composed of proteasome-generated peptides and polymorphic presenting molecules, that are related to the major histocompatibility complex (MHC) family (e.g., MHC class I/II molecules), the antigenic activation of γδ T cells is mostly MHC-independent, which strengthens their therapeutical interest (i.e., lack of alloreactivity) (11). The antigenic activation of γδ T cells is linked with their tissue residency and the Vδ chain expressed (12, 13). Interestingly, several studies have now reported that γδ T lymphocyte subsets can be activated by various native or modified molecules that mainly derive from a *Self* origin, including MHC-like molecules in mice (e.g., T10–T22) and in humans (e.g., MICA/B, CD1c, CD1d, and EPCR) (14–18) and yet unrelated native molecules, such as F_0–F_1 ATP synthase, phycoerythrin, and apolipoprotein A-I (19). More recently, Annexin-A2, which is expressed in tumor cell(s) upon oxidative stress, has been shown to be directly recognized by human Vγ8Vδ3 T lymphocytes (20). TLRs, dectins, and NLRs may act as γδ TCR costimulator (21). Of note, in most cases, the γδ TCR-dependent activation is also tightly regulated by a set of various molecules, including TLRs, dectins, and NLRs, killer Ig-like receptors (e.g., KIR2D, KIR3D), C-type lectins (CD94/NKG2A-C, NKG2D), and several costimulatory molecules shared with αβ T cells (e.g., LFA1, CD2, CD27, and CD28) (22). In this review, we focus our analysis on the γδ TCR-dependent activation modalities of the major peripheral Vγ9Vδ2 T cell subset.

2. HUMAN Vγ9Vδ2 T CELLS ARE SPECIFICALLY ACTIVATED BY PHOSPHOANTIGENS

In healthy adult primates, the major peripheral γδ T cell subset, which expresses a TCR composed of Vγ9 and Vδ2 chains, does not account for more than 10% of the total peripheral T cell pool. Interestingly, this lymphocyte subset expands upon microbial infections (e.g., *Mycobacterium leprae*, *Mycobacterium tuberculosis*) (23, 24). *In vitro* assays that rely on the incubation of peripheral lymphoid cells with mycobacterial lysates have evidenced Vγ9Vδ2 T cell expansion mediated by protease-resistant and phosphatase-sensitive components, hereafter called phosphoantigens (pAg) (25). These low molecular weight agonists are constituted of alkyl esters associated with a diphosphate moiety that carries their bioactivity (26–28). Isopentenyl PyroPhosphate (IPP), which was the first natural pAg identified from the mycobacteria *M. smegmatis*, is also synthesized in eukaryotic cells where it is an intermediate metabolite of the isoprenoid mevalonate (MVA) pathway leading to cholesterol synthesis (29). Several natural pAg have been further identified and characterized from vertebrates (e.g., DMAPP, dimethylallyl pyrophosphate) and microbes (e.g., HDMAPP/HMBPP, 4-hydroxy-3-dimethylallyl pyrophosphate). These microbial metabolites, produced from the DOXP/MEP (1-deoxy-D-xylulose-5-phosphate/2-C-methyl-D-erythritol-4-phosphate) pathway (30–32), are much more efficient to activate Vγ9Vδ2 T cells than MVA-derived IPP. This property could explain the strong reactivity displayed by Vγ9Vδ2 T cells in infectious contexts (33). Dysregulation of the eukaryotic MVA pathway, which leads to an intracellular accumulation of IPP, has been reported in various types of tumor cells (34). For example, the over-expression of HMG-CoA reductase, in non-Hodgkin B cell lymphoma cell-line Daudi or breast adenocarcinoma cells, induces their spontaneous recognition by γ9Vδ2 T cells (35). Accordingly, pharmacological MVA pathway inhibitors that target upstream (e.g., statins) or downstream (e.g., aminobisphosphonates) IPP synthesis, respectively, suppress or trigger pAg-induced Vγ9Vδ2 T cell activation (36).

Primate Vγ9Vδ2 T cells can specifically sense weak modifications of the expression of *Self* molecules, such as pAg, in a contact- and TCR-dependent manner. However, the mechanisms and pathways involved in this peculiar antigenic activation process remain ill-defined. Despite several attempts, direct interactions between pAg and Vγ9Vδ2 TCR have never been clearly evidenced. While the contribution of additional molecules to this species-specific process has been suggested by various complementary studies [e.g., implication of TCR CDRs (37)], this had not been shown until the groundbreaking evidence that butyrophilins could represent a first group of key molecules.

3. THE BUTYROPHILIN BTN3A1 ORCHESTRATES Vγ9Vδ2 T CELL ANTIGENIC ACTIVATION INDUCED BY PHOSPHOANTIGENS

Following the key identification of pAg as potent and specific agonist compounds, the clear evidence that butyrophilin-3A (BTN3A/CD277) molecules also play a mandatory role in the antigenic activation of primate Vγ9Vδ2 T cells was a groundbreaking step to better understand this peculiar and mysterious immunological process (38). Phylogenetically, ubiquitously expressed type I glycoprotein butyrophilin (BTN) molecules share a common ancestor with other members of the B7-CD28 superfamily, which thus suggests that they display immunological functions (39).

Indeed, various studies suggest that BTN, as well as BTN-like (BTNL) molecules are involved in some regulatory processes by triggering yet unclear pathways (40). In humans, BTN genes (>10) are located in the telomeric part close to HLA class I region of the chromosome 6p. BTN molecules, which are structurally highly homologous, are divided in three subfamilies (BTN1, BTN2, and BTN3). The BTN3A (CD277) subfamily, then contains three isoforms BTN3A1, -A2, and -A3, belonging to the immunoglobulin (Ig) superfamily and sharing a high structural homology for the extracellular domain composed of an Ig-like IgV and an IgC domain (39) (**Figure 1**). Of note, the sequences of both B7 and BTN receptors are sufficiently distinct to prevent the latter ones from binding to known costimulatory T ligands, such as CD28 or CTLA-4 (41, 42). While the ectodomain of the three BTN3A isoforms have a very high homology (>95%), only BTN3A1 and BTN3A3 isoforms express an intracellular portion which is composed of a poorly conserved PRY/SPRY B30.2 (hereafter called B30.2) (43). The B30.2 domain, described as a key region for mediating protein–protein interactions, is shared by other BTN family members, as well as various "immunological" proteins, such as TRIM (TRIpartite Motif) and pyrin families (44). The human genome contains four identified *btnl* genes, with the designations of BTNL2, -3, -8, and -9. *btnl2*, the best characterized family member, is clustered with the *btn* genes on chromosome 6, but near to human MHC class II region, whereas the least explored family members *btnl3*, *btnl8,* and *btnl9* are localized on chromosome 5 (45). Interestingly, BTNL molecules share an homology with the murine Skint family molecules and more particulary with Skint1, which drives the intrathymic differentiation of murine Vγ5Vδ1 T cells (46). The biological function of BTN3A1 molecules is elusive. A recent report shows that BTN3A1 is a positive regulator of the nucleic acid-mediated type I IFN signaling pathway. Upon nucleic acid stimulation, BTN3A1 moves along microtubules toward the perinuclear region, where it directs the interaction of TBK1 with IRF3, thereby facilitating the phosphorylation of IRF3. This process is controlled by microtubule-associated protein 4 (MAP4) (47). Our group described the specific and mandatory contribution of BTN3A1, expressed at the membrane of cellular targets, to the pAg-induced reactivity of primate Vγ9Vδ2 T cells (38). BTN3A1 is ubiquitously expressed in primates, which seems associated with the presence of pAg-reactive γδ T cells in these species (48, 49). Accordingly, BTN3A1 orthologs are not expressed in the rodent lineage that lacks Vγ9Vδ2 T cell counterparts specific for pAg. The emergence of Vγ9Vδ2 TCR and BTN3 molecules with eutherian placental mammals has been reported, suggesting a strong co-evolutionary link (50).

The combined mode of action of BTN3A1 and pAg molecules for triggering a strong and specific antigenic activation of primate Vγ9Vδ2 T cells remains unclear and controversial. BTN3A1 has been first proposed as a "classical" antigen-presenting molecule for pyrophosphate compounds. In this model, pAg would bind a shallow groove within the distal IgV extracellular domain, which induces the formation of stable complexes that then directly interact and stimulate the Vγ9Vδ2 TCR, similarly to the peptide-MHC molecules and αβ TCR system (51). This model, which implies cognate physical interactions between a conserved portion of the IgV domain of BTN3A1, pAg, and the Vγ9Vδ2 TCR, diverges from the data published in several studies that clearly show the key specific requirement for the BTN3A1 isoform in the pAg-mediated activation of Vγ9Vδ2 T cells. In line with these observations, our model proposes that the intracellular B30.2 domain of the BTN3A1 isoform, but not BTN3A3, drives Vγ9Vδ2 T cell antigenic activation through a direct binding of pAg to a charged groove. This model, based on the intracellular sensing of pAg by BTN3A1 molecules, has been supported by several complementary observations. Depletion, domain swapping, and mutation experiments indicate that BTN3A1 lacking its intracellular domain B30.2, or expressing a BTN3A3 B30.2 domain, or at least mutated on some of its critical pAg-binding residues, fail to trigger an efficient pAg-induced Vγ9Vδ2 T cell stimulation. Conversely, chimeric BTN3A3 molecules that expressed the B30.2 domain of BTN3A1 efficiently trigger a pAg-mediated activation (52, 53). Together, these results support the mandatory role played by the intracellular BTN3A1 B30.2 domain in the pAg-binding and sensing by Vγ9Vδ2 T cells.

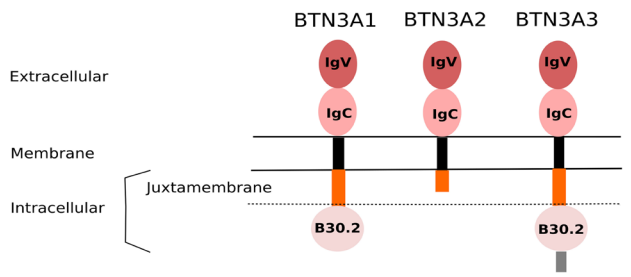

FIGURE 1 | Domain organization of BTN3A isoforms. The BTN3A family proteins share a high structural homology, mainly through their extracellular domain comprising a membrane-proximal IgC and a N-terminal IgV domains. They are linked to a poorly conserved intracellular part *via* a single transmembrane structure (black). The submembrane region (orange) represents the juxtamembrane domain (JTM). BTN3A1 and BTN3A3, but not BTN3A2, contain an intracellular B30.2 domain. The BTN3A3 isoform is further composed of an additional C-terminal extension (gray).

4. B30.2, THE LOCK/KEY SYSTEM OF INTRACELLULAR PHOSPHOANTIGEN SENSING

While the B30.2 domains of BTN3A1 and BTN3A3 display a strong homology (approximately 87% amino acid identity), the domain of BTN3A3 fails to efficiently bind pAg and to trigger a significant antigenic activation of Vγ9Vδ2 T cells. The crystal structure of the B30.2 domain of BTN3A1 gave key information about pAg binding site. Importantly, specificity of the BTN3A1 B30.2 domain is a highly positive charged pocket which is constituted by basic residues, including arginines (R^{442}, R^{448}, and R^{499}), histidines (H^{381} and H^{408}), and lysine (K^{423}). Positively charged B30.2 domain represents an ideal pocket candidate for binding negatively charged pAg. Accordingly, the mutation from basic to (negatively charged) acidic residues completely abrogates pAg-binding and Vγ9Vδ2 T cell activation (53, 54). However, these

results did not entirely explain the differences between the capacity of BTN3A1 and BTN3A3 to bind pAg. Close examination of the amino acid differences between these isoforms revealed a single amino acid difference in position 381 within the binding pocket: a histidine in BTN3A1 and an arginine in BTN3A3 (**Figure 2**). Swapping this single amino acid between the domains of each isoform (i.e., mutating the H into R in BNT3A1 and R into H in BTN3A3) transferred both binding and functional abilities to stimulate Vγ9Vδ2 T cells. Affinity differences have been measured between endogenous and exogenous pAg by a technique called Isothermal Titration Calorimetry (ITC): KD ≃1 mM for endogenous and KD ≃1 mM for exogenous pAg (55). These results also confirmed that the functional potency of those compounds in mediating activation of Vγ9Vδ2 T cells despite is not directly proportional to the affinity (56). The endogenous IPP is typically 100,000-fold weaker potency than the exogenous HMBPP (57).

Adams and colleagues have investigated the effects of pAg binding to the intracellular domain B30.2 of BTN3A1 by NMR spectrometry and molecular dynamics simulation. Using a BTN3A1 full-length intracellular domain model, they have shown that pAg binding induces conformational changes of the BTN3A1 B30.2 domain. The Y^{382} residue, close to the positive pocket, has been identified as critical by showing the largest perturbation induced by pAg binding. ABP-treated Y352A mutants are less capable of mediating Vγ9Vδ2 T cell activation than the wild-type B30.2-containing protein (58). These conformational changes could represent the first signals delivered to distinguish activating or non-activating molecules. In fact, the BTN3A1 B30.2 domain is able to bind additional negatively charged small molecules, like malonate, citrate, adenosine-diphosphate (ADP), and nucleotidic pAg (59). Exogenous pAg (e.g., HMBPP/HDMAPP) induce a chemical shift into the B30.2 domain that extended to the binding site. IPP binding, a less affine pAg, induces similar shift perturbations but qualitatively smaller in magnitude. These results confirmed the antigenic potential difference between exogenous and endogenous pAg. In contrast, titration of the B30.2 domain with malonate and citrate revealed only few chemical shifts with a small magnitude. Both of these nonantigenic molecules failed to induce perturbations in residues more distal to the pAg-binding site. Strikingly, the conformational changes induced by ADP occur in a different direction than those with pAg (60). NMR and crystallography studies suggest that a precise conformation of BTN3A1 B30.2 domain is required to induce Vγ9Vδ2 T cell activation.

Studies from Massaia's group provided further mechanistic inputs about the contribution of BTN3A1 in pAg-induced Vγ9Vδ2 T lymphocyte activation. They showed that ABP-treated dendritic cells (DC) release extracellular IPP that can induce a significant Vγ9Vδ2 T cell proliferation (61). They identified the ATP-binding cassette transporter 1 (ABCA1) as a major complex involved in this extracellular release of IPP by ABP-treated DCs, with the physical cooperation of BTN3A1 and apolipoprotein A-I (ApoA-I) molecules (62). BTN3A1 is physically linked to ABCA1 but not associated with ApoA-I. Gene silencing of BTN3A1 in ABP-treated DCs slightly decreased the amounts of IPP released. This important study highlighted the existence of pAg membrane transporter complexes that are involved in the export of these compounds. Conversely, the ways by which external charged pAg could cross the plasmic membrane to reach intracellular butyrophilins and then induce the reactivity of Vγ9Vδ2 T cells remain unclear and will need to be further defined.

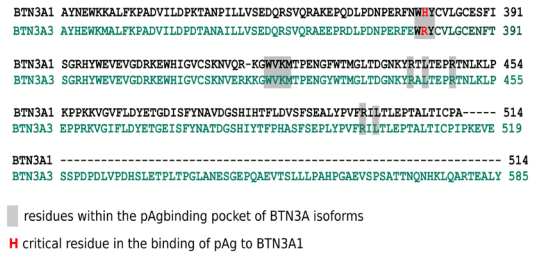

FIGURE 2 | Alignment of the intracellular B30.2 domain sequences of BTN3A1 and BTN3A3 isoforms. Amino acid sequence alignment of the B30.2 domains of BTN3A1 (top line) and BTN3A3 (bottom line). Dashes indicate absent residues in BTN3A1. Amino acids are shown in the single letter designations and numbered according full length nomenclature. Gray boxes indicate residues which constitute the pAg-binding positively charged pocket. Red font highlights the single amino acid difference between pAg-binding pocket, in position 381, H in BTN3A1, and R in BTN3A3 isoforms adapted from Ref. (53).

5. THE JUXTAMEMBRANE DOMAIN OF BTN3A1, ANOTHER KEY PLAYER IN THE SENSING OF PHOSPHOANTIGENS

The role played by the extracellular and intracellular B30.2 domains of BTN3A1 in the antigenic activation of human Vγ9Vδ2 T cells has been extensively studied. Moreover, the contribution of additional portions of these molecules, such as the juxtamembrane (JTM) domain, has also been carefully analyzed. The JTM domain of many transmembrane receptors, such as growth factor receptors, has been shown to be involved in signaling processes (63). The intracellular JTM region of BTN3A, which is a rather flexible structure, connects the transmembrane domain to the B30.2 one. Our functional activation assays performed with BTN3A1 chimeras swapped for their JTM region support that this intracellular part is a strong regulator of the Vγ9Vδ2 T cell activation. Indeed, BTN3A1 chimeras that express the JTM domains from BTN1A1, BTN2A2, BTNL3, or BTNL9 fail to trigger the antigenic activation of Vγ9Vδ2 T cells. Interestingly, chimeric BTN3A1 molecules expressing the JTM domain of BTN3A3 induce a massive antigenic activation of Vγ9Vδ2 T cells more efficiently than wild-type BTN3A1 (64) (**Figure 3**). Accordingly, a very recent report further supports these observations by showing that the binding of pAg, such as HMBPP, to the B30.2 domain perturbs residues within the JTM region, suggesting ligand-induced conformational changes. Interestingly, HMBPP could interact with residues within both the B30.2 and the JTM region at different contact points. Furthermore, this report also indicates that both key residues Ser/$Thr^{296/297}$ and Thr^{304} fall within a critical functional BTN3A1 JTM region (65).

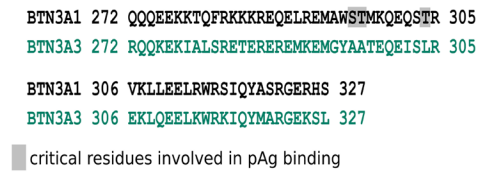

FIGURE 3 | Alignment of sequences encoded by the intracellular juxtamembrane (JTM) domain from BTN3A1 and BTN3A3 isoforms. Amino acids sequence alignment of the JTM domains of BTN3A1 (top line) and BTN3A3 (bottom line). Amino acids are shown in the single letter designation and numbered according to full length nomenclature. Gray boxes show key residues, Ser/Thr$^{296/297}$ and Thr^{304}, involved in pAg binding in the JTM region due to the folding of the B30.2 domain in Vγ9Vδ2 T cell antigenic activation adapted from Ref. (64).

The binding of pAg to the intracellular B30.2 domain has been shown to induce conformational changes of the JTM that could have important functional consequences (55). For example, these modifications could either spread to the extracellular domain of BTN3A molecules or alter its membrane topology and dynamics, leading to their recognition by γδ T cells.

6. THE HOLY GRAIL: UNDERSTANDING THE CRYPTIC MECHANISM OF ANTIGENIC ACTIVATION OF Vγ9Vδ2 T CELLS

Despite representing significant advances by suggesting that butyrophilins do not operate as "classical" antigen-presenting partners, such as MHC and MHC-like molecules, these recent observations rather complicated the poor understanding of this peculiar antigenic activation process. Ultimately, γδ T lymphocyte immunologists will need to answer to the challenging question about the mechanism(s) by which the Vγ9Vδ2 TCR exquisitely and specifically sense them, following the increase of pAg levels and their association(s) to butyrophilins, to deliver strong and rapid activation signals. From a fundamental point of view, these future analyses should provide evidences about the intracellular trafficking, the dynamics of these molecules (e.g., intracellular/membrane multimeric complexes), the regulation of this process in normal vs. pathological contexts (e.g., tumor cells). Basically, these results should bring some important information about the still unclear biological functions displayed by these molecules. On a more evolutionary side, these results should help to finally provide an unified overview of the antigenic activation process of human and murine γδ T lymphocyte subsets, some of the latter ones being also regulated by non-BTN3A1 butyrophilin-related molecules (e.g., Skint or BTNL8) (66, 67).

To assist these complex deciphering steps, novel elements have been recently brought, such as the recruitment of BTN3A1 partners and the contribution of other isoforms and conformational changes. As BTN3A1 isoforms have not been shown to directly interact with the Vγ9Vδ2 TCR, various independent studies have been conducted to identify and to characterize extra- and intracellular partner molecules. Consequently, different groups first confirmed that the expression of human BTN3A1 molecules in rodent cells may not be sufficient to simply induce the reactivity of primate Vγ9Vδ2 T cells (68). The transfer of human chromosome 6 in those cells, which triggers this species-specific activation, then suggested that partner molecule(s) are encoded by gene(s) located within this chromosome (69). Two studies recently reported that molecular partners, such as RhoB or periplakin, cognately interact with BTN3A molecules (70). RhoB is a small G protein of the Rho GTPase family that regulates actin reorganization, vesicles transport, and apoptosis in transformed cells following DNA damage. RhoB contributes to various cellular events, including cancer progression through multiple pathways by regulating DNA damage responses, apoptosis, cell cycle progression, migration, and invasion (71). Lipid modifications affect main subcellular localizations (i.e., endosomes, Golgi vesicles, and nucleus) of RhoB and its levels are acutely regulated in response to a variety of stimuli. Using a biolayer interferometry approach, Kuball's group demonstrated that RhoB binds to the full-length BTN3A1 intracellular domain, while binding was significantly reduced to the B30.2 domain alone. However, the precise contribution of RhoB, which is conserved between humans and rodents and encoded by a gene located in chromosome 2, to the activation of Vγ9Vδ2 T lymphocytes is yet unclear and will require a deeper analysis.

The plakin family member, cytoskeleton adaptor protein periplakin (PPL), whose gene is located in chromosome 16, has also been shown to bind to the BTN3A1 JTM (72). PPL might contribute to the formation of responsive and dynamic structures which could implicate both cytoskeleton components (e.g., intermediate filaments, actin) and pAg. Accordingly, our results from fluorescence recovery after photobleaching (FRAP) experiments have shown an immobilization of BTN3A1 molecules linked to pAg sensitization (53). This suggests that the antigenic activation of Vγ9Vδ2 T lymphocytes is linked to the recruitment and containment of BTN3A1 proteins in selected subcellular domains which are located in the vicinity of the plasma membrane and focal adhesions (LB & ES, unpublished observations). However, PPL knockdown using siRNAs had no clearly interpretable effects on BTN3A1-mediated activation of Vγ9Vδ2 T cells. In this work, the main evidence for a functional contribution of these interactions is a correlation between loss of PPL binding and loss of activation, induced by a deletion of either the VKLLEEL JTM stretch (located in exon 5 of BTN3A1) or only of its di-leucine motif. In so far as PPL does not bind to BTN3A3, while active BTN3A3 carrying the R351H mutation efficiently activates Vγ9Vδ2 T lymphocytes, it seems unlikely that PPL is required for the Vγ9Vδ2 T lymphocyte antigenic activation process.

Initial experiments evidenced that agonist #20.1 BNT3A-specific mAbs bind the IgV ectodomain of BTN3A glycoproteins, which leads to the activation of Vγ9Vδ2 T lymphocytes (38, 73). Among various hypotheses, the possibility of mAb-induced conformational changes, which could mimic pAg-induced modifications, deserves attention. The functional impact of pAg-induced changes of the intracellular B30.2 and JTM domains, that could be then transduced to the extracellular domain and trigger the sensing of these modified *Self* complexes by Vγ9Vδ2 T lymphocytes,

has been investigated. Accordingly, independent studies have shown that the conformation of both the B30.2 domain and its upstream JTM region vary upon pAg binding (58, 60). An important study has shown that pAg bind the B30.2 pocket and weakly interact with some residues constituting the JTM region. Based on both length and flexibility characteristics, the authors propose that the B30.2 domain of BTN3A1 is moved toward the JTM region and closer to the membrane upon ligand binding. Such intracellular changes would be sensed by γδ T cells through modifications of either the extracellular domain or interactions with other molecular partners (65). Non-BTN3A proteins composed of an intracellular B30.2 domain have been shown to naturally multimerize and this status is important to fulfill their functions (74, 75).

While first studies proposed that the ectodomain of BTN3A exist at the surface into either V-shaped or head-to-tail conformations (49, 76), recent experiments suggest that only the ectodomain adopts a V-shaped conformation (58). Strikingly, this study indicates that the expression of BTN3A1–BTN3A2 heterodimers in lipid nanodiscs is more stable than BTN3A1 homodimers, which suggest a role for the BTN3A2 isoform (which contains no intracellular B30.2 domain). A growing set of studies from various laboratories confirmed that BTN3A1 molecules are mandatory for pAg-dependent activation of Vγ9Vδ2 T lymphocytes. The contribution of BTN3A2 and BTN3A3 isoforms to this process remained to be understood and was analyzed. Initial functional studies, using global, and likely incomplete, BTN3A-knockdown (shRNA delivered by lentivirus) combined to a forced expression of selected isoforms (transfection), first showed that the expression of BTN3A2 and BTN3A3 isoforms is not sufficient to induce the activation of Vγ9Vδ2 T lymphocytes by pAg. So far, the results failed to demonstrate any inhibitory or activatory role played by non-BTN3A1 isoforms. A work from Hayday's group proposes that BTN3A1 and BTN3A2 heterodimers would contribute to this process according to this model. The ectodomain and the B30.2 domain of BTN3A1 would represent active entities in Vγ9Vδ2 T lymphocyte stimulation, while BTN3A2 isoforms would rather participate by regulating the appropriate routing (e.g., ER trafficking), kinetics, and/or stability of BTN3A1 (77).

Despite these major breakthroughs, the main question remains yet unsolved: how could such conformational changes and heterodimeric associations be specifically sensed by the TCR of Vγ9Vδ2 T lymphocytes. This issue represents major future research tracks in this field (**Figure 4**). To summarize, complementary research issues can be identified: (i) the subcellular localization for the interactions of pAg with BTN3A molecules; (ii) the role played by additional intra- vs. extracellular partners

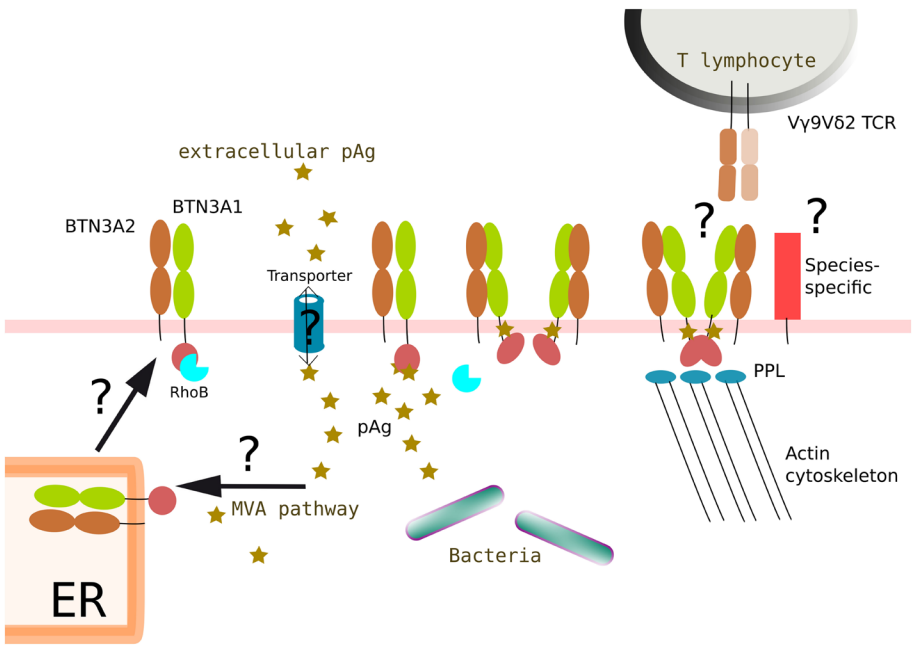

FIGURE 4 | Proposed integrated model of BTN3A1 modifications induced by phosphoantigens and leading to the antigenic activation of Vγ9Vδ2 T lymphocytes. Intracellular accumulation of pAg could originate from a dysregulation of the *Self* mevalonate (MVA) pathway in pathological situations (e.g., cancer, infections) and/or be from exogenous origin (e.g., pathogens). In some situations, negatively charged pAg would need to be routed (e.g., import/export) *via* active processes (e.g., ABC transporters). pAg would then bind to intracellular parts of butyrophilin molecules (e.g., B30.2 ± juxtamembrane domains) at different sub-cellular locations during synthesis and routing steps of the molecules (e.g., ER, cell membrane). The binding of pAg to butyrophilins induces structural modifications that affect the dynamics of the molecules (e.g., membrane diffusion) and the immunological visibility of these molecules. Accordingly, the transition from resting to activatory state of these molecular complexes might also be linked to the nature of the multimerization of BTN3A1 glycoproteins (e.g., homodimers, heterodimers). The contribution of additional partner molecules, some of them being species-specific, regulating actin cytoskeleton modifications (e.g., RhoB, PPL) might also be important. The mechanisms that drive this unique antigenic activation process of human Vγ9Vδ2 T lymphocytes sensing these subtle molecular changes though a specific, contact-, and Vγ9Vδ2 TCR-dependent process remain a major conundrum. The question marks (?) refer to unsolved or yet unclear issues.

(e.g., cargo ?); (iii) the characterization of BTN3A antigenic complexes and their dynamics, linked to the antigenic activation status; (iv) the conformation(s)/multimerization of integral BTN3A molecules; and (v) the specific role played by BTN3A2 and BTN3A3 isoforms in these processes.

AUTHOR CONTRIBUTIONS

Both authors contributed to the writing process, prepared the manuscript, and approved the final version.

ACKNOWLEDGMENTS

The authors thank the staff of the cellular and tissular imaging core (MicroPICell) and the cytometry facility (Cytocell) from Nantes CRCINA, SFRF. Bonamy and Université de Nantes for their expert assistance. The authors thank Quentin Ayoul-Guilmard for critical reading of the manuscript.

FUNDING

This work was supported by funds from INSERM, CNRS, Université de Nantes, Institut National du Cancer (INCa, PLBio2014), Agence Nationale de la Recherche (ANR, GDSTRESS), Ligue Nationale contre le Cancer (AO InterRégional 2017), Fondation pour la Recherche Médicale (FRM Equipe 2017), Cancéropôle Grand-Ouest, and SANOFI. The work was realized in the context of the LabEX IGO and the IHU-Cesti programs, supported by the National Research Agency Investissements d'Avenir *via* the programs ANR-11-LABX-0016-01 and ANR-10-IBHU-005, respectively. The IHU-Cesti project is also supported by Nantes Métropole and Région Pays de la Loire.

REFERENCES

1. Hayday AC. [gamma][delta] cells: a right time and a right place for a conserved third way of protection. *Annu Rev Immunol* (2000) 18:975–1026. doi:10.1146/annurev.immunol.18.1.975
2. Chien Y-H, Meyer C, Bonneville M. γδ T cells: first line of defense and beyond. *Annu Rev Immunol* (2014) 32:121–55. doi:10.1146/annurev-immunol-032713-120216
3. Groh V, Porcelli S, Fabbi M, Lanier LL, Picker LJ, Anderson T, et al. Human lymphocytes bearing T cell receptor gamma/delta are phenotypically diverse and evenly distributed throughout the lymphoid system. *J Exp Med* (1989) 169(4):1277–94. doi:10.1084/jem.169.4.1277
4. Davis WC, Brown WC, Hamilton MJ, Wyatt CR, Orden JA, Khalid AM, et al. Analysis of monoclonal antibodies specific for the gamma delta TcR. *Vet Immunol Immunopathol* (1996) 52(4):275–83. doi:10.1016/0165-2427(96)05578-X
5. Hayday AC. Gammadelta T cells and the lymphoid stress-surveillance response. *Immunity* (2009) 31(2):184–96. doi:10.1016/j.immuni.2009.08.006
6. Bonneville M, O'Brien RL, Born WK. Gammadelta T cell effector functions: a blend of innate programming and acquired plasticity. *Nat Rev Immunol* (2010) 10(7):467–78. doi:10.1038/nri2781
7. Devilder M-C, Maillet S, Bouyge-Moreau I, Donnadieu E, Bonneville M, Scotet E. Potentiation of antigen-stimulated V gamma 9v delta 2 T cell cytokine production by immature dendritic cells (DC) and reciprocal effect on DC maturation. *J Immunol* (2006) 176(3):1386–93. doi:10.4049/jimmunol.176.3.1386
8. Devilder M-C, Allain S, Dousset C, Bonneville M, Scotet E. Early triggering of exclusive IFN-gamma responses of human Vgamma9vdelta2 T cells by TLR-activated myeloid and plasmacytoid dendritic cells. *J Immunol* (2009) 183(6):3625–33. doi:10.4049/jimmunol.0901571
9. Conti L, Casetti R, Cardone M, Varano B, Martino A, Belardelli F, et al. Reciprocal activating interaction between dendritic cells and pamidronate-stimulated gammadelta T cells: role of CD86 and inflammatory cytokines. *J Immunol* (2005) 174(1):252–60. doi:10.4049/jimmunol.174.1.252
10. Brandes M, Willimann K, Moser B. Professional antigen-presentation function by human gammadelta T cells. *Science* (2005) 309(5732):264–8. doi:10.1126/science.1110267
11. Allison TJ, Winter CC, Fournié JJ, Bonneville M, Garboczi DN. Structure of a human gammadelta T-cell antigen receptor. *Nature* (2001) 411(6839):820–4. doi:10.1038/35081115
12. Kisielow J, Kopf M. The origin and fate of γδ T cell subsets. *Curr Opin Immunol* (2013) 25(2):181–8. doi:10.1016/j.coi.2013.03.002
13. Vantourout P, Hayday A. Six-of-the-best: unique contributions of γδ T cells to immunology. *Nat Rev Immunol* (2013) 13(2):88–100. doi:10.1038/nri3384
14. Willcox CR, Pitard V, Netzer S, Couzi L, Salim M, Silberzahn T, et al. Cytomegalovirus and tumor stress surveillance by binding of a human γδ T cell antigen receptor to endothelial protein C receptor. *Nat Immunol* (2012) 13(9):872–9. doi:10.1038/ni.2394
15. Spada FM, Grant EP, Peters PJ, Sugita M, Melián A, Leslie DS, et al. Self-recognition of CD1 by gamma/delta T cells: implications for innate immunity. *J Exp Med* (2000) 191(6):937–48. doi:10.1084/jem.191.6.937
16. Luoma AM, Castro CD, Mayassi T, Bembinster LA, Bai L, Picard D, et al. Crystal structure of Vδ1 T cell receptor in complex with CD1d-sulfatide shows MHC-like recognition of a self-lipid by human γδ T cells. *Immunity* (2013) 39(6):1032–42. doi:10.1016/j.immuni.2013.11.001
17. Shin S, El-Diwany R, Schaffert S, Adams EJ, Garcia KC, Pereira P, et al. Antigen recognition determinants of gammadelta T cell receptors. *Science* (2005) 308(5719):252–5. doi:10.1126/science.1106480
18. Adams EJ, Chien Y-H, Garcia KC. Structure of a gammadelta T cell receptor in complex with the nonclassical MHC T22. *Science* (2005) 308(5719):227–31. doi:10.1126/science.1106885
19. Scotet E, Martinez LO, Grant E, Barbaras R, Jenö P, Guiraud M, et al. Tumor recognition following Vgamma9vdelta2 T cell receptor interactions with a surface F1-ATPase-related structure and apolipoprotein A-I. *Immunity* (2005) 22(1):71–80. doi:10.1016/j.immuni.2004.11.012
20. Marlin R, Pappalardo A, Kaminski H, Willcox CR, Pitard V, Netzer S, et al. Sensing of cell stress by human γδ TCR-dependent recognition of annexin A2. *Proc Natl Acad Sci U S A* (2017) 114(12):3163–8. doi:10.1073/pnas.1621052114
21. Wesch D, Peters C, Oberg H-H, Pietschmann K, Kabelitz D. Modulation of γδ T cell responses by TLR ligands. *Cell Mol Life Sci* (2011) 68(14):2357–70. doi:10.1007/s00018-011-0699-1
22. Ribot JC, debarros A, Silva-Santos B. Searching for "signal 2": costimulation requirements of γδ T cells. *Cell Mol Life Sci* (2011) 68(14):2345–55. doi:10.1007/s00018-011-0698-2
23. Balbi B, Valle MT, Oddera S, Giunti D, Manca F, Rossi GA, et al. T-lymphocytes with gamma delta+ V delta 2+ antigen receptors are present in increased proportions in a fraction of patients with tuberculosis or with sarcoidosis. *Am Rev Respir Dis* (1993) 148(6 Pt 1):1685–90. doi:10.1164/ajrccm/148.6_Pt_1.1685
24. Morita CT, Mariuzza RA, Brenner MB. Antigen recognition by human gamma delta T cells: pattern recognition by the adaptive immune system. *Springer Semin Immunopathol* (2000) 22(3):191–217. doi:10.1007/s002810000042
25. Pfeffer K, Schoel B, Gulle H, Kaufmann SH, Wagner H. Primary responses of human T cells to mycobacteria: a frequent set of gamma/delta T cells are stimulated by protease-resistant ligands. *Eur J Immunol* (1990) 20(5):1175–9. doi:10.1002/eji.1830200534
26. Constant P, Davodeau F, Peyrat MA, Poquet Y, Puzo G, Bonneville M, et al. Stimulation of human gamma delta T cells by nonpeptidic mycobacterial ligands. *Science* (1994) 264(5156):267–70. doi:10.1126/science.8146660
27. Espinosa E, Belmant C, Pont F, Luciani B, Poupot R, Romagné F, et al. Chemical synthesis and biological activity of bromohydrin pyrophosphate, a potent stimulator of human gamma delta T cells. *J Biol Chem* (2001) 276(21):18337–44. doi:10.1074/jbc.M100495200
28. Zhang Y, Song Y, Yin F, Broderick E, Siegel K, Goddard A, et al. Structural studies of Vgamma2vdelta2 T cell phosphoantigens. *Chem Biol* (2006) 13(9):985–92. doi:10.1016/j.chembiol.2006.08.007

29. Tanaka Y, Morita CT, Tanaka Y, Nieves E, Brenner MB, Bloom BR. Natural and synthetic non-peptide antigens recognized by human gamma delta T cells. *Nature* (1995) 375(6527):155–8. doi:10.1038/375155a0
30. Rohmer M, Knani M, Simonin P, Sutter B, Sahm H. Isoprenoid biosynthesis in bacteria: a novel pathway for the early steps leading to isopentenyl diphosphate. *Biochem J* (1993) 295(Pt 2):517–24. doi:10.1042/bj2950517
31. Jomaa H, Feurle J, Lühs K, Kunzmann V, Tony HP, Herderich M, et al. Vgamma9/Vdelta2 T cell activation induced by bacterial low molecular mass compounds depends on the 1-deoxy-D-xylulose 5-phosphate pathway of isoprenoid biosynthesis. *FEMS Immunol Med Microbiol* (1999) 25(4):371–8. doi:10.1016/S0928-8244(99)00110-8
32. Belmant C, Espinosa E, Poupot R, Peyrat MA, Guiraud M, Poquet Y, et al. 3-Formyl-1-butyl pyrophosphate A novel mycobacterial metabolite-activating human gammadelta T cells. *J Biol Chem* (1999) 274(45):32079–84. doi:10.1074/jbc.274.45.32079
33. Eberl M, Altincicek B, Kollas A-K, Sanderbrand S, Bahr U, Reichenberg A, et al. Accumulation of a potent gammadelta T-cell stimulator after deletion of the lytB gene in *Escherichia coli*. *Immunology* (2002) 106(2):200–11. doi:10.1046/j.1365-2567.2002.01414.x
34. Gober H-J, Kistowska M, Angman L, Jenö P, Mori L, De Libero G. Human T cell receptor gammadelta cells recognize endogenous mevalonate metabolites in tumor cells. *J Exp Med* (2003) 197(2):163–8. doi:10.1084/jem.20021500
35. Asslan R, Pradines A, Pratx C, Allal C, Favre G, Le Gaillard F. Epidermal growth factor stimulates 3-hydroxy-3-methylglutaryl-coenzyme A reductase expression via the ErbB-2 pathway in human breast adenocarcinoma cells. *Biochem Biophys Res Commun* (1999) 260(3):699–706. doi:10.1006/bbrc.1999.0945
36. Kunzmann V, Bauer E, Wilhelm M. Gamma/delta T-cell stimulation by pamidronate. *N Engl J Med* (1999) 340(9):737–8. doi:10.1056/NEJM199903043400914
37. Wang H, Fang Z, Morita CT. Vgamma2vdelta2 T cell receptor recognition of prenyl pyrophosphates is dependent on all CDRs. *J Immunol* (2010) 184(11):6209–22. doi:10.4049/jimmunol.1000231
38. Harly C, Guillaume Y, Nedellec S, Peigné C-M, Mönkkönen H, Mönkkönen J, et al. Key implication of CD277/butyrophilin-3 (BTN3a) in cellular stress sensing by a major human γδ T-cell subset. *Blood* (2012) 120(11):2269–79. doi:10.1182/blood-2012-05-430470
39. Arnett HA, Escobar SS, Viney JL. Regulation of costimulation in the era of butyrophilins. *Cytokine* (2009) 46(3):370–5. doi:10.1016/j.cyto.2009.03.009
40. Rhodes DA, Reith W, Trowsdale J. Regulation of immunity by butyrophilins. *Annu Rev Immunol* (2016) 34:151–72. doi:10.1146/annurev-immunol-041015-055435
41. Schwartz JC, Zhang X, Fedorov AA, Nathenson SG, Almo SC. Structural basis for co-stimulation by the human CTLA-4/B7-2 complex. *Nature* (2001) 410(6828):604–8. doi:10.1038/35069112
42. Stamper CC, Zhang Y, Tobin JF, Erbe DV, Ikemizu S, Davis SJ, et al. Crystal structure of the B7-1/CTLA-4 complex that inhibits human immune responses. *Nature* (2001) 410(6828):608–11. doi:10.1038/35069118
43. D'Cruz AA, Babon JJ, Norton RS, Nicola NA, Nicholson SE. Structure and function of the SPRY/B30.2 domain proteins involved in innate immunity. *Protein Sci* (2013) 22(1):1–10. doi:10.1002/pro.2185
44. Rhodes DA, de Bono B, Trowsdale J. Relationship between SPRY and B30.2 protein domains. Evolution of a component of immune defence? *Immunology* (2005) 116(4):411–7. doi:10.1111/j.1365-2567.2005.02248.x
45. Abeler-Dörner L, Swamy M, Williams G, Hayday AC, Bas A. Butyrophilins: an emerging family of immune regulators. *Trends Immunol* (2012) 33(1):34–41. doi:10.1016/j.it.2011.09.007
46. Boyden LM, Lewis JM, Barbee SD, Bas A, Girardi M, Hayday AC, et al. Skint1, the prototype of a newly identified immunoglobulin superfamily gene cluster, positively selects epidermal gammadelta T cells. *Nat Genet* (2008) 40(5):656–62. doi:10.1038/ng.108
47. Seo M, Lee S-O, Kim J-H, Hong Y, Kim S, Kim Y, et al. MAP4-regulated dynein-dependent trafficking of BTN3a1 controls the TBK1-IRF3 signaling axis. *Proc Natl Acad Sci U S A* (2016) 113(50):14390–5. doi:10.1073/pnas.1615287113
48. Compte E, Pontarotti P, Collette Y, Lopez M, Olive D. Frontline: characterization of BT3 molecules belonging to the B7 family expressed on immune cells. *Eur J Immunol* (2004) 34(8):2089–99. doi:10.1002/eji.200425227
49. Palakodeti A, Sandstrom A, Sundaresan L, Harly C, Nedellec S, Olive D, et al. The molecular basis for modulation of human Vγ9vδ2 T cell responses by CD277/butyrophilin-3 (BTN3a)-specific antibodies. *J Biol Chem* (2012) 287(39):32780–90. doi:10.1074/jbc.M112.384354
50. Karunakaran MM, Göbel TW, Starick L, Walter L, Herrmann T. Vγ9 and Vδ2 T cell antigen receptor genes and butyrophilin 3 (BTN3) emerged with placental mammals and are concomitantly preserved in selected species like alpaca (*Vicugna pacos*). *Immunogenetics* (2014) 66(4):243–54. doi:10.1007/s00251-014-0763-8
51. Vavassori S, Kumar A, Wan GS, Ramanjaneyulu GS, Cavallari M, El Daker S, et al. Butyrophilin 3a1 binds phosphorylated antigens and stimulates human γδ T cells. *Nat Immunol* (2013) 14(9):908–16. doi:10.1038/ni.2665
52. Wang H, Henry O, Distefano MD, Wang Y-C, Räikkönen J, Mönkkönen J, et al. Butyrophilin 3a1 plays an essential role in prenyl pyrophosphate stimulation of human Vγ2vδ2 T cells. *J Immunol* (2013) 191(3):1029–42. doi:10.4049/jimmunol.1300658
53. Sandstrom A, Peigné C-M, Léger A, Crooks JE, Konczak F, Gesnel M-C, et al. The intracellular B30.2 domain of butyrophilin 3a1 binds phosphoantigens to mediate activation of human Vγ9vδ2 T cells. *Immunity* (2014) 40(4):490–500. doi:10.1016/j.immuni.2014.03.003
54. Wang H, Morita CT. Sensor function for butyrophilin 3a1 in prenyl pyrophosphate stimulation of human Vγ2vδ2 T cells. *J Immunol* (2015) 195(10):4583–94. doi:10.4049/jimmunol.1500314
55. Hsiao C-HC, Lin X, Barney RJ, Shippy RR, Li J, Vinogradova O, et al. Synthesis of a phosphoantigen prodrug that potently activates Vγ9δ2 T-lymphocytes. *Chem Biol* (2014) 21(8):945–54. doi:10.1016/j.chembiol.2014.06.006
56. Shippy RR, Lin X, Agabiti SS, Li J, Zangari BM, Foust BJ, et al. Phosphinophosphonates and their tris-pivaloyloxymethyl prodrugs reveal a negatively cooperative butyrophilin activation mechanism. *J Med Chem* (2017) 60(6):2373–82. doi:10.1021/acs.jmedchem.6b00965
57. Altincicek B, Moll J, Campos N, Foerster G, Beck E, Hoeffler JF, et al. Cutting edge: human gamma delta T cells are activated by intermediates of the 2-C-methyl-D-erythritol 4-phosphate pathway of isoprenoid biosynthesis. *J Immunol* (2001) 166(6):3655–8. doi:10.4049/jimmunol.166.6.3655
58. Gu S, Sachleben JR, Boughter CT, Nawrocka WI, Borowska MT, Tarrasch JT, et al. Phosphoantigen-induced conformational change of butyrophilin 3a1 (BTN3a1) and its implication on Vγ9vδ2 T cell activation. *Proc Natl Acad Sci U S A* (2017) 114(35):E7311–20. doi:10.1073/pnas.1707547114
59. Moulin M, Alguacil J, Gu S, Mehtougui A, Adams EJ, Peyrottes S, et al. Vγ9vδ2 T cell activation by strongly agonistic nucleotidic phosphoantigens. *Cell Mol Life Sci* (2017) 74(23):4353–67. doi:10.1007/s00018-017-2583-0
60. Salim M, Knowles TJ, Baker AT, Davey MS, Jeeves M, Sridhar P, et al. BTN3a1 discriminates γδ T cell phosphoantigens from nonantigenic small molecules via a conformational sensor in its B30.2 domain. *ACS Chem Biol* (2017) 12(10):2631–43. doi:10.1021/acschembio.7b00694
61. Castella B, Riganti C, Fiore F, Pantaleoni F, Canepari ME, Peola S, et al. Immune modulation by zoledronic acid in human myeloma: an advantageous cross-talk between Vγ9vδ2 T cells, αβ CD8+ T cells, regulatory T cells, and dendritic cells. *J Immunol* (2011) 187(4):1578–90. doi:10.4049/jimmunol.1002514
62. Castella B, Kopecka J, Sciancalepore P, Mandili G, Foglietta M, Mitro N, et al. The ATP-binding cassette transporter A1 regulates phosphoantigen release and Vγ9vδ2 T cell activation by dendritic cells. *Nat Commun* (2017) 8:15663. doi:10.1038/ncomms15663
63. Kovacs E, Das R, Wang Q, Collier TS, Cantor A, Huang Y, et al. Analysis of the role of the C-terminal tail in the regulation of the epidermal growth factor receptor. *Mol Cell Biol* (2015) 35(17):3083–102. doi:10.1128/MCB.00248-15
64. Peigné C-M, Léger A, Gesnel M-C, Konczak F, Olive D, Bonneville M, et al. The juxtamembrane domain of butyrophilin BTN3a1 controls phosphoantigen-mediated activation of human Vγ9vδ2 T cells. *J Immunol* (2017) 198(11):4228–34. doi:10.4049/jimmunol.1601910
65. Nguyen K, Li J, Puthenveetil R, Lin X, Poe MM, Hsiao C-HC, et al. The butyrophilin 3a1 intracellular domain undergoes a conformational change involving the juxtamembrane region. *FASEB J* (2017) 31(11):4697–706. doi:10.1096/fj.201601370RR
66. Barbee SD, Woodward MJ, Turchinovich G, Mention J-J, Lewis JM, Boyden LM, et al. Skint-1 is a highly specific, unique selecting component for epidermal T cells. *Proc Natl Acad Sci U S A* (2011) 108(8):3330–5. doi:10.1073/pnas.1010890108
67. Di Marco Barros R, Roberts NA, Dart RJ, Vantourout P, Jandke A, Nussbaumer O, et al. Epithelia use butyrophilin-like molecules to shape organ-specific γδ T cell compartments. *Cell* (2016) 167(1):203–18.e17. doi:10.1016/j.cell.2016.08.030

68. Morita CT, Jin C, Sarikonda G, Wang H. Nonpeptide antigens, presentation mechanisms, and immunological memory of human Vgamma2vdelta2 T cells: discriminating friend from foe through the recognition of prenyl pyrophosphate antigens. *Immunol Rev* (2007) 215:59–76. doi:10.1111/j.1600-065X.2006.00479.x
69. Riaño F, Karunakaran MM, Starick L, Li J, Scholz CJ, Kunzmann V, et al. Vγ9vδ2 TCR-activation by phosphorylated antigens requires butyrophilin 3 A1 (BTN3a1) and additional genes on human chromosome 6. *Eur J Immunol* (2014) 44(9):2571–6. doi:10.1002/eji.201444712
70. Sebestyen Z, Scheper W, Vyborova A, Gu S, Rychnavska Z, Schiffler M, et al. RhoB mediates phosphoantigen recognition by Vγ9vδ2â T cell receptor. *Cell Rep* (2016) 15(9):1973–85. doi:10.1016/j.celrep.2016.04.081
71. Vega FM, Ridley AJ. The RhoB small GTPase in physiology and disease. *Small GTPases* (2016):1–10. doi:10.1080/21541248.2016.1253528
72. Rhodes DA, Chen H-C, Price AJ, Keeble AH, Davey MS, James LC, et al. Activation of human γδ T cells by cytosolic interactions of BTN3a1 with soluble phosphoantigens and the cytoskeletal adaptor periplakin. *J Immunol* (2015) 194(5):2390–8. doi:10.4049/jimmunol.1401064
73. Starick L, Riano F, Karunakaran MM, Kunzmann V, Li J, Kreiss M, et al. Butyrophilin 3a (BTN3a, CD277)-specific antibody 20.1 differentially activates Vγ9vδ2 TCR clonotypes and interferes with phosphoantigen activation. *Eur J Immunol* (2017) 47(6):982–92. doi:10.1002/eji.201646818
74. Jeong J, Rao AU, Xu J, Ogg SL, Hathout Y, Fenselau C, et al. The PRY/SPRY/B30.2 domain of butyrophilin 1a1 (BTN1a1) binds to xanthine oxidoreductase: implications for the function of BTN1a1 in the mammary gland and other tissues. *J Biol Chem* (2009) 284(33):22444–56. doi:10.1074/jbc.M109.020446
75. Nepveu-Traversy M-E, Bérubé J, Berthoux L. TRIM5alpha and TRIMCyp form apparent hexamers and their multimeric state is not affected by exposure to restriction-sensitive viruses or by treatment with pharmacological inhibitors. *Retrovirology* (2009) 6:100. doi:10.1186/1742-4690-6-100
76. Gu S, Nawrocka W, Adams EJ. Sensing of pyrophosphate metabolites by Vγ9vδ2 T cells. *Front Immunol* (2014) 5:688. doi:10.3389/fimmu.2014.00688
77. Vantourout P, Laing A, Woodward MJ, Zlatareva I, Apolonia L, Jones AW, et al. Heteromeric interactions regulate butyrophilin (BTN) and BTN-like molecules governing γδ T cell biology. *Proc Natl Acad Sci U S A* (2018) 115(5):1039–44. doi:10.1073/pnas.1701237115

Conflict of Interest Statement: LB was employed by company Sanofi-Aventis R&D. All other authors declare no competing interests.

Copyright © 2018 Boutin and Scotet. This is an open-access article distributed under the terms of the Creative Commons Attribution License (CC BY). The use, distribution or reproduction in other forums is permitted, provided the original author(s) and the copyright owner are credited and that the original publication in this journal is cited, in accordance with accepted academic practice. No use, distribution or reproduction is permitted which does not comply with these terms.

frontiers in Immunology

REVIEW
published: 20 April 2018
doi: 10.3389/fimmu.2018.00796

The Emerging Complexity of γδT17 Cells

Duncan R. McKenzie[1†], Iain Comerford[1], Bruno Silva-Santos[2] and Shaun R. McColl[1]**

[1] Department of Molecular & Cellular Biology, University of Adelaide, Adelaide, SA, Australia, [2] Faculdade de Medicina, Instituto de Medicina Molecular, Universidade de Lisboa, Lisboa, Portugal

Preprogrammed IL-17-producing γδ T cells constitute a poorly understood class of lymphocytes that express rearranged antigen receptors but appear to make little use of them. γδT17 cells were first characterized as tissue-resident sentinels with innate effector function. However, ongoing research continues to reveal unexpected complexity to this unusual subset, including phenotypic plasticity, memory-like activity and unique migratory behavior. Despite these advances, at the core of γδT17 cell biology remain fundamental gaps in knowledge: Are γδT17 cells truly innate or has the importance of the T cell receptor been overlooked? How unique are they among IL-17-producing lymphocytes? How similar are these cells between mice and humans? We speculate that answering these unresolved questions is key to successful manipulation of γδ T cells in clinical settings.

Keywords: γδ T cells, IL-17, T cell receptor signaling, migration, plasticity, immunological memory, translation

OPEN ACCESS

Edited by:
Francisco Sanchez-Madrid, Universidad Autonoma de Madrid, Spain

Reviewed by:
Maria L. Toribio, Centro de Biología Molecular Severo Ochoa (CSIC), Spain
Vasileios Bekiaris, Technical University of Denmark, Denmark

****Correspondence:***
Bruno Silva-Santos
bssantos@medicina.ulisboa.pt;
Shaun R. McColl
shaun.mccoll@adelaide.edu.au

†Present address:
Duncan R. McKenzie, The Francis Crick Institute, London, United Kingdom

Specialty section:
This article was submitted to T Cell Biology, a section of the journal Frontiers in Immunology

Received: *12 February 2018*
Accepted: *03 April 2018*
Published: *20 April 2018*

Citation:
McKenzie DR, Comerford I, Silva-Santos B and McColl SR (2018) The Emerging Complexity of γδT17 Cells. Front. Immunol. 9:796. doi: 10.3389/fimmu.2018.00796

INTRODUCTION

Whereas conventional αβ T cells expressing diverse T cell receptors (TCRs) continuously patrol lymphoid tissues and extensively proliferate and differentiate to generate pathogen-tailored effector responses upon detection of cognate antigen, numerous innate-like lymphocyte subsets constitutively occupy barrier tissues and respond far more rapidly to tissue stress and infection. γδ T cells that produce interleukin 17 (IL-17, termed γδT17 or alternatively γδ17, Tγδ17) are one such population attracting increasing attention. Peripheral tissue localization coupled with preprogrammed effector function and a capacity for rapid antigen-independent activation enables γδT17 cells to respond within hours of infection. As such, γδ T cell-derived IL-17 is critical for control of pathogen load during the earliest stages of infection in a range of models. However, this innate-like response is not unique to γδT17 cells, as innate lymphoid cells (ILCs) and some invariant αβ T cell subsets also contribute to early production of Type 3 cytokines, which include IL-17, IL-22 and granulocyte-macrophage colony stimulating factor (GM-CSF). Thus, why these different lymphocyte subsets have co-evolved to fill the same protective niche remains unclear, although some of the features of γδT17 cells discussed throughout this review may highlight functions unique to these cells. Moreover, while γδT17 cells have been identified in humans, they exhibit some apparently fundamental differences from their murine counterparts that require further clarification before findings in mice may be exploited to understand human biology and ultimately influence clinical practice.

γδT17 cells express receptors for the innate-derived inflammatory cytokines IL-23 and IL-1β, enabling immediate activation *in situ* following detection of invading microbes by myeloid and stromal cells (1–3). The contribution of γδT17 cells to antimicrobial immunity is most predominant in tissues harboring high frequencies of these cells at homeostasis: lung, skin, liver, peritoneal cavity, and lymph nodes (LNs) (**Figure 1**). However, aberrant γδT17 cell activity promotes autoimmune inflammation in numerous murine models (4). Unlike protective scenarios, many of these

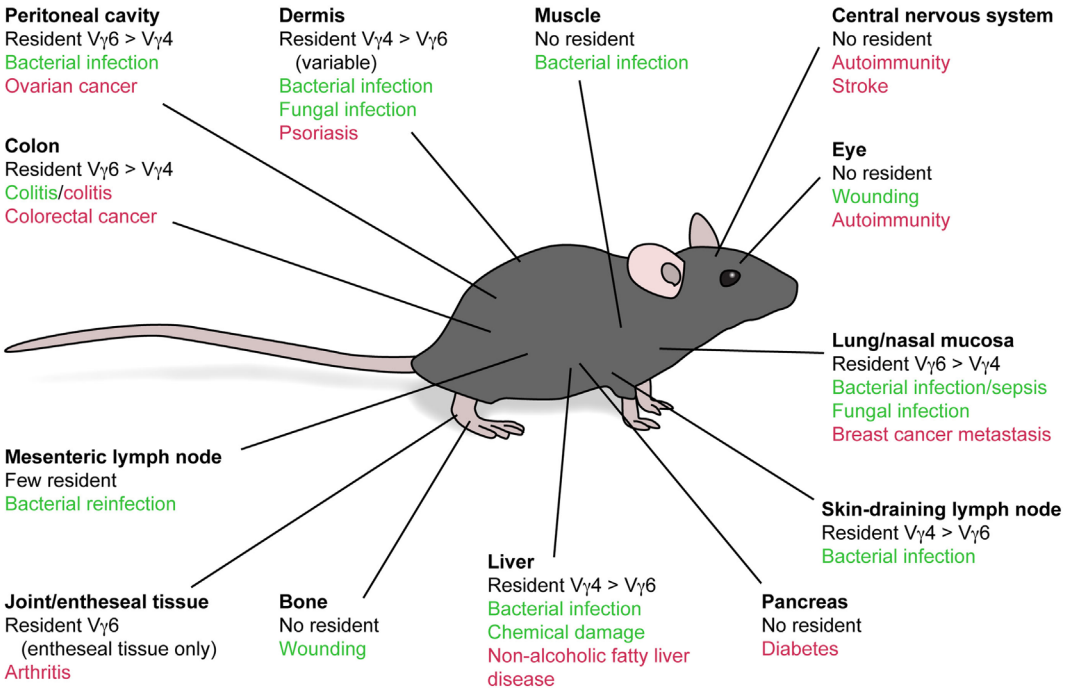

FIGURE 1 | Beneficial and detrimental functions of local and infiltrating γδT17 cells. Vγ4$^+$ and Vγ6$^+$ γδT17 cells distribute to numerous peripheral tissues following development, although with differential bias. These cells are implicated in beneficial (green) and detrimental (red) immune responses both in these tissues and those that do not evidently harbor a resident γδT17 cell population. This suggests that migratory behavior of γδT17 cells, particularly during autoimmune conditions, exerts a strong influence on the outcome of inflammation.

pathological responses involve target tissues that lack substantial local γδT17 cell populations, suggesting that γδT17 cells expand and subsequently home into autoimmune inflammatory foci. A key exception is psoriatic dermatitis, which manifests in the γδT17 cell-replete dermis. However, skin-resident γδT17 cells still appear to migrate between layers of the skin in this setting, and recent studies suggest a poorly understood interplay between local and infiltrating cells in the pathogenesis of skin inflammation (5, 6). γδT17 cell activity also promotes tumor growth in multiple murine models, which may arise from recruitment of myeloid cells and promotion of angiogenesis (7). The role of γδT17 cells in beneficial or detrimental immune responses has been extensively reviewed and will not be discussed further except where directly relevant (8).

γδT17 cells are further divided into two subsets as defined by the variable γ chain usage of their TCR. Those expressing the invariant Vγ6Vδ1 TCR strictly develop during embryogenesis and subsequently home to the dermis, lung, intestine, peritoneal cavity, and uterus (9). Alternatively, γδT17 cells expressing Vγ4 TCRs may develop in the adult thymus, are not invariant (although are fairly restricted) and represent only a fraction of the total Vγ4$^+$ γδ T cell pool (10, 11). Vγ4$^+$ γδT17 cells home to LNs, lung, liver, and the dermis alongside Vγ6$^+$ cells, although the ratio of these two subsets in the dermal γδT17 cell population is variable and may be microbiota dependent (10, 12, 13). The contribution of particular γδT17 cell subsets to defense against infection or pathogenic activity during cancer often reflects the local subset bias at the effector site. Why two populations with such similar effector function develop separately and inhabit different tissues remains an open question. It is possible that the more tissue-biased Vγ6$^+$ subset prioritizes immunosurveillance of barrier sites, while the lymphoid organ-skewed Vγ4$^+$ subset serves as a pool that is mobilized to distal sites during local and systemic challenges, although this remains to be formally demonstrated. Intriguingly, these two populations can respond to distinct stimuli even within the same location, as demonstrated by dermal Vγ4$^+$ and Vγ6$^+$ cells which selectively expand following skin colonization with *Corynebacterium accolens* and *Staphylococcus epidermidis*, respectively (14).

Understanding of γδT17 cell development and function is far from complete, as we know little about many key aspects of their basic biology that are well established in conventional T cells. For example, the function and specificity of the Vγ4 and Vγ6 TCRs remain undefined. It is still unknown whether ligand–TCR interactions are relevant to thymic selection or peripheral function of γδT17 cells, nor whether potential ligands are host-derived or foreign. Understanding how and when the TCR functions in γδT17 cell biology should clarify whether these cells occupy a niche closer to ILCs or invariant αβ T cells in terms of fundamental biology and may shed light on the recent descriptions of memory-like γδT17 cell responses during infection and chronic inflammation (6, 15). Moreover, elucidation of the previously unappreciated plasticity and migratory dynamics of γδT17 cells is underway but remains incompletely

defined (16, 17). Here, we review the current state of knowledge in these emerging concepts, in the form of the key questions that should be answered to progress knowledge of γδT17 cells toward clinical application.

WHAT IS THE ROLE OF TCR SIGNALING IN γδT17 CELL DEVELOPMENT?

While recent work has somewhat clarified the role of TCR signaling in γδT17 ontogeny, whether true ligand-driven selection, akin to that experienced by αβ T cells, occurs during their thymic development remains unclear. A number of transcription factors, cytokine signals, and surface receptor interactions are essential for γδT17 cell development and have been reviewed recently elsewhere (18). However, it is worth reiterating that γδT17 cell ontogeny requires RORγt and TGF-β, two factors also crucial to *de novo* polarization of Th17 cells from naïve αβ T cells, suggesting that the induction of the Type 3 program in these cell types is fundamentally conserved despite occurring under different conditions, in different sites and with some divergent signal requirements (19, 20).

Shifting Views on Instructive TCR Signaling in γδT17 Cell Development

Early studies suggested that γδT17 cells do not receive antigen-driven TCR signals development, as TCR engagement promotes alternate fates. Initially, the Chien laboratory proposed that TCR activation in the thymus drives γδ T cells toward the interferon (IFN)-γ program (γδT1) at the expense of the γδT17 pathway (21). This conclusion derived from the observation that unlike γδT1 cells, peripheral γδT17 cells lack surface CD122 expression, a marker previously associated with antigen recognition by αβ thymocytes (22). Further support for this concept arose from studies of dendritic epidermal T cells (DETCs). Mice with a loss-of-function mutation in *Skint1*, a butyrophilin-like transmembrane protein, lack prototypic Vγ5Vδ1$^+$ DETCs as their precursors fail to mature in the embryonic thymus (23). However, the immature DETC precursors in these mice exhibit an abnormal γδT17 phenotype rather than the wild-type IFN-γ/IL-13 program (24). This may suggest that the IL-17 fate is the default program of γδ T cells, which is normally avoided by instructive signals such as Skint1. However, as it remains unknown whether Skint1 is a Vγ5Vδ1 TCR ligand, this does not demonstrate that TCR signaling *per se* instructs developing γδ T cells away from the IL-17 fate, nor whether this concept applies to naturally developing γδT17 cells.

More recently, the concept that γδT17 cells do not experience TCR engagement in the thymus has been challenged by three key studies of mice with genetic deficiencies in this pathway. First, there is a striking lack of Vγ4$^+$ and Vγ6$^+$ γδT17 cells in mice with reduced TCR signal strength due to a hypomorphic mutation in the TCR signaling intermediate Zap70 (25). Second, mice haploinsufficient for TCR signaling components CD3γ and CD3δ have reduced numbers of Vγ6$^+$ but not Vγ4$^+$ γδT17 cells (26). Third, mice deficient in Syk, a kinase classically associated with B cell receptor signaling, and downstream PI3 kinase, lack all γδT17 cells. Strangely, Zap70-deficient mice here showed a deficit only in Vγ6$^+$ γδT17 cells, whereas both Vγ4$^+$ and Vγ6$^+$ cells were affected in the hypomorphic mutant (27). A solid explanation for the differential effects of these mutations upon Vγ4$^+$ γδT17 cells is lacking. However, it has been posited that developing αβ T cells undergo stronger TCR signaling during the fetal period, which may suggest that fetal-derived Vγ6$^+$ cells require higher threshold signaling than their adult Vγ4$^+$ counterparts (28). Alterations in the Vγ6$^+$ to Vγ4$^+$ γδT17 cell ratio are also observed in mice with mutations affecting cortical thymic epithelial cell function (29, 30).

Further dissection of the specific nature of TCR signaling during γδT17 cell development has stemmed from more detailed understanding of surface marker expression during this process. Coffey and colleagues identified surface CD73 as a selective marker of TCR–ligand experienced γδ T cells by interrogating KN6 γδ-TCR transgenic thymocytes, which recognize known ligands T10 and T22 (31). As the majority of γδT17 cells in the wild-type adult thymus are CD73$^+$, this suggested that TCR–ligand interaction naturally occurs during their ontogeny. Furthermore, this study showed that KN6 transgenic γδT17 cells do not develop in the absence of T10 and T22 (31). Subsequently, fetal γδ thymocytes lacking CD24, CD44, and CD45RB expression were identified as the common precursor of both CD44$^+$ γδT17-committed cells and CD45RB$^+$ γδT1-committed cells. However, antibody-mediated TCR crosslinking drives these precursors selectively to the IFN-γ program, inhibiting γδT17 cell development (32). This report may therefore explain the apparently contradictory results from earlier studies by clarifying that γδT17 cells receive "weaker" TCR signals than other subsets. Together, these studies provide clear evidence that TCR engagement of a certain nature is required for γδT17 cell development. It is likely that the discrete signaling pathways engaged by different modes of TCR activation are crucial for the successful programming of γδT17 cell effector function, although this requires further investigation.

TCR-Independent Facets of γδT17 Cell Development

Further dissection of γδT17 cell development has revealed that a requirement for TCR signaling may only exist for certain elements of this process. While most developing γδT17 cells express the antigen-experience marker CD73 in adulthood (31), this is not the case during early life. Anderson and colleagues recently determined that the majority of both Vγ4$^+$ and Vγ6$^+$ γδT17 cells developing during the fetal and perinatal period progress directly from a CD24$^+$ immature to CD24$^-$ mature phenotype without ever inducing CD73 (33). These CD73$^-$ γδT17 cells are completely dependent upon the transcription factor HEB for induction of γδT17 cell lineage-specifying factors *Sox4*, *Sox13*, and *Rorc*. Mature CD73$^-$ γδT17 cells are also detectable in peripheral tissue, although the majority of tissue γδT17 cells remain CD73$^+$ (33). Although direct analysis of TCR signaling was not undertaken, this report suggests that while most postnatally derived Vγ4$^+$ γδT17 cells experience thymic antigen, γδT17 cells developing during the fetal period do not. It will be important to reconcile conclusions from CD73 studies with mice deficient in TCR signaling intermediates to clarify whether particular subpopulations of

γδT17 cells show distinct requirements for TCR signals during development.

Taken together, the evidence outlined so far suggests that the emergence of mature γδT17 cells from the thymus is largely TCR dependent. An important but distinct question is whether induction of IL-17 effector function in normally developing γδ T cells is explicitly dependent upon TCR engagement. IL-17 expression in the fetal thymus coincides with *Tcrd* locus opening and rearrangement, before the expression of a functional TCR in T cell-committed progenitors (34). Moreover, the expression of key γδT17 lineage-specifying transcription factors in developing Vγ4$^+$ cells is largely unaffected by deficiency of ITK, a protein crucial for γδ-TCR signal transduction (35). These reports thus far indicate that the IL-17 effector program arises before, and therefore independently of, expression of the γδ-TCR. In context of the prior discussion, this suggests that any role for TCR signaling in γδT17 cell development is subsequent to the IL-17 fate decision, instead promoting ensuing survival, proliferation, and/or further maturation.

Importantly, the most mechanistic studies to date identify a role for TCR signaling but not necessarily ligand encounter during γδT17 cell thymic development. As solid information regarding the ligand(s) of the Vγ4 and Vγ6 γδT17 TCRs is lacking, it is difficult to distinguish TCR signals driven by ligation of physiological antigen from TCR assembly driven signals, which have been reported (36). Therefore, the identification of γδ-TCR ligands remains critical for understanding thymic selection, preprogramming, and antigen specificity in the context of peripheral responses.

DO MATURE γδT17 CELLS USE THEIR TCR?

Whether TCR signaling fulfils an important physiological function in mature murine γδT17 cells is unclear, a critical question to answer given the more obvious function of human γδ-TCRs. Murine γδT17 cells can be activated solely by innate-derived cytokines, predominantly IL-23 and IL-1β, but also IL-7 and IL-18 (2, 37, 38). This is reminiscent of Th17 cells, which can also be activated independently of TCR stimulation by IL-23 and IL-1β once polarized (39). This observation is consistent with the programmed "effector memory"-like phenotype of γδT17 cells. However, as TCR signaling is patently implicated in Th17 effector function, it also hints that the TCR may modulate γδT17 cell activity when combined with innate signals.

Evidence for TCR Signaling in Preprogrammed γδT17 Cell Responses

While not essential, it is clear that crosslinking of the TCR by anti-CD3 or pan anti-γδ-TCR antibodies does activate γδT17 cells. *In vitro* TCR stimulation alone is sufficient to induce IL-17 secretion by γδ T cells, and TCR signals enhance the amount of IL-17 produced in response to innate cytokines (21, 40–42). In addition, TCR crosslinking enhances IL-7-driven proliferation of γδT17 cells and promotes their efficient *in vitro* expansion (17, 38). *In vivo*, administration of anti-Vγ4 antibodies exacerbates experimental autoimmune encephalomyelitis (EAE) symptoms as it activates pathogenic Vγ4$^+$ γδT17 cells rather than depleting them (43). However, while suggestive, these data do not prove a physiological function for TCR signaling in γδT17 cell responses. Several studies (discussed below) have utilized the Nur77-GFP reporter mouse, commonly used to measure αβ-TCR signal strength, to determine whether TCR signaling underpins γδT17 memory-like responses. However, *in vitro* stimulation with IL-23 and IL-1β alone also induces some level of reporter expression (6), and so additional methods are required to investigate whether physiological Vγ4$^+$ or Vγ6$^+$ TCR signaling occurs during γδT17 cell responses *in vivo*. Inducible deletion of the γδ-TCR in mature, fluorescently labeled γδ T cells would help to address this important question.

A key clarification is that the threshold required for activation of downstream TCR signaling is significantly greater in γδT17 cells than other lymphoid γδ T cell subsets. CD27$^+$ γδ T cells, which are biased toward IFN-γ production and are predominantly found in lymphoid organs, undergo a conventional αβ T cell-like response to TCR crosslinking, showing rapid Ca^{2+} flux and phosphorylation of Erk. By contrast, very little response to this stimulation is observed in γδT17 cells, and a substantially higher concentration of crosslinking antibody is required to induce Nur77-GFP expression (25). A similar hyporesponsive TCR is documented for DETCs and a subset of innate-like γδT1 cells. Considering that tonic TCR engagement is observed in DETCs (44), it is possible that a higher signaling threshold is needed to ensure that they are only activated upon upregulation or relocalization of cognate self-antigen during tissue stress. This in itself is merely speculative, so whether the higher TCR threshold in γδT17 cells reflects the nature of their putative antigen(s) is unknown.

A recent study reported that γδT17 cells appear to directly recognize microbiota-derived lipids presented by the non-classical MHC molecule CD1d (45). The maintenance of peritoneal cavity and gut-associated γδT17 cells is dependent upon the microbiome, as they are diminished in mice treated with antibiotics or raised in germ-free conditions (46). Tian and colleagues extended these findings to hepatic γδT17 cells, which are similarly depleted upon antibiotic treatment (45). Moreover, hepatic γδT17 cells are deficient in *Cd1d*$^{-/-}$ mice, independent of microbiota composition. CD1d is well known to present microbial-derived lipids to NKT cells expressing an invariant αβ-TCR, although it has also been crystallized presenting lipid to a human Vδ1$^+$ TCR (47, 48). Murine hepatic, but not splenic, γδT17 cells bind CD1d tetramers loaded with various bacterial lipids, and when purified are activated *in vitro* by hepatocytes in a CD1d-dependent manner (45). While no biochemical data have yet been reported to confirm presentation of lipids directly to murine γδT17 TCRs, it will be of great importance to pursue this intriguing possibility as it is not only a strong lead in the hunt for γδ-TCR ligands but may be immediately relevant to human γδ T cells.

Induction of γδT17 Effector Function in Peripheral γδ T Cells

While the general consensus is that γδT17 cell function is preprogrammed, some notable studies have documented inducible γδT17 cells that develop from naïve precursors following antigen

engagement. These instances are intriguing because they more closely reflect the human system, where γδT17 cell effector phenotype can be induced from "naïve" precursors upon TCR stimulation and exposure to appropriate cytokines (49, 50). Chien and colleagues reported populations of murine γδ T cells specific for phycoerythrin (PE) and haptens cyanine 3 and 4-hydroxy-3-nitrophenylacetyl, which induce key γδT17 genes including *Il17a*, *Il17f*, *Rorc*, and *Ccr6* following antigen-specific immunization (41, 51). Moreover, immunization with PE drives upregulation of *Il23r* and *Il1r1* in PE-specific γδ T cells, suggesting that IL-23 and IL-1β may boost antigen-driven IL-17 production in these cells. These studies were also notable in that they identified the first genuine γδT17 TCR ligands, unequivocally demonstrated by surface plasmon resonance. However, the natural frequency of PE- and hapten-specific γδ T cells is on the order of 0.1% of splenic γδ T cells, which more closely reflects clonal frequencies of naïve conventional antigen-specific αβ T cells than the highly restricted TCR diversity observed in "natural" γδT17 cells. How these rare "inducible" γδT17 cell clones, which express diverse Vγ1 and Vγ4 TCRs, relate to the 100-fold more abundant invariant and semi-invariant Vγ6$^+$ and Vγ4$^+$ γδT17 cells is unclear.

Conversely, two recent complementary reports identified inducible γδT17 cells on a larger scale. Both used radiation bone marrow chimeras to reveal *de novo* differentiation of γδT17 cells from precursors in the periphery, as thymus-derived "natural" γδT17 cells do not arise from adult bone marrow progenitors in many laboratories. First, induced γδT17 cells were identified during EAE following bone marrow reconstitution of *Tcrd*$^{-/-}$ hosts (42). These were dependent upon IL-23 signaling alone, which is somewhat unexpected given the requirement of naïve αβ T cells to first experience IL-6 to upregulate the IL-23 receptor during Th17 polarization (52). Second, IL23R$^+$ γδT17 cells developed from peripheral IL23R$^-$ γδ T cells during imiquimod (IMQ)-induced psoriasis (53). In this case, both IL-23 and IL-1β signals were essential. Notably, the former report determined that while TCR stimulation was not essential for induction of γδT17 cells *in vitro*, it did synergize with cytokine signals to promote their development. The latter report utilized TCR stimulation throughout, thus it is unclear whether it is essential in that case. It will be important to determine the broader contribution of inducible γδT17 cells to murine pathophysiology, given their more immediate relevance to humans as discussed below.

ARE γδT17 CELLS CAPABLE OF MEMORY RESPONSES?

Conventional memory responses involve the persistence of a quiescent population of antigen-specific effector T or B cells following resolution of infection, which rapidly expand during antigenic rechallenge and efficiently control reinfection. Therefore, a central tenet of classical memory is antigen specificity. However, as discussed earlier, γδT17 cell antigens are unknown and may even be irrelevant to their biology. Thus, it is fascinating that reports continue to emerge of enhanced γδT17 cell frequency and activity upon secondary rechallenge in bacterial infection. In addition, memory-like γδT17 cell responses are observed during psoriatic dermatitis models, where there is no immunizing antigen (although stress-induced self-antigens would be abundant).

A "memory" response involving γδT17 cells was first documented in the mesenteric LNs of mice previously infected with oral *Listeria monocytogenes*. Here, Vγ6$^+$ cells remained at elevated frequencies following primary infection and proliferated rapidly when specifically rechallenged with the same pathogen only *via* the same route (15). This "memory" response was later shown to be dependent on IL-17-driven formation of γδT17 and myeloid cell clusters around *L. monocytogenes* replication foci (54). As purported antibody-mediated internalization of the γδ-TCR inhibited this recall Vγ6$^+$ γδT17 cell response *in vivo*, it was suggested that memory-like γδT17 cells are reactivated in a TCR-dependent manner (15). However, more definitive demonstration of a TCR-specific response is lacking in this scenario.

This memory-like behavior has subsequently been observed in other bacterial infections. First, Vγ6$^+$ γδT17-dependent "memory" responses against *Staphylococcus aureus* rechallenge were identified in the peritoneal cavity, and transfer of peritoneal γδ T cells from previously challenged mice led to reduced bacterial load in newly challenged recipients. Here, activation of Vγ6$^+$ "memory" cells *in vitro* by coculture with infected macrophages is not inhibited by blockade of IL-23 or IL-1β signaling, indirectly suggesting that the TCR may be involved (55). Most recently, expanded lung Vγ4$^+$ γδT17 cells were shown to proliferate more rapidly upon rechallenge with *Bordetella pertussis*, and these memory-like cells, when purified, respond to heat-killed *B. pertussis in vitro* (56). These examples demonstrate that both Vγ4$^+$ and Vγ6$^+$ γδT17 cells can remain in target tissues at higher frequency following resolution of infection, and therefore expand more rapidly to control pathogen colonization upon rechallenge. However, whether this represents *bona fide* TCR-dependent, antigen-specific memory or instead to corresponds to memory-like behavior observed in natural killer (NK) or myeloid cells remains to be established (57, 58).

γδT17 cell memory-like responses have also been observed during IMQ-induced psoriasis, where activated Vγ4Vδ4$^+$ cells redistribute to distal uninflamed skin, thus driving enhanced pathology upon subsequent challenge of previously unaffected skin (5, 6). Both studies reporting this phenomenon demonstrated induction of Nur77, a marker of early TCR signaling, specifically within the "memory" population upon rechallenge. However, Nur77 is also induced by IL-23 and IL-1β signaling alone *in vitro*, suggesting that these results should be cautiously interpreted. Regardless, the selective response of γδT17 cells bearing a specific γδ-TCR chain pairing, given that Vγ4 may pair with multiple δ chains, does hint at a TCR-selective response. Memory-like skin Vγ4$^+$ γδT17 cells also show elevated IL-1R1 expression, suggesting that in this scenario, heightened sensitivity to cytokine stimulation may contribute to the recall behavior (6). This experimental system also uncovered novel γδT17 trafficking dynamics which will be discussed below.

From current evidence, it is clear that γδT17 cells can respond with heightened kinetics upon repeated inflammatory challenge or infection. These responses profoundly influence the outcome of inflammation, be it worsening psoriatic dermatitis or enhancing bacterial clearance. Determining whether these phenomena are

examples of true immunological memory will require comprehensive demonstration of a TCR- and antigen-dependent response. If this is in fact the case, it will be an excellent opportunity to elucidate the antigens recognized by γδT17 TCRs. They are likely to be either self-stress signals and/or conserved bacterial products, given the broad reactivity of Vγ6$^+$ cells bearing invariant receptors. Alternatively, these memory-like responses may more resemble trained immunity, the memory-like behavior observed in NK cells, myeloid cells, and most recently epithelial stem cells, due to epigenetic changes facilitating more powerful activation upon re-exposure to inflammatory stimuli (57–59). Further research into this area will be of great use to the field.

WHEN AND HOW DO γδT17 CELLS EXHIBIT PLASTICITY?

While generally "rigid" in effector function, some reports of plasticity have emerged suggesting that γδT17 cell responses can be fine tuned over the course of inflammation. Their αβ counterparts, CD4$^+$ Th17 cells, display marked phenotypic plasticity during *in vivo* responses. Although IFN-γ is the defining effector cytokine produced by Th1 cells, Th17 cells are induced to co-express IFN-γ and IL-17 by signals such as IL-12 and IL-23 (60, 61). Furthermore, by generating a mouse capable of permanently marking cells that had transcribed the *Il17a* locus at some point in their history, Stockinger and colleagues discovered that the majority of central nervous system-infiltrating, IFN-γ-producing CD4$^+$ T cells during EAE were formerly Th17 cells that had subsequently extinguished IL-17 production (62). IFN-γ production by Th17 cells is dependent upon transcription factors T-bet, Runx1, and Runx3 (62, 63). Notably, Th17 cells do not lose IL-17 nor gain IFN-γ expression during cutaneous fungal infection, suggesting that a particular inflammatory milieu dictates the plasticity of Th17 cells. Analysis of γδ T cells alongside Th17 cells in EAE and fungal infection revealed negligible plasticity in either setting (62).

These findings cemented the view that γδT17 cells are fixed in phenotype until several studies began to describe IFN-γ$^+$IL-17$^+$ γδ T cells in select scenarios. First, Vγ6$^+$ "memory" γδT17 cells in oral *L. monocytogenes* rechallenge were shown to co-produce IFN-γ, alongside induction of the classically Type 1-associated chemokine receptor CXCR3 (15, 54). Subsequently, a large proportion of late-stage tumor-infiltrating Vγ6$^+$ γδT17 cells in a peritoneal model of ovarian cancer were also identified to produce IFN-γ (16). These reports of *in vivo* plasticity of γδT17 cells support *in vitro* evidence of IFN-γ production by γδT17 cells when stimulated with IL-23 and IL-1β (40). As both described examples hitherto feature Vγ6$^+$ γδT17 cells, whether this subset is more plastic than Vγ4$^+$ γδT17 cells is unclear. It is important to clarify at this point that while plasticity of γδT17 cells in the above scenarios is clear, γδT17 cells do not produce IFN-γ in the majority of settings investigated, suggesting that this behavior is tightly regulated.

Insight into the potential for γδT17 cells to induce a Type 1 phenotype arose from comparative genome-wide epigenetic analysis of CD27$^+$ (γδT1-enriched) and CD27$^-$ (γδT17-enriched) γδ T cells (16). As anticipated, γδT1 cells exhibit permissive H3K4 dimethylation marks upon characteristic genes *Ifng*, *Tbx21*, and *Eomes* and repressive H3K4 trimethylation on γδT17 lineage genes *Rorc*, *Il17a*, *Il17f*, and *Il22*. However, γδT17 cells display permissive marks not only on γδT17 lineage genes as expected but also on *Ifng* and *Tbx21*. These data indicate that γδT17 cells are epigenetically "primed" to induce γδT1 factors, but not *vice versa*. It will be insightful to elucidate the stimuli responsible for inducing T-bet expression and IFN-γ production in γδT17 cells, as this may influence their protective and/or pathogenic behavior akin to Th17 cells. While IL-23 and IL-1β stimulation promotes IFN-γ secretion by γδT17 cells in some reports, additional signals are likely required, as these two cytokines direct γδT17 cell activity during *in vivo* settings both with and without evidence of plasticity. Moreover, while IL-12 promotes IFN-γ expression by Th17 cells, γδT17 cells do not express its receptor and do not respond in this manner (61, 64). While the upstream signals are somewhat unclear, it is now evident that γδT17 cell plasticity is restricted by post-transcriptional mechanisms. Specifically, γδT17 cells were recently found to selectively express high levels of microRNA miR-146, which targets Nod1 to suppress IFN-γ production (65). Considerable co-expression of IL-17A and IFN-γ is evident from *in vitro* polarized human γδT17 cells (49, 50), therefore understanding the mechanism and relevance of γδT17 cell plasticity is another worthy pursuit in the path to therapeutic manipulation of human γδ T cells.

HOW AND WHY DO γδT17 CELLS ESTABLISH THEIR MIGRATION PATTERNS?

γδT17 cells may be considered innate-like cousins of tissue-resident memory T cells as they similarly inhabit barrier tissues in a poised state, primed to initiate inflammation upon microbial (re)invasion. However, even the earliest studies implied that γδT17 cells are distinct in their ability to traffic to distant sites. Indeed, several key murine autoimmune models in which γδT17 cells are implicated involve their migration to and infiltration of target sites that do not harbor resident populations (**Figure 1**). Moreover, new evidence suggests that γδT17 cells adopt an unusual hybrid homeostatic migration pattern that spans true tissue residency and free naïve αβ T cell recirculation.

γδT17 cells are selectively enriched in skin-draining lymph nodes (sLNs) but are also detected in circulation. Cyster and colleagues first hinted at constitutive γδT17 cell trafficking by detecting dermis-derived Vγ4$^+$ T cells in sLNs in under homeostatic conditions, using Kaede photoconvertible reporter mice (66). Subsequently, sphingosine-1-phosphate antagonism demonstrated that the circulating γδT17 cell population is LN-derived (67). This loop is completed by recruitment of blood-borne γδT17 cells back into the dermis by constitutively expressed chemokine receptor CCR6, probably in concert with cutaneous lymphocyte antigen (CLA) (6, 10, 17). Whether CCR6 directs γδT17 cells to other uninflamed barrier tissues is unclear, although their frequency is unaltered in the lung and liver of *Ccr6*$^{-/-}$ mice (17). CCR6 also positions Vγ4$^+$ cells in the LN subcapsular sinus and is critical for their response to lymph-borne *S. aureus* (68). However, recent parabiosis experiments have demonstrated that while

γδT17 cells indeed move between sLNs, blood, and dermis, their trafficking is fairly restricted compared with αβ T cells (68, 69). This limited motility appears to be imposed by LN macrophages, whose blebs are acquired by γδT17 cells at steady state (70).

γδT17 cells constitutively express a range of homing receptors which enable their rapid recruitment to sites of inflammation (**Table 1**). In particular, CCR2, a receptor predominantly associated with mononuclear phagocyte migration, drives γδT17 cell infiltration of numerous inflamed tissues and is crucial for their protection against *S. pneumoniae* infection (6, 17, 71). Whereas most unambiguous descriptions of γδT17 cell trafficking during inflammation involve sites lacking a resident population, findings in *S. pneumoniae* infection and psoriasitic dermatitis models suggest that blood-borne γδT17 cells also infiltrate tissues already hosting local γδT17 cells. Intriguingly, dermal Vγ4$^+$ γδT17 cells migrate from inflamed skin to draining LNs during IMQ psoriasis, proliferate, and then migrate both to the original inflamed tissue and to distal uninflamed skin (5, 6). As discussed earlier, this memory-like behavior appears to be based upon increases in tissue γδT17 cell frequency, indicating that migratory characteristics define the influence of γδT17 cells on the outcome of inflammation. While γδT17 cell redistribution to unaffected skin predisposes that area to more severe inflammation, the influence of LN-expanded γδT17 cell homing back to already inflamed skin is unclear, as retention of these cells in LNs by sphingosine-1-phosphate antagonism does not affect the progression of skin inflammation (72).

Unlike conventional T cell responses, which involve induction of inflammatory homing receptors during time-consuming expansion and polarization of effector cells, γδT17 cells constitutively express both homeostatic and inflammatory chemokine receptors. Unusually, they do not express the typical homeostatic receptor CCR7, and so most likely can only enter LNs from afferent lymph rather than directly from circulation (81). Instead γδT17 cells express CCR6, which is an unusual receptor as it directs recruitment of lymphocytes and myeloid cells both to homeostatic sites and inflamed tissues (82). It is important to clarify that the "homeostatic" sites where the sole CCR6 ligand CCL20 is expressed may not necessarily be uninflamed in the technical sense, as these mucocutaneous tissues are constantly exposed to environmental and microbial stress. Nevertheless, in multiple inflammatory scenarios, γδT17 cells downregulate CCR6 expression rapidly upon activation. This loss of CCR6 is beneficial for homing during inflammation as it prevents recruitment to uninflamed skin and thereby concentrates their homing toward inflamed tissues (17). However, CCR6 is implicated in the recruitment of γδT17 cells to inflammatory lesions in several scenarios, such as psoriasis, liver inflammation, and corneal damage, suggesting that modulation of its expression is context specific (76–78). Although CCR6 has been suggested to influence γδT17 cell migration during skin inflammation (**Table 1**), activated γδT17 cells either emigrating from inflamed dermis during psoriasis or migrating into inflamed epidermis during a transgenic model of oncogenesis have lost CCR6 expression (66, 83). It will be useful to reconcile these results given the expression of CCR6 by human skin-infiltrating γδ T cells, as discussed below. By contrast, memory-like Vγ6$^+$ γδT17 cells in oral *L. monocytogenes* infection upregulate CXCR3 expression (54), which may be linked to their plasticity toward the IFN-γ program rather than an intrinsic property of chronically activated γδT17 cells.

Despite advances in elucidating when and how γδT17 cells migrate, we still lack a solid understanding of why they establish such patterns. Dermal γδT17 cells are intrinsically motile, which

TABLE 1 | Homing receptors involved in murine γδT17 cell migration.

Homing receptor *Ligands*	Tissue	Setting	Evidence	Reference
CCR2 *CCL2, CCL7, CCL12*	Skin	IMQ psoriasis	*Ccr2*$^{-/-}$ cell transfer	(6)
	Joints	*Il1rn*$^{-/-}$ arthritis	CCL2 neutralization	(71)
	CNS	EAE	*Ccr2*$^{-/-}$ cell transfer	(17)
	Tumor	B16 melanoma	*Ccr2*$^{-/-}$ cell transfer	(17)
		KEP breast cancer	CCL2 neutralization	(73)
	Nasal mucosa	*S. pneumoniae*	*Ccr2*$^{-/-}$ cell transfer	(17)
CCR6 *CCL20*	Skin	Homeostasis	*Ccr6*$^{-/-}$ cell transfer	(10)
			Ccr6$^{-/-}$ cell transfer	(17)
		IL-23 psoriasis	*Ccr6*$^{-/-}$ mice, CCL20 neutralization	(74)
		IMQ psoriasis	*Ccr6*$^{-/-}$ mice	(75)
			CCR6 antagonist, *Ccr6*$^{-/-}$ mice	(76)
	Cornea	Corneal abrasion	CCL20 neutralization	(77)
	Liver	CCl_4, methionine–choline-deficient fibrosis	*Ccr6*$^{-/-}$ mice	(78)
	Brain	Stroke	*Ccr6*$^{-/-}$ mice	(79)
CCR9 *CCL25*	Lung	OVA challenge	CCL25 neutralization	(80)
CXCR3 *CXCL9, CXCL10, CXCL11*	mLN	*Listeria monocytogenes* rechallenge	CXCR3 neutralization	(54)
$S1P_1$ *S1P*	Blood	Homeostasis	$S1P_1$ antagonist	(67)
	Skin (*via* blood)	IMQ psoriasis	$S1P_1$ antagonist	(6, 67)
	CNS (*via* blood)	EAE	$S1P_1$ antagonist	(67)
$\alpha_4\beta_7$ *MadCAM-1, VCAM-1*	Lung	OVA challenge	$\alpha_4\beta_7$ neutralization	(80)

IMQ, imiquimod; CNS, central nervous system; EAE, experimental autoimmune encephalomyelitis; IL-23, interleukin 23; OVA, ovalbumin; mLN, mesenteric lymph node.

may facilitate their surveillance of the skin (84). The purpose of draining to sLNs *via* afferent lymphatics, entering circulation, and returning to skin is less clear. It is not obvious that γδT17 cells need to scan LNs for antigen, especially considering their highly restricted TCRs. Instead, this process may serve to constantly redistribute γδT17 cells to other skin sites or maintain a constant peripheral blood pool that could act as an immediate reservoir of effector cells when inflammation arises. During tissue inflammation, γδT17 cells proliferate in draining LNs and home toward the inflammatory foci (85). While largely observed in autoimmune scenarios where the target tissue lacks resident γδT17 cells, there is evidence that this process also occurs during psoriatic dermatitis and *S. pneumonia* infection of nasal mucosa (6, 17). Thus, local γδT17 cells may initiate inflammation, stimulating proliferation of LN γδT17 cells which then home to the target site in a second wave of innate-like IL-17 production. This working model (**Figure 2**) should be tested in additional pathophysiological settings, as again it is reminiscent of the human system where expansion of circulating γδT17 cells is documented during inflammation.

CAN WE TRANSLATE OUR KNOWLEDGE OF γδT17 CELLS FROM MICE TO HUMANS?

The relevance of extensive research into murine tissue-resident γδT17 cells may be questioned by their conspicuous absence in many human tissues. Moreover, key features of γδT17 cell biology in mice appear to clash with their rare human counterparts. While murine γδT17 cells gain their effector function in the thymus and can be subsequently activated independently of the TCR (2), human thymic γδ T cells are immature and γδT17 cells are presumably polarized from "naïve" peripheral blood precursors when provided with antigen, costimulatory, and inflammatory signals (49, 50, 86). These induced γδT17 cells express CCR6, RORγt, and receptors for IL-23 and IL-1β like their murine counterparts, as well as CD161, an NK receptor shared with human Th17 cells (50, 87). Human γδT17 cells do not appear to show the highly restricted TCR expression found in mice, as both those expressing typical peripheral blood Vγ9Vδ2 TCRs and tissue-biased Vδ1 TCRs (with varied and undefined γ chain pairing) have been identified in patient samples (50, 88). Accumulating evidence suggests that human γδT17 cells may perform similar functions to those in mice, including host defense and exacerbation of autoimmunity and cancer. In addition, some of the emerging concepts discussed earlier suggest that γδT17 cells may not be as different between species as initially thought (**Figure 3**).

Whereas mouse γδT17 cells comprise the majority of γδ T cells found in certain tissues (such as dermis, peritoneal cavity, and lung), γδ T cells in humans are largely IFN-γ producing and/or cytotoxic in function (7). However, γδT17 cells have been observed in some pathological scenarios that echo the mouse system. Human γδT17 cells have been identified in the cerebrospinal fluid of multiple sclerosis patients, and infiltrating

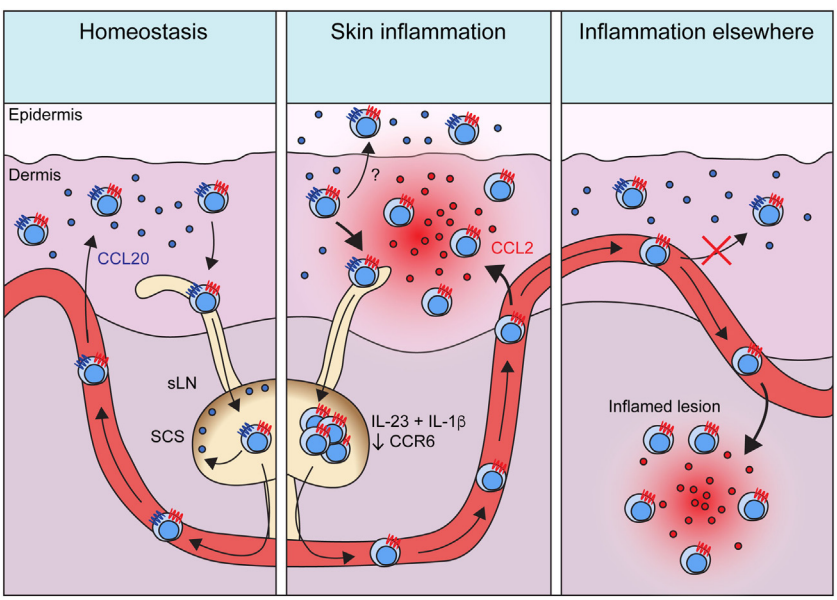

FIGURE 2 | Migratory dynamics of γδT17 cells. Under homeostasis, γδT17 cells largely reside in barrier tissues such as the dermis, but also drain slowly into sLNs and are detectable in the blood. Circulating γδT17 cells return to the skin using CCR6 which directs them toward CCL20 expressed in the dermis. CCR6 also positions γδT17 cells in the sLN SCS to scan for invading microbes. During skin inflammation, γδT17 cell trafficking from the dermis to sLNs is increased. γδT17 cells undergo proliferation driven by IL-23 and IL-1β in sLNs, where they lose CCR6 expression. Activated and expanded γδT17 cells then home *via* the blood to inflamed skin using CCR2, which senses ligands such as CCL2 induced during inflammation. CCR6 probably recruits γδT17 cells into the epidermis during skin inflammation, but how its expression is maintained in this scenario is unknown. During inflammation in other peripheral organs, γδT17 cells similarly proliferate in LNs *via* IL-23 and IL-1β and become CCR6^{-}. They then traffic *via* circulation to infiltrate the inflamed site *via* CCR2. Loss of CCR6 expression is required for optimal γδT17 cell recruitment to such inflammatory sites, as it prevents activated γδT17 cells from instead homing to unaffected dermis. Abbreviations: sLN, skin-draining lymph node; SCS, subcapsular sinus.

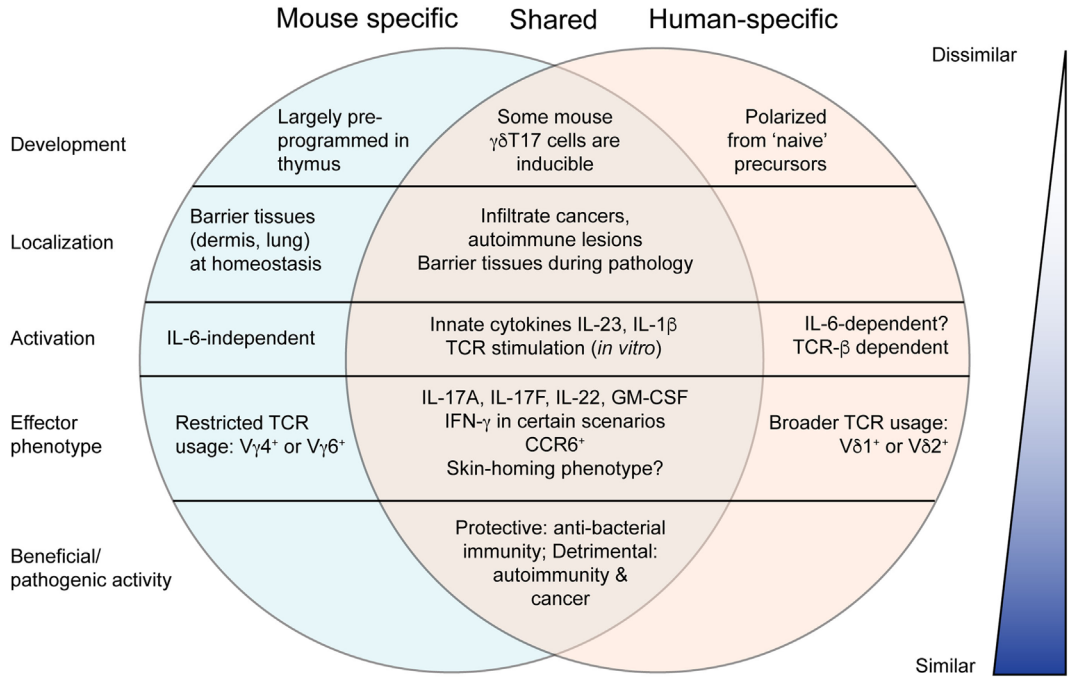

FIGURE 3 | Comparison of murine and human γδT17 cells. Murine γδT17 cells are preprogrammed, tissue-localized innate-like sentinels that respond to innate cytokines. Human γδT17 cells are very rare and develop from naïve precursors upon T cell receptor (TCR) stimulation. However, there are many similarities between mouse and human as outlined. Most notably, mouse and human γδT17 cells are beneficial or pathogenic in highly similar scenarios, suggesting that knowledge from mice may be useful to promote antibacterial immunity or treat autoimmunity and cancer in humans. Moreover, further research to clarify emerging concepts discussed in this review may reveal greater similarity.

colorectal and gallbladder cancer, similar to mouse γδT17 cells in EAE and cancer models (88–90). Human γδT17 cells have also been identified in lesional psoriasis skin, although not in healthy tissue (91). Circulating γδT17 cells are rare in healthy individuals but are present in bacterial meningitis patients and disappear upon successful treatment (50). Moreover, they are elevated in the peripheral blood of patients with active tuberculosis or HIV (92, 93). Thus, while γδT17 cells are particularly rare in healthy humans, it is likely that they will prove relevant in wider infectious and pathological settings upon further investigation.

It is also possible that the equivalent population of mouse γδT17 cells in humans is not necessarily defined by IL-17 production. After all, many alternative traits identify mouse γδT17 cells, such as expression of specific homing molecules, activation markers and other subset-specific surface markers, participation in particular immune responses and specific tissue localization. It is important to consider that immune cell populations are generally named in reference to an effector molecule or function relevant at the time of their discovery, and not necessarily that most critical to their function which may become evident in light of further research. For example, Th17 cells were named after their production of IL-17, although in the context of autoimmunity, this nomenclature may be misleading as it is their production of GM-CSF that may contribute more to their pathological function (94, 95). With this in mind, consider that IL-17-producing γδ T cells are scarce in healthy human skin or blood. However, a significant proportion of circulating γδ T cells in healthy individuals expresses skin-homing molecules such as CLA, CCR4, CCR6, and CCR10 (96). Moreover, it is these cells that home to psoriatic skin, and in doing so decrease in blood frequency. Therefore, are these CCR6$^+$ γδ T cells equivalent to mouse γδT17 cells? Further investigation is clearly warranted, perhaps first by performing comparative transcriptomic analyses.

A non-mutually exclusive alternate explanation for the discrepancy between mouse and human γδT17 cells is that Type 3 innate lymphoid cells (ILC3s) in humans have evolved to fill the niche occupied by γδT17 cells in mice. Already in the mouse there is substantial overlap in the functions of ILC3s and γδT17 cells: both are tissue-localized, innate-like responders to bacterial infection with preprogrammed IL-17- and IL-22-secreting effector function (97, 98). Apart from a slight differential bias in specific tissue responses, such as the preferential involvement of ILC3s in intestinal protection or γδT17 cells in skin infection, it is possible that the only basic features distinguishing the functional niche of these populations are the emerging concepts discussed throughout this review. Without a thorough understanding of γδT17 cell TCR responses, memory, migratory behavior, and functional plasticity, it is unclear why γδT17 cells and ILC3s have co-evolved in the mouse. In humans, where the TCR plays a more obvious role in γδT17 cell biology, it is conceivable that ILC3s have evolved to occupy the entire innate(-like) IL-17 effector niche. Perhaps it is most pertinent to further investigate inducible murine γδT17 cells, as these appear to more closely reflect their human counterparts. Given the dearth of information

BOX 1 | Research priorities in γδT17 cell biology.

1. Defining, if any, the *in vivo* antigens recognized by mouse/human γδT17 cells
2. Determining the relative influence of T cell receptor vs. inflammatory cytokine signaling in γδT17 (patho)physiological responses, in mouse and human
3. Establishing whether γδT17 cells are resident in normal human tissues. If so, do they develop from naïve precursors upon inflammation or are they preprogrammed?
4. Clarifying the extent of interplay between tissue-localized and circulating γδT17 cells
5. Assessing whether γδT17 cells are capable of mounting *bona fide* memory responses to pathogens
6. Investigating the extent of γδT17 cell plasticity and how it influences immunity

about human γδT17 cells, whether the emerging themes of mouse γδT17 cell biology outlined here could be exploited for therapeutic benefit will require a more focused effort to extend findings in mice to humans (**Box 1**).

CONCLUDING REMARKS

The γδT17 cell subset, discovered just over 10 years ago, is proving more and more complex and intriguing every year. This review has given an overview of the key emerging concepts that may improve our understanding of how γδT17 cells fit into the grand scheme of tissue immunity. Thus, by considering the latest trends in immune–microbiota interactions, immunometabolism, and single cell transcriptomics, we may soon clarify where γδT17 cells sit on the innate/adaptive spectrum. This will likely explain why they constitute a major source of IL-17 at particular stages of multiple experiment models of disease, and their non-redundant roles in relation to ILC3s and Th17 cells. Finally, we strongly believe that our improved knowledge of murine γδT17 cells will carry across to their human counterparts, and thus be exploited for clinical benefit.

AUTHOR CONTRIBUTIONS

DM conceptualized the review, wrote the manuscript, and prepared figures. BS-S, IC, and SM conceptualized the review, provided essential discussion, and edited the manuscript.

FUNDING

This work was supported by grant 1066871 from the National Health and Medical Research Council of Australia to IC and SM and European Research Council CoG_646701 to BS-S.

REFERENCES

1. Shibata K, Yamada H, Hara H, Kishihara K, Yoshikai Y. Resident Vdelta1+ gammadelta T cells control early infiltration of neutrophils after *Escherichia coli* infection via IL-17 production. *J Immunol* (2007) 178(7):4466–72. doi:10.4049/jimmunol.178.7.4466
2. Sutton CE, Lalor SJ, Sweeney CM, Brereton CF, Lavelle EC, Mills KH. Interleukin-1 and IL-23 induce innate IL-17 production from gammadelta T cells, amplifying Th17 responses and autoimmunity. *Immunity* (2009) 31(2):331–41. doi:10.1016/j.immuni.2009.08.001
3. Kashem SW, Riedl MS, Yao C, Honda CN, Vulchanova L, Kaplan DH. Nociceptive sensory fibers drive interleukin-23 production from CD301b+ dermal dendritic cells and drive protective cutaneous immunity. *Immunity* (2015) 43(3):515–26. doi:10.1016/j.immuni.2015.08.016
4. Papotto PH, Reinhardt A, Prinz I, Silva-Santos B. Innately versatile: gammadelta17 T cells in inflammatory and autoimmune diseases. *J Autoimmun* (2017) 87:26–37. doi:10.1016/j.jaut.2017.11.006
5. Hartwig T, Pantelyushin S, Croxford AL, Kulig P, Becher B. Dermal IL-17-producing gammadelta T cells establish long-lived memory in the skin. *Eur J Immunol* (2015) 45(11):3022–33. doi:10.1002/eji.201545883
6. Ramirez-Valle F, Gray EE, Cyster JG. Inflammation induces dermal Vgamma4+ gammadeltaT17 memory-like cells that travel to distant skin and accelerate secondary IL-17-driven responses. *Proc Natl Acad Sci USA* (2015) 112(26):8046–51. doi:10.1073/pnas.1508990112
7. Silva-Santos B, Serre K, Norell H. gammadelta T cells in cancer. *Nat Rev Immunol* (2015) 15(11):683–91. doi:10.1038/nri3904
8. Papotto PH, Ribot JC, Silva-Santos B. IL-17+ gammadelta T cells as kick-starters of inflammation. *Nat Immunol* (2017) 18(6):604–11. doi:10.1038/ni.3726
9. Shibata K, Yamada H, Nakamura R, Sun X, Itsumi M, Yoshikai Y. Identification of CD25+ gamma delta T cells as fetal thymus-derived naturally occurring IL-17 producers. *J Immunol* (2008) 181(9):5940–7. doi:10.4049/jimmunol.181.9.5940
10. Cai Y, Xue F, Fleming C, Yang J, Ding C, Ma Y, et al. Differential developmental requirement and peripheral regulation for dermal Vgamma4 and Vgamma6T17 cells in health and inflammation. *Nat Commun* (2014) 5:3986. doi:10.1038/ncomms4986
11. Kashani E, Fohse L, Raha S, Sandrock I, Oberdorfer L, Koenecke C, et al. A clonotypic Vgamma4Jgamma1/Vdelta5Ddelta2Jdelta1 innate gammadelta T-cell population restricted to the CCR6(+)CD27(-) subset. *Nat Commun* (2015) 6:6477. doi:10.1038/ncomms7477
12. Naik S, Bouladoux N, Wilhelm C, Molloy MJ, Salcedo R, Kastenmuller W, et al. Compartmentalized control of skin immunity by resident commensals. *Science* (2012) 337(6098):1115–9. doi:10.1126/science.1225152
13. Wei YL, Han A, Glanville J, Fang F, Zuniga LA, Lee JS, et al. A highly focused antigen receptor repertoire characterizes gammadelta T cells that are poised to make IL-17 rapidly in naive animals. *Front Immunol* (2015) 6:118. doi:10.3389/fimmu.2015.00118
14. Ridaura VK, Bouladoux N, Claesen J, Chen YE, Byrd AL, Constantinides MG, et al. Contextual control of skin immunity and inflammation by *Corynebacterium*. *J Exp Med* (2018) 215(3):785–99. doi:10.1084/jem.20171079
15. Sheridan BS, Romagnoli PA, Pham QM, Fu HH, Alonzo F III, Schubert WD, et al. gammadelta T cells exhibit multifunctional and protective memory in intestinal tissues. *Immunity* (2013) 39(1):184–95. doi:10.1016/j.immuni.2013.06.015
16. Schmolka N, Serre K, Grosso AR, Rei M, Pennington DJ, Gomes AQ, et al. Epigenetic and transcriptional signatures of stable versus plastic differentiation of proinflammatory gammadelta T cell subsets. *Nat Immunol* (2013) 14(10):1093–100. doi:10.1038/ni.2702
17. McKenzie DR, Kara EE, Bastow CR, Tyllis TS, Fenix KA, Gregor CE, et al. IL-17-producing gammadelta T cells switch migratory patterns between resting and activated states. *Nat Commun* (2017) 8:15632. doi:10.1038/ncomms15632
18. Munoz-Ruiz M, Sumaria N, Pennington DJ, Silva-Santos B. Thymic determinants of gammadelta T cell differentiation. *Trends Immunol* (2017) 38(5):336–44. doi:10.1016/j.it.2017.01.007
19. Do JS, Fink PJ, Li L, Spolski R, Robinson J, Leonard WJ, et al. Cutting edge: spontaneous development of IL-17-producing gamma delta T cells in the thymus occurs via a TGF-beta 1-dependent mechanism. *J Immunol* (2010) 184(4):1675–9. doi:10.4049/jimmunol.0903539
20. Shibata K, Yamada H, Sato T, Dejima T, Nakamura M, Ikawa T, et al. Notch-Hes1 pathway is required for the development of IL-17-producing gammadelta T cells. *Blood* (2011) 118(3):586–93. doi:10.1182/blood-2011-02-334995

21. Jensen KD, Su X, Shin S, Li L, Youssef S, Yamasaki S, et al. Thymic selection determines gammadelta T cell effector fate: antigen-naive cells make interleukin-17 and antigen-experienced cells make interferon gamma. *Immunity* (2008) 29(1):90–100. doi:10.1016/j.immuni.2008.04.022
22. Hanke T, Mitnacht R, Boyd R, Hunig T. Induction of interleukin 2 receptor beta chain expression by self-recognition in the thymus. *J Exp Med* (1994) 180(5):1629–36. doi:10.1084/jem.180.5.1629
23. Lewis JM, Girardi M, Roberts SJ, Barbee SD, Hayday AC, Tigelaar RE. Selection of the cutaneous intraepithelial gammadelta+ T cell repertoire by a thymic stromal determinant. *Nat Immunol* (2006) 7(8):843–50. doi:10.1038/ni1363
24. Turchinovich G, Hayday AC. Skint-1 identifies a common molecular mechanism for the development of interferon-gamma-secreting versus interleukin-17-secreting gammadelta T cells. *Immunity* (2011) 35(1):59–68. doi:10.1016/j.immuni.2011.04.018
25. Wencker M, Turchinovich G, Di Marco Barros R, Deban L, Jandke A, Cope A, et al. Innate-like T cells straddle innate and adaptive immunity by altering antigen-receptor responsiveness. *Nat Immunol* (2014) 15(1):80–7. doi:10.1038/ni.2773
26. Munoz-Ruiz M, Ribot JC, Grosso AR, Goncalves-Sousa N, Pamplona A, Pennington DJ, et al. TCR signal strength controls thymic differentiation of discrete proinflammatory gammadelta T cell subsets. *Nat Immunol* (2016) 17(6):721–7. doi:10.1038/ni.3424
27. Buus TB, Odum N, Geisler C, Lauritsen JPH. Three distinct developmental pathways for adaptive and two IFN-gamma-producing gammadelta T subsets in adult thymus. *Nat Commun* (2017) 8(1):1911. doi:10.1038/s41467-017-01963-w
28. Dong M, Artusa P, Kelly SA, Fournier M, Baldwin TA, Mandl JN, et al. Alterations in the thymic selection threshold skew the self-reactivity of the TCR repertoire in neonates. *J Immunol* (2017) 199(3):965–73. doi:10.4049/jimmunol.1602137
29. Nitta T, Muro R, Shimizu Y, Nitta S, Oda H, Ohte Y, et al. The thymic cortical epithelium determines the TCR repertoire of IL-17-producing gammadeltaT cells. *EMBO Rep* (2015) 16(5):638–53. doi:10.15252/embr.201540096
30. Wang HX, Shin J, Wang S, Gorentla B, Lin X, Gao J, et al. mTORC1 in thymic epithelial cells is critical for thymopoiesis, T-cell generation, and temporal control of gammadeltaT17 development and TCRgamma/delta recombination. *PLoS Biol* (2016) 14(2):e1002370. doi:10.1371/journal.pbio.1002370
31. Coffey F, Lee SY, Buus TB, Lauritsen JP, Wong GW, Joachims ML, et al. The TCR ligand-inducible expression of CD73 marks gammadelta lineage commitment and a metastable intermediate in effector specification. *J Exp Med* (2014) 211(2):329–43. doi:10.1084/jem.20131540
32. Sumaria N, Grandjean CL, Silva-Santos B, Pennington DJ. Strong TCR-gammadelta signaling prohibits thymic development of IL-17A-secreting gammadelta T cells. *Cell Rep* (2017) 19(12):2469–76. doi:10.1016/j.celrep.2017.05.071
33. In TSH, Trotman-Grant A, Fahl S, Chen ELY, Zarin P, Moore AJ, et al. HEB is required for the specification of fetal IL-17-producing gammadelta T cells. *Nat Commun* (2017) 8(1):2004. doi:10.1038/s41467-017-02225-5
34. Haas JD, Ravens S, Duber S, Sandrock I, Oberdorfer L, Kashani E, et al. Development of interleukin-17-producing gammadelta T cells is restricted to a functional embryonic wave. *Immunity* (2012) 37(1):48–59. doi:10.1016/j.immuni.2012.06.003
35. Malhotra N, Narayan K, Cho OH, Sylvia KE, Yin C, Melichar H, et al. A network of high-mobility group box transcription factors programs innate interleukin-17 production. *Immunity* (2013) 38(4):681–93. doi:10.1016/j.immuni.2013.01.010
36. Mahtani-Patching J, Neves JF, Pang DJ, Stoenchev KV, Aguirre-Blanco AM, Silva-Santos B, et al. PreTCR and TCRgammadelta signal initiation in thymocyte progenitors does not require domains implicated in receptor oligomerization. *Sci Signal* (2011) 4(182):ra47. doi:10.1126/scisignal.2001765
37. Lalor SJ, Dungan LS, Sutton CE, Basdeo SA, Fletcher JM, Mills KH. Caspase-1-processed cytokines IL-1beta and IL-18 promote IL-17 production by gammadelta and CD4 T cells that mediate autoimmunity. *J Immunol* (2011) 186(10):5738–48. doi:10.4049/jimmunol.1003597
38. Michel ML, Pang DJ, Haque SF, Potocnik AJ, Pennington DJ, Hayday AC. Interleukin 7 (IL-7) selectively promotes mouse and human IL-17-producing gammadelta cells. *Proc Natl Acad Sci U S A* (2012) 109(43):17549–54. doi:10.1073/pnas.1204327109
39. Guo L, Wei G, Zhu J, Liao W, Leonard WJ, Zhao K, et al. IL-1 family members and STAT activators induce cytokine production by Th2, Th17, and Th1 cells. *Proc Natl Acad Sci U S A* (2009) 106(32):13463–8. doi:10.1073/pnas.0906988106
40. Ribot JC, deBarros A, Pang DJ, Neves JF, Peperzak V, Roberts SJ, et al. CD27 is a thymic determinant of the balance between interferon-gamma- and interleukin 17-producing gammadelta T cell subsets. *Nat Immunol* (2009) 10(4):427–36. doi:10.1038/ni.1717
41. Zeng X, Wei YL, Huang J, Newell EW, Yu H, Kidd BA, et al. gammadelta T cells recognize a microbial encoded B cell antigen to initiate a rapid antigen-specific interleukin-17 response. *Immunity* (2012) 37(3):524–34. doi:10.1016/j.immuni.2012.06.011
42. Papotto PH, Goncalves-Sousa N, Schmolka N, Iseppon A, Mensurado S, Stockinger B, et al. IL-23 drives differentiation of peripheral gammadelta17 T cells from adult bone marrow-derived precursors. *EMBO Rep* (2017) 18(11):1957–67. doi:10.15252/embr.201744200
43. Blink SE, Caldis MW, Goings GE, Harp CT, Malissen B, Prinz I, et al. gammadelta T cell subsets play opposing roles in regulating experimental autoimmune encephalomyelitis. *Cell Immunol* (2014) 290(1):39–51. doi:10.1016/j.cellimm.2014.04.013
44. Chodaczek G, Papanna V, Zal MA, Zal T. Body-barrier surveillance by epidermal gammadelta TCRs. *Nat Immunol* (2012) 13(3):272–82. doi:10.1038/ni.2240
45. Li F, Hao X, Chen Y, Bai L, Gao X, Lian Z, et al. The microbiota maintain homeostasis of liver-resident gammadeltaT-17 cells in a lipid antigen/CD1d-dependent manner. *Nat Commun* (2017) 7:13839. doi:10.1038/ncomms13839
46. Duan J, Chung H, Troy E, Kasper DL. Microbial colonization drives expansion of IL-1 receptor 1-expressing and IL-17-producing gamma/delta T cells. *Cell Host Microbe* (2010) 7(2):140–50. doi:10.1016/j.chom.2010.01.005
47. Luoma AM, Castro CD, Mayassi T, Bembinster LA, Bai L, Picard D, et al. Crystal structure of Vdelta1 T cell receptor in complex with CD1d-sulfatide shows MHC-like recognition of a self-lipid by human gammadelta T cells. *Immunity* (2013) 39(6):1032–42. doi:10.1016/j.immuni.2013.11.001
48. Uldrich AP, Le Nours J, Pellicci DG, Gherardin NA, McPherson KG, Lim RT, et al. CD1d-lipid antigen recognition by the gammadelta TCR. *Nat Immunol* (2013) 14(11):1137–45. doi:10.1038/ni.2713
49. Ness-Schwickerath KJ, Jin C, Morita CT. Cytokine requirements for the differentiation and expansion of IL-17A- and IL-22-producing human Vgamma2Vdelta2 T cells. *J Immunol* (2010) 184(12):7268–80. doi:10.4049/jimmunol.1000600
50. Caccamo N, La Mendola C, Orlando V, Meraviglia S, Todaro M, Stassi G, et al. Differentiation, phenotype, and function of interleukin-17-producing human Vgamma9Vdelta2 T cells. *Blood* (2011) 118(1):129–38. doi:10.1182/blood-2011-01-331298
51. Zeng X, Meyer C, Huang J, Newell EW, Kidd BA, Wei YL, et al. Gamma delta T cells recognize haptens and mount a hapten-specific response. *Elife* (2014) 3:e03609. doi:10.7554/eLife.03609
52. Ghoreschi K, Laurence A, Yang XP, Tato CM, McGeachy MJ, Konkel JE, et al. Generation of pathogenic T(H)17 cells in the absence of TGF-beta signalling. *Nature* (2010) 467(7318):967–71. doi:10.1038/nature09447
53. Muschaweckh A, Petermann F, Korn T. IL-1beta and IL-23 promote extrathymic commitment of CD27+CD122- gammadeltaT17 cells. *J Immunol* (2017) 199(8):2668–79. doi:10.4049/jimmunol.1700287
54. Romagnoli PA, Sheridan BS, Pham QM, Lefrancois L, Khanna KM. IL-17A-producing resident memory gammadelta T cells orchestrate the innate immune response to secondary oral *Listeria monocytogenes* infection. *Proc Natl Acad Sci U S A* (2016) 113(30):8502–7. doi:10.1073/pnas.1600713113
55. Murphy AG, O'Keeffe KM, Lalor SJ, Maher BM, Mills KH, McLoughlin RM. *Staphylococcus aureus* infection of mice expands a population of memory gammadelta T cells that are protective against subsequent infection. *J Immunol* (2014) 192(8):3697–708. doi:10.4049/jimmunol.1303420
56. Misiak A, Wilk MM, Raverdeau M, Mills KH. IL-17-producing innate and pathogen-specific tissue resident memory gammadelta T cells expand in the lungs of bordetella pertussis-infected mice. *J Immunol* (2017) 198(1):363–74. doi:10.4049/jimmunol.1601024

57. Cerwenka A, Lanier LL. Natural killer cell memory in infection, inflammation and cancer. *Nat Rev Immunol* (2016) 16(2):112–23. doi:10.1038/nri.2015.9
58. Netea MG, Joosten LA, Latz E, Mills KH, Natoli G, Stunnenberg HG, et al. Trained immunity: a program of innate immune memory in health and disease. *Science* (2016) 352(6284):aaf1098. doi:10.1126/science.aaf1098
59. Naik S, Larsen SB, Gomez NC, Alaverdyan K, Sendoel A, Yuan S, et al. Inflammatory memory sensitizes skin epithelial stem cells to tissue damage. *Nature* (2017) 550(7677):475–80. doi:10.1038/nature24271
60. McGeachy MJ, Chen Y, Tato CM, Laurence A, Joyce-Shaikh B, Blumenschein WM, et al. The interleukin 23 receptor is essential for the terminal differentiation of interleukin 17-producing effector T helper cells in vivo. *Nat Immunol* (2009) 10(3):314–24. doi:10.1038/ni.1698
61. Mukasa R, Balasubramani A, Lee YK, Whitley SK, Weaver BT, Shibata Y, et al. Epigenetic instability of cytokine and transcription factor gene loci underlies plasticity of the T helper 17 cell lineage. *Immunity* (2010) 32(5):616–27. doi:10.1016/j.immuni.2010.04.016
62. Hirota K, Duarte JH, Veldhoen M, Hornsby E, Li Y, Cua DJ, et al. Fate mapping of IL-17-producing T cells in inflammatory responses. *Nat Immunol* (2011) 12(3):255–63. doi:10.1038/ni.1993
63. Wang Y, Godec J, Ben-Aissa K, Cui K, Zhao K, Pucsek AB, et al. The transcription factors T-bet and Runx are required for the ontogeny of pathogenic interferon-gamma-producing T helper 17 cells. *Immunity* (2014) 40(3): 355–66. doi:10.1016/j.immuni.2014.01.002
64. Kulig P, Musiol S, Freiberger SN, Schreiner B, Gyulveszi G, Russo G, et al. IL-12 protects from psoriasiform skin inflammation. *Nat Commun* (2016) 7:13466. doi:10.1038/ncomms13466
65. Schmolka N, Papotto PH, Romero PV, Amado T, Enguita FJ, Amorim A, et al. MicroRNA-146a controls functional plasticity in gamma-delta T cells by targeting Nod1. *Sci Immunol* (in press).
66. Gray EE, Ramirez-Valle F, Xu Y, Wu S, Wu Z, Karjalainen KE, et al. Deficiency in IL-17-committed Vgamma4(+) gammadelta T cells in a spontaneous Sox13-mutant CD45.1(+) congenic mouse substrain provides protection from dermatitis. *Nat Immunol* (2013) 14(6):584–92. doi:10.1038/ni.2585
67. Maeda Y, Seki N, Kataoka H, Takemoto K, Utsumi H, Fukunari A, et al. IL-17-producing Vgamma4+ gammadelta T cells require sphingosine 1-phosphate receptor 1 for their egress from the lymph nodes under homeostatic and inflammatory conditions. *J Immunol* (2015) 195(4):1408–16. doi:10.4049/jimmunol.1500599
68. Zhang Y, Roth TL, Gray EE, Chen H, Rodda LB, Liang Y, et al. Migratory and adhesive cues controlling innate-like lymphocyte surveillance of the pathogen-exposed surface of the lymph node. *Elife* (2016) 5:e18156. doi:10.7554/eLife.18156
69. Jiang X, Park CO, Geddes Sweeney J, Yoo MJ, Gaide O, Kupper TS. Dermal gammadelta T cells do not freely re-circulate out of skin and produce IL-17 to promote neutrophil infiltration during primary contact hypersensitivity. *PLoS One* (2017) 12(1):e0169397. doi:10.1371/journal.pone.0169397
70. Audemard-Verger A, Riviere M, Durand A, Peranzoni E, Guichard V, Hamon P, et al. Macrophages induce long-term trapping of gammadelta T cells with innate-like properties within secondary lymphoid organs in the steady state. *J Immunol* (2017) 199(6):1998–2007. doi:10.4049/jimmunol.1700430
71. Akitsu A, Ishigame H, Kakuta S, Chung SH, Ikeda S, Shimizu K, et al. IL-1 receptor antagonist-deficient mice develop autoimmune arthritis due to intrinsic activation of IL-17-producing CCR2(+)Vgamma6(+)gammadelta T cells. *Nat Commun* (2015) 6:7464. doi:10.1038/ncomms8464
72. Riol-Blanco L, Ordovas-Montanes J, Perro M, Naval E, Thiriot A, Alvarez D, et al. Nociceptive sensory neurons drive interleukin-23-mediated psoriasiform skin inflammation. *Nature* (2014) 510(7503):157–61. doi:10.1038/nature13199
73. Kersten K, Coffelt SB, Hoogstraat M, Verstegen NJM, Vrijland K, Ciampricotti M, et al. Mammary tumor-derived CCL2 enhances pro-metastatic systemic inflammation through upregulation of IL1beta in tumor-associated macrophages. *Oncoimmunology* (2017) 6(8):e1334744. doi:10.1080/2162402X.2017.1334744
74. Mabuchi T, Singh TP, Takekoshi T, Jia GF, Wu X, Kao MC, et al. CCR6 is required for epidermal trafficking of gammadelta-T cells in an IL-23-induced model of psoriasiform dermatitis. *J Invest Dermatol* (2013) 133(1):164–71. doi:10.1038/jid.2012.260
75. Cochez PM, Michiels C, Hendrickx E, Dauguet N, Warnier G, Renauld JC, et al. Ccr6 is dispensable for the development of skin lesions induced by imiquimod despite its effect on epidermal homing of IL-22-producing cells. *J Invest Dermatol* (2017) 137(5):1094–103. doi:10.1016/j.jid.2016.12.023
76. Campbell JJ, Ebsworth K, Ertl LS, McMahon JP, Newland D, Wang Y, et al. IL-17-secreting gammadelta T cells are completely dependent upon CCR6 for homing to inflamed skin. *J Immunol* (2017) 199(9):3129–36. doi:10.4049/jimmunol.1700826
77. Li Z, Burns AR, Miller SB, Smith CW. CCL20, gammadelta T cells, and IL-22 in corneal epithelial healing. *FASEB J* (2011) 25(8):2659–68. doi:10.1096/fj.11-184804
78. Hammerich L, Bangen JM, Govaere O, Zimmermann HW, Gassler N, Huss S, et al. Chemokine receptor CCR6-dependent accumulation of gammadelta T cells in injured liver restricts hepatic inflammation and fibrosis. *Hepatology* (2014) 59(2):630–42. doi:10.1002/hep.26697
79. Arunachalam P, Ludewig P, Melich P, Arumugam TV, Gerloff C, Prinz I, et al. CCR6 (CC chemokine receptor 6) is essential for the migration of detrimental natural interleukin-17-producing gammadelta T cells in stroke. *Stroke* (2017) 48(7):1957–65. doi:10.1161/STROKEAHA.117.016753
80. Costa MF, Bornstein VU, Candea AL, Henriques-Pons A, Henriques MG, Penido C. CCL25 induces alpha(4)beta(7) integrin-dependent migration of IL-17(+) gammadelta T lymphocytes during an allergic reaction. *Eur J Immunol* (2012) 42(5):1250–60. doi:10.1002/eji.201142021
81. Nakamizo S, Egawa G, Tomura M, Sakai S, Tsuchiya S, Kitoh A, et al. Dermal Vgamma4(+) gammadelta T cells possess a migratory potency to the draining lymph nodes and modulate CD8(+) T-cell activity through TNF-alpha production. *J Invest Dermatol* (2015) 135(4):1007–15. doi:10.1038/jid.2014.516
82. Comerford I, Bunting M, Fenix K, Haylock-Jacobs S, Litchfield W, Harata-Lee Y, et al. An immune paradox: how can the same chemokine axis regulate both immune tolerance and activation? CCR6/CCL20: a chemokine axis balancing immunological tolerance and inflammation in autoimmune disease. *Bioessays* (2010) 32(12):1067–76. doi:10.1002/bies.201000063
83. Van Hede D, Polese B, Humblet C, Wilharm A, Renoux V, Dortu E, et al. Human papillomavirus oncoproteins induce a reorganization of epithelial-associated gammadelta T cells promoting tumor formation. *Proc Natl Acad Sci U S A* (2017) 114(43):E9056–65. doi:10.1073/pnas.1712883114
84. Gray EE, Suzuki K, Cyster JG. Cutting edge: identification of a motile IL-17-producing gammadelta T cell population in the dermis. *J Immunol* (2011) 186(11):6091–5. doi:10.4049/jimmunol.1100427
85. Wohler JE, Smith SS, Zinn KR, Bullard DC, Barnum SR. Gammadelta T cells in EAE: early trafficking events and cytokine requirements. *Eur J Immunol* (2009) 39(6):1516–26. doi:10.1002/eji.200839176
86. Ribot JC, Ribeiro ST, Correia DV, Sousa AE, Silva-Santos B. Human gammadelta thymocytes are functionally immature and differentiate into cytotoxic type 1 effector T cells upon IL-2/IL-15 signaling. *J Immunol* (2014) 192(5): 2237–43. doi:10.4049/jimmunol.1303119
87. Maggi L, Santarlasci V, Capone M, Peired A, Frosali F, Crome SQ, et al. CD161 is a marker of all human IL-17-producing T-cell subsets and is induced by RORC. *Eur J Immunol* (2010) 40(8):2174–81. doi:10.1002/eji.200940257
88. Wu P, Wu D, Ni C, Ye J, Chen W, Hu G, et al. gammadeltaT17 cells promote the accumulation and expansion of myeloid-derived suppressor cells in human colorectal cancer. *Immunity* (2014) 40(5):785–800. doi:10.1016/j.immuni.2014.03.013
89. Schirmer L, Rothhammer V, Hemmer B, Korn T. Enriched CD161high CCR6+ gammadelta T cells in the cerebrospinal fluid of patients with multiple sclerosis. *JAMA Neurol* (2013) 70(3):345–51. doi:10.1001/2013.jamaneurol.409
90. Patil RS, Shah SU, Shrikhande SV, Goel M, Dikshit RP, Chiplunkar SV. IL17 producing gammadeltaT cells induce angiogenesis and are associated with poor survival in gallbladder cancer patients. *Int J Cancer* (2016) 139(4):869–81. doi:10.1002/ijc.30134
91. Cai Y, Shen X, Ding C, Qi C, Li K, Li X, et al. Pivotal role of dermal IL-17-producing gammadelta T cells in skin inflammation. *Immunity* (2011) 35(4):596–610. doi:10.1016/j.immuni.2011.08.001
92. Peng MY, Wang ZH, Yao CY, Jiang LN, Jin QL, Wang J, et al. Interleukin 17-producing gamma delta T cells increased in patients with active pulmonary tuberculosis. *Cell Mol Immunol* (2008) 5(3):203–8. doi:10.1038/cmi.2008.25
93. Fenoglio D, Poggi A, Catellani S, Battaglia F, Ferrera A, Setti M, et al. Vdelta1 T lymphocytes producing IFN-gamma and IL-17 are expanded in HIV-1-infected patients and respond to *Candida albicans*. *Blood* (2009) 113(26):6611–8. doi:10.1182/blood-2009-01-198028

94. Codarri L, Gyulveszi G, Tosevski V, Hesske L, Fontana A, Magnenat L, et al. RORgammat drives production of the cytokine GM-CSF in helper T cells, which is essential for the effector phase of autoimmune neuroinflammation. *Nat Immunol* (2011) 12(6):560–7. doi:10.1038/ni.2027
95. Lee Y, Awasthi A, Yosef N, Quintana FJ, Xiao S, Peters A, et al. Induction and molecular signature of pathogenic TH17 cells. *Nat Immunol* (2012) 13(10):991–9. doi:10.1038/ni.2416
96. Laggner U, Di Meglio P, Perera GK, Hundhausen C, Lacy KE, Ali N, et al. Identification of a novel proinflammatory human skin-homing Vgamma9Vdelta2 T cell subset with a potential role in psoriasis. *J Immunol* (2011) 187(5):2783–93. doi:10.4049/jimmunol.1100804
97. Satoh-Takayama N, Vosshenrich CA, Lesjean-Pottier S, Sawa S, Lochner M, Rattis F, et al. Microbial flora drives interleukin 22 production in intestinal NKp46+ cells that provide innate mucosal immune defense. *Immunity* (2008) 29(6):958–70. doi:10.1016/j.immuni.2008.11.001
98. Sonnenberg GF, Monticelli LA, Elloso MM, Fouser LA, Artis D. CD4(+) lymphoid tissue-inducer cells promote innate immunity in the gut. *Immunity* (2011) 34(1):122–34. doi:10.1016/j.immuni.2010.12.009

Conflict of Interest Statement: The authors declare that the research was conducted in the absence of any commercial or financial relationships that could be construed as a potential conflict of interest.

Copyright © 2018 McKenzie, Comerford, Silva-Santos and McColl. This is an open-access article distributed under the terms of the Creative Commons Attribution License (CC BY). The use, distribution or reproduction in other forums is permitted, provided the original author(s) and the copyright owner are credited and that the original publication in this journal is cited, in accordance with accepted academic practice. No use, distribution or reproduction is permitted which does not comply with these terms.

frontiers in Immunology

MINI REVIEW
published: 09 April 2018
doi: 10.3389/fimmu.2018.00731

Coreceptors and Their Ligands in Epithelial γδ T Cell Biology

*Deborah A. Witherden, Margarete D. Johnson and Wendy L. Havran**

Department of Immunology and Microbiology, The Scripps Research Institute, La Jolla, CA, United States

Epithelial tissues line the body providing a protective barrier from the external environment. Maintenance of these epithelial barrier tissues critically relies on the presence of a functional resident T cell population. In some tissues, the resident T cell population is exclusively comprised of γδ T cells, while in others γδ T cells are found together with αβ T cells and other lymphocyte populations. Epithelial-resident γδ T cells function not only in the maintenance of the epithelium, but are also central to the repair process following damage from environmental and pathogenic insults. Key to their function is the crosstalk between γδ T cells and neighboring epithelial cells. This crosstalk relies on multiple receptor–ligand interactions through both the T cell receptor and accessory molecules leading to temporal and spatial regulation of cytokine, chemokine, growth factor, and extracellular matrix protein production. As antigens that activate epithelial γδ T cells are largely unknown and many classical costimulatory molecules and coreceptors are not used by these cells, efforts have focused on identification of novel coreceptors and ligands that mediate pivotal interactions between γδ T cells and their neighbors. In this review, we discuss recent advances in the understanding of functions for these coreceptors and their ligands in epithelial maintenance and repair processes.

Keywords: epithelial, γδ T cell, activation, costimulation, inhibition, epidermis, intestine, lung

OPEN ACCESS

Edited by:
Pierre Vantourout, King's College London, United Kingdom

Reviewed by:
Tomasz Zal, University of Texas MD Anderson Cancer Center, United States
Jessica Strid, Imperial College London, United Kingdom
Nathalie Jacobs, University of Liège, Belgium

****Correspondence:***
Wendy L. Havran
havran@scripps.edu

Specialty section:
This article was submitted to T Cell Biology, a section of the journal Frontiers in Immunology

Received: *15 February 2018*
Accepted: *23 March 2018*
Published: *09 April 2018*

Citation:
Witherden DA, Johnson MD and Havran WL (2018) Coreceptors and Their Ligands in Epithelial γδ T Cell Biology. Front. Immunol. 9:731. doi: 10.3389/fimmu.2018.00731

INTRODUCTION

The epithelial tissues are home to populations of T cells that function to protect the body from environmental pathogens and other insults. A major portion of T cells in many of these tissues expresses the γδ T cell antigen receptor (TCR) (1). The importance of these cells to homeostasis and wound repair has been evident for several years and exemplified by studies in skin, intestine, and lung (2–9). An absence of epithelial-resident γδ T cells in these tissues results in dysregulation of the epithelium, more severe damage or disease, and a delay in repair processes (2, 6, 8, 10, 11). Constant communication between resident γδ T cells and their neighboring epithelia is crucial for homeostasis and repair processes following damage or disease. Recent studies have begun to define the role of distinct molecular interactions in the rapid and localized response of epithelial-resident γδ T cells to tissue injury, yet much of the triggers and sequence of events remain a mystery.

EPITHELIAL TISSUES

The resident T cell population in the epidermal layer of the murine skin is a highly dendritic γδ T cell termed dendritic epidermal T cell (DETC). DETC express a canonical Vγ3Vδ1 TCR [nomenclature according to Garman et al. (12); alternative nomenclature Vγ5Vδ1 (13)] and make numerous contacts with surrounding epithelial cells, in particular keratinocytes and Langerhans

cells. Under homeostatic conditions, their individual dendrites extend between surrounding cells allowing for constant contact with numerous adjacent cells. This feature allows for regulated interactions between both cell surface receptors and soluble molecules facilitating homeostasis in the skin and allowing for rapid repair following damage or disease. Although differing in T cell composition, human epidermis also contains resident T cells that make crucial contributions to wound repair (9). As such, it is reasonable to suggest that similar mechanisms of communication exist in human epidermis.

The intestinal mucosal barrier is also occupied by resident T cells. These T cells are termed intraepithelial lymphocytes (IEL) that, as their name suggests, are found residing between epithelial cells and include subsets of both αβ and γδ T cells. The intestinal γδ T cell subset expresses predominantly a Vγ5 TCR [alternative nomenclature Vγ7 (13)] that is able to pair with a number of different Vδ chains. Although not dendritic like γδ T cells in the skin, γδ IEL are able to make contact with multiple epithelial cells through active migration within the intestinal epithelium. This gives a single γδ IEL the ability to surveil large areas of epithelium (14, 15) and defend against pathogenic assault (16). Although not as clearly defined, resistance to infection and repair from damage in the lung also relies on resident γδ T cells (3, 11, 17–20), again likely through numerous contacts with surrounding cells (21).

Continual interaction with neighboring epithelia is thus required for epithelial γδ T cells to perform their functions in homeostasis, resistance to infection, and damage repair. While the importance of the TCR is clear (22–25), it is becoming evident that additional distinct molecular interactions drive these functions of epithelial γδ T cells. Discussion of some of these interactions (**Table 1**) will be the focus of the remainder of this review.

TABLE 1 | Non-TCR receptor–ligand pairs in epithelial γδ T cell function.

γδ T cell	Epithelial cell	Species	Function	Reference
Junctional adhesion molecule-like	Coxsackie and adenovirus receptor	Mouse and human	Costimulation	(64, 65)
NKG2D	MICA/MICB Rae1, H60c, MULT-1	Human Mouse	Costimulation	(71–74, 78, 79)
?	Skints Butyrophilins	Mouse Mouse/human	Activation Activation	(81) (82)
CD200R	CD200	Mouse	Inhibition	(85)
CD94/NKG2	HLA-E Qa-1	Human Mouse	Inhibition	(86–89)
G protein-coupled receptor 55	L-α-lysophosphatidylinositol	Mouse	Inhibition	(15)
Lymphocyte function-associated antigen-1	Intercellular adhesion molecule 1	Mouse and human	Adhesion	(26, 27)
E-cadherin	?	Mouse	Adhesion	(42–44, 48, 49)
αEβ7	E-cadherin	Mouse	Adhesion	(45–50)
CD100	Plexin B2	Mouse	Morphology/migration	(58–60)
Aryl hydrocarbon receptor	?	Mouse	γδ T cell maintenance	(55–57)
TLR 2, 4, 9	?	Mouse	?	(83)
?	CD98hc	Mouse	?	(53)
CCR4		Mouse	γδ T cell maintenance	(54)

?, unknown.

ADHESION

The maintenance of epithelial-resident γδ T cells within the epithelium is known to involve adhesion through integrin and cadherin-mediated interactions. Expression of these molecules is also modulated in response to epithelial damage suggesting their functions may extend beyond maintenance to roles in repair processes as well.

Intercellular adhesion molecule 1 (ICAM-1), also known as CD54, is a membrane-bound adhesion molecule that is a ligand for leukocyte-expressed lymphocyte function-associated antigen-1 (LFA-1). This protein is well known to recruit leukocytes to sites of inflammation, but its interaction with tissue-resident γδ T cells is less understood. ICAM-1 is upregulated by the corneal epithelium following wounding and is required for γδ T cell recruitment to the site of damage in an LFA-1-dependent process (26). While ICAM-1 is also upregulated by endothelial cells and keratinocytes following wounding (27), and ICAM-1-deficient mice are known to exhibit delayed wound repair (27, 28), it is unknown whether the protein plays any role in DETC-mediated epithelial repair. ICAM-1 has also been shown to be important in shaping the gut lymphocyte populations, with ICAM-1-deficient mice displaying a relatively higher proportion of γδ T cells and a lower proportion of αβ T cells, though the biological effects of this population shift are unclear (29). Interestingly, the effect of ICAM-1/LFA-1 interactions on γδ T cells is not limited to leukocyte migration. Costimulation of peripheral mouse γδ T cells through TCR and LFA-1 was demonstrated to trigger apoptosis of these cells (30, 31), in contrast to the proliferative response observed in αβ T cells (30). However, ICAM-1/LFA-1 interaction has been shown to be involved in peripheral γδ T cell recognition of tumor cells and subsequent cytolytic response (32–36), so the outcome appears to be context dependent. While the majority of this work has focused on γδ T cell recognition of target cell-expressed ICAM-1, it should be noted that γδ T cells also express ICAM-1 (37). Blocking ICAM-1 expressed on the epithelial-associated Vδ1 T cell population has been reported to reduce cytotoxicity against myeloma cells (34). Studies in αβ T cells have shown ICAM-1 to be a costimulatory molecule promoting proliferation, IL-2 and IFNγ secretion, phosphatidylinositol-3 kinase activation, and a shift toward a memory phenotype (38–40). However, it remains to be seen whether epithelial-resident γδ T cells also have the ability to receive costimulatory signals through ICAM-1, and what the effects of LFA-1 engagement are in this population.

E-cadherin is an adhesion molecule that supports adhesion between keratinocytes (41). Interestingly, DETC also express E-cadherin as well as another E-cadherin ligand, αEβ7. Following

wounding, DETC downregulate expression of E-cadherin, but maintain their level of expression of αEβ7 (42–44). *In vitro* and *in vivo* studies have demonstrated a role for αEβ7 in DETC activation with possible functions in adhesion and epidermal retention, dendrite anchoring, morphology and motility, cytotoxicity and costimulation (22, 45–47). In contrast, DETC-expressed E-cadherin functions as an inhibitory receptor for DETC activation (47). Murine intestinal IEL also express both E-cadherin and αEβ7 (48, 49), and αEβ7 is expressed on most γδ T cells in the bleomycin-induced mouse model of lung fibrosis (50), suggesting similar functions for these adhesion molecules on γδ T cells in other epithelial sites. Furthermore, the expression of both E-cadherin and αEβ7 on fetal thymic precursors of DETC (43, 44) indicates that inhibitory and costimulatory signals, respectively through these molecules may also influence thymic development and maturation of DETC precursors. This is further supported by the observation of diminished DETC numbers in the epidermis of αE deficient mice (46), although thymic populations were not directly analyzed in this study.

CD98hc is an amino acid transporter that associates with both cadherins and β1 integrins (51, 52). As such, it is perhaps not surprising that it too has been implicated in the regulation of skin homeostasis and wound healing (53), although it is unknown whether this involves direct interaction of CD98hc with DETC. In addition to adhesive interactions, the chemokine receptor CCR4 has been shown to be important for DETC retention in the epidermis (54). Additionally, the aryl hydrocarbon receptor (AhR) transcription factor is essential for maintaining both DETC and IEL in their respective tissues (55–57), although just how AhR signals lead to tissue retention of DETC and IEL, and whether AhR plays a role in epithelial γδ T cell activation and the wound repair process, is unknown.

MORPHOLOGY AND MIGRATION

γδ IEL actively migrate within the intestinal epithelium and this migration is dependent on occludin expression in both IEL and the epithelium (14). In contrast, DETC in the epidermis are sessile under homeostatic conditions, communicating with surrounding keratinocytes through their numerous dendritic processes. Upon keratinocyte damage, DETC rapidly pull back these processes and adopt a more rounded morphology (6). Interestingly, downregulation of E-cadherin in keratinocytes can contribute to this rounding either through disruption of E-cadherin-mediated homophilic binding and/or αEβ7 integrin-mediated heterophilic binding (45).

In addition, binding of the semaphorin, CD100, to one of its ligands, Plexin B2, contributes to the DETC rounding response through activation of ERK kinase and cofilin (58). In the absence of CD100, the DETC rounding response to keratinocyte damage is delayed resulting in subsequent delayed wound closure (58). It has been suggested that the rounding of DETC permits them to migrate within the epidermis during wound repair, yet this remains to be demonstrated. Interestingly, in the intestinal epithelium, where IEL are in constant motion, CD100-plexin B2 interactions still play an important role as CD100-deficiency results in more severe damage as well as delayed repair in a mouse model of DSS-induced colitis (59). Similarly, a role for CD100 in lung allergic inflammation has been described (60). Whether CD100 is involved in γδ T cell migration in these epithelial tissues is yet to be determined.

ACTIVATION

To become fully activated, αβ T cells require engagement of molecules in addition to the TCR, such as CD4, CD8, and CD28 together with other costimulatory and adhesion molecules. Unlike αβ T cells, epithelial-resident γδ T cells do not express CD4, CD8 (although the CD8aa homodimer is expressed by some γδ IEL), or CD28 (61), however, a number of other molecules have recently been described to participate in the activation of these cells.

Striking similarities between CD28 and the junctional adhesion molecule-like (JAML) (62–64) suggest that JAML may play the role of primary costimulator for epithelial-resident γδ T cells through interaction with its ligand coxsackie and adenovirus receptor (CAR) (64, 65), expressed on epithelial cells. Like CD28 on αβ T cells, JAML is able to induce proliferation and cytokine production in epithelial γδ T cells. This response is mediated through PI3K which is recruited to JAML following CAR ligation (63). The PI3K binding motif in CD28 (66), similarly mediates delivery of a costimulatory signal. Although JAML expression has been demonstrated on activated peripheral γδ T cells, a population of activated $CD8^+$ αβ T cells and other cell types of both the innate and adaptive arms of the immune system, including neutrophils, monocytes, and some memory T cells (64, 65, 67), the function of JAML as a costimulatory molecule appears confined to the epithelial subsets of γδ T cells.

Blocking of JAML-CAR costimulation *in vivo* impairs DETC activation and delays wound closure (64), demonstrating the importance of this interaction to DETC function. Just how this interaction might function in response to other perturbations to the skin, such as infection or malignancy, is unknown. A parallel role in IEL activation in the mouse intestine (64) is suggested by the similarity in expression patterns of JAML and CAR in the intestine. Whether this costimulatory pair also functions in human skin and intestinal T cell activation and tissue repair is still not known.

The NKG2D receptor (discussed in detail elsewhere) is an activating receptor expressed on NK, γδ, and $CD8^+$ T cells (10, 68–70). In the mouse epidermis, NKG2D is expressed on DETC and ligation to its ligands Rae-1, H60, and MULT-1 on keratinocytes activates DETC (10). A reliance on PI3K signaling has been demonstrated, however, whether activation through NKG2D also requires simultaneous TCR stimulation or can stimulate DETC directly is somewhat controversial (71–75). Nevertheless, the importance of NKG2D signaling in epithelial γδ T cells has been demonstrated in models of wound healing, carcinogenesis, and contact hypersensitivity responses (72, 76, 77). Whether the difference in T cell receptor requirement for NKG2D-mediated DETC activation is due to differences in the induced ligand resulting from the type of damage elicited, is unclear at this time. In humans, there is evidence to suggest that recognition of MIC by Vδ1 expressing intestinal epithelial T cells (76, 78, 79) can

either be direct, *via* the TCR, through NKG2D, or sequentially using both molecules (80). This idea, however, requires experimental confirmation.

It is increasingly evident that additional molecules are also important for the activation of epithelial-resident γδ T cells. A recent analysis of defective wound healing in aged mice highlighted the importance of Skint molecules (to be reviewed in detail elsewhere) in DETC activation and epidermal re-epithelialization (81). A role for the closely related butyrophilin (Btnl) molecules in the activation of intestinal γδ T cells in both mice and humans has recently been demonstrated (82). In addition, other molecules, such as toll-like receptors 2, 4, and 9 have been shown to be upregulated on γδ T cells following skin injury (83), suggesting a role in their activation, however, a precise function has yet to be defined.

INHIBITION

The role of inhibitory signals in the control of αβ T cell activation is well established. Emerging evidence points to similar signals playing an important role in regulating the activation of epithelial-resident γδ T cells. The transmembrane glycoprotein CD200 expressed on keratinocytes has been implicated in the protection of hair follicles from autoimmune attack (84). Interestingly, resting DETC express low levels of the CD200-receptors 1, 2, and 3, but expression of CD200R1 is increased following activation *in vitro*. In functional assays, ligation of DETC-expressed CD200R with immobilized CD200 inhibits DETC proliferation and cytokine secretion highlighting an important role for CD200–CD200R interactions in the control of DETC activation (85). How this interaction may function during wound repair is unknown.

Inhibitory receptors expressed by NK cells are also found on γδ T cells, and appear to have similar inhibitory functions on these cells (86). The Ly49E and CD94/NKG2 receptors are expressed on mature fetal thymic DETC as well as those residing in the epidermis (86). DETC do not express other members of the Ly49 family. DETC cytotoxicity is inhibited by ligation of CD94/NKG2 and monoclonal antibody cross-linking of CD94/NKG2 prevents mature DETC thymocytes from killing $FcγR^+$ target cells demonstrating a role for CD94/NKG2 as an inhibitory receptor on DETC (86). Just how these and other inhibitory interactions may function in epithelial wound repair processes warrants further investigation.

A recent report has identified an inhibitory role for G protein-coupled receptor 55 (GPR55) on intestinal IEL (15). GPR55 is highly expressed on γδ IEL and more modestly on αβ IEL and intestinal dendritic cells. Through interaction with its receptor L-α-lysophosphatidylinositol expressed on intestinal epithelial cells, GPR55 regulates the interaction between IEL and the epithelium and inhibits the accumulation of $GPR55^+$ cells in the small intestine. Analysis of GPR55-deficient animals revealed increased γδ IEL migration within, and retention in, the small intestine, and enhanced IEL-epithelial cell crosstalk (15). Although the precise inhibitory role of GPR55 in the intestine is yet to be determined, Sumida et al. (15) propose that it may constrain IEL movement in the epithelium to allow normal epithelial cell functions to proceed.

CONCLUSION

By analogy with skin, gut, and lung, the existence of a resident γδ T cell population in all epithelial barrier tissues implies a crucial function for these cells throughout the body. An increasing number of receptor-ligand pairs are being identified as vital for the homeostasis and repair functions of these resident γδ T cells. An understanding of the precise mechanisms of action of these various molecules in the crosstalk between T cells and their adjacent epithelial cells will help to elucidate their roles throughout the epithelia.

AUTHOR CONTRIBUTIONS

DW, MJ, and WH all contributed to the writing of the manuscript.

REFERENCES

1. Allison JP, Havran WL. The immunobiology of T cells with invariant γδ antigen receptors. *Annu Rev Immunol* (1991) 9:679–705. doi:10.1146/annurev.iy.09.040191.003335
2. Chen Y, Chou K, Fuchs E, Havran WL, Boismenu R. Protection of the intestinal mucosa by intraepithelial γδ T cells. *Proc Natl Acad Sci U S A* (2002) 99(22):14338–43. doi:10.1073/pnas.212290499
3. Cheng M, Hu S. Lung-resident gammadelta T cells and their roles in lung diseases. *Immunology* (2017) 151(4):375–84. doi:10.1111/imm.12764
4. Dalton JE, Cruickshank SM, Egan CE, Mears R, Newton DJ, Andrew EM, et al. Intraepithelial gammadelta+ lymphocytes maintain the integrity of intestinal epithelial tight junctions in response to infection. *Gastroenterology* (2006) 131(3):818–29. doi:10.1053/j.gastro.2006.06.003
5. Inagaki-Ohara K, Chinen T, Matsuzaki G, Sasaki A, Sakamoto Y, Hiromatsu K, et al. Mucosal T cells bearing TCRγδ play a protective role in intestinal inflammation. *J Immunol* (2004) 173(2):1390–8. doi:10.4049/jimmunol.173.2.1390
6. Jameson J, Ugarte K, Chen N, Yachi P, Fuchs E, Boismenu R, et al. A role for skin γδ T cells in wound repair. *Science* (2002) 296(5568):747–9. doi:10.1126/science.1069639
7. Komano H, Fujiura Y, Kawaguchi M, Matsumoto S, Hashimoto Y, Obana S, et al. Homeostatic regulation of intestinal epithelia by intraepithelial gamma delta T cells. *Proc Natl Acad Sci U S A* (1995) 92(13):6147–51. doi:10.1073/pnas.92.13.6147
8. Sharp LL, Jameson JM, Cauvi G, Havran WL. Dendritic epidermal T cells regulate skin homeostasis through local production of insulin-like growth factor 1. *Nat Immunol* (2005) 6(1):73–9. doi:10.1038/ni1152
9. Toulon A, Breton L, Taylor KR, Tenenhaus M, Bhavsar D, Lanigan C, et al. A role for human skin-resident T cells in wound healing. *J Exp Med* (2009) 206(4):743–50. doi:10.1084/jem.20081787
10. Girardi M, Oppenheim DE, Steele CR, Lewis JM, Glusac E, Filler R, et al. Regulation of cutaneous malignancy by γδ T cells. *Science* (2001) 294(5542):605–9. doi:10.1126/science.1063916
11. King DP, Hyde DM, Jackson KA, Novosad DM, Ellis TN, Putney L, et al. Cutting edge: protective response to pulmonary injury requires γδ T lymphocytes. *J Immunol* (1999) 162(9):5033–6.
12. Garman RD, Doherty PJ, Raulet DH. Diversity, rearrangement, and expression of murine T cell gamma genes. *Cell* (1986) 45(5):733–42. doi:10.1016/0092-8674(86)90787-7
13. Heilig JS, Tonegawa S. Diversity of murine gamma genes and expression in fetal and adult T lymphocytes. *Nature* (1986) 322(6082):836–40. doi:10.1038/322836a0
14. Edelblum KL, Shen L, Weber CR, Marchiando AM, Clay BS, Wang Y, et al. Dynamic migration of γδ intraepithelial lymphocytes requires occludin. *Proc Natl Acad Sci U S A* (2012) 109(18):7097–102. doi:10.1073/pnas.1112519109

15. Sumida H, Lu E, Chen H, Yang Q, Mackie K, Cyster JG. GPR55 regulates intraepithelial lymphocyte migration dynamics and susceptibility to intestinal damage. *Sci Immunol* (2017) 2(18):eaao1135. doi:10.1126/sciimmunol.aao1135
16. Edelblum KL, Singh G, Odenwald MA, Lingaraju A, El Bissati K, McLeod R, et al. gammadelta intraepithelial lymphocyte migration limits transepithelial pathogen invasion and systemic disease in mice. *Gastroenterology* (2015) 148(7):1417–26. doi:10.1053/j.gastro.2015.02.053
17. Born W, Cady C, Jones-Carson J, Mukasa A, Lahn M, O'Brien R. Immunoregulatory functions of γδ T cells. *Adv Immunol* (1999) 71:77–144. doi:10.1016/S0065-2776(08)60400-9
18. Born WK, Lahn M, Takeda K, Kanehiro A, O'Brien RL, Gelfand EW. Role of γδ T cells in protecting normal airway function. *Respir Res* (2000) 1(3):151–8. doi:10.1186/rr26
19. Hahn YS, Taube C, Jin N, Takeda K, Park JW, Wands JM, et al. Vγ4$^+$ γδ T cells regulate airway hyperreactivity to methacholine in ovalbumin-sensitized and challenged mice. *J Immunol* (2003) 171(6):3170–8. doi:10.4049/jimmunol.171.6.3170
20. Lahn M, Kanehiro A, Takeda K, Konowal A, O'Brien RL, Gelfand EW, et al. γδ T cells as regulators of airway hyperresponsiveness. *Int Arch Allergy Immunol* (2001) 125(3):203–10. doi:10.1159/000053817
21. Wands JM, Roark CL, Aydintug MK, Jin N, Hahn YS, Cook L, et al. Distribution and leukocyte contacts of γδ T cells in the lung. *J Leukoc Biol* (2005) 78(5):1086–96. doi:10.1189/jlb.0505244
22. Chodaczek G, Papanna V, Zal MA, Zal T. Body-barrier surveillance by epidermal γδ TCRs. *Nat Immunol* (2012) 13(3):272–82. doi:10.1038/ni.2240
23. Jameson JM, Cauvi G, Witherden DA, Havran WL. A keratinocyte-responsive γδ TCR is necessary for dendritic epidermal T cell activation by damaged keratinocytes and maintenance in the epidermis. *J Immunol* (2004) 172(6):3573–9. doi:10.4049/jimmunol.172.6.3573
24. Mallick-Wood CA, Lewis JM, Richie LI, Owen MJ, Tigelaar RE, Hayday AC. Conservation of T cell receptor conformation in epidermal γδ cells with disrupted primary Vγ gene usage. *Science* (1998) 279(5357):1729–33. doi:10.1126/science.279.5357.1729
25. Zhang B, Wu J, Jiao Y, Bock C, Dai M, Chen B, et al. Differential requirements of TCR signaling in homeostatic maintenance and function of dendritic epidermal T cells. *J Immunol* (2015) 195(9):4282–91. doi:10.4049/jimmunol.1501220
26. Byeseda SE, Burns AR, Dieffenbaugher S, Rumbaut RE, Smith CW, Li Z. ICAM-1 is necessary for epithelial recruitment of gammadelta T cells and efficient corneal wound healing. *Am J Pathol* (2009) 175(2):571–9. doi:10.2353/ajpath.2009.090112
27. Nagaoka T, Kaburagi Y, Hamaguchi Y, Hasegawa M, Takehara K, Steeber DA, et al. Delayed wound healing in the absence of intercellular adhesion molecule-1 or L-selectin expression. *Am J Pathol* (2000) 157(1):237–47. doi:10.1016/S0002-9440(10)64534-8
28. Gay AN, Mushin OP, Lazar DA, Naik-Mathuria BJ, Yu L, Gobin A, et al. Wound healing characteristics of ICAM-1 null mice devoid of all isoforms of ICAM-1. *J Surg Res* (2011) 171(1):e1–7. doi:10.1016/j.jss.2011.06.053
29. Steinhoff U, Klemm U, Greiner M, Bordasch K, Kaufmann SH. Altered intestinal immune system but normal antibacterial resistance in the absence of P-selectin and ICAM-1. *J Immunol* (1998) 160(12):6112–20.
30. Kobayashi N, Hiromatsu K, Matsuzaki G, Harada M, Matsumoto Y, Nomoto K, et al. A sustained increase of cytosolic Ca2+ in gammadelta T cells triggered by co-stimulation via TCR/CD3 and LFA-1. *Cell Calcium* (1997) 22(6):421–30. doi:10.1016/S0143-4160(97)90069-5
31. Matsumoto Y, Hiromatsu K, Sakai T, Kobayashi Y, Kimura Y, Usami J, et al. Co-stimulation with LFA-1 triggers apoptosis in gamma delta T cells on T cell receptor engagement. *Eur J Immunol* (1994) 24(10):2441–5. doi:10.1002/eji.1830241027
32. Corvaisier M, Moreau-Aubry A, Diez E, Bennouna J, Mosnier JF, Scotet E, et al. V gamma 9V delta 2 T cell response to colon carcinoma cells. *J Immunol* (2005) 175(8):5481–8. doi:10.4049/jimmunol.175.8.5481
33. Ensslin AS, Formby B. Comparison of cytolytic and proliferative activities of human gamma delta and alpha beta T cells from peripheral blood against various human tumor cell lines. *J Natl Cancer Inst* (1991) 83(21):1564–9. doi:10.1093/jnci/83.21.1564
34. Knight A, Mackinnon S, Lowdell MW. Human Vdelta1 gamma-delta T cells exert potent specific cytotoxicity against primary multiple myeloma cells. *Cytotherapy* (2012) 14(9):1110–8. doi:10.3109/14653249.2012.700766
35. Liu Z, Guo B, Lopez RD. Expression of intercellular adhesion molecule (ICAM)-1 or ICAM-2 is critical in determining sensitivity of pancreatic cancer cells to cytolysis by human gammadelta-T cells: implications in the design of gammadelta-T-cell-based immunotherapies for pancreatic cancer. *J Gastroenterol Hepatol* (2009) 24(5):900–11. doi:10.1111/j.1440-1746.2008.05668.x
36. Uchida R, Ashihara E, Sato K, Kimura S, Kuroda J, Takeuchi M, et al. Gamma delta T cells kill myeloma cells by sensing mevalonate metabolites and ICAM-1 molecules on cell surface. *Biochem Biophys Res Commun* (2007) 354(2):613–8. doi:10.1016/j.bbrc.2007.01.031
37. Chao CC, Sandor M, Dailey MO. Expression and regulation of adhesion molecules by gamma delta T cells from lymphoid tissues and intestinal epithelium. *Eur J Immunol* (1994) 24(12):3180–7. doi:10.1002/eji.1830241240
38. Chirathaworn C, Kohlmeier JE, Tibbetts SA, Rumsey LM, Chan MA, Benedict SH. Stimulation through intercellular adhesion molecule-1 provides a second signal for T cell activation. *J Immunol* (2002) 168(11):5530–7. doi:10.4049/jimmunol.168.11.5530
39. Kohlmeier JE, Chan MA, Benedict SH. Costimulation of naive human CD4 T cells through intercellular adhesion molecule-1 promotes differentiation to a memory phenotype that is not strictly the result of multiple rounds of cell division. *Immunology* (2006) 118(4):549–58. doi:10.1111/j.1365-2567.2006.02396.x
40. Kohlmeier JE, Rumsey LM, Chan MA, Benedict SH. The outcome of T-cell costimulation through intercellular adhesion molecule-1 differs from costimulation through leucocyte function-associated antigen-1. *Immunology* (2003) 108(2):152–7. doi:10.1046/j.1365-2567.2003.01578.x
41. Gumbiner BM. Regulation of cadherin-mediated adhesion in morphogenesis. *Nat Rev Mol Cell Biol* (2005) 6(8):622–34. doi:10.1038/nrm1699
42. Aiba S, Nakagawa S, Ozawa H, Tagami H. Different expression of E-cadherin by two cutaneous gamma/delta TcR+ T-cell subsets, V gamma 5− and V gamma 5+ gamma/delta TcR+ T cells. *J Invest Dermatol* (1995) 105(3):379–82. doi:10.1111/1523-1747.ep12320959
43. Lee MG, Tang A, Sharrow SO, Udey MC. Murine dendritic epidermal T cells (DETC) express the homophilic adhesion molecule E-cadherin. *Epithelial Cell Biol* (1994) 3(4):149–55.
44. Lefrancois L, Barrett TA, Havran WL, Puddington L. Developmental expression of the alpha IEL beta 7 integrin on T cell receptor gamma delta and T cell receptor alpha beta T cells. *Eur J Immunol* (1994) 24(3):635–40. doi:10.1002/eji.1830240322
45. Schlickum S, Sennefelder H, Friedrich M, Harms G, Lohse MJ, Kilshaw P, et al. Integrin alpha E(CD103)beta 7 influences cellular shape and motility in a ligand-dependent fashion. *Blood* (2008) 112(3):619–25. doi:10.1182/blood-2008-01-134833
46. Schon MP, Schon M, Parker CM, Williams IR. Dendritic epidermal T cells (DETC) are diminished in integrin alphaE(CD103)-deficient mice. *J Invest Dermatol* (2002) 119(1):190–3. doi:10.1046/j.1523-1747.2002.17973.x
47. Uchida Y, Kawai K, Ibusuki A, Kanekura T. Role for E-cadherin as an inhibitory receptor on epidermal γδ T cells. *J Immunol* (2011) 186(12):6945–54. doi:10.4049/jimmunol.1003853
48. Cepek KL, Shaw SK, Parker CM, Russell GJ, Morrow JS, Rimm DL, et al. Adhesion between epithelial cells and T lymphocytes mediated by E-cadherin and the alpha E beta 7 integrin. *Nature* (1994) 372(6502):190–3. doi:10.1038/372190a0
49. Inagaki-Ohara K, Sawaguchi A, Suganuma T, Matsuzaki G, Nawa Y. Intraepithelial lymphocytes express junctional molecules in murine small intestine. *Biochem Biophys Res Commun* (2005) 331(4):977–83. doi:10.1016/j.bbrc.2005.04.025
50. Braun RK, Sterner-Kock A, Kilshaw PJ, Ferrick DA, Giri SN. Integrin alpha E beta 7 expression on BAL CD4+, CD8+, and gamma delta T-cells in bleomycin-induced lung fibrosis in mouse. *Eur Respir J* (1996) 9(4):673–9. doi:10.1183/09031936.96.09040673
51. Lemaitre G, Stella A, Feteira J, Baldeschi C, Vaigot P, Martin MT, et al. CD98hc (SLC3A2) is a key regulator of keratinocyte adhesion. *J Dermatol Sci* (2011) 61(3):169–79. doi:10.1016/j.jdermsci.2010.12.007
52. Nakamura E, Sato M, Yang H, Miyagawa F, Harasaki M, Tomita K, et al. 4F2 (CD98) heavy chain is associated covalently with an amino acid transporter and controls intracellular trafficking and membrane topology of 4F2 heterodimer. *J Biol Chem* (1999) 274(5):3009–16. doi:10.1074/jbc.274.5.3009
53. Boulter E, Estrach S, Errante A, Pons C, Cailleteau L, Tissot F, et al. CD98hc (SLC3A2) regulation of skin homeostasis wanes with age. *J Exp Med* (2013) 210(1):173–90. doi:10.1084/jem.20121651

54. Nakamura K, White AJ, Parnell SM, Lane PJ, Jenkinson EJ, Jenkinson WE, et al. Differential requirement for CCR4 in the maintenance but not establishment of the invariant Vgamma5(+) dendritic epidermal T-cell pool. *PLoS One* (2013) 8(9):e74019. doi:10.1371/journal.pone.0074019
55. Esser C, Rannug A, Stockinger B. The aryl hydrocarbon receptor in immunity. *Trends Immunol* (2009) 30(9):447–54. doi:10.1016/j.it.2009.06.005
56. Kadow S, Jux B, Zahner SP, Wingerath B, Chmill S, Clausen BE, et al. Aryl hydrocarbon receptor is critical for homeostasis of invariant γδ T cells in the murine epidermis. *J Immunol* (2011) 187(6):3104–10. doi:10.4049/jimmunol.1100912
57. Li Y, Innocentin S, Withers DR, Roberts NA, Gallagher AR, Grigorieva EF, et al. Exogenous stimuli maintain intraepithelial lymphocytes via aryl hydrocarbon receptor activation. *Cell* (2011) 147(3):629–40. doi:10.1016/j.cell.2011.09.025
58. Witherden DA, Watanabe M, Garijo O, Rieder SE, Sarkisyan G, Cronin SJ, et al. The CD100 receptor interacts with its plexin B2 ligand to regulate epidermal γδ T cell function. *Immunity* (2012) 37(2):314–25. doi:10.1016/j.immuni.2012.05.026
59. Meehan TF, Witherden DA, Kim CH, Sendaydiego K, Ye I, Garijo O, et al. Protection against colitis by CD100-dependent modulation of intraepithelial γδ T lymphocyte function. *Mucosal Immunol* (2014) 7(1):134–42. doi:10.1038/mi.2013.32
60. Shanks K, Nkyimbeng-Takwi EH, Smith E, Lipsky MM, DeTolla LJ, Scott DW, et al. Neuroimmune semaphorin 4D is necessary for optimal lung allergic inflammation. *Mol Immunol* (2013) 56(4):480–7. doi:10.1016/j.molimm.2013.05.228
61. Hayday A, Theodoridis E, Ramsburg E, Shires J. Intraepithelial lymphocytes: exploring the third way in immunology. *Nat Immunol* (2001) 2(11):997–1003. doi:10.1038/ni1101-997
62. Moog-Lutz C, Cave-Riant F, Guibal FC, Breau MA, Di Gioia Y, Couraud PO, et al. JAML, a novel protein with characteristics of a junctional adhesion molecule, is induced during differentiation of myeloid leukemia cells. *Blood* (2003) 102(9):3371–8. doi:10.1182/blood-2002-11-3462
63. Verdino P, Witherden DA, Havran WL, Wilson IA. The molecular interaction of CAR and JAML recruits the central cell signal transducer PI3K. *Science* (2010) 329(5996):1210–4. doi:10.1126/science.1187996
64. Witherden DA, Verdino P, Rieder SE, Garijo O, Mills RE, Teyton L, et al. The junctional adhesion molecule JAML is a costimulatory receptor for epithelial γδ T cell activation. *Science* (2010) 329(5996):1205–10. doi:10.1126/science.1192698
65. Zen K, Liu Y, McCall IC, Wu T, Lee W, Babbin BA, et al. Neutrophil migration across tight junctions is mediated by adhesive interactions between epithelial coxsackie and adenovirus receptor and a junctional adhesion molecule-like protein on neutrophils. *Mol Biol Cell* (2005) 16(6):2694–703. doi:10.1091/mbc.E05-01-0036
66. Rudd CE, Schneider H. Unifying concepts in CD28, ICOS and CTLA4 co-receptor signalling. *Nat Rev Immunol* (2003) 3(7):544–56. doi:10.1038/nri1131
67. Luissint AC, Lutz PG, Calderwood DA, Couraud PO, Bourdoulous S. JAM-L-mediated leukocyte adhesion to endothelial cells is regulated in cis by α4β1 integrin activation. *J Cell Biol* (2008) 183(6):1159–73. doi:10.1083/jcb.200805061
68. Bauer S, Groh V, Wu J, Steinle A, Phillips JH, Lanier LL, et al. Activation of NK cells and T cells by NKG2D, a receptor for stress-inducible MICA. *Science* (1999) 285(5428):727–9. doi:10.1126/science.285.5428.727
69. Jamieson AM, Diefenbach A, McMahon CW, Xiong N, Carlyle JR, Raulet DH. The role of the NKG2D immunoreceptor in immune cell activation and natural killing. *Immunity* (2002) 17(1):19–29. doi:10.1016/S1074-7613(02)00333-3
70. Raulet DH. Roles of the NKG2D immunoreceptor and its ligands. *Nat Rev Immunol* (2003) 3(10):781–90. doi:10.1038/nri1199
71. Whang MI, Guerra N, Raulet DH. Costimulation of dendritic epidermal γδ T cells by a new NKG2D ligand expressed specifically in the skin. *J Immunol* (2009) 182(8):4557–64. doi:10.4049/jimmunol.0802439
72. Yoshida S, Mohamed RH, Kajikawa M, Koizumi J, Tanaka M, Fugo K, et al. Involvement of an NKG2D ligand H60c in epidermal dendritic T cell-mediated wound repair. *J Immunol* (2012) 188(8):3972–9. doi:10.4049/jimmunol.1102886
73. Nitahara A, Shimura H, Ito A, Tomiyama K, Ito M, Kawai K. NKG2D ligation without T cell receptor engagement triggers both cytotoxicity and cytokine production in dendritic epidermal T cells. *J Invest Dermatol* (2006) 126(5):1052–8. doi:10.1038/sj.jid.5700112
74. Strid J, Roberts SJ, Filler RB, Lewis JM, Kwong BY, Schpero W, et al. Acute upregulation of an NKG2D ligand promotes rapid reorganization of a local immune compartment with pleiotropic effects on carcinogenesis. *Nat Immunol* (2008) 9(2):146–54. doi:10.1038/ni1556
75. Ibusuki A, Kawai K, Yoshida S, Uchida Y, Nitahara-Takeuchi A, Kuroki K, et al. NKG2D triggers cytotoxicity in murine epidermal gammadelta T cells via PI3K-dependent, Syk/ZAP70-independent signaling pathway. *J Invest Dermatol* (2014) 134(2):396–404. doi:10.1038/jid.2013.353
76. Groh V, Steinle A, Bauer S, Spies T. Recognition of stress-induced MHC molecules by intestinal epithelial γδ T cells. *Science* (1998) 279(5357):1737–40. doi:10.1126/science.279.5357.1737
77. Nielsen MM, Dyring-Andersen B, Schmidt JD, Witherden D, Lovato P, Woetmann A, et al. NKG2D-dependent activation of dendritic epidermal T cells in contact hypersensitivity. *J Invest Dermatol* (2015) 135(5):1311–9. doi:10.1038/jid.2015.23
78. Das H, Groh V, Kuijl C, Sugita M, Morita CT, Spies T, et al. MICA engagement by human Vγ2Vδ2 T cells enhances their antigen-dependent effector function. *Immunity* (2001) 15(1):83–93. doi:10.1016/S1074-7613(01)00168-6
79. Groh V, Rhinehart R, Secrist H, Bauer S, Grabstein KH, Spies T. Broad tumor-associated expression and recognition by tumor-derived γδ T cells of MICA and MICB. *Proc Natl Acad Sci U S A* (1999) 96(12):6879–84. doi:10.1073/pnas.96.12.6879
80. Xu B, Pizarro JC, Holmes MA, McBeth C, Groh V, Spies T, et al. Crystal structure of a γδ T-cell receptor specific for the human MHC class I homolog MICA. *Proc Natl Acad Sci U S A* (2011) 108(6):2414–9. doi:10.1073/pnas.1015433108
81. Keyes BE, Liu S, Asare A, Naik S, Levorse J, Polak L, et al. Impaired epidermal to dendritic T cell signaling slows wound repair in aged skin. *Cell* (2016) 167(5):1323–38e14. doi:10.1016/j.cell.2016.10.052
82. Di Marco Barros R, Roberts NA, Dart RJ, Vantourout P, Jandke A, Nussbaumer O, et al. Epithelia use butyrophilin-like molecules to shape organ-specific gammadelta T cell compartments. *Cell* (2016) 167(1):203–18e17. doi:10.1016/j.cell.2016.08.030
83. Rani M, Zhang Q, Scherer MR, Cap AP, Schwacha MG. Activated skin gammadelta T-cells regulate T-cell infiltration of the wound site after burn. *Innate Immun* (2015) 21(2):140–50. doi:10.1177/1753425913519350
84. Rosenblum MD, Olasz EB, Yancey KB, Woodliff JE, Lazarova Z, Gerber KA, et al. Expression of CD200 on epithelial cells of the murine hair follicle: a role in tissue-specific immune tolerance? *J Invest Dermatol* (2004) 123(5):880–7. doi:10.1111/j.0022-202X.2004.23461.x
85. Rosenblum MD, Woodliff JE, Madsen NA, McOlash LJ, Keller MR, Truitt RL. Characterization of CD 200-receptor expression in the murine epidermis. *J InvestDermatol*(2005)125(6):1130–8.doi:10.1111/j.0022-202X.2005.23948.x
86. Van Beneden K, De Creus A, Stevenaert F, Debacker V, Plum J, Leclercq G. Expression of inhibitory receptors Ly49E and CD94/NKG2 on fetal thymic and adult epidermal TCR V gamma 3 lymphocytes. *J Immunol* (2002) 168(7):3295–302. doi:10.4049/jimmunol.168.7.3295
87. Lanier LL. NK cell receptors. *Annu Rev Immunol.* (1998) 16:359–93. doi:10.1146/annurev.immunol.16.1.359
88. Lee N, Llano M, Carretero M, Ishitani A, Navarro F, Lopez-Botet M, et al. HLA-E is a major ligand for the natural killer inhibitory receptor CD94/NKG2A. *Proc Natl Acad Sci U S A* (1998) 95(9):5199–204. doi:10.1073/pnas.95.9.5199
89. Vance RE, Kraft JR, Altman JD, Jensen PE, Raulet DH. Mouse CD94/NKG2A is a natural killer cell receptor for the nonclassical major histocompatibility complex (MHC) class I molecule Qa-1(b). *J Exp Med* (1998) 188(10):1841–8. doi:10.1084/jem.188.10.1841

Conflict of Interest Statement: The authors declare that the research was conducted in the absence of any commercial or financial relationships that could be construed as a potential conflict of interest.

Copyright © 2018 Witherden, Johnson and Havran. This is an open-access article distributed under the terms of the Creative Commons Attribution License (CC BY). The use, distribution or reproduction in other forums is permitted, provided the original author(s) and the copyright owner are credited and that the original publication in this journal is cited, in accordance with accepted academic practice. No use, distribution or reproduction is permitted which does not comply with these terms.

frontiers in Immunology

ORIGINAL RESEARCH
published: 04 April 2018
doi: 10.3389/fimmu.2018.00662

Regulation of Human γδ T Cells by BTN3A1 Protein Stability and ATP-Binding Cassette Transporters

David A. Rhodes[1], Hung-Chang Chen[2†], James C. Williamson[3], Alfred Hill[1], Jack Yuan[1], Sam Smith[1], Harriet Rhodes[1], John Trowsdale[1], Paul J. Lehner[3], Thomas Herrmann[4] and Matthias Eberl[2,5]*

[1] Department of Pathology, University of Cambridge, Cambridge, United Kingdom, [2] Division of Infection and Immunity, School of Medicine, Cardiff University, Cardiff, United Kingdom, [3] Cambridge Institute for Medical Research, University of Cambridge School of Clinical Medicine, Cambridge, United Kingdom, [4] Institut für Virologie und Immunbiologie, Julius-Maximilians-Universität Würzburg, Würzburg, Germany, [5] Systems Immunity Research Institute, Cardiff University, Cardiff, United Kingdom

OPEN ACCESS

Edited by:
David Vermijlen, Université libre de Bruxelles, Belgium

Reviewed by:
Andrew Wiemer, University of Connecticut, United States
Massimo Massaia, Università degli Studi di Torino, Italy

***Correspondence:**
David A. Rhodes
dar32@cam.ac.uk

†Present address:
Hung-Chang Chen, Cancer Research UK Cambridge Institute, University of Cambridge, Cambridge, United Kingdom

Specialty section:
This article was submitted to T Cell Biology, a section of the journal Frontiers in Immunology

Received: 23 January 2018
Accepted: 19 March 2018
Published: 04 April 2018

Citation:
Rhodes DA, Chen H-C, Williamson JC, Hill A, Yuan J, Smith S, Rhodes H, Trowsdale J, Lehner PJ, Herrmann T and Eberl M (2018) Regulation of Human γδ T Cells by BTN3A1 Protein Stability and ATP-Binding Cassette Transporters. Front. Immunol. 9:662. doi: 10.3389/fimmu.2018.00662

Activation of human Vγ9/Vδ2 T cells by "phosphoantigens" (pAg), the microbial metabolite (*E*)-4-hydroxy-3-methyl-but-2-enyl pyrophosphate (HMB-PP) and the endogenous isoprenoid intermediate isopentenyl pyrophosphate, requires expression of butyrophilin BTN3A molecules by presenting cells. However, the precise mechanism of activation of Vγ9/Vδ2 T cells by BTN3A molecules remains elusive. It is not clear what conformation of the three BTN3A isoforms transmits activation signals nor how externally delivered pAg accesses the cytosolic B30.2 domain of BTN3A1. To approach these problems, we studied two HLA haplo-identical HeLa cell lines, termed HeLa-L and HeLa-M, which showed marked differences in pAg-dependent stimulation of Vγ9/Vδ2 T cells. Levels of IFN-γ secretion by Vγ9/Vδ2 T cells were profoundly increased by pAg loading, or by binding of the pan-BTN3A specific agonist antibody CD277 20.1, in HeLa-M compared to HeLa-L cells. IL-2 production from a murine hybridoma T cell line expressing human Vγ9/Vδ2 T cell receptor (TCR) transgenes confirmed that the differential responsiveness to HeLa-L and HeLa-M was TCR dependent. By tissue typing, both HeLa lines were shown to be genetically identical and full-length transcripts of the three BTN3A isoforms were detected in equal abundance with no sequence variation. Expression of BTN3A and interacting molecules, such as periplakin or RhoB, did not account for the functional variation between HeLa-L and HeLa-M cells. Instead, the data implicate a checkpoint controlling BTN3A1 stability and protein trafficking, acting at an early time point in its maturation. In addition, plasma membrane profiling was used to identify proteins upregulated in HMB-PP-treated HeLa-M. ABCG2, a member of the ATP-binding cassette (ABC) transporter family was the most significant candidate, which crucially showed reduced expression in HeLa-L. Expression of a subset of ABC transporters, including ABCA1 and ABCG1, correlated with efficiency of T cell activation by cytokine secretion, although direct evidence of a functional role was not obtained by knockdown experiments. Our findings indicate a link between members of the ABC protein superfamily and the BTN3A-dependent activation of γδ T cells by endogenous and exogenous pAg.

Keywords: butyrophilins, T cells, phosphoantigens, mevalonate pathway, ABCG2, NRF2

INTRODUCTION

Gammadelta (γδ) T cells are a lineage of innate-like "unconventional" T lymphocytes with potent cytotoxic, pro-inflammatory, and regulatory properties. They express, as a defining feature, a T cell receptor (TCR) composed of a γ and δ chain heterodimer, both products of V(D)J recombination, which distinguishes them from conventional αβ T cells (1).

Although often restricted to distinct anatomical locations including skin and intestinal epithelium, both major sites of host interaction with the microbiota and of pathogen entry, the role of γδ T cells in tissue immune surveillance is not fully understood (2, 3). Butyrophilins (BTNs) appear to be pivotal in the maintenance of immune homeostasis in tissue epithelium by controlling the activation of γδ T cells (4). The observed homology to co-receptors, such as CD80, CD86, and PD-L1 (5), initially suggested the possibility of ligands for BTN molecules expressed on the surface of T cells, although identification of such receptors has remained elusive so far (6). Some data are consistent with a direct interaction with the γδ TCR, although this remains to be confirmed (7–9).

Our work aims to understand the function of BTNs in the regulation of γδ T cells and how their dysregulation may contribute to disease. We study the human BTN3A proteins and their role in the activation of Vγ9/Vδ2 T cells, a prominent γδ T cell lineage in human blood and tissues (10). A mandatory role for paired BTN3A molecules in controlling Vγ9/Vδ2 T cell activation has been shown recently (11), and other BTN and BTN-like molecules both in mouse and in humans may similarly control defined γδ T cell subsets. For example, Skint1 determines the Vγ5/Vδ1 dendritic epidermal T cell lineage in murine skin (12, 13), Btnl1 controls the Vγ7+ mouse enterocyte γδ T cell compartment, and BTNL3 and BTNL8 control human colonic Vγ4+ γδ T cells (4). Therefore, this work is likely to be relevant to other systems of γδ T cell selection, homeostasis, and antigen-dependent activation.

The Vγ9/Vδ2 lineage of γδ T cells is known to be activated by exposure to specific "phosphoantigens" (pAg), isopentenyl pyrophosphate (IPP) and (*E*)-4-hydroxy-3-methyl-but-2-enyl pyrophosphate (HMB-PP). IPP is a ubiquitous metabolite in all living cells and the common end product both of the classical mevalonate (also called the HMG-CoA reductase) pathway in eukaryotes and some bacteria and of the alternative non-mevalonate pathway in Gram-negative bacteria, mycobacteria, and malaria parasites. The microbial metabolite HMB-PP is an intermediate of the non-mevalonate pathway, showing 4log10 greater activity over IPP (14, 15). While IPP has a lower bioactivity on Vγ9/Vδ2 T cells in cell culture and lower affinity for the B30.2 domain of BTN3A1 in binding assays compared to HMB-PP, IPP may still play a physiological role *in vivo*. This may be the case where intracellular IPP levels are elevated as a result of dysregulation of the mevalonate pathway, for instance upon treatment of target cells with aminobisphosphonate drugs such as zoledronate, by infection or cellular transformation (16, 17).

In addition to cytokine production and cytotoxicity, Vγ9/Vδ2 cells promote conventional peptide antigen presentation *via* MHC-I- and MHC-II-dependent mechanisms (18–20) and are being investigated as potential tools in cancer immunotherapy (21–26). Further, while γδ T cells generally are linked to inflammatory and autoimmune responses (27, 28), the contribution of the Vγ9/Vδ2 lineage to autoimmune pathology has not been addressed. In these contexts, understanding the molecular basis of their activation by BTN3A-dependent pAg presentation should facilitate their therapeutic manipulation (29).

In initial screens, we identified two HeLa cell lines which differed markedly in their ability to elicit cytokine from cocultured γδ T cells. We have used this model to investigate the function of BTN3A molecules in this process and to identify novel components. The data indicate that environmental exposure, such as treatment of cells with the cytotoxic anticancer drug doxorubicin (DOX), may influence γδ T cell activation by regulation of BTN3A protein stability or trafficking and expression of ATP-binding cassette (ABC) transporters *via* the KEAP1/NRF2 stress response pathway.

MATERIALS AND METHODS

Expression Constructs

Primer sequences are listed in Table S1 in Supplementary Material. DNA encoding specific shRNA oligos directed to BTN3A isoforms, periplakin, and ABCG2 were cloned into pHR-SIREN/puro using *Bam*HI/*Eco*RI as described previously (30). Virus particles were produced by co-transfection of 293T cells with pCMV8.91 (gag-pol) and pMDG (VSV-G env) plasmids. Supernatant was harvested after 48 h, filtered, and used to transduce HeLa cells. Clones were selected by puromycin (1 μg/ml) for 24 h. shRNA oligonucleotide sequence targeting all BTN3A isoforms was: shBTN3A.CGTGTATGCAGATGGAAAG. For re-expression, HeLa shRNA^{BTN3A} cells were co-transduced with lentivirus carrying variant BTN3A1 sequences. Green fluorescent protein (GFP) positive cells were sorted using BD FACSAria cell sorter.

Cell Lines and DNA Constructs

HeLa-M (a gift from Dick van den Boomen CIMR, Cambridge) and HeLa-L (from Will McEwan, MRC-LMB, Cambridge) cervical carcinoma cells were grown in standard tissue culture conditions using RPMI-1640 medium plus 10% FCS, penicillin/streptomycin (100 U/ml) and L-glutamine (2 mM). Cells were routinely checked for mycoplasma (MycoAlert Lonza LT07-218). HLA typing was performed by Addenbrooke's Hospital Histocompatibility and Immunogenetics (Tissue Typing) laboratory. Human embryonic kidney 293T and bladder carcinoma EJ28 cells were also grown in supplemented RPMI-1640 medium. Human foreskin fibroblasts HFF-T and fetal lung MRC-5T, both immortalized by expression of hTERT, the catalytic subunit of human telomerase (a gift of Stephen Graham, Department of Pathology) were grown in supplemented DMEM medium.

Cells (1×10^5) growing in six-well plates were transfected with DNA expression constructs using Fugene (Promega). For RT-PCR, total RNA was prepared from cultured cells using RNAeasy mini (Qiagen) and Superscript III (Invitrogen) used to

produce first strand cDNA. Amplification was carried out using 2× BiomixRed Taq polymerase (Bioline). RT-PCR products were analyzed by gel electrophoresis and cloned using Zero-Blunt Topo (Invitrogen).

Killing assay was by propidium iodide (PI) dye exclusion in cells treated with doxorubicin DOX (Cell Signaling). Cells were harvested and stained in 100 µl PBS (2.5 µg/ml PI) for 5 min before washing and analysis by fluorescence activated cell sorting (FACS) on a BD FACScalibur and data points collected on FL3/FSC. Inhibitors MG132 (5 µM for 5 h) and bafilomycin A (bafA) (5 µM 10 h) were used in cell assays. For activation, supernatants were collected from 24 h cocultures of Vγ9/Vδ2 T and HeLa-M cells containing 10 nM HMB-PP (Echelon) and used at a 1/10 dilution for 24 and 48 h.

Immunoblot and Quantitative Mass Spectroscopy of Surface-Biotinylated Proteins

Cell lysates were prepared in buffer (50 mM Tris–Cl pH 7.5, 150 mM NaCl, 1% Triton-X, EDTA-free protease inhibitor, Roche) by incubation for 10 min at 4°C, then pre-cleared by centrifugation. For immune blots, cleared lysates were solubilized in SDS-PAGE buffer (5 min, 95°C) and separated in 10% SDS-PAGE gels (NextGel) then transferred to PVDF membrane. Antibodies were added directly to blocked membranes (5% Marvel/PBS 0.1% Tween 20) and incubated for 1 h with primary and HRP-conjugated secondary antibodies. Blots were visualized with ECL reagent (GEhealthcare) before exposure to X-ray film (Fuji). Monoclonal CD277 20.1 (LifeSpanBio), NRF2 (AF3925 R&D Systems), ABCG2 (ab108312) anti-calnexin (3811-100), and anti-GFP (SAB4301138) were used as well as 056 and B6 rabbit anti-B30.2 polyclonal sera at concentration between 0.5 and 1 µg/ml (30). Cell fractionation was carried out using Qproteome cell compartment kit (Qiagen).

For plasma membrane profiling (PMP), HeLa-M cells (5×10^7) in large T175 flasks were either left untreated or treated with HMB-PP (10 nM for 10 h). Cells were washed (1× PBS) then biotinylation reagents added (30 min at 4°C). After quenching, cells were harvested by scraping and processed for immunoprecipitation, by lysis in 1% Tx-100 TBS pH 8 buffer with protease inhibitor (Complete EDTA free, Roche) and end-over-end rotation for 30 min at 4°C. After centrifugation (10,000 *g* for 10 min), Streptavidin agarose resin (Thermo Fisher) was added to supernatants, with incubation for 2 h at 4°C. Agarose beads were washed (20×) in lysis buffer, 20× in 0.5% SDS in PBS, 20× in 6 M urea/triethylammonium bicarbonate (TEAB) pH 8.5, 5× in TEAB pH 8.5 before digestion overnight with 0.5 µg trypsin in a final volume of 50 µl TEAB (31). Resulting peptides were analyzed by LC-MS/MS analysis using an Orbitrap Fusion instrument (Thermo Fisher) utilizing a 60-min gradient. Raw data were searched using MASCOT from within Proteome Discoverer (Thermo Fisher) v2.0 against the Uniprot human reference proteome. Peptide identifications were controlled at 1% FDR using Mascot Percolator. Proteins were quantified in a label-free manner using the precursor ion quantifier node.

T Cell Assays

Ethical approval for working with blood samples from healthy donors was obtained from the South East Wales Local Ethics Committee (08/WSE04/17) and the Cambridge Local Ethics Committee (HBREC.2015.27). All volunteers provided written informed consent.

Vγ9/Vδ2 T cells were expanded from peripheral blood mononuclear cells of healthy donors with 1 µM zoledronate (Zometa; Novartis) and 50 U/ml IL-2 (Proleukin, Chiron) for 14 days and further enriched to purities >98% CD3+ Vγ9+ by negative selection using a modified human γδ T cell isolation kit that depletes B cells, αβ T cells, NK cells, dendritic cells, stem cells, granulocytes, and monocytes (Stem Cell Technologies). Unless otherwise stated, target HeLa cells were pretreated with 10 µM zoledronate or 10 nM HMB-PP, then washed extensively before coculture with γδ T cells at a ratio of 1:10 (10^4 target: 10^5T effector cells). The amount of IFN-γ secreted into the culture supernatant over 24 h was measured by ELISA (eBioscience). Mobilization of CD107a onto the cell surface over the first 5 h of coculture was determined using a PE-conjugated anti-CD107a antibody (H4A3; BD Biosciences) in the presence of monensin at a 1:2,000 dilution (GolgiStop). Cells were acquired on a FACS Canto II and analyzed with FlowJo. HeLa cells were also incubated with agonist CD277 20.1 monoclonal antibody (eBioscence) to induce activation independently of phosphoantigen.

The murine T cell hybridoma 53/4r/mCD28 TCR MOP was used to test Vγ9/Vδ2 TCR mediated activation, as described (32). In these experiments, HeLa cells used as stimulators (10^4) were seeded in 96-well flat bottom tissue culture plate, allowed to adhere for 1 day before addition of T cells in fresh culture medium. Production of mouse IL-2 in culture supernatants was tested with a commercial mouse IL-2 ELISA kit.

RESULTS

Two Haplo-Identical HeLa Cell Lines, HeLa-L and HeLa-M, Show Marked Variation in Their Ability to Activate Vγ9/Vδ2 T Cells *via* BTN3A

Various tumor-derived and primary epithelial cell lines were tested for their ability to respond to the aminobisphosphonate drug zoledronate and present the microbial compound HMB-PP to Vγ9/Vδ2 T cells (Figure S1A in Supplementary Material). Two HeLa cervical epithelium carcinoma cell lines, HeLa-L and HeLa-M, showed profound differences in their ability to elicit cytokine (**Figure 1**; Figure S1 in Supplementary Material). HeLa-M cells were far more potent than HeLa-L cells in stimulating release of IFN-γ (**Figure 1A**; Figure S1B in Supplementary Material) and TNF-α (Figure S1C in Supplementary Material) upon pretreatment with HMB-PP. Responses to zoledronate similarly differed between the two cell lines (data not shown). Responses to either HeLa cell line were abrogated by expression of a single shRNA targeting the three BTN3A isoforms (shRNA^{BTN3A} cells), confirming the importance of BTN3A in mediating

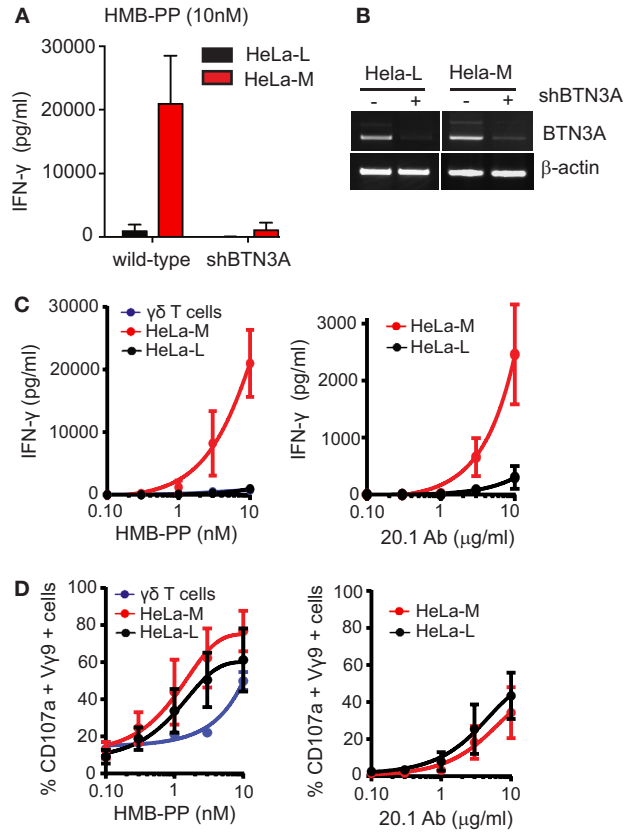

FIGURE 1 | HLA haplo-identical HeLa-L and HeLa-M cells vary in their ability to present phosphoantigens to Vγ9Vδ2 T cells. **(A)** Vγ9/Vδ2 T cell activation as detected by production of IFN-γ. Wild-type and shRNA^{BTN3A} HeLa-L and HeLa-M cells were pretreated with hydroxy-3-methyl-but-2-enyl pyrophosphate (HMB-PP) (10 nM for 5 h) before addition of expanded Vγ9/Vδ2 T cells at E:T ratio of 10:1. After overnight incubation, culture supernatants were analyzed by ELISA. Bar chart shows mean and SD from triplicate measurements using T cells from one donor and is representative of three independent experiments using T cells from separate donors. **(B)** Knockdown of BTN3A expression by shRNA expression in HeLa cells. Transcripts for BTN3A and β-actin were amplified by RT-PCR from wild-type and shRNA^{BTN3A} HeLa-L and HeLa-M cDNA template and products analyzed by gel electrophoresis. PCR results shown are representative of three independent experiments. **(C)** Activation of Vγ9/Vδ2 T cells detected by ELISA for IFN-γ as in **(A)** using a concentration gradient of HMB-PP, agonist antibody CD277 20.1 and T cells expanded from two separate donors. Activation was induced by pretreatment of HeLa cells using HMB-PP for 5 h (left panel) and anti-BTN3A monoclonal antibody 20.1 for 30 min (right panel). Graphs show mean and SD from $n = 2$ and are representative of two independent measurements. **(D)** Activation of Vγ9/Vδ2 T cells as detected by flow cytometry for percent double positive Vγ9 and CD107a cells after coculture experiments as in **(C)**.

Vγ9/Vδ2 T cell responses to both HMB-PP and zoledronate (**Figures 1A,B**).

The differential responsiveness of Vγ9/Vδ2 T cells to HeLa-L and HeLa-M cells was replicated when using the pan-BTN3A specific agonist antibody CD277 20.1, which induces BTN3A-dependent activation of Vγ9/Vδ2 T cell activation in the absence of HMB-PP or zoledronate (**Figure 1C**). In addition, production of IL-2 from a murine T cell hybridoma expressing human Vγ9/Vδ2 transgenes showed a similar differential response to HMB-PP (Figure S1D in Supplementary Material).

In striking contrast to these findings of cytokine secretion as a functional read-out for T cell responses, surface mobilization of CD107a/LAMP1 did not differ between Vγ9/Vδ2 T cells responding to the two HeLa lines, upon HMB-PP or CD277 20.1 antibody pretreatment (**Figure 1D**), indicating differential signaling requirements for the induction of cytokine secretion versus CD107a mobilization.

Taken together, these experiments demonstrated that HeLa-M cells were more efficient at activating Vγ9/Vδ2 T cells *via* BTN3A than HeLa-L cells, with regard to the induction of cytokine expression but not CD107a mobilization. These cell lines, therefore, represent a useful experimental model to investigate the molecular mechanism underlying the specific Vγ9/Vδ2 T cell responses to endogenous and exogenous pAg.

BTN3A Transcripts Are Identical in HeLa-L and HeLa-M

In order to account for the functional differences between HeLa-L and HeLa-M cells, full-length BTN3A transcripts were amplified by RT-PCR from HeLa cDNA, cloned, and sequenced (**Figure 2**). As shown in **Figure 2A**, transcripts of all three BTN3A isoforms were expressed at comparable levels in both HeLa-L and HeLa-M, with no differences in splicing and all were targeted with equal efficiently by shRNA. No sequence variation or mutation was detected when six clones from each cell line for each BTN3A isoform were compared to consensus sequences (BTN3A1 NM_007048, BTN3A2 NM_007047, BTN3A3 NM_006994) (data not shown). Known synonymous SNPs common in sub-Saharan Africa, but rare in other populations, were identified in all BTN3A1 sequences (dbSNP rs3857550, rs2393650, and rs537072716), suggesting that both HeLa lines were homozygous for these polymorphisms. BTN3A2 and BTN3A3 nucleotide sequences showed no polymorphisms; however, allelic exclusion or haplotype bias in transcript expression was not assessed. By tissue typing of genomic DNA, both HeLa cell lines were HLA-A68-B15:03/15 -Bw6 -C12 -DR 01:02/01:2601 haplo-identical. These data provided convincing authentication of the HeLa lines by conformation of their common genetic origin.

Cellular Markers of Activation Are Unaffected

Transcripts for BTN3A1 were shown to be induced by type I and type II interferons and HeLa-L and HeLa-M cells did not differ in this regard (**Figure 2B** and data not shown). By cytometry, there was comparable upregulation of surface MHC-I and MHC-II by IFN-γ treatment; however surface staining using CD277 20.1 antibody was not detected, indicating a discrepancy between transcriptional regulation and protein expression (**Figure 2C**).

In order to investigate the possibility of a soluble factor influencing T cell activation and also a more physiologically relevant stimulus potentially influencing BTN3A1 expression, we studied the response of both HeLa lines to treatment with supernatants collected from 24 h cocultures of Vγ9/Vδ2 T cells activated with HMB-PP (10 nM) loaded HeLa-M cells. Transcripts for a

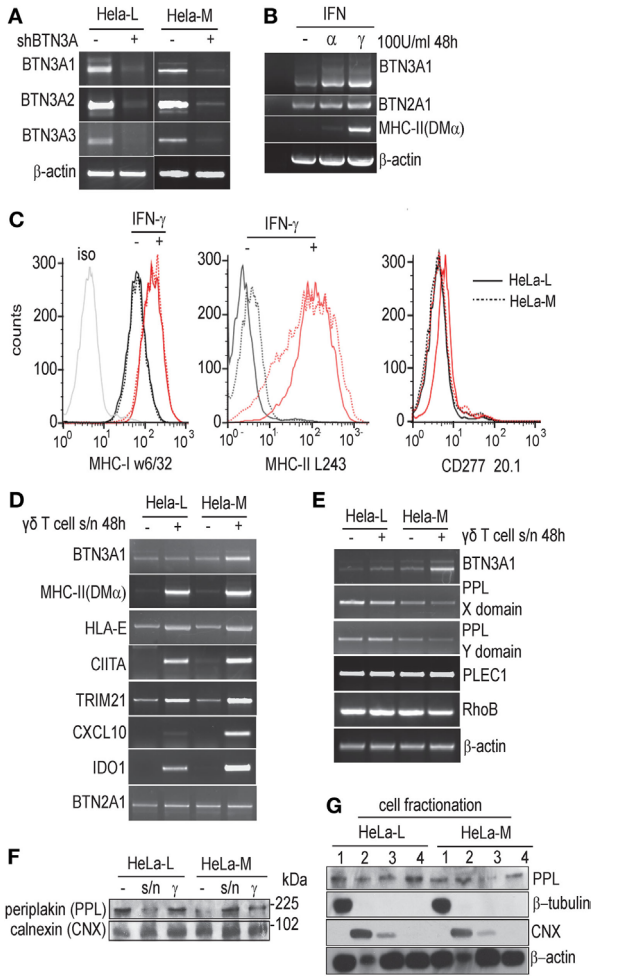

FIGURE 2 | Transcripts for the three BTN3A isoforms are unchanged in HeLa-L and HeLa-M. **(A)** Amplification of full-length BTN3A1, BTN3A2, and BTN3A3 transcripts by RT-PCR from wild-type and shRNA^{BTN3A} HeLa-L and HeLa-M cDNA template. **(B)** RT-PCR for BTN3A1, BTN2A1, and MHC-II (DMα) from cDNA derived from HeLa-M cells either left untreated or treated with IFN-α or IFN-γ. RT-PCR products were analyzed by gel electrophoresis, with β-actin as loading control. Results are representative of three experiments. **(C)** Analysis of activation markers MHC-I (w6/32), MHC-II (L243), and BTN3A (CD277 20.1) by flow cytometry in HeLa cells treated with or without IFN-γ. Results representative of triplicate experiments. Red lines indicate IFN-γ treated and black lines untreated samples. Solid lines are HeLa-M and dotted lines HeLa-L. **(D)** Expression of activation markers as detected by RT-PCR in HeLa-L and HeLa-M cells left untreated or treated with γδ T/HeLa-M cell coculture supernatant collected as described (see Materials and Methods). Transcripts for BTN3A1, HLA-E, DMα, CIITA, TRIM21, CXCL10, IDO-1, and BTN2A1 were amplified and visualized by gel electrophoresis. Results are representative of duplicate experiments. **(E)** Expression of the BTN3A1 interacting molecules protein periplakin (PPL) and RhoB in treated and untreated HeLa-L and HeLa-M cells analyzed by RT-PCR, as in **(C)**, with transcripts for β-actin as a loading control. Results are representative of duplicate experiments. **(F)** Lysates from HeLa-L and HeLa-M cells left untreated or treated with γδ T/HeLa-M cell coculture supernatant or IFN-γ, were analyzed by western blot for expression of PPL protein. Duplicate blots were probed with calnexin (CNX) antibody as a loading control. **(G)** Cell fractionation to compare the sub-cellular distribution of PPL protein in HeLa-L and HeLa-M cells. Fractions for soluble (1), membrane (2), nuclear (3), and cytoskeletal/detergent resistant membrane (4) fractions were prepared and analyzed by western blot using anti-PPL, β-tubulin, CNX, and β-actin antibodies.

number of activation markers, including MHC-II DMα, HLA-E, MHC-II trans-activator CIITA, and TRIM21 were analyzed by RT-PCR in addition to BTN3A1 (**Figure 2D**). Some variation in HeLa-derived transcripts was detected, particularly CXCL10 and IDO-1 and a slight increase in BTN3A1 transcripts upon activation in HeLa-M was not seen in HeLa-L. However, convincing BTN3A expression or activation at the cell surface was not detected by cytometry using CD277 20.1 antibody as for **Figure 2C** (data not shown). BTN2A1 transcripts did not vary between samples, and there was no correlation between butyrophilin BTN2A or BTN3A expression and CIITA/MHC-II in HeLa cells (6). A more detailed quantitative analysis of some transcripts, for example CXCL10 or IDO-1 may be warranted, but the data so far were not consistent with a major signaling defect in either HeLa line which could account for differential responses in T cell assays or with transcriptional control affecting BTN3A1 activation.

No Variation in Expression of BTN3A1 Interactors

The cytoskeletal adaptor protein periplakin (PPL) and the RAS-superfamily GTPase RhoB were recently identified as BTN3A1 interacting molecules (30, 33). We tested whether the differential BTN3A1-dependent responsiveness of Vγ9/Vδ2 T cells to HMB-PP loaded HeLa-L and HeLa-M might be due to variation in PPL and/or RhoB expression. In duplicated RT-PCR experiments, transcripts for PPL were slightly more abundant in HeLa-L compared to HeLa-M. By analyzing separate domains of the mRNA, no variation in splicing which conceivably could affect protein interactions or shRNA-mediated transcript suppression was detected (**Figure 2E**). In addition to PPL itself, we detected transcripts for the PPL interacting molecule PLEC1 (**Figure 2E**) but not for kazrin or envoplakin (34–36). RhoB transcripts were detected abundantly in both HeLa lines and were not obviously affected by activation with γδ T cell/HeLa-M coculture supernatants. By western blot, major variation in PPL protein level was not detected between the HeLa cell lines either with, or without, activation using IFN-γ or using T cell supernatants (**Figure 2F**). Neither did we see any discrepancy in cellular distribution by cell fractionation; PPL was distributed equally in soluble, membrane, nuclear, and cytoskeletal/detergent resistant membrane fractions as shown previously (**Figure 2G**) (30).

These experiments suggested that differences in the expression of BTN3A1 interacting molecules did not account for the functional variation between HeLa-L and HeLa-M cells. By contrast, in a direct comparison in T cell assays of HeLa-L and HeLa-M PPL knockdown lines, produced by expression of three different PPL targeting shRNA (Figure S2 in Supplementary Material), wide variation in responses as measured by IFN-γ was detected. The PPL knockdown experiments were consistent with our initial conclusion of a regulatory rather than mandatory role for PPL in transmitting activation signals to T cells (30).

Detection of BTN3A1 by Re-Expression in shRNA^{BTN3A} Cells

Although mRNA transcripts were detectable, BTN3A proteins were not abundantly expressed in HeLa cells. In addition, CD277 20.1 antibody binding to HeLa cells was not convincing

by cytometry (**Figure 2C**), despite the fact that this agonistic antibody elicited potent Vγ9/Vδ2 T cell activation (**Figure 1B**). In order to overcome the limitations posed by low expression levels, we re-expressed BTN3A isoforms in wild-type and BTN3A knockdown (shRNA^{BTN3A}) cells using a lentiviral vector which afforded an independent marker of transgene expression via detection of GFP (**Figures 3A,B**).

By transient transfection of either HeLa-L or HeLa-M with expression vectors for BTN3A1, BTN3A2, and BTN3A3, significant surface CD277 20.1 antibody staining was not detected for any of the three BTN3A isoforms, even with high GFP transgene expression (Figure S2A in Supplementary Material). In contrast, BTN3A2 and BTN3A3, but not BTN3A1, were productively expressed on the surface of 293T cells using the same transfection strategy, indicating that surface expression of BTN3A/CD277 was tightly regulated, by a mechanism which targeted BTN3A1 preferentially and which differed between cell lines.

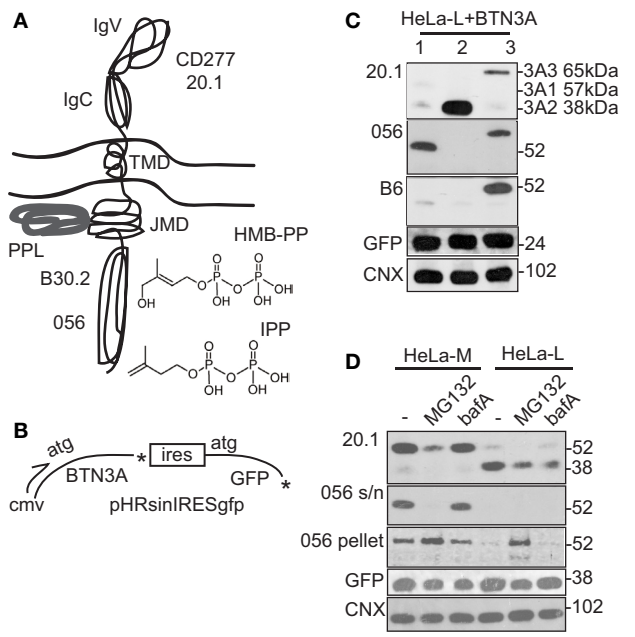

FIGURE 3 | Detection of BTN3A1 by re-expression in shRNA^{BTN3A} cells. **(A)** Diagram of BTN3A1 protein and structure of the two principal stimulatory phosphoantigens (pAg) hydroxy-3-methyl-but-2-enyl pyrophosphate (HMB-PP) and isopentenyl pyrophosphate (IPP). Sites of pAg interaction in the BTN3A1 B30.2 domain, protein periplakin (PPL) interaction at the juxta-membrane domain (JMD) and the antibodies used for detection are highlighted. BTN3A3 has a structure similar to BTN3A1, whereas BTN3A2 is truncated after the JMD and lacks the B30.2 domain. **(B)** Diagram of BTN3A pHRsinIRESgfp lentiviral expression vector used in re-expression studies. Independent measure of transgene expression is provided by internal ribosome entry site (IRES) driven green fluorescent protein (GFP). **(C)** Western blot of HeLa-L cells transiently transfected with expression vectors for BTN3A1, BTN3A2, and BTN3A3. Monoclonal anti-BTN3A (CD277 20.1) antibody and polyclonal sera 056 and B6, directed to B30.2 domains of BTN3A1 and BTN3A3, respectively, were used. Anti-GFP and calnexin (CNX) antibodies provided loading controls for expression of transgene and endogenous proteins, respectively. **(D)** Western blot analysis of stable BTN3A1 re-expression lines of HeLa-L and HeLa-M shRNA^{BTN3A} cells, either left untreated or treated with MG132 or bafilomycin A (bafA). Anti-CD277 20.1 antibody and polyclonal sera 056 were used, together with anti-GFP and CNX control antibodies as in **(C)**. Detection of CD277 20.1 and 056 reactive protein bands required extended exposure to X-ray film.

By western blot analysis of lysates from transiently transfected cells, there was marked variation in the ability of CD277 20.1 antibody to detect the different BTN3A isoforms (**Figure 3C**; Figure S2B in Supplementary Material). While BTN3A1 was barely detectable, BTN3A2 was abundant (at levels expected from transgene expression) and BTN3A3 was expressed at intermediate levels. Authentic expression of full-length proteins was confirmed in some experiments using isoform specific antisera directed against the B30.2 domains of BTN3A1 and BTN3A3 (**Figure 3C**; Figure S2 in Supplementary Material), requiring extended exposure to X-ray film.

The above experiments indicated an intracellular checkpoint to BTN3A1 expression. To determine if this was mediated by protein degradation, we tested the effect of the proteasome inhibitor MG132 and bafA, an inhibitor of lysosome/autophagy pathways, on BTN3A1 expression in lentivirally transduced HeLa-L and HeLa-M shRNA^{BTN3A} cells (**Figure 3D**). By western blot using CD277 20.1 antibody, full-length soluble BTN3A1 (57 kDa) was detected in the untreated HeLa-M re-expression line, but was barely detectable in the HeLa-L lysate. Instead, a lower molecular weight band of 38 kDa was detected in HeLa-L samples, indicative of BTN3A1 protein cleavage. Alternatively, the 38-kDa protein could represent endogenous BTN3A2, although BTN3A2 was not detected abundantly in un-transfected cell lines (Figure S3 in Supplementary Material). Levels of detergent-soluble, full-length BTN3A1 were reduced by MG132 treatment, but were unaffected by bafA. In contrast, MG132 treatment of HeLa-L cells led to the appearance of full-length BTN3A1 (57 kDa) in the detergent resistant fractions from Tx-100 lysates, suggesting a potential redistribution of BTN3A1 in the membrane by proteasome inhibition.

Taken together, these results were consistent with a mechanism controlling surface expression of BTN3A protein isoforms, in particular BTN3A1, by protein production, stability, or trafficking.

PMP of HMB-PP Treated Cells Identifies ABCG2

We next searched for differences in cellular factors that might influence pAg presentation in the two HeLa cell lines using surface biotinylation, followed by immunoprecipitation and quantitative mass spectroscopy (37). Bulk HeLa-M cells were allowed to adhere (10 h), then were either left untreated or treated with HMB-PP (10 nM for 10 h) prior to PMP as described (38).

By this approach, ABCG2 (also called breast cancer resistance protein) was identified as a candidate whose expression was significantly influenced by HMB-PP in HeLa-M cells (**Figure 4A**). ABCG2 is a member of the superfamily of ABC transporters and was originally characterized as a drug efflux pump (39). Variation in expression was modest (log2 = 2.69 increase), but several independent peptides of ABCG2 were detected. FAM129B, a molecule involved in RAS activation, was another candidate potentially affected by HMB-PP treatment (log2 = 2.15 increase) (40). By RT-PCR from the panel of untreated versus treated HeLa cDNA (**Figure 4B**), transcripts for

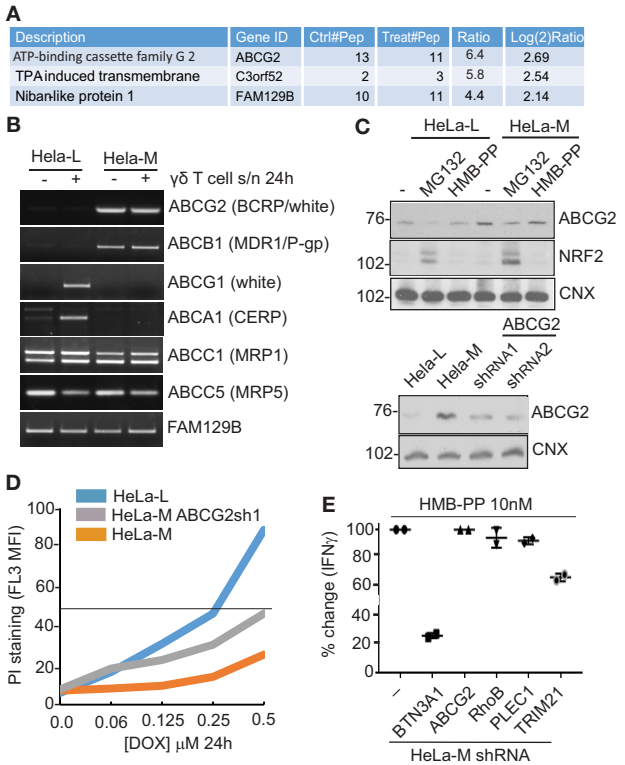

FIGURE 4 | Plasma membrane profiling (PMP) by mass spectroscopy identifies ABCG2. **(A)** Table of top hits identified using PMP to compare HMB-PP treated and untreated HeLa-M cells. Several independent peptides of ATP-binding cassette (ABC) transporter ABCG2 were detected, with modest increase (log_2 2.69) by treatment. Other potential candidates by these criteria (C3orf52 and FAM129B) are listed and were less significant. **(B)** Dysregulation of a subset of ABC transporters, including ABCG2, in HeLa cells detected by RT-PCR. Template cDNA was prepared from total RNA from HeLa-L and HeLa-M cells left untreated or treated with γδ T cell supernatant for 24 h. RT-PCR products were analyzed by gel electrophoresis. **(C)** Variation in ABCG2 protein expression in HeLa cells by western blot. Top panel: HeLa-L and HeLa-M cells were left untreated or treated with MG132 (5 μM for 10 h) or HMB-PP (10 nM for 10 h). Cell lysates were prepared and analyzed using antibodies directed to ABCG2, NRF2, and calnexin (CNX), which acts as a loading control. Bottom panel: western blot analysis of $shRNA^{ABCG2}$ cells confirms reduction in ABCG2 protein expression. **(D)** HeLa-M cells show ABCG2-dependent resistance to cytotoxic drug doxorubicin (DOX). Wild-type HeLa-M, HeLa-L, and $shRNA^{ABCG2}$ HeLa-M cells were incubated (24 h) with DOX at the indicated concentrations. Cells were stained using propidium iodide (PI) (2.5 μg/ml for 5 min) as a marker of plasma membrane integrity. After washing, cells were analyzed by cytometry. Chart shows mean fluorescence intensity (MFI) of PI staining. **(E)** No effect on T cell activation using $shRNA^{ABCG2}$ HeLa-M cells. The effect on the efficiency of Vγ9/Vδ2 T cell activation for a series of HeLa-M gene knockdown lines, including shRNA BTN3A1, ABCG2, RhoB, PLEC1, and TRIM21. Cells were pretreated with HMB-PP (10 nM for 6 h) before Vγ9/Vδ2 T cells from a single donor were applied. Coculture was allowed to proceed overnight when culture supernatants were analyzed by ELISA. Chart shows percent (%) change in detected IFN-γ relative to wild-type HeLa-M cells of duplicate determinations for each cell line.

ABCG2 were reduced in HeLa-L compared to HeLa-M samples, an observation not seen for other candidates, while FAM129B transcripts did not vary (**Figures 2C,D**). Reduced expression of ABCG2 total protein in HeLa-L compared to HeLa-M cell lysate was confirmed by western blot (**Figure 4C**), but variation in expression by HMB-PP treatment was not and surface ABCG2 was not detected by flow cytometry. However, reduced levels of ABCG2 by MG132 treatment was seen (**Figure 4C**), similar to that detected for BTN3A1 (**Figure 3D**). Expression of NRF2 (nuclear factor erythroid 2-related factor 2), a basic leucine zipper (bZIP) protein and major transcriptional regulator of ABCG2, was stabilized in the MG132 treated samples as expected, with increased levels of NRF2 evident in HeLa-M versus HeLa-L samples, consistent with the higher expression of ABCG2 in these cells (**Figure 4C**).

From these data, ABCG2 was the most promising candidate to account for the differential effects of the HeLa cell lines in T cell assays, implicating this molecule in pAg presentation. Therefore, HeLa-M cells expressing shRNA targeting ABCG2 ($shRNA^{ABCG2}$) were constructed. Reduced ABCG2 expression in $shRNA^{ABCG2}$ cells was confirmed by western blot (**Figure 4C** bottom panel) as was a functional effect in killing assays, by increased sensitivity to DOX, a major target substrate of ABCG2 (**Figure 4D**). However, in coculture assays with Vγ9/Vδ2 T cells, no effect on the efficiency of T cell activation of HMB-PP loaded HeLa-M $shRNA^{ABCG2}$ cells was detected, as measured by ELISA for IFN-γ (**Figure 4E**). With $shRNA^{BTN3A}$ cells acting as control, a modest effect of $shRNA^{TRIM21}$ cells was detected in these experiments, but no effect of $shRNA^{RhoB}$ or $shRNA^{PLEC1}$ cells. RhoB has been implicated previously in pAg presentation using similar shRNA-mediated knockdown (33), so the lack of specific effects in our experiments may be indicative of ineffective transcript suppression or variation between different cell lines. The mechanism by which TRIM21 may be affecting γδ T cell activation is unexplained (41).

Expression of a number of functionally related ABC transporters was examined by RT-PCR in the activated HeLa cell panel, including ABCB1 (multidrug resistance 1, MDR1), ABCG1 (white), ABCA1 (cholesterol export regulatory protein, CERP), ABCC1 (multi-resistance protein 1), and ABCC5 (multi-resistance protein 5). While expression of the latter two (ABCC1 and ABCC5) did not vary, transcripts for ABCB1, ABCG1, and ABCA1 did (**Figure 4B**). ABCB1 showed a pattern of expression similar to ABCG2, while ABCG1 and ABCA1 transcripts were only detected in treated samples of HeLa-L, and not in HeLa-M.

Taken together, the results revealed dysregulated expression of a subset of ABC transporters, which correlated with efficiency of γδ T cell activation, suggesting a link between these members of the ABC protein superfamily and pAg-dependent γδ T cell activation.

DISCUSSION

Butyrophilin BTN3A proteins are the critical determinants of pAg presentation to Vγ9/Vδ2 T cells, but their precise role and how they are regulated is not fully understood. In order to address this issue and with a view to identifying novel effectors, we studied two HeLa cell lines which showed marked differences in their ability to activate Vγ9/Vδ2 T cells in response to pAg loading. Endogenous levels of all BTN3A isoforms were low in HeLa cells

and were not detected by western blotting or flow cytometry. By PMP using quantitative mass spectroscopy in HeLa-M cells that were untreated or treated with HMB-PP, BTN3A1 and BTN3A2 isoforms were detected at low levels, with minor variation by treatment. Subsequent experiments using PMP may allow for interrogation of endogenous BTN3A proteins, their regulation by pAg and correlation with T cell activation in different presenting cells (42).

BTN3A1 protein stability at steady state, where BTN3A1 transgene re-expression was carefully controlled by GFP, was reduced significantly compared to that of the other isoforms, BTN3A2 and BTN3A3. We also detected differences in BTN3A1 protein between the two HeLa cell lines. The data are consistent with regulation of BTN3A1 at the level of protein stability. Protein truncation, presumably resulting from proteolytic cleavage to remove the B30.2 domain was also evident using anti-BTN3A antibodies. The possibility that posttranslational modification, for instance by N-linked glycosylation, may be influencing CD277 20.1 antibody recognition of BTN3A1 by affecting protein trafficking and stability cannot be ruled out. It is also unclear whether the free B30.2 domain, a potential degradation intermediate, has a separate function.

It is possible that specific miRNA or mRNA processing, resulting in a block or premature stop in translation could account for truncated and/or reduced protein levels, although no effect on BTN3A1 transcripts in re-expression lines was detected by RT-PCR. Since inhibitor MG132 did not give a clear picture of protein stabilization, as exemplified here by stabilization of NRF2, it is not clear whether BTN3A1 instability is due to proteasome function. Lysosomal inhibition also had no effect. Therefore, another mechanism of protein maturation and trafficking, acting at the level of protein translation or membrane insertion may be involved.

Control of BTN3A1 stability would provide a dynamic mechanism to control Vγ9/Vδ2 T cell activation, similar to that shown for the homologous molecule PD-L1 in controlling αβ T cell responses (43). The fact that BN3A1 expression appears to be limiting over BTN3A2 will also influence interactions between the two isoforms, proposed recently to be essential for Vγ9/Vδ2 T cell activation (11). Regulation of BTN3A1 stability would also offer a means to modulate immune-surveillance by Vγ9/Vδ2 T cells, representing a potential immune-evasion mechanism exploited by tumors and intracellular pathogens.

ABCG2 was identified as a potential candidate protein in pAg-dependent T cell activation using PMP of HMB-PP treated HeLa-M cells. ABCG2 correlates functionally with dye negative side population, a biomarker of cancer stem cells (44) and was considered an interesting functional candidate in pAg presentation because of the known association with statins, cholesterol metabolism, and the HMG-CoA reductase pathway (45, 46). However $shRNA^{ABCG2}$ knockdown cells showed no functional defect in T cell assays. It is possible that shRNA did not reduce ABCG2 levels sufficiently in HeLa-M^{ABCG2} cells to influence this assay, or that other members of the ABC transporter family with similar expression and substrate profile (for example, ABCB1) compensated for its absence in these cells.

In addition to ABCG2 and ABCB1, transcription of ABCA1 and ABCG1 was dysregulated. ABCA1 and ABCG1 are also linked functionally to cholesterol metabolism, acting as regulators of cholesterol transport (47, 48). Since these molecules are not known to be induced by pro-inflammatory cytokines, it is unclear what signals from the γδ T cell supernatant, derived from cocultures with HeLa-M cells containing 10 nM HMB-PP, induced transcription of ABCA1 and ABCG1 in HeLa-L cells but not in HeLa-M. Published data describe a role in γδ T cell activation for ABCA1 acting together with BTN3A1 as a pAg efflux transporter in myeloid cells, linked to the LXR (liver X receptor) transcription factor (49). In the ABCA1 efflux model (49), ABCA1 drives IPP into the extracellular compartment to activate γδ T cells *in trans*. In our system, ABCA1 expression in activated HeLa-L cells would theoretically reduce intracellular HMB-PP concentration to thereby limit the pool available to activate BTN3A1. However, ABCA1 did not enhance T cell activation by HMB-PP-loaded HeLa-M because it did not appear to be expressed in these cells. Therefore, ABCA1 alone cannot account for the effects we detected, and it is also difficult to resolve an extracellular pAg delivery and sensing mechanism with the binding of pAg to the cytosolic B30.2 domain of BTN3A1 (9), unless this interaction promotes pAg export to bind BTN3A1 externally, as proposed by other workers (7, 50).

Conventional MHC restricted antigen presentation to TCR expressed on αβ T cells relies on peptide transport by the heterodimeric TAP1/2 transporter, and it is plausible that pAg transport similarly requires ABC family members. Other workers have investigated ABCC5 (51) in addition to ABCA1 (49). Although most are described as drug or xenobiotic efflux pumps contributing to a multidrug resistance phenotype, endogenous substrates for many ABC transporters are largely uncharacterized. If these ABC transporters are involved, evidently there is more complexity in this system than current models of pAg presentation allow, in particular whether pAg transport is into or out of cells (or both) (50, 52) and whether they influence BTN3A expression by direct interaction (49). Further analysis of these ABC transporters seems warranted.

HeLa cells were the first cell line to be used for biomedical research, originating in the 1950s (53). HeLa-L and HeLa-M are two sublines the origins of which are obscure but which our data so far indicate are genetically identical. The cell lines were free of mycoplasma or other detectable infection and the chance observation of differences in pAg presentation and interaction with expanded Vγ9/Vδ2 T cells derived from different donors were stable for over 3 years with repeat samples acquired from original sources. The HeLa-M line historically showed elevated responses to IFN-γ (54) and in our hands showed resistance to the anticancer drug DOX in dye-exclusion killing assay, an effect reversed to some extent by ABCG2 knockdown. A feasible scenario, therefore, would be selection by an anticancer drug such as DOX resulting in DNA mutation (55), permanent activation of the KEAP1/NRF2 stress response pathway and increased ABCG2 expression in these cells (56). A similar approach was used to identify ABCG2 from a drug-resistant MCF-7 line (57).

Alternatively, signaling defects of the hedgehog pathway or LXR transcriptional regulation may be involved in ABC transporter expression (47, 58–60). If DOX impacts regulation of

BTN3A-dependent pAg sensing, then the use of such cytotoxic drugs in cancer treatment could impact immunotherapy strategies based on γδ T cells (23) by selecting clones with increased expression of survival factors which promote tumor growth. In any event, expression of this subset of ABC transporters may act as a biomarker for enhanced Vγ9/Vδ2 T cell activation by cytokine secretion, and it will be interesting to test this correlation in other cells and with other markers of activation. Current experiments are underway to identify a more comprehensive catalog of differences between HeLa-L and HeLa-M cells.

AUTHOR CONTRIBUTIONS

DR, ME, and TH designed research; DR, H-CC, JW, AH, JY, SS, HR, and TH performed research; DR, ME, H-CC, and TH analyzed data, JT and PL provided capacity; DR and ME wrote the paper with input from all authors.

ACKNOWLEDGMENTS

This work was supported by MRC Project Grants MR/M020290/1 and MR/N023145/1, a Cardiff Incoming Visiting Fellowship (TH) and a Wilhelm Sander Stiftung Grant 2013.907.2. TH thanks L. Starick and A. Nöhren for excellent technical assistance.

SUPPLEMENTARY MATERIAL

The Supplementary Material for this article can be found online at https://www.frontiersin.org/articles/10.3389/fimmu.2018.00662/full#supplementary-material.

REFERENCES

1. Allison JP, Havran WL. The immunobiology of T cells with invariant gamma delta antigen receptors. *Annu Rev Immunol* (1991) 9:679–705. doi:10.1146/annurev.iy.09.040191.003335
2. Hayday AC. Gammadelta T cells and the lymphoid stress-surveillance response. *Immunity* (2009) 31:184–96. doi:10.1016/j.immuni.2009.08.006
3. Nielsen MM, Witherden DA, Havran WL. Gammadelta T cells in homeostasis and host defence of epithelial barrier tissues. *Nat Rev Immunol* (2017) 17:733–45. doi:10.1038/nri.2017.101
4. Di Marco Barros R, Roberts NA, Dart RJ, Vantourout P, Jandke A, Nussbaumer O, et al. Epithelia use butyrophilin-like molecules to shape organ-specific gammadelta T cell compartments. *Cell* (2016) 167:203–18.e17. doi:10.1016/j.cell.2016.08.030
5. Henry J, Miller MM, Pontarotti P. Structure and evolution of the extended B7 family. *Immunol Today* (1999) 20:285–8. doi:10.1016/S0167-5699(98)01418-2
6. Sarter K, Leimgruber E, Gobet F, Agrawal V, Dunand-Sauthier I, Barras E, et al. Btn2a2, a T cell immunomodulatory molecule coregulated with MHC class II genes. *J Exp Med* (2016) 213:177–87. doi:10.1084/jem.20150435
7. Vavassori S, Kumar A, Wan GS, Ramanjaneyulu GS, Cavallari M, El Daker S, et al. Butyrophilin 3A1 binds phosphorylated antigens and stimulates human gammadelta T cells. *Nat Immunol* (2013) 14:908–16. doi:10.1038/ni.2665
8. Decaup E, Duault C, Bezombes C, Poupot M, Savina A, Olive D, et al. Phosphoantigens and butyrophilin 3A1 induce similar intracellular activation signaling in human TCRVgamma9+ gammadelta T lymphocytes. *Immunol Lett* (2014) 161:133–7. doi:10.1016/j.imlet.2014.05.011
9. Sandstrom A, Peigne CM, Leger A, Crooks JE, Konczak F, Gesnel MC, et al. The intracellular B30.2 domain of butyrophilin 3A1 binds phosphoantigens to mediate activation of human Vgamma9Vdelta2 T cells. *Immunity* (2014) 40:490–500. doi:10.1016/j.immuni.2014.03.003
10. Harly C, Guillaume Y, Nedellec S, Peigne CM, Monkkonen H, Monkkonen J, et al. Key implication of CD277/butyrophilin-3 (BTN3A) in cellular stress sensing by a major human gammadelta T-cell subset. *Blood* (2012) 120:2269–79. doi:10.1182/blood-2012-05-430470
11. Vantourout P, Laing A, Woodward MJ, Zlatareva I, Apolonia L, Jones AW, et al. Heteromeric interactions regulate butyrophilin (BTN) and BTN-like molecules governing γδ T cell biology. *Proc Natl Acad Sci U S A* (2018) 115:1039–44. doi:10.1073/pnas.1701237115
12. Boyden LM, Lewis JM, Barbee SD, Bas A, Girardi M, Hayday AC, et al. Skint1, the prototype of a newly identified immunoglobulin superfamily gene cluster, positively selects epidermal gammadelta T cells. *Nat Genet* (2008) 40:656–62. doi:10.1038/ng.108
13. Barbee SD, Woodward MJ, Turchinovich G, Mention JJ, Lewis JM, Boyden LM, et al. Skint-1 is a highly specific, unique selecting component for epidermal T cells. *Proc Natl Acad Sci U S A* (2011) 108:3330–5. doi:10.1073/pnas.1010890108
14. Hintz M, Reichenberg A, Altincicek B, Bahr U, Gschwind RM, Kollas AK, et al. Identification of (E)-4-hydroxy-3-methyl-but-2-enyl pyrophosphate as a major activator for human gammadelta T cells in *Escherichia coli*. *FEBS Lett* (2001) 509:317–22. doi:10.1016/S0014-5793(01)03191-X
15. Eberl M, Hintz M, Reichenberg A, Kollas AK, Wiesner J, Jomaa H. Microbial isoprenoid biosynthesis and human gammadelta T cell activation. *FEBS Lett* (2003) 544:4–10. doi:10.1016/S0014-5793(03)00483-6
16. Castella B, Riganti C, Fiore F, Pantaleoni F, Canepari ME, Peola S, et al. Immune modulation by zoledronic acid in human myeloma: an advantageous cross-talk between Vgamma9Vdelta2 T cells, alphabeta CD8+ T cells, regulatory T cells, and dendritic cells. *J Immunol* (2011) 187:1578–90. doi:10.4049/jimmunol.1002514
17. Fowler DW, Copier J, Dalgleish AG, Bodman-Smith MD. Zoledronic acid renders human M1 and M2 macrophages susceptible to Vdelta2(+) gammadelta T cell cytotoxicity in a perforin-dependent manner. *Cancer Immunol Immunother* (2017) 66:1205–15. doi:10.1007/s00262-017-2011-1
18. Brandes M, Willimann K, Moser B. Professional antigen-presentation function by human gammadelta T cells. *Science* (2005) 309:264–8. doi:10.1126/science.1110267
19. Brandes M, Willimann K, Bioley G, Levy N, Eberl M, Luo M, et al. Cross-presenting human gammadelta T cells induce robust CD8+ alphabeta T cell responses. *Proc Natl Acad Sci U S A* (2009) 106:2307–12. doi:10.1073/pnas.0810059106
20. Tyler CJ, Doherty DG, Moser B, Eberl M. Human Vgamma9/Vdelta2 T cells: innate adaptors of the immune system. *Cell Immunol* (2015) 296:10–21. doi:10.1016/j.cellimm.2015.01.008
21. Wilhelm M, Kunzmann V, Eckstein S, Reimer P, Weissinger F, Ruediger T, et al. Gammadelta T cells for immune therapy of patients with lymphoid malignancies. *Blood* (2003) 102:200–6. doi:10.1182/blood-2002-12-3665
22. Meraviglia S, Eberl M, Vermijlen D, Todaro M, Buccheri S, Cicero G, et al. In vivo manipulation of Vgamma9Vdelta2 T cells with zoledronate and low-dose interleukin-2 for immunotherapy of advanced breast cancer patients. *Clin Exp Immunol* (2010) 161:290–7. doi:10.1111/j.1365-2249.2010.04167.x
23. Gertner-Dardenne J, Castellano R, Mamessier E, Garbit S, Kochbati E, Etienne A, et al. Human Vgamma9Vdelta2 T cells specifically recognize and kill acute myeloid leukemic blasts. *J Immunol* (2012) 188:4701–8. doi:10.4049/jimmunol.1103710
24. Hannani D, Ma Y, Yamazaki T, Dechanet-Merville J, Kroemer G, Zitvogel L. Harnessing gammadelta T cells in anticancer immunotherapy. *Trends Immunol* (2012) 33:199–206. doi:10.1016/j.it.2012.01.006
25. Moser B. Tumor-killing gammadelta-TCRs take center stage. *Blood* (2012) 120:5093–4. doi:10.1182/blood-2012-10-460378
26. Khan MW, Eberl M, Moser B. Potential use of gammadelta T cell-based vaccines in cancer immunotherapy. *Front Immunol* (2014) 5:512. doi:10.3389/fimmu.2014.00512
27. McCarthy NE, Hedin CR, Sanders TJ, Amon P, Hoti I, Ayada I, et al. Azathioprine therapy selectively ablates human Vdelta2(+) T cells in Crohn's disease. *J Clin Invest* (2015) 125:3215–25. doi:10.1172/JCI80840

28. Papotto PH, Reinhardt A, Prinz I, Silva-Santos B. Innately versatile: gamma-delta17 T cells in inflammatory and autoimmune diseases. *J Autoimmun* (2018) 87:26–37. doi:10.1016/j.jaut.2017.11.006
29. Benyamine A, Le Roy A, Mamessier E, Gertner-Dardenne J, Castanier C, Orlanducci F, et al. BTN3A molecules considerably improve Vgamma9V-delta2T cells-based immunotherapy in acute myeloid leukemia. *Oncoimmunology* (2016) 5:e1146843. doi:10.1080/2162402X.2016.1146843
30. Rhodes DA, Chen HC, Price AJ, Keeble AH, Davey MS, James LC, et al. Activation of human gammadelta T cells by cytosolic interactions of BTN3A1 with soluble phosphoantigens and the cytoskeletal adaptor periplakin. *J Immunol* (2015) 194:2390–8. doi:10.4049/jimmunol.1401064
31. Weekes MP, Tomasec P, Huttlin EL, Fielding CA, Nusinow D, Stanton RJ, et al. Quantitative temporal viromics: an approach to investigate host-pathogen interaction. *Cell* (2014) 157:1460–72. doi:10.1016/j.cell.2014.04.028
32. Starick L, Riano F, Karunakaran MM, Kunzmann V, Li J, Kreiss M, et al. Butyrophilin 3A (BTN3A, CD277)-specific antibody 20.1 differentially activates Vgamma9Vdelta2 TCR clonotypes and interferes with phosphoantigen activation. *Eur J Immunol* (2017) 47:982–92. doi:10.1002/eji.201646818
33. Sebestyen Z, Scheper W, Vyborova A, Gu S, Rychnavska Z, Schiffler M, et al. RhoB mediates phosphoantigen recognition by Vgamma9Vdelta2 T cell receptor. *Cell Rep* (2016) 15:1973–85. doi:10.1016/j.celrep.2016.04.081
34. Groot KR, Sevilla LM, Nishi K, DiColandrea T, Watt FM. Kazrin, a novel periplakin-interacting protein associated with desmosomes and the keratinocyte plasma membrane. *J Cell Biol* (2004) 166:653–9. doi:10.1083/jcb.200312123
35. Boczonadi V, McInroy L, Maatta A. Cytolinker cross-talk: periplakin N-terminus interacts with plectin to regulate keratin organisation and epithelial migration. *Exp Cell Res* (2007) 313:3579–91. doi:10.1016/j.yexcr.2007.07.005
36. Sevilla LM, Nachat R, Groot KR, Klement JF, Uitto J, Djian P, et al. Mice deficient in involucrin, envoplakin, and periplakin have a defective epidermal barrier. *J Cell Biol* (2007) 179:1599–612. doi:10.1083/jcb.200706187
37. Weekes MP, Antrobus R, Lill JR, Duncan LM, Hor S, Lehner PJ. Comparative analysis of techniques to purify plasma membrane proteins. *J Biomol Tech* (2010) 21:108–15.
38. Weekes MP, Tan SY, Poole E, Talbot S, Antrobus R, Smith DL, et al. Latency-associated degradation of the MRP1 drug transporter during latent human cytomegalovirus infection. *Science* (2013) 340:199–202. doi:10.1126/science.1235047
39. Doyle LA, Yang W, Abruzzo LV, Krogmann T, Gao Y, Rishi AK, et al. A multidrug resistance transporter from human MCF-7 breast cancer cells. *Proc Natl Acad Sci U S A* (1998) 95:15665–70. doi:10.1073/pnas.95.26.15665
40. Ji H, Lee JH, Wang Y, Pang Y, Zhang T, Xia Y, et al. EGFR phosphorylates FAM129B to promote Ras activation. *Proc Natl Acad Sci U S A* (2016) 113:644–9. doi:10.1073/pnas.1517112113
41. Mallery DL, McEwan WA, Bidgood SR, Towers GJ, Johnson CM, James LC. Antibodies mediate intracellular immunity through tripartite motif-containing 21 (TRIM21). *Proc Natl Acad Sci U S A* (2010) 107:19985–90. doi:10.1073/pnas.1014074107
42. Hsu JL, van den Boomen DJ, Tomasec P, Weekes MP, Antrobus R, Stanton RJ, et al. Plasma membrane profiling defines an expanded class of cell surface proteins selectively targeted for degradation by HCMV US2 in cooperation with UL141. *PLoS Pathog* (2015) 11:e1004811. doi:10.1371/journal.ppat.1004811
43. Burr ML, Sparbier CE, Chan YC, Williamson JC, Woods K, Beavis PA, et al. CMTM6 maintains the expression of PD-L1 and regulates anti-tumour immunity. *Nature* (2017) 549:101–5. doi:10.1038/nature23643
44. Zhou S, Schuetz JD, Bunting KD, Colapietro AM, Sampath J, Morris JJ, et al. The ABC transporter Bcrp1/ABCG2 is expressed in a wide variety of stem cells and is a molecular determinant of the side-population phenotype. *Nat Med* (2001) 7:1028–34. doi:10.1038/nm0901-1028
45. Tomlinson B, Hu M, Lee VW, Lui SS, Chu TT, Poon EW, et al. ABCG2 polymorphism is associated with the low-density lipoprotein cholesterol response to rosuvastatin. *Clin Pharmacol Ther* (2010) 87:558–62. doi:10.1038/clpt.2009.232
46. Hu M, To KK, Mak VW, Tomlinson B. The ABCG2 transporter and its relations with the pharmacokinetics, drug interaction and lipid-lowering effects of statins. *Expert Opin Drug Metab Toxicol* (2011) 7:49–62. doi:10.1517/17425255.2011.538383
47. Kaneko T, Kanno C, Ichikawa-Tomikawa N, Kashiwagi K, Yaginuma N, Ohkoshi C, et al. Liver X receptor reduces proliferation of human oral cancer cells by promoting cholesterol efflux via up-regulation of ABCA1 expression. *Oncotarget* (2015) 6:33345–57. doi:10.18632/oncotarget.5428
48. Qian H, Zhao X, Cao P, Lei J, Yan N, Gong X. Structure of the human lipid exporter ABCA1. *Cell* (2017) 169:1228–39.e10. doi:10.1016/j.cell.2017.05.020
49. Castella B, Kopecka J, Sciancalepore P, Mandili G, Foglietta M, Mitro N, et al. The ATP-binding cassette transporter A1 regulates phosphoantigen release and Vgamma9Vdelta2 T cell activation by dendritic cells. *Nat Commun* (2017) 8:15663. doi:10.1038/ncomms15663
50. De Libero G, Lau SY, Mori L. Phosphoantigen presentation to TCR gammadelta cells, a conundrum getting less gray zones. *Front Immunol* (2014) 5:679. doi:10.3389/fimmu.2014.00679
51. Kistowska M. *Antigen Recognition and Thymic Maturation of Human TCR Vgamma9-Vdelta2 Cells*. Ph.D. thesis, Basel: Universität Basel (2007).
52. Gu S, Nawrocka W, Adams EJ. Sensing of pyrophosphate metabolites by Vgamma9Vdelta2 T cells. *Front Immunol* (2014) 5:688. doi:10.3389/fimmu.2014.00688
53. Adey A, Burton JN, Kitzman JO, Hiatt JB, Lewis AP, Martin BK, et al. The haplotype-resolved genome and epigenome of the aneuploid HeLa cancer cell line. *Nature* (2013) 500:207–11. doi:10.1038/nature12064
54. Tiwari RK, Kusari J, Sen GC. Functional equivalents of interferon-mediated signals needed for induction of an mRNA can be generated by double-stranded RNA and growth factors. *EMBO J* (1987) 6:3373–8.
55. Calcagno AM, Fostel JM, To KK, Salcido CD, Martin SE, Chewning KJ, et al. Single-step doxorubicin-selected cancer cells overexpress the ABCG2 drug transporter through epigenetic changes. *Br J Cancer* (2008) 98:1515–24. doi:10.1038/sj.bjc.6604334
56. Hayes JD, McMahon M. NRF2 and KEAP1 mutations: permanent activation of an adaptive response in cancer. *Trends Biochem Sci* (2009) 34:176–88. doi:10.1016/j.tibs.2008.12.008
57. Doyle L, Ross DD. Multidrug resistance mediated by the breast cancer resistance protein BCRP (ABCG2). *Oncogene* (2003) 22:7340–58. doi:10.1038/sj.onc.1206938
58. Singh RR, Kunkalla K, Qu C, Schlette E, Neelapu SS, Samaniego F, et al. ABCG2 is a direct transcriptional target of hedgehog signaling and involved in stroma-induced drug tolerance in diffuse large B-cell lymphoma. *Oncogene* (2011) 30:4874–86. doi:10.1038/onc.2011.195
59. Chen Y, Bieber MM, Teng NN. Hedgehog signaling regulates drug sensitivity by targeting ABC transporters ABCB1 and ABCG2 in epithelial ovarian cancer. *Mol Carcinog* (2014) 53:625–34. doi:10.1002/mc.22015
60. Ito A, Hong C, Rong X, Zhu X, Tarling EJ, Hedde PN, et al. LXRs link metabolism to inflammation through Abca1-dependent regulation of membrane composition and TLR signaling. *Elife* (2015) 4:e08009. doi:10.7554/eLife.08009

Conflict of Interest Statement: The authors are not aware of any financial holdings or other personal and professional relationships which could be construed as affecting the objectivity of this manuscript.

The handling Editor declared a past co-authorship with one of the authors (ME).

Copyright © 2018 Rhodes, Chen, Williamson, Hill, Yuan, Smith, Rhodes, Trowsdale, Lehner, Herrmann and Eberl. This is an open-access article distributed under the terms of the Creative Commons Attribution License (CC BY). The use, distribution or reproduction in other forums is permitted, provided the original author(s) and the copyright owner are credited and that the original publication in this journal is cited, in accordance with accepted academic practice. No use, distribution or reproduction is permitted which does not comply with these terms.

frontiers in Immunology

ORIGINAL RESEARCH
published: 16 March 2018
doi: 10.3389/fimmu.2018.00510

Human γδ T Cell Receptor Repertoires in Peripheral Blood Remain Stable Despite Clearance of Persistent Hepatitis C Virus Infection by Direct-Acting Antiviral Drug Therapy

Sarina Ravens[1†], Julia Hengst[2†], Verena Schlapphoff[2], Katja Deterding[2], Akshay Dhingra[3], Christian Schultze-Florey[1,4], Christian Koenecke[1,4], Markus Cornberg[2], Heiner Wedemeyer[2,5‡] and Immo Prinz[1*‡]*

[1] Institute of Immunology, Hannover Medical School, Hannover, Germany, [2] Department of Gastroenterology, Hepatology and Endocrinology, Hannover Medical School, Hannover, Germany, [3] Institute of Virology, Hannover Medical School, Hannover, Germany, [4] Department of Hematology, Hemostasis, Oncology and Stem Cell Transplantation, Hannover Medical School, Hannover, Germany, [5] Department of Gastroenterology and Hepatology, Essen University Hospital, Essen, Germany

OPEN ACCESS

Edited by:
David Vermijlen,
Université Libre de Bruxelles, Belgium

Reviewed by:
Robert Thimme,
Albert Ludwigs Universität Freiburg, Germany
Tom Taghon,
Ghent University, Belgium

***Correspondence:**
Sarina Ravens
ravens.sarina@mh-hannover.de;
Immo Prinz
prinz.immo@mh-hannover.de

[†]These authors have contributed equally to this work.

[‡]Shared senior authorship.

Specialty section:
This article was submitted to T Cell Biology, a section of the journal Frontiers in Immunology

Received: 11 January 2018
Accepted: 26 February 2018
Published: 16 March 2018

Citation:
Ravens S, Hengst J, Schlapphoff V, Deterding K, Dhingra A, Schultze-Florey C, Koenecke C, Cornberg M, Wedemeyer H and Prinz I (2018) Human γδ T Cell Receptor Repertoires in Peripheral Blood Remain Stable Despite Clearance of Persistent Hepatitis C Virus Infection by Direct-Acting Antiviral Drug Therapy. Front. Immunol. 9:510. doi: 10.3389/fimmu.2018.00510

Human γδ T cells can contribute to clearance of hepatitis C virus (HCV) infection but also mediate liver inflammation. This study aimed to understand the clonal distribution of γδ T cells in peripheral blood of chronic HCV patients and following HCV clearance by interferon-free direct-acting antiviral drug therapies. To this end, γδ T cell receptor (TCR) repertoires were monitored by mRNA-based next-generation sequencing. While the percentage of Vγ9$^+$ T cells was higher in patients with elevated liver enzymes and a few expanded Vδ3 clones could be identified in peripheral blood of 23 HCV-infected non-cirrhotic patients, overall clonality and complexity of γδ TCR repertoires were largely comparable to those of matched healthy donors. Monitoring eight chronic HCV patients before, during and up to 1 year after therapy revealed that direct-acting antiviral (DAA) drug therapies induced only minor alterations of TRG and TRD repertoires of Vγ9$^+$ and Vγ9$^-$ cells. Together, we show that peripheral γδ TCR repertoires display a high stability (1) by chronic HCV infection in the absence of liver cirrhosis and (2) by HCV clearance in the course of DAA drug therapy.

Keywords: γδ T cells, chronic hepatitis C virus, TRG, TRD, next-generation sequencing, direct-acting antivirals

INTRODUCTION

The majority of hepatitis C virus (HCV) infection results in chronicity and only 10–50% of cases are cleared in the acute phase (1, 2). Failing cytotoxic T cell activity due to exhaustion of expanded T cells causes chronic viral persistence and continuous activation of liver-infiltrating lymphocytes progressively leading to liver cirrhosis and development of hepatocellular carcinoma (3–5). However, the contribution of γδ T cells to HCV control is largely unknown.

γδ T cells are innate immune cells expressing a T cell receptor (TCR) consisting of a γ- and a δ-chain, each composed of a variable (V), diversity (D), and joining (J) gene segment generated by "VDJ recombination." The random rearrangement of different gene segments creates a high clonal

diversity, which is particularly reflected in the junctional regions (CDR3 sequence) of TCR chains. γδ T cells can be classified based on their expressed Vγ or Vδ chains functionality and distribution within the body. The Vγ9JP$^+$Vδ2$^+$ subset is the main population of γδ T cells within the peripheral blood of most adult healthy individuals (6). Vγ9JP$^+$Vδ2$^+$ cells are activated through small phosphoantigens, like microbial-derived HMB-PP or host-derived isopentyl pyrophosphate (IPP) (7, 8) and are involved in anti-cancer surveillance, pathogen clearance, or inflammatory diseases (9). By contrast, the identity of molecules activating non-Vγ9JP$^+$Vδ2$^+$ cells is largely unknown. Nevertheless, a few studies revealed that these could be stress molecules exposed by virus-infected or tumor cells (10–14). Overall, non-Vγ9JP$^+$Vδ2$^+$ γδ T cells exert a high degree of antiviral and antitumor activity (15, 16), which is for instance reflected in the expansion of Vδ1$^+$ γδ T cells in response to viral infection in immunocompromised patients, stem cell transplant recipients, and during pregnancy (17–21).

The functional role of different γδ T cell populations in HCV persistence and associated liver malignancies remains to be understood. *Per se*, γδ T cells are enriched not only in liver tissues of healthy persons but also in patients with hepatitis infections (22). Hepatic γδ T cell populations express the NK-cell marker CD56, the liver-homing marker CD161, produce INF-γ, and demonstrate an effector/memory phenotype (23–25). Especially, chronic HCV patients with liver cirrhosis display elevated γδ T cell numbers and their cytokine production and cytotoxicity was suggested to play a role in inflammatory necrotic processes (26–29). Studies analyzing matched blood and liver specimens from patients with chronic liver diseases indicated that Vδ2$^+$ and/or Vδ1$^+$ can infiltrate the liver (25, 28). Increased Vδ1$^+$ cell frequencies in liver transplant recipient were associated with high viral loads (HCV, CMV) (30). Likewise, patients infected with only HCV, or co-infected with HIV undergoing active antiretroviral therapy (HAART), had elevated Vδ1$^+$ γδ T cells in the blood and liver, which was linked to liver inflammation (28, 31). Of note, HAART therapy did not restore intrahepatic Vδ1$^+$ T cells to normal levels within HCV/HIV co-infected patients (31). Especially, Vγ9JP$^+$Vδ2$^+$ cells have been revealed to inhibit viral replication (32). Other studies connect HCV persistence to low Vγ9JP$^+$Vδ2$^+$ frequencies, impaired IFN-γ production, and γδ T cell exhaustion (24, 25, 33, 34), while the cytotoxicity and continuous activation of Vγ9JP$^+$Vδ2$^+$ during chronic HCV infection contributes to liver inflammation and cirrhosis (24). The therapeutic application of zoledronate to activate Vγ9JP$^+$Vδ2$^+$ γδ T cells through cellular accumulation of IPP was suggested as a strategy to apply γδ T cells to inhibit viral replication during interferon-based therapies (32, 34, 35).

Over the past few years, conventional HCV therapy based on PEG-INFα/ribavirin has been replaced by direct-acting antiviral (DAA) drugs. These DAA therapies result in increased cure rates defined by virus clearance and improve liver inflammation and cirrhosis in HCV-infected patients (36–38). Effects of DAAs and HCV clearance on the restoration of different immune cell subsets including HCV-specific T cells, NK cells, and MAIT cells have been analyzed in patients (39–43). However, to the best of our knowledge, no study addressed the effect of DAA on γδ T cell composition.

Next-generation sequencing (NGS) of TCR repertoires has the advantage to monitor γδ T cell populations at the clonal level and to identify disease-related TRG (γ-chain) and TRD (δ-chain) sequences (19, 44). To understand the clonal distribution of γδ T cells in patients with chronic HCV and to investigate in the influence of DAA on γδ T cell repertoires, we used flow cytometric cell sorting and NGS to profile γδ TCRs from total as well as Vγ9$^+$ and Vγ9$^-$ isolated γδ T cell populations from peripheral blood.

RESULTS

Healthy and Chronic HCV Patients Show Similar γδ T Cell Repertoire Complexity

We monitored peripheral γδ T cell repertoires in 10 patients with chronic HCV infections before, during, and after therapy with DAAs and in additional 13 patients at a single time point during therapeutic DAA treatments. All patients had persistent viral infection with the HCV genotype 1 (**Table 1** for patients' characteristics). Even though parameters for liver inflammation, such as alanine aminotransferase (ALT) and aspartate aminotransferase (AST) level, were above normal levels in 4 of 10 patients (**Table 1**), it is important to note that all patients included in this study had not yet developed liver cirrhosis. After flow cytometric sorting of γδ T cells, the highly diverse CDR3 regions of the TCR γ- and δ-chain were PCR amplified through gene-specific primers and subjected to NGS analysis (19). The workflow to analyze multiple samples from 14 healthy controls (HC) and 23 chronic HCV patients is depicted in Figure S1A in Supplementary Material. Flow cytometric analyses showed slightly decreased total γδ T cell frequencies, but a higher percentage of Vγ9$^+$ T cells, in patients with higher ALT levels when compared with HC and chronic HCV patients having low ALT levels (**Figures 1A,B**). NGS of functional Vγ or Vδ chain usage of TCR repertoires

TABLE 1 | Baseline characteristics of healthy individuals and both cohorts of chronic HCV patients.

	Healthy	Chronic HCV (longitudinal samples)	Chronic HCV (one time-point)
n (m/f)	9 (4/5), 5 (3/2)	10 (5/5)	14 (8/6)
Age (years)	41 (26–51), 44 (21–66)	54 (47–60)	54 (25–79)
HCV RNA (IU/mL)		2,913,000 (140,000–6,700,000)	1,893,000 (76,000–6,300,000)
HCV genotype		1	1
ALT (U/L)		96.2 (51–289)	65.4 (22–138)
AST (U/L)		54.6 (24–108)	52.3 (24–108)
gGT (U/L)		55.9 (21–107)	108.6 (14–558)
Fibroscan (kPa)		7.4 (5.4–12.3)	7.9 (2.2–24.3)
Abs. lymphocyte count		2,150 (1,600–3,300)	2,121 (1,200–3,200)

ALT, alanine aminotransferase; AST, aspartate aminotransferase; gGT, gamma-glutamyl transpeptidase; HCV, hepatitis C virus.

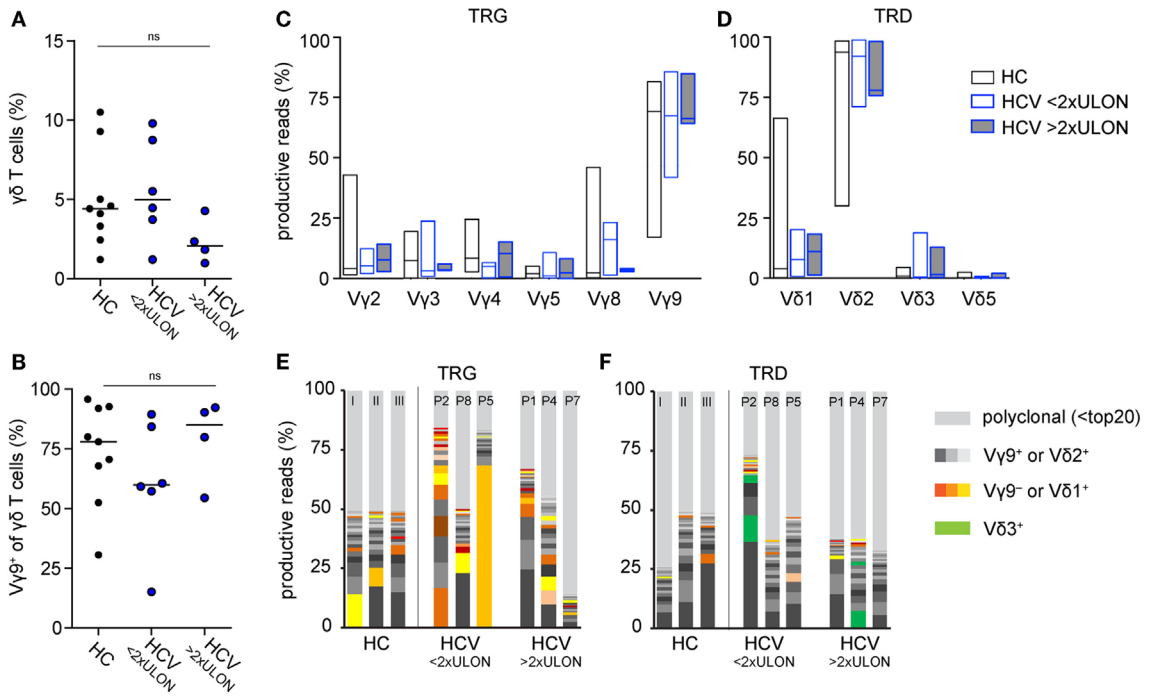

FIGURE 1 | Comparison of peripheral γδ T cell repertoires in chronic hepatitis C virus (HCV) patients and healthy controls (HC). **(A,B)** Flow cytometric sorting results of 9 HC (black dots) and 10 chronic HCV patients at baseline (blue dots), which were grouped based on their alanine aminotransferase (ALT) values, are summarized in dot plots representing **(A)** total γδ T cell frequencies of $CD14^-/CD19^-$ lymphocytes and **(B)** $Vγ9^+$ cell frequencies of total γδ T cells. Six patients had ALT levels two times lower than upper limit of normal (<2× ULON) and four patients had increased ALT levels (>2× ULON). Horizontal lines present median values. Data were analyzed by Mann–Whitney test. **(C,D)** Sorted γδ T cells of eight HC and eight chronic HCV patients, the latter grouped based on their ALT levels, were subjected to next-generation sequencing (NGS) analysis. Floating bars from minimum to maximum represent the distribution of functional V-genes of analyzed **(C)** TRG or **(D)** TRD repertoires. Lines represent median values. **(E,F)** The most expanded top 20 **(E)** TRG or **(F)** TRD clones are highlighted in stacked area graphs of three representative HC and six HCV patients who were stratified due to their ALT levels. $Vγ9^-$ or $Vδ1^+$ clones are highlighted in orange, $Vγ9^+$ or $Vδ2^+$ in gray, $Vδ3^+$ clones in green color, and non-top 20 clones in light gray. NGS samples were normalized to the percentage of all productive sequences per sample.

(**Figures 1C,D**) further indicated almost no difference of V-chain distributions between HC and chronic HCV patients. Of note, box plots in **Figure 1D** suggest that at least some of the chronic HCV-infected patients had higher peripheral $Vδ3^+$ frequencies and this was independent of ALT levels. To characterize γδ T cell repertoires in more detail, we analyzed the clonal distribution and diversity of TRG and TRD repertoires (**Figures 1E,F**). As observed in previous datasets of HC (19, 44, 45) and as illustrated by three HC of this study and six representative chronic HCV patients with different ALT levels, the 20 most expanded clones collectively made up between 25 and 60% of whole TRG or TRD repertoires (**Figures 1E,F**). Thus, γδ TCR repertoires of chronic HCV patients largely resembled HC and were highly diverse with few expanded clones, that are not necessarily $Vγ9JP^+$ and $Vδ2^+$ (**Figures 1E,F**). All datasets were summarized by depicting the median frequency of top 20 clones and median Shannon index, a parameter used to measure TCR repertoire diversity, and showed no significant differences between the given groups (Figures S2A,B in Supplementary Material). Together, these NGS results indicate that peripheral TRG and TRD repertoires of healthy persons and chronic HCV patients have a similar complexity and clonal composition.

DAA Drugs Lead to Minor Changes on γδ T Cell Numbers

Next, we investigated the effect of DAA-induced viral clearance on peripheral γδ T cell lymphocytes. Patients were treated for 8 weeks with a combination of sofosbuvir and ledipasvir. All patients achieved a sustained virological response (Figure S1A in Supplementary Material). Six of ten patients were virus-negative at therapy week 4 (w4); HCV RNA levels of the other four patients were already very low at this time point (<20 IU/mL) (**Figure 2A**). Some patients had mild liver fibrosis indicated by fibroscan values ranging from 5.4 to 12.3 kPa, which decreased significantly from therapy start (TS) to follow-up week 12 (fu12) (**Table 1**; **Figure 2B**). Some parameters for liver inflammation, such as ALT and AST levels, were slightly increased at TS (**Table 1**; **Figure 2C**), while bilirubin values were ranging in the normal level below 17 μmol/L (3.0–14.0 μmol/L) (**Table 1**). During DAA therapy, ALT levels decreased significantly within the first therapy week and reached normal levels at week 4 (**Figure 2C**). After initiation of DAA therapy, a slight increase of absolute lymphocyte numbers and γδ T cells/μL blood was observed (**Figures 2D,E**), which declined then until follow-up week 12 (**Figure 2D**). Furthermore, small changes in the number of $Vγ9^+$ and $Vγ9^-$ γδ T cells/μL blood were detected during

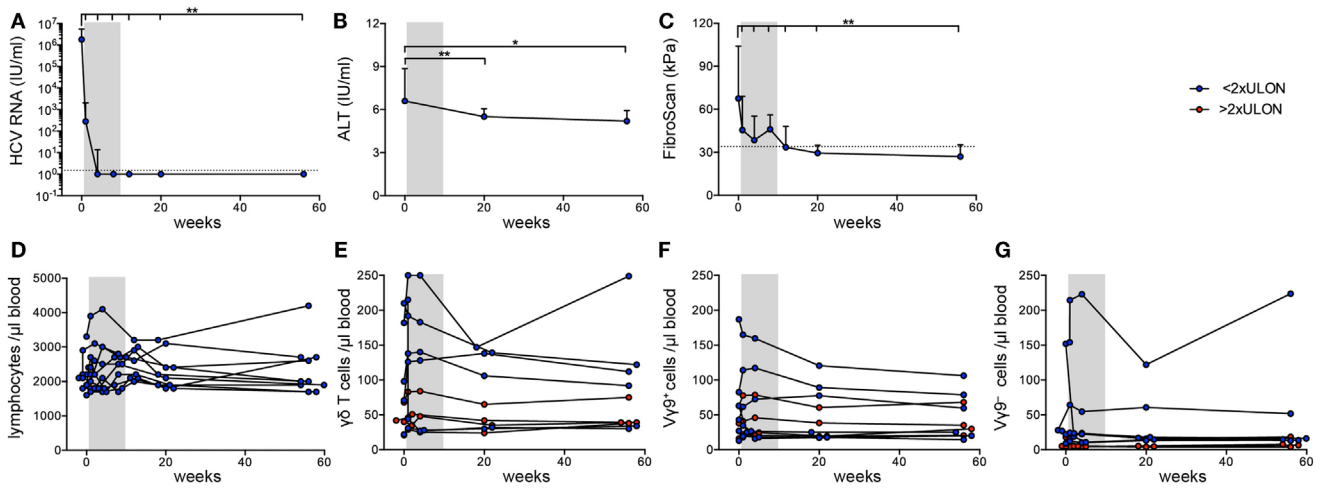

FIGURE 2 | Clinical parameters and γδ T cell numbers in chronic hepatitis C virus (HCV) patients receiving DAA therapy. Graphs represent **(A)** HCV RNA levels in IU/mL and **(B)** alanine aminotransferase (ALT) levels in IU/mL, statistical analysis for both parameters with Wilcoxon test, as well as **(C)** fibroscan values in kPa, statistical analysis with paired *t*-test. **(A–C)** Median values with interquartile range from 10 chronic HCV patients before, during, and after DAA therapy are summarized. **(D)** Absolute lymphocyte counts were assessed for 10 chronic HCV patients at given time points. **(E–G)** The number of total **(E)**, Vγ9$^+$ **(F)**, or Vγ9$^-$ **(G)** γδ T cells per µL blood were determined from FACS data and lymphocyte counts shown for each of the 10 HCV patients individually. Gray shaded areas highlight the 8 weeks of DAA treatment. The number of total **(E)**, Vγ9$^+$ **(F)**, or Vγ9$^-$ **(G)** γδ T cells per µL blood were separated based on the ALT levels (red shows patients who have ALT levels >2 times ULON, blue indicates patients who have ALT levels <2 times ULON). Gray shaded areas highlight the 8-week DAA treatment.

the first therapy weeks while staying stable during the follow-up year (**Figures 2F,G**). Of note, patients with ALT values higher than twofold ULON had very low numbers of Vγ9$^-$ γδ T cells/µL blood (**Figure 2G**), whereas the number of Vγ9$^+$ γδ T cells/µL blood and their progression was similar to patients with ALT values lower than twofold ULON (**Figure 2F**). Altogether, patients improved with regard to liver inflammation and stiffness following successful eradication of HCV infection, while total numbers of Vγ9$^+$ and Vγ9$^-$ γδ T cells remained highly stable after viral clearance. This suggests that potential alterations in γδ T cell numbers and repertoire composition in response to HCV infection were sustained for the observation period of 48 weeks.

TRD Repertoires of Vγ9$^+$ and Vγ9$^-$ γδ T Cells Are Distinct

Next, we investigated Vγ9$^+$ and Vγ9$^-$ cells separately. Flow cytometric profiling of γδ T cells specified a fraction of Vγ9$^-$Vδ2$^+$ cells in the peripheral blood of adults and chronic HCV patients (**Figure 3A**), which is in line with the identification of expanded Vγ9$^-$Vδ2$^+$ clones in HC and transplant recipients (19). In adults, TRD repertoires are highly individual, while all TRG repertoires comprise public Vγ9JP rearrangements shared between all persons (19, 45). Here, we analyzed TRD repertoires of sorted Vγ9$^+$ and Vγ9$^-$ γδ T cells from 11 HC and 20 chronic HCV patients receiving DAA therapy (**Table 1**; Figure S1 in Supplementary Material). First, we studied the distribution of δ-chains within the Vγ9$^+$ and Vγ9$^-$ subsets in HC and chronic HCV patients. As depicted by boxplots (**Figures 3B,C**), Vγ9$^+$ cells paired mainly with Vδ2$^+$ sequences, while Vγ9$^-$ cells paired with Vδ1, Vδ2, and Vδ3 sequences. In addition, the proportion of Vγ9$^-$Vδ3$^+$ cells was on average slightly increased in chronic HCV patients when compared with HC (**Figures 1D** and **3C**) and could be associated with the identification of some expanded Vγ9$^-$Vδ3$^+$ clones (**Figure 3D**). Next, we analyzed the clonal distribution of the 20 most expanded TRD clones of Vγ9$^+$ and Vγ9$^-$ sorted cells from three representative HC (**Figure 3E**) and three chronic HCV patients (**Figure 3F**). Similar to total γδ T cell populations, TRD repertoires of Vγ9$^+$ and Vγ9$^-$ cell subsets were diverse and depicted an oligoclonal expansion of particular Vγ9$^+$Vδ2$^+$, Vγ9$^-$Vδ2$^-$, and Vγ9$^-$Vδ2$^+$ clones (**Figures 3E,F**). Comparison of the combined median frequency of the top 20 Vγ9$^+$ and Vγ9$^-$ TRD clones between HC and chronic HCV patients pointed to lower frequencies of top 20 clones in Vγ9$^+$ cells of the HC group (**Figure 3G**). However, individual TRD repertoires were very diverse in the analyzed groups and thus differences in top 20 frequencies (**Figure 3G**) and TRD repertoire diversities as measured by Shannon indices (**Figure 3H**) were not statistically significant. Still, separate analyses of Vγ9$^+$ and Vγ9$^-$ sorted γδ T cells revealed that Vγ9$^-$ TRD repertoires displayed a high Vδ-chain diversity and that expanded Vγ9$^-$Vδ3$^+$ clones existed in some chronic HCV patients, while the overall clonal composition of Vγ9$^+$ and Vγ9$^-$ TRD repertoires was comparable between healthy persons and chronic HCV patients. Further studies, preferably also including patients with more severe HCV disease, will be required to support or refute the hypothesis that Vγ9$^-$Vδ3$^+$ clones selectively expand in response to HCV infection.

Stability of Vγ9$^+$ and Vγ9$^-$ TRD Repertoires During DAA Drug Therapy

Finally, we asked whether chronic HCV infection and DAA-driven viral clearance would affect γδ T cell repertoires, which

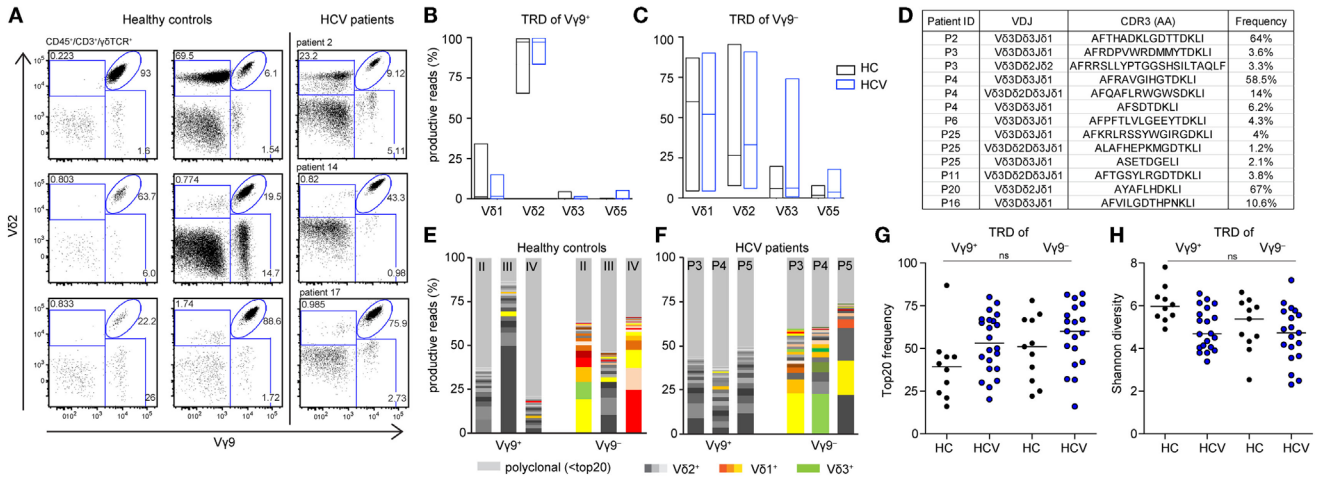

Patient ID	VDJ	CDR3 (AA)	Frequency
P2	Vδ3Dδ3Jδ1	AFTHADKLGDTTDKLI	64%
P3	Vδ3Dδ3Jδ1	AFRDPVWRDMMYTDKLI	3.6%
P3	Vδ3Dδ2Jδ2	AFRRSLLYPTGGSHSILTAQLF	3.3%
P4	Vδ3Dδ3Jδ1	AFRAVGIHGTDKLI	58.5%
P4	Vδ3Dδ2Dδ3Jδ1	AFQAFLRWGWSDKLI	14%
P4	Vδ3Dδ3Jδ1	AFSDTDKLI	6.2%
P6	Vδ3Dδ3Jδ1	AFPFTLVLGEEYTDKLI	4.3%
P25	Vδ3Dδ3Jδ1	AFKRLRSSYWGIRGDKLI	4%
P25	Vδ3Dδ2Dδ3Jδ1	ALAFHEPKMGDTKLI	1.2%
P25	Vδ3Dδ3Jδ1	ASETDGELI	2.1%
P11	Vδ3Dδ2Dδ3Jδ1	AFTGSYLRGDTDKLI	3.8%
P20	Vδ3Dδ2Jδ1	AYAFLHDKLI	67%
P16	Vδ3Dδ3Jδ1	AFVILGDTHPNKLI	10.6%

FIGURE 3 | Differences between TRD repertoires of sorted Vγ9$^+$ and Vγ9$^-$ cells in healthy controls (HC) and chronic hepatitis C virus (HCV) patients. **(A)** Flow cytometric analysis of total γδ T cells for expression of Vγ9 and Vδ2 in six HC and three chronic HCV patients. **(B–H)** TRD next-generation sequencing analysis of sorted Vγ9$^+$ and Vγ9$^-$ γδ T cells from 11 HC and 23 HCV patients. **(B,C)** Fractions of V-delta chains within the sorted **(B)** Vγ9$^+$ and **(C)** Vγ9$^-$ populations of HC and HCV patients are represented as floating bars from minimum to maximum with the line representing the median. **(D)** Identified Vδ3$^+$ sequences within sorted Vγ9$^-$ cells of chronic HCV patients. **(E,F)** Top 20 expanded TRD clones of either Vγ9$^+$ or Vγ9$^-$ cells are plotted in stacked area graphs for **(E)** three HC or **(F)** three HCV patients. Vδ2$^+$ are depicted in gray, Vδ1$^+$ clones in orange, and Vδ3$^+$ clones in green. Light gray represents non-top 20 TRD clones. Data sets were normalized to the percentage of productive reads per sample. **(G)** Dot plot displays the proportion of top 20 TRD clones within the Vγ9$^+$ or Vγ9$^-$ γδ T cell compartments for each analyzed sample. **(H)** TRD repertoire diversity of either Vγ9$^+$ or Vγ9$^-$ analyzed samples were determined by Shannon diversity indices. Samples were normalized to 10,000 productive reads. Median values are depicted as horizontal lines. Statistical analysis was performed using one-way ANOVA.

otherwise stay relatively stable over time (19, 44, 46). For this, we analyzed γδ TCR repertoires at TS, during DAA treatment and up to 1 year after therapy (illustrated in Figure S1A in Supplementary Material). We studied the TRD repertoires of sorted Vγ9$^+$ or Vγ9$^-$ cells as well as TRG and TRD repertoires of total γδ T cells. First, no significant changes in median frequencies of the top 20 clones and Shannon diversity indices of the analyzed cell subsets reflected that γδ TCR repertoires retained the overall complexity during the course of DAA drug therapy (**Figures 4A,B**; Figures S3A,B in Supplementary Material). Plotting the most expanded 20 TRD clones of either Vγ9$^+$ or Vγ9$^-$ sorted cells (**Figure 4C**) and the top 20 TRG and TRD clones of total γδ T cells (Figure S3C in Supplementary Material) over time, it turned out that only one patient (patient 3) showed notable changes in the distribution of expanded clones after TS. Importantly, this instability was caused by changes in Vδ2$^+$ sequences of Vγ9$^+$ sorted cells (**Figure 4C**). These might have been associated with increased γδ T cell counts starting from w1, but no other clinical parameters. Furthermore, γδTCR repertoire stability can be described in similarities between two given time points as calculated by Morisita–Horn indices. Notably, the Morisita–Horn index considers all clones of the given repertoire, while zero means no overlap and one represents complete overlap between all clones of given samples. Median values of calculated Morisita–Horn similarity indices revealed only minor changes of γδ T cell repertoires before, during, and after DAA drug therapy (**Figure 4D**; Figure S3D in Supplementary Material). In summary, γδ TCR repertoires of total, Vγ9$^+$ or Vγ9$^-$ γδ T cells retained their overall complexity during DAA therapy and were highly stable up to 1 year after viral clearance and normalization of liver enzymes.

MATERIALS AND METHODS

Patient Characteristics

All 23 patients chronically infected with HCV as well as 9 HC were recruited at the Department of Gastroenterology, Hepatology and Endocrinology at Hannover Medical School, Germany. In addition, five HC were recruited at the Institute of Immunology/Department of Hematology, Hemostasis, Oncology and Stem Cell Transplantation at Hannover Medical School, Germany. The chronic HCV patients were analyzed over time before, during, and after novel DAA therapy for 8 weeks with a combination of sofosbuvir and ledipasvir. From 10 patients, peripheral blood mononuclear cells were collected at treatment start (TS), therapy week 1 (w1), therapy week 4 (w4), follow-up week 12 (fu12), and 1 year after treatment cessation (fu48), isolated and cryopreserved for deferred analysis. Further, 13 chronic HCV patients who were treated for 8 or 12 weeks with a combination of sofosbuvir and ledipasvir were included in the study with only one time-point during or after treatment to determine their TRD repertoires.

The ethics committee of Hannover Medical School approved this study (Study number: 2148-2014 and 2604-2014), and all patients provided written confirmed consent before enrollment. The clinical characteristics of the chronic HCV patients and the HC are summarized in **Table 1**.

Flow Cytometric Analysis and Sorting

PBMCs were thawed, washed twice, and stained for 20 min at room temperature for flow cytometric analysis and cell sorting with the following antibodies: LIVE/DEAD Fixable Green Dead cell Stain Kit, Thermofisher or DAPI; CD14-FITC, clone M5E2,

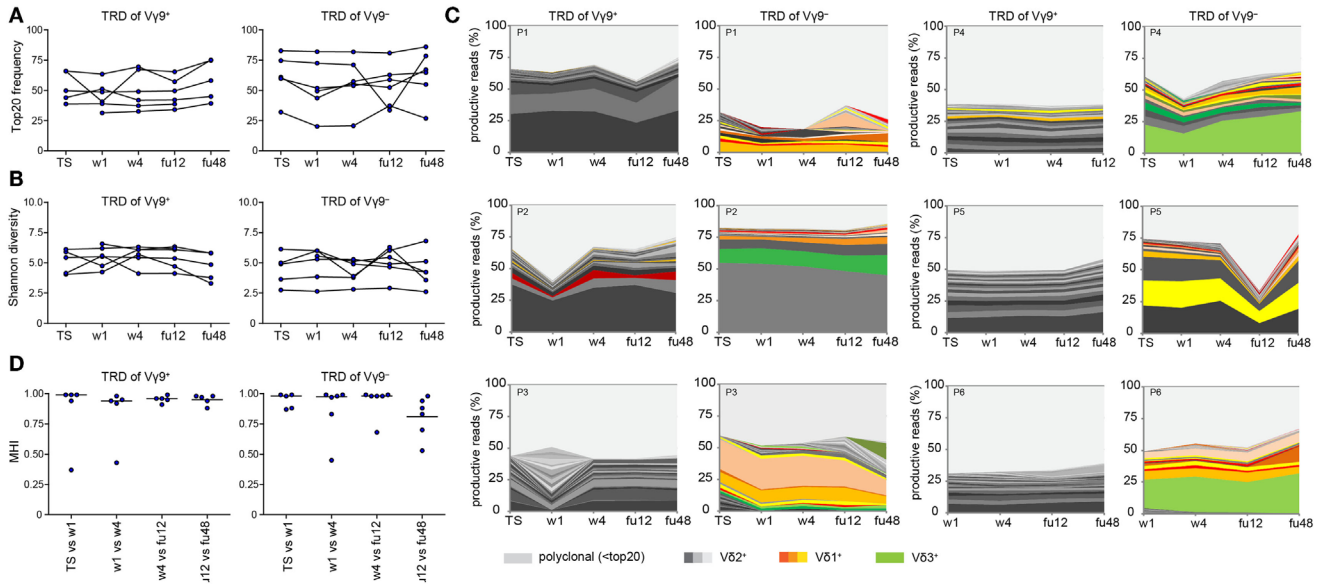

FIGURE 4 | Monitoring of TRD repertoires of Vγ9+ and Vγ9− γδ T cells in hepatitis C virus (HCV) patients over time. Next-generation sequencing results of TRD repertoires from sorted Vγ9+ or Vγ9− cells of six chronic HCV patients receiving DAA therapy overtime (TS: therapy start; therapy week 1 and week 4: w1, w4; follow-up weeks: fu12, fu48). **(A)** TRD repertoire diversities were determined by Shannon values for Vγ9+ (left side) and Vγ9− (right side) cells. Samples were normalized to 10,000 productive reads. **(B)** Frequency of top 20 TRD clones of sorted Vγ9+ (left side) and Vγ9− (right side) cells. **(C)** Stacked area graphs illustrate the distribution of top 20 TRD clones within sorted Vγ9+ (left side) or Vγ9− (right side) cells of chronic HCV patients from TS up to 1 year after DAA treatment (fu48). Vδ2+ clones are highlighted in gray, Vδ1+ clones in orange, and Vδ3+ clones in green. Light gray stands for non-top 20 TRD clones. Data sets were normalized to the percentage of productive reads. Horizontal lines represent median values. **(D)** To compare the TRD repertoire similarity between the given time points of either Vγ9+ (left side) or Vγ9− (right side) cells, Morisita–Horn indices were calculated and visualized as dot plots. Zero means no overlap and one total overlap between all CDR3 sequences of two samples.

BD Biosciences; CD19-FITC, clone HIB19, BD Biosciences; γδ TCR-PE, clone 11F2, eBiosciences; Vγ9-PE-Cy5, clone IMMU 360, Beckman Coulter; Vδ2-APC, clone 123R4, Miltenyi; CD45-APC-Cy7, clone 5B1, Miltenyi; CD3-BV786 and CD3-PECy7, clone UCHT1, BD Biosciences. After staining, PBMCs were washed twice and stored on ice until acquisition and sorting on a FACSAria Fusion cell sorter (BD Biosciences). HC and patients recruited at the Department of Gastroenterology, Hepatology and Endocrinology were sorted for $CD14^-/CD19^-$ γδ T cells and HC recruited at the Institute for Immunology were sorted for $CD45^+/CD3^+$ γδ T cells. Flow cytometry data were analyzed using the Flow Jo software V.9.8 (Tree Star Inc., Ashland, OR, USA).

TCR Amplicon Generation and NGS

For cDNA synthesis, extracted mRNA using the RNAeasy mini kit (Qiagen) of flow cytometric sorted Vγ9+ and Vγ9− cells, 5 µL mRNA of both subsets was pooled equally for analysis of total γδ T cells. CDR3 TRG and TRD sequencing amplicons were generated as described previously (19), while using 25–30 PCR cycles. According to Illumina guidelines 96 samples were labeled with Nextera XT indices and subjected to Illumina MiSeq analysis using 500 cycle paired-end sequencing. 20% PhIX was added as an internal control and to increase library complexity. Illumina output fastq files were processed using ea-utils.

TCR Repertoire Analysis

All sequencing files were annotated according to IMGT/High-Vquest. Only productive reads were taken into consideration for downstream processing of annotated sequences. Repertoire analyses were based on CDR3 amino acid sequences. Annotated V-chains were counted and CDR3 sequences were ranked according to their abundance to finally normalize the results to the percentage of productive reads within the given sample. All bioinformatics analysis was conducted using R (version 3.2.2) and bash shell commands. Shannon indices were calculated with the R library "vegan" and Morisita–Horn indices with VDJtools (47) and TcR (48). Analysis scripts are available upon request.

Statistical Analysis

Data were analyzed using the GraphPad Prism version 6.0b and 4.0. To test for normal distribution of data, D'Agostino and Pearson omnibus normality test was applied. Normally distributed data of multiple or two groups was analyzed using the one-way ANOVA, paired *t*-test, or unpaired *t*-test depending on the data sets that were compared. Regarding non-normally distributed data, the Mann–Whitney test or Wilcoxon matched-pairs signed rank test was used.

Data Availability

SRA files have been deposited at SRP128752.

DISCUSSION

In this study, we monitored peripheral γδ T cell repertoire dynamics in a homogenous cohort of chronic HCV patients before and during DAA therapy. All HCV patients had similar characteristics by being persistently infected with the HCV genotype 1, by no development of liver cirrhosis and by receiving a short 8 weeks therapeutic drug treatment. It was reasonable to expect an impact of chronic HCV infection and its clearance on γδ T cell dynamics, because γδ T cells play a role in the antiviral defense of CMV, HCV, and other viruses (22, 49, 50). During HCV infection, cytokine release (IFN-γ) by Vγ9JP$^+$Vδ2$^+$ and non-Vγ9JP$^+$Vδ2$^+$ may contribute to virus clearance, while HCV persistence is associated with low γδ T cell numbers and an impaired cytokine production (22). By contrast, chronic HCV patients with high liver inflammation rather have increased frequencies of cytotoxic γδ T cells when compared with healthy subjects or patients with no liver inflammation. In our study, all chronic HCV patients included had no or only mild liver fibrosis and mild liver inflammation, which might explain that they displayed no significantly, elevated numbers of γδ T cells. Importantly, eradication of the viral infection resulted in significant improvement of liver stiffness and inflammation as revealed by fibroscan values and ALT levels. Overall, our TCR analyses showed that uncomplicated chronic HCV infection and rapid viral clearance had only minor effects on the peripheral γδ T cell compartment, indicating that more drastic immunological events are required for perturbation of peripheral γδ T cell repertoires (19). However, we cannot exclude that TCR repertoires in the liver might be more affected by HCV clearance. Also, patients with liver cirrhosis may show more pronounced alterations of TCR repertoires during DAA therapy.

This study characterized, in addition to the analysis of total γδ T cell populations in peripheral blood, TRD repertoires of sorted Vγ9$^+$ and Vγ9$^-$ cells separately. As already demonstrated in preterm-infants and neonates, Vδ2 sequences pair mainly, but not exclusively with Vγ9JP$^+$ TRG sequences (51). Flow cytometric results and TRD repertoire analysis of this study pointed out that Vγ9$^-$Vδ2$^+$ T cells are maintained until adulthood. While Vγ9$^+$ cells displayed a more homogenous Vδ-chain usage (mainly Vδ2), TRD repertoires of Vγ9$^-$ cells were more diverse and consisted of Vδ1$^+$, Vδ2$^+$, Vδ3$^+$, but very little Vδ5$^+$ sequences. Clonal distributions and the complete absence of any shared expanded TRD clones collectively illustrated that similar to all γδ T cells (19), Vγ9$^+$ and Vγ9$^-$ TRD repertoires are generally oligoclonal and individual. Although γδ TCR repertoires showed only minor alterations within patients with mild HCV infections, we identified several expanded Vγ9$^-$Vδ3$^+$ γδ T cell clones present in the peripheral blood of some chronic HCV patients. In general, Vδ3$^+$ cells are highly enriched in the liver, but not in the blood, of healthy persons (23). Since in routine clinical practice liver biopsies are no longer performed in uncomplicated HCV infection and patient sampling starts only after diagnosis of persistent HCV infection, we can only speculate that these liver-specific Vδ3$^+$ cells might undergo a HCV-induced clonal expansion to finally circulate in the peripheral blood of chronic HCV patients. Presence of NK cell markers and liver-homing markers (e.g., CD161) could strengthen the hypothesis Vδ3$^+$ γδ T cell clones can be associated with liver specificity. In addition, it should be worthwhile to investigate a potential HCV-related antigen specificity of expanded Vγ9$^-$Vδ3$^+$ γδ T cell clones in future *in vitro* studies.

Another important finding of this study was the absence of significant and detectable effects of novel DAA therapy on γδ T cell frequencies and their TCR repertoires in peripheral blood. This is remarkable as the systemic inflammatory milieu shows profound changes already early during antiviral therapy—even though no complete restoration of various soluble inflammatory parameters occurs (40). The effect of spontaneous clearance of acute HCV infection and a longitudinal follow-up would be an appropriate control; however, those patients are rarely seen in the clinics. It is conceivable that γδ T cells might contribute to successful resolution of the disease. Nevertheless, the finding that peripheral γδ T cell compartments and their associated TCR repertoires were highly stable even 1 year after viral elimination is in line with previous observations for other cell types. This may suggest that distinct imprints on the immune system by long-lasting HCV infection can persist for years despite eradication of HCV, which may have clinical implications for some hepatic and extrahepatic disease manifestations. For instance, no changes in the short-term risk to develop hepatocellular carcinoma upon DAA treated were observed in the analyzed cohort of HCV patients (52). With regard to NK cells, it has been suggested that phenotypic and functional alterations during chronic HCV infections could be restored upon DAA therapy (53). NK cell phenotypes were altered upon IFN-free DAA treatment further resulting in modifications of the transcription factor profiles (54, 55). T cells have also been studied in HCV infection and during DAA-related viral eradication. The proliferative capacity of HCV-responsive CD8$^+$ T cells could be restored in part (56) and a decrease in PD-1 expression on CD8$^+$ T cells was observed upon successful DAA treatment (55). On the other hand, neither the frequency nor the phenotype of regulatory T cells was rescued upon viral clearance (57). Likewise, MAIT cells were reduced in frequency and their functions are affected by chronic HCV infection (58), and in particular peripheral MAIT cells could not be restored upon viral eradication (39, 40). All these studies were analyzing the phenotypic and functional changes of given immune cells by flow cytometry. Our data now contribute that the frequency of peripheral γδ T cell populations is neither affected by uncomplicated chronic HCV infection with no liver inflammation *per se* nor by rapid viral eradication upon DAA therapy. Likewise, conventional PEG-IFNα/Ribavirin therapy might not significantly change γδ T cell numbers; however, the presence of IFNα during this treatment regime may stimulate cytokine production by Vγ9$^+$Vδ2$^+$ (24, 34, 35). In this study, peripheral Vγ9$^+$ and Vγ9$^-$ cell TCR repertoires were largely undisturbed with regard to oligoclonality and TCR diversity by rapid viral clearance using IFN-free DAA therapies. During and after DAA treatment, peripheral γδ TCR repertoires displayed a high stability for up to 1 year, indicating that there is no dominant acute anti-HCV response of γδ T cells in patients with chronic HCV infection and also consistent with the assumption that chronic viral infection might leave a sustained footprint on the γδ T cell compartment in peripheral blood.

ETHICS STATEMENT

The ethics committee of Hannover Medical School approved this study (Study number: 2148-2014 and 2604-2014), and all patients provided written confirmed consent before enrollment.

AUTHOR CONTRIBUTIONS

SR, JH, and VS conducted, analyzed, and interpreted experiments. CS-F recruited and organized healthy controls. SR and AD performed NGS. KD collected and organized HCV patient samples. CK, MC, HW, and IP discussed data and designed the study. SR, JH, HW, and IP wrote the manuscript.

ACKNOWLEDGMENTS

We would like to thank Matthias Ballmeier of the MHH cell sorting facility for flow cytometric sorting, Solaiman Raha for bioinformatics support, Melanie Drenker for isolation of peripheral blood lymphocytes of healthy control samples and the Genomics platform of the HZI Braunschweig as well as Z1-project of the Sonderforschungsbereich 900 for Illumina MiSeq sequencing.

FUNDING

The study was supported by Deutsche Forschungsgemeinschaft (CRC900 to IP), CK, MC, and HW and IRTG1273 to JH; by Hannover Medical School young investigator funds (MHH-HILF to SR); by DZIF to HW; and by HepNet study house for HW and MC. Deutsche Forschungsgemeinschaft DFG PR727/4-1 to IP, COALITION to SR and IP.

SUPPLEMENTARY MATERIAL

The Supplementary Material for this article can be found online at http://www.frontiersin.org/articles/10.3389/fimmu.2018.00510/full#supplementary-material.

REFERENCES

1. Deterding K, Gruner N, Buggisch P, Wiegand J, Galle PR, Spengler U, et al. Delayed versus immediate treatment for patients with acute hepatitis C: a randomised controlled non-inferiority trial. *Lancet Infect Dis* (2013) 13:497–506. doi:10.1016/S1473-3099(13)70059-8
2. Santantonio T, Wiegand J, Gerlach JT. Acute hepatitis C: current status and remaining challenges. *J Hepatol* (2008) 49:625–33. doi:10.1016/j.jhep.2008.07.005
3. Klenerman P, Thimme R. T cell responses in hepatitis C: the good, the bad and the unconventional. *Gut* (2012) 61:1226–34. doi:10.1136/gutjnl-2011-300620
4. Rehermann B. Pathogenesis of chronic viral hepatitis: differential roles of T cells and NK cells. *Nat Med* (2013) 19:859–68. doi:10.1038/nm.3251
5. Debes JD, de Knegt RJ, Boonstra A. The Path to cancer and back: immune modulation during hepatitis C virus infection, progression to fibrosis and cancer, and unexpected roles of new antivirals. *Transplantation* (2017) 101:910–5. doi:10.1097/TP.0000000000001623
6. Vermijlen D, Prinz I. Ontogeny of innate T lymphocytes – some innate lymphocytes are more innate than others. *Front Immunol* (2014) 5:486. doi:10.3389/fimmu.2014.00486
7. Puan KJ, Jin C, Wang H, Sarikonda G, Raker AM, Lee HK, et al. Preferential recognition of a microbial metabolite by human Vgamma2Vdelta2 T cells. *Int Immunol* (2007) 19:657–73. doi:10.1093/intimm/dxm031
8. Tanaka Y, Morita CT, Tanaka Y, Nieves E, Brenner MB, Bloom BR. Natural and synthetic non-peptide antigens recognized by human gamma delta T cells. *Nature* (1995) 375:155–8. doi:10.1038/375155a0
9. Kabelitz D, He W. The multifunctionality of human Vgamma9Vdelta2 gammadelta T cells: clonal plasticity or distinct subsets? *Scand J Immunol* (2012) 76:213–22. doi:10.1111/j.1365-3083.2012.02727.x
10. Marlin R, Pappalardo A, Kaminski H, Willcox CR, Pitard V, Netzer S, et al. Sensing of cell stress by human gammadelta TCR-dependent recognition of annexin A2. *Proc Natl Acad Sci U S A* (2017) 114:3163–8. doi:10.1073/pnas.1621052114
11. Willcox CR, Pitard V, Netzer S, Couzi L, Salim M, Silberzahn T, et al. Cytomegalovirus and tumor stress surveillance by binding of a human gammadelta T cell antigen receptor to endothelial protein C receptor. *Nat Immunol* (2012) 13:872–9. doi:10.1038/ni.2394
12. Luoma AM, Castro CD, Mayassi T, Bembinster LA, Bai L, Picard D, et al. Crystal structure of Vdelta1 T cell receptor in complex with CD1d-sulfatide shows MHC-like recognition of a self-lipid by human gammadelta T cells. *Immunity* (2013) 39:1032–42. doi:10.1016/j.immuni.2013.11.001
13. Uldrich AP, Le Nours J, Pellicci DG, Gherardin NA, McPherson KG, Lim RT, et al. CD1d-lipid antigen recognition by the gammadelta TCR. *Nat Immunol* (2013) 14:1137–45. doi:10.1038/ni.2713
14. Xu B, Pizarro JC, Holmes MA, McBeth C, Groh V, Spies T, et al. Crystal structure of a gammadelta T-cell receptor specific for the human MHC class I homolog MICA. *Proc Natl Acad Sci U S A* (2011) 108:2414–9. doi:10.1073/pnas.1015433108
15. Silva-Santos B, Serre K, Norell H. γδ T cells in cancer. *Nat Rev Immunol* (2013) 15:683–91. doi:10.1038/nri3904
16. Vantourout P, Hayday A. Six-of-the-best: unique contributions of gammadelta T cells to immunology. *Nat Rev Immunol* (2013) 13:88–100. doi:10.1038/nri3384
17. Dechanet J, Merville P, Lim A, Retiere C, Pitard V, Lafarge X, et al. Implication of gammadelta T cells in the human immune response to cytomegalovirus. *J Clin Invest* (1999) 103:1437–49. doi:10.1172/JCI5409
18. Knight A, Madrigal AJ, Grace S, Sivakumaran J, Kottaridis P, Mackinnon S, et al. The role of Vdelta2-negative gammadelta T cells during cytomegalovirus reactivation in recipients of allogeneic stem cell transplantation. *Blood* (2010) 116:2164–72. doi:10.1182/blood-2010-01-255166
19. Ravens S, Schultze-Florey C, Raha S, Sandrock I, Drenker M, Oberdorfer L, et al. Human gammadelta T cells are quickly reconstituted after stem-cell transplantation and show adaptive clonal expansion in response to viral infection. *Nat Immunol* (2017) 18:393–401. doi:10.1038/ni.3686
20. Pitard V, Roumanes D, Lafarge X, Couzi L, Garrigue I, Lafon ME, et al. Long-term expansion of effector/memory Vdelta2-gammadelta T cells is a specific blood signature of CMV infection. *Blood* (2008) 112:1317–24. doi:10.1182/blood-2008-01-136713
21. Vermijlen D, Brouwer M, Donner C, Liesnard C, Tackoen M, Van Rysselberge M, et al. Human cytomegalovirus elicits fetal gammadelta T cell responses in utero. *J Exp Med* (2010) 207:807–21. doi:10.1084/jem.20090348
22. Rajoriya N, Fergusson JR, Leithead JA, Klenerman P. Gamma delta T-lymphocytes in hepatitis C and chronic liver disease. *Front Immunol* (2014) 5:400. doi:10.3389/fimmu.2014.00400
23. Kenna T, Golden-Mason L, Norris S, Hegarty JE, O'Farrelly C, Doherty DG. Distinct subpopulations of gamma delta T cells are present in normal and tumor-bearing human liver. *Clin Immunol* (2004) 113:56–63. doi:10.1016/j.clim.2004.05.003
24. Yin W, Tong S, Zhang Q, Shao J, Liu Q, Peng H, et al. Functional dichotomy of Vdelta2 gammadelta T cells in chronic hepatitis C virus infections: role in cytotoxicity but not for IFN-gamma production. *Sci Rep* (2016) 6:26296. doi:10.1038/srep26296
25. Cimini E, Bordoni V, Sacchi A, Visco-Comandini U, Montalbano M, Taibi C, et al. Intrahepatic Vgamma9Vdelta2 T-cells from HCV-infected patients show an exhausted phenotype but can inhibit HCV replication. *Virus Res* (2018) 243:31–5. doi:10.1016/j.virusres.2017.10.008
26. Kanayama K, Morise K, Nagura H. Immunohistochemical study of T cell receptor gamma delta cells in chronic liver disease. *Am J Gastroenterol* (1992) 87:1018–22.

27. Tseng CT, Miskovsky E, Houghton M, Klimpel GR. Characterization of liver T-cell receptor gammadelta T cells obtained from individuals chronically infected with hepatitis C virus (HCV): evidence for these T cells playing a role in the liver pathology associated with HCV infections. *Hepatology* (2001) 33:1312–20. doi:10.1053/jhep.2001.24269
28. Agrati C, D'Offizi G, Narciso P, Abrignani S, Ippolito G, Colizzi V, et al. Vdelta1 T lymphocytes expressing a Th1 phenotype are the major gammadelta T cell subset infiltrating the liver of HCV-infected persons. *Mol Med* (2001) 7:11–9.
29. Deignan T, Curry MP, Doherty DG, Golden-Mason L, Volkov Y, Norris S, et al. Decrease in hepatic CD56(+) T cells and V alpha 24(+) natural killer T cells in chronic hepatitis C viral infection. *J Hepatol* (2002) 37:101–8. doi:10.1016/S0168-8278(02)00072-7
30. Puig-Pey I, Bohne F, Benitez C, Lopez M, Martinez-Llordella M, Oppenheimer F, et al. Characterization of gammadelta T cell subsets in organ transplantation. *Transpl Int* (2010) 23:1045–55. doi:10.1111/j.1432-2277.2010.01095.x
31. Agrati C, D'Offizi G, Narciso P, Selva C, Pucillo LP, Ippolito G, et al. Gammadelta T cell activation by chronic HIV infection may contribute to intrahepatic vdelta1 compartmentalization and hepatitis C virus disease progression independent of highly active antiretroviral therapy. *AIDS Res Hum Retroviruses* (2001) 17:1357–63. doi:10.1089/08892220152596614
32. Agrati C, Alonzi T, De Santis R, Castilletti C, Abbate I, Capobianchi MR, et al. Activation of Vgamma9Vdelta2 T cells by non-peptidic antigens induces the inhibition of subgenomic HCV replication. *Int Immunol* (2006) 18:11–8. doi:10.1093/intimm/dxh337
33. Par G, Rukavina D, Podack ER, Horanyi M, Szekeres-Bartho J, Hegedus G, et al. Decrease in CD3-negative-CD8dim(+) and Vdelta2/Vgamma9 TcR+ peripheral blood lymphocyte counts, low perforin expression and the impairment of natural killer cell activity is associated with chronic hepatitis C virus infection. *J Hepatol* (2002) 37:514–22. doi:10.1016/S0168-8278(02)00218-0
34. Cimini E, Bonnafous C, Bordoni V, Lalle E, Sicard H, Sacchi A, et al. Interferon-alpha improves phosphoantigen-induced Vgamma9Vdelta2 T-cells interferon-gamma production during chronic HCV infection. *PLoS One* (2012) 7:e37014. doi:10.1371/journal.pone.0037014
35. Cimini E, Bonnafous C, Sicard H, Vlassi C, D'Offizi G, Capobianchi MR, et al. In vivo interferon-alpha/ribavirin treatment modulates Vgamma9Vdelta2 T-cell function during chronic HCV infection. *J Interferon Cytokine Res* (2013) 33:136–41. doi:10.1089/jir.2012.0050
36. Wedemeyer H. Towards interferon-free treatment for all HCV genotypes. *Lancet* (2015) 385:2443–5. doi:10.1016/S0140-6736(15)60605-5
37. Deterding K, Honer Zu Siederdissen C, Port K, Solbach P, Sollik L, Kirschner J, et al. Improvement of liver function parameters in advanced HCV-associated liver cirrhosis by IFN-free antiviral therapies. *Aliment Pharmacol Ther* (2015) 42:889–901. doi:10.1111/apt.13343
38. Columbo M, Forner A, Ijzermans J, Paradis VL, Reeves H, Vilgrain VL, et al. EASL clinical practice guidelines on the management of benign liver tumours. *J Hepatol* (2016) 65:386–98. doi:10.1016/j.jhep.2016.04.001
39. Bolte FJ, O'Keefe AC, Webb LM, Serti E, Rivera E, Liang TJ, et al. Intrahepatic depletion of mucosal-associated invariant T cells in hepatitis C virus-induced liver inflammation. *Gastroenterology* (2017) 153:1392–403.e1392. doi:10.1053/j.gastro.2017.07.043
40. Hengst J, Strunz B, Deterding K, Ljunggren HG, Leeansyah E, Manns MP, et al. Nonreversible MAIT cell-dysfunction in chronic hepatitis C virus infection despite successful interferon-free therapy. *Eur J Immunol* (2016) 46:2204–10. doi:10.1002/eji.201646447
41. Hengst J, Falk CS, Schlaphoff V, Deterding K, Manns MP, Cornberg M, et al. Direct-acting antiviral-induced hepatitis C virus clearance does not completely restore the altered cytokine and chemokine milieu in patients with chronic hepatitis C. *J Infect Dis* (2016) 214:1965–74. doi:10.1093/infdis/jiw457
42. Spaan M, Hullegie SJ, Beudeker BJ, Kreefft K, van Oord GW, Groothuismink ZM, et al. Frequencies of circulating MAIT cells are diminished in chronic HCV, HIV and HCV/HIV co-infection and do not recover during therapy. *PLoS One* (2016) 11:e0159243. doi:10.1371/journal.pone.0159243
43. Serti E, Park H, Keane M, O'Keefe AC, Rivera E, Liang TJ, et al. Rapid decrease in hepatitis C viremia by direct acting antivirals improves the natural killer cell response to IFNalpha. *Gut* (2017) 66:724–35. doi:10.1136/gutjnl-2015-310033
44. Davey MS, Willcox CR, Joyce SP, Ladell K, Kasatskaya SA, McLaren JE, et al. Clonal selection in the human Vdelta1 T cell repertoire indicates gammadelta TCR-dependent adaptive immune surveillance. *Nat Commun* (2017) 8:14760. doi:10.1038/ncomms14760
45. Sherwood AM, Desmarais C, Livingston RJ, Andriesen J, Haussler M, Carlson CS, et al. Deep sequencing of the human TCRgamma and TCRbeta repertoires suggests that TCRbeta rearranges after alphabeta and gammadelta T cell commitment. *Sci Transl Med* (2011) 3:90ra61. doi:10.1126/scitranslmed.3002536
46. Ryan PL, Sumaria N, Holland CJ, Bradford CM, Izotova N, Grandjean CL, et al. Heterogeneous yet stable Vdelta2(+) T-cell profiles define distinct cytotoxic effector potentials in healthy human individuals. *Proc Natl Acad Sci U S A* (2016) 113:14378–83. doi:10.1073/pnas.1611098113
47. Shugay M, Bagaev DV, Turchaninova MA, Bolotin DA, Britanova OV, Putintseva EV, et al. VDJtools: unifying post-analysis of T cell receptor repertoires. *PLoS Comput Biol* (2015) 11:e1004503. doi:10.1371/journal.pcbi.1004503
48. Nazarov VI, Pogorelyy MV, Komech EA, Zvyagin IV, Bolotin DA, Shugay M, et al. tcR: an R package for T cell receptor repertoire advanced data analysis. *BMC Bioinformatics* (2015) 16:175. doi:10.1186/s12859-015-0613-1
49. Pauza CD, Poonia B, Li H, Cairo C, Chaudhry S. γδ T cells in HIV disease: past, present, and future. *Front Immunol* (2015) 5:687. doi:10.3389/fimmu.2014.00687
50. Khairallah C, Dechanet-Merville J, Capone M. γδ T cell-mediated immunity to cytomegalovirus infection. *Front Immunol* (2015) 8:105. doi:10.3389/fimmu.2017.00105
51. Dimova T, Brouwer M, Gosselin F, Tassignon J, Leo O, Donner C, et al. Effector Vgamma9Vdelta2 T cells dominate the human fetal gammadelta T-cell repertoire. *Proc Natl Acad Sci U S A* (2015) 112:E556–65. doi:10.1073/pnas.1412058112
52. Mettke F, Schlevogt B, Deterding K, Wranke A, Smith A, Port K, et al. Interferon-free therapy of chronic hepatitis C with direct-acting antivirals does not change the short-term risk for de novo hepatocellular carcinoma in patients with liver cirrhosis. *Aliment Pharmacol Ther* (2017) 47(4): 516–25. doi:10.1111/apt.14427
53. Serti E, Chepa-Lotrea X, Kim YJ, Keane M, Fryzek N, Liang TJ, et al. Successful interferon-free therapy of chronic hepatitis C virus infection normalizes natural killer cell function. *Gastroenterology* (2015) 149:190–200.e2. doi:10.1053/j.gastro.2015.03.004
54. Spaan M, van Oord G, Kreefft K, Hou J, Hansen BE, Janssen HL, et al. Immunological analysis during interferon-free therapy for chronic hepatitis C virus infection reveals modulation of the natural killer cell compartment. *J Infect Dis* (2016) 213:216–23. doi:10.1093/infdis/jiv391
55. Burchill MA, Golden-Mason L, Wind-Rotolo M, Rosen HR. Memory re-differentiation and reduced lymphocyte activation in chronic HCV-infected patients receiving direct-acting antivirals. *J Viral Hepat* (2015) 22:983–91. doi:10.1111/jvh.12465
56. Martin B, Hennecke N, Lohmann V, Kayser A, Neumann-Haefelin C, Kukolj G, et al. Restoration of HCV-specific CD8+ T cell function by interferon-free therapy. *J Hepatol* (2014) 61:538–43. doi:10.1016/j.jhep.2014.05.043
57. Langhans B, Nischalke HD, Kramer B, Hausen A, Dold L, van Heteren P, et al. Increased peripheral CD4(+) regulatory T cells persist after successful direct-acting antiviral treatment of chronic hepatitis C. *J Hepatol* (2017) 66:888–96. doi:10.1016/j.jhep.2016.12.019
58. van Wilgenburg B, Scherwitzl I, Hutchinson EC, Leng T, Kurioka A, Kulicke C, et al. MAIT cells are activated during human viral infections. *Nat Commun* (2016) 7:11653. doi:10.1038/ncomms11653

Conflict of Interest Statement: The authors declare that the research was conducted in the absence of commercial or financial relationships that could be construed as a potential conflict of interest.

Copyright © 2018 Ravens, Hengst, Schlapphoff, Deterding, Dhingra, Schultze-Florey, Koenecke, Cornberg, Wedemeyer and Prinz. This is an open-access article distributed under the terms of the Creative Commons Attribution License (CC BY). The use, distribution or reproduction in other forums is permitted, provided the original author(s) and the copyright owner are credited and that the original publication in this journal is cited, in accordance with accepted academic practice. No use, distribution or reproduction is permitted which does not comply with these terms.

frontiers in Immunology

MINI REVIEW
published: 13 March 2018
doi: 10.3389/fimmu.2018.00521

Integral Roles for Integrins in γδ T Cell Function

*Gabrielle M. Siegers**

Experimental Oncology, University of Alberta, Edmonton, AB, Canada

Integrins are adhesion receptors on the cell surface that enable cells to respond to their environment. Most integrins are heterodimers, comprising α and β type I transmembrane glycoprotein chains with large extracellular domains and short cytoplasmic tails. Integrins deliver signals through multiprotein complexes at the cell surface, which interact with cytoskeletal and signaling proteins to influence gene expression, cell proliferation, morphology, and migration. Integrin expression on γδ T cells (γδTc) has not been systematically investigated; however, reports in the literature dating back to the early 1990s reveal an understated role for integrins in γδTc function. Over the years, integrins have been investigated on resting and/or activated peripheral blood-derived polyclonal γδTc, γδTc clones, as well as γδ T intraepithelial lymphocytes. Differences in integrin expression have been found between αβ T cells (αβTc) and γδTc, as well as between Vδ1 and Vδ2 γδTc. While most studies have focused on human γδTc, research has also been carried out in mouse and bovine models. Roles attributed to γδTc integrins include adhesion, signaling, activation, migration, tissue localization, tissue retention, cell spreading, cytokine secretion, tumor infiltration, and involvement in tumor cell killing. This review attempts to encompass all reports of integrins expressed on γδTc published prior to December 2017, highlights areas warranting further investigation, and discusses the relevance of integrin expression for γδTc function.

Keywords: gamma delta T cells, adhesion and signaling molecules, cellular migration, tissue retention, tissue localization, tumor infiltrating lymphocytes, cytotoxicity, cytokine secretion

OPEN ACCESS

Edited by:
Pierre Vantourout, King's College London, United Kingdom

Reviewed by:
Vicky Morrison, University of Glasgow, United Kingdom
Wendy L. Havran, The Scripps Research Institute, United States
C. David Pauza, American Gene Technologies International Inc., United States

***Correspondence:**
Gabrielle M. Siegers
siegers@ualberta.ca

Specialty section:
This article was submitted to T Cell Biology, a section of the journal Frontiers in Immunology

Received: *15 January 2018*
Accepted: *28 February 2018*
Published: *13 March 2018*

Citation:
Siegers GM (2018) Integral Roles for Integrins in γδ T Cell Function. Front. Immunol. 9:521. doi: 10.3389/fimmu.2018.00521

INTRODUCTION

Although much was known about integrins on lymphocytes as early as 1990 (1), integrin expression on γδTc has been only sporadically, and often indirectly, investigated. Considered all together, these reports reveal an understated role for integrins in γδTc function (**Table 1**).

Integrins are heterodimeric adhesion receptors comprising non-covalently linked α and β chains (2). Greek letters indicating chain pairings for β1 and cluster of differentiation designations for β2 integrins are used throughout this review; cited works may have used alternative nomenclature.

INTEGRIN ACTIVATION AND FUNCTIONS

Integrins play a role in many cellular functions including development, activation, differentiation, proliferation, mobility, and survival (1, 3). Integrins enable two-way communication between cells (cytoskeleton) and their surroundings [extracellular matrix (ECM), other cells]. ECM proteins with which integrins interact include collagen, a structural protein, and adhesion proteins fibronectin (FN) and vitronectin (4). Signaling through integrins can be "inside-out," regulating extracellular interaction between integrins and their ligands, but also "outside-in," influencing actin cytoskeleton

TABLE 1 | Integrin expression reported on γδ T cells; cells used were blood-derived unless otherwise indicated.

	α	β	a.k.a	Binds	Function	spp	Reference
β1							
α1β1	CD49a	CD29	VLA-1	Collagen IV	Extravasation, tumor infiltration, cellular morphology	H	(16)
α2β1	CD49b	CD29	VLA-2	Collagen	n.d.	H	(15)
α4β1	CD49d	CD29	VLA-4	FN	n.d.	H	(15)
					Signaling, adhesion	H	(17)
					Adhesion to endothelial cells	H	(9)
				VCAM-1	Endothelial layer permeability	H	(29)
					Transendothelial migration?	H	(30)
					Adhesion to fibroblasts	H	(49)
α5β1	CD49e	CD29	VLA-5	FN	n.d.	H	(15)
					Signaling, adhesion	H	(17)
					Transendothelial migration?	H	(30)
					Vδ1 activation, localization, retention	H	(9)
					Adhesion to fibroblasts	H	(49)
α6β1	CD49f	CD29	VLA-6		Transendothelial migration	H	(30)
β2							
αLβ2	CD11a	CD18	LFA-1	CD54/ICAM-1	Adhesion to endothelial and epithelial cells, fibroblasts	H	(9)
					Naive αβTc activation?	H	(19)
					Endothelial layer permeability	H	(29)
					Transendothelial migration?	H	(30)
					Trafficking to infected airways (TB)?	NHP	(33)
					Adhesion to fibroblasts	H	(49)
					K562 leukemia cell binding	H	(54)
					Cytotoxicity against Burkitt Lymphoma, prostate cancer, Daudi B cell lymphoma	H	(55–58)
					CNS trafficking in EAE? (LN, spleen-derived)	M	(22)
αMβ2	CD11b	CD18	Mac-1		Naive αβTc activation?	H	(19)
			Mo-1		Early fetal thymocyte differentiation?	M	(67)
					CNS trafficking in EAE? (LN, spleen-derived)	M	(22)
αXβ2	CD11c	CD18	P150,95		Naive αβTc activation?	H	(19)
					Homing, activation, interferon γ secretion	H	(20)
					CNS trafficking in EAE? (LN, spleen-derived)	M	(22)
αDβ2	CD11d	CD18		ICAM-1	Vδ1 cell spreading?	H	(25)
				VCAM-1	Inflammatory response? Vδ1 tissue retention?	H	(23)
					Proliferation?	M	(22)
					Early fetal thymocyte differentiation?	M	(67)
					CNS trafficking in EAE? (LN, spleen-derived)	M	(22)
β3							
αvβ3	αv	β3	VNR	RGD sequence	IL-4 production (DETC)	M	(71)
β7							
αEβ7	CD103	β7		E-cadherin	Epithelial retention of γδTc IEL?	H	(37)
						M	(78, 79)
					Proliferation? IL-9 production?	H	(40)
					Vδ1 binding SCC	H	(49)
					Vδ1 tumor retention?	H	(49)
					Homing to gut? (mLN, colitis)	M	(80)
					Homing to and retention in gut?	R	(81)
α4β7	CD49d	β7		MadCAM	Susceptibility to HIV infection on $CCR5^{+}Vδ2$	H	(60)
					Homing to gut (TDL, RTE)	M	(76, 80)
					Migration to inflamed tissue in allergic reaction	M	(77)
					Migration to tissues	B	(7)

Question marks denote suggested functions that require further validation. a.k.a., also known as; B, bovine; CNS, central nervous system; DETC, dendritic epidermal T cells; EAE, experimental autoimmune encephalitis; ECM, extracellular matrix; FN, fibronectin; H, human; ICAM, intercellular adhesion molecule; IEL, intraepithelial lymphocyte; IL, interleukin; LFA-1, lymphocyte function-associated antigen-1; LN, lymph node; M, murine; MAdCAM-1, mucosal addressin cell adhesion molecule 1; mLN, mesenteric lymph node; n.d., not determined in this report (with respect to γδ T cells); NHP, nonhuman primate; ref, reference; RTE, recent thymic emigrant; SCC, squamous cell carcinoma; spp, species; TB, tuberculosis; TDL, thoracic duct lymphocytes; VCAM-1, vascular cell adhesion molecule-1; VLA, very late antigen; VNR, vitronectin receptor.

rearrangement as well as gene expression and transcription of associated proteins, including cytokines, to impact cellular processes (5, 6).

Integrins are integral to lymphocyte homing to tissues and migration within tissues; they—together with selectins and their respective ligands—participate in tethering, rolling, and adhesion

(7). Integrins respond to chemokine signaling arresting migration of lymphocytes and facilitating transmigration into tissues (8). In contrast to other cell types, β1 integrins on conventional T cells require activation for adhesion to occur (9, 10). Basal adhesion levels reflect inactive or low-affinity status of integrins; stimulus with 12-O-tetradecanoylphorbol-13-acetate, anti-CD3 or anti-CD2 activates β1 integrins, converting them to a high-affinity state without necessitating greater surface expression (10). Such activation dependence is also true for the β2 integrin CD11a/CD18 in T cell adhesion and de-adhesion (11). Indeed, several integrins serve as costimulatory molecules in concert with T cell antigen receptor (TCR) engagement (10, 12–14). Much occurs downstream of integrin-mediated cell adhesion, including phosphorylation of proteins in signaling pathways for cell cycle, cytokine expression, and cytoskeletal remodeling enabling processes such as proliferation and migration (3, 6).

Integrins on human γδTc will first be considered, loosely grouped according to function, and then findings in other species will be discussed. **Figure 1** depicts integrins found on γδTc and some of their functions.

ADHESION AND SIGNALING

In 1992, α4, β1, and CD18 were identified on human Vγ9 γδTc derived from stimulated peripheral blood mononuclear cells (PBMCs). While no α3, αv, or β3 expression was observed, less than 30% expressed α1, α2, or α5 chains. $CD8^+$ γδTc clones expressed high β1, and consistent α4 and α5 levels. Phorbol 12-myristate 13-acetate (PMA)-induced adhesion *via* integrin activation; while α2β1 was required for collagen binding, FN binding relied on both α4β1 and α5β1. Most polyclonal γδTc only expressed α4β1, whereas individual clones showed variation attributed to extended culturing and selection during cloning (15), corroborating evidence that β1 expression on T cells increases qualitatively and quantitatively over time in culture (1, 16). Admittedly, these studies used activated γδTc and may not have reflected the state of cells in circulation (15).

Expression of α4 and α5 on $CD3^+CD4^-CD8^-$ γδTc, and lack of α3 or α6 was confirmed. Activated $CD25^{hi}$ γδTc bound FN better than resting $CD25^{low}$ γδTc, mediated mostly by α4 and partly by α5. Culturing cells on immobilized anti-γδ TCR antibodies together with FN enhanced proliferation and increased CD25 expression, suggesting both signaling and adhesion roles for α4 and α5 integrins. While γδTc adhesion required activation through the TCR, surface levels of α4 and α5 remained unaltered (17). Cytokines such as interleukin (IL)-1β and TNF-α may influence γδTc integrin expression and/or activation (18); this has yet to be explored.

Compared to αβTc, fresh primary γδTc were more adhesive (~2:1 to 4:1) to endothelial cells, fibroblasts, and epithelial cells independent of activation. Both αβTc and γδTc required CD11a/CD18 and α4β1 to bind endothelial cells, whereas CD11a/CD18-ICAM-1 interaction facilitated adherence to fibroblasts and epithelial cells. Phorbol dibutyrate treatment of PBMCs and cytokine stimulation of monolayers greatly enhanced T cell adhesion, correlated with their expression of CD11a/CD18 and α4β1 (9). CD11a, b, c, and CD18 were detected on isopentenyl pyrophosphate (IPP)-stimulated γδTc, in parallel with markers indicating antigen presenting potential; integrins were likely involved in clustering between γδTc and naïve αβTc in an activation capacity, but their role was not directly addressed (19). It would be of interest to determine whether loss of one or more integrins might impact γδTc antigen presentation.

In healthy women, constitutively high CD11c levels were observed on circulating $CCR7^-CD4^-$ populations co-expressing γδTCR and CD8; cervical γδTc (>20%) also expressed CD11c. α1β1 and α4β7 were co-expressed on $CD11c^+CCR7^-CD4^-$ T cells, of which γδTc were a part, but unfortunately not specifically analyzed. CD11c expression was associated with T cell homing and activation, and interferon γ (IFNγ) secretion in a fraction of

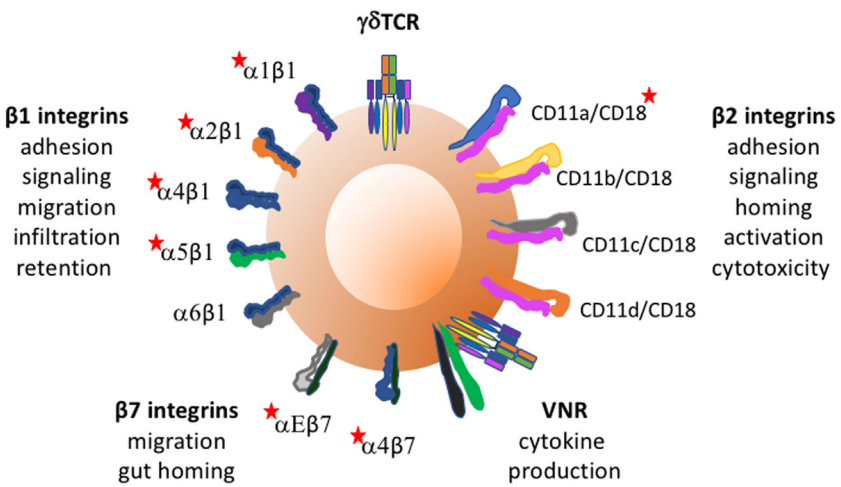

FIGURE 1 | Integrins found on γδ T cells and some of their functions. Red stars indicate integrins whose expression and/or function on γδTc has been reported to require activation. Vitronectin receptor signals through CD3 zeta of the TCR.

(E)-4-hydroxy-3-methyl-but-2-enyl pyrophosphate-stimulated γδTc (20).

CD11d, first described in 1995 (21), has now been identified on both murine (22) and human γδTc (23). CD11d/CD18 binds vascular cell adhesion molecule (VCAM-)1 (24) and intercellular adhesion molecule (ICAM-)3 (21). Vδ1 clones cultured on anti-ICAM-3 plates in the presence of IL-2 underwent spreading; however, the participating receptor on γδTc had not yet been identified (25). Since ICAM-3 is a CD11d ligand, and CD11d is highly expressed on Vδ1 γδTc (23), it was likely CD11d-ICAM-3 interaction mediating this response. ICAM-3 may play a role in inflammatory response initiation, potentially aiding in such processes as antigen presentation and cytotoxicity (26). ICAM-3 on neutrophils participates in IFNγ production but not cytotoxicity of NK cells (27) and has some predictive value in perioperative systemic inflammatory response syndrome (28). Thus, CD11d on γδTc may play a role in inflammation, but this requires further investigation.

TRANSENDOTHELIAL MIGRATION

In the first report investigating mechanisms by which γδTc cross the endothelium to migrate into inflamed tissue from the circulation, CD11a/CD18 and α4β1 on γδTc bound to endothelial cell ligands CD54/ICAM-1 and VCAM-1, respectively, increasing endothelial cell permeability. While cytotoxicity of γδTc clones to endothelial cells surely contributed to endothelial layer permeability, it was thought unlikely to occur with autologous cells *in vivo* (29).

An immunophenotyping study showed that γδTc had greater transendothelial migratory capacity than αβTc (30), explaining γδTc enrichment in chronic inflammation (31, 32), attributed to CD11a/CD18 expression, and increased α4, α5, and α6 β1 integrin density on migrating compared to non-migrating T cells; blocking assays were not performed to confirm functional relevance here (30). While CD11d expression on PBMC-derived γδTc was higher compared to αβTc (freshly isolated or expanded), their migratory ability was not compared (23). In a non-human primate tuberculosis model, adoptively transferred Vδ2 cells trafficking to infected airways expressed CD11a/CD18 (33). In contrast, increased numbers of peripheral γδTc expressing reduced CD18 levels were identified in patients suffering acute psoriasis, suggesting a role in disease pathogenesis (34).

INTEGRINS ON Vδ1 VERSUS Vδ2 DIRECTING LOCALIZATION AND TISSUE RETENTION

Integrins likely play a role in the tissue specificity of γδTc subsets. In Galéa's study, Vδ1 and Vδ2 migrated similarly, suggesting that Vδ1 tissue accumulation relates to their retention rather than migratory abilities (30). Indeed, higher CD11d expression on Vδ1 compared to Vδ2 cells may also account for preferential Vδ1 retention (23), as well as Vδ1 prevalence in large intestinal mucosal epithelium (35) and conditions such as rheumatoid arthritis (31, 32, 36).

An E-cadherin binding integrin associated with epithelial retention, αEβ7 (CD103), was found on human γδTc intraepithelial lymphocytes (IELs). While peripheral blood T cells did not express much αEβ7 the authors posited its upregulation after T cells extravasate in the lamina propria, since αEβ7 expression positively correlated with nearer proximity to epithelium (37). IL-2 and phytohemagglutinin (PHA) stimulation activated αEβ7 on cultured $CD4^+CD8^+$ IEL, and TCR crosslinking enhanced αEβ7-E-cadherin avidity (38). On αβTc, this transforming growth factor β (TGF-β)-induced integrin is associated with pro- and anti-inflammatory conditions, tissue retention, and both cytotoxic and regulatory T lymphocyte tumor infiltration and function, expertly reviewed in Ref. (39). Peters and colleagues noted upregulation of *ITGAE*, the gene encoding αEβ7, and corresponding surface expression on expanded Vδ2 cells treated with TGF-β and IL-15 correlating with enhanced proliferation and IL-9 production (40).

Subset variation exists for α5β1, with Vδ1 expressing more than Vδ2, providing an explanation for previous reports of low α5β1 expression in studies focusing on Vδ2 cells. High α5β1 expression accounted for increased Vδ1 binding to FN, potentially reflecting Vδ1 adhesion to fibroblasts *in vivo*, and the importance of this interaction for Vδ1 activation and localization (9). During inflammation, mucosal epithelial cells display increased FN levels (41), which may increase Vδ1 retention. Similar ICAM-1 and VCAM-1-mediated binding of Vδ1 and Vδ2 cells could be explained by their comparable expression of CD11a/CD18 and α4β1 (9). Thus, γδTc tissue recruitment may be achieved through CD11a/CD18 and α4β1 binding to endothelial cell ligands, and cells retained in tissue *via* CD11a/CD18 and α5β1 interactions with epithelial cell-, fibroblast-, and ECM ligands (9).

TUMOR INFILTRATION

Increased α1β1 expression may facilitate γδTc migration out of vessels and infiltration into tumors (16). A known receptor for the basement membrane protein collagen IV, α1β1 has been observed on IL-2-activated T cells invading tumors (42–47). While resting peripheral blood T cells expressed little α1β1, its expression increased over time in culture; γδTc clones expressed higher α1β1 than polyclonal T cells (16), corroborating observed α1β1 expression on long-term activated T cells (48). Anti-α1β1 inhibited $CD8^+$ γδTc interaction with collagen IV, but not FN or collagen I, in a concentration-dependent manner. Cellular morphology was impacted, as Mg^{2+} cation-dependent spreading of long-term cultured $CD8^+$ $\alpha1\beta1^{high}$ αβTc or γδTc on collagen IV-coated slides was inhibited by anti-α1β1 antibodies (16).

Compared to αβTc, γδTc derived from patient blood bound squamous carcinoma (SCC) and fibroblast cells more tightly (49), confirming previous results (9). While CD11a/CD18 played a role in both cases, SCC binding was mediated *via* L-selectin and CD44v6; fibroblast binding was achieved though α4β1 and α5β1 (49).

Vδ1 predominance has been reported in tumor infiltrating lymphocytes from lung (50), colon (51), renal carcinoma (52), and esophageal tumors (49). Preferential extravasation, infiltration, and retention of Vδ1 cells in esophageal tumors was attributed to higher expression and a greater variety of integrins such as CD11a/CD18, α4β1, α5β1, and αEβ7 on Vδ1 compared to Vδ2. In particular, Vδ1 used αEβ7 to bind SCC. Since esophageal

tumors also express E-cadherin, αEβ7 expression may provide a mechanism of lymphocyte retention in tumors (49).

CYTOTOXICITY

CD11a/CD18 facilitates effector-target cell conjugation (53). This interaction, integral to γδTc cytotoxicity, has been confirmed in binding assays with K562 leukemia (54), and blocking assays with Burkitt Lymphoma (55), prostate cancer (56, 57), and Daudi B cell lymphoma cells (58). We have observed significant γδTc apoptosis induced by anti-γδTCR (59) antibodies; thus, this may also occur with antibodies blocking CD18 and should be considered when designing controls and interpreting results from blocking assays using such antibodies. Activation of αβTCR changes CD11a/CD18 avidity from low to high transiently, to allow adhesion, but then also de-adhesion of T cells, promoting continued serial killing (11). If this holds true for the γδTCR, then this mechanism greatly contributes to γδTc cytotoxicity and could be therapeutically relevant.

SUSCEPTIBILITY TO VIRAL INFECTION

In the absence of CD4, high α4 and β7 levels on IPP-expanded Vδ2 cells formed a complex with high levels of CCR5 (fivefold higher than αβTc); this inferred HIV envelope glycoprotein susceptibility resulting in $CD4^-$ Vδ2 cells' demise (60). While Vδ1 express as much α4β7 as Vδ2, they do not express CCR5, thus rendering Vδ1 immune to HIV-envelope-mediated killing (61).

IMMUNOLOGICAL MEMORY

CD11b (complement receptor 3, Mac-1) expression on peripheral blood T cells increased with age, leveling out later in life. γδTc expressed more CD11b than αβTc across all ages; and while not shown, CD11b was thought important for migration to spleen and liver, and to indicate antigen-specific memory T cells (62). Later studies suggested roles associated with T cell immunoregulation, proliferation, and homing (63, 64), but the significance of CD11b on human γδTc remains unknown. Increased αβTc integrin levels and adherence have been associated with memory $CD4^+$ T cells (10, 65), but the only study addressing this with respect to γδTc equated Vδ1 with naïve and Vδ2 with memory cells, then compared Vδ1 to Vδ2 expression of CD11a, α4β1, and α5β1 (not CD11b), finding no correlation between adhesion/integrin levels and maturation (9). A longitudinal study following integrin expression and function during the course of γδTc maturation would be more appropriate to address this question, keeping in mind the influence of *in vitro* culture.

OF RODENTS AND RUMINANTS IN HEALTH AND DISEASE…

β1 Integrins

In mice, β1 integrins play an important role in thymocyte differentiation into $CD4^+$ and $CD8^+$ αβTc; however, their role in γδTc development remains unknown (66).

β2 Integrins

While not found on thymocytes in adult wild-type mice, transient co-expression of CD11b and CD11d on fetal thymocytes suggests an important role for β2 integrins in early differentiation (67).

In the context of experimental autoimmune encephalitis (EAE), murine γδTc differentially expressed β2 integrins and produced more IFNγ and tumor necrosis factor α in lymph nodes, spleen, and spinal cord compared to αβTc (22). At baseline, most γδTc expressed CD11a, b, and d. Both γδTc frequency and upregulation of β2 integrins, including CD11c, were noted after EAE induction; γδTc infiltration of the central nervous system (CNS) followed that of αβTc, but was more rapid (22). Thus, β2 integrin expression on γδTc affected their trafficking into the CNS, thereby impacting EAE development kinetics (22). In a follow-up study, EAE disease severity was similar in $\gamma\delta Tc^{-/-}$ mice reconstituted with γδTc lacking CD11a, b, or c suggesting that β2 integrins were not important for CNS trafficking; however, CD11d was still present on γδTc, pointing to this integrin's potential role in trafficking. $CD11a/CD18^{-/-}$ γδTc displayed reduced CNS retention and expansion during EAE, suggesting CD11a involvement in both retention and co-stimulation (68). While not specific to γδTc, it is interesting that CD3 expression was reduced in $CD11b^{-/-}$ and $CD11d^{-/-}$ mice compared to wildtype. Furthermore, CD11b and CD11d seem important for proliferation of murine T cells stimulated with PHA and Concanavalin A or superantigen, but not for their response to PMA (67). Indeed, β2 integrin expression seems concomitant with T cell expansion, in line with observations of increased CD11d expression on human γδTc expanded under higher IL-2 levels (23). In a murine spontaneous psoriasis model, reduced CD18 resulted in loss of $V\gamma5^+$ skin-resident γδTc and expansion of lymph node derived skin-homing $V\gamma4^+$ γδTc contributing to disease initiation and progression. $CD18^{low}$ γδTc expressed higher IL-7Rα levels and increased IL-7-induced proliferation generating inflammatory memory $CD44^+CD27^-$ capable of IL-17 production (34). Adoptive transfer experiments confirmed that low levels of CD18 did not impair γδTc trafficking to the skin in healthy mice (34). *Itgax*, the gene encoding integrin CD11c, is common to γδTc and NK cells, yet, differentiates γδTc from iNKT and αβTc in the mouse (69). Murine CD11c was identified on γδTc in the blood and genital tract, most predominantly on γδTc co-expressing NK1.1. Vaginal *Chlamydia* infection expanded circulating $CD11c^+$ γδTc (20).

The Vitronectin Receptor (VNR)

An integrin later identified as the VNR, or αvβ3, was found on murine dendritic epidermal T cell lines (DETC); its expression on splenic T cells was only observed after a minimum of 1 week of stimulation (70). VNR expression was soon further confirmed on autoreactive DETC-derived cell lines (6, 71, 72). A subset of these γδTc (Vγ1.1/Cγ4-Vδ6/Cδ1) secreted IL-4 in a VNR-dependent manner (71). In a follow-up report using a $TCR^{-/-}$ hybridoma line transfected with CD3ζ fusion proteins, VNR- but not TCR-engagement by ligand was required in conjunction with CD3ζ chain signaling for IL-2 production (73). VNR recognizes the adhesive peptide sequence RGD in ECM proteins (74). While human αβTc can be induced to express VNR upon stimulation

with PHA and/or PMA (75), VNR has not been found on polyclonal or clonal human γδTc (15).

α4β7 and αEβ7

High levels of α4β7 were associated with gut-tropism of murine γδTc trafficking from adult thymus to the small intestine epithelium, whereupon reaching their destination, α4β7 was subsequently downregulated, through interaction with its counter-receptor mucosal addressin cell adhesion molecule 1 (MadCAM) on the lamina propria (76). In a model of allergic reaction, IL-17$^+$ γδTc expressed α4β7 that enabled their mobilization by CCL25 in inflamed tissue, which in turn modulated IL-17 levels (77). Blocking α4β7 *in vivo* prevented the migration of IL-17$^+$ γδTc but not αβTc into mouse pleura, and also blocked transmigration of γδTc across VCAM-1- and MadCAM-1-expressing endothelium toward CCL25 or cell-free pleural washes from mice in whom an allergic reaction had been induced (77). Bovine peripheral blood-derived CD8$^+$ γδTc accumulated in MAdCAM-1-expressing tissues in a dose-dependent manner. CD8$^+$ γδTc expressed 1.5-fold more α4β7 than CD8$^-$ γδTc but similar β_1 and β_2 levels. While adding CXCL12 increased MAdCAM binding of all γδTc, CCL21 activated integrins and increased CD8$^+$ γδTc binding to recombinant MAdCAM1 more so than CD8$^-$ γδTc. Circulating human CD8$^-$ and CD8$^+$ γδTc migrated similarly in response to CCL21, and expressed comparable α4β7; this species-specific discrepancy was attributed to CD8 chain usage differences in humans (αα) versus cows (αβ) (7).

Prevalence of "inflammatory" γδTc (iγδTc) co-expressing high levels of gut-homing α4β7 and αEβ7 correlated with disease severity in both spontaneous and induced murine colitis models. Cytotoxicity, cytokine production, and NK cell receptor genes were upregulated on iγδTc compared to other γδTc subsets (expressing α4β7 or αEβ7) isolated from mesenteric lymph nodes in induced colitis, suggesting profound functional relevance of integrin co-expression on these cells (78).

In αEβ7-knockout mice, γδTc IEL migration within the intraepithelial compartment was enhanced (79) and remained so when challenged with *Salmonella typhimurium* or *Toxoplasma gondii*, drastically reducing pathogen translocation and emphasizing the ability of αEβ7 to limit γδTc IEL migration and impact host defense against infection (80). In a study on suckling Lewis rats, probiotics significantly increased both CD62L-positive and negative CD4$^-$CD8$^-$ T cells expressing αEβ7 in mesenteric lymph nodes; in IEL, significantly increased CD62L$^-$ αEβ7-expressing CD4$^-$CD8$^-$ cells were observed, hypothesized to result from enhanced homing and retention, respectively (81).

CONCLUDING REMARKS

T cells use classical cell biological pathways in new ways (82). Thus, understanding integrin functions on other cell types, including αβTc, suggests but does not dictate their roles on γδTc. Some roles suspected in human γδTc have been confirmed in other species, whereas interspecies variation also exists. Some integrin functions are expected and others surprising, such as HIV-induced Vδ2 demise enabled by α4β7 complexed with CCR5 (60). This review describes the tip of the iceberg with respect to integrins on γδTc; some have yet to be explored at all, and others are worthy of further study. Understanding integrin contributions to γδTc activation, proliferation, and cytotoxicity could inform better expansion protocols and improve γδTc immunotherapy for a variety of indications. We have much to learn about integrin involvement in the myriad functions of these fascinating cells.

AUTHOR CONTRIBUTIONS

GS reviewed the literature, wrote the manuscript, and designed both the table and the figure.

ACKNOWLEDGMENTS

Special thanks to Dr. Gregory Dekaban, who introduced me to the exciting world of integrins, and Dr. Lynne-Marie Postovit, for continued support. Thanks to Indrani Dutta for critical reading of the manuscript.

FUNDING

This work has been supported by the London Regional Cancer Program, London, ON (Translational Breast Cancer Postdoctoral award) and the Cancer Research Society.

REFERENCES

1. Hemler ME. VLA proteins in the integrin family: structures, functions, and their role on leukocytes. *Annu Rev Immunol* (1990) 8:365–400. doi:10.1146/annurev.iy.08.040190.002053
2. Stewart M, Thiel M, Hogg N. Leukocyte integrins. *Curr Opin Cell Biol* (1995) 7:690–6. doi:10.1016/0955-0674(95)80111-1
3. Streuli CH. Integrins as architects of cell behavior. *Mol Biol Cell* (2016) 27:2885–8. doi:10.1091/mbc.E15-06-0369
4. Derya M, Yilmaz I, Aytekin M. The role of extracellular matrix in lung diseases. *Biol Med* (2014) 6:1–8. doi:10.4172/0974-8369.1000200
5. Lub M, van Kooyk Y, Figdor CG. Ins and outs of LFA-1. *Immunol Today* (1995) 16:479–83. doi:10.1016/0167-5699(95)80031-X
6. Halvorson MJ, Coligan JE, Sturmhofel K. The vitronectin receptor (alpha V beta 3) as an example for the role of integrins in T lymphocyte stimulation. *Immunol Res* (1996) 15:16–29. doi:10.1007/BF02918281
7. Wilson E, Hedges JF, Butcher EC, Briskin M, Jutila MA. Bovine gamma delta T cell subsets express distinct patterns of chemokine responsiveness and adhesion molecules: a mechanism for tissue-specific gamma delta T cell subset accumulation. *J Immunol* (2002) 169:4970–5. doi:10.4049/jimmunol.169.9.4970
8. Campbell JJ, Hedrick J, Zlotnik A, Siani MA, Thompson DA, Butcher EC. Chemokines and the arrest of lymphocytes rolling under flow conditions. *Science* (1998) 279:381–4. doi:10.1126/science.279.5349.381
9. Nakajima S, Roswit WT, Look DC, Holtzman MJ. A hierarchy for integrin expression and adhesiveness among T cell subsets that is linked to TCR gene usage and emphasizes V delta 1+ gamma delta T cell adherence and tissue retention. *J Immunol* (1995) 155:1117–31.
10. Shimizu Y, Van Seventer GA, Horgan KJ, Shaw S. Regulated expression and binding of three VLA (beta 1) integrin receptors on T cells. *Nature* (1990) 345:250–3. doi:10.1038/345250a0
11. Dustin ML, Springer TA. T-cell receptor cross-linking transiently stimulates adhesiveness through LFA-1. *Nature* (1989) 341:619–24. doi:10.1038/341619a0

12. Matsuyama T, Yamada A, Kay J, Yamada KM, Akiyama SK, Schlossman SF, et al. Activation of CD4 cells by fibronectin and anti-CD3 antibody. A synergistic effect mediated by the VLA-5 fibronectin receptor complex. *J Exp Med* (1989) 170:1133–48. doi:10.1084/jem.170.4.1133
13. Yamada A, Nikaido T, Nojima Y, Schlossman SF, Morimoto C. Activation of human CD4 T lymphocytes. Interaction of fibronectin with VLA-5 receptor on CD4 cells induces the AP-1 transcription factor. *J Immunol* (1991) 146:53–6.
14. Damle NK, Aruffo A. Vascular cell adhesion molecule 1 induces T-cell antigen receptor-dependent activation of CD4+T lymphocytes. *Proc Natl Acad Sci U S A* (1991) 88:6403–7. doi:10.1073/pnas.88.15.6403
15. Wilkins J, Selin L, Stewart S, Sivananthan K, Stupack D. The interactions of gamma delta T cells with extracellular matrix: receptor expression and utilization patterns. *Scand J Immunol* (1992) 36:213–9. doi:10.1111/j.1365-3083.1992.tb03093.x
16. Bank I, Book M, Ware R. Functional role of VLA-1 (CD49A) in adhesion, cation-dependent spreading, and activation of cultured human T lymphocytes. *Cell Immunol* (1994) 156:424–37. doi:10.1006/cimm.1994.1187
17. Avdalovic M, Fong D, Formby B. Adhesion and costimulation of proliferative responses of human gamma delta T cells by interaction of VLA-4 and VLA-5 with fibronectin. *Immunol Lett* (1993) 35:101–8. doi:10.1016/0165-2478(93)90077-F
18. Meager A. Cytokine regulation of cellular adhesion molecule expression in inflammation. *Cytokine Growth Factor Rev* (1999) 10:27–39. doi:10.1016/S1359-6101(98)00024-0
19. Brandes M, Willimann K, Moser B. Professional antigen-presentation function by human gammadelta T Cells. *Science* (2005) 309:264–8. doi:10.1126/science.1110267
20. Qualai J, Li LX, Cantero J, Tarrats A, Fernández MA, Sumoy L, et al. Expression of CD11c is associated with unconventional activated T cell subsets with high migratory potential. *PLoS One* (2016) 11:e0154253. doi:10.1371/journal.pone.0154253
21. Van der Vieren M, Le Trong H, Wood CL, Moore PF, St John T, Staunton DE, et al. A novel leukointegrin, alpha d beta 2, binds preferentially to ICAM-3. *Immunity* (1995) 3:683–90. doi:10.1016/1074-7613(95)90058-6
22. Smith SS, Barnum SR. Differential expression of beta 2-integrins and cytokine production between gammadelta and alphabeta T cells in experimental autoimmune encephalomyelitis. *J Leukoc Biol* (2008) 83:71–9. doi:10.1189/jlb.0407263
23. Siegers GM, Barreira CR, Postovit LM, Dekaban GA. CD11d beta2 integrin expression on human NK, B, and gammadelta T cells. *J Leukoc Biol* (2017) 101:1029–35. doi:10.1189/jlb.3AB0716-326RR
24. Van der Vieren M, Crowe DT, Hoekstra D, Vazeux R, Hoffman PA, Grayson MH, et al. The leukocyte integrin alpha D beta 2 binds VCAM-1: evidence for a binding interface between I domain and VCAM-1. *J Immunol* (1999) 163:1984–90.
25. Hernandez-Caselles T, Rubio G, Campanero MR, del Pozo MA, Muro M, Sanchez-Madrid F, et al. ICAM-3, the third LFA-1 counterreceptor, is a co-stimulatory molecule for both resting and activated T lymphocytes. *Eur J Immunol* (1993) 23:2799–806. doi:10.1002/eji.1830231112
26. Knudsen H, Andersen CB, Ladefoged SD. Expression of the intercellular adhesion molecule-3 (ICAM-3) in human renal tissue with relation to kidney transplants and various inflammatory diseases. *APMIS* (1995) 103:593–6. doi:10.1111/j.1699-0463.1995.tb01411.x
27. Costantini C, Calzetti F, Perbellini O, Micheletti A, Scarponi C, Lonardi S, et al. Human neutrophils interact with both 6-sulfo LacNAc+ DC and NK cells to amplify NK-derived IFN{gamma}: role of CD18, ICAM-1, and ICAM-3. *Blood* (2011) 117:1677–86. doi:10.1182/blood-2010-06-287243
28. Litmathe J, Boeken U, Bohlen G, Gursoy D, Sucker C, Feindt P. Systemic inflammatory response syndrome after extracorporeal circulation: a predictive algorithm for the patient at risk. *Hellenic J Cardiol* (2011) 52:493–500.
29. Mohagheghpour N, Bermudez LE, Khajavi S, Rivas A. The VLA-4/VCAM-1 molecules participate in gamma delta cell interaction with endothelial cells. *Cell Immunol* (1992) 143:170–82. doi:10.1016/0008-8749(92)90014-G
30. Galea P, Brezinschek R, Lipsky PE, Oppenheimer-Marks N. Phenotypic characterization of CD4-/alpha beta TCR+ and gamma delta TCR+ T cells with a transendothelial migratory capacity. *J Immunol* (1994) 153:529–42.
31. Brennan FM, Londei M, Jackson AM, Hercend T, Brenner MB, Maini RN, et al. T cells expressing gamma delta chain receptors in rheumatoid arthritis. *J Autoimmun* (1988) 1:319–26. doi:10.1016/0896-8411(88)90002-9
32. Meliconi R, Pitzalis C, Kingsley GH, Panayi GS. Gamma/delta T cells and their subpopulations in blood and synovial fluid from rheumatoid arthritis and spondyloarthritis. *Clin Immunol Immunopathol* (1991) 59:165–72. doi:10.1016/0090-1229(91)90090-W
33. Qaqish A, Huang D, Chen CY, Zhang Z, Wang R, Li S, et al. Adoptive transfer of phosphoantigen-specific gammadelta T cell subset attenuates *Mycobacterium tuberculosis* infection in nonhuman primates. *J Immunol* (2017) 198:4753–63. doi:10.4049/jimmunol.1602019
34. Gatzka M, Hainzl A, Peters T, Singh K, Tasdogan A, Wlaschek M, et al. Reduction of CD18 promotes expansion of inflammatory gammadelta T cells collaborating with CD4+ T cells in chronic murine psoriasiform dermatitis. *J Immunol* (2013) 191(11):5477–88. doi:10.4049/jimmunol.1300976
35. Deusch K, Lüling F, Reich K, Classen M, Wagner H, Pfeffer K. A major fraction of human intraepithelial lymphocytes simultaneously expresses the gamma/delta T cell receptor, the CD8 accessory molecule and preferentially uses the V delta 1 gene segment. *Eur J Immunol* (1991) 21:1053–9. doi:10.1002/eji.1830210429
36. Sioud M, Kjeldsen-Kragh J, Quayle A, Kalvenes C, Waalen K, Førre O, et al. The V delta gene usage by freshly isolated T lymphocytes from synovial fluids in rheumatoid synovitis: a preliminary report. *Scand J Immunol* (1990) 31:415–21. doi:10.1111/j.1365-3083.1990.tb02787.x
37. Farstad IN, Halstensen TS, Lien B, Kilshaw PJ, Lazarovits AI, Brandtzaeg P. Distribution of beta 7 integrins in human intestinal mucosa and organized gut-associated lymphoid tissue. *Immunology* (1996) 89:227–37. doi:10.1046/j.1365-2567.1996.d01-727.x
38. Higgins JM, Mandlebrot DA, Shaw SK, Russell GJ, Murphy EA, Chen YT, et al. Direct and regulated interaction of integrin alphaEbeta7 with E-cadherin. *J Cell Biol* (1998) 140:197–210. doi:10.1083/jcb.140.1.197
39. Hardenberg JB, Braun A, Schon MP. A Yin and Yang in epithelial immunology: the roles of the alphaE(CD103)beta7 integrin in T cells. *J Invest Dermatol* (2018) 138:23–31. doi:10.1016/j.jid.2017.05.026
40. Peters C, Hasler R, Wesch D, Kabelitz D. Human Vdelta2 T cells are a major source of interleukin-9. *Proc Natl Acad Sci U S A* (2016) 113:12520–5. doi:10.1073/pnas.1607136113
41. Campbell AM, Chanez P, Vignola AM, Bousquet J, Couret I, Michel FB, et al. Functional characteristics of bronchial epithelium obtained by brushing from asthmatic and normal subjects. *Am Rev Respir Dis* (1993) 147:529–34. doi:10.1164/ajrccm/147.3.529
42. Chan BM, Wong JG, Rao A, Hemler ME. T cell receptor-dependent, antigen-specific stimulation of a murine T cell clone induces a transient, VLA protein-mediated binding to extracellular matrix. *J Immunol* (1991) 147:398–404.
43. Alcocer-Varela J, Aleman-Hoey D, Alarcon-Segovia D. Interleukin-1 and interleukin-6 activities are increased in the cerebrospinal fluid of patients with CNS lupus erythematosus and correlate with local late T-cell activation markers. *Lupus* (1992) 1:111–7. doi:10.1177/096120339200100209
44. Saltini C, Hemler ME, Crystal RG. T lymphocytes compartmentalized on the epithelial surface of the lower respiratory tract express the very late activation antigen complex VLA-1. *Clin Immunol Immunopathol* (1988) 46:221–33. doi:10.1016/0090-1229(88)90185-7
45. Choy MY, Richman PI, Horton MA, MacDonald TT. Expression of the VLA family of integrins in human intestine. *J Pathol* (1990) 160:35–40. doi:10.1002/path.1711600109
46. Konter U, Kellner I, Hoffmeister B, Sterry W. Induction and upregulation of adhesion receptors in oral and dermal lichen planus. *J Oral Pathol Med* (1990) 19:459–63. doi:10.1111/j.1600-0714.1990.tb00787.x
47. Hermann GG, Geertsen PF, von der Maase H, Steven K, Andersen C, Hald T, et al. Recombinant interleukin-2 and lymphokine-activated killer cell treatment of advanced bladder cancer: clinical results and immunological effects. *Cancer Res* (1992) 52:726–33.
48. Hemler ME. Adhesive protein receptors on hematopoietic cells. *Immunol Today* (1988) 9:109–13. doi:10.1016/0167-5699(88)91280-7
49. Thomas ML, Badwe RA, Deshpande RK, Samant UC, Chiplunkar SV. Role of adhesion molecules in recruitment of Vdelta1 T cells from the peripheral blood to the tumor tissue of esophageal cancer patients. *Cancer Immunol Immunother* (2001) 50:218–25. doi:10.1007/s002620100190
50. Zocchi MR, Ferrarini M, Rugarli C. Selective lysis of the autologous tumor by delta TCS1+ gamma/delta+ tumor-infiltrating lymphocytes from human lung carcinomas. *Eur J Immunol* (1990) 20:2685–9. doi:10.1002/eji.1830201224

51. Maeurer MJ, Martin D, Walter W, Liu K, Zitvogel L, Halusczcak K, et al. Human intestinal Vdelta1+ lymphocytes recognize tumor cells of epithelial origin. *J Exp Med* (1996) 183:1681–96. doi:10.1084/jem.183.4.1681
52. Choudhary A, Davodeau F, Moreau A, Peyrat MA, Bonneville M, Jotereau F. Selective lysis of autologous tumor cells by recurrent gamma delta tumor-infiltrating lymphocytes from renal carcinoma. *J Immunol* (1995) 154:3932–40.
53. Springer TA. Adhesion receptors of the immune system. *Nature* (1990) 346:425–34. doi:10.1038/346425a0
54. Arancia G, Malorni W, Iosi F, Zarcone D, Cerruti G, Favre A, et al. Morphological features of cloned lymphocytes expressing gamma/delta T cell receptors. *Eur J Immunol* (1991) 21:173–8. doi:10.1002/eji.1830210126
55. Nelson EL, Kim HT, Mar ND, Goralski TJ, McIntyre BW, Clayberger C, et al. Novel tumor-associated accessory molecules involved in the gamma/delta cytotoxic T-lymphocyte-Burkitt's lymphoma interaction. *Cancer* (1995) 75:886–93. doi:10.1002/1097-0142(19950201)75:3<886::AID-CNCR2820750321>3.0.CO;2-G
56. Liu Z, Guo BL, Gehrs BC, Nan L, Lopez RD. Ex vivo expanded human Vgamma9Vdelta2+ gammadelta-T cells mediate innate antitumor activity against human prostate cancer cells in vitro. *J Urol* (2005) 173:1552–6. doi:10.1097/01.ju.0000154355.45816.0b
57. Siegers GM, Ribot EJ, Keating A, Foster PJ. Extensive expansion of primary human gamma delta T cells generates cytotoxic effector memory cells that can be labeled with Feraheme for cellular MRI. *Cancer Immunol Immunother* (2013) 62:571–83. doi:10.1007/s00262-012-1353-y
58. Wang P, Malkovsky M. Different roles of the CD2 and LFA-1 T-cell co-receptors for regulating cytotoxic, proliferative, and cytokine responses of human V gamma 9/V delta 2 T cells. *Mol Med* (2000) 6:196–207.
59. Dutta I, Postovit LM, Siegers GM. Apoptosis induced via gamma delta T cell antigen receptor "blocking" antibodies: a cautionary tale. *Front Immunol* (2017) 8:776. doi:10.3389/fimmu.2017.00776
60. Li H, Pauza CD. HIV envelope-mediated, CCR5/alpha4beta7-dependent killing of CD4-negative gammadelta T cells which are lost during progression to AIDS. *Blood* (2011) 118:5824–31. doi:10.1182/blood-2011-05-356535
61. Li H, Pauza CD. The alpha4beta7 integrin binds HIV envelope but does not mediate bystander killing of gammadelta T cells. *Blood* (2012) 120:698–9. doi:10.1182/blood-2012-03-420117
62. Hoshino T, Yamada A, Honda J, Imai Y, Nakao M, Inoue M, et al. Tissue-specific distribution and age-dependent increase of human CD11b+ T cells. *J Immunol* (1993) 151:2237–46.
63. Wagner C, Hänsch GM, Stegmaier S, Denefleh B, Hug F, Schoels M. The complement receptor 3, CR3 (CD11b/CD18), on T lymphocytes: activation-dependent up-regulation and regulatory function. *Eur J Immunol* (2001) 31:1173–80. doi:10.1002/1521-4141(200104)31:4<1173::AID-IMMU1173>3.0.CO;2-9
64. Nielsen HV, Christensen JP, Andersson EC, Marker O, Thomsen AR. Expression of type 3 complement receptor on activated CD8+ T cells facilitates homing to inflammatory sites. *J Immunol* (1994) 153:2021–8.
65. Shimizu Y, Newman W, Gopal TV, Horgan KJ, Graber N, Beall LD, et al. Four molecular pathways of T cell adhesion to endothelial cells: roles of LFA-1, VCAM-1, and ELAM-1 and changes in pathway hierarchy under different activation conditions. *J Cell Biol* (1991) 113:1203–12. doi:10.1083/jcb.113.5.1203
66. Schmeissner PJ, Xie H, Smilenov LB, Shu F, Marcantonio EE. Integrin functions play a key role in the differentiation of thymocytes in vivo. *J Immunol* (2001) 167:3715–24. doi:10.4049/jimmunol.167.7.3715
67. Wu H, Rodgers JR, Perrard XY, Perrard JL, Prince JE, Abe Y, et al. Deficiency of CD11b or CD11d results in reduced staphylococcal enterotoxin-induced T cell response and T cell phenotypic changes. *J Immunol* (2004) 173:297–306. doi:10.4049/jimmunol.173.1.297
68. Wohler JE, Smith SS, Zinn KR, Bullard DC, Barnum SR. Gammadelta T cells in EAE: early trafficking events and cytokine requirements. *Eur J Immunol* (2009) 39:1516–26. doi:10.1002/eji.200839176
69. Bezman NA, Kim CC, Sun JC, Min-Oo G, Hendricks DW, Kamimura Y, et al. Molecular definition of the identity and activation of natural killer cells. *Nat Immunol* (2012) 13:1000–9. doi:10.1038/ni.2395
70. Maxfield SR, Moulder K, Koning F, Elbe A, Stingl G, Coligan JE, et al. Murine T cells express a cell surface receptor for multiple extracellular matrix proteins. Identification and characterization with monoclonal antibodies. *J Exp Med* (1989) 169:2173–90. doi:10.1084/jem.169.6.2173
71. Roberts K, Yokoyama WM, Kehn PJ, Shevach EM. The vitronectin receptor serves as an accessory molecule for the activation of a subset of gamma/delta T cells. *J Exp Med* (1991) 173:231–40. doi:10.1084/jem.173.1.231
72. Wilde DB, Roberts K, Sturmhöfel K, Kikuchi G, Coligan JE, Shevach EM. Mouse autoreactive gamma/delta T cells. I. Functional properties of autoreactive T cell hybridomas. *Eur J Immunol* (1992) 22:483–9. doi:10.1002/eji.1830220229
73. Sturmhofel K, Brando C, Martinon F, Shevach EM, Coligan JE. Antigen-independent, integrin-mediated T cell activation. *J Immunol* (1995) 154:2104–11.
74. Ruoslahti E, Pierschbacher MD. Arg-Gly-Asp: a versatile cell recognition signal. *Cell* (1986) 44:517–8. doi:10.1016/0092-8674(86)90259-X
75. Huang S, Endo RI, Nemerow GR. Upregulation of integrins alpha v beta 3 and alpha v beta 5 on human monocytes and T lymphocytes facilitates adenovirus-mediated gene delivery. *J Virol* (1995) 69:2257–63.
76. Guy-Grand D, Vassalli P, Eberl G, Pereira P, Burlen-Defranoux O, Lemaitre F, et al. Origin, trafficking, and intraepithelial fate of gut-tropic T cells. *J Exp Med* (2013) 210:1839–54. doi:10.1084/jem.20122588
77. Costa MF, Bornstein VU, Candéa AL, Henriques-Pons A, Henriques MG, Penido C. CCL25 induces alpha(4)beta(7) integrin-dependent migration of IL-17(+) gammadelta T lymphocytes during an allergic reaction. *Eur J Immunol* (2012) 42:1250–60. doi:10.1002/eji.201142021
78. Do JS, Kim S, Keslar K, Jang E, Huang E, Fairchild RL, et al. γδ T cells coexpressing gut homing alpha4beta7 and alphaE integrins define a novel subset promoting intestinal inflammation. *J Immunol* (2017) 198:908–15. doi:10.4049/jimmunol.1601060
79. Edelblum KL, Shen L, Weber CR, Marchiando AM, Clay BS, Wang Y, et al. Dynamic migration of gammadelta intraepithelial lymphocytes requires occludin. *Proc Natl Acad Sci U S A* (2012) 109:7097–102. doi:10.1073/pnas.1112519109
80. Edelblum KL, Singh G, Odenwald MA, Lingaraju A, El Bissati K, McLeod R, et al. γδ Intraepithelial lymphocyte migration limits transepithelial pathogen invasion and systemic disease in mice. *Gastroenterology* (2015) 148:1417–26. doi:10.1053/j.gastro.2015.02.053
81. Rigo-Adrover MD, Franch A, Castell M, Perez-Cano FJ. Preclinical immunomodulation by the probiotic *Bifidobacterium breve* M-16V in early life. *PLoS One* (2016) 11:e0166082. doi:10.1371/journal.pone.0166082
82. Dustin ML. T-cells play the classics with a different spin. *Mol Biol Cell* (2014) 25:1699–703. doi:10.1091/mbc.E13-11-0636

Conflict of Interest Statement: The author declares that the research was conducted in the absence of any commercial or financial relationships that could be construed as a potential conflict of interest.

Copyright © 2018 Siegers. This is an open-access article distributed under the terms of the Creative Commons Attribution License (CC BY). The use, distribution or reproduction in other forums is permitted, provided the original author(s) and the copyright owner are credited and that the original publication in this journal is cited, in accordance with accepted academic practice. No use, distribution or reproduction is permitted which does not comply with these terms.

frontiers in Immunology

ORIGINAL RESEARCH
published: 23 February 2018
doi: 10.3389/fimmu.2018.00265

The Armadillo (*Dasypus novemcinctus*): A Witness but Not a Functional Example for the Emergence of the Butyrophilin 3/Vγ9Vδ2 System in Placental Mammals

*Alina Suzann Fichtner[1], Mohindar Murugesh Karunakaran[1], Lisa Starick[1], Richard W. Truman[2] and Thomas Herrmann[1]**

[1] Institut für Virologie und Immunbiologie, Julius-Maximilians-Universität Würzburg, Würzburg, Germany, [2] National Hansen's Disease Program, Louisiana State University, Baton Rouge, LA, United States

OPEN ACCESS

Edited by:
Pierre Vantourout, King's College London, United Kingdom

Reviewed by:
Jim Kaufman, University of Cambridge, United Kingdom
Jacques A. Nunes, Center de Recherche en Cancerologie de Marseille, France

***Correspondence:**
Thomas Herrmann
herrmann-t@vim.uni-wuerzburg.de

Specialty section:
This article was submitted to T Cell Biology, a section of the journal Frontiers in Immunology

Received: *29 September 2017*
Accepted: *30 January 2018*
Published: *23 February 2018*

Citation:
Fichtner AS, Karunakaran MM, Starick L, Truman RW and Herrmann T (2018) The Armadillo (Dasypus novemcinctus): A Witness but Not a Functional Example for the Emergence of the Butyrophilin 3/Vγ9Vδ2 System in Placental Mammals. Front. Immunol. 9:265. doi: 10.3389/fimmu.2018.00265

1–5% of human blood T cells are Vγ9Vδ2 T cells whose T cell receptor (TCR) contain a *TRGV9/TRGJP* rearrangement and a *TRDV2* comprising Vδ2-chain. They respond to phosphoantigens (PAgs) like isopentenyl pyrophosphate or (E)-4-hydroxy-3-methyl-but-2-enyl-pyrophosphate (HMBPP) in a butyrophilin 3 (BTN3)-dependent manner and may contribute to the control of mycobacterial infections. These cells were thought to be restricted to primates, but we demonstrated by analysis of genomic databases that *TRGV9*, *TRDV2*, and *BTN3* genes coevolved and emerged together with placental mammals. Furthermore, we identified alpaca (*Vicugna pacos*) as species with typical Vγ9Vδ2 TCR rearrangements and currently aim to directly identify Vγ9Vδ2 T cells and BTN3. Other candidates to study this coevolution are the bottlenose dolphin (*Tursiops truncatus*) and the nine-banded armadillo (*Dasypus novemcinctus*) with genomic sequences encoding open reading frames for *TRGV9*, *TRDV2*, and the extracellular part of *BTN3*. Dolphins have been shown to express Vγ9- and Vδ2-like TCR chains and possess a predicted *BTN3*-like gene homologous to human *BTN3A3*. The other candidate, the armadillo, is of medical interest since it serves as a natural reservoir for *Mycobacterium leprae*. In this study, we analyzed the armadillo genome and found evidence for multiple non-functional *BTN3* genes including genomic context which closely resembles the organization of the human, alpaca, and dolphin *BTN3A3* loci. However, no *BTN3* transcript could be detected in armadillo cDNA. Additionally, attempts to identify a functional *TRGV9/TRGJP* rearrangement *via* PCR failed. In contrast, complete *TRDV2* gene segments preferentially rearranged with a *TRDJ4* homolog were cloned and co-expressed with a human Vγ9-chain in murine hybridoma cells. These cells could be stimulated by immobilized anti-mouse CD3 antibody but not with human RAJI-RT1B^{l} cells and HMBPP. So far, the

Abbreviations: BTN, butyrophilin; BTN3-V, BTN3 IgV-like region; BTN3-C, BTN3 IgC-like region; HMBPP, (E)-4-hydroxy-3-methyl-but-2-enyl pyrophosphate; PAg, phosphoantigen; wgs, whole genome shotgun contigs.

lack of expression of *TRGV9* rearrangements and *BTN3* renders the armadillo an unlikely candidate species for PAg-reactive Vγ9Vδ2 T cells. This is in line with the postulated coevolution of the three genes, where occurrence of Vγ9Vδ2 TCRs coincides with a functional BTN3 molecule.

Keywords: Vγ9Vδ2, TRGV9, TRDV2, butyrophilin 3, coevolution, nine-banded armadillo, placental mammals

INTRODUCTION

With up to 5% of T cells, Vγ9Vδ2 T cells constitute a major γδ T cell population in the human blood (1, 2). Their T cell receptor (TCR) is characterized by a pairing of a Vγ9 chain, encoded by a *TRGV9/TRGJP* gene rearrangement and a *TRGC1* constant region, and a Vδ2 chain using a *TRDV2* variable region. This cell subset recognizes and rapidly reacts to endogenous or exogenous phosphoantigens (PAgs) in a MHC-unrestricted fashion (1). PAgs are small molecules with pyrophosphate groups produced during isoprenoid synthesis. The most important naturally occurring PAgs are isopentenyl pyrophosphate and (E)-4-hydroxy-3-methyl-but-2-enyl pyrophosphate (HMBPP). The importance of the Vγ9Vδ2 T cell subset lies within their multitude of effector functions such as production of cytokines, killing of cells (*via* TCR, NKG2D, CD16), B cell help and APC-like functions (2). Their reactivity to aminobisphosphonates and PAgs makes them a potential tool for tumor treatment (3) and involvement in infections with HMBPP-producing pathogens like *Mycobacterium tuberculosis* (4–8), *Mycobacterium leprae* (9), *Listeria monocytogenes* (10) and in malaria (11) and toxoplasmosis (12) was observed. The implication of Vγ9Vδ2 T cells in infections has been reviewed elsewhere (13, 14). Recently, Butyrophilin 3 (BTN3) (CD277) has been proven essential for the PAg-dependent activation of Vγ9Vδ2 T cells (15). The three human BTN3 isoforms belong to the immunoglobulin superfamily and their expression has been shown on T and B cells, monocytes, NK cells, dendritic cells (16–18), and non-hematopoietic cells (19). In humans and other primates, the *BTN3* gene was subject to two successive duplications resulting in three isoforms BTN3A1, A2, and A3 (20). These share the same overall structure: two extracellular immunoglobulin-like domains (BTN3-V and BTN3-C) and a transmembrane region. The isoforms BTN3A1 and A3 additionally possess an intracellular B30.2 domain, which is missing in BTN3A2 (21). Regarding Vγ9Vδ2 T cells, BTN3A1 seems to mediate PAg recognition through the B30.2 domain containing a positively charged surface pocket, which can accommodate PAgs (15). The molecule BTN3A1, however, is not sufficient to induce PAg-mediated Vγ9Vδ2 T cell activation and other unknown molecules on the human chromosome 6 are currently investigated (22).

The long-standing belief that Vγ9Vδ2 T cells are a primate-specific T cell subset has lately been challenged through studies in other placental mammals. Genomic surveys demonstrated the existence of *TRGV9*, *TRDV2*, and *BTN3* genes in several species of placental mammals but not in other mammals or vertebrates (23, 24). Therefore, an emergence of those genes with Placentalia seems evident. The best candidate for a non-primate species bearing PAg-reactive γδ T cells is, so far, the alpaca (*Vicugna pacos*), which possesses transcripts of γδ TCR rearrangements with features typical of human PAg-reactive cells (23) and transcripts of a BTN3 ortholog with high homology to primate BTN3. In line with this, our group generated first evidence for PAg-reactive γδ T cells in this species (25).

Apart from that, the bottlenose dolphin (*Tursiops truncatus*) has recently been found to express *TRGV9*- and *TRDV2*-like productive rearrangements (26) and a *BTN3A3*-like gene was predicted *via* Gnomon gene prediction tool (GenBank: XM_004332447.2). Another candidate with in-frame *TRGV9*, *TRDV2*, and *BTN3* extracellular domain genes is the nine-banded armadillo (*Dasypus novemcinctus*), which belongs to the Xenarthra superorder. Armadillos are a natural reservoir of *M. leprae* and, therefore, a valuable tool for leprosy research (27, 28). In addition, the neurological involvement and dissemination in armadillos infected with *M. leprae* is similar to the one observed in humans and could not be reproduced in rodent models, as reviewed elsewhere (29). Karunakaran et al. (23) predicted armadillo *TRGV9* and *TRDV2* genes with rather high identities to their human homologs as well as a *BTN3-V*-like domain. In this study, we tested the expression of those genes in armadillo PBMCs. Here, we report the expression of *in silico* translatable *TRDV2* chains but the apparent lack of expression for productive *TRGV9* rearrangements and of a complete *BTN3*-like transcript and discuss the implications of these findings for the coevolution of *Vγ9*, *Vδ2*, and *BTN3* genes.

MATERIALS AND METHODS

Armadillo/Alpaca/Dolphin Homologs for *TRGV9*, *TRDV2*, and *BTN3*

Dasypus novemcinctus (taxid 9361) whole genomic shotgun sequences (wgs) were taken from the National Center for Biotechnology Information (NCBI) databases (BioProject: PRJNA12594/PRJNA196486; BioSample: SAMN02953623; GenBank: gb|AAGV00000000.3). Homologous sequences to human Vγ9Vδ2 TCR MOP (GenBank: KC170727.1/KC196073.1) or G115 (PDB: 1HXM_A) (30) and BTN3A1/2/3 (GenBank: NM_007048.5/NM_007047.4/NM_006994.4) were predicted using the NCBI Basic Local Alignment Tool (BLAST) (31). Accession numbers of identified armadillo homologs are: *TRGV9* AAGV03121505.1 nt402-695; *TRGC-A* Ex1 AAGV03121543.1 nt3646-3947; *TRGC-B* Ex1 AAGV03121550.1 nt3170-3471; *TRGC-C* Ex1 AAGV03121548.1 nt6289-6590; *TRGC-D* Ex1 AAGV03173223.1 nt672-373; *TRDV2* AAGV03208792.1 nt2277-1994; *TRDC* Ex1/2 AAGV03208782.1 nt782-510/nt95-27;

TRDC Ex3 AAGV03208781.1 nt 1291-1218; 1st *BTN3-V-ID* AAGV03145787.1; 2nd *BTN3-V* AAGV03287843.1; 3rd *BTN3-V* AAGV03240336.1; 2nd *BTN3-C* AAGV03240337.1; 3rd *BTN3-C* AAGV03010207.1.

Vicugna pacos (taxid 30538) whole genomic shotgun sequences were obtained from NCBI databases (BioProject: PRJNA30567, BioSample: SAMN01096418). A full-length alpaca BTN3-like sequence amplified from *V. pacos* cDNA (MG029164) (32) and an alpaca *BTN3* gene predicted by NCBI via Gnomon (XM_015251744.1) were used to analyze the genomic organization of the alpaca *BTN3* locus in the contig ABRR02153549.1.

Tursiops truncatus (taxid 9739) wgs sequences were obtained from NCBI databases (BioProject: PRJNA356464 and PRJNA20367, BioSample: SAMN06114300 and SAMN00000070) and two loci with *BTN3*-like genomic regions were found (*BTN3-V-ID* MRVK01002630.1 and *BTN3-V-C* ABRN02485746.1). A predicted *BTN3*-like molecule (XM_004332447.2) was used for BLAST analysis of wgs data.

Gene regions in *BTN3* loci were assigned according to consensus splice donor and acceptor sites. If no consensus splice site was found, the exon length was determined *via* homologies to human *BTN3A3* exons. If not otherwise indicated, the IMGT nomenclature was used for *TRG* and *TRD* genes and transcripts from human and mouse and if possible, armadillo genes were named according to their homologies to human genes. If not, letters were used to indicate different isoforms. The proteins encoded by *TRGV9* and *TRDV2* rearrangements are referred to as Vγ9 and Vδ2 TCR chains, respectively.

Amplification of Armadillo *TRGV9*, *TRDV2* Rearrangements, and *BTN3* Transcripts

Armadillo PBMCs in RNAlater and genomic liver DNA were provided by the National Hansen's Disease Program, Baton Rouge, LA, USA. Armadillos were maintained and samples collected in accordance with all ethical guidelines of the U.S. Public Health Service under protocols approved by the IACUC of the National Hansen's Disease Program, assurance number A3032-1.

RNA isolation was performed with RNeasy Mini Kit (Qiagen) and First Strand cDNA Synthesis (Thermo Fisher Scientific) was performed with Oligo dT primer after DNase digestion with DNase I (Thermo Fisher Scientific). Unknown 5′ and 3′ ends of transcripts were determined using the GeneRacer Kit with SuperScript III RT (Invitrogen) according to the manufacturer's instructions. Touchdown PCR with RACE-ready cDNA was performed with Q5 Hot Start Polymerase (NEB) and Phusion Polymerase (Thermo Fisher Scientific) was used for other PCR experiments. TOPO TA cloning set for sequencing with pCR4-TOPO vector (Thermo Fisher Scientific) was used for cloning and sequencing of PCR products. Armadillo genomic liver DNA was used as a control for PCR amplifications. Primer sequences are given in Supplementary Table S1 in Supplementary Material.

TRDV2

TRDV2/*TRDC* amplification was performed with the primers A21 and A72, nested PCR with A71 and A73. The 5′ end of *TRDV2* was determined *via* 5′RACE PCR with the primer A118 and nested primer A119. The primers A94 and A95 were applied for 3′RACE PCR starting from *TRDV2*. The PCR products of those amplifications were subsequently cloned and clones were analyzed.

TRGV9

Attempts to amplify a *TRGV9* rearrangement included amplification of *TRGV9*/*TRGC* with different primer combinations and 3′RACE PCR starting from *TRGV9*. The 5′ end of *TRGC* transcripts was, therefore, amplified using 5′RACE PCR and the primers A86 and A87, and the PCR product was cloned with the TOPO TA cloning kit. The 3′ sequence of *TRGC* was analyzed with 3′RACE PCR using the primers A103 and A104.

Butyrophilin 3

Expression of a *BTN3* homolog in armadillo PBMCs was analyzed with the partial amplification of *BTN3* from the *BTN3-V* to *BTN3-C* domain with primers specific for all three armadillo homologs (A122 + A123). Furthermore, RACE PCR to obtain the 5′ sequence of *BTN3-V* (A165, A166) and the 3′ sequence from *BTN3-V* (A163, A164) and *BTN3-C* (A167, A168) was conducted.

Sequence Analysis

Sequence analysis of genomic sequence data or PCR amplifications was performed with NCBI BLAST and Clustal Omega software. Alignments were calculated with Clustal Omega and BioEdit software was used for editing of alignments.

Expression of Armadillo Vδ2 TCR Chains

A murine TCR-negative T cell hybridoma cell line (BW58 r/mCD28) expressing a rat/mouse chimeric CD28 molecule (33, 34) was used to express armadillo Vδ2 TCR chains and test for surface expression, CD3 signaling, and HMBPP-reactivity. Full-length armadillo Vδ2 chains were amplified using the primers A193 and A194 and cloning in pMSCV-IRES-mCherry FP (a gift from Dario Vignali, Addgene plasmid # 52114) was performed using the In-Fusion® HD Cloning Kit (Takara Bio). The clones 7 and 9 were selected for co-expression with the human Vγ9 TCR MOP chain (35). Retroviral transduction of BW58 r/mCD28 cells was used to stably express TCR chains (36) and vector-encoded EGFP (pEGN huVγ9) and mCherry (pMSCV dnVδ2 cl7 or cl9) indicated successful transduction. TCR surface expression was confirmed in a flow cytometry staining of human Vγ9 (2.5 µg/ml anti-Vγ9 TCR 4D7 mAb) (37) detected by a secondary antibody [1 µg/ml F(ab')2 Fragment Donkey α-Mouse IgG (H + L)] (BD Pharmingen) and anti-mouse CD3 (1 µg/ml biotin hamster anti-mouse CD3ε clone 145-2C11) detected by streptavidin [0.4 µg/ml Streptavidin-APC (BD Pharmingen)]. BW58 r/m CD28 cells overexpressing transduced TCR chains can be applied as responder cell lines in various *in vitro* models of antigen recognition and their activity can be measured by mouse IL-2 ELISA (38, 39). Thus, the human/armadillo TCR transductants (hu/dnTCR cl7 or cl9) were tested for functional TCR signaling by CD3 crosslinking and PAg reactivity (HMBPP, Sigma-Aldrich) in co-culture with Raji RT1B^1 cells (23, 38, 40). TCR-negative BW58 cells expressing r/mCD28 (TCR$^-$), the same cells transduced with only the human Vγ9 chain (hu/-TCR), and the human TCR MOP

(hu/huTCR) were used as controls for stainings and stimulations. Cells were cultured in 200 µl/well RPMI 1640 supplemented with 5 or 10% FCS, 100 mM sodium pyruvate, 0.05% w/v glutamine, 10 mM nonessential amino acids, and 5×10^{-5} M mercaptoethanol (Invitrogen). Stimulations were carried out for 22 h with 5×10^4/well responder cells cultured in 96-well round bottom plates (Greiner) in co-culture with 5×10^4/well RAJI-RT1B[1] cells. For CD3 crosslinking, 96 well flat bottom plates (Greiner) were coated with anti-mouse CD3ε (clone 145-2C11, BD Pharmingen) in PBS for 24 h at 4°C before stimulations. Mouse IL-2 sandwich ELISA (BD) was used to determine IL-2 secretion in the culture supernatants and appropriate dilutions were measured if the upper detection limit was reached.

RESULTS

Genomic Organization of a Close Homolog of Human *BTN3* loci in Armadillo

Previous studies reported armadillo genomic regions homologous to the human *BTN3A1* extracellular and intracellular domains (24). After more detailed homology analysis of those armadillo genes, a closer resemblance to human *BTN3A3* was confirmed. Through the NCBI Basic local alignment (BLAST) tool (31), we, therefore, compared the human *BTN3A3* mRNA sequence (GenBank: NM_006994.4) to the *D. novemcinctus* whole genomic shotgun sequences (wgs) and could identify three homologous regions for the *BTN3*-V and *BTN3*-C domains, respectively. To compare these with homologous *BTN3* genes in other species, we additionally analyzed the *BTN3*-like loci of the two other candidate species alpaca (*V. pacos*) and bottlenose dolphin (*Tursiops truncatus*). For those species, predicted *BTN3A3*-like sequences are published in NCBI databases (alpaca: XM_015251744.1, dolphin: XM_004332447.2). Those predicted sequences were compared to the respective wgs databases to analyze *BTN3*-like loci and isoforms. Whole genome shotgun sequence databases are comprised of contigs with unique accession numbers and contain incomplete non-annotated genomic information. Whole genomic shotgun sequences were taken from the NCBI databases and allow full or partial reconstruction of *BTN3* encoding genomic regions (**Figure 1**). The corresponding nucleotide and amino acid sequence alignments and armadillo locus information are supplied in the Figures S1–S5 in Supplementary Material.

The human *BTN3A3* gene is comprised of nine protein-coding exons with exon 2 encoding the BTN3-V region, exon 3 encoding BTN3-C, exon 4 representing part of the transmembrane region, followed by four relatively small exons (5–8) and the B30.2 exon (9) (**Figure 1A**) (42). The alpaca *BTN3*-like genomic sequence is organized in a locus strikingly homologous to human *BTN3A3* (**Figure 1B**), showing exons with nucleotide sequence identities to human *BTN3A3* ranging from 73 to 93% and conserved intron lengths. The intracellular B30.2 domain is slightly shorter (81 nt) than the human counterpart. *In silico* splicing and translation of this alpaca *BTN3*-like gene with an overall nucleotide identity of 81% to human *BTN3A3* results in a protein sequence, which shares 72% amino acids with the human homolog. The expression of an alpaca BTN3-like molecule (GenBank: MG029164), with a conservation of 81% on the nucleotide and 73% on the amino acid level to human BTN3A3, has been confirmed before (32). We could, however, identify minor differences between the genomic alpaca *BTN3* and the *BTN3* transcript amplified from cDNA on the nucleotide and amino acid level (Figures S1 and S2 in Supplementary Material). This can be explained by inter-individual polymorphisms that also exist in humans (20). Both available alpaca BTN3 protein sequences carry six conserved amino acids each in the BTN3-V (Glu37, Lys39, Arg61, Tyr100, Gln102, and Tyr107) and B30.2 domain (His351, His378, Lys393, Arg412, Arg418, Arg469) (Figure S2 in Supplementary Material) predicted to be involved in PAg recognition in human BTN3A1 (15, 23, 24, 43).

Dolphins have been found to express *TRGV9*- and *TRDV2*-like mRNA transcripts (26), however, *BTN3* expression has not yet been proven. Here, we report the existence of one locus in the dolphin wgs database that comprises a full-length *BTN3*-like sequence predicted by NCBI *via* Gnomon (GenBank: XM_004332447.2) and a remarkably conserved locus organization (**Figure 1C**). Comparable to the alpaca *BTN3*-like locus, the dolphin locus features nine exons with nucleotide (nt) identities from 72 to 93% compared to human *BTN3A3* and intron lengths similar to the one in the human *BTN3A3* locus. However, the intron between exon 6 and 7 is only about half in size compared to the human intron at this location and the intracellular B30.2 exon (9) is 33 nucleotides shorter. The dolphin *BTN3*-like sequence *is in silico* translatable and exhibits a nucleotide identity of 81% and an amino acid (aa) identity of 73% with human *BTN3A3* (Figure S1 and S2 in Supplementary Material). This *BTN3A3*-like gene carries five out of six conserved amino acids in the BTN3-V domain and a substitution (Lys39Thr) (Figure S2 in Supplementary Material). All six predicted PAg-binding residues in the B30.2 domain (15, 43) are identical. Interestingly, we report the existence of another *BTN3*-like partial locus in the dolphin genomic sequences (**Figure 1D**). This contig is only long enough to comprise exons 1 to 3 of a *BTN3*-like gene structure. The *BTN3*-V (exon 2) of this locus (**Figure 1D**) is 92% identical to and shorter than the other *BTN3*-V found for the dolphin (**Figure 1C**), which indicates possible deletions in this exon. Consequently, this locus seems to code for a *BTN3*-like pseudogene.

Database analysis of the armadillo wgs database resulted in a total of three *BTN3*-V, three *BTN3*-C homologous regions, and one exon similar to the human *BTN3A3* B30.2 domain. One pair of *BTN3-V* and *BTN3-C* is comprised in one single contig of the nine-banded armadillo wgs database (AAGV03145787.1), which also includes a partial hit for the transmembrane region in exon 4 of *BTN3A3*, three small exons, homologous to human exons 6–8, and a downstream B30.2-like region (**Figure 1E**; Figure S5A in Supplementary Material). All those homologous regions show a nucleotide conservation of more than 70% compared to human *BTN3A3* domains and are also remarkably similar to human *BTN3A3* with respect to intron lengths and genomic organization. Two other *BTN3-V* domains (AAGV03287843.1 and AAGV03240336.1) were found as well as two other *BTN3-C* domains (AAGV03240337.1 and AAGV03010207.1). However, the *BTN3-C* containing contig AAGV03240337.1 does not seem to include a B30.2-like region and shows a truncated

***Homo sapiens BTN3A3*, chromosome 6, alternate assembly CHM1 1.1 (NC_018917.2)**

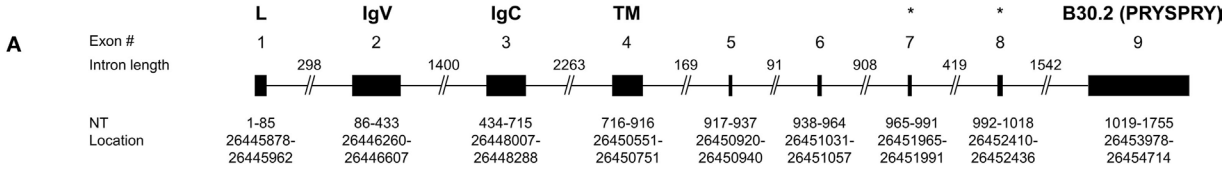

***Vicugna pacos* (taxid:30538) BTN3 homologous region, whole-genome shotgun contig ABRR02153549.1**

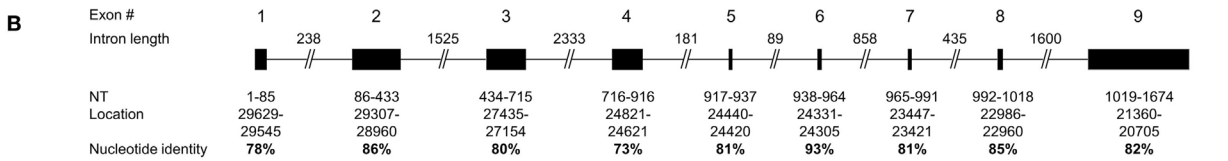

***Tursiops truncatus* (taxid:9739) BTN3 homologous region, whole-genome shotgun contigs**

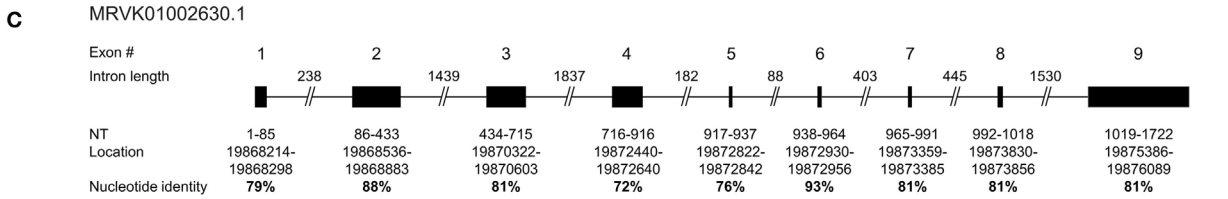

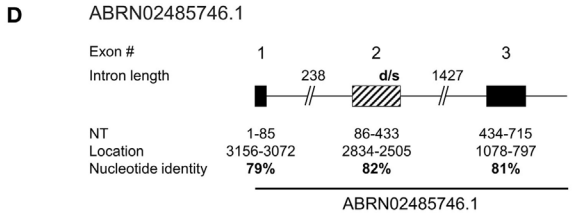

***Dasypus novemcinctus* (taxid:9361) BTN3 homologous regions, whole-genome shotgun contigs**

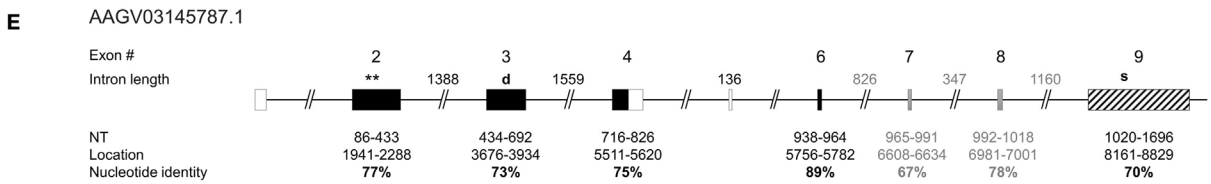

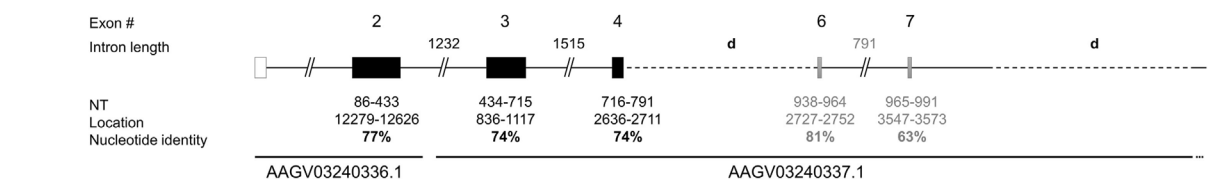

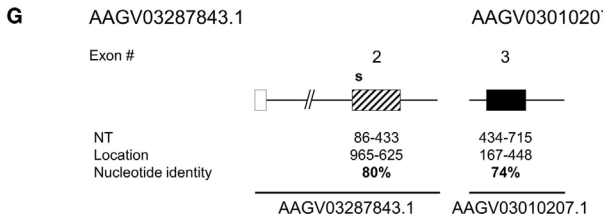

FIGURE 1 | Continued.

FIGURE 1 | Genomic organization of armadillo Butyrophilin 3 (*BTN3*) homologous regions *BTN3-V*, *BTN3-C*, and B30.2 show similarities to human, alpaca, and dolphin *BTN3* loci. The human *BTN3A3* locus **(A)** was determined by National Center for Biotechnology Information (NCBI) megablast of BTN3A3 (GenBank: NM_006994.4) to Human G + T database (GenBank/Assembly: NC_018917.2). The alpaca *BTN3*-like locus **(B)** was mapped using NCBI blastn of the predicted alpaca *BTN3A3* (XM_015251744.1) to *Vicugna pacos* wgs database. Dolphin *BTN3*-like loci **(C,D)** were identified using NCBI blastn of the predicted dolphin *BTN3A3* (XM_004332447.2) to *Tursiops truncatus* wgs. Armadillo *BTN3* homologous regions **(E–G)** were identified by NCBI blastn of human BTN3A3 to *Dasypus novemcinctus* whole genome shotgun contigs database (taxid: 9361). Exons are represented by boxes: translatable (solid black), non-translatable (striped black), missing (solid white) found by intron homologies (solid gray). The size of the exon, location in assembly/contig, and nucleotide identity of the regions to human *BTN3A3* are indicated in bold. Intron lengths were calculated based on location in contigs and putative deletions are shown by dashed lines and "d". Stop codons are indicated by "s" at the approximate location in the gene (*location of the proposed juxtamembrane motif important for PAg recognition (41); **location of the putative ATG at nt 1982).

transmembrane homolog directly followed by another exon similar to the transmembrane region of human *BTN3A3* (**Figure 1F**; Figure S5B in Supplementary Material). No homologous intracellular regions could be found in AAGV03010207.1 due to the short contig length (**Figure 1G**). Owing to the abundant use of SPRY/B30.2 domains in several families of molecules (44), prediction of *BTN3*-related B30.2 regions is difficult, except for the one found in contig AAGV03145787.1 (**Figure 1E**; Figure S4 in Supplementary Material). Additionally, conserved leader sequences encoded by exon 1 and another part of human *BTN3A3* encoded by exon 5 could not be predicted in all contigs through Blast using *BTN3A3* and it is noteworthy that gene prediction tools like Gnomon used for a predicted armadillo *BTN3A3* entry (GenBank: XM_012528284.1) or FGENESH+ (reference protein: huBTN3A1/2/3; GenBank: NM_007048.5/NM_007047.4/NM_006994.4) (45) also fail to predict a leader sequence in the AAGV03145787.1 contig. The published predicted *BTN3A3* homolog calculated by Gnomon software and our own calculations with FGENESH+ locate the start codon within the *BTN3-V* region (**Figure 1E**). *In silico* translation was successful for two *BTN3-V*-like regions (Figure S3A in Supplementary Material). The third *BTN3-V* homolog in AAGV03287843.1 (**Figure 1G**) carries a stop codon, if translated in the same frame. All three *BTN3-C* homologs were translatable; however, the respective region in AAGV03145787.1, although not having any stop codons, exhibits one nucleotide deletion leading to a frameshift (**Figure 1E**; Figure S3B in Supplementary Material). The only intracellular B30.2 domain found in this setting in the armadillo is identical with the previously reported one (24), but reexamination of the nucleotide to protein translation reveals several stop codons if the human B30.2 frame is used (Figure S4 in Supplementary Material). Yet, nucleotide alignments show the conservation of codons encoding all of the six conserved PAg-binding residues in the B30.2 domain of BTN3A1 described by Sandstrom et al. (15) including His351. Six extracellular PAg-binding residues have been proposed for the BTN3-V domain of BTN3A1 (43) and codons for these amino acids are partially conserved in the armadillo. Here, four out of six codons are conserved in the *BTN3*-V exons found in AAGV03240336.1 and AAGV03287843.1, and three out of six in AAGV03145787.1.

In addition to database analysis, we tested for expression of potential *BTN3* isoforms, as well as *TRGV9* and *TRDV2* transcripts, in cDNA of armadillo PBMCs. *D. novemcinctus* PBMCs dissolved in RNAlater were provided by the National Hansen's Disease Program, Baton Rouge, LA, USA and tested for transcripts of *BTN3*, *TRGV9*, and *TRDV2*. These PCR approaches included the amplifications of *BTN3* performed with primers specific for all *BTN3*-V and *BTN3*-C regions and the RACE PCR amplification of the 5′ and 3′ sequences starting in several domains of the predicted genes (Table S1 in Supplementary Material). No transcripts of *BTN3* were found, but we were able to amplify *BTN3*-V to *BTN3*-C including a corresponding intron from genomic liver DNA using the same primers. TOPO TA cloning of this PCR product resulted in five clones of apparently two distinct types (GenBank: cl1: MG600558; cl3: MG600559; cl5: MG600560; cl4/6: MG600561). One type was strikingly like the *BTN3*-V containing contig AAGV03240336.1 and the *BTN3*-C comprising contig AAGV03240337.1, which lead us to link those two contigs together (**Figure 1F**). However, the three TOPO clones of this subtype were not nucleotide-identical (cl1, cl3, cl5). The two remaining TOPO clones (cl4, cl6) were identical but could not be mapped to an armadillo wgs database contig and those clones were only 92–95% identical to the previously predicted *BTN3* loci. This could indicate the existence of even more loci for *BTN3* homologs in the armadillo. Closer comparison of the two predicted *BTN3* loci in the armadillo showed an apparent deletion in the AAGV03240337.1 contig when blasted with AAGV03145787.1 (**Figure 1F**). The first deletion results from a fusion of a truncated exon 4 with exon 6, the second deletion includes exon 8 and the B30.2 domain encoded by exon 9. In summary, no evidence was found for the expression of a *BTN3* homolog and even in the unlikely case that expression of such a gene was missed, we do not expect that these transcripts yield functional proteins. This is especially evident compared to the loci of alpaca and dolphin *BTN3*-like genomic regions, which feature not only homologous regions to all nine *BTN3A3* exons, but are also *in silico* translatable and in the case of alpaca also expressed on cDNA level.

In Silico Translatable *TRDV2* Rearrangements Are Expressed in Armadillo

In contrast to the lack of expression of a *BTN3*-like gene by *D. novemcinctus*, we demonstrate the expression of *in silico* translatable *TRDV2* TCR chains (IMGT nomenclature if not otherwise indicated). Full-length armadillo *TRDV2*-like variable regions preferentially recombined with a *TRDJ4* homolog could be assembled through the amplifications of *TRDV2/TRDC* from armadillo PBMCs, RACE PCR and cloning of full-length *TRDV2* chains into the pMSCV-IRES-mCherry FP plasmid. The overall amino acid identities of two clones carrying *TRDV2/TRDJ4*

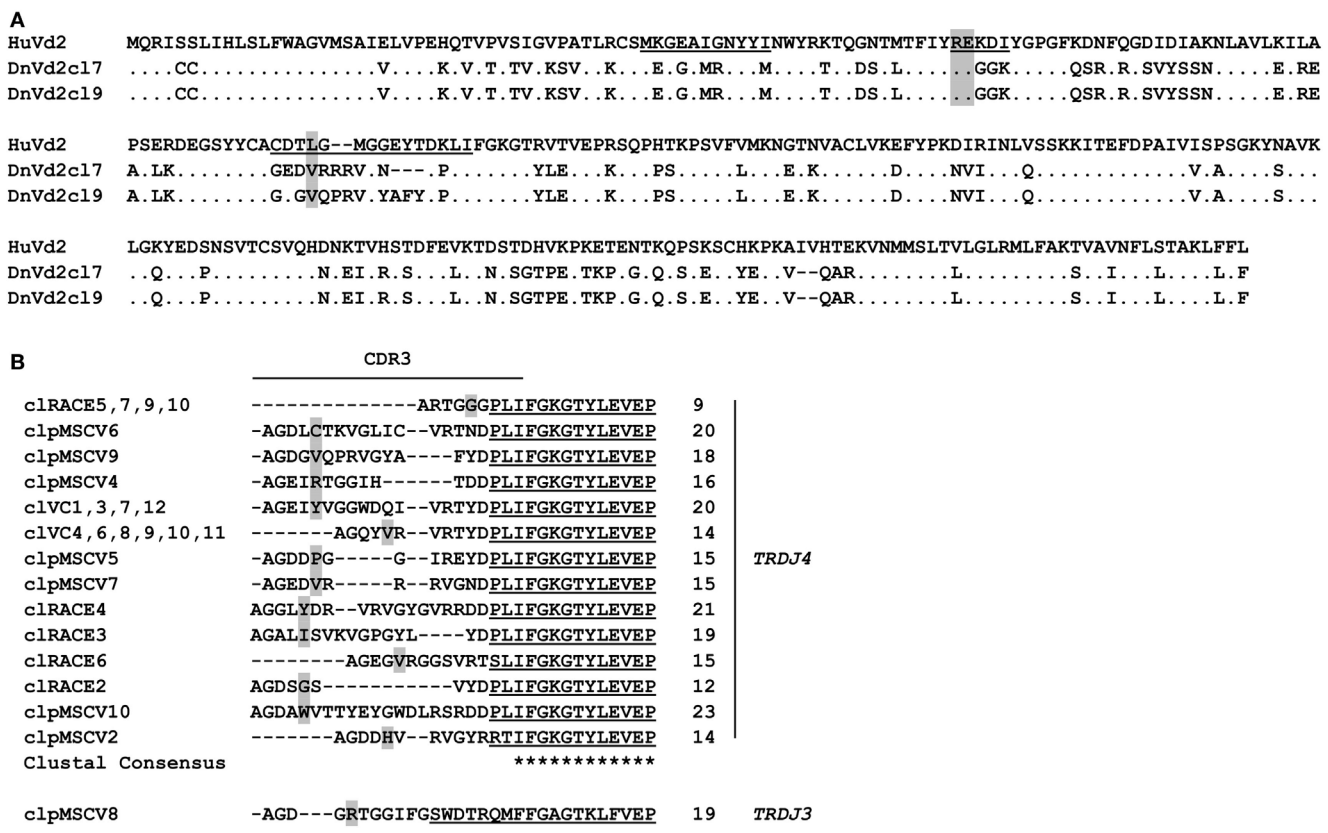

FIGURE 2 | *In silico* translatable Vδ2 T cell receptor chains are expressed in *Dasypus novemcinctus* PBMCs. **(A)** Alignment of human G115 Vδ2 chain (PDB: 1HXM_A) (30) and two representative armadillo Vδ2 chains (obtained from cloning of full-length armadillo Vδ2 chains into pMSCV-IRES-mCherry FP). CDR regions appear underscored and positions δ51/52 and δ97 (gray) are highlighted. **(B)** CDR3 regions of TRDV2 clones obtained by TRDV2/TRDC PCR (clVC1, 3, 4, and 6–12), TRDV2 3′RACE PCR (cl2-7, 9, 10), and cloning (clpMSCV2, 4–10). CDR3 lengths and TRDJ-usage are indicated on the right. Alignments were calculated with Clustal Omega webtool, identical amino acids (dots), J region (underscored), and positions δ51/52 and δ97 (gray) are highlighted. The GenBank Accession numbers of unique clones are: cl2 (MG021118); clVC1 (MG021131); clVC4 (MG021132); cl3 (MG021127); cl4 (MG021128); cl5 (MG021129); cl6 (MG021130); clpMSCV2 (MG807648); clpMSCV4 (MG807649); clpMSCV5 (MG807650); clpMSCV6 (MG807651); clpMSCV7 (MG807652); clpMSCV8 (MG807653); clpMSCV9 (MG807654); clpMSCV10 (MG807655).

homologs to the human G115 Vδ2 chain were 65% for both clones (**Figure 2A**). The armadillo V region shares a 77% nucleotide and a 59% aa identity with the human G115 Vδ2 chain, the J region is 86% (nt) and 86% (aa) identical to the human *TRDJ4*, *TRDC* of armadillo and human show a conservation of 82% (nt) and 69% (aa). A single clone was found to carry a *TRDV2* rearrangement with a *TRDJ* region homologous to human *TRDJ3*, with 88% (nt) and 89% (aa) identity (**Figure 2B**). PAg-reactive Vδ2 chains in humans commonly use *TRDJ1*, *2* or *3* (46), however, preferential but not exclusive rearrangement of *TRDV2* with a *TRDJ4*-like J segment has been shown in *V. pacos* (23). Other conserved features of PAg-reactive Vδ2 chains are varying CDR3 lengths (46), the residues Arg51 (30, 46, 47) and Glu52 (30), and the presence of a hydrophobic amino acid (Leu, Ile, Val) at position δ97 (46, 48). Partial armadillo *TRDV2*-like rearrangements were amplified either through 3′ RACE (8 clones) or *TRDV2/TRDC* amplification (10 clones) and PCR products were cloned with the TOPO TA cloning set for sequencing with pCR4-TOPO vector (Thermo Fisher Scientific). Another eight unique *TRDV2* clones were obtained from cloning of full-length rearranged armadillo *TRDV2* transcripts into the pMSCV-IRES-mCherry FP vector. All those partial clones were in frame with CDR3 lengths of 9-23 aa (**Figure 2B**). The positions Arg51 and Glu52 are conserved in all our armadillo clones and 5 out of 15 unique CDR3 sequences carry valine or isoleucine at δ97. Two armadillo Vδ2 chains amplified by PCR from cDNA were co-expressed with a human Vγ9 chain (TCR MOP) in a TCR-negative mouse cell line (BW58 r/mCD28) (33, 34). Surface expression of heterodimeric TCRs was confirmed by flow cytometry staining of the Vγ9 and Vδ2 chain and mouse CD3, as well as vector-encoded EGFP (human Vγ9) and mCherry (armadillo Vδ2) (**Figure 3**). CD28 expression of all cell lines was confirmed to be equal. The Vγ9 and CD3 expression of both cell lines overexpressing human/armadillo TCRs (hu/dnTCR cl7 or cl9) was significant but lower in comparison with human Vγ9Vδ2 TCR (huTCR) overexpressed in the same cell line. Thus, structural features important for pairing of armadillo Vδ2 chains with human Vγ9 chains seem to be conserved. Transduction of only the human Vγ9 chain did not

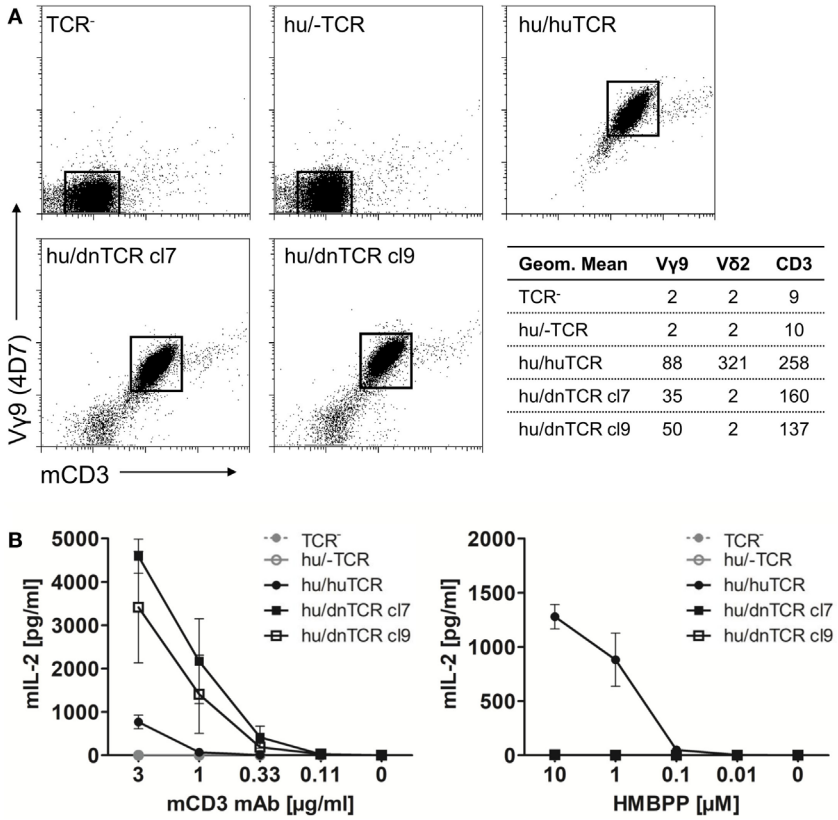

Geom. Mean	Vγ9	Vδ2	CD3
TCR-	2	2	9
hu/-TCR	2	2	10
hu/huTCR	88	321	258
hu/dnTCR cl7	35	2	160
hu/dnTCR cl9	50	2	137

FIGURE 3 | Surface expression of a functional armadillo Vδ2 T cell receptor (TCR) chain. **(A)** Armadillo Vδ2 TCR chains (pMSCV-IRES-mCherry FP armadillo Vδ2 cl7 or cl9) were retrovirally transduced into TCR-negative murine cell lines (BW58 r/mCD28). The human Vγ9 TCR MOP chain (pEGN huVγ9, GenBank: KC170727.1) was co-transduced and TCR surface expression was confirmed with flow cytometry stainings of the human Vγ9 chain, Vδ2 chain, and mouse CD3. Dotplots of Vγ9 (*Y*-axis, log) and CD3 (*X*-axis, log) co-stainings are shown and geometric means of Vγ9, Vδ2, and CD3 stainings are indicated. **(B)** BW58 r/mCD28 cells and TCR transductants were cultured for 22 h in 96-well plates coated with α-mCD3 mAb or with RAJI-RT1B[1] cells in the presence of increasing amounts of HMBPP. Mean + SEM of three independent experiments is shown for each cell line. Stimulation of hu/huTCR with 10 µg/ml α-mCD3 mAb resulted in 651 pg/ml (SEM: 129).

result in surface expression of Vγ9 or CD3. Signal transduction of huVγ9/dnVδ2 TCRs was studied with *in vitro* stimulation assays. Crosslinking of CD3 by plate-bound anti-mouse CD3 mAb was performed as described before (23, 40) and resulted in a substantial mIL-2 production of TCR transductants but no detectable IL-2 secretion of TCR- cells or cells transduced with the human Vγ9 chain only (**Figure 3B**). Anti-CD3 mediated stimulation of hu/huTCR reached saturation at 3 µg/ml anti-CD3 as indicated by stimulation with 10 µg/ml. Reactivity to the PAg HMBPP was not observed in a stimulation assay with RAJI-RT1B[1] cells, although human TCR transductants (hu/huTCR) readily recognized HMBPP in this context (**Figure 3B**). In summary, we report functional Vδ2 chains in the armadillo, that pair with TCR γ chains and show no crossreactivity to human BTN3.

Functional *TRG* Chain Rearrangements Lack Homologs to Human *TRGV9*

Genomic surveys revealed a *TRGV9*-like gene (Accession: AAGV03121505.1 nt402-695) in *D. novemcinctus*, which is *in silico* translatable and shares 80% of its nucleotides and 69% of its amino acids with the human G115 TCR γ. We were, however, not able to amplify a *TRGV9* transcript from armadillo PBMCs *via* PCR of *TRGV9/TRGC* or 3′RACE PCR from *TRGV9*. Notably, we found four different regions (*TRGC-A, -B, -C, -D*) homologous to the first exon of the TCR γ constant region in the armadillo wgs database. Armadillo *TRGC-A, -B,* and -C (Accession: *TRGC-A* Ex1 AAGV03121543.1; *TRGC-B* Ex1 AAGV03121550.1; *TRGC-C* Ex1 AAGV03121548.1) can be fully translated, however, *TRGC-D* (Accession: *TRGC-D* Ex1 AAGV03173223.1 nt672-373) contains stop codons and is most likely a *TRGC* pseudogene. The first exons of *TRGC-A* and *TRGC-B/C* share 94% nucleotide identity, *TRGC-B*, and *TRGC-C* are 98% identical on the nucleotide level and all of them are 80% identical to exon 1 of the human *TRGC1*. Amplification of the 3′ end and 5′RACE PCR of *TRGC-A/B/C* exon 1 confirmed *TRGC-A* and *TRGC-B*, but not *TRGC-C* transcripts on cDNA level. It appears that *TRGC-A* is encoded by 3 exons, which are all represented in the contig AAGV03121543.1 (exon1: nt3646-3953, exon2: nt7499–7548, exon3: nt9731-9871),

A

V regions of *TRGC* 5′RACE clones	Name	*D. novemcinctus* wgs Location	Identities %	*Homo sapiens* homologs	*Bos taurus* homologs
AAGV03121491.1 (2/23)	*TRGV2*	1977-2285	100	TRGV2 46%	TRGV8-1 47%
AAGV03121484.1 (3/23)	*TRGV4.1*	40190-40506	99/100	TRGV4 48%	TRGV8-3 46%
AAGV03121485.1 (4/23)	*TRGV4.2*	6942-7251	98/99/100	TRGV4 48%	TRGV8-1 45%
AAGV03121495.1 (6/23)	*TRGV4.3*	4127-4438	99/100	TRGV4 46%	TRGV8-1 51%
AAGV03121497.1 (1/23)	*TRGV8.1*	7075-7385	100	TRGV8 54%	TRGV9-2 53%
AAGV03121496.1 (4/23)	*TRGV8.2*	20045-20356	99	TRGV8 50%	TRGV9-2 48%
	TRGV8.4	20045-20356	90	TRGV8 46%	TRGV5-1 49%
AAGV03121492.1 (2/23)	*TRGV8.3*	14807-15113	100	TRGV8 47%	TRGV5-1 43%
AAGV03121542.1 (1/23)	*TRGmV6*	2171-2485	100	IGLV3-12 38%	TRGV10-1 64% *Canis lupus* TRGV5-2 65% *Mus musculus* TRGV6 56%

B

J Regions of *TRGC* 5′RACE clones	Name	*D. novemcinctus* wgs Location	Identities %	*Homo sapiens* homologs	Other species
AAGV03121547.1 (6/23)	*TRGJ-A*	2929-2991	97/98/100	TRGJP1 71% (73%) TRGJP2 63% (84%)	79% *Myotis davidii* (GenBank: ELK34092.1, 100%)
AAGV03121549.1 (15/23)	*TRGJ-B*	14544-14609	96/98/100	TRGJP 80% (52%) TRGJP1 73% (57%)	79% *Ovis aries* (PIR: S36294, 73%)
AAGV03121543.1 (2/23)	*TRGJ-C*	184-238	94/98	TRGJP 75% (60%)	72% *Tursiops truncatus* (GenBank: CDG24288.1, 90%)

C

Gene usage *in silico* translatable clones

TRGV	*TRGJ*	*TRGC*
TRGV4.2	*TRGJ-A*	*TRGC-B/C*
TRGV2 (2x)	*TRGJ-B*	*TRGC-B/C*
TRGV4.1	*TRGJ-B*	*TRGC-B/C*
TRGV8.4 (2x)	*TRGJ-B*	*TRGC-B/C*
TRGV8.1	*TRGJ-C*	*TRGC-A*
TRGmV6	*TRGJ-C*	*TRGC-A*

FIGURE 4 | Gamma chain transcripts homologous to human IMGT subgroup TRGV1 are expressed in armadillo PBMCs. **(A)** *Dasypus novemcinctus TRGV* regions used by 5′ RACE PCR products (Accession: *TRGC-A* Ex1 AAGV03121543.1; *TRGC-B* Ex1 AAGV03121550.1; *TRGC-C* Ex1 AAGV03121548.1) with associated wgs accession numbers based on sequence homologies and location of those in the respective contigs. Armadillo *TRGV* segments were labeled according to their closest homolog in human or mouse. Varying nucleotide identities to genomic sequences and putative AA homologs in human and other species are indicated. AA homologs were determined with IMGT/DomainGapAlign (57, 58). **(B)** J regions of *TRGC* 5′ RACE clones with location in wgs contigs and identities. Designations of J regions of the armadillo are random as distinct homologs to human *TRGJ* could not be determined. Homologies were determined by NCBI blastp to AA sequence of human germline encoded J regions or the NCBI non-redundant protein sequence database for other species. **(C)** Gene usage of *in silico* translatable *TRGC* 5′ RACE clones. The GenBank accession numbers of productive rearrangements are supplied in Table S2 in Supplementary Material.

whereas *TRGC-B* and *TRGC-C* are encoded by 4 exons with exon 1 and 2 in the contigs AAGV03121548.1 (nt6277–6590 and nt7441–7491) and AAGV03121550.1 (nt3170–3478 and nt7125-7178), and exon 3 and 4 in AAGV03121549.1 (nt101-152 and nt 2384–2525) and AAGV03121551.1 (nt1733-1784 and nt3978–4119), respectively. However, we were not able to assemble full-length *TRGC*-like regions from those contigs. Through 5′RACE PCR of *TRGC*, we can additionally report the existence of several armadillo *TRGV* transcripts. Of 23 clones used for the analysis (Table S2 in Supplementary Material), only eight were fully translatable, which corresponds to other findings of a multitude of non-productive TCR γ chain rearrangements, which can be expressed by cells that later commit to the αβ lineage (49, 50). The transcripts were compared to the armadillo wgs database and genomic location and accession numbers of contigs indicated the existence of nine different *TRGV* regions in our clones (**Figure 4A**). Those regions were found to be homologous to the human TRGV1 cluster (*TRGV1-8*) with amino acid identities ranging from 46% up to 54%. Higher similarities were found with *Bos taurus TRGV* (43–64%). One particular armadillo V segment could not be assigned to a human *TRGV*; however, it shares 56% identity with the mouse *TRGV6*. These V genes were rearranged with three different J regions (*TRGJ-A*, *TRGJ-B*, and *TRGJ-C*) (**Figure 4B**) sharing amino acid homologies of 63–80% with human *TRGJ* segments. Query cover with human homologs varied from 52 to 84%, which made a definite assignment difficult and lowers amino acid identities. Concerning the translatable clones resulting from the 5′RACE PCR (**Figure 4C**), it is interesting that *TRGJ-A* and *TRGJ-B* from *D. novemcinctus* seem to associate with other *TRGV* than *TRGJ-C*. Additionally, the *TRGC* usage of *TRGJ-C* is restricted to *TRGC-A*, the other J segments use either *TRGC-B* or *TRGC-C*, which could not be distinguished in this 5′RACE PCR. This apparent bias in C region usage is reminiscent of a cassette structure of the armadillo *TRG* locus comparable to artiodactyls or the bottlenose dolphin (IMGT-Locus representations) (26). Due to the lack of any evidence for a functional *TRGV9* rearrangement in armadillo PBMCs, together with the fact that we found other *TRGV* in a functional rearrangement with *TRGJ* in the armadillo, we propose the lack of expression of Vγ9Vδ2 TCRs in this species.

DISCUSSION

In this study, we report for the first time, an analysis of the expression of the essential components of the BTN3/Vγ9Vδ2 TCR system in the nine-banded armadillo (*D. novemcinctus*) and a comparison with homologous genes of other mammalian species. Studies of the distribution of the *TRGV9*, *TRDV2*, and *BTN3* genes identified this animal as a candidate for a functional Vγ9Vδ2 T cell population with a corresponding BTN3 molecule, which is essential for PAg recognition. However, we observed that aside from expression of *in silico* translatable *TRDV2* chains, the armadillo does most likely not express a functional *TRGV9* rearrangement. Surface expression of armadillo Vδ2 and human Vγ9 chains was achieved and signaling after CD3 stimulation was observed. This is an interesting finding, as apparently structural features, which allow pairing of armadillo Vδ2 with

Vγ9 are conserved, although no evidence for *TRGV9* expression was found. However, pairing of Vδ2 chains is not restricted to Vγ9 TCR chains in humans (51) even though there are certain pairings of γδ chains in mice that fail to be expressed (52). PAg-reactivity of human/armadillo heterodimeric γδ TCRs could not be shown. This was not surprising given that previous alanine-scanning mutagenesis showed contribution of all six CDR3 to PAg-reactivity (46). Nevertheless, armadillo Vδ2 chains might become a valuable model for future mutagenesis and structural studies, e.g., by transplanting human CDR into the armadillo Vδ2 chain. Moreover, the fact that in a species, which lacks bona fide PAg-reactive Vγ9Vδ2 TCR a third of the clones expresses the amino acids isoleucine or valine at position 97 suggest that the common use of these amino acids might not be taken as an indicator for a certain PAg-reactivity but may be largely random or a result of selection by structural requirements or other ligands (23, 48).

In addition to the lack of evidence for *TRGV9* rearrangements, no full-length *BTN3* transcript seems to be expressed in the armadillo. Based on genomic data, we report evidence for the existence of a multigene family of *BTN3*-like genes in the armadillo. Assessment of numbers of genes and their structural analysis is not possible to this date due to lack of genomic data and transcripts. We identified one locus that closely resembles the human *BTN3A3* locus and another one carrying deletions of transmembrane domains and the B30.2 domain, which could be more like a *BTN3A2* gene. However, the lack of signal sequences and multiple deletions and frameshifts as well as the overall lack of transcripts of a BTN3-like molecule speaks against functional BTN3 molecules in armadillo. The lack of leader sequences for all identified *BTN3-V* segments might indicate that loss of function preceded the duplication events. In contrast, in primates a duplication of the *BTN3* loci occurred (20) and led to new BTN3 molecules such as BTN3A1. This isoform is not only essential for the mediation of PAg-dependent stimulation of Vγ9Vδ2 T cells but also contributes to signaling to induce type I interferon transcription (15, 53). The fact that the non-functional armadillo B30.2 domain has preserved the codons for all six amino acids contacting the PAg in the proposed PAg binding sites and the existence of a translatable, although not expressed, *TRGV9* homolog may indicate the loss of functional elements for PAg sensing by γδ T cells in the armadillo ancestor. With the armadillo as an animal model for *M. leprae* in mind (27), one could speculate that a non-functional Vγ9Vδ2 T cell subset leads to higher susceptibility for this pathogen. In armadillos, however, low core body temperatures of 33–35°C could be seen as a factor that favors *M. leprae* proliferation *in vivo* (54, 55). Furthermore, other species like rodents, which have lost the BTN3/Vγ9Vδ2 system do not exhibit higher susceptibility to leprosy manifestations (29, 56). Regarding our observations of lacking transcripts of the BTN3/Vγ9Vδ2 system, we can only state that the armadillo cannot be used as a model for this T cell subset.

So far, there are two other non-primate species that can be considered prime candidates for possessing PAg-sensing Vγ9Vδ2 T cells. First, the alpaca (*V. pacos*), which not only expresses transcripts but also possesses a Vγ9Vδ2-like cell population that expands upon HMBPP stimulation (25). This species shows not only functional rearrangements of *TRGV9* and *TRDV2* but additionally a single BTN3 molecule (23, 24). Interestingly, this more primordial BTN3 possesses the predicted PAg-binding sites of both BTN3-V and B30.2 domain of the human BTN3A1 within a protein more closely related to human BTN3A3. The second species, the bottlenose dolphin shows functional *TRDV2* rearrangements as well as *TRG* rearrangements homolog to human *TRGV9/TRGJP* containing TCR-chains and a single *BTN3*-like gene. With these candidates in mind, it seems even more likely that *D. novemcinctus* cannot be considered a model organism for PAg-reactive Vγ9Vδ2 T cells, but stands as a witness for the emergence of this system with placental mammals.

ETHICS STATEMENT

Armadillos were maintained and samples collected in accordance with all ethical guidelines of the U.S. Public Health Service under protocols approved by the IACUC of the National Hansen's Disease Program, assurance number A3032-1.

AUTHOR CONTRIBUTIONS

AF planned, performed, and analyzed experiments, and wrote the manuscript. MK reviewed the manuscript and provided the sequence for *Vicugna pacos* BTN3. LS performed experiments. RT provided samples and reviewed the manuscript. TH conceived the study, planned and analyzed experiments, and wrote the manuscript.

ACKNOWLEDGMENTS

We greatly appreciate the technical assistance of Anna Nöhren and want to thank Niklas Beyersdorf for reviewing the manuscript and valuable input.

FUNDING

This study was funded by the DFG HE 2346/7-1 grant. The publication of this manuscript was funded by the German Research Foundation (DFG) and the University of Wuerzburg in the funding program Open Access Publishing.

SUPPLEMENTARY MATERIAL

The Supplementary Material for this article can be found online at https://www.frontiersin.org/articles/10.3389/fimmu.2018.00265/full#supplementary-material.

REFERENCES

1. Morita CT, Jin C, Sarikonda G, Wang H. Nonpeptide antigens, presentation mechanisms, and immunological memory of human Vgamma2Vdelta2 T cells: discriminating friend from foe through the recognition of prenyl pyrophosphate antigens. *Immunol Rev* (2007) 215:59–76. doi:10.1111/j.1600-065X.2006.00479.x
2. Kabelitz D, He W. The multifunctionality of human Vgamma9Vdelta2 gammadelta T cells: clonal plasticity or distinct subsets? *Scand J Immunol* (2012) 76(3):213–22. doi:10.1111/j.1365-3083.2012.02727.x
3. Fournie JJ, Sicard H, Poupot M, Bezombes C, Blanc A, Romagne F, et al. What lessons can be learned from gammadelta T cell-based cancer immunotherapy trials? *Cell Mol Immunol* (2013) 10(1):35–41. doi:10.1038/cmi.2012.39
4. Li B, Rossman MD, Imir T, Oner-Eyuboglu AF, Lee CW, Biancaniello R, et al. Disease-specific changes in gammadelta T cell repertoire and function in patients with pulmonary tuberculosis. *J Immunol* (1996) 157(9):4222–9.
5. Shen Y, Zhou D, Qiu L, Lai X, Simon M, Shen L, et al. Adaptive immune response of Vgamma2Vdelta2+ T cells during mycobacterial infections. *Science* (2002) 295(5563):2255–8. doi:10.1126/science.1068819
6. Huang D, Chen CY, Zhang M, Qiu L, Shen Y, Du G, et al. Clonal immune responses of *Mycobacterium*-specific gammadelta T cells in tuberculous and non-tuberculous tissues during *M. tuberculosis* infection. *PLoS One* (2012) 7(2):e30631. doi:10.1371/journal.pone.0030631
7. Abate G, Spencer CT, Hamzabegovic F, Blazevic A, Xia M, Hoft DF. *Mycobacterium*-specific gamma9delta2 T cells mediate both pathogen-inhibitory and CD40 ligand-dependent antigen presentation effects important for tuberculosis immunity. *Infect Immun* (2015) 84(2):580–9. doi:10.1128/IAI.01262-15
8. Qaqish A, Huang D, Chen CY, Zhang Z, Wang R, Li S, et al. Adoptive transfer of phosphoantigen-specific gammadelta T cell subset attenuates *Mycobacterium tuberculosis* infection in nonhuman primates. *J Immunol* (2017) 198(12):4753–63. doi:10.4049/jimmunol.1602019
9. Modlin RL, Pirmez C, Hofman FM, Torigian V, Uyemura K, Rea TH, et al. Lymphocytes bearing antigen-specific gamma delta T-cell receptors accumulate in human infectious disease lesions. *Nature* (1989) 339(6225):544–8. doi:10.1038/339544a0
10. Ryan-Payseur B, Frencher J, Shen L, Chen CY, Huang D, Chen ZW. Multieffector-functional immune responses of HMBPP-specific Vgamma2Vdelta2 T cells in nonhuman primates inoculated with *Listeria monocytogenes* DeltaactA prfA*. *J Immunol* (2012) 189(3):1285–93. doi:10.4049/jimmunol.1200641
11. Ho M, Webster HK, Tongtawe P, Pattanapanyasat K, Weidanz WP. Increased gamma delta T cells in acute *plasmodium falciparum* malaria. *Immunol Lett* (1990) 25(1–3):139–41. doi:10.1016/0165-2478(90)90104-X
12. De Paoli P, Basaglia G, Gennari D, Crovatto M, Modolo ML, Santini G. Phenotypic profile and functional characteristics of human gamma and delta T cells during acute toxoplasmosis. *J Clin Microbiol* (1992) 30(3):729–31.
13. Chen ZW. Multifunctional immune responses of HMBPP-specific Vgamma2Vdelta2 T cells in M. tuberculosis and other infections. *Cell Mol Immunol* (2013) 10(1):58–64. doi:10.1038/cmi.2012.46
14. Lawand M, Dechanet-Merville J, Dieu-Nosjean MC. Key features of gamma-delta T-cell subsets in human diseases and their immunotherapeutic implications. *Front Immunol* (2017) 8:761. doi:10.3389/fimmu.2017.00761
15. Sandstrom A, Peigne CM, Leger A, Crooks JE, Konczak F, Gesnel MC, et al. The intracellular B30.2 domain of butyrophilin 3A1 binds phosphoantigens to mediate activation of human Vgamma9Vdelta2 T cells. *Immunity* (2014) 40(4):490–500. doi:10.1016/j.immuni.2014.03.003
16. Compte E, Pontarotti P, Collette Y, Lopez M, Olive D. Frontline: characterization of BT3 molecules belonging to the B7 family expressed on immune cells. *Eur J Immunol* (2004) 34(8):2089–99. doi:10.1002/eji.200425227
17. Yamashiro H, Yoshizaki S, Tadaki T, Egawa K, Seo N. Stimulation of human butyrophilin 3 molecules results in negative regulation of cellular immunity. *J Leukoc Biol* (2010) 88(4):757–67. doi:10.1189/jlb.0309156
18. Messal N, Mamessier E, Sylvain A, Celis-Gutierrez J, Thibult ML, Chetaille B, et al. Differential role for CD277 as a co-regulator of the immune signal in T and NK cells. *Eur J Immunol* (2011) 41(12):3443–54. doi:10.1002/eji.201141404
19. Rhodes DA, Chen HC, Price AJ, Keeble AH, Davey MS, James LC, et al. Activation of human gammadelta T cells by cytosolic interactions of BTN3A1 with soluble phosphoantigens and the cytoskeletal adaptor periplakin. *J Immunol* (2015) 194(5):2390–8. doi:10.4049/jimmunol.1401064
20. Afrache H, Pontarotti P, Abi-Rached L, Olive D. Evolutionary and polymorphism analyses reveal the central role of BTN3A2 in the concerted evolution of the BTN3 gene family. *Immunogenetics* (2017) 69(6):379–90. doi:10.1007/s00251-017-0980-z
21. Rhodes DA, Stammers M, Malcherek G, Beck S, Trowsdale J. The cluster of BTN genes in the extended major histocompatibility complex. *Genomics* (2001) 71(3):351–62. doi:10.1006/geno.2000.6406
22. Riano F, Karunakaran MM, Starick L, Li J, Scholz CJ, Kunzmann V, et al. Vgamma9Vdelta2 TCR-activation by phosphorylated antigens requires butyrophilin 3 A1 (BTN3A1) and additional genes on human chromosome 6. *Eur J Immunol* (2014) 44(9):2571–6. doi:10.1002/eji.201444712
23. Karunakaran MM, Gobel TW, Starick L, Walter L, Herrmann T. Vgamma9 and Vdelta2 T cell antigen receptor genes and butyrophilin 3 (BTN3) emerged with placental mammals and are concomitantly preserved in selected species like alpaca (Vicugna pacos). *Immunogenetics* (2014) 66(4):243–54. doi:10.1007/s00251-014-0763-8
24. Karunakaran MM, Herrmann T. The Vgamma9Vdelta2 T cell antigen receptor and butyrophilin-3 A1: models of interaction, the possibility of co-evolution, and the case of dendritic epidermal T cells. *Front Immunol* (2014) 5:648. doi:10.3389/fimmu.2014.00648
25. Fichtner AS, Karunakaran MM, Starick L, Goebel T, Herrmann T. Functional and molecular conservation of activation of T cells by phosphorylated metabolites between humans and the new world camelid alpaca (*Vicugna pacos*). *Eur J Immunol* (2017) 47(S2):211 (abstract p. 248). doi:10.1002/eji.201770300
26. Linguiti G, Antonacci R, Tasco G, Grande F, Casadio R, Massari S, et al. Genomic and expression analyses of *Tursiops truncatus* T cell receptor gamma (TRG) and alpha/delta (TRA/TRD) loci reveal a similar basic public gammadelta repertoire in dolphin and human. *BMC Genomics* (2016) 17(1):634. doi:10.1186/s12864-016-2841-9
27. Kirchheimer WF, Storrs EE. Attempts to establish the armadillo (*Dasypus novemcinctus* Linn.) as a model for the study of leprosy. I. Report of lepromatoid leprosy in an experimentally infected armadillo. *Int J Lepr Other Mycobact Dis* (1971) 39(3):693–702.
28. Truman R. Leprosy in wild armadillos. *Lepr Rev* (2005) 76(3):198–208.
29. Scollard DM, Adams LB, Gillis TP, Krahenbuhl JL, Truman RW, Williams DL. The continuing challenges of leprosy. *Clin Microbiol Rev* (2006) 19(2):338–81. doi:10.1128/CMR.19.2.338-381.2006
30. Allison TJ, Winter CC, Fournie JJ, Bonneville M, Garboczi DN. Structure of a human gammadelta T-cell antigen receptor. *Nature* (2001) 411(6839):820–4. doi:10.1038/35081115
31. Altschul SF, Madden TL, Schaffer AA, Zhang J, Zhang Z, Miller W, et al. Gapped BLAST and PSI-BLAST: a new generation of protein database search programs. *Nucleic Acids Res* (1997) 25(17):3389–402. doi:10.1093/nar/25.17.3389
32. Karunakaran MM. *The Evolution of Vγ9Vδ2 T Cells [Dissertation]*. Julius-Maximilians-Universität Würzburg (2014). Available from: urn:nbn:de:bvb:20-opus-99871;https://opus.bibliothek.uni-wuerzburg.de/opus4-wuerzburg/frontdoor/deliver/index/docId/9987/file/MMKarunakaran_Doctoral_Thesis.pdf
33. Letourneur F, Malissen B. Derivation of a T cell hybridoma variant deprived of functional T cell receptor alpha and beta chain transcripts reveals a nonfunctional alpha-mRNA of BW5147 origin. *Eur J Immunol* (1989) 19(12):2269–74. doi:10.1002/eji.1830191214
34. Luhder F, Huang Y, Dennehy KM, Guntermann C, Muller I, Winkler E, et al. Topological requirements and signaling properties of T cell-activating, anti-CD28 antibody superagonists. *J Exp Med* (2003) 197(8):955–66. doi:10.1084/jem.20021024
35. Harly C, Guillaume Y, Nedellec S, Peigne CM, Monkkonen H, Monkkonen J, et al. Key implication of CD277/butyrophilin-3 (BTN3A) in cellular stress sensing by a major human gammadelta T-cell subset. *Blood* (2012) 120(11):2269–79. doi:10.1182/blood-2012-05-430470
36. Soneoka Y, Cannon PM, Ramsdale EE, Griffiths JC, Romano G, Kingsman SM, et al. A transient three-plasmid expression system for the production of high titer retroviral vectors. *Nucleic Acids Res* (1995) 23(4):628–33. doi:10.1093/nar/23.4.628

37. Deusch K, Lüling F, Reich K, Classen M, Wagner H, Pfeffer K. A major fraction of human intraepithelial lymphocytes simultaneously expresses the γ/δ T cell receptor, the CD8 accessory molecule and preferentially uses the Vδ1 gene segment. *Eur J Immunol* (1991) 21(4):1053–9. doi:10.1002/eji.1830210429
38. Kreiss M, Asmuss A, Krejci K, Lindemann D, Miyoshi-Akiyama T, Uchiyama T, et al. Contrasting contributions of complementarity-determining region 2 and hypervariable region 4 of rat BV8S2+ (Vbeta8.2) TCR to the recognition of myelin basic protein and different types of bacterial superantigens. *Int Immunol* (2004) 16(5):655–63. doi:10.1093/intimm/dxh068
39. Pyz E, Naidenko O, Miyake S, Yamamura T, Berberich I, Cardell S, et al. The complementarity determining region 2 of BV8S2 (V beta 8.2) contributes to antigen recognition by rat invariant NKT cell TCR. *J Immunol* (2006) 176(12):7447–55. doi:10.4049/jimmunol.176.12.7447
40. Starick L, Riano F, Karunakaran MM, Kunzmann V, Li J, Kreiss M, et al. Butyrophilin 3A (BTN3A, CD277)-specific antibody 20.1 differentially activates Vgamma9Vdelta2 TCR clonotypes and interferes with phosphoantigen activation. *Eur J Immunol* (2017) 47(6):982–92. doi:10.1002/eji.201646818
41. Peigne CM, Leger A, Gesnel MC, Konczak F, Olive D, Bonneville M, et al. The juxtamembrane domain of butyrophilin BTN3A1 controls phosphoantigen-mediated activation of human Vgamma9Vdelta2 T cells. *J Immunol* (2017) 198(11):4228–34. doi:10.4049/jimmunol.1601910
42. Nguyen K, Li J, Puthenveetil R, Lin X, Poe MM, Hsiao CC, et al. The butyrophilin 3A1 intracellular domain undergoes a conformational change involving the juxtamembrane region. *FASEB J* (2017) 31(11):4697–706. doi:10.1096/fj.201601370RR
43. Vavassori S, Kumar A, Wan GS, Ramanjaneyulu GS, Cavallari M, El Daker S, et al. Butyrophilin 3A1 binds phosphorylated antigens and stimulates human gammadelta T cells. *Nat Immunol* (2013) 14(9):908–16. doi:10.1038/ni.2665
44. Rhodes DA, de Bono B, Trowsdale J. Relationship between SPRY and B30.2 protein domains. Evolution of a component of immune defence? *Immunology* (2005) 116(4):411–7. doi:10.1111/j.1365-2567.2005.02248.x
45. Solovyev VV. Statistical approaches in eukaryotic gene prediction. 3rd ed. In: Cannings C, Balding D, Bishop M, editors. *Handbook of Statistical Genetics*. West Sussex: John Wiley & Sons Ltd (2007). p. 97–159.
46. Wang H, Fang Z, Morita CT. Vgamma2Vdelta2 T cell receptor recognition of prenyl pyrophosphates is dependent on all CDRs. *J Immunol* (2010) 184(11):6209–22. doi:10.4049/jimmunol.1000231
47. Miyagawa F, Tanaka Y, Yamashita S, Mikami B, Danno K, Uehara M, et al. Essential contribution of germline-encoded lysine residues in Jgamma1.2 segment to the recognition of nonpeptide antigens by human gammadelta T cells. *J Immunol* (2001) 167(12):6773–9. doi:10.4049/jimmunol.167.12.6773
48. Yamashita S, Tanaka Y, Harazaki M, Mikami B, Minato N. Recognition mechanism of non-peptide antigens by human gammadelta T cells. *Int Immunol* (2003) 15(11):1301–7. doi:10.1093/intimm/dxg129
49. Alexandre D, Lefranc MP. The human gamma/delta + and alpha/beta + T cells: a branched pathway of differentiation. *Mol Immunol* (1992) 29(4):447–51. doi:10.1016/0161-5890(92)90001-E
50. Sherwood AM, Desmarais C, Livingston RJ, Andriesen J, Haussler M, Carlson CS, et al. Deep sequencing of the human TCRgamma and TCRbeta repertoires suggests that TCRbeta rearranges after alphabeta and gammadelta T cell commitment. *Sci Transl Med* (2011) 3(90):90ra61. doi:10.1126/scitranslmed.3002536
51. Solomon KR, Krangel MS, McLean J, Brenner MB, Band H. Human T cell receptor-gamma and -delta chain pairing analyzed by transfection of a T cell receptor-delta negative mutant cell line. *J Immunol* (1990) 144(3):1120–6.
52. Boucontet L, Grana M, Alzari PM, Pereira P. Mechanisms determining cell membrane expression of different gammadelta TCR chain pairings. *Eur J Immunol* (2009) 39(7):1937–46. doi:10.1002/eji.200939345
53. Seo M, Grana M, Alzari PM, Pereira P. MAP4-regulated dynein-dependent trafficking of BTN3A1 controls the TBK1–IRF3 signaling axis. *Proceedings of the National Academy of Sciences* (2016) 113(50):14390–5. doi:10.1073/pnas.1615287113
54. Truman RW, Krahenbuhl JL. Viable *M. leprae* as a research reagent. *Int J Lepr Other Mycobact Dis* (2001) 69(1):1–12.
55. Truman RW, Ebenezer GJ, Pena MT, Sharma R, Balamayooran G, Gillingwater TH, et al. The armadillo as a model for peripheral neuropathy in leprosy. *ILAR J* (2014) 54(3):304–14. doi:10.1093/ilar/ilt050
56. Johnstone PA. The search for animal models of leprosy. *Int J Lepr Other Mycobact Dis* (1987) 55(3):535–47.
57. Ehrenmann F, Kaas Q, Lefranc MP. IMGT/3Dstructure-DB and IMGT/DomainGapAlign: a database and a tool for immunoglobulins or antibodies, T cell receptors, MHC, IgSF and MhcSF. *Nucleic Acids Research* (2010) 38(Suppl 1):D301–7. doi:10.1093/nar/gkp946
58. Ehrenmann F, Lefranc MP. IMGT/DomainGapAlign: the IMGT® tool for the analysis of IG, TR, MH, IgSF, and MhSF domain amino acid polymorphism. *Methods Mol Biol* (2012) 882:605–33. doi:10.1007/978-1-61779-842-9_33

Conflict of Interest Statement: The authors declare that the research was conducted in the absence of any commercial or financial relationships that could be construed as a potential conflict of interest.

Copyright © 2018 Fichtner, Karunakaran, Starick, Truman and Herrmann. This is an open-access article distributed under the terms of the Creative Commons Attribution License (CC BY). The use, distribution or reproduction in other forums is permitted, provided the original author(s) and the copyright owner are credited and that the original publication in this journal is cited, in accordance with accepted academic practice. No use, distribution or reproduction is permitted which does not comply with these terms.

Advantages of publishing in Frontiers

OPEN ACCESS
Articles are free to read for greatest visibility and readership

FAST PUBLICATION
Around 90 days from submission to decision

HIGH QUALITY PEER-REVIEW
Rigorous, collaborative, and constructive peer-review

TRANSPARENT PEER-REVIEW
Editors and reviewers acknowledged by name on published articles

Frontiers
Avenue du Tribunal-Fédéral 34
1005 Lausanne | Switzerland

Visit us: www.frontiersin.org
Contact us: info@frontiersin.org | +41 21 510 17 00

REPRODUCIBILITY OF RESEARCH
Support open data and methods to enhance research reproducibility

DIGITAL PUBLISHING
Articles designed for optimal readership across devices

FOLLOW US
@frontiersin

IMPACT METRICS
Advanced article metrics track visibility across digital media

EXTENSIVE PROMOTION
Marketing and promotion of impactful research

LOOP RESEARCH NETWORK
Our network increases your article's readership